

# High-Throughput Calculations of Magnetic Topological Materials

Yuanfeng Xu,<sup>1</sup> Luis Elcoro,<sup>2</sup> Zhida Song,<sup>3</sup> Benjamin J. Wieder,<sup>4,5,3</sup> M. G. Vergniory,<sup>6,7</sup>  
Nicolas Regnault,<sup>8,3</sup> Yulin Chen,<sup>9,10,11,12</sup> Claudia Felser,<sup>13,14</sup> and B. Andrei Bernevig<sup>3,1,15,\*</sup>

<sup>1</sup>Max Planck Institute of Microstructure Physics, 06120 Halle, Germany

<sup>2</sup>Department of Condensed Matter Physics, University of the Basque Country UPV/EHU, Apartado 644, 48080 Bilbao, Spain

<sup>3</sup>Department of Physics, Princeton University, Princeton, New Jersey 08544, USA

<sup>4</sup>Department of Physics, Massachusetts Institute of Technology, Cambridge, MA 02139, USA

<sup>5</sup>Department of Physics, Northeastern University, Boston, MA 02115, USA

<sup>6</sup>Donostia International Physics Center, P. Manuel de Lardizabal 4, 20018 Donostia-San Sebastian, Spain

<sup>7</sup>IKERBASQUE, Basque Foundation for Science, Bilbao, Spain

<sup>8</sup>Laboratoire de Physique de l'Ecole normale supérieure,

ENS, Université PSL, CNRS, Sorbonne Université,

Université Paris-Diderot, Sorbonne Paris Cité, Paris, France

<sup>9</sup>School of Physical Science and Technology, ShanghaiTech University, Shanghai 201210, China

<sup>10</sup>ShanghaiTech Laboratory for Topological Physics, Shanghai 200031, China

<sup>11</sup>Clarendon Laboratory, Department of Physics, University of Oxford, Oxford OX1 3PU, UK

<sup>12</sup>State Key Laboratory of Low Dimensional Quantum Physics,

Department of Physics and Collaborative Innovation Center of Quantum Matter, Tsinghua University, Beijing 100084, China

<sup>13</sup>Max Planck Institute for Chemical Physics of Solids, Dresden D-01187, Germany

<sup>14</sup>Center for Nanoscale Systems, Faculty of Arts and Science,

Harvard University, 11 Oxford Street, LISE 308Cambridge, MA 021138, USA

<sup>15</sup>Physics Department, Freie Universität Berlin, Arnimallee 14, 14195 Berlin, Germany

(Dated: February 11, 2023)

The discoveries of intrinsically magnetic topological materials, including semimetals with a large anomalous Hall effect and axion insulators [1–3], have directed fundamental research in solid-state materials. Topological Quantum Chemistry [4] has enabled the understanding of and the search for paramagnetic topological materials [5, 6]. Using magnetic topological indices obtained from magnetic topological quantum chemistry (MTQC) [7], here we perform the first high-throughput search for magnetic topological materials. here we perform a high-throughput search for magnetic topological materials based on first-principles calculations. We use as our starting point the Magnetic Materials Database on the Bilbao Crystallographic Server, which contains more than 549 magnetic compounds with magnetic structures deduced from neutron-scattering experiments, and identify 130 enforced semimetals (for which the band crossings are implied by symmetry eigenvalues), and topological insulators. For each compound, we perform complete electronic structure calculations, which include complete topological phase diagrams using different values of the Hubbard potential. Using a custom code to find the magnetic co-representations of all bands in all magnetic space groups, we generate data to be fed into the algorithm of MTQC to determine the topology of each magnetic material. Several of these materials display previously unknown topological phases, including symmetry-indicated magnetic semimetals, three-dimensional anomalous Hall insulators and higher-order magnetic semimetals. We analyse topological trends in the materials under varying interactions: 60 per cent of the 130 topological materials have topologies sensitive to interactions, and the others have stable topologies under varying interactions. We provide a materials database for future experimental studies and open-source code for diagnosing topologies of magnetic materials.

## CONTENTS

I. Introduction	2	VI. Chemical Categories	7
II. Workflow	3	VII. Discussion	7
III. Topological phase diagrams	3	VIII. Conclusion	8
IV. High-quality topological materials	4	IX. Methods	9
V. Consistency with previous works	6	A. A brief introduction to Magnetic Topological Quantum Chemistry (MTQC)	12
		B. Material statistics in the BCSMD	14
		C. Computational methods	17
		1. Convention setting of the magnetic unit cell	17

\* bernevig@princeton.edu

2. Parameters setting in <i>ab initio</i> calculations	17	M. Band structures and detailed information	123
3. Magnetic VASP2trace package	18	References	225
4. Construction of Wannier tight-binding Hamiltonian and surface states calculation	18		
D. Comparison of the ground state energy between different magnetic configurations of several compounds	18		
E. Comparisons between different exchange-correlation potentials	19		
1. Band structure calculations with GGA functional	19		
2. Band structure calculations with meta-GGA functional	19		
F. Comparisons between LDA+U and LDA+Gutzwiller methods	28		
G. Topological phase diagrams of the topological materials that predicted by MTQC	28		
H. Physical interpretations for the TI classified by MTQC	34		
1. Definitions for the stable indices of MSG 2.4	34		
2. Definitions for the stable indices of MSG 47.249	35		
3. Definitions for the stable indices of MSG 81.33	35		
4. Definitions for the stable indices of MSG 83.43	35		
5. Definitions for the stable indices of MSG 143.1	36		
6. Stable indices of the magnetic TIs	36		
I. Compatibility-relations along high-symmetry paths of the symmetry enforced semimetals	45		
J. Detailed discussion of the ideal magnetic TI and SMs	94		
1. Higher-order topology of the ideal Axion insulator NpBi	94		
2. Topological phase diagram of the ideal antiferromagnetic nodal-line semimetal CeCo <sub>2</sub> P <sub>2</sub>	95		
3. Topological phase diagram of the antiferromagnetic Dirac semimetal MnGeO <sub>3</sub>	95		
4. Weyl nodes, Nodal-lines and Anomalous Hall effect in Mn <sub>3</sub> ZnC	96		
K. Fragile bands in the magnetic materials	98		
L. Magnetic moments for each materials with different Coulomb interactions	103		
1. Ferro(Ferri)magnetic materials	123		
		I. INTRODUCTION	
		Non-magnetic topological materials have dominated the landscape of topological physics for the past two decades. Research in this field has led to a rapid succession of theoretical and experimental discoveries; notable examples include the theoretical prediction of the first topological insulators (TIs) in two [8, 9] and three spatial dimensions [10], topological crystalline insulators [11], Dirac and Weyl semimetals [12–18], and non-symmorphic topological insulators and semimetals [19–23]. Though topological materials were once believed to be rare and esoteric, recent advances in nonmagnetic topological materials have found that TIs and enforced semimetals (ESs) are much more prevalent than initially thought. In 2017 <i>Topological Quantum Chemistry</i> (TQC) and the equivalent method of symmetry-based indicators provided a description of the universal global properties of all possible atomic limit band structures in all non-magnetic symmetry groups, in real and momentum space [4, 24–27]. This allowed for a classification of the non-magnetic, non-trivial (topological) band structures through high-throughput methods that have changed our understanding of the number of topological materials existent in nature. About 40%–50% of all non-magnetic materials can be classified as topological at the Fermi level [5, 6, 28], leading to a “periodic table” of topological materials.	
		These breakthroughs in non-magnetic materials have not yet been matched by similar advances in magnetic compounds, due to a multitude of challenges. First, although a method for classifying band topology in the 1651 magnetic and nonmagnetic space groups (MSGs and SGs, respectively) was recently introduced [29], there still does not exist a theory similar to TQC or equivalent methods [4, 24–27] by which the indicator groups in Ref. [29] can be linked to topological (anomalous) surface (and hinge) states. Second, a full classification of the magnetic co-representations and compatibility relations has not yet been tabulated. Third, code to compute the magnetic co-representations from <i>ab initio</i> band structures does not exist. Fourth, and finally, even if all the above were available, the <i>ab initio</i> calculation of magnetic compounds is notoriously inaccurate for complicated magnetic structures beyond ferromagnets. Specifically, unless the magnetic structure of a material is known a priori, then the <i>ab initio</i> calculation will likely converge to a misleading ground state. This has rendered the number of accurately predicted magnetic topological materials to be less than 10 [1–3, 30–39].	
		In the present work and in ref. [7], we present substantial advances towards solving all of the above challenges—which we have made freely	

available to the public on internet repositories (<https://www.cryst.ehu.es/cryst/checktopologicalmagnet>) -covering four years of our work on the subject, and over 70 years [40] of research on the group theory, symmetry, and topology of magnetic materials. We present a full theory of magnetic indices, co-representations, compatibility relations, code with which to compute the magnetic co-representations directly from ab initio calculations, and we perform full local density approximation (LDA) + Hubbard U calculations on 549 magnetic structures, which have been accurately tabulated through the careful analysis of neutron-scattering data. We predict several novel magnetic topological phases in real materials, including higher-order magnetic Dirac semimetals with hinge arcs [41], magnetic chiral crystals with long Fermi arcs, Dirac semimetals with nodes not related by time-reversal symmetry, Weyl points and nodal lines in non-collinear antiferrimagnets, and ideal axion insulators with gapped surface states and chiral hinge modes [42, 43].

## II. WORKFLOW

Starting from the material database MAGNDATA MAGNDATA on the Bilbao Crystallographic Server (BCS) (the BCSMD), which contains portable magnetic structure files determined by neutron scattering experiments of more than 707 magnetic structures, we select 549 high-quality magnetic structures for the ab initio calculations. We take the magnetic configurations provided by BCSMD as the initial inputs and then perform ab initio calculations incorporating spin-orbit coupling. LDA + U are applied for each material with different Hubbard U parameters to obtain a full phase diagram. Then, we calculate the character tables of the valence bands of each material using the MagVasp2trace package. By feeding the character tables into the machinery of MTQC, that is, the Check Topological Magnetic Mat. (<https://www.cryst.ehu.es/cryst/checktopologicalmagnet>) function on BCS [7], we identify the corresponding magnetic co-representations (irreps) and classify the materials into different topological categories. Here we define six topological categories:

1. Band representation. Insulating phase consistent with atomic insulators.
2. Enforced semimetal with Fermi degeneracy (ESFD). Semimetal phase with a partially filled degenerate level at a high symmetry point in the Brillouin zone.
3. Enforced semimetal. Semimetal phase with un-avoidable level crossings along high symmetry lines or in high-symmetry planes in the Brillouin zone.

4. Smith-index semimetal (SISM). Semimetal phase with un-avoidable level crossings at generic points (away from high symmetry points/lines/planes) in the Brillouin zone.
5. Stable topological insulator. Insulating phase inconsistent with atomic insulators. The topology (inconsistency with atomic insulators) is stable against being coupled to atomic insulators.
6. Fragile topological insulator. Insulating phase inconsistent with atomic insulators. The topology is unstable against being coupled to certain atomic insulators.

Further details about BCSMD, the calculation methods, the MagVasp2trace package, the identification of magnetic irreps, and definitions of the topological categories are given in the Methods.

## III. TOPOLOGICAL PHASE DIAGRAMS

With the irreps successfully identified, we classify 403 magnetic structures with convergent ground states into the six topological categories. We find that there are 130 materials (about 32% of the total) that exhibit nontrivial topology for at least one of the U values in the phase diagram. We sort these materials into four groups based on their U-dependence: (1) 50 materials belong to the same topological categories for all values of U. These are the most robust topological materials. (2) 49 materials, on the other hand, are nontrivial at  $U = 0$  but become trivial when U is larger than a critical value. (3) 20 materials have non-monotonous dependence on U: they belong to one topologically nontrivial categories at  $U = 0$  and change to a different topologically nontrivial category at a larger value of U. (4) Six materials are trivial at  $U = 0$  but become nontrivial after a critical value of U. The topology of these six interesting materials is thus driven by electron-electron interactions. The materials in this category are: CaCo<sub>2</sub>P<sub>2</sub>, YbCo<sub>2</sub>Si<sub>2</sub>, Ba<sub>5</sub>Co<sub>5</sub>ClO<sub>13</sub>, U<sub>2</sub>Ni<sub>2</sub>Sn, CeCoGe<sub>3</sub>, and CeMnAsO. The self-consistent calculations of the remaining 5 materials do not converge for at least one value of U, and hence the phase diagrams are not complete. Complete classifications of the converged materials are tabulated in Appendix G; the corresponding band structures are given in Appendix M. In Table Table I, we summarize the total number of topological materials in each magnetic space group (MSG) at different values of U. We have also provided full topological classifications and band structures of each material on the Topological Magnetic Materials Database (<https://www.topologicalquantumchemistry.fr/magnetic>).

In the scheme of MTQC, the stable magnetic topological insulators and SISMs are characterized by non-zero stable indices. These indices can be understood as generalizations of the Fu-Kane parity criterion for

a three-dimensional topological insulator [44]. A complete table of the stable indices and the index-implied topological invariants, which include (weak) Chern numbers, the axion  $\theta$  angle, and magnetic higher-order topological insulator (HOTI) indices, is given in ref. [7]. In Appendix H, we present examples of stable indices relevant to the present work, as well as their physical interpretations. Although there are many (1,651) magnetic and nonmagnetic space groups, we find in ref. [7] that the stable indices of all of the MSGs are dependent on minimal indices in the set of the so-called minimal groups. Thus, to determine the stable indices of a material, we first subduce the representation of the MSG formed by the material to a representation of the corresponding minimal group—a subgroup of the MSG on which the indices are dependent. We then calculate the indices in the minimal group. Using this method, we find a tremendous variety of topological phases among the magnetic materials studied in this work, including axion insulators [45–48], mirror topological crystalline insulators [11], three-dimensional quantum anomalous Hall insulators, and SISMs. A complete table of the topology of all of the magnetic materials studied in this work is provided in Appendix G.

We additionally discover many ESFD and enforced semimetal materials, in which unavoidable electronic band crossings respectively occur at high-symmetry  $\mathbf{k}$  points or on high-symmetry lines or planes in the Brillouin zone. For each of the ESFD and enforced semimetal magnetic materials, we tabulate the  $\mathbf{k}$  points where unavoidable crossings occur (see Appendix I).

We did not discover any examples of magnetic materials for which the entire valence manifold is fragile topological. However, as will be discussed below, we discovered many magnetic materials with well isolated fragile bands in their valence manifolds, thereby providing examples of magnetic fragile bands in real materials.

#### IV. HIGH-QUALITY TOPOLOGICAL MATERIALS

We here select several representative “high-quality” topological materials with clean band structures at the Fermi level: NpBi in MSG 224.113 ( $Pn\bar{3}m'$ ) (antiferromagnetic stable topological insulator), CaFe<sub>2</sub>As<sub>2</sub> in MSG 64.480 ( $C_{Amca}$ ) (antiferromagnetic stable topological insulator), NpSe in MSG 228.139 ( $F_Sd\bar{3}c$ ) (antiferromagnetic ESFD), CeCo<sub>2</sub>P<sub>2</sub> in MSG 126.386 ( $P_14/nnc$ ) (antiferromagnetic enforced semimetal), MnGeO<sub>3</sub> in MSG 148.19 ( $R\bar{3}'$ ) (antiferromagnetic enforced semimetal), Mn<sub>3</sub>ZnC in MSG 139.537 ( $I4/mm'm'$ ) (non-collinear ferrimagnetic enforced semimetal), as shown in Fig. 1.

To identify the stable topologies of the antiferromagnets NpBi and CaFe<sub>2</sub>As<sub>2</sub>, we calculate the stable indices subduced onto MSG 2.4 ( $P\bar{1}$ ),

a subgroup of MSG 224.113 ( $Pn\bar{3}m'$ ) and 64.480 ( $C_{Amca}$ ).

The stable indices in MSG 2.4 ( $P\bar{1}$ ) are defined using only parity (inversion) eigenvalues [7, 29, 42, 49–51]:

$$\eta_{4I} = \sum_K n_K^- \bmod 4, \quad (1)$$

$$z_{2I,i} = \sum_{K, K_i=\pi} n_K^- \bmod 2 \quad (2)$$

where  $K$  sums over the eight inversion-invariant momenta, and  $n_K^-$  is the number of occupied states with odd parity eigenvalues at momentum  $K$ .  $z_{2I,i}$  is the parity of the Chern number of the Bloch states in the plane  $k_i = \pi$ . As explained in Appendix H 1,  $\eta_{4I} = 1, 3$  correspond to Weyl semimetal (WSM) phases with odd-numbered Weyl points in each half of the BZ;  $\eta_{4I} = 2$  indicates an axion insulator phase provided that the band structure is fully gapped and the weak Chern numbers in all directions are zero. The inversion eigenvalues of NpBi with  $U=2$  eV and CaFe<sub>2</sub>As<sub>2</sub> with  $U=2$  eV are tabulated in Table II. The corresponding band structures are shown in Fig. 2a and Fig. 2b, respectively. Both NpBi and CaFe<sub>2</sub>As<sub>2</sub> have the indices  $(\eta_{4I}, z_{2I,1}, z_{2I,2}, z_{2I,3}) = (2, 0, 0, 0)$ . As shown in Appendix H 6, the  $\eta_{4I}$  index of NpBi is the same for  $U=0, 2, 4, 6$  eV; whereas the  $\eta_{4I}$  index of CaFe<sub>2</sub>As<sub>2</sub> is 2 for  $U=0, 1, 2$  eV and 0 for  $U=3, 4$  eV. We have confirmed that both NpBi and CaFe<sub>2</sub>As<sub>2</sub> have vanishing weak Chern numbers, implying that the  $\eta_{4I} = 2$  phases must be axion insulators.

An axion insulator is defined by a nontrivial  $\theta$  angle, which necessitates a quantized magneto-electric response in the bulk and chiral hinge modes on the boundary [43, 45–48]. We have calculated the surface states of NpBi and find that, as expected, the (001) surface is fully gapped (Fig. 2a). Owing to the  $C_3$ -rotation symmetry of the MSG 224.113, the (100) and (010) surfaces are also gapped. Therefore, a cubic sample with terminating surfaces in the (100), (010) and (001) directions, as shown in Fig. 2a, exhibits completely gapped surfaces. However, as an axion insulator, it must exhibit chiral hinge modes when terminated in an inversion-symmetric geometry [42, 43]. We predict that the chiral hinge modes exist on the edges shown in Fig. 2a. More details about NpBi are provided in Appendix J 1.

Next, we discuss representative examples of magnetic topological semimetals. The antiferromagnet NpSe with  $U=2$  eV, 4 eV and 6 eV is an ESFD with a partially-filled degenerate band at the  $\Gamma$  point, where the lowest conduction bands and the highest valence bands meet in a fourfold degeneracy (Fig. 1c). The antiferromagnet CeCo<sub>2</sub>P<sub>2</sub> is an enforced semimetal at all the  $U$  values used in our calculations. For  $U = 0$  eV and 2 eV, we predict CeCo<sub>2</sub>P<sub>2</sub> to be a Dirac semimetal protected by  $C_4$  rotation symmetry. Because the Dirac points in CeCo<sub>2</sub>P<sub>2</sub> lie along a high-symmetry line ( $\Gamma Z$ ) whose little group contains  $4mm$ , we see that

TABLE I. Topological categories vary with  $U$ . Shown are the number of magnetic topological insulators/SISMs and enforced semimetals/ESFDs in each MSG for different values of the Hubbard interaction  $U = 0$  eV, 2 eV and 4 eV. For  $U = 0$ , there are 38 topological insulators/SISMs and 73 enforced semimetals/ESFDs in total. For  $U = 2$  eV, the numbers of topological insulators/SISMs and enforced semimetals/ESFDs decrease to 27 and 58, respectively. For  $U = 4$  eV, the numbers of topological insulators/SISMs and enforced semimetals/ESFDs decrease to 24 and 57, respectively. Choosing the value of  $U$  for each material for which the magnetic moments calculated ab initio lie closest to their experimentally measured values, there are 29 topological insulators/SISMs and 62 enforced semimetals/ESFDs.

MSG	TIs/SISMs			ESs/ESFDs			MSG	TIs/SISMs			ESs/ESFDs			MSG	TIs/SISMs			ESs/ESFDs		
	U=0	U=2	U=4	U=0	U=2	U=4		U=0	U=2	U=4	U=0	U=2	U=4		U=0	U=2	U=4	U=0	U=2	U=4
2.7	1	0	1	0	1	0	62.447	0	1	0	1	0	0	129.416	0	0	1	0	1	0
4.7	0	1	0	0	0	0	62.450	2	2	1	2	1	2	130.432	0	1	0	1	0	1
11.54	1	0	1	0	0	0	63.462	0	2	0	2	0	2	132.456	0	1	0	1	0	1
11.57	1	0	0	0	0	0	63.463	0	1	0	1	0	1	134.481	3	0	1	1	2	0
12.62	2	0	1	0	1	0	63.464	1	1	1	1	0	1	135.492	0	2	0	2	0	2
12.63	0	0	0	0	0	0	63.466	0	0	2	0	1	1	138.528	1	0	1	0	1	0
13.73	2	0	2	0	1	0	63.467	0	0	0	0	1	0	139.536	0	1	0	1	0	1
14.75	0	1	0	0	0	0	64.480	3	0	2	0	0	1	139.537	0	1	0	1	0	1
14.80	1	0	0	0	0	0	65.486	0	0	0	1	0	1	140.550	0	2	1	2	1	2
15.89	2	1	3	0	3	0	65.489	1	0	0	1	0	1	141.556	0	1	0	0	1	0
15.90	4	0	0	0	0	0	67.510	0	0	1	0	0	0	141.557	1	4	0	1	0	1
18.22	0	1	0	0	0	0	70.530	0	1	0	0	0	0	148.19	0	1	0	1	0	1
33.154	0	1	0	0	0	0	71.536	0	1	0	1	0	1	155.48	0	0	0	0	0	1
36.178	0	0	0	0	0	1	73.553	1	0	1	0	1	0	161.69	0	1	0	1	0	0
38.191	0	1	0	0	0	0	74.559	0	1	0	1	0	1	161.71	0	2	0	2	0	0
49.270	0	1	0	1	0	1	85.59	0	1	0	1	0	1	165.95	0	1	0	0	0	0
49.273	0	1	1	0	1	0	88.81	0	1	0	0	0	0	166.101	1	3	0	3	1	2
51.295	0	1	0	1	0	1	92.114	0	1	0	1	0	1	166.97	0	1	0	1	0	1
51.298	0	1	0	1	0	1	107.231	0	0	0	1	0	1	167.108	0	1	0	0	0	0
53.334	0	0	0	0	1	0	114.282	0	1	0	0	0	0	185.201	1	0	0	0	0	0
57.391	1	0	1	0	1	0	123.345	0	1	0	1	0	1	192.252	0	2	0	2	0	2
58.398	0	1	0	0	0	0	124.360	1	3	0	4	0	4	194.268	0	0	0	0	0	1
58.399	0	2	0	2	0	2	125.373	0	1	0	1	0	1	205.33	1	0	0	0	0	0
59.407	0	1	0	0	0	0	126.386	0	1	0	1	0	1	222.103	0	1	0	1	0	1
59.416	0	0	1	0	1	0	127.394	1	1	1	1	1	1	224.113	2	1	2	0	2	0
60.431	1	0	0	0	0	0	127.397	0	1	0	1	0	1	227.131	0	1	0	0	0	0
61.439	0	0	1	0	0	0	128.408	0	1	0	1	0	1	228.139	2	1	0	3	0	3
62.441	0	3	0	0	0	0	128.410	0	4	0	4	0	4	Total	38	27	24	73	58	57

TABLE II. Parities and topological indices of two magnetic topological insulators. Shown are the numbers of occupied bands with odd/even parity eigenvalues at the eight inversion-invariant points ( $\eta_\alpha$ ) for the magnetic topological insulators NpX (where X = Sb, Bi) and XFe<sub>2</sub>As<sub>2</sub> (where X = Ca, Ba) with  $U = 2$  eV. The  $\eta_{4I} = 2$  phase corresponds to an axion insulator or Weyl semimetal phase with even pairs of Weyl points at generic locations in the Brillouin zone interior (given vanishing weak Chern numbers), and  $\eta_{4I} = 1, 3$  corresponds to a Weyl semimetal phase with odd number of Weyl points at generic locations within each half of the Brillouin zone. We have confirmed that the weak Chern numbers vanish in NpX and XFe<sub>2</sub>As<sub>2</sub>, implying that both materials are axion insulators.

$\Lambda_\alpha$	(0,0,0)	( $\pi$ ,0,0)	(0, $\pi$ ,0)	( $\pi$ , $\pi$ ,0)	(0,0, $\pi$ )	( $\pi$ ,0, $\pi$ )	(0, $\pi$ , $\pi$ )	( $\pi$ , $\pi$ , $\pi$ )	( $\eta_{4I}, z_{2I,1}, z_{2I,2}, z_{2I,3}$ )
NpX	58/22	40/40	40/40	40/40	40/40	40/40	40/40	48/32	(2,0,0,0)
XFe <sub>2</sub> As <sub>2</sub>	50/46	48/48	48/48	52/44	48/48	52/44	52/44	48/48	(2,0,0,0)

CeCo<sub>2</sub>P<sub>2</sub> is a higher-order topological semimetal that exhibits flat-band-like higher-order Fermi-arc states on mirror-invariant hinges, analogous to the hinge states recently predicted [41] and experimentally observed [52] in the non-magnetic Dirac semimetal Cd<sub>3</sub>As<sub>2</sub>. For  $U = 4$  eV and 6 eV, CeCo<sub>2</sub>P<sub>2</sub> becomes a nodal ring semimetal protected by the mirror symmetry  $M_z$ . As detailed in Appendix J 2, the transition between the two enforced semimetal phases is completed by two successively band inversions at  $\Gamma$  and Z, which removes the Dirac node

and creates the nodal ring, respectively. The band structure of the nodal ring semimetal phase at  $U=6$  eV is plotted in Fig. 1d. The antiferromagnet MnGeO<sub>3</sub> is a  $C_3$ -rotation-protected Dirac semimetal, in which the number of Dirac nodes changes with the value of  $U$ . For  $U=0$  eV, 1 eV, 3 eV and 4 eV, we predict MnGeO<sub>3</sub> to have two Dirac nodes along the high-symmetry line GF; for  $U=2$  eV, we observe four Dirac nodes along the same high-symmetry line. In Fig. 1e, we plot the band structure of MnGeO<sub>3</sub> using  $U=4$  eV. We next

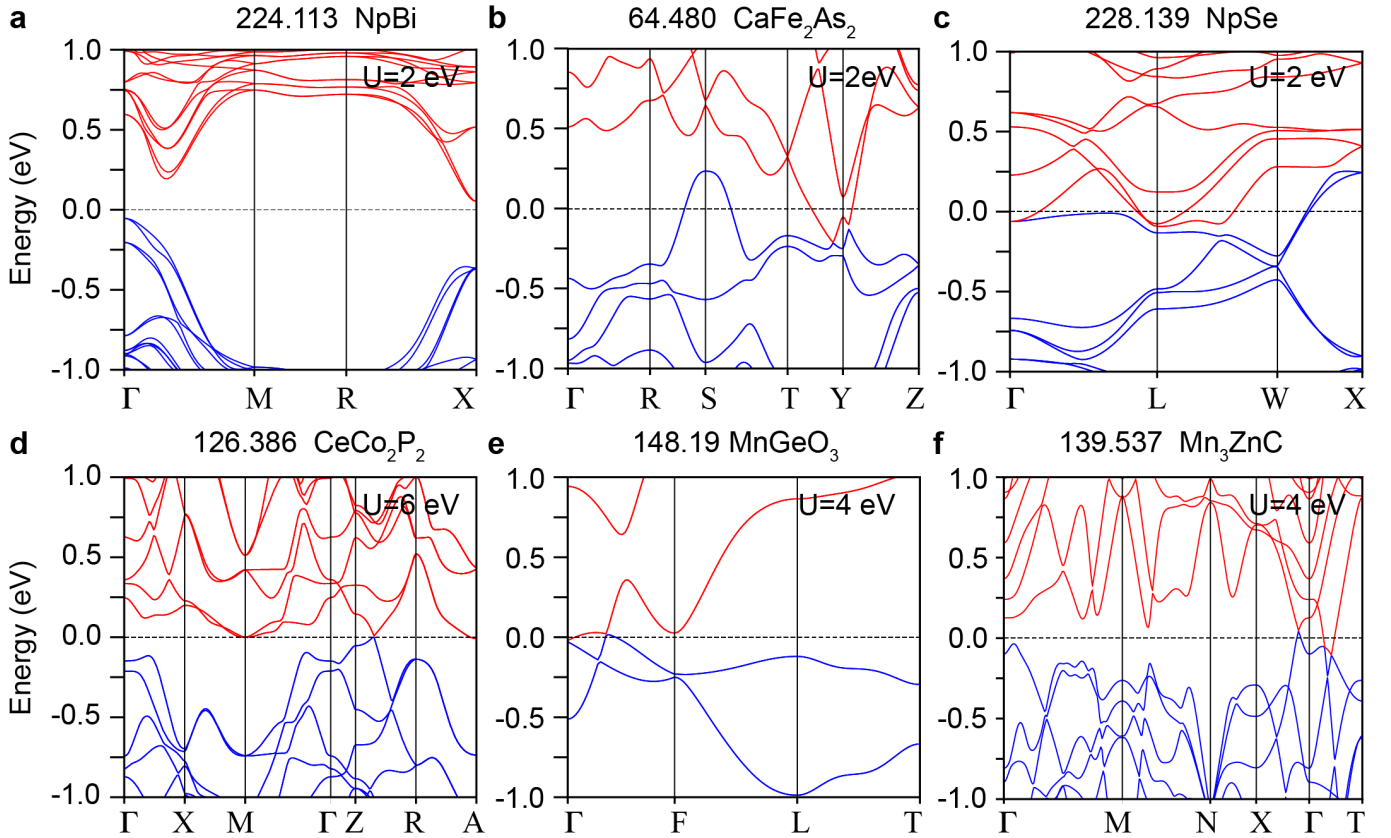


FIG. 1. Band structures of the ‘high-quality’ magnetic topological materials predicted by MTQC. (a, b) The antiferromagnetic axion topological insulators, NpBi and CaFe<sub>2</sub>As<sub>2</sub>. Although there are Fermi pockets around S and Y in CaFe<sub>2</sub>As<sub>2</sub>, the insulating compatibility relations are fully satisfied. We note that there is a small gap (about 5 meV) along the path T–Y; this indicates that the valence bands are well separated from the conduction bands, and thus have a well defined topology. (c) The antiferromagnetic ESFD NpSe, which has a partially filled fourfold degeneracy at  $\Gamma$ . (d) The antiferromagnetic nodal-line semimetal CeCo<sub>2</sub>P<sub>2</sub>. A gapless nodal ring protected by mirror symmetry lies in the Z–R–A plane. (e) The antiferromagnetic Dirac semimetal MnGeO<sub>3</sub>. One of the two Dirac nodes protected by the  $C_3$ -rotation symmetry lies along the high-symmetry line  $\Gamma$ –F. Note that there is a small bandgap at the  $\Gamma$  point. (f) The non-collinear ferrimagnetic Weyl semimetal Mn<sub>3</sub>ZnC. Two Weyl points are pinned to the rotation-invariant line  $\Gamma$ –T by  $C_4$ -rotation symmetry. Mn<sub>3</sub>ZnC also hosts nodal lines at the Fermi level  $E_F$ ; we specifically observe five nodal rings protected by the mirror symmetry ( $M_z$ ) in the plane  $k_z = 0$ . The sequential number of each MSG in the BNS setting and the chemical formula of each material are provided on the top of each panel.

predict the non-collinear ferrimagnet Mn<sub>3</sub>ZnC to be an ES with symmetry-enforced Weyl points coexisting with the Weyl nodal rings (Fig. 1f). Two of the Weyl points in Mn<sub>3</sub>ZnC are pinned by the  $C_4$ -rotation symmetry to the high-symmetry line  $\Gamma$ T, and we observe five nodal rings protected by the mirror symmetry  $M_z$  in the  $k_z = 0$  plane. In time-reversal-breaking Weyl semimetals, divergent Berry curvature near Weyl points can give rise to a large intrinsic anomalous Hall conductivity [1, 2, 33, 34, 53]. We thus expect there to be a large anomalous Hall effect in Mn<sub>3</sub>ZnC. As detailed in Appendix J4, we have specifically calculated the the anomalous Hall conductivity of Mn<sub>3</sub>ZnC to be about 123  $\Omega^{-1} \cdot \text{cm}^{-1}$ .

The surface states of the enforced semimetals CeCo<sub>2</sub>P<sub>2</sub> and MnGeO<sub>3</sub> are shown in Fig. 2b,c, respectively. Because the bulk states of CeCo<sub>2</sub>P<sub>2</sub> and MnGeO<sub>3</sub> have

clean Fermi surfaces, the surface states are well separated from the bulk states, and should be observable in experiment. For the Dirac semimetal MnGeO<sub>3</sub>, we observe a discontinuous Fermi surface (Fermi-arc) on the surface (Fig. 2d). In Appendix J, we provide further details of our surface-state calculations.

## V. CONSISTENCY WITH PREVIOUS WORKS

Our magnetic materials database (<https://www.topologicalquantumchemistry.fr/magnetic>) includes several topological materials that have previously been reported but whose topology was not known to be protected by symmetry eigenvalues. For example, the non-collinear magnet Mn<sub>3</sub>Sn in MSG 63.463 ( $Cm'cm'$ ) has been reported as a magnetic

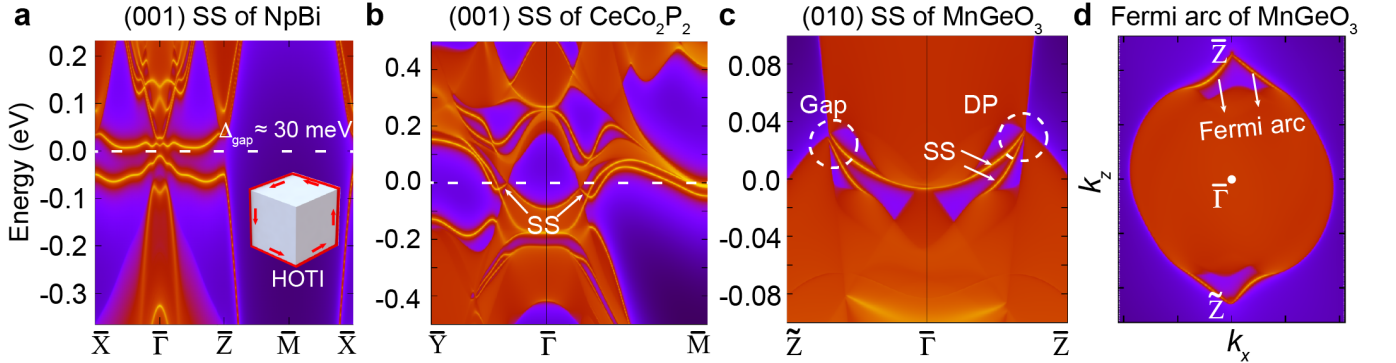


FIG. 2. Topological surface states of representative magnetic topological insulator and enforced semimetal phases. (a) The (001) surface state of the axion insulator NpBi, which has an energy gap of 30 meV. The inset shows a schematic of the chiral hinge states on a cubic sample. (b) The (001) surface state of the enforced semimetal CeCo<sub>2</sub>P<sub>2</sub>. The drumhead-like topological surface states connect the projections of the bulk nodal rings. (c) The (010) surface state of the enforced semimetal MnGeO<sub>3</sub>. The bulk Dirac point along the  $\bar{\Gamma} - \bar{Z}$  line is protected by  $C_3$  symmetry. However, because time-reversal symmetry is broken, the projected band crossing on  $\bar{\Gamma} - \bar{Z}$  (along  $-k_z$ ) is no longer protected, and is instead weakly gapped. The coordinates of  $\bar{Z}$  and  $\bar{Z}$  on the (010) surface are  $(0, k_z = \pi/c)$  and  $(0, k_z = -\pi/c)$ , respectively. The (d) Fermi arc of MnGeO<sub>3</sub> on the (010) surface, connecting the two Dirac points.

Weyl semimetal candidate with six pairs of Weyl points [31, 54]. In our LDA+U calculation, for  $U = 0$  eV, 1 eV and 2 eV, we find Mn<sub>3</sub>Sn to be classified instead as a magnetic topological insulator category with the index  $\eta_{4I} = 2$ .  $\eta_{4I} = 2$  can correspond to several different topological phases (which we emphasize are not all topological insulators): (1) an axion insulator, (2) a three-dimensional quantum anomalous Hall state with even weak Chern number (not determinable from symmetry eigenvalues) [55], or (3) a Weyl semimetal phase with an *even* number of Weyl points in half of the BZ (not determinable from symmetry eigenvalues). Thus our calculations on Mn<sub>3</sub>Sn for  $U = 0, 1, 2$  eV are consistent with the results in refs.[31, 54]. We emphasize that if the six Weyl points in half of the Brillouin zone were pairwise annihilated without closing a gap at the inversion-invariant momenta, then the gapped phase would either be an axion insulator or a three-dimensional quantum anomalous Hall state. When U is further increased to 3 eV and 4 eV, a topological phase transition occurs, driving the  $\eta_{4I} = 2$  phase into a gapless enforced semimetal phase.

## VI. CHEMICAL CATEGORIES

In Table III, we classify the topological magnetic materials predicted by MTQC into three main chemical categories, and 11 sub-categories, through a consideration of their magnetic ions and chemical bonding. Detailed descriptions of each category are given in the Methods. Of the materials listed in Table III, most antiferromagnetic insulators, which are well studied experimentally in the case of the so-called Mott insulators, appear to be trivial. We observe that

most of the materials in Table III are identified as topological enforced semimetals or ESFDs, which are defined by small densities of states at the Fermi level, and hence lie chemically at the border between insulators and metals.

## VII. DISCUSSION

A large number of the topological materials predicted in this work (see Appendix G for a complete tabulation) can readily be synthesized into single crystals for the exploration of their unusual physical properties and the confirmation of their topological electronic structures in different phase categories. These include materials with non-trivial topology over the full range of U values used in our calculations (for example, Mn<sub>3</sub>Ge, Mn<sub>3</sub>Sn, Mn<sub>3</sub>Ir, LuFe<sub>4</sub>Ge<sub>2</sub>, and YFe<sub>4</sub>Ge<sub>2</sub>), materials sensitive to U (for example, NdCo<sub>2</sub> and NdCo<sub>2</sub>P<sub>2</sub>), and interaction-driven topological materials (for example, U<sub>2</sub>Ni<sub>2</sub>Sn and CeCuGe<sub>3</sub>).

We did not find any examples of materials whose entire valence manifolds are fragile topological. However, it is still possible for well isolated bands within the valence manifold to be fragile topological if they can be expressed as a difference of band representations. We find many examples of energetically well isolated fragile branches among the occupied bands. We tabulate all the fragile branches close to the Fermi level in Appendix K.

We emphasize that there also exist topological insulators and topological semimetals (for example, Weyl semimetals) that cannot be diagnosed through symmetry eigenvalues, which in this work are classified as trivial band representations [4]. It is worth mentioning that even the topologically trivial bands may also be

Categories	Properties	Materials
I-A	Non-collinear Manganese compounds	Mn <sub>3</sub> GaC, Mn <sub>3</sub> ZnC, Mn <sub>3</sub> CuN, Mn <sub>3</sub> Sn, Mn <sub>3</sub> Ge, Mn <sub>3</sub> Ir, Mn <sub>3</sub> Pt, Mn <sub>5</sub> Si <sub>3</sub>
I-B	Actinide Intermetallic	UNiGa <sub>5</sub> , UPtGa <sub>5</sub> , NpRhGa <sub>5</sub> , NpNiGa <sub>5</sub>
I-C	Rare earth intermetallic	NdCo <sub>2</sub> , TbCo <sub>2</sub> , NpCo <sub>2</sub> , PrAg, DyCu, NdZn, TbMg, NdMg, Nd <sub>5</sub> Si <sub>4</sub> , Nd <sub>5</sub> Ge <sub>4</sub> , Ho <sub>2</sub> RhIn <sub>8</sub> , Er <sub>2</sub> CoGa <sub>8</sub> , Nd <sub>2</sub> RhIn <sub>8</sub> , Tm <sub>2</sub> CoGa <sub>8</sub> , Ho <sub>2</sub> RhIn <sub>8</sub> , DyCo <sub>2</sub> Ge <sub>8</sub> , TbCo <sub>2</sub> Ge <sub>8</sub> , Er <sub>2</sub> Ni <sub>2</sub> In, CeRu <sub>2</sub> Al <sub>10</sub> , Nd <sub>3</sub> Ru <sub>4</sub> Al <sub>12</sub> , Pr <sub>3</sub> Ru <sub>4</sub> Al <sub>12</sub> , ScMn <sub>6</sub> Ge <sub>6</sub> , YFe <sub>4</sub> Ge <sub>4</sub> , LuFe <sub>4</sub> Ge <sub>4</sub> , CeCoGe <sub>3</sub>
II-A	Metallic Iron pnictides	LaFeAsO, CaFe <sub>2</sub> As <sub>2</sub> , EuFe <sub>2</sub> As <sub>2</sub> , BaFe <sub>2</sub> As <sub>2</sub> , Fe <sub>2</sub> As, CaFe <sub>4</sub> As <sub>3</sub> , LaCrAsO, Cr <sub>2</sub> As, CrAs, CrN
II-B	Semiconducting manganese pnictides	BaMn <sub>2</sub> As <sub>2</sub> , BaMn <sub>2</sub> Bi <sub>2</sub> , CaMnBi <sub>2</sub> , SrMnBi <sub>2</sub> , CaMn <sub>2</sub> Sb <sub>2</sub> , CuMnAs, CuMnSb, Mn <sub>2</sub> As
II-C	Rare earth intermetallic compounds with the composition 1:2:2	PrNi <sub>2</sub> Si <sub>2</sub> , YbCo <sub>2</sub> Si <sub>2</sub> , DyCo <sub>2</sub> Si <sub>2</sub> , PrCo <sub>2</sub> P <sub>2</sub> , CeCo <sub>2</sub> P <sub>2</sub> , NdCo <sub>2</sub> P <sub>2</sub> , DyCu <sub>2</sub> Si <sub>2</sub> , CeRh <sub>2</sub> Si <sub>2</sub> , UAu <sub>2</sub> Si <sub>2</sub> , U <sub>2</sub> Pd <sub>2</sub> Sn, U <sub>2</sub> Pd <sub>2</sub> In, U <sub>2</sub> Ni <sub>2</sub> Sn, U <sub>2</sub> Ni <sub>2</sub> In, U <sub>2</sub> Rh <sub>2</sub> Sn
II-D	Rare earth ternary compounds of the composition 1:1:1	CeMgPb, PrMgPb, NdMgPb, TmMgPb
III-A	Semiconducting Actinides/Rare earth Pnictides	HoP, UP, UP <sub>2</sub> , UAs, NpS, NpSe, NpTe, NpSb, NpBi, U <sub>3</sub> As <sub>4</sub> , U <sub>3</sub> P <sub>4</sub>
III-B	Metallic oxides	Ag <sub>2</sub> NiO <sub>2</sub> , AgNiO <sub>2</sub> , Ca <sub>3</sub> Ru <sub>2</sub> O <sub>7</sub> , Double perovskite Sr <sub>3</sub> CoIrO <sub>6</sub>
III-C	Metal to insulator transition compounds	NiS <sub>2</sub> , Sr <sub>2</sub> Mn <sub>3</sub> As <sub>2</sub> O <sub>2</sub>
III-D	Semiconducting and insulating oxides, borates, hydroxides, silicates, phosphate	LuFeO <sub>3</sub> , PdNiO <sub>3</sub> , ErVO <sub>3</sub> , DyVO <sub>3</sub> , MnGeO <sub>3</sub> , Tm <sub>2</sub> Mn <sub>2</sub> O <sub>7</sub> , Yb <sub>2</sub> Sn <sub>2</sub> O <sub>7</sub> , Tb <sub>2</sub> Sn <sub>2</sub> O <sub>7</sub> , Ho <sub>2</sub> Ru <sub>2</sub> O <sub>7</sub> , Er <sub>2</sub> Ti <sub>2</sub> O <sub>7</sub> , Tb <sub>2</sub> Ti <sub>2</sub> O <sub>7</sub> , Cd <sub>2</sub> Os <sub>2</sub> O <sub>7</sub> , Ho <sub>2</sub> Ru <sub>2</sub> O <sub>7</sub> , Cr <sub>2</sub> ReO <sub>6</sub> , NiCr <sub>2</sub> O <sub>4</sub> , MnV <sub>2</sub> O <sub>4</sub> , Co <sub>2</sub> SiO <sub>4</sub> , Fe <sub>2</sub> SiO <sub>4</sub> , PrFe <sub>3</sub> (BO <sub>3</sub> ) <sub>4</sub> , KCo <sub>4</sub> (PO <sub>4</sub> ) <sub>3</sub> , CoPS <sub>3</sub> , SrMn(VO <sub>4</sub> )(OH), Ba <sub>5</sub> Co <sub>5</sub> ClO <sub>13</sub> , FeI <sub>2</sub>

TABLE III. The magnetic topological materials identified in this work.

interesting if the occupied bands form Wannier functions centred at positions away from the atoms, because a Wannier centre shift in three-dimensional insulators leads to the appearance of topological corner states, like those of quantized ‘quadrupole’ insulators [41]. Topological phases characterized by displaced Wannier functions are known as obstructed atomic limits; we leave their high-throughput calculation for future studies.

## VIII. CONCLUSION

We have performed LDA + U calculations on 549 existent magnetic structures and have successfully classified 403 using the machinery of MTQC [7]. We find that 130 materials (about 32% of the total) have topological phases as we scan the U parameter. Our results suggest that a large number of previously synthesized magnetic materials are topologically nontrivial. We highlight several ‘high-quality’ magnetic topological materials that should be experimentally examined for topological response effects and surface (and hinge) states.

**Acknowledgements** We thank U. Schmidt, I. Weidl, W. Shi and Y. Zhang. We acknowledge the computational resources Cobra in the Max Planck Computing and Data Facility (MPCDF), the HPC Platform of ShanghaiTech University and Atlas in the Donostia International Physics Center (DIPC). Y.X. is grateful to D. Liu for help in plotting some diagrammatic sketches. B.A.B., N.R., B.J.W. and Z.S. were primarily supported

by a Department of Energy grant (DE-SC0016239), and partially supported by the National Science Foundation (EAGER grant DMR 1643312), a Simons Investigator grant (404513), the Office of Naval Research (ONR; grant N00014-14-1-0330), the NSF-MRSEC (grant DMR-142051), the Packard Foundation, the Schmidt Fund for Innovative Research, the BSF Israel US foundation (grant 2018226), the ONR (grant N00014-20-1-2303) and a Guggenheim Fellowship (to B.A.B.). Additional support was provided by the Gordon and Betty Moore Foundation through grant GBMF8685 towards the Princeton theory programme. L.E. was supported by the Government of the Basque Country (Project IT1301-19) and the Spanish Ministry of Science and Innovation (PID2019-106644GB-I00). M.G.V. acknowledges support from the Diputacion Foral de Gipuzkoa (DFG; grant INCIEN2019-000356) from Gipuzkoako Foru Aldundia and the Spanish Ministerio de Ciencia e Innovación (grant PID2019-109905GB-C21). Y.C. was supported by the Shanghai Municipal Science and Technology Major Project (grant 2018SHZDZX02) and a Engineering and Physical Sciences Research Council (UK) Platform Grant (grant EP/M020517/1). C.F. acknowledges financial support by the DFG under Germany’s Excellence Strategy through the Würzburg-Dresden Cluster of Excellence on Complexity and Topology in Quantum Matter (ct.qmat EXC 2147, project-id 390858490), an ERC Advanced Grant (742068 ‘TOPMAT’). Y.X. and B.A.B. were also supported by the Max Planck Society.

**Author contributions** B.A.B. conceived this work; Y.X. and M.G.V. performed the first-principles

calculations. L.E. wrote the code for calculating the irreducible representations and checking the topologies of materials. Y.X., Z.S., B.J.W. and B.A.B. analysed the calculated results, B.J.W. determined the physical meaning of the topological indices with help from L.E., Z.S. and Y.X. C.F. performed chemical analysis of the magnetic topological materials. N.R. built the topological material database. All authors wrote the main text and Y.X. and Z.S. wrote the Methods and the Supplementary Information.

#### Competing interests

The authors declare no competing interests.

**Correspondence and requests for materials**  
should be addressed to B.A.B.

#### Corresponding authors

Correspondence to B. Andrei Bernevig.

## IX. METHODS

**Concepts** Here we give a brief introduction to MTQC [4, 7, 56–58] and the definitions of six topological classes. A magnetic band structure below the Fermi level is partially described by the irreducible co-representations (irreps) formed by the occupied electronic states at the high-symmetry  $\mathbf{k}$  points, which are defined as the momenta whose little groups – the groups that leave the momenta unchanged – are maximal subgroups of the space group. If the highest occupied (valence) band and the lowest unoccupied (conduction) band are degenerate at a high-symmetry  $\mathbf{k}$  point, then we refer to the material as an enforced semimetal with Fermi degeneracy (ESFD) [4]. Depending on whether the irreps at high-symmetry points satisfy the so-called compatibility relations [4, 24, 25, 58] – which determine whether the occupied bands must cross with unoccupied bands along high-symmetry lines or planes (whose little groups are non-maximal) – band structures can then be further classified as insulating (along high-symmetry lines and planes) or enforced semimetals (ES). ES-classified materials generically feature band crossings along high-symmetry lines or planes. If a band structure satisfies the compatibility relations, it can be a trivial insulator, whose occupied bands form a BR [4], a topological semimetal with crossing nodes at generic momenta [Smith-index semimetal (SISM)] or non-symmetry-indicated topological semimetal – a system which satisfies all compatibility relations but exhibits Weyl-type nodes], or a TI. Some of the topological semimetals and insulators can be diagnosed through their irreps: If the irreps do not match a BR, then the band structure must be a topological insulator or a SISM. There are two types of topological insulators: Stable TIs [26, 27, 59, 60], which include crystalline and higher-order TIs (TCIs and HOTIs, respectively) [61–65], and fragile TIs [60, 66–70]. Stable TIs remain topological when coupled to trivial or fragile bands, whereas fragile

TIs, on the other hand, can be trivialized by being coupled to certain trivial bands, or even other fragile bands [41, 43]. In the accompanying paper [7], we explicitly identify all of the symmetry-indicated stable electronic (fermionic) TIs and topological semimetals, specifically detailing the bulk, surface, and hinge states of all symmetry-indicated stable TIs, TCIs, and HOTIs in all 1651 spinful (double) SGs and MSGs.

To summarize, using MTQC, we divide an electronic band structure into one of six topological classes: BRs, ESFD, ES, SISM, stable TI, and fragile TI, among which only BRs are considered to be topologically trivial. If a band structure satisfies the compatibility relations along high-symmetry lines and planes, and has a nontrivial value of a stable index, then, unlike in the nonmagnetic SGs, it is possible for the bulk to be a topological (semi)metal [7]. We label these cases as Smith-index semimetals (SISMs). See Appendix A for a more detailed description of the six topological classes.

**Magnetic Materials Database** We perform high-throughput calculations of the magnetic structures listed on BCSMD [71]. BCSMD contains portable structure files, including magnetic structure data and symmetry information, for 707 magnetic structures. The magnetic structures of all the materials are determined by neutron scattering experiments. We thus consider it reasonable and experimentally motivated to use the crystal and magnetic structures provided on the BCSMD as the initial inputs for *ab initio* calculations, instead of letting our theoretical ab-initio codes predict the magnetic ground-state. We emphasize that predictions of topological magnetic materials based on theoretically calculated magnetic structures, rather than experimentally measured structures, are more likely to predict unphysical (and possibly incorrect) magnetic ground states. From the 707 magnetic structures on the BCSMD, we omit 63 structures with lattice-incommensurate magnetism and 95 alloys, as they do not have translation symmetry and hence are not invariant under any MSG. We apply *ab initio* calculations for the remaining 549 structures. These magnetic structures belong to 261 different MSGs, including 29 chiral MSGs and 232 achiral MSGs (chiral MSGs are defined as MSGs without improper rotations or combinations of improper rotations and time reversal; all other MSGs are achiral). In Appendix B, we list the number of materials with experimentally obtained magnetic structures in each MSG.

**Calculation Methods** We performed *ab initio* calculations incorporating spin-orbital coupling (SOC) using VASP [72]. Because all of the magnetic materials on BCSMD with translation symmetry contain at least one correlated atom with  $3d$ ,  $4d$ ,  $4f$ , or  $5f$  electrons, we apply a series of LDA+ $U$  calculations for each material with different Hubbard- $U$  parameters to obtain a full phase diagram. For all of the  $3d$  valence orbitals and the atom Ru with  $4d$  valence orbitals, we take  $U$  as 0 eV, 1 eV, 2 eV, 3 eV and 4 eV. The other atoms with  $4d$  valence

electrons usually do not exhibit magnetism or have weak correlation effects, and hence are not considered to be correlated in our calculations. Conversely, atoms with  $4f$  and  $5f$  valence electrons have stronger correlation effects, so we take  $U$  for atoms with  $4f$  or  $5f$  valence electrons to be 0 eV, 2 eV, 4 eV and 6 eV. If a material has both  $d$  and  $f$  electrons near the Fermi level, we fix the  $U$  parameter of the  $d$  electrons as 2 eV, and take  $U$  of the  $f$  electrons to be 0 eV, 2 eV, 4 eV and 6 eV sequentially. We also adopt four other exchange-correlation functionals in the LDA +  $U$  scheme to check the consistency between different functionals. Further details of our first-principles calculations are provided in Appendix C,D, E and F.

Of the 549 magnetic structures that we examined, 403 converged self-consistently to a magnetic ground state within an energy threshold of  $10^{-5}$ eV per cell. For 324 of the 403 converged materials, magnetic moments matching the experimental values (up to an average error of 50%) were obtained for at least one of the values of  $U$  used to obtain the material phase diagram. We stress that these are good agreements for calculations on these strongly correlated states. However, for the other 79 materials, the calculated magnetic momenta always notably diverged from the experimental values (see Appendix L for a complete comparison of the experimental and ab initio magnetic moments). The differences can be explained as follows. First, we consider only the spin components, but not the orbital components, of the magnetic moments in our current ab initio calculations. This can result in a large average error for compounds with large spin-orbital coupling. Second, because the average error is defined relative to the experimental moments, the ‘error’ (measured as a percentage) is likely to be larger when the experimental moments are small. In this case, the random, slight changes in the numerically calculated moments have an outsized effect on the reported error percentage. Last but not least, mean-field theory applied in the LDA+ $U$  calculations is not a good approximation for some strongly correlated materials, which should be checked further with more advanced methods. Although the prediction of magnetic structure with mean-field theory is sometimes not reliable for strongly correlated materials, it is worth comparing the energy difference between the magnetic structures from neutron scattering and the other possible magnetic structures. In Appendix D, we selected several topological materials and compared their energies with some possible magnetic configurations and different  $U$ . We find that their experimental magnetic configurations have the lowest energies, and hence are theoretically favoured. Finally, we have additionally performed self-consistent calculations of the charge density at different values of  $U$ , which we used as input for our band structure calculations. In Appendix M, we provide a complete summary of results.

Considering the possible underestimation of the band gap by generalized gradient approximations (GGA),

electronic structures of 23 topological mateirals are further confirmed by the calculations using the modified Becke–Johnson potential [73]. As shown in Appendix E2, both the features of bands near Fermi level and the topological classes obtained from modified Becke–Johnson potential are consistent with LDA+ $U$  calculations. Because of the limitations of the LDA+ $U$  method, we have also performed the more costly LDA+Gutzwiller [74] calculations in two of the topological materials identified in this work-CeCo<sub>2</sub>P<sub>2</sub> and MnGeO<sub>3</sub>, both classified as enforced semimetal-to confirm the bulk topology. As shown in Appendix F, the strong correlations renormalize the quasiparticle spectrum by a factor of quasiparticle weight, but do not change the band topology. The surface-state calculations have been performed using the WannierTools package ??.

**Identification of the magnetic irreps** Using the self-consistent charge density and potentials, we calculate the Bloch wavefunctions at the high-symmetry momenta in the Brillouin zone and then identify the corresponding magnetic irreps using the MagVasp2trace package, which is the magnetic version of Vasp2trace package [75]. (See Appendix C for details about MagVasp2trace). The little group  $G_{\mathbf{k}}$  of a high symmetry point  $\mathbf{k}$  is in general isomorphic to an MSG. For little groups without anti-unitary operations, we calculate the traces of the symmetry representations formed by the wavefunctions, and then decompose the traces into the characters of the small irreps of the little group  $G_{\mathbf{k}}$ . For little groups with anti-unitary operations, we calculate only the traces of the unitary operations and decompose the representations into the irreps of the maximal unitary subgroup  $G_{\mathbf{k}}^U$  of  $G_{\mathbf{k}}$ . Since anti-unitary operations in general lead to additional degeneracies, specifically enforcing two irreps of  $G_{\mathbf{k}}^U$  to become degenerate and form a co-representation, we check whether the additional degeneracies hold in the irreps obtained. Because VASP does not impose anti-unitary (magnetic) symmetries, degeneracies labelled by magnetic co-representations may exhibit very small splittings in band structures generated by VASP. In these cases, we reduce the convergence threshold and re-run the self-consistent calculation until the splitting is specifically small ( $\leq 10\%$ ) compared to the smallest energy gap across all of the high-symmetry momenta.

The algorithm and methods designed in this work are also applicable to future high-throughput searches for magnetic topological materials [76].

**Details of the chemical catagories** Considering the magnetic ions and chemical bonding of the magnetic materials, we classify the topological magnetic materials predicted in this work into the following 11 chemical categories.

(I-A) Non-collinear manganese compounds, which have received considerable recent attention owing to their unusual combination of a large anomalous Hall effect and net-zero magnetic moments. The symmetry of the non-collinear antiferromagnet spin structure allows

for a non-vanishing Berry curvature, the origin of the unusual anomalous Hall effect. Examples of non-collinear manganese compounds include the hexagonal Weyl semimetals  $Mn_3Sn$ ,  $Mn_3Ge$  and the well-studied cubic antiferromagnetic spintronic-material  $Mn_3Ir$ , as well as the inverse perovskite compounds  $Mn_3Y$ , which represent ‘stuffed’ versions of the cubic  $Mn_3Y$  compounds.

(I-B,C) Intermetallic materials, containing rare-earth atoms or actinide atoms, which are typically antiferromagnets. The variation of the Hubbard  $U$  changes the band structures slightly in these materials, but not the topological character.

(II-A) The  $ThCr_2Si_2$  structure and related structures, which have received attention because of the high-temperature iron pnictide superconductors in this group. In these materials, the transition-metal layers and the pnictide layers form square lattices. The square nets of the pnictides act as a driving force for a topological band structure [77]. Several of the antiferromagnetic undoped prototypes, such as  $CaFe_2As_2$ , are topological antiferromagnets. This suggests the possibility of topological superconductivity in these materials, like that recently found in  $FeTe_{0.55}Se_{0.45}$  [78].

(II-B) Semiconducting manganese pnictines, which occur when iron is substituted with manganese, leading to materials that are trivial when insulating and gapped, but which become topological antiferromagnets when their gap is closed. By increasing the Hubbard  $U$ , the antiferromagnetic phases of these compounds can be converted into trivial insulators. The antiferromagnetic insulators and semimetals in this class can also be converted into ferromagnetic metals by doping.

(II-C) Transition metals in combination with rare earth or actinide atoms form compounds of the  $ThCr_2Si_2$  structure type. Here the antiferromagnetic ordering comes from the Thorium-position in the  $ThCr_2Si_2$  structure type.

(II-D) Rare earth ternary compounds of the composition 1:1:1.

(III-A,B,C,D) The third class of magnetic materials are ionic compounds, of which most have been experimentally determined to be insulating. Within the density functional approximation, several of the compounds have been identified as topological nontrivial metals, such as oxides, borates, hydroxides, silicates, phosphates and  $FeI_2$ . By increasing the Hubbard  $U$ , a topologically trivial gap can be opened in these materials.

Additional data and discussion can be found online in the Supplementary information.

**Data availability** All data are available in the Supplementary Information and at <https://www.topologicalquantumchemistry.fr/magnetic>. The codes required to calculate the character table of magnetic materials are available at <https://www.cryst.ehu.es/cryst/checktopologicalmagma>.

## Appendix A: A brief introduction to Magnetic Topological Quantum Chemistry (MTQC)

The symmetry group property of a band structure is fully described by the multiplicities of the irreducible co-representations (irreps) formed by the occupied bands at all the maximal  $K$ -points. In the present paper, we define the 1st band to the  $N_e$ th band as the “occupied” bands, where  $N_e$  is the number of electrons. Maximal  $k$ -points are defined as the high symmetry momenta whose little groups are maximal subgroups of the magnetic space group. The maximal  $K$ -points of each magnetic space group are supplied in the magnetic vasp2trace package. We denote the little group at the momentum  $K$  as  $G_K$ , the  $i$ th irrep of  $G_K$  as  $\rho_K^i$ , and its multiplicity of  $\rho_K^i$  formed by the occupied bands as  $m(\rho_K^i)$ . For example, the Brillouin zone (BZ) of the 2D space group generated from inversion ( $I$ ) and translations has four maximal  $k$ -points:  $\Gamma(0,0)$ ,  $X(\pi,0)$ ,  $Y(0,\pi)$ ,  $M(\pi,\pi)$ , all of which have the same little group:  $C_i = \{E, I\}$ . Here  $E$  is the identity.  $C_i$  has two types of irreps: the even(+) and the odd(−). Thus a band structure is characterized by the eight integers  $m(\rho_{\Gamma,X,Y,M}^{+, -})$ . For convenience, we introduce the symmetry-data-vector[4]

$$B = (m(\rho_{\Gamma}^{+}), m(\rho_{\Gamma}^{-}), m(\rho_X^{+}), m(\rho_X^{-}), m(\rho_Y^{+}), m(\rho_Y^{-}), m(\rho_M^{+}), m(\rho_M^{-}))^T. \quad (\text{A1})$$

The symmetry property of a band structure is fully described by the symmetry-data-vector.

**Enforced semimetal with Fermi degeneracy.** In some materials, the highest occupied band and the lowest empty band are degenerate at some maximal  $K$ -points, and the degeneracy is protected by the MSG. We call such states enforced semimetals with Fermi degeneracy (ESFD)[4, 79]. ESFD does not have a well defined symmetry-data-vector  $B$ . See FIG. 1c of the main text for examples of ESFD.

For band structures where the occupied bands are gapped from the empty bands along all the high symmetry lines, the multiplicities  $m$  necessarily satisfy the compatibility relations [4, 25, 29, 56–58, 80]. We consider two maximal  $k$ -points  $K_{1,2}$  and a path  $k$  between them. On the one hand, since  $G_k$  is a subgroup of  $G_{K_1}$ , the irreps of  $G_k$  formed by the occupied bands in  $k$  near to  $K_1$  can be obtained by subduction of the irreps of  $G_{K_1}$  formed by occupied bands at  $K_1$ . On the other hand, the irreps of  $G_k$  formed by the occupied bands in  $k$  near to  $K_2$  can also be obtained by subduction of the irreps at  $K_2$ . If the irreps of  $G_k$  obtained at the two ends  $K_1$  and  $K_2$  are not the same, then there must be a symmetry protected level crossing along the path  $k$ . In other words, in order to guarantee the path  $k$  is gapped, the irreps at  $K_1$  and  $K_2$  must reduce to the same set of irreps of  $G_k$ . This requirement establishes the compatibility relations along  $k$ . The full compatibility relations can be obtained by applying this analysis to all the inequivalent paths in the BZ.[56]

In the example of 2D space group with inversion  $P\bar{1}$ , all the momenta except  $\Gamma$ ,  $X$ ,  $Y$ ,  $M$  have the same little group: the identity group. Thus for any two maximal  $k$ -points, there is only one inequivalent path connecting them, and both even and odd irreps reduce to the identity irrep of the identity group. The compatibility-relation is nothing but the restriction that the two maximal  $k$ -points have the same number of occupied bands. We can write the compatibility relations as

$$m(\rho_{\Gamma}^{+}) + m(\rho_{\Gamma}^{-}) = m(\rho_X^{+}) + m(\rho_X^{-}) = m(\rho_Y^{+}) + m(\rho_Y^{-}) = m(\rho_M^{+}) + m(\rho_M^{-}). \quad (\text{A2})$$

Since we define the “occupied” bands as the 1st band to the  $N_e$ th band, there are always  $N_e$  occupied levels at any momentum and hence Eq.(A2) is automatically satisfied. However, most other magnetic space groups have more compatibility relations than the band number restriction; these compatibility relations can be broken in materials.

**Enforced Semimetals.** Band structures breaking the compatibility relations are referred to as enforced semimetals (ESs). The inversion case is not a good example for ES because the compatibility-relation is satisfied by definition. Please see J for example of ES.

We now classify the possible band structures allowed by compatibility relations. The strategy is that we first enumerate all the atomic insulators and then, for any given band structure from DFT, compare its irreps with those of the atomic insulators. A band structure must be topologically nontrivial if its irreps are not consistent with any atomic insulator; otherwise can be either trivial/nontrivial. Following the terminology of Zak [81–83], we refer to atomic insulators as band representations (BRs) and to the generators of the BRs as elementary BRs (EBRs).

We take the 2D space group with inversion  $P\bar{1}$  as an example to illustrate the concept of EBRs. There are four maximal Wyckoff positions in each unit cell,  $a(0,0)$ ,  $b(\frac{1}{2},0)$ ,  $c(0,\frac{1}{2})$ ,  $d(\frac{1}{2},\frac{1}{2})$ . Maximal Wyckoff positions are defined as positions with site-symmetry-groups which are maximal subgroups of the space group. In this example, the site-symmetry-groups of  $a, b, c, d$  are all isomorphic to  $C_i = \{E, I\}$ . Since  $C_i$  only has two types of irreps (even and odd), we can add either  $s$  orbital (even)/ $p$  orbital (odd) at each position. We can then obtain eight different EBRs. To see that they are EBRs, we consider an atomic insulator formed by two orbitals at two general positions,  $(x,y)$ ,  $(1-x,1-y)$ , which transform into each other under the inversion operation at  $d$  position. We can recombine the two orbitals to form a bonding state and an anti-bonding state at the  $d$  position. Thus this atomic insulator can be generated from two EBRs at the  $d$  position. The symmetry-data-vectors of the eight EBRs can be calculated by acting

the symmetry operators on the corresponding Bloch wave functions. The wave functions are Fourier transformations of the local orbitals

$$|\phi_{\xi,\alpha,\mathbf{k}}\rangle = \frac{1}{\sqrt{N}} \sum_{\mathbf{R}} e^{i\mathbf{k}\cdot(\mathbf{R}+\mathbf{t}_\alpha)} |\xi, \mathbf{R} + \mathbf{t}_\alpha\rangle \quad (\text{A3})$$

Here  $\xi = \pm$  is the parity of the local orbital,  $\alpha = a, b, c, d$  is the Wyckoff position,  $\mathbf{t}_\alpha$  is the position vector of the Wyckoff position,  $\mathbf{R}$  sums over all lattice vectors, and  $N$  is the system size. Since  $I|\xi, \mathbf{R} + \mathbf{t}_\alpha\rangle = \xi|\xi, -\mathbf{R} - \mathbf{t}_\alpha\rangle$ , we obtain

$$I|\phi_{\xi,\alpha,\mathbf{k}}\rangle = \xi \frac{1}{\sqrt{N}} \sum_{\mathbf{R}} e^{i\mathbf{k}\cdot(\mathbf{R}+\mathbf{t}_\alpha)} |\xi, -\mathbf{R} - \mathbf{t}_\alpha\rangle = \xi \frac{1}{\sqrt{N}} \sum_{\mathbf{R}'} e^{-i\mathbf{k}\cdot(\mathbf{R}'+\mathbf{t}_\alpha)} |\xi, \mathbf{R}' + \mathbf{t}_\alpha\rangle, \quad (\text{A4})$$

where the lattice vector  $\mathbf{R}'$  is  $-\mathbf{R} - 2\mathbf{t}_\alpha$ . If  $\mathbf{k}$  is one of the maximal  $k$ -points ( $\Gamma, X, Y, M$ ), we can calculate the parity of the Bloch wave function as

$$\langle \phi_{\xi,\alpha,\mathbf{k}} | I | \phi_{\xi,\alpha,\mathbf{k}} \rangle = \xi \frac{1}{N} \sum_{\mathbf{R}'} e^{-i2\mathbf{k}\cdot(\mathbf{R}'+\mathbf{t}_\alpha)} = \xi e^{-i2\mathbf{k}\cdot\mathbf{t}_\alpha}. \quad (\text{A5})$$

We have made use of the fact that  $2\mathbf{k}$  is a reciprocal lattice vector and hence  $2\mathbf{k}\cdot\mathbf{R} = 0 \pmod{2\pi}$ . For  $\alpha = a$ , the Bloch wave function has the same parity at all the four maximal  $k$ -points because  $e^{-i2\mathbf{k}\cdot\mathbf{t}_a} = 1$ . Thus the EBR induced from the orbital with parity  $\pm$  at the  $a$  position form the irreps  $\rho_\Gamma^\pm, \rho_X^\pm, \rho_Y^\pm, \rho_M^\pm$ . The symmetry-data-vectors (A1) of these two EBRs are

$$EBR_{+,a} = (1, 0, 1, 0, 1, 0, 1, 0)^T, \quad EBR_{-,a} = (0, 1, 0, 1, 0, 1, 0, 1)^T. \quad (\text{A6})$$

For  $\alpha = b, c, d$ , the Bloch wave function has different parities at the four maximal  $k$ -points because  $e^{-i2\mathbf{k}\cdot\mathbf{t}_\alpha}$  can be either  $1/-1$ . For example, for  $\alpha = b$ ,  $e^{-i2\mathbf{k}\cdot\mathbf{t}_b}$  equals to 1 and  $-1$  at  $\Gamma, Y$  and  $X, M$ , respectively. Thus the EBR induced from the orbital with parity  $\pm$  at the  $b$  position form the irreps  $\rho_\Gamma^\pm, \rho_X^\mp, \rho_Y^\pm, \rho_M^\mp$ . The corresponding symmetry-data-vectors are

$$EBR_{+,b} = (1, 0, 0, 1, 1, 0, 0, 1)^T, \quad EBR_{-,b} = (0, 1, 1, 0, 1, 0, 1, 0)^T. \quad (\text{A7})$$

Similarly, one can derive the symmetry-data-vectors of EBRs induced from  $c, d$  positions as

$$EBR_{+,c} = (1, 0, 1, 0, 0, 1, 0, 1)^T, \quad EBR_{-,c} = (0, 1, 0, 1, 1, 0, 1, 0)^T, \quad (\text{A8})$$

$$EBR_{+,d} = (1, 0, 0, 1, 0, 1, 1, 0)^T, \quad EBR_{-,d} = (0, 1, 1, 0, 1, 0, 0, 1)^T. \quad (\text{A9})$$

**Stable TI.** We consider an example where the occupied band form a single odd irrep at  $\Gamma$  and three even irreps at  $X, Y, M$  respectively. The corresponding symmetry-data-vector can be written as

$$B_1 = (0, 1, 1, 0, 1, 0, 1, 0)^T. \quad (\text{A10})$$

$B_1$  is not one of the EBRs; It is also not a sum of EBRs, because all EBRs have even number of odd irreps in Eqs. (A6) to (A9). It is also not a sum of EBRs because  $B_1$  has only one band but any sum of EBRs has at least two bands. Thus  $B_1$  must be topological. According to the Fu-Kane-like formula for Chern insulators [84]

$$(-1)^C = \prod_{K=\Gamma,X,Y,M} \prod_n \lambda_n(K), \quad (\text{A11})$$

where  $C$  is the Chern number,  $n$  is the index of occupied bands, and  $\lambda_n(K)$  is the parity of  $n$ th band at the momentum  $K$ , the band structure has an odd Chern number.

One notices that  $B_1$  can be written as a linear combination of EBRs with fractional coefficients

$$B_1 = -\frac{1}{2} EBR_{-,a} + \frac{1}{2} EBR_{-,d} + \frac{1}{2} EBR_{-,c} + \frac{1}{2} EBR_{-,d}, \quad (\text{A12})$$

but cannot be written as an integer combination of EBRs. It is a general principle that if a band structure cannot be written as a linear combination of EBRs unless the coefficients are fractional numbers, the band structure must have stable topology. Such stable topology implied by symmetry eigenvalues is characterized by the stable index (SI) (also

referred to as symmetry-based indicator [60, 80]). Eq. (A11) can be thought as an example of SI. Readers can refer to supplementary information of Ref. [60, 70] for technical details.

**Smith-index semimetal.** In magnetic space groups, some symmetry-data-vectors are not compatible with gapped state and implies topological Weyl semimetal (WSM), even when all of the compatibility relations are satisfied. In this work, the WSM phase implied by symmetry eigenvalue is named as Smith-index semimetal (SISM).

From the MTQC theory, we have found several MSGs with SI corresponding to WSM phase. All of these MSGs have a minimal subgroup MSG 2.4 ( $P\bar{1}$ )/MSG 81.33 ( $P\bar{4}$ ). For the MSGs with minimal subgroup  $P\bar{1}$  (with only inversion symmetry), the topologies are described by the stable indices group  $\mathbb{Z}_4 \times \mathbb{Z}_2^3$ . We found the stable index  $\eta_{4I} mod 2$  is the parity of the Chern number difference between  $k_z = 0$  and  $k_z = \pi$  planes. Thus  $\eta_{4I} = 1, 3$  correspond to the WSM phase with odd number of Weyl points in one half Brillouin zone [7]. For the MSGs with minimal subgroup  $P4$ , they have the SI group  $\mathbb{Z}_4 \times \mathbb{Z}_2^2$ . We find one of the two  $z_2$  indices can be interpreted as [7]  $\delta_{2S} = \frac{c_\pi - c_0}{2} mod 2$ , where  $c_{0,\pi}$  are the Chern numbers in the  $k_z = 0, \pi$  planes. Thus, when this  $\delta_{2S}$  index is nonzero,  $k_z = 0, \pi$  planes must have different Chern numbers and hence Weyl nodes must appear in between the two planes.

**Fragile TI.** If the  $B$  vector of a state cannot be written as a sum of EBRs, but can be written as a difference of EBRs, then the state is at least a fragile TI. [60, 66–70, 85–87] We say “at least” because the state can also have a stable topology which cannot be diagnosed through symmetry eigenvalues but through Berry phases. Now we give an example in the inversion case. We consider that the occupied bands form two odd irreps at  $\Gamma$  and three pairs of even irreps at X, Y, M respectively. The corresponding symmetry-data-vector is double of  $B_1$ , i.e.,

$$B_2 = (0, 2, 2, 0, 2, 0, 2, 0)^T. \quad (\text{A13})$$

Since  $B_2 = 2B_1$ , we can write the  $B_2$  as a linear combination of EBRs with integer coefficients, and one of the coefficients is negative

$$B_2 = -EBR_{-,a} + EBR_{-,d} + EBR_{-,c} + EBR_{-,d}. \quad (\text{A14})$$

This decomposition implies that, after being coupled to a trivial band forming the  $EBR_{-,a}$ ,  $B_2$  becomes trivial because it can be written as a sum of EBRs as  $EBR_{-,d} + EBR_{-,c} + EBR_{-,d}$ . Therefore,  $B_2$  is at least a fragile TI. Readers can refer to Ref. [70] for more examples and complete classifications of eigenvalue implied fragile TIs.

## Appendix B: Material statistics in the BCSMD

Ignoring the magnetic materials with incommensurate structures, there are 644 materials (including 95 alloys) with 261 different MSGs in the Bilbao Crystallographic Server Magnetic database(BCSMD)[71, 88]. We provide the number of materials in each MSG in Table IV. Detailed information about each of the magnetic materials can be obtained on the BCSMD website (<http://webbdccristal.ehu.es/magnadata>). Based on the stable topological classifications of MSGs [7, 29], we classify the MSGs into four types.

**Type A** The MSGs that have stable topological indices, which are indicated by red color. There are 435 materials in BCSMD with Type A MSGs.

**Type B** In this type of MSGs, given the electron number, one can immediately identify whether a material is ESFD. This type of MSGs are indicated by blue color. There are 34 materials with Type B MSGs in BCSMD.

**Type C** Among Type B MSGs, some also have stable topological indices, which are indicated by green color. There are 19 materials in BCSMD with Type C MSG.

**Type D** The other MSGs that do not belong to Type A/Type B are indicated by black color. There are 183 materials with Type D MSG.

We also emphasize that for an ES/ESFD, if the crossing point occurs at a k-point whose little co-group is chiral, the crossing point must necessarily carry a nonzero chiral charge [89–91]. The chiral MSGs have been tagged in Table IV.

TABLE IV: The number of magnetic materials per magnetic space group in BCSMD

MSG	Count	MSG	Count	MSG	Count	MSG	Count
1.3 $P_s1^*$	4	33.144 $Pna2_1$	3	63.462 $Cm'c'm$	2	138.528 $P_c4_2/ncm$	1
2.4 $P\bar{1}$	4	33.147 $Pna'2'_1$	2	63.463 $Cmc'm'$	1	138.529 $P_C4_2/ncm$	1
2.6 $P\bar{1}'$	3	33.148 $Pn'a'2_1$	3	63.464 $Cm'cm'$	4	139.535 $I4'/mmm'$	1
2.7 $P_s\bar{1}$	34	33.149 $P_a na2_1$	1	63.466 $C_c mcm$	2	139.536 $I4'/m'm'm'$	4
4.10 $P_a2_1^*$	7	33.150 $P_b na2_1$	1	63.467 $C_a mcm$	1	139.537 $I4/mm'm'$	2
4.12 $P_c2_1^*$	1	33.154 $P_c na2_1$	3	63.468 $C_A mcm$	1	140.550 $I_c4/mcm$	6

4.7 $P_{2_1}^*$	3	35.167 $Cm'm2'$	1	64.476 $Cm'ca'$	1	141.554 $I4'_1/am'd$	2
4.9 $P_{2_1'}^*$	3	36.174 $Cm'c2'_1$	2	64.479 $C_amca$	1	141.555 $I4'_1/am'd'$	3
5.13 $C_{2^*}$	1	36.176 $Cm'c'2_1$	1	64.480 $C_Amca$	13	141.556 $I4'_1/a'm'd$	3
5.15 $C2'^*$	1	36.178 $C_amc2_1$	4	65.483 $Cm'mm$	1	141.557 $I4_1/am'd'$	8
5.16 $C_c2^*$	3	38.191 $Am'm'2$	1	65.486 $Cmm'm'$	2	142.568 $I4'_1/a'cd'$	1
6.20 $Pm'$	1	38.192 $A_ammm2$	1	65.489 $C_ammm$	2	146.10 $R3^*$	2
7.27 $P_{ac}$	1	39.201 $A_bb2$	1	66.500 $C_{accm}$	5	146.12 $R_I3^*$	2
7.29 $P_{bc}$	1	41.217 $A_bba2$	1	67.510 $C_{amma}$	1	148.17 $R\bar{3}$	5
8.35 $C_{cm}$	1	42.223 $F_{somm2}$	1	69.523 $Fm'mm$	1	148.19 $R\bar{3}'$	2
8.36 $C_am$	4	43.227 $Fd'd'2$	1	69.526 $Fsmmm$	3	148.20 $R_I\bar{3}$	1
9.39 $Cc'$	2	45.237 $Ib'a2'$	1	70.530 $Fd'd'd$	2	152.35 $P_{3_1}2'1^*$	1
9.40 $C_{cc}$	3	46.243 $Im'a2'$	1	71.536 $Im'm'm$	2	154.41 $P_{3_2}21^*$	1
9.41 $C_a c$	3	49.270 $Pc'cm'$	1	72.543 $Ib'a'm$	1	154.44 $P_{c3_2}21^*$	3
10.49 $P_{C2/m}$	1	49.273 $P_{eccm}$	1	73.551 $Ib'c'a$	1	155.48 $R_I32^*$	1
11.54 $P_{2_1'/m'}$	2	50.282 $Pb'an'$	1	73.553 $I_cbea$	2	157.53 $P_{31m}$	1
11.55 $P_{a21/m}$	2	51.295 $Pmm'a'$	1	74.559 $Imm'a'$	1	157.55 $P_{31m'}$	1
11.57 $P_{C21/m}$	3	51.298 $P_{amma}$	1	74.562 $I_bmma$	1	159.64 $P_{c31c}$	3
12.58 $C2/m$	1	52.310 $Pn'n'a$	1	83.50 $P_{I4}/m$	2	161.69 $R3c$	2
12.60 $C2'/m$	4	52.312 $Pn'na'$	1	84.58 $P_{I4_2}/m$	1	161.71 $R3c'$	2
12.62 $C2'/m'$	9	52.315 $P_bnna$	1	85.59 $P4/n$	1	161.72 $R_I3c$	2
12.63 $C_c2/m$	8	53.334 $P_{Bmna}$	1	85.64 $P_c4/n$	1	162.78 $P_c\bar{3}1m$	1
12.64 $C_a2/m$	5	53.335 $P_{Cmna}$	1	86.67 $P_{4_2}/n$	1	164.89 $P\bar{3}m'$	2
13.67 $P2'/c$	1	54.350 $P_{Bcca}$	1	86.73 $P_{C4_2}/n$	3	165.94 $P\bar{3}'c'1$	1
13.69 $P2'/c'$	1	54.352 $P_{Iccca}$	3	87.75 $I4/m$	1	165.95 $P\bar{3}c'1$	2
13.70 $P_{a2/c}$	1	55.355 $Pb'am$	1	87.78 $I4/m'$	3	165.96 $P_c\bar{3}c1$	1
13.73 $P_{A2/c}$	3	55.356 $Pbam'$	1	88.81 $I_{4_1}/a$	1	166.101 $R\bar{3}m'$	5
13.74 $P_{C2/c}$	4	55.361 $P_{cbam}$	1	88.86 $I_c4_1/a$	1	166.102 $R_I\bar{3}m$	1
14.75 $P_{2_1/c}$	9	56.369 $Pc'c'n$	1	92.111 $P_{4_12_1}2^*$	1	166.97 $R\bar{3}m$	2
14.77 $P_{2_1'/c}$	3	56.372 $P_{bccn}$	1	92.114 $P_{4_12'_1}2'^*$	1	167.103 $R\bar{3}c$	1
14.78 $P_{2_1/c'}$	5	56.373 $P_{cccn}$	2	94.132 $P_{c4_22_1}2^*$	1	167.106 $R\bar{3}'c'$	1
14.79 $P_{2_1'/c'}$	8	56.374 $'P_{accn'}$	2	96.150 $P_{I4_32_1}2^*$	1	167.107 $R\bar{3}c'$	1
14.80 $P_{a21/c}$	20	57.389 $P_{Abcm}$	1	107.231 $I4m'm'$	1	167.108 $R_I\bar{3}c$	5
14.81 $P_{b21/c}$	1	57.391 $P_{Cbcm}$	1	111.255 $P\bar{4}2'm'$	1	173.129 $P_{6_3}$	1
14.82 $P_{c21/c}$	6	58.395 $Pn'nm$	5	113.267 $P\bar{4}2_1m$	1	173.131 $P_{6'_3}$	1
14.83 $P_{A2_1/c}$	1	58.398 $Pnn'm'$	4	114.282 $P_I\bar{4}2_1c$	1	174.136 $P_c\bar{6}$	1
14.84 $P_{C2_1/c}$	10	58.399 $Pn'n'm'$	2	117.305 $P_C\bar{4}b2$	1	176.145 $P_{6'_3}/m$	1
15.85 $C2/c$	6	58.404 $P_{Innm}$	1	119.319 $I4m'2'$	1	185.197 $P_{6_3cm}$	3
15.87 $C2'/c$	4	59.407 $Pm'mn$	2	122.338 $I_c\bar{4}2d$	1	185.199 $P_{6'_3}c'm$	2
15.88 $C2/c'$	2	59.409 $Pm'm'n$	1	123.345 $P4/mm'm'$	1	185.200 $P_{6'_3}cm'$	1
15.89 $C2'/c'$	11	59.410 $Pmm'n'$	1	124.360 $P_c4/mcc$	4	185.201 $P_{6_3}c'm'$	3
15.90 $C_c2/c$	28	59.416 $P_{Immn}$	1	125.367 $P4'/nbm'$	1	186.207 $P_{6_3}m'c'$	1
15.91 $C_a2/c$	3	60.419 $Pb'cn$	2	125.373 $P_{c4}/nbm$	1	188.220 $P_c\bar{6}c2$	1
18.19 $P_{2_12_1'2^*}$	1	60.422 $Pb'c'n$	1	126.384 $P_c4/nnc$	1	189.223 $P\bar{6}'2'm$	1
18.22 $P_{B2_12_12^*}$	1	60.431 $P_{Cbcn}$	1	126.386 $P_{I4}/nnc$	1	189.224 $P\bar{6}'2m'$	1
19.25 $P_{2_12_12_1^*}$	2	61.433 $Pbca$	2	127.394 $P4'/m'bm'$	2	192.252 $P_c6/mcc$	2
19.27 $P_{2_1'2_1'2_1^*}$	1	61.437 $Pb'c'a'$	3	127.395 $P4/m'b'm'$	1	193.259 $P_{6'_3}/m'cm'$	1
19.28 $P_{c2_12_12_1^*}$	1	61.439 $P_{Cbc}$	1	127.397 $P_{c4}/mbm$	1	193.260 $P_{6_3}/mc'm'$	3
19.29 $P_{C2_12_12_1^*}$	1	62.441 $Pnma$	11	128.408 $P_{c4}/mnc$	1	194.268 $P_{6'_3}/m'm'c$	1
20.34 $C22'2_1^*$	1	62.443 $Pn'ma$	2	128.410 $P_{I4}/mnc$	5	203.26 $Fd\bar{3}$	1
20.37 $C_{A2221^*}$	1	62.444 $Pnm'a$	4	129.416 $P4'/n'm'm'$	3	205.33 $Pa\bar{3}$	2
26.66 $Pmc2_1$	2	62.445 $Pnma'$	5	129.419 $P4/n'm'm'$	1	216.77 $F_S\bar{4}3m$	1
26.68 $Pm'c21'$	2	62.446 $Pn'm'a$	9	130.432 $P_{c4}/ncc$	2	222.103 $P_{In}\bar{3}n$	1
26.72 $P_bmc2_1$	3	62.447 $Pnm'a'$	3	131.440 $P4'_2/m'm'c$	1	224.113 $Pn\bar{3}m'$	4

27.82 <i>P<sub>ccc</sub>2</i>	1	<b>62.448</b> <i>Pn'ma'</i>	5	<b>132.456</b> <i>P<sub>c</sub>4<sub>2</sub>/mcm</i>	1	<b>227.131</b> <i>Fd<sub>3</sub>m'</i>	1
29.101 <i>Pc'a2'_1</i>	4	62.449 <i>Pn'm'a'</i>	4	<b>134.481</b> <i>P<sub>c</sub>4<sub>2</sub>/nnm</i>	3	<b>228.139</b> <i>F<sub>S</sub>d<sub>3</sub>c</i>	3
29.104 <i>P<sub>a</sub>ca2<sub>1</sub></i>	5	<b>62.450</b> <i>P<sub>a</sub>nma</i>	5	<b>135.492</b> <i>P<sub>c</sub>4<sub>2</sub>/mbe</i>	2	<b>229.143</b> <i>Im<sub>3</sub>m'</i>	1
29.105 <i>P<sub>b</sub>ca2<sub>1</sub></i>	1	<b>62.452</b> <i>P<sub>c</sub>nma</i>	1	<b>136.499</b> <i>P4'_2/mnm'</i>	2	<b>230.148</b> <i>Ia<sub>3</sub>d'</i>	1
29.110 <i>P<sub>I</sub>ca2<sub>1</sub></i>	1	<b>62.453</b> <i>P<sub>A</sub>nma</i>	1	<b>136.503</b> <i>P4<sub>2</sub>/m'n'm'</i>	1		
31.129 <i>P<sub>b</sub>mn2<sub>1</sub></i>	3	63.459 <i>Cm'cm</i>	1	<b>136.506</b> <i>P<sub>I</sub>4<sub>2</sub>/mnm</i>	1		
32.137 <i>Pb'a2'</i>	1	63.461 <i>Cmcm'</i>	1	<b>138.525</b> <i>P4<sub>2</sub>/nc'm'</i>	1		

\* Chiral MSG

In the magnetic material database, all of the materials have distinct chemical formulae/different MSGs except for the 15 materials tabulated in Table V. The 15 compounds are reported having the same chemical formulae and MSGs but different magnetic moments in two independent neutron experiments. The differences between them have been described in Table V. These differences consist in the experimental temperature/lattice parameters. In this work, we have performed the *ab initio* calculations for all of them.

TABLE V: The 15 compounds that have the same chemical formulae and MSG but with different magnetic moments are tabulated together.

No.	Chemical Formula	MSG	BSCID	$(M_x, M_y, M_z)(\mu_B)$	Differences
1	CoSe <sub>2</sub> O <sub>5</sub>	60.419	0.119	Co(3.1,0.0,0.8)	Small canting along <i>z</i> axis
			0.161	Co(3,0,0)	
2	Er <sub>2</sub> BaNiO <sub>5</sub>	15.90	1.15	Er(7.89,0,0.25), Ni(-1.4,0,-0.64)	Small difference between the magnetic moments
			1.53	Er(7.23,0,0.32), Ni(-1.38,0,-0.18)	
3	Cr <sub>2</sub> TeO <sub>6</sub>	58.395	0.76	Cr(1,0,0)	Experimental temperature is different; <i>T</i> = 93K for BCSID-58.395, <i>T</i> = 4.2K for BCSID-0.143
			0.143	Cr(2.45,0,0)	
4	Cr <sub>2</sub> WO <sub>6</sub>	58.395	0.75	Cr(1,0,0)	Experimental temperature is different; <i>T</i> = 45K for BCSID-58.395, <i>T</i> = 4.2K for BCSID-0.143
			0.144	Cr(2.14,0,0)	
5	Ho <sub>2</sub> Ru <sub>2</sub> O <sub>7</sub>	141.557	0.49	Ru(0.56,0.56,0.9)	Experimental temperature is different; <i>T</i> = 20K for BCSID-141.557, <i>T</i> = 0.1K for BCSID-0.51
			0.51	Ho(-4.26,-4.26,-1.84), Ru(0.22,0.22,1.77)	
6	Ni <sub>2</sub> SiO <sub>4</sub>	14.82	1.203	Ni(1,0,1)	Small difference on the lattice parameter and experimental temperature
			1.204	Ni(1.82,0,-0.9)	
7	ScMn <sub>6</sub> Ge <sub>6</sub>	192.252	1.110	Mn(0,0,1.96)	Experimental temperature is different; <i>T</i> = 309K for BCSID-1.110, <i>T</i> = 149 for BCSID-1.225
			1.225	(0,0,2.08)	
8	Sr <sub>2</sub> IrO <sub>4</sub>	54.352	1.3	Ir(0.24,0,0)	Small canting along <i>y</i> axis
			1.77	Ir(0.202,0,0.048,0)	
9	U <sub>2</sub> Rh <sub>2</sub> Sn	135.492	1.103	U(0,0,0.53)	Small poloarization on Rh
			1.207	U(0,0,0.5), Rh(0.04,0.04,0)	
10	Mn <sub>2</sub> O <sub>3</sub>	61.433	0.40	Mn1(2.6,0,-1.6), Mn2(3.4,0,0.7)	Experimental temperature is different; <i>T</i> = 2K for BCSID-0.40, <i>T</i> = 40K for BCSID-0.41
			0.41	Mn1(2.4,0,-1.4), Mn2(3.0,0,0.8)	
11	Co <sub>4</sub> Nb <sub>2</sub> O <sub>9</sub>	15.88	0.196	Co1(3.7,1.85,1.42), Co2(2.78,1.39,0.97)	Small difference on the lattice parameter and experimental temperature
			0.197	Co1(2.677,1.312,0), Co(2.842,1.953,0)	
12	HoMnO <sub>3</sub>	185.197	0.32	Mn(1.72,3.44,0)	Experimental temperature is different; <i>T</i> = 32K for BCSID-0.32, <i>T</i> = 1.7K for BCSID-0.33

			0.33	Mn(1.76,3.52,0),Ho(0,0,2.87)	
13	FeI2	12.62	3.14	Fe(0,0,1)	Different lattice parameters
			1.0.13	Fe(0,0,1)	
14	Co2SiO4	62.441	0.218	Co1(0.94,3.14,0.47),Co2(0,3.64,0)	Small difference on the experimental temperature
			0.219	Co1(1.2,3.64,0.57),Co2(0,3.35,0)	
15	CuMnSb	16.72	1.233	Mn(2.53,1.39,2.53)	Small difference on the lattice parameter and experimental temperature
			1.265	Mn(2.25,2.25,2.25)	

## Appendix C: Computational methods

### 1. Convention setting of the magnetic unit cell

We read the crystalline parameters and magnetic moments from the magnetic structure files, whose datatype are 'mcif', provided by BCSMD. In the BCSMD website, lattice parameters of the magnetic unit cell are in the convention called working setting ( $\vec{a}$ ,  $\vec{b}$ ,  $\vec{c}$ ) and it can be transformed to the standard convention ( $\vec{a}_s$ ,  $\vec{b}_s$ ,  $\vec{c}_s$ ) by the transformation matrix  $T_s = \{T|\vec{\tau}\}$  as,

$$(\vec{a}_s, \vec{b}_s, \vec{c}_s) = T \cdot (\vec{a}, \vec{b}, \vec{c}) + \vec{\tau} \quad (C1)$$

where the transformation matrix  $T_s = \{T|\vec{\tau}\}$  of each material has been supplied in the BCSMD website.

While, in the *ab initio* calculations, we adopt the primitive magnetic unit cell. The primitive lattice vectors ( $\vec{p}_1$ ,  $\vec{p}_2$ ,  $\vec{p}_3$ ) can be obtained by transforming the lattice vectors in standard convention ( $\vec{a}_s$ ,  $\vec{b}_s$ ,  $\vec{c}_s$ ) with the transformation matrix  $M_X$ ,

$$(\vec{p}_1, \vec{p}_2, \vec{p}_3) = (\vec{a}_s, \vec{b}_s, \vec{c}_s) \cdot M_X \quad (C2)$$

where  $M_X$  has been supplied in the VASP2trace package ([www.cryst.ehu.es/crust/checktopologicalmat](http://www.cryst.ehu.es/crust/checktopologicalmat)) and  $X$  is the lattice type of the magnetic unit cell.

### 2. Parameters setting in *ab initio* calculations

We perform all of the first-principle calculations using the Vienna *ab initio* simulation package(VASP); the generalized gradient approximation (GGA) with the Perdew-Burke-Ernzerhof (PBE) type exchange-correlation potential was adopted. For each material, we set the cutoff energy for plane wave basis as 1.2 times larger than the suggested value in the pseudo-potential files. In the *ab initio* calculations, the initial magnetic moments are set to the experimental values provided by BCSMD website. The convergence accuracy of self-consistent calculations is  $10^{-5}$ eV and spin-orbital coupling (SOC) has been included. For magnetic cells containing less than 50 atoms, the Brillouin zone (BZ) sampling is performed by using k grids with a  $9 \times 9 \times 9$  mesh in self-consistent calculations. We reduce the grids to  $5 \times 5 \times 5$  if there are more than 50 atoms in the magnetic primitive cell to save calculational costs. We implement the *ab initio* calculations on the MPG supercomputer Cobra and Draco with 960 CPU cores in total and the supercomputer in ShanghaiTech University with 560 CPU cores. For benchmarking, we calculate the simple compound CeCo<sub>2</sub>P<sub>2</sub> (with 10 atoms per magnetic primitive cell) on the Cobra supercomputer with 80 Skylake cores at 2.4GHz. The time used is 15 min 34s for the self consistent calculations and 15 min 45s for the band structure calculations with 240 k points. For the complex compound Sr<sub>3</sub>CoIrO<sub>6</sub> with 66 atoms per magnetic primitive cell, it costs 7h 50min for the self consistent calculations and 6h 42 min 53s for the band structure calculation with 200 k points.

Since all of the magnetic materials contain at least one correlated element, we also perform the L(S)DA+U calculations for all of the magnetic materials using the VASP. For the L(S)DA+U calculations, we adopt the simplified (rotationally invariant) approach and set the Hubbard U as 1, 2, 3, 4 eV for the *d* electrons and 2, 4, 6 eV for the *f* electrons. For the materials which have both *d* and *f* electron, we set U of *d* electron as 2 eV and the U of *f* electron as 2, 4, 6 eV.

Similar with the TQC for paramagnetic materials, we also provide the maximal  $\mathbf{k}$  vectors for each magnetic space group in the BCS website. Based on the self-consistent charge density files, we calculate the wave functions at the magnetic maximal  $\mathbf{k}$  vectors and obtain the characters using the MagVASP2trace package.

### 3. Magnetic VASP2trace package

In TQC, the in house VASP2trace package [75] is used to calculate the character tables of paramagnetic materials. It read the unitary symmetry operators from the output files of VASP and can identify the space group. While the anti-unitary symmetries are absent and VASP2trace cannot identify the magnetic space groups (MSGs).

In the MTQC, we revise the VASP2trace package to calculate the character tables of magnetic materials and supply the symmetry file for each MSG. The magnetic VASP2trace (MagVASP2trace) [?] reads the magnetic symmetries from the symmetry files that we supply, instead of reading them from the output files of VASP. The symmetry file contains both unitary operations and anti-unitary operations. Both SO(3) and SU(2) matrix in the symmetry files are written in the basis of primitive lattice vectors.

MagVASP2trace adopts both SO(3) and SU(2) matrix in the convention used in the BCS website (<https://www.cryst.ehu.es/>) and generate the **trace.txt** file that contains all of the magnetic symmetry operators and the character tables of the occupied bands at the magnetic maximal  $\mathbf{k}$  vectors.

### 4. Construction of Wannier tight-binding Hamiltonian and surface states calculation

We construct the tight-binding Hamiltonians of NpBi, CeCo<sub>2</sub>P<sub>2</sub>, MnGeO<sub>3</sub> and Mn<sub>3</sub>ZnC using the Wannier90 package [92]. We generate the maximally localized Wannier functions (MLWFs) for 5p orbitals on Bi, 5f and 6d orbitals on Np for the magnetic TI NpBi. For the magnetic NLSM CeCo<sub>2</sub>P<sub>2</sub>, the MLWFs for 3p orbitals on P, 3d orbitals on Co, 4f and 5d orbitals on Ce are constructed. For the magnetic DSM MnGeO<sub>3</sub>, we generate the MLWFs for 4s orbitals on Ge, 2p orbitals on O, and 3d orbitals on Mn. For the ferrimagnetic ES Mn<sub>3</sub>ZnC, we generate the MLWFs for 4s, 4p and 3d orbitals on Zn, 2p orbitals on C and 3d orbitals on Mn.

The surface states are calculated with the Green's function method using the WannierTools package [93, 94], and the results are shown in FIG. 2 of main text and FIG. 32-33.

### Appendix D: Comparison of the ground state energy between different magnetic configurations of several compounds

We select the three magnetic topological materials NpBi with BCSID-3.7, CeCo<sub>2</sub>P<sub>2</sub> with BCSID-1.253 and MnGeO<sub>3</sub> with BCSID-0.125 to compare the energy difference between different magnetic structures, respectively. As shown in Figure 3, there are three possible magnetic structures for each material, where AFM-I and AFM-II are the assumed configurations and the AFM-III phase is the one obtained from neutron experiments. The relative ground state energies at each U for the three materials are tabulated in Table VI. For NpBi and CeCo<sub>2</sub>P<sub>2</sub>, AFM-III phase always has the lowest ground state energy at different U. For MnGeO<sub>3</sub>, there is only one exception, i.e. the AFM-I phase of MnGeO<sub>3</sub> with U=0, that has lower energy than the AFM-III phase. With increasing U, the experimental AFM-III phase lowers its energy to become the lowest.

The comparisons in Table VI indicate that the magnetic configurations obtained from neutron experiments are favorable with the lowest ground state energy.

TABLE VI: The relative ground state energy of NpBi, CeCo<sub>2</sub>P<sub>2</sub> and MnGeO<sub>3</sub> in three possible magnetic structures with different U added. The magnetic structures are shown in Figure 3, where the magnetic configurations AFM-III are obtained from neutron scattering experiments.

Materials (BCSID)	U(eV)	E(AFM-I) (eV)	E(AFM-II) (eV)	E(AFM-III) (eV)
NpBi (BCSID: 3.7)	0	0.079	0.091	0
	2	2.108	2.125	1.995
	4	3.049	3.05	2.999
	6	3.538	3.543	3.525
	0	0.388	0.388	0

CeCo<sub>2</sub>P<sub>2</sub> (BCSID: 1.253)

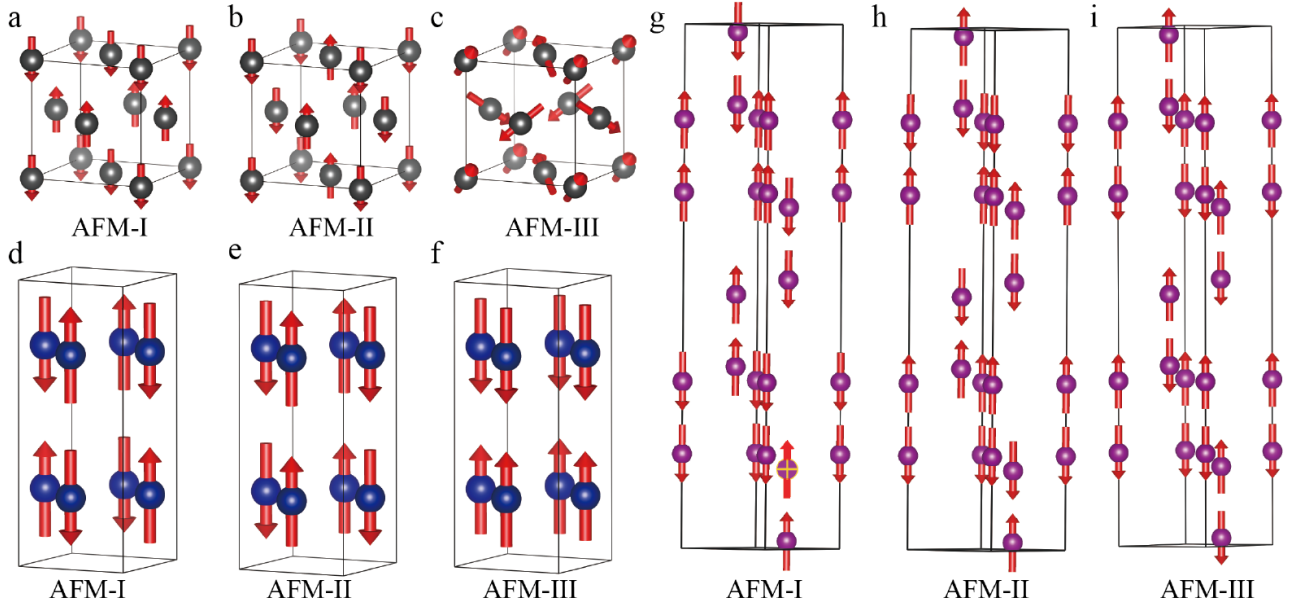


FIG. 3. Three possible magnetic structures for (a-c)NpBi, (d-f)CeCo<sub>2</sub>P<sub>2</sub> and (g-i) MnGeO<sub>3</sub>, where the AFM-III phase in (c)(f)(i) are the ones from neutron scattering experiments.

	2	9.159	9.243	8.468
	4	10.666	10.729	9.973
	6	11.955	12.098	11.263
MnGeO <sub>3</sub> (BCSID: 0.125)	0	-0.4	0.164	0
	1	6.845	6.532	6.437
	2	12.713	12.151	12.068
	3	17.703	17.132	17.068
	4	22.095	21.589	21.529

## Appendix E: Comparisons between different exchange-correlation potentials

### 1. Band structure calculations with GGA functional

We adopt five different exchange-correlation functional methods, including Perdew-Wang 91 (91), AM05 (AM), revised PBE (RE), revised PBE with Pade Approximation (RP) and Ceperley-Alder functional (CA), to check the topologies and the band structures that obtained by the PBE (PE) method. The topology and band structure comparisons of the topological materials BaFe<sub>2</sub>As<sub>2</sub>, CeCo<sub>2</sub>P<sub>2</sub>, NpBi, and MnGeO<sub>3</sub> are shown in the FIG. 4-7. The comparisons indicate that different exchange-correlation functional methods have minor effect on the band structures but do not change the topologies of these materials.

### 2. Band structure calculations with meta-GGA functional

To further check the band structures and topologies obtained from LDA+U calculations, we have also performed ab initio calculations with the modified Becke-Johnson (mBJ) [73] potential for 23 topological compounds. They are Mn<sub>3</sub>Ir (BCSID-0.108), Mn<sub>3</sub>Sn (BCSID-0.200), Mn<sub>3</sub>Pt (BCSID-1.143), MnGeO<sub>3</sub> (BCSID-0.125), Mn<sub>2</sub>As (BCSID-1.132), CaFe<sub>2</sub>As<sub>2</sub> (BCSID-1.52), Cd<sub>2</sub>O<sub>2</sub>S<sub>2</sub>O<sub>7</sub> (BCSID-0.2), NiCr<sub>2</sub>O<sub>4</sub> (BCSID-0.4), PbNiO<sub>3</sub> (BCSID-0.21), LuFeO<sub>3</sub> (BCSID-0.117), LuFe<sub>4</sub>Ge<sub>2</sub> (BCSID-0.140), NiS<sub>2</sub> (BCSID-0.150), Mn<sub>3</sub>Ge (BCSID-0.203), Co<sub>2</sub>SiO<sub>4</sub> (BCSID-0.218), CrN (BCSID-1.28), ScMn<sub>6</sub>Ge<sub>6</sub> (BCSID-1.110), CaCo<sub>2</sub>P<sub>2</sub> (BCSID-1.252), CeCo<sub>2</sub>P<sub>2</sub> (BCSID-1.253), GdIn<sub>3</sub> (BCSID-1.81), Mn<sub>3</sub>ZnC (BCSID-2.19), NpBi (BCSID-3.7), NpSe (BCSID-3.10) and NpSb (BCSID-3.12).

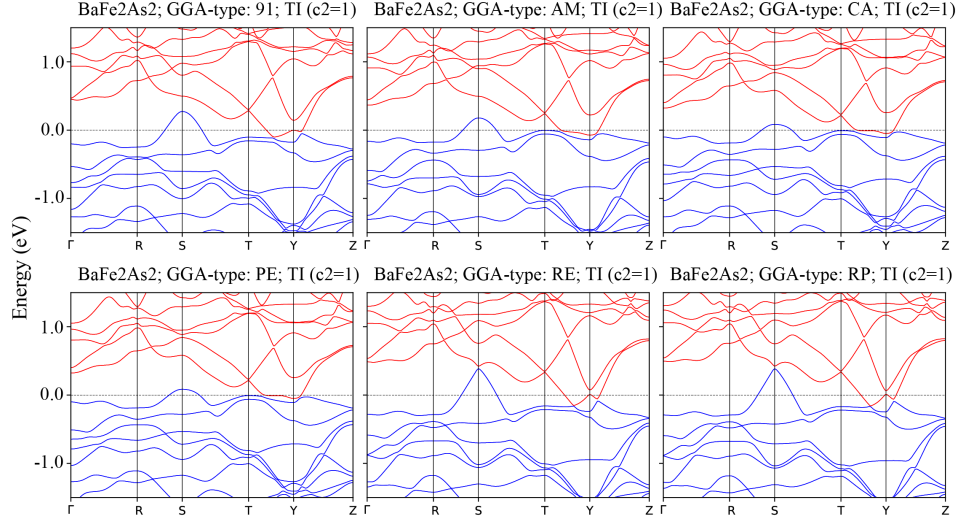


FIG. 4. The band structures and topology of  $\text{BaFe}_2\text{As}_2$  obtained by different exchange-correlation functional methods. The topology is maintained for different methods, indicating a TI with topological index  $c_2 = 1$ . The Hubbard  $U$  of  $3d$  electron is set to 1 eV.

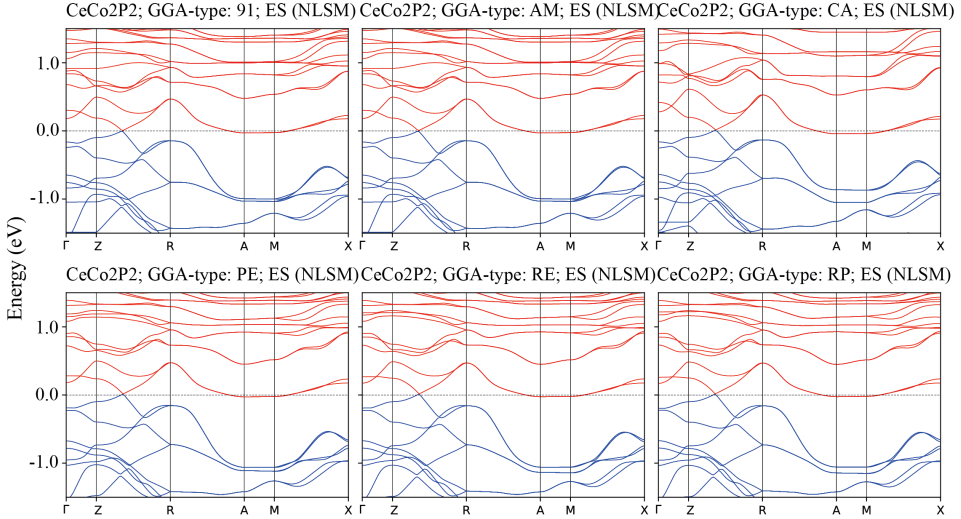


FIG. 5. The band structures and topology of  $\text{CeCo}_2\text{P}_2$  obtained by different exchange-correlation functional methods. The topology is maintained ES (also NLSM) for the different methods. The Hubbard  $U$  of  $3d$  and  $4f$  electron are set to 2 and 6 eV, respectively.

Apart from NpSe (BCSID-3.10), we find slightly different band structures with MBJ and LDA+U methods. However, comparing these 2 band structures and its topology, we can always find a value of  $U$  that reproduces the MBJ calculations. As shown in FIG. 8–29, we have found the correct value of  $U$  for each compound. Using the correct value of  $U$ , we can reproduce the the band structures and topology at the Fermi level consistent with the results obtained from mBJ.

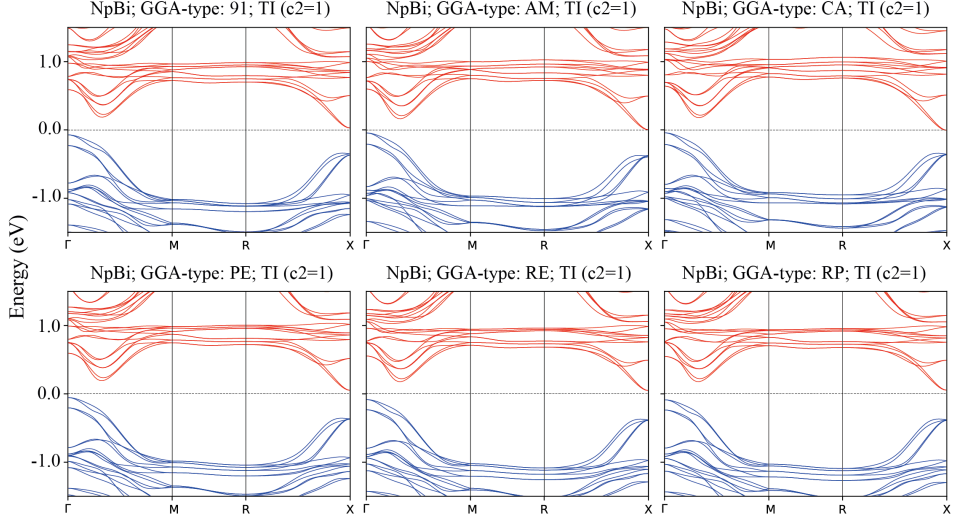


FIG. 6. The band structures and topology of NpBi obtained by different exchange-correlation functional methods. The topology is maintained TI with topological index  $c_2 = 1$  for the different methods. The Hubbard U of  $5f$  electron is set to 2 eV.

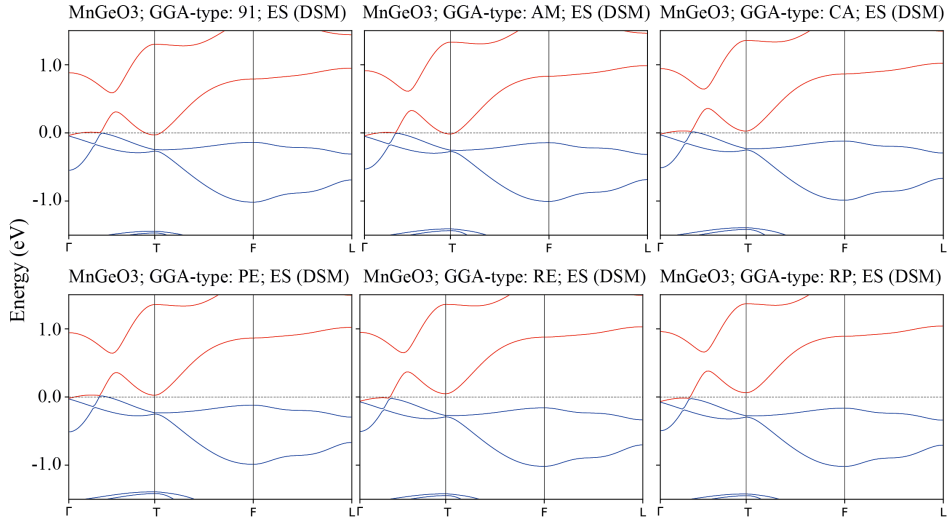


FIG. 7. The band structures and topology of MnGeO<sub>3</sub> obtained by different exchange-correlation functional methods. The topology is maintained ES (also DSM) for the different methods. The Hubbard U of  $3d$  electron is set to 4 eV.

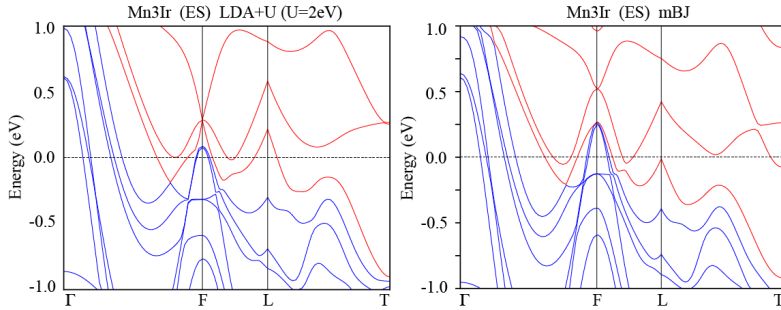


FIG. 8. Band structures of the ES Mn<sub>3</sub>Ir obtained from LDA+U ( $U = 2\text{eV}$ ) and mBJ methods.

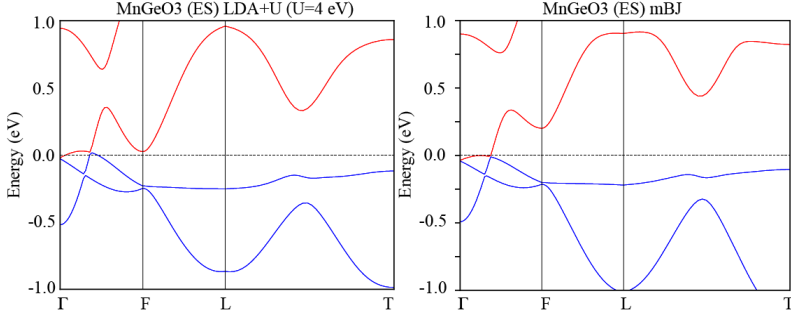


FIG. 9. Band structures of the ES MnGeO<sub>3</sub> obtained from LDA+U ( $U = 4\text{ eV}$ ) and mBJ methods.

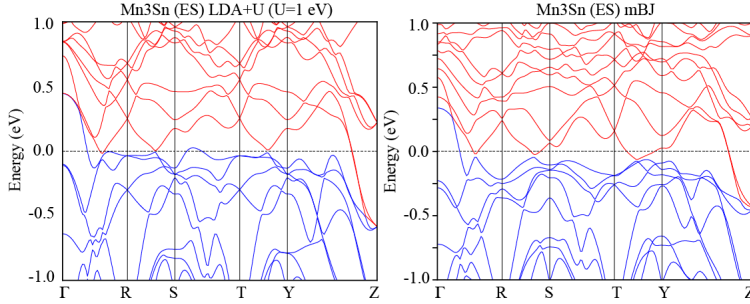


FIG. 10. Band structures of the ES Mn<sub>3</sub>Sn obtained from LDA+U ( $U = 1\text{ eV}$ ) and mBJ methods.

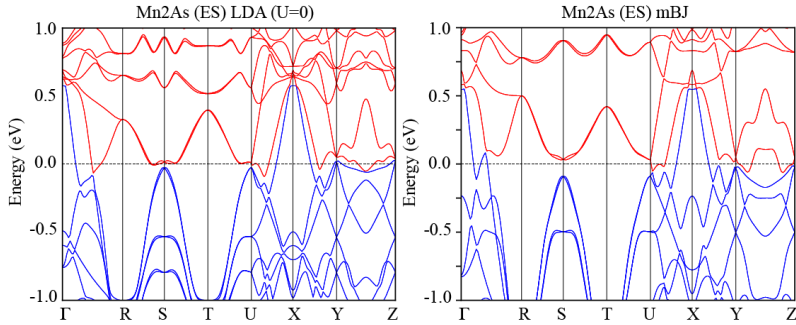


FIG. 11. Band structures of the ES Mn<sub>2</sub>As obtained from LDA+U ( $U = 0\text{ eV}$ ) and mBJ methods.

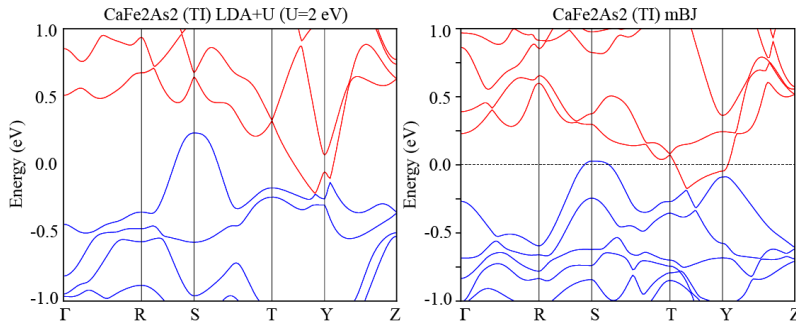


FIG. 12. Band structures of the TI CaFe<sub>2</sub>As<sub>2</sub> obtained from LDA+U ( $U = 2\text{ eV}$ ) and mBJ methods.

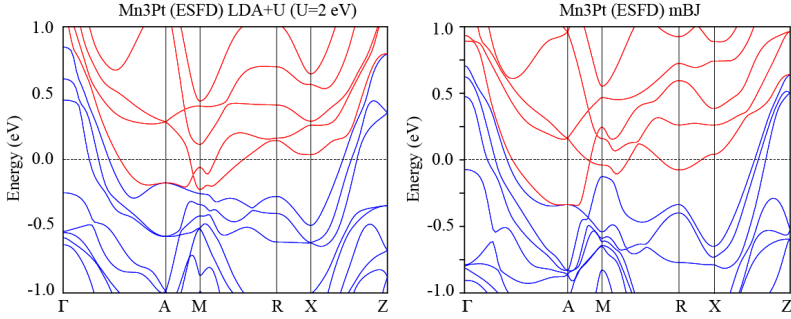


FIG. 13. Band structures of the ESFD Mn<sub>3</sub>Pt obtained from LDA+U ( $U = 2\text{ eV}$ ) and mBJ methods.

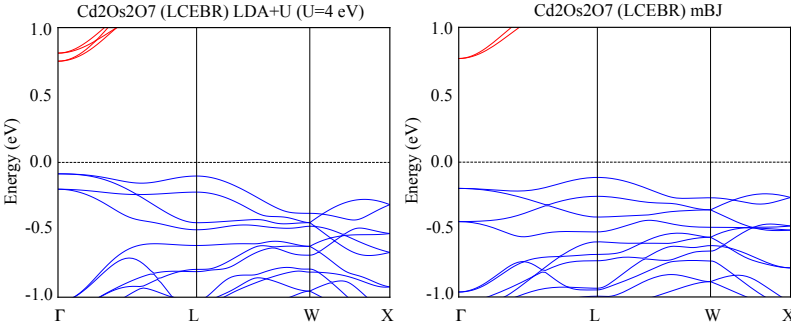


FIG. 14. Band structures of Cd<sub>2</sub>O<sub>7</sub> obtained from LDA+U ( $U = 2\text{ eV}$ ) with LCEBR phase and mBJ method with LCEBR phase.

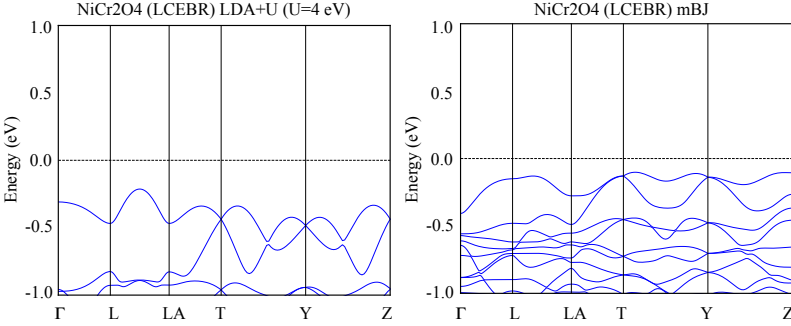


FIG. 15. Band structures of the NiCr<sub>2</sub>O<sub>4</sub> obtained from LDA+U ( $U = 4\text{ eV}$ ) with LCEBR phase and mBJ method with LCEBR phase.

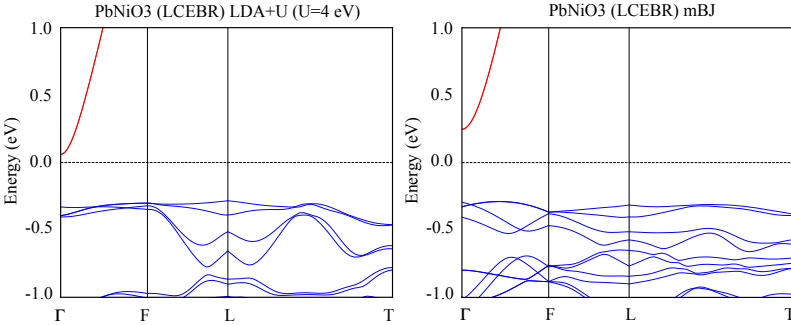


FIG. 16. Band structures of PbNiO<sub>3</sub> obtained from LDA+U ( $U = 4\text{ eV}$ ) with LCEBR phase and mBJ methods with LCEBR phase.

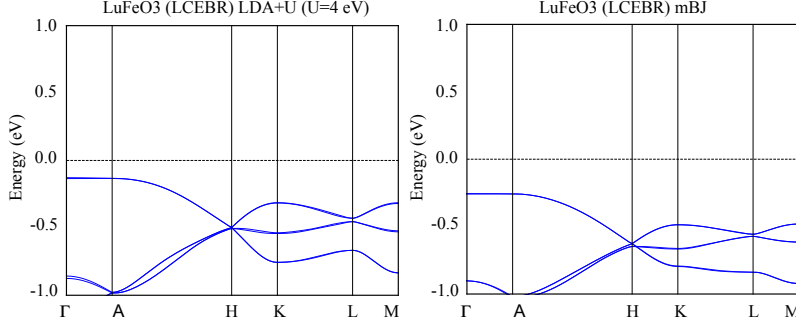


FIG. 17. Band structures of the LuFeO<sub>3</sub> obtained from LDA+U ( $U = 4\text{ eV}$ ) with LCEBR phase and mBJ methods with LCEBR phase.

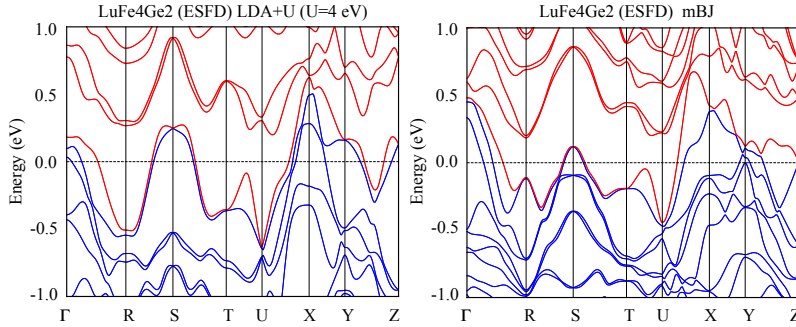


FIG. 18. Band structures of the ESFD LuFe<sub>4</sub>Ge<sub>2</sub> obtained from LDA+U ( $U = 4\text{ eV}$ ) and mBJ methods.

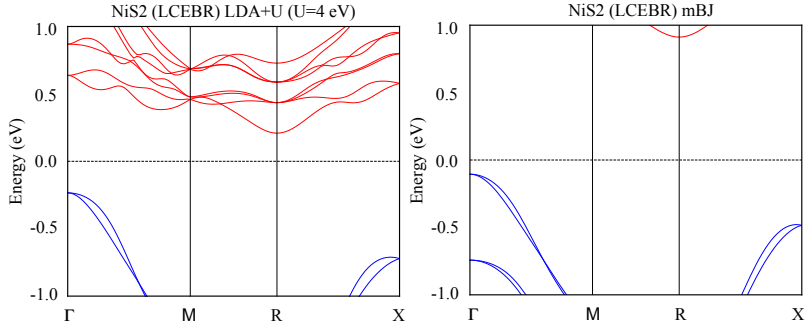


FIG. 19. Band structures of NiS<sub>2</sub> obtained from LDA+U ( $U = 2\text{ eV}$ ) with LCEBR phase and mBJ methods with LCEBR phase.

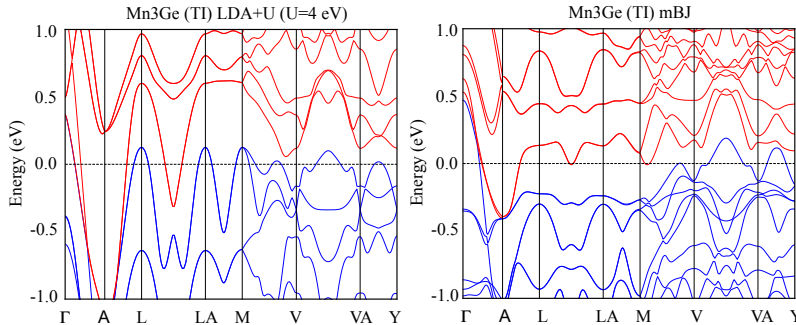


FIG. 20. Band structures of the TI Mn<sub>3</sub>Ge obtained from LDA+U ( $U = 4\text{ eV}$ ) and mBJ methods.

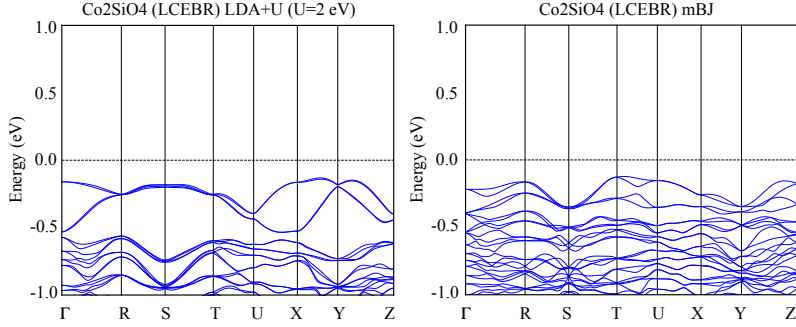


FIG. 21. Band structures of  $\text{Co}_2\text{SiO}_4$  obtained from LDA+U ( $U = 2\text{eV}$ ) with LCEBR phase and mBJ methods with LCEBR phase.

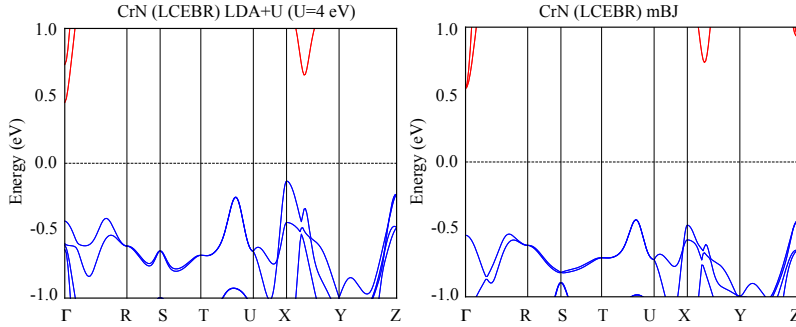


FIG. 22. Band structures of CrN obtained from LDA+U ( $U = 2\text{eV}$ ) with LCEBR phase and mBJ methods with LCEBR phase.

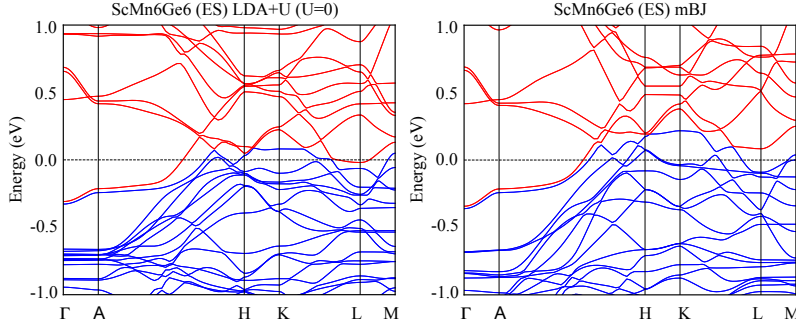


FIG. 23. Band structures of the ES  $\text{ScMn}_6\text{Ge}_6$  obtained from LDA+U ( $U = 0$ ) and mBJ methods.

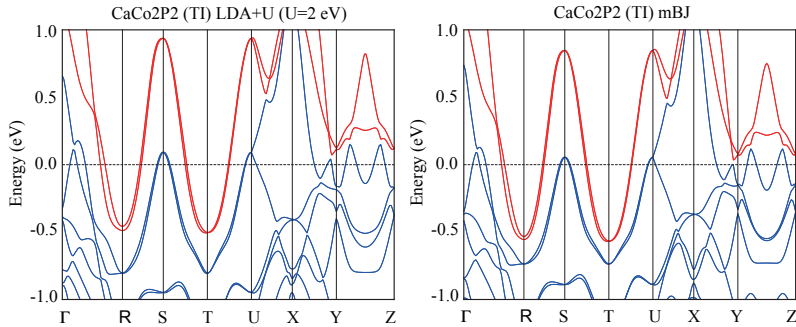


FIG. 24. Band structures of the TI  $\text{CaCo}_2\text{P}_2$  obtained from LDA+U ( $U = 2\text{eV}$ ) and mBJ methods.

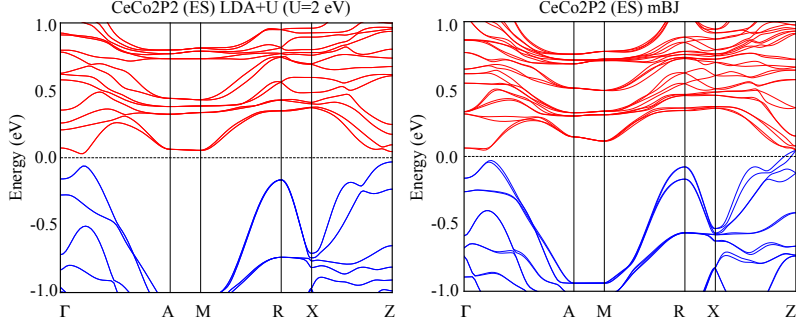


FIG. 25. Band structures of the ESFD CeCo<sub>2</sub>P<sub>2</sub> obtained from LDA+U ( $U = 2\text{eV}$ ) and mBJ methods.

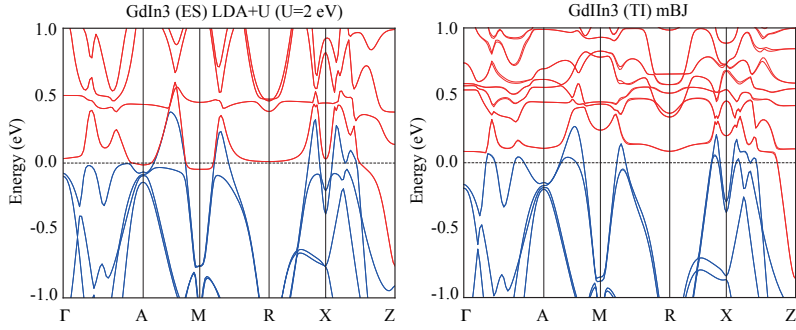


FIG. 26. Band structures of the ES GdIn<sub>3</sub> obtained from LDA+U ( $U = 2\text{eV}$ ) and mBJ methods.

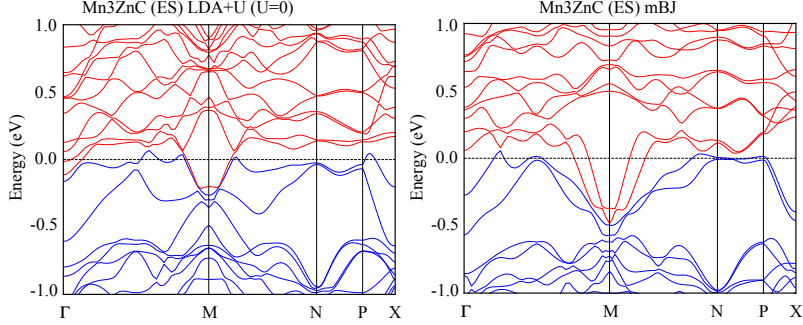


FIG. 27. Band structures of the ES Mn<sub>3</sub>ZnC obtained from LDA+U ( $U = 2\text{eV}$ ) and mBJ methods.

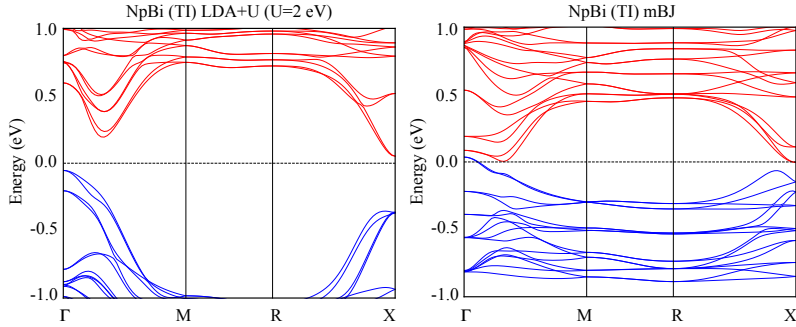


FIG. 28. Band structures of the TI NpBi obtained from LDA+U ( $U = 2\text{eV}$ ) and mBJ methods.

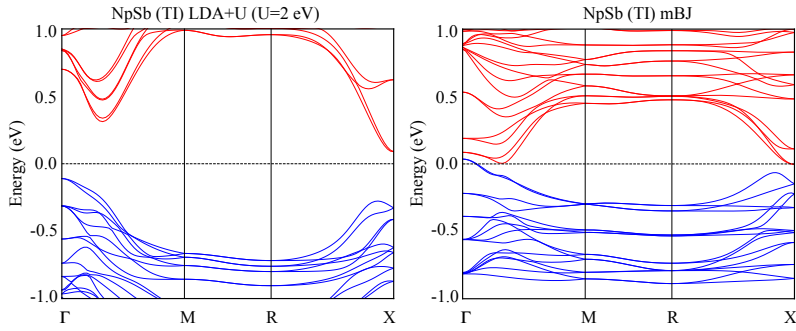


FIG. 29. Band structures of the TI NpSb obtained from LDA+U ( $U = 2\text{ eV}$ ) and mBJ methods.

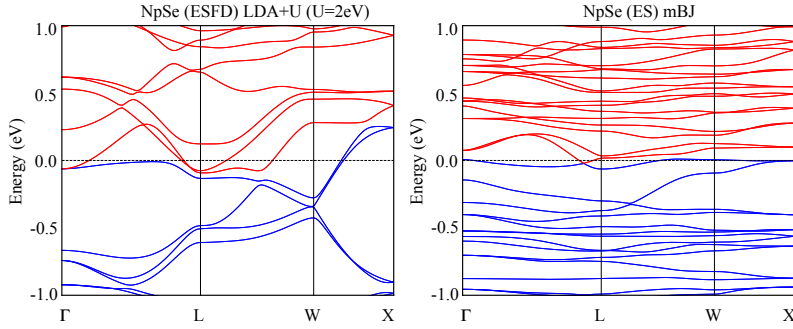


FIG. 30. Band structures of NpSe obtained from LDA+U ( $U = 2\text{eV}$ ) with ESFD phase and mBJ methods with ES phase. In LDA+U calculations, the irreps of the bands at  $\Gamma$  point on the Fermi level is 2-fold degenerate and half-filled. So, it's in ESFD phase. While, in mBJ calculations, the valence band that crossing the Fermi level is 1-dimentional. It's in the ES phase with a symmetry protected crossing point on the  $\Gamma L$  path.

#### Appendix F: Comparisons between LDA+U and LDA+Gutzwiller methods

To further check the robustness of the results obtained from LDA+U calculations, we have performed the LDA+Gutzwiller calculations [74] for the two stable magnetic topological semimetals, MnGeO<sub>3</sub> and CeCo<sub>2</sub>P<sub>2</sub>.

LDA+Gutzwiller is a many-body technics combined with DFT calculations, which has been successfully applied to predict correlated topological materials [95–97]. Similar to other post-LDA methods, i.e. LDA+U and LDA+DMFT, the total Hamiltonian adopt in LDA+Gutzwiller can be written as,

$$H_{total} = H_{LDA} + H_{int} + H_{dc} \quad (\text{F1})$$

with  $H_{LDA}$  being the non-interacting Hamiltonian obtained by LDA+SOC, the atomic spin orbital coupling and  $H_{int}$  being the interacting Hamiltonian. The last term in Eq. (F1) is the double counting Hamiltonian, which needs to be included to remove the local interaction energy treated by LDA already in the mean field manner. In the present study, the Kanamori-type interaction and the fully localized limit scheme for the double counting energy [98] are adopted.

In the LDA+Gutzwiller method, the Gutzwiller type wave function  $|\psi_G\rangle = \hat{P}|\psi_0\rangle$  has been proposed for the trial wave function to minimize the ground state energy, where  $|\psi_0\rangle$  is the non-interacting wave function and  $\hat{P}$  is the local projector applied to adjust the probability of the local atomic configuration (in the many-particle Fock space). In addition, the Gutzwiller approximation is applied to evaluate the ground state energy and an effective Hamiltonian  $H_{eff} \approx \hat{P}H_{LDA}\hat{P}$  describing the quasi-particle dispersion can be obtained. For detailed description for the method please refer to references [74, 99, 100].

In the LDA+Gutzwiller calculation, we adopt the same parameter U as LDA+U calculation. For MnGeO<sub>3</sub>, the quasi-particle weight of the *d* electron on Mn is about 0.8 and the local magnetic moment on Mn is about  $4.6 \mu_B/\text{Mn}$  which is consistent with LDA+U calculation ( $4.3 \mu_B/\text{Mn}$ ). Compared with the band structure obtained from LDA+U calculations in Figure 31(a), the quasi-particle band structure in LDA+Gutzwiller are renormalized by a factor of 0.86, as shown in Figure 31(b).

For CeCo<sub>2</sub>P<sub>2</sub>, the quasi-particle weight of the *f* electron on Ce is about 0.25 and the occupation of *f* electron is about 1.0/Ce. Compared with the band structure obtained from LDA+U calculations in Figure 31(c), the quasi-particle band structure in LDA+Gutzwiller are strongly renormalized by a factor of 0.25, as shown in Figure 31(d). Although the large-size renormalization on *f* orbitals changes the quasi-particle bands a lot, the symmetry enforced band crossing along  $Z A$  path is stable.

Both comparisons for MnGeO<sub>3</sub> and CeCo<sub>2</sub>P<sub>2</sub> indicate that strong correlations only renormalize the band width by a factor of quasi-particle weight but don't change the topologies for the stable topological materials MnGeO<sub>3</sub> and CeCo<sub>2</sub>P<sub>2</sub>.

#### Appendix G: Topological phase diagrams of the topological materials that predicted by MTQC

We tabulate the topological categories at different *U*'s for all the magnetic materials. In the Table VII and VIII, each material list is represented by different colors based on their phase transition trends with increasing *U*. The tables

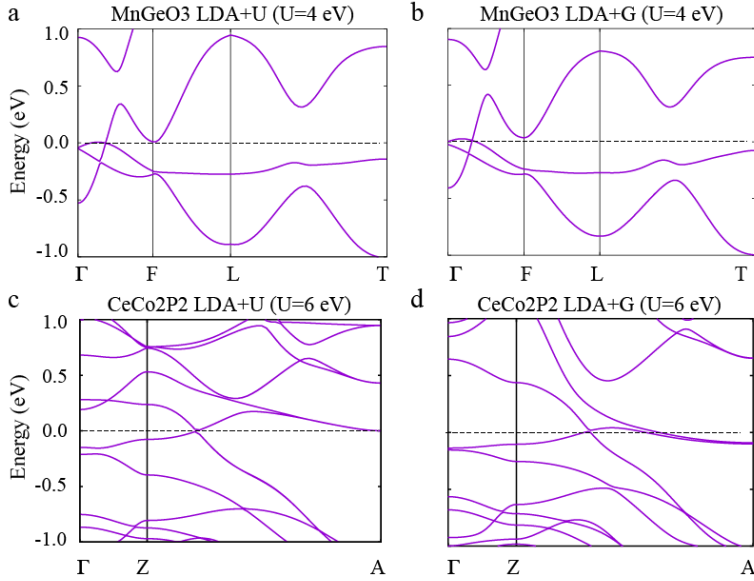


FIG. 31. (a) Electronic band structures of  $\text{MnGeO}_3$  obtained from LDA+U and (b) LDA+Gutzwiller (b) with the on-site Coulomb interaction  $U = 4\text{ eV}$  and the Hund's coupling  $J = 0.8\text{ eV}$ . From LDA+Gutzwiller calculations, the quasi-particle weight of the  $d$  electron on Mn is about 0.86 and the magnetic moments on Mn is about  $4.8 \mu_B$ (c)-(d) Electronic band structures of  $\text{CeCo}_2\text{P}_2$  obtained from LDA+U and LDA+Gutzwiller, respectively. The on-site interaction of  $f$  orbitals is taken as  $U = 6\text{ eV}$ . From LDA+Gutzwiller calculations, the quasi-particle weight of the  $f$  electron on Ce is about 0.25. The magnetic moments on Ce and Co are  $0.0$  and  $0.9 \mu_B$ , respectively.

contain the material identification number in BCSMD (BCSID), chemical formula (Formula), magnetic space group (MSG), the correlated atoms (CA) that exhibit added  $U$  in the *ab initio* calculations, topological phases with different  $U$  and the link to our plotted band structures (BS).

In Tables VII and VIII, the interaction parameter  $U$  is varied in the range of 0, 1, 2, 3, 4 eV for  $d$  electron and 0, 2, 4, 6 eV for  $f$  electron, respectively. Upon adding and increasing  $U$ , there are 49 of the 130 topological materials that have stable topology (remain the same topology for all  $U$ ), and 49 materials have nontrivial topology for weak correlation, while becoming topological trivial with strong correlations. There are 20 materials whose topologies are sensitive to the interaction and have topological phase transitions between TI and ES in a small interaction range. There are only 5 materials that belong to trivial class in the weak correlated case and become topological nontrivial when the correlation is strong enough. The trend of 'Topological  $\rightarrow$  Trivial' upon large  $U$  is clear in our data.

The green color stands for nontrivial topology stable in the whole range of  $U$  considered in the calculations. The blue color stands for topology nontrivial for weak correlation effect, but trivial with strong correlation. The yellow color stands for topology sensitive to correlations and for topological phase transitions between TI and ES in a small interaction range. The red color stands for topology trivial in weak correlations, but nontrivial with increasing  $U$ . The grey color stands for the cases where the self consistent calculations are not converged and the topological phase diagrams are not completed. We have separated the material list into two parts: one for  $d$  electron with Coulomb in the range of  $0 \sim 4\text{ eV}$ , another for  $f$  electron with Coulomb in the range of  $0 \sim 6\text{ eV}$ . The materials are ordered by the MSG. We also tag the ESs/ESFDs with chiral MSGs, in which the crossing points carry nonzero chiral charges.

We emphasize that if a symmetry-data-vector cannot be written as an integer combination of EBRs (LCEBR) and the compatibility relations are satisfied, it is diagnosed as a TI in Table VII and VIII. This TI can be stable TI/SISM with stable topological index. In H, we interpret all the TIs by their topological indices. We also find that some of the ES phases can be changed to TI/SISM phase by symmetry breaking. For example, the ES phase ( $U = 3, 4\text{ eV}$ ) of  $\text{Mn}_3\text{Sn}$  (with BCSID-0.200) can be calssified as SISM phase (with indice  $\eta_{4I} = 3$ ) if its MSG 63.464 ( $Cm/cm$ ) is subducted to the minimal subgroup MSG 2.4 ( $P\bar{1}$ ).

TABLE VII: Topological phase diagram of the magnetic materials that have transition elements.. The interaction parameter  $U$  of  $d$  electrons on the correlated atoms have been set to 0, 1, 2, 3 and 4 eV. For the material  $\text{EuFe}_2\text{As}_2$  (BCS-ID: 2.1), since the local magnetic moments on Eu are about  $7.0 \mu_B$ , which is fully spin-polarized, we take the  $U$  of  $f$  electron on Eu as 4 eV and the  $U$  of  $d$  electron on Fe as 0, 1, 2, 3, 4 eV.

BCS-ID	Formula	MSG	CA	$U=0$	$U=1$	$U=2$	$U=3$	$U=4$	BS
0.165	$\text{SrMn}(\text{VO}_4)(\text{OH})$	$4.7(P2_1)^*$	Mn,V	ES	LCEBR	LCEBR	LCEBR	LCEBR	Table [Li]

1.264	CoPS3	$11.57(P_C 2_1/m)$	Co	TI	LCEBR	LCEBR	LCEBR	LCEBR	Table [LXVI]
0.203	Mn3Ge	$12.62(C2'/m')$	Mn	TI	TI	TI	TI	TI	Table [LXX]
1.0.13	FeI2	$12.62(C2'/m')$	Fe	TI	LCEBR	LCEBR	LCEBR	LCEBR	Table [LXXI]
1.201	Cr2ReO6	$14.80(P_a 2_1/c)$	Cr	TI	LCEBR	LCEBR	TBD	TBD	Table [XCVII]
1.49	Ag2NiO2	$15.90(C_c 2/c)$	Ni	TI	LCEBR	LCEBR	LCEBR	LCEBR	Table [CXXXIV]
1.50	AgNiO2	$18.22(P_B 2_1 2_1 2)^*$	Ni	ES	ES	LCEBR	LCEBR	LCEBR	Table [CXXXIX]
1.263	Ca3Ru2O7	$33.154(P_C n a 2_1)$	Ru	ES	ES	LCEBR	LCEBR	LCEBR	Table [CLV]
0.85	KCo4(PO4)3	$58.398(P_{nn'} m')$	Co	ES	LCEBR	LCEBR	LCEBR	LCEBR	Table [CLXXIX]
0.140	LuFe4Ge2	$58.399(P_{n'n'm'})$	Fe	ESFD	ESFD	ESFD	ESFD	ESFD	Table [CLXXX]
0.27	YFe4Ge2	$58.399(P_{n'n'm'})$	Fe	ESFD	ESFD	ESFD	ESFD	ESFD	Table [CLXXXI]
1.252	CaCo2P2	$59.416(P_I mmn)$	Co	LCEBR	TI	TI	TI	TI	Table [CLXXXIV]
1.88	Mn5Si3	$60.431(P_C bcn)$	Mn	TI	ES	LCEBR	LCEBR	LCEBR	Table [CLXXXVII]
2.1	EuFe2As2	$61.439(P_C bca)$	Eu,Fe	LCEBR	ES	TI	TI	LCEBR	Table [CXCI]
0.218	Co2SiO4	$62.441(P_{nma})$	Co	ES	LCEBR	LCEBR	LCEBR	LCEBR	Table [CXCV]
0.219	Co2SiO4	$62.441(P_{nma})$	Co	ES	ES	LCEBR	LCEBR	LCEBR	Table [CXCVI]
0.221	Fe2SiO4	$62.441(P_{nma})$	Fe	ES	LCEBR	LCEBR	LCEBR	LCEBR	Table [CXCVII]
1.130	Cr2As	$62.450(P_a nma)$	Cr	LCEBR	TI	LCEBR	LCEBR	LCEBR	Table [CCXIII]
1.131	Fe2As	$62.450(P_a nma)$	Fe	TI	TI	ES	TI	TI	Table [CCXIV]
1.132	Mn2As	$62.450(P_a nma)$	Mn	ES	ES	ES	ES	ES	Table [CCXV]
1.28	CrN	$62.450(P_a nma)$	Cr	TI	TI	LCEBR	LCEBR	LCEBR	Table [CCXVI]
0.199	Mn3Sn	$63.463(Cmc'm')$	Mn	ES	ES	ES	ES	ES	Table [CCXIX]
0.200	Mn3Sn	$63.464(Cm'cm')$	Mn	TI	TI	TI	ES	ES	Table [CCXX]
1.16	BaFe2As2	$64.480(C_A mca)$	Fe	TI	TI	TI	TI	LCEBR	Table [CCXXIV]
1.52	CaFe2As2	$64.480(C_A mca)$	Fe	TI	TI	TI	LCEBR	LCEBR	Table [CCXXVI]
2.15	Mn3Ni20P6	$65.486(Cmm'm')$	Mn,Ni	TBD	ES	ES	TI	ES	Table [CCXXVII]
0.4	NiCr2O4	$70.530(Fd'd'd)$	Ni,Cr	ES	LCEBR	LCEBR	LCEBR	LCEBR	Table [CCXXX]
1.125	LaFeAsO	$73.553(I_c bca)$	Fe	TI	LCEBR	LCEBR	LCEBR	LCEBR	Table [CCXXXI]
1.176	YbCo2Si2	$73.553(I_c bca)$	Co	LCEBR	TI	TI	TI	TI	Table [CCXXXII]
2.5	Mn3CuN	$85.59(P4/n)$	Mn	ES	ES	ES	ES	ES	Table [CCXXXIV]

0.64	MnV2O4	88.81( $I4_1/a$ )	Mn,V	ES	LCEBR	LCEBR	LCEBR	LCEBR	Table [CCXXXVII]
1.85	alpha-Mn	114.282( $P_1\bar{4}2_1c$ )	Mn	ES	LCEBR	LCEBR	LCEBR	TBD	Table [CCXLII]
1.143	Mn3Pt	132.456( $P_c4_2/mcm$ )	Mn	ESFD	ESFD	ESFD	ESFD	ESFD	Table [CCXLV]
1.146	LaCrAsO	138.528( $P_c4_2/nbm$ )	Cr	TI	TI	TI	TI	TI	Table [CCXLIX]
0.212	Sr2Mn3As2O2	139.536( $I4'/m'm'm$ )	Mn	ESFD	ESFD	ESFD	ESFD	ESFD	Table [CCLI]
2.19	Mn3ZnC	139.537( $I4/mm'm'$ )	Mn	ES	ES	ES	ES	ES	Table [CCLIV]
0.125	MnGeO3	148.19( $R\bar{3}'$ )	Mn	ES	ES	ES	ES	ES	Table [CCLXI]
0.21	PbNiO3	161.69( $R3c$ )	Ni	ESFD	ESFD	ESFD	LCEBR	LCEBR	Table [CCLXVII]
1.0.5	Sr3CoIrO6	165.95( $P\bar{3}c'1$ )	Co	ES	LCEBR	LCEBR	LCEBR	LCEBR	Table [CCLXXIII]
0.108	Mn3Ir	166.101( $R\bar{3}m'$ )	Mn	ES	ES	ES	ES	ES	Table [CCLXXV]
0.109	Mn3Pt	166.101( $R\bar{3}m'$ )	Mn	ES	ES	ES	ES	ES	Table [CCLXXVI]
0.177	Mn3GaN	166.97( $R\bar{3}m$ )	Mn	ES	ES	ES	ES	ESFD	Table [CCLXXVII]
1.153	Mn3GaC	167.108( $R_I\bar{3}c$ )	Mn	ES	LCEBR	LCEBR	LCEBR	LCEBR	Table [CCLXXX]
0.117	LuFeO3	185.201( $P6_3c'm'$ )	Fe	TI	LCEBR	LCEBR	LCEBR	LCEBR	Table [CCLXXXV]
1.110	ScMn6Ge6	192.252( $P_c6/mcc$ )	Mn	ES	ES	ES	ES	ES	Table [CCLXXXVIII]
1.225	ScMn6Ge6	192.252( $P_c6/mcc$ )	Mn	ES	ES	ES	ES	ES	Table [CCLXXXIX]
0.118	Ba5Co5ClO13	194.268( $P6'_3/m'm'c$ )	Co	LCEBR	LCEBR	LCEBR	LCEBR	ES	Table [CCXCI]
0.150	NiS2	205.33( $Pa\bar{3}$ )	Ni	TI	LCEBR	LCEBR	LCEBR	LCEBR	Table [CCXCIII]
0.2	Cd2Os2O7	227.131( $Fd\bar{3}m'$ )	Os	ES	LCEBR	LCEBR	LCEBR	LCEBR	Table [CCXCV]

\* Chiral MSG. The crossing points in the ES/ESFD phase with Chiral MSG must carry nonzero chiral charges. [90, 91]

TABLE VIII: Topological phase diagram of the magnetic materials that have Rare-earth elements. The interaction parameter  $U$  of  $f$  electrons on Rare-earth elements have been set to 0, 2, 4 and 6 eV. If the material also have transition elements, we take  $U$  of  $d$  electron as 2 eV.

BCS-ID	Formula	MSG	CA	U=0	U=2	U=4	U=6	BS
1.206	Dy2Fe2Si2C	2.7( $P_S\bar{1}$ )	Dy,Fe	TI	TI	TI	TI	Table. [CCXCVII]
0.104	ErVO3	11.54( $P2'_1/m'$ )	Er,V	LCEBR	TI	LCEBR	LCEBR	Table. [CCCII]
0.106	DyVO3	11.54( $P2'_1/m'$ )	Dy,V	TI	LCEBR	LCEBR	LCEBR	Table. [CCCIII]
1.22	DyCu2Si2	12.63( $C_c2/m$ )	Dy,Cu	TBD	TBD	LCEBR	ES	Table. [CCCV]
1.140	PrMgPb	13.73( $P_A2/c$ )	Pr	TI	TI	TI	TI	Table. [CCCVII]
1.141	NdMgPb	13.73( $P_A2/c$ )	Nd	TI	TI	LCEBR	LCEBR	Table. [CCCVIII]
0.105	ErVO3	14.75( $P2_1/c$ )	Er,V	ES	LCEBR	LCEBR	LCEBR	Table. [CCCX]
0.174	Pr3Ru4Al12	15.89( $C2'/c'$ )	Pr,Ru	TI	TI	TI	TI	Table. [CCCXVI]
0.226	NdCo2	15.89( $C2'/c'$ )	Nd,Co	ES	TI	TI	TI	Table. [CCCXVII]
2.10	HoP	15.89( $C2'/c'$ )	Ho	TI	TI	TI	TI	Table. [CCCXVIII]

1.211	Dy2O2S	15.90( $C_c2/c$ )	Dy	TI	LCEBR	LCEBR	LCEBR	Table. [CCCXXI]
1.216	Nd2BaNiO5	15.90( $C_c2/c$ )	Nd,Ni	TI	LCEBR	LCEBR	LCEBR	Table. [CCCXXXIII]
1.217	Tb2BaNiO5	15.90( $C_c2/c$ )	Tb,Ni	TI	LCEBR	LCEBR	LCEBR	Table. [CCCXXIV]
1.43	PrNiO3	36.178( $C_amc2_1$ )	Pr,Ni	LCEBR	LCEBR	ES	LCEBR	Table. [CCCXXIX]
0.26	TmAgGe	38.191( $Am'm'2$ )	Tm	ES	TBD	TBD	TBD	Table. [CCCXXX]
2.12	TbMg	49.270( $P_c'm'$ )	Tb	ES	ES	ES	ES	Table. [CCCXXXI]
1.139	Ho2RhIn8	49.273( $P_ccm$ )	Ho	ES	TI	TI	ES	Table. [CCCXXXII]
2.11	TbMg	51.295( $Pmm'a'$ )	Tb	ES	ES	ES	ES	Table. [CCCXXXIII]
1.222	Er2CoGa8	51.298( $P_{amma}$ )	Er,Co	ES	ES	ES	ES	Table. [CCCXXXIV]
1.150	PrAg	53.334( $P_Bmna$ )	Pr	LCEBR	TBD	TI	TBD	Table. [CCCXXXV]
1.8	CeRu2Al10	57.391( $P_Cbcm$ )	Ce,Ru	TI	TI	TI	LCEBR	Table. [CCCXXXVIII]
0.187	CeMnAsO	59.407( $Pm'mn$ )	Ce,Mn	ES	LCEBR	LCEBR	LCEBR	Table. [CCCXXXIX]
0.185	Nd5Ge4	62.447( $Pnm'a'$ )	Nd	ES	ES	TBD	ES	Table. [CCCXLII]
1.179	NdCoAsO	62.450( $P_anma$ )	Nd,Co	ES	TI	ES	ES	Table. [CCCXLV]
0.149	Nd3Ru4Al12	63.462( $Cm'c'm$ )	Nd,Ru	ES	ES	ES	ES	Table. [CCCXLVII]
0.173	Pr3Ru4Al12	63.462( $Cm'c'm$ )	Pr,Ru	ES	ES	ES	ES	Table. [CCCXLVIII]
3.3	Ho2RhIn8	63.464( $Cm'cm'$ )	Ho	ES	ES	TBD	TBD	Table. [CCCXLIX]
1.200	U2Ni2Sn	63.466( $C_cmc_m$ )	U,Ni	LCEBR	TI	TI	TI	Table. [CCCL]
1.262	NpRhGa5	63.466( $C_cmc_m$ )	Np	LCEBR	TI	ES	LCEBR	Table. [CCCLI]
1.195	Er2Ni2In	63.467( $C_amcm$ )	Er,Ni	LCEBR	LCEBR	TI	LCEBR	Table. [CCCLII]
1.188	CeRh2Si2	64.480( $C_Amca$ )	Ce	TI	LCEBR	ES	TI	Table. [CCCLIV]
1.223	Tm2CoGa8	65.489( $C_ammm$ )	Tm,Co	TI	ES	ES	ES	Table. [CCCLVI]
1.142	CeMgPb	67.510( $C_{amma}$ )	Ce	LCEBR	TI	TBD	TBD	Table. [CCCLVIII]
1.0.12	UAu2Si2	71.536( $Im'm'm$ )	U	ES	ES	ES	ES	Table. [CCCLX]
2.28	NpNiGa5	74.559( $Imm'a'$ )	Np,Ni	ES	ES	ES	ES	Table. [CCCLXI]
0.184	Nd5Si4	92.114( $P4_12'_12'$ )*	Nd	ES	ES	ES	ES	Table. [CCCLXIV]
1.0.11	CeCoGe3	107.231( $I4m'm'$ )	Ce,Co	LCEBR	ES	ES	TBD	Table. [CCCLXV]
2.26	PrCo2P2	123.345( $P4/mm'm'$ )	Pr,Co	ES	ES	ES	ES	Table. [CCCLXVI]
1.162	NdMg	124.360( $P_c4/mcc$ )	Nd	ES	ES	ES	ES	Table. [CCCLXVII]
1.251	NdCo2P2	124.360( $P_c4/mcc$ )	Nd,Co	ES	ES	ES	TI	Table. [CCCLXVIII]
1.255	UPtGa5	124.360( $P_c4/mcc$ )	U	TI	ES	ES	ES	Table. [CCCLXIX]
1.261	NpRhGa5	124.360( $P_c4/mcc$ )	Np	ES	ES	ES	ES	Table. [CCCLXX]
2.14	NdMg	125.373( $P_c4/nbm$ )	Nd	ES	ES	ES	ES	Table. [CCCLXXII]
1.253	CeCo2P2	126.386( $P_I4/nnc$ )	Ce,Co	ES	ES	ES	ES	Table. [CCCLXXIII]
0.80	U2Pd2In	127.394( $P4'/m/bm'$ )	U	ESFD	ESFD	ESFD	ESFD	Table. [CCCLXXIV]
0.81	U2Pd2Sn	127.394( $P4'/m/bm'$ )	U	TI	TI	TI	TI	Table. [CCCLXXV]
1.81	GdIn3	127.397( $P_C4/mbm$ )	Gd	ES	ES	ES	ES	Table. [CCCLXXVII]
1.102	U2Ni2In	128.408( $P_c4/mnc$ )	U,Ni	ES	ES	ES	ES	Table. [CCCLXXVIII]
1.160	UP	128.410( $P_I4/mnc$ )	U	ES	ES	ES	ES	Table. [CCCLXXIX]
1.187	TbRh2Si2	128.410( $P_I4/mnc$ )	Tb	ES	ES	ES	ES	Table. [CCCLXXX]
1.208	UAs	128.410( $P_I4/mnc$ )	U	ES	ES	ES	TI	Table. [CCCLXXXI]
1.21	DyCo2Si2	128.410( $P_I4/mnc$ )	Dy,Co	ES	ES	ES	ES	Table. [CCCLXXXII]
0.186	CeMnAsO	129.416( $P4'/n'm'm$ )	Ce,Mn	LCEBR	TI	TI	TI	Table. [CCCLXXXIII]
1.215	UP2	130.432( $P_c4/ncc$ )	U	ES	ES	ES	ES	Table. [CCCLXXXV]
2.13	UP	134.481( $P_C4_2/nnm$ )	U	TI	TI	TI	TI	Table. [CCCLXXXVII]
2.20	UAs	134.481( $P_C4_2/nnm$ )	U	TI	ES	TI	TI	Table. [CCCLXXXVIII]
2.6	Nd2CuO4	134.481( $P_C4_2/nnm$ )	Nd	TI	LCEBR	LCEBR	LCEBR	Table. [CCCLXXXIX]
1.103	U2Rh2Sn	135.492( $P_c4_2/mbc$ )	U	ES	ES	ES	ES	Table. [CCCXC]
1.207	U2Rh2Sn	135.492( $P_c4_2/mbc$ )	U	ES	ES	ES	ES	Table. [CCCXCII]
1.254	UNiGa5	140.550( $I_c4/mcm$ )	U,Ni	ES	TI	TI	LCEBR	Table. [CCCXCII]
1.82	Nd2RhIn8	140.550( $I_c4/mcm$ )	Nd	LCEBR	ES	ES	ES	Table. [CCCXCIII]

1.87	TbCo2Ga8	140.550( $I_c4/mcm$ )	Tb,Co	ES	ES	ES	ES	Table. [CCCXCIV]
0.126	NpCo2	141.556( $I4'_1/a'm'd'$ )	Np,Co	ES	TBD	TI	TI	Table. [CCCXCVIII]
0.151	Tm2Mn2O7	141.557( $I4_1/am'd'$ )	Tm,Mn	ES	LCEBR	LCEBR	LCEBR	Table. [CD]
0.227	NdCo2	141.557( $I4_1/am'd'$ )	Nd,Co	ES	ES	ES	ES	Table. [CDII]
0.48	Tb2Sn2O7	141.557( $I4_1/am'd'$ )	Tb	ES	LCEBR	LCEBR	LCEBR	Table. [CDIII]
0.49	Ho2Ru2O7	141.557( $I4_1/am'd'$ )	Ho,Ru	ES	LCEBR	LCEBR	ES	Table. [CDIV]
0.51	Ho2Ru2O7	141.557( $I4_1/am'd'$ )	Ho,Ru	TI	LCEBR	LCEBR	LCEBR	Table. [CDV]
1.161	PrFe3(BO3)4	155.48( $R_{I32}$ )*	Pr,Fe	LCEBR	TBD	ES	LCEBR	Table. [CDVI]
0.169	U3As4	161.71( $R_{3c'}$ )	U	ES	ES	LCEBR	LCEBR	Table. [CDVII]
0.170	U3P4	161.71( $R_{3c'}$ )	U	ES	ES	LCEBR	LCEBR	Table. [CDVIII]
0.228	TbCo2	166.101( $R\bar{3}m'$ )	Tb,Co	TI	ES	TI	TI	Table. [CDX]
0.77	Tb2Ti2O7	166.101( $R\bar{3}m'$ )	Tb,Ti	ES	LCEBR	LCEBR	LCEBR	Table. [CDXI]
3.8	NdZn	222.103( $P_{1n}\bar{3}n$ )	Nd	ESFD	ES	ES	ESFD	Table. [CDXV]
3.12	NpSb	224.113( $Pn\bar{3}m'$ )	Np	TI	TI	TI	TI	Table. [CDXVI]
3.2	UO2	224.113( $Pn\bar{3}m'$ )	U	ES	LCEBR	LCEBR	LCEBR	Table. [CDXVII]
3.7	NpBi	224.113( $Pn\bar{3}m'$ )	Np	TI	TI	TI	TI	Table. [CDXVIII]
3.10	NpSe	228.139( $F_{sd}\bar{3}c$ )	Np	TI	ESFD	ESFD	ESFD	Table. [CDXIX]
3.11	NpTe	228.139( $F_{sd}\bar{3}c$ )	Np	TI	ESFD	ESFD	ESFD	Table. [CDXX]
3.9	NpS	228.139( $F_{sd}\bar{3}c$ )	Np	ES	ESFD	ESFD	ESFD	Table. [CDXXI]
3.6	DyCu	229.143( $Im\bar{3}m'$ )	Dy	TBD	ES	ES	ES	Table. [CDXXII]

\* Chiral MSG. The crossing points in the ES/ESFD phase with Chiral MSG must carry nonzero chiral charges. [90, 91]

Some of the topological compounds in Table VIII contain both  $3d$  element and  $4f/5f$  element, where we set the U value of  $d$  electron as 2eV. For comparisons, we have also considered the empirical U values for the  $3d$  electron and identified the topological phase diagram using MTQC theory. In the Table IX, we chose 15 materials, each of which contains the  $3d$  element V, Co, Ni/Mn. The empirical U values of V, Co, Ni and Mn are set as 3.25, 3.7, 6.2 and 3.9eV, respectively[? ]. As tabulated in Table IX, the results indicate that interaction of  $3d$  electron almost doesn't change the topological phase diagram for the compounds containing  $4f/5f$  element.

TABLE IX: Comparisons of the topological phase diagrams for some of the topological compounds containing both  $3d$  element and  $4f/5f$  element. For each material, the U value of  $3d$  element ( $U_{3d}$ ) is set as 2eV and an empirical value. The U value of  $4f/5f$  element ( $U_f$ ) is set as 2, 4 and 6eV. The cases that have different topologies when  $U_{3d}$  is taken 2eV and an empirical value are marked by red color.

BCSID	Formula	MSG	CA	$U_{3d}(eV)$	$U_f = 2eV$	$U_f = 4eV$	$U_f = 6eV$
2.26	PrCo2P2	123.345( $P4/mm'm'$ )	Pr,Co	2	ES	ES	ES
				3.7	ES	ES	ES
1.251	NdCo2P2	124.360( $P_c4/mcc$ )	Nd,Co	2	ES	ES	TI
				3.7	ES	ES	ES
1.253	CeCo2P2	126.386( $P_I4/nnc$ )	Ce,Co	2	ES	ES	ES
				3.7	ES	ES	ES
1.102	U2Ni2In	128.408( $P_c4/mnc$ )	U,Ni	2	ES	ES	ES
				6.2	ES	ES	ES
1.21	DyCo2Si2	128.410( $P_I4/mnc$ )	Dy,Co	2	ES	ES	ES
				3.7	ES	ES	ES
0.105	ErVO3	14.75( $P_{21}/c$ )	Er,V	2	LCEBR	LCEBR	LCEBR
				3.25	LCEBR	LCEBR	LCEBR
1.254	UNiGa5	140.550( $I_c4/mcm$ )	U,Ni	2	TI	TI	LCEBR
				6.2	TI	TI	TI
0.151	Tm2Mn2O7	141.557( $I4_1/am'd'$ )	Tm,Mn	2	LCEBR	LCEBR	LCEBR
				3.9	LCEBR	LCEBR	LCEBR
0.227	NdCo2	141.557( $I4_1/am'd'$ )	Nd,Co	2	ES	ES	ES
				3.7	ES	ES	ES
1.222	Er2CoGa8	51.298( $P_amma$ )	Er,Co	2	ES	ES	ES

				3.7	ES	ES	ES
0.187	CeMnAsO	59.407( $Pm'mn$ )	Ce,Mn	2	LCEBR	LCEBR	LCEBR
				3.9	LCEBR	LCEBR	LCEBR
1.200	U2Ni2Sn	63.466( $C_c mcm$ )	U,Ni	2	TI	TI	TI
				6.2	LCEBR	TI	TI
1.195	Er2Ni2In	63.467( $C_a mcm$ )	Er,Ni	2	LCEBR	TI	LCEBR
				6.2	LCEBR	LCEBR	LCEBR
1.223	Tm2CoGa8	65.489( $C_a mmm$ )	Tm,Co	2	ES	ES	ES
				3.7	ES	ES	ES
2.28	NpNiGa5	74.559( $Imm'a'$ )	Np,Ni	2	ES	ES	ES
				6.2	ES	ES	ES

## Appendix H: Physical interpretations for the TI classified by MTQC

In MTQC theory [7], in order to have a physical interpretation for the SI, we reduce the SI of MSG to one of its subgroup, and then interpret the SI of the subgroup using the layer construction approach [26]. In this work, all the involved SI are subduced onto MSG 2.4 ( $P\bar{1}$ ), MSG 47.24 ( $Pmmm$ ), MSG 81.33 ( $P4$ ), MSG 83.43 ( $P4/m$ ),/MSG 143.1 ( $P3$ ). In the following, we provide the definitions of SI of these groups.

### 1. Definitions for the stable indices of MSG 2.4

**MSG 2.4 ( $P\bar{1}$ )** has the SI group  $\mathbb{Z}_4 \times \mathbb{Z}_2^3$ . The four SI  $(\eta_{4I}, z_{2I,1}, z_{2I,2}, z_{2I,3})$  are defined as

$$\eta_{4I} = \sum_K n_K^- = \sum_K \frac{1}{2}(n_K^- - n_K^+) \mod 4, \quad (H1)$$

$$z_{2I,i=1,2,3} = C_{k_i=\pi} \mod 2 = \sum_{K, K_i=\pi} n_K^- \mod 2, \quad (H2)$$

where  $K$  sums over the eight inversion-invariant momenta, and  $n_K^\pm$  means the number of occupied even/odd states at the momentum  $K$ .  $z_{2I,i}$  is the parity of Chern number in the plane  $k_i = \pi$ .  $\eta_{4I} \mod 2$  is the parity of the Chern number difference between  $k_z = 0$  and  $k_z = \pi$  planes. Thus  $\eta_{4I} = 1, 3$  correspond to Weyl semimetal (WSM) phase. For  $\eta_{4I} = 2$  corresponds to an axion insulator phase/3D QAH, which can not be distinguished from SI but from Wilson loop [?]/surface state calculations.

**Layer constructions** Now make use of the layer constructions of the gapped states to build a mapping from the SI to topological invariants. Here we first give the SI of several layer constructions.

1. A Chern layer with  $C = \pm 1$  at  $x = 0$  gives the SI (2100).
2. A Chern layer with  $C = \pm 1$  at  $x = \frac{1}{2}$  gives the SI (0100).
3. A Chern layer with  $C = \pm 1$  at  $y = 0$  gives the SI (2010).
4. A Chern layer with  $C = \pm 1$  at  $y = \frac{1}{2}$  gives the SI (0010).
5. A Chern layer with  $C = \pm 1$  at  $z = 0$  gives the SI (2001).
6. A Chern layer with  $C = \pm 1$  at  $z = \frac{1}{2}$  gives the SI (0001).

We take the Chern layers with  $C = 1$  at  $z = 0$  and  $\frac{1}{2}$  as two examples to show how to calculate the SI of layer-constructed states. Since the SI indicate stable topological invariants (rather than fragile topological invariants), states having the same stable topological invariants must have the same SI. For layer-constructed states, the stable topological invariants are completely determined by the positions and directions of the layers [26] and the Chern numbers of layers. Other details about the layer constructions are irrelevant to determine the SI. We first consider a single layer with  $C = 1$  at  $z = 0$ . The  $z = 0$  plane is inversion-invariant, and there are four momenta in the 2D Brillouin zone, *i.e.*,  $(k_x, k_y) = (0, 0), (0, \pi), (\pi, 0), (\pi, \pi)$ . The Bloch states at these four momenta are either even/odd under the inversion. According to the Fu-Kane formula

$$(-1)^C = \prod_K \prod_{n \in \text{occ}} \lambda'_n(K), \quad (H3)$$

where  $K$  goes over the four inversion-invariant momenta and  $\lambda'_{K,n}$  is the parity of the  $n$ th occupied band at  $K$ , in a  $C = 1$  state, the total parity of the Bloch states at the four momenta must be odd. Here we assume the Chern layer has a single occupied band and the parities at  $(0, 0), (0, \pi), (\pi, 0), (\pi, \pi)$  are  $-+, +, +, +$ , respectively. Then we copy the layer to all the integer  $z$  positions, *i.e.*,  $z = 0, \pm 1, \pm 2, \dots$ , to construct the 3D state. Supposing the 2D Bloch state of a single layer at  $z$  is  $|\psi_{k_x, k_y, z}\rangle$ , then the 3D state Bloch state is given by

$$|\psi_{\mathbf{k}}\rangle = \frac{1}{\sqrt{N_z}} \sum_{z=0, \pm 1, \dots} e^{izk_z} |\psi_{k_x, k_y, z}\rangle, \quad (H4)$$

where  $N_z$  is the period in the  $z$ -direction. Let us calculate the inversion eigenvalues of the 3D state. For  $(k_x, k_y) = (0, 0), (0, \pi), (\pi, 0), (\pi, \pi)$ , under the inversion operator  $\hat{P}$ , the 2D state at  $z$  first gains a factor  $\lambda'(k_x, k_y)$  and then transforms to  $-z$ . Thus we obtain

$$\hat{P}|\psi_{\mathbf{k}}\rangle = \lambda'(k_x, k_y) \frac{1}{\sqrt{N_z}} \sum_{z=0, \pm 1, \dots} e^{-izk_z} |\psi_{k_x, k_y, z}\rangle. \quad (\text{H5})$$

For  $k_z = 0, \pi$ , we further obtain

$$\hat{P}|\psi_{\mathbf{k}}\rangle = \lambda'(k_x, k_y) \frac{1}{\sqrt{N_z}} \sum_{z=0, \pm 1, \dots} e^{izk_z} |\psi_{k_x, k_y, z}\rangle = \lambda'(k_x, k_y) |\psi_{\mathbf{k}}\rangle. \quad (\text{H6})$$

Thus the parities of the 3D state are given by  $\lambda(k_x, k_y, k_z) = \lambda'(k_x, k_y)$ . We obtain the parities of the 3D state at  $(k_x, k_y, k_z) = (0, 0, 0), (\pi, 0, 0), (0, \pi, 0), (\pi, \pi, 0), (0, 0, \pi), (\pi, 0, \pi), (0, \pi, \pi), (\pi, \pi, \pi)$  as  $-+, +, +, +, -, +, +, +$ , respectively. Substituting the parities into Eqs. (H1) and (H2), we obtain the SI as (2001).

Then we consider the same 2D layers locating at half-integer positions, *i.e.*,  $z = \pm \frac{1}{2}, \pm \frac{3}{2}, \dots$ . The 3D Bloch state can be written as

$$|\psi_{\mathbf{k}}\rangle = \frac{1}{\sqrt{N_z}} \sum_{z=\pm \frac{1}{2}, \pm \frac{3}{2}, \dots} e^{izk_z} |\psi_{k_x, k_y, z}\rangle. \quad (\text{H7})$$

For  $(k_x, k_y) = (0, 0), (0, \pi), (\pi, 0), (\pi, \pi)$ , we have the inversion action as

$$\hat{P}|\psi_{\mathbf{k}}\rangle = \lambda'(k_x, k_y) \frac{1}{\sqrt{N_z}} \sum_{z=\pm \frac{1}{2}, \pm \frac{3}{2}, \dots} e^{-izk_z} |\psi_{k_x, k_y, z}\rangle. \quad (\text{H8})$$

For  $k_z = 0, \pi$ , we have  $e^{-izk_z} = e^{-2izk_z} \times e^{izk_z} = e^{ik_z} \times e^{izk_z}$  and hence

$$\hat{P}|\psi_{\mathbf{k}}\rangle = \lambda'(k_x, k_y) e^{ik_z} \frac{1}{\sqrt{N_z}} \sum_{z=\pm \frac{1}{2}, \pm \frac{3}{2}, \dots} e^{izk_z} |\psi_{k_x, k_y, z}\rangle = \lambda'(k_x, k_y) e^{ik_z} |\psi_{\mathbf{k}}\rangle. \quad (\text{H9})$$

Thus the parities of the 3D state are given by  $\lambda(k_x, k_y, k_z) = \lambda'(k_x, k_y) e^{ik_z}$ . We obtain the parities of the 3D state at  $(k_x, k_y, k_z) = (0, 0, 0), (\pi, 0, 0), (0, \pi, 0), (\pi, \pi, 0), (0, 0, \pi), (\pi, 0, \pi), (0, \pi, \pi), (\pi, \pi, \pi)$  as  $-+, +, +, +, +, -, -, -$ , respectively. Substituting the parities into Eqs. (H1) and (H2), we obtain the SI as (0001).

The SI of other layer constructions can be similarly calculated.

**The inversion  $\mathbb{Z}_2$  invariant and axion insulator** We find that  $\eta_{4I} = 2$  iff the origin point (000) is occupied by odd Chern layers. Hence, for gapped state, we define the inversion- $\mathbb{Z}_2$  invariant as

$$\eta'_{2I} = \frac{1}{2} \eta_{4I} \mod 2. \quad (\text{H10})$$

When the total Chern number is zero, the axion  $\theta$ -angle is given by  $\theta = \eta_{2I} \pi$ . For example, the state consists of  $C = 1$  layer at the  $z = 0$  plane and  $C = -1$  Chern layer at the  $z = \frac{1}{2}$  plane, which has the SI (2000), has zero total Chern number and  $\eta'_{2I} = 1$ . This state is axion insulator. One can see this from the boundary state: for a finite centrosymmetric sample centered at the origin, the Chern layer at  $z = 0$  contributes to a chiral hinge mode, whereas the chiral modes from all the other layers cancel each pairwise. On the other hand, the state consists of  $C = 1$  Chern layers at both the  $z = 0, \frac{1}{2}$  planes, which also has the SI (2000), has total Chern number 2 and also  $\eta'_{2I} = 1$ . This state is a 3D QAH, for which the  $\theta$ -angle is ill-defined. ( $\theta$  can still be constructed if the Chern numbers are non-zero, but will be origin-dependent [101] and loses the physical meaning of magnetoelectric response.)

In the rest, we will directly give the SI and the corresponding interpretations. Readers might refer to [7] for more details.

## 2. Definitions for the stable indices of MSG 47.249

**MSG 47.249** (*Pmmm*) has the SI group  $\mathbb{Z}_4 \times \mathbb{Z}_2^3$ . Because of the anti-commuting mirror symmetries, all states at the inversion-invariant momenta are doubly degenerate. The SI can be chosen as same as the MSG 47.250 *Pmmm1'* [26] because for this group TRS does not change the irreps. The  $\mathbb{Z}_4$  factor is

$$z_4 = \sum_K \frac{1}{4} (n_K^- - n_K^+) \mod 4, \quad (\text{H11})$$

where  $K$  sums over all inversion-invariant momenta and  $n_K^\pm$  is the number of occupied even/odd states at  $K$ .  $z_4$  can be thought as Eq. (H1) except that  $n_K^-$  are replaced by the number of odd doublets. Odd  $z_4$  corresponds to axion insulator and  $z_4 = 2$  corresponds to a higher-order TI (HOTI) jointly protected by mirrors and  $C_2$  rotations [7]. The three  $\mathbb{Z}_2$  factors are the mirror Chern number parities in the  $k_{1,2,3} = \pi$  planes

$$z_{2w, i=1,2,3} = C_{m, k_i=\pi} \mod 2 = \sum_{K, K_i=\pi} \frac{1}{2} n_K^- \mod 2. \quad (\text{H12})$$

Because of the anti-commuting mirror symmetries, net Chern numbers in all the directions vanishes.

## 3. Definitions for the stable indices of MSG 81.33

**MSG 81.33** (*P̄4*) has the SI group  $\mathbb{Z}_4 \times \mathbb{Z}_2^2$ . We choose the  $\mathbb{Z}_4$  factor as the Chern number in the  $k_z = \pi$  plane mod 4

$$z_{4S} = C_\pi \mod 4 = 2N_{\text{occ}} - \frac{1}{2} n_Z^{\frac{1}{2}} + \frac{1}{2} n_Z^{-\frac{1}{2}} - \frac{3}{2} n_Z^{\frac{3}{2}} + \frac{3}{2} n_Z^{-\frac{3}{2}} - \frac{1}{2} n_A^{\frac{1}{2}} + \frac{1}{2} n_A^{-\frac{1}{2}} - \frac{3}{2} n_A^{\frac{3}{2}} + \frac{3}{2} n_A^{-\frac{3}{2}} - n_R^{\frac{1}{2}} + n_R^{-\frac{1}{2}} \mod 4, \quad (\text{H13})$$

where  $n_{Z,A}^{\frac{1}{2}, -\frac{1}{2}, \frac{3}{2}, -\frac{3}{2}}$  are the numbers of occupied states with  $S_4$  eigenvalues  $e^{-i\frac{\pi}{4}}, e^{i\frac{\pi}{4}}, e^{-i\frac{3\pi}{4}}, e^{i\frac{3\pi}{4}}$ , and  $n_R^{\frac{1}{2}, -\frac{1}{2}}$  are the numbers of occupied states with  $C_2$  eigenvalues  $e^{-i\frac{\pi}{4}}, e^{i\frac{\pi}{4}}$ . We choose the first  $\mathbb{Z}_2$  factor as the difference of Chern numbers in the  $k_z = \pi$  plane and the  $k_z = 0$  plane over 2 mod 2

$$\delta_{2S} = -n_Z^{\frac{3}{2}} + n_Z^{-\frac{3}{2}} - n_A^{\frac{3}{2}} + n_A^{-\frac{3}{2}} + n_{\Gamma}^{\frac{3}{2}} - n_{\Gamma}^{-\frac{3}{2}} + n_M^{\frac{3}{2}} - n_M^{-\frac{3}{2}} \pmod{2}. \quad (\text{H14})$$

The  $\delta_{2S} = 1$  phase is a WSM with 2 Weyl points between  $k_z = 0$  and  $k_z = \pi$ . One may be curious why  $C_{\pi} - C_0$  is an even number. The answer is that it is enforced by the compatibility relations: the  $k_z = 0$  and  $k_z = \pi$  planes must have the same  $C_2$  eigenvalues and hence the same parity of Chern numbers. The second  $\mathbb{Z}_2$  factor is

$$z_2 = \sum_{K=\Gamma, M, Z, A} \frac{n_K^{\frac{1}{2}} - n_K^{-\frac{3}{2}}}{2} \pmod{2}. \quad (\text{H15})$$

For  $z_{4S} = 0$  and  $\delta_{2S} = 0$ ,  $z_2$  corresponds to axion insulator/3D QAH state [7].

#### 4. Definitions for the stable indices of MSG 83.43

**MSG 83.43** ( $P4/m$ ) has the SI group  $\mathbb{Z}_4^3$ . We choose the three SI as

$$\begin{aligned} \delta_{4m} = C_{\pi}^+ - C_0^- \pmod{4} &= \sum_{K=Z, A} \left( -\frac{1}{2} n_K^{\frac{1}{2}, +i} + \frac{1}{2} n_K^{-\frac{1}{2}, +i} - \frac{3}{2} n_K^{\frac{3}{2}, +i} + \frac{3}{2} n_K^{-\frac{3}{2}, +i} \right) - n_R^{\frac{1}{2}, +i} + n_R^{-\frac{1}{2}, +i} \\ &\quad - \sum_{K=\Gamma, M} \left( -\frac{1}{2} n_K^{\frac{1}{2}, -i} + \frac{1}{2} n_K^{-\frac{1}{2}, -i} - \frac{3}{2} n_K^{\frac{3}{2}, -i} + \frac{3}{2} n_K^{-\frac{3}{2}, -i} \right) + n_X^{\frac{1}{2}, -i} + n_X^{-\frac{1}{2}, -i} \pmod{4}, \end{aligned} \quad (\text{H16})$$

$$z_{4m, \pi}^+ = C_{\pi}^+ \pmod{4} = N_{occ} + \sum_{K=Z, A} \left( -\frac{1}{2} n_K^{\frac{1}{2}, +i} + \frac{1}{2} n_K^{-\frac{1}{2}, +i} - \frac{3}{2} n_K^{\frac{3}{2}, +i} + \frac{3}{2} n_K^{-\frac{3}{2}, +i} \right) - n_R^{\frac{1}{2}, +i} + n_R^{-\frac{1}{2}, +i} \pmod{4}, \quad (\text{H17})$$

$$z_{4m, \pi}^- = C_{\pi}^- \pmod{4} = N_{occ} + \sum_{K=Z, A} \left( -\frac{1}{2} n_K^{\frac{1}{2}, -i} + \frac{1}{2} n_K^{-\frac{1}{2}, -i} - \frac{3}{2} n_K^{\frac{3}{2}, -i} + \frac{3}{2} n_K^{-\frac{3}{2}, -i} \right) - n_R^{\frac{1}{2}, -i} + n_R^{-\frac{1}{2}, -i} \pmod{4}. \quad (\text{H18})$$

Here  $C_{0, \pi}^{\pm i}$  represents Chern number in the  $\pm i$  mirror sector in the  $k_z = 0, \pi$  plane.

#### 5. Definitions for the stable indices of MSG 143.1

**MSG 143.1** ( $P3$ ) has the SI group  $\mathbb{Z}_3$ . According to the Chern number formula, the Chern number  $C$  is related to the  $C_3$  eigenvalues

$$e^{i\frac{2\pi}{3}C} = (-1)^{N_{occ}} \prod_{n \in occ} \theta_n(\Gamma) \theta_n(K) \theta_n(KA), \quad (\text{H19})$$

where  $\theta_n(\Gamma, K, K')$  is the  $C_3$  eigenvalue of the  $n$ th occupied state at the corresponding momentum. (One should not confuse the  $C_3$  eigenvalues  $\theta_n$  with the axion theta angle  $\theta$ ). We define the SI as,

$$z_{3R} = \sum_{K=A, H, HA} \left( n_K^{-\frac{1}{2}} - n_K^{\frac{3}{2}} \right) \pmod{3}. \quad (\text{H20})$$

#### 6. Stable indices of the magnetic TIs

Using the SI defined above, we have explained the physical meaning for all of the TIs obtained from MTQC. We tabulate all of the TIs diagnosed by MTQC in Table X. For each material, we list the identification number in BCSMD (BCSID), chemical formula (Formula), Coulomb interaction strength in LDA+U calculations (U), magnetic space group (MSG), SI of the MSG calculated by the machinery of MTQC (Indices(MTQC)), whose physical meaning is unclear, the SI and the corresponding subgroup (Min-sMSG), and the physical interpretation of the Indices (Interpretations).

TABLE X: Topological indices and the physical interpretations of the TIs predicted by MTQC.

BCSID	Formula	U(eV)	MSG	Indices(MTQC)	Min-sMSG	Indices	Interpretations
1.206	Dy2Fe2Si2C	0	2.7 ( $P_S \bar{I}$ )	$c2 = 1$	2.4 ( $P\bar{I}$ )	$z_{2I,1} = 0, z_{2I,2} = 0, z_{2I,3} = 0, \eta_{4I} = 2$	AXI/3D QAH
1.206	Dy2Fe2Si2C	2	2.7 ( $P_S \bar{I}$ )	$c2 = 1$	2.4 ( $P\bar{I}$ )	$z_{2I,1} = 0, z_{2I,2} = 0, z_{2I,3} = 0, \eta_{4I} = 2$	AXI/3D QAH

1.206	Dy2Fe2Si2C	4	2.7 ( $P_S\bar{1}$ )	$c2 = 1$	2.4 ( $P\bar{1}$ )	$z_{2I,1} = 0,$ $z_{2I,2} = 0,$ $z_{2I,3} = 0,$ $\eta_{4I} = 2$	AXI/3D QAH
1.206	Dy2Fe2Si2C	6	2.7 ( $P_S\bar{1}$ )	$c2 = 1$	2.4 ( $P\bar{1}$ )	$z_{2I,1} = 0,$ $z_{2I,2} = 0,$ $z_{2I,3} = 0,$ $\eta_{4I} = 2$	AXI/3D QAH
0.104	ErVO <sub>3</sub>	2	11.54 ( $P2'_1/m'$ )	$c2_1 = 0, c2_2 = 0,$ $c4 = 2$	2.4 ( $P\bar{1}$ )	$z_{2I,1} = 0,$ $z_{2I,2} = 0,$ $z_{2I,3} = 0,$ $\eta_{4I} = 2$	AXI/3D QAH
0.106	DyVO <sub>3</sub>	0	11.54 ( $P2'_1/m'$ )	$c2_1 = 1, c2_2 = 1,$ $c4 = 1$	2.4 ( $P\bar{1}$ )	$z_{2I,1} = 1,$ $z_{2I,2} = 0,$ $z_{2I,3} = 1,$ $\eta_{4I} = 1$	SISM
1.264	CoPS <sub>3</sub>	0	11.57 ( $P_C2_1/m$ )	$c2 = 1$	2.4 ( $P\bar{1}$ )	$z_{2I,1} = 0,$ $z_{2I,2} = 0,$ $z_{2I,3} = 0,$ $\eta_{4I} = 2$	AXI/3D QAH
0.203	Mn <sub>3</sub> Ge	0	12.62 ( $C2'/m'$ )	$c2_1 = 0, c2_2 = 0,$ $c4 = 2$	2.4 ( $P\bar{1}$ )	$z_{2I,1} = 0,$ $z_{2I,2} = 0,$ $z_{2I,3} = 0,$ $\eta_{4I} = 2$	AXI/3D QAH
0.203	Mn <sub>3</sub> Ge	1	12.62 ( $C2'/m'$ )	$c2_1 = 0, c2_2 = 0,$ $c4 = 2$	2.4 ( $P\bar{1}$ )	$z_{2I,1} = 0,$ $z_{2I,2} = 0,$ $z_{2I,3} = 0,$ $\eta_{4I} = 2$	AXI/3D QAH
0.203	Mn <sub>3</sub> Ge	2	12.62 ( $C2'/m'$ )	$c2_1 = 0, c2_2 = 0,$ $c4 = 2$	2.4 ( $P\bar{1}$ )	$z_{2I,1} = 0,$ $z_{2I,2} = 0,$ $z_{2I,3} = 0,$ $\eta_{4I} = 2$	AXI/3D QAH
0.203	Mn <sub>3</sub> Ge	3	12.62 ( $C2'/m'$ )	$c2_1 = 0, c2_2 = 0,$ $c4 = 2$	2.4 ( $P\bar{1}$ )	$z_{2I,1} = 0,$ $z_{2I,2} = 0,$ $z_{2I,3} = 0,$ $\eta_{4I} = 2$	AXI/3D QAH
0.203	Mn <sub>3</sub> Ge	4	12.62 ( $C2'/m'$ )	$c2_1 = 0, c2_2 = 0,$ $c4 = 2$	2.4 ( $P\bar{1}$ )	$z_{2I,1} = 0,$ $z_{2I,2} = 0,$ $z_{2I,3} = 0,$ $\eta_{4I} = 2$	AXI/3D QAH
1.0.13	FeI <sub>2</sub>	0	12.62 ( $C2'/m'$ )	$c2_1 = 1, c2_2 = 1,$ $c4 = 3$	2.4 ( $P\bar{1}$ )	$z_{2I,1} = 0,$ $z_{2I,2} = 0,$ $z_{2I,3} = 0,$ $\eta_{4I} = 1$	SISM
1.140	PrMgPb	0	13.73 ( $P_A2/c$ )	$c2 = 1$	2.4 ( $P\bar{1}$ )	$z_{2I,1} = 0,$ $z_{2I,2} = 0,$ $z_{2I,3} = 0,$ $\eta_{4I} = 2$	AXI/3D QAH
1.140	PrMgPb	2	13.73 ( $P_A2/c$ )	$c2 = 1$	2.4 ( $P\bar{1}$ )	$z_{2I,1} = 0,$ $z_{2I,2} = 0,$ $z_{2I,3} = 0,$ $\eta_{4I} = 2$	AXI/3D QAH
1.140	PrMgPb	4	13.73 ( $P_A2/c$ )	$c2 = 1$	2.4 ( $P\bar{1}$ )	$z_{2I,1} = 0,$ $z_{2I,2} = 0,$ $z_{2I,3} = 0,$ $\eta_{4I} = 2$	AXI/3D QAH

1.140	PrMgPb	6	13.73 ( $P_A 2/c$ )	$c2 = 1$	2.4 ( $P\bar{1}$ )	$z_{2I,1} = 0,$ $z_{2I,2} = 0,$ $z_{2I,3} = 0,$ $\eta_{4I} = 2$	AXI/3D QAH
1.141	NdMgPb	0	13.73 ( $P_A 2/c$ )	$c2 = 1$	2.4 ( $P\bar{1}$ )	$z_{2I,1} = 0,$ $z_{2I,2} = 0,$ $z_{2I,3} = 0,$ $\eta_{4I} = 2$	AXI/3D QAH
1.141	NdMgPb	2	13.73 ( $P_A 2/c$ )	$c2 = 1$	2.4 ( $P\bar{1}$ )	$z_{2I,1} = 0,$ $z_{2I,2} = 0,$ $z_{2I,3} = 0,$ $\eta_{4I} = 2$	AXI/3D QAH
1.201	Cr <sub>2</sub> ReO <sub>6</sub>	0	14.80 ( $P_a 2_1/c$ )	$c2 = 1$	2.4 ( $P\bar{1}$ )	$z_{2I,1} = 0,$ $z_{2I,2} = 0,$ $z_{2I,3} = 0,$ $\eta_{4I} = 2$	AXI/3D QAH
0.174	Pr <sub>3</sub> Ru <sub>4</sub> Al <sub>12</sub>	0	15.89 ( $C2'/c'$ )	$c2 = 1, c4 = 1$	2.4 ( $P\bar{1}$ )	$z_{2I,1} = 0,$ $z_{2I,2} = 0,$ $z_{2I,3} = 0,$ $\eta_{4I} = 1$	SISM
0.174	Pr <sub>3</sub> Ru <sub>4</sub> Al <sub>12</sub>	2	15.89 ( $C2'/c'$ )	$c2 = 1, c4 = 1$	2.4 ( $P\bar{1}$ )	$z_{2I,1} = 0,$ $z_{2I,2} = 0,$ $z_{2I,3} = 0,$ $\eta_{4I} = 1$	SISM
0.174	Pr <sub>3</sub> Ru <sub>4</sub> Al <sub>12</sub>	4	15.89 ( $C2'/c'$ )	$c2 = 1, c4 = 1$	2.4 ( $P\bar{1}$ )	$z_{2I,1} = 0,$ $z_{2I,2} = 0,$ $z_{2I,3} = 0,$ $\eta_{4I} = 1$	SISM
0.174	Pr <sub>3</sub> Ru <sub>4</sub> Al <sub>12</sub>	6	15.89 ( $C2'/c'$ )	$c2 = 1, c4 = 1$	2.4 ( $P\bar{1}$ )	$z_{2I,1} = 0,$ $z_{2I,2} = 0,$ $z_{2I,3} = 0,$ $\eta_{4I} = 1$	SISM
0.226	NdCo <sub>2</sub>	2	15.89 ( $C2'/c'$ )	$c2 = 1, c4 = 3$	2.4 ( $P\bar{1}$ )	$z_{2I,1} = 0,$ $z_{2I,2} = 0,$ $z_{2I,3} = 0,$ $\eta_{4I} = 3$	SISM
0.226	NdCo <sub>2</sub>	4	15.89 ( $C2'/c'$ )	$c2 = 0, c4 = 2$	2.4 ( $P\bar{1}$ )	$z_{2I,1} = 0,$ $z_{2I,2} = 0,$ $z_{2I,3} = 0,$ $\eta_{4I} = 2$	AXI/3D QAH
0.226	NdCo <sub>2</sub>	6	15.89 ( $C2'/c'$ )	$c2 = 1, c4 = 3$	2.4 ( $P\bar{1}$ )	$z_{2I,1} = 0,$ $z_{2I,2} = 0,$ $z_{2I,3} = 0,$ $\eta_{4I} = 3$	SISM
2.10	HoP	0	15.89 ( $C2'/c'$ )	$c2 = 1, c4 = 3$	2.4 ( $P\bar{1}$ )	$z_{2I,1} = 0,$ $z_{2I,2} = 0,$ $z_{2I,3} = 0,$ $\eta_{4I} = 3$	SISM
2.10	HoP	2	15.89 ( $C2'/c'$ )	$c2 = 1, c4 = 0$	2.4 ( $P\bar{1}$ )	$z_{2I,1} = 1,$ $z_{2I,2} = 1,$ $z_{2I,3} = 0,$ $\eta_{4I} = 0$	3D QAH
2.10	HoP	4	15.89 ( $C2'/c'$ )	$c2 = 1, c4 = 0$	2.4 ( $P\bar{1}$ )	$z_{2I,1} = 1,$ $z_{2I,2} = 1,$ $z_{2I,3} = 0,$ $\eta_{4I} = 0$	3D QAH

2.10	HoP	6	15.89 ( $C2'/c'$ )	$c2 = 1, c4 = 0$	2.4 ( $P\bar{1}$ )	$z_{2I,1} = 1,$ $z_{2I,2} = 1,$ $z_{2I,3} = 0,$ $\eta_{4I} = 0$	3D QAH
1.211	Dy <sub>2</sub> O <sub>2</sub> S	0	15.90 ( $C_c2/c$ )	$c2 = 1$	2.4 ( $P\bar{1}$ )	$z_{2I,1} = 0,$ $z_{2I,2} = 0,$ $z_{2I,3} = 0,$ $\eta_{4I} = 2$	AXI/3D QAH
1.216	Nd <sub>2</sub> BaNiO <sub>5</sub>	0	15.90 ( $C_c2/c$ )	$c2 = 1$	2.4 ( $P\bar{1}$ )	$z_{2I,1} = 0,$ $z_{2I,2} = 0,$ $z_{2I,3} = 0,$ $\eta_{4I} = 2$	AXI/3D QAH
1.217	Tb <sub>2</sub> BaNiO <sub>5</sub>	0	15.90 ( $C_c2/c$ )	$c2 = 1$	2.4 ( $P\bar{1}$ )	$z_{2I,1} = 0,$ $z_{2I,2} = 0,$ $z_{2I,3} = 0,$ $\eta_{4I} = 2$	AXI/3D QAH
1.49	Ag <sub>2</sub> NiO <sub>2</sub>	0	15.90 ( $C_c2/c$ )	$c2 = 1$	2.4 ( $P\bar{1}$ )	$z_{2I,1} = 0,$ $z_{2I,2} = 0,$ $z_{2I,3} = 0,$ $\eta_{4I} = 2$	AXI/3D QAH
1.139	Ho <sub>2</sub> RhIn <sub>8</sub>	2	49.273 ( $P_cccm$ )	$c2 = 1$	2.4 ( $P\bar{1}$ )	$z_{2I,1} = 0,$ $z_{2I,2} = 0,$ $z_{2I,3} = 0,$ $\eta_{4I} = 2$	AXI
1.139	Ho <sub>2</sub> RhIn <sub>8</sub>	4	49.273 ( $P_cccm$ )	$c2 = 1$	2.4 ( $P\bar{1}$ )	$z_{2I,1} = 0,$ $z_{2I,2} = 0,$ $z_{2I,3} = 0,$ $\eta_{4I} = 2$	AXI
1.150	PrAg	4	53.334 ( $P_Bmna$ )	$c2 = 1$	2.4 ( $P\bar{1}$ )	$z_{2I,1} = 0,$ $z_{2I,2} = 0,$ $z_{2I,3} = 0,$ $\eta_{4I} = 2$	AXI
1.8	CeRu <sub>2</sub> Al <sub>10</sub>	0	57.391 ( $P_Cbcm$ )	$c2 = 1$	2.4 ( $P\bar{1}$ )	$z_{2I,1} = 0,$ $z_{2I,2} = 0,$ $z_{2I,3} = 0,$ $\eta_{4I} = 2$	AXI
1.8	CeRu <sub>2</sub> Al <sub>10</sub>	2	57.391 ( $P_Cbcm$ )	$c2 = 1$	2.4 ( $P\bar{1}$ )	$z_{2I,1} = 0,$ $z_{2I,2} = 0,$ $z_{2I,3} = 0,$ $\eta_{4I} = 2$	AXI
1.8	CeRu <sub>2</sub> Al <sub>10</sub>	4	57.391 ( $P_Cbcm$ )	$c2 = 1$	2.4 ( $P\bar{1}$ )	$z_{2I,1} = 0,$ $z_{2I,2} = 0,$ $z_{2I,3} = 0,$ $\eta_{4I} = 2$	AXI
1.252	CaCo <sub>2</sub> P <sub>2</sub>	1	59.416 ( $P_Immn$ )	$c2 = 1$	2.4 ( $P\bar{1}$ )	$z_{2I,1} = 0,$ $z_{2I,2} = 0,$ $z_{2I,3} = 0,$ $\eta_{4I} = 2$	AXI
1.252	CaCo <sub>2</sub> P <sub>2</sub>	2	59.416 ( $P_Immn$ )	$c2 = 1$	2.4 ( $P\bar{1}$ )	$z_{2I,1} = 0,$ $z_{2I,2} = 0,$ $z_{2I,3} = 0,$ $\eta_{4I} = 2$	AXI
1.252	CaCo <sub>2</sub> P <sub>2</sub>	3	59.416 ( $P_Immn$ )	$c2 = 1$	2.4 ( $P\bar{1}$ )	$z_{2I,1} = 0,$ $z_{2I,2} = 0,$ $z_{2I,3} = 0,$ $\eta_{4I} = 2$	AXI

1.252	CaCo2P2	4	59.416 ( $P_I mmn$ )	$c2 = 1$	2.4 ( $P\bar{1}$ )	$z_{2I,1} = 0,$ $z_{2I,2} = 0,$ $z_{2I,3} = 0,$ $\eta_{4I} = 2$	AXI
1.88	Mn5Si3	0	60.431 ( $P_C bcn$ )	$c2 = 1$	2.4 ( $P\bar{1}$ )	$z_{2I,1} = 0,$ $z_{2I,2} = 0,$ $z_{2I,3} = 0,$ $\eta_{4I} = 2$	AXI
2.1	EuFe2As2	2	61.439 ( $P_C bca$ )	$c2 = 1$	2.4 ( $P\bar{1}$ )	$z_{2I,1} = 0,$ $z_{2I,2} = 0,$ $z_{2I,3} = 0,$ $\eta_{4I} = 2$	AXI
2.1	EuFe2As2	3	61.439 ( $P_C bca$ )	$c2 = 1$	2.4 ( $P\bar{1}$ )	$z_{2I,1} = 0,$ $z_{2I,2} = 0,$ $z_{2I,3} = 0,$ $\eta_{4I} = 2$	AXI
1.130	Cr2As	1	62.450 ( $P_a nma$ )	$c2 = 1$	2.4 ( $P\bar{1}$ )	$z_{2I,1} = 0,$ $z_{2I,2} = 0,$ $z_{2I,3} = 0,$ $\eta_{4I} = 2$	AXI
1.131	Fe2As	0	62.450 ( $P_a nma$ )	$c2 = 1$	2.4 ( $P\bar{1}$ )	$z_{2I,1} = 0,$ $z_{2I,2} = 0,$ $z_{2I,3} = 0,$ $\eta_{4I} = 2$	AXI
1.131	Fe2As	1	62.450 ( $P_a nma$ )	$c2 = 1$	2.4 ( $P\bar{1}$ )	$z_{2I,1} = 0,$ $z_{2I,2} = 0,$ $z_{2I,3} = 0,$ $\eta_{4I} = 2$	AXI
1.131	Fe2As	3	62.450 ( $P_a nma$ )	$c2 = 1$	2.4 ( $P\bar{1}$ )	$z_{2I,1} = 0,$ $z_{2I,2} = 0,$ $z_{2I,3} = 0,$ $\eta_{4I} = 2$	AXI
1.131	Fe2As	4	62.450 ( $P_a nma$ )	$c2 = 1$	2.4 ( $P\bar{1}$ )	$z_{2I,1} = 0,$ $z_{2I,2} = 0,$ $z_{2I,3} = 0,$ $\eta_{4I} = 2$	AXI
1.179	NdCoAsO	2	62.450 ( $P_a nma$ )	$c2 = 1$	2.4 ( $P\bar{1}$ )	$z_{2I,1} = 0,$ $z_{2I,2} = 0,$ $z_{2I,3} = 0,$ $\eta_{4I} = 2$	AXI
1.28	CrN	0	62.450 ( $P_a nma$ )	$c2 = 1$	2.4 ( $P\bar{1}$ )	$z_{2I,1} = 0,$ $z_{2I,2} = 0,$ $z_{2I,3} = 0,$ $\eta_{4I} = 2$	AXI
1.28	CrN	1	62.450 ( $P_a nma$ )	$c2 = 1$	2.4 ( $P\bar{1}$ )	$z_{2I,1} = 0,$ $z_{2I,2} = 0,$ $z_{2I,3} = 0,$ $\eta_{4I} = 2$	AXI
0.200	Mn3Sn	0	63.464 ( $Cm'cm'$ )	$c2_1 = 1, c2_2 = 0$	2.4 ( $P\bar{1}$ )	$z_{2I,1} = 0,$ $z_{2I,2} = 0,$ $z_{2I,3} = 0,$ $\eta_{4I} = 2$	AXI/3D QAH
0.200	Mn3Sn	1	63.464 ( $Cm'cm'$ )	$c2_1 = 1, c2_2 = 0$	2.4 ( $P\bar{1}$ )	$z_{2I,1} = 0,$ $z_{2I,2} = 0,$ $z_{2I,3} = 0,$ $\eta_{4I} = 2$	AXI/3D QAH

0.200	Mn3Sn	2	63.464 ( $Cm'm'$ )	$c2_1 = 1, c2_2 = 0$	2.4 ( $P\bar{1}$ )	$z_{2I,1} = 0,$ $z_{2I,2} = 0,$ $z_{2I,3} = 0,$ $\eta_{4I} = 2$	AXI/3D QAH
1.200	U2Ni2Sn	2	63.466 ( $C_c mcm$ )	$c2 = 1$	2.4 ( $P\bar{1}$ )	$z_{2I,1} = 0,$ $z_{2I,2} = 0,$ $z_{2I,3} = 0,$ $\eta_{4I} = 2$	AXI
1.200	U2Ni2Sn	4	63.466 ( $C_c mcm$ )	$c2 = 1$	2.4 ( $P\bar{1}$ )	$z_{2I,1} = 0,$ $z_{2I,2} = 0,$ $z_{2I,3} = 0,$ $\eta_{4I} = 2$	AXI
1.200	U2Ni2Sn	6	63.466 ( $C_c mcm$ )	$c2 = 1$	2.4 ( $P\bar{1}$ )	$z_{2I,1} = 0,$ $z_{2I,2} = 0,$ $z_{2I,3} = 0,$ $\eta_{4I} = 2$	AXI
1.262	NpRhGa5	2	63.466 ( $C_c mcm$ )	$c2 = 1$	2.4 ( $P\bar{1}$ )	$z_{2I,1} = 0,$ $z_{2I,2} = 0,$ $z_{2I,3} = 0,$ $\eta_{4I} = 2$	AXI
1.195	Er2Ni2In	4	63.467 ( $C_a mcm$ )	$c2 = 1$	2.4 ( $P\bar{1}$ )	$z_{2I,1} = 0,$ $z_{2I,2} = 0,$ $z_{2I,3} = 0,$ $\eta_{4I} = 2$	AXI
1.16	BaFe2As2	0	64.480 ( $C_A mca$ )	$c2 = 1$	2.4 ( $P\bar{1}$ )	$z_{2I,1} = 0,$ $z_{2I,2} = 0,$ $z_{2I,3} = 0,$ $\eta_{4I} = 2$	AXI
1.16	BaFe2As2	1	64.480 ( $C_A mca$ )	$c2 = 1$	2.4 ( $P\bar{1}$ )	$z_{2I,1} = 0,$ $z_{2I,2} = 0,$ $z_{2I,3} = 0,$ $\eta_{4I} = 2$	AXI
1.16	BaFe2As2	2	64.480 ( $C_A mca$ )	$c2 = 1$	2.4 ( $P\bar{1}$ )	$z_{2I,1} = 0,$ $z_{2I,2} = 0,$ $z_{2I,3} = 0,$ $\eta_{4I} = 2$	AXI
1.16	BaFe2As2	3	64.480 ( $C_A mca$ )	$c2 = 1$	2.4 ( $P\bar{1}$ )	$z_{2I,1} = 0,$ $z_{2I,2} = 0,$ $z_{2I,3} = 0,$ $\eta_{4I} = 2$	AXI
1.188	CeRh2Si2	0	64.480 ( $C_A mca$ )	$c2 = 1$	2.4 ( $P\bar{1}$ )	$z_{2I,1} = 0,$ $z_{2I,2} = 0,$ $z_{2I,3} = 0,$ $\eta_{4I} = 2$	AXI
1.188	CeRh2Si2	6	64.480 ( $C_A mca$ )	$c2 = 1$	2.4 ( $P\bar{1}$ )	$z_{2I,1} = 0,$ $z_{2I,2} = 0,$ $z_{2I,3} = 0,$ $\eta_{4I} = 2$	AXI
1.52	CaFe2As2	0	64.480 ( $C_A mca$ )	$c2 = 1$	2.4 ( $P\bar{1}$ )	$z_{2I,1} = 0,$ $z_{2I,2} = 0,$ $z_{2I,3} = 0,$ $\eta_{4I} = 2$	AXI
1.52	CaFe2As2	1	64.480 ( $C_A mca$ )	$c2 = 1$	2.4 ( $P\bar{1}$ )	$z_{2I,1} = 0,$ $z_{2I,2} = 0,$ $z_{2I,3} = 0,$ $\eta_{4I} = 2$	AXI

1.52	CaFe2As2	2	64.480 ( $C_A mca$ )	$c2 = 1$	2.4 ( $P\bar{1}$ )	$z_{2I,1} = 0,$ $z_{2I,2} = 0,$ $z_{2I,3} = 0,$ $\eta_{4I} = 2$	AXI
2.15	Mn3Ni20P6	3	65.486 ( $Cmm'm'$ )	$c2_1 = 1, c2_2 = 0$	2.4 ( $P\bar{1}$ )	$z_{2I,1} = 0,$ $z_{2I,2} = 0,$ $z_{2I,3} = 0,$ $\eta_{4I} = 2$	AXI/3D QAH
1.142	CeMgPb	2	67.510 ( $C_A mma$ )	$c2 = 1$	2.4 ( $P\bar{1}$ )	$z_{2I,1} = 0,$ $z_{2I,2} = 0,$ $z_{2I,3} = 0,$ $\eta_{4I} = 2$	AXI
1.125	LaFeAsO	0	73.553 ( $I_c bca$ )	$c2 = 1$	2.4 ( $P\bar{1}$ )	$z_{2I,1} = 0,$ $z_{2I,2} = 0,$ $z_{2I,3} = 0,$ $\eta_{4I} = 2$	AXI
1.176	YbCo2Si2	1	73.553 ( $I_c bca$ )	$c2 = 1$	2.4 ( $P\bar{1}$ )	$z_{2I,1} = 0,$ $z_{2I,2} = 0,$ $z_{2I,3} = 0,$ $\eta_{4I} = 2$	AXI
1.176	YbCo2Si2	2	73.553 ( $I_c bca$ )	$c2 = 1$	2.4 ( $P\bar{1}$ )	$z_{2I,1} = 0,$ $z_{2I,2} = 0,$ $z_{2I,3} = 0,$ $\eta_{4I} = 2$	AXI
1.176	YbCo2Si2	3	73.553 ( $I_c bca$ )	$c2 = 1$	2.4 ( $P\bar{1}$ )	$z_{2I,1} = 0,$ $z_{2I,2} = 0,$ $z_{2I,3} = 0,$ $\eta_{4I} = 2$	AXI
1.176	YbCo2Si2	4	73.553 ( $I_c bca$ )	$c2 = 1$	2.4 ( $P\bar{1}$ )	$z_{2I,1} = 0,$ $z_{2I,2} = 0,$ $z_{2I,3} = 0,$ $\eta_{4I} = 2$	AXI
2.13	UP	0	134.481 ( $P_C 4_2/nnm$ )	$c2 = 1$	2.4 ( $P\bar{1}$ )	$z_{2I,1} = 0,$ $z_{2I,2} = 0,$ $z_{2I,3} = 0,$ $\eta_{4I} = 2$	AXI
2.13	UP	2	134.481 ( $P_C 4_2/nnm$ )	$c2 = 1$	2.4 ( $P\bar{1}$ )	$z_{2I,1} = 0,$ $z_{2I,2} = 0,$ $z_{2I,3} = 0,$ $\eta_{4I} = 2$	AXI
2.13	UP	4	134.481 ( $P_C 4_2/nnm$ )	$c2 = 1$	2.4 ( $P\bar{1}$ )	$z_{2I,1} = 0,$ $z_{2I,2} = 0,$ $z_{2I,3} = 0,$ $\eta_{4I} = 2$	AXI
2.13	UP	6	134.481 ( $P_C 4_2/nnm$ )	$c2 = 1$	2.4 ( $P\bar{1}$ )	$z_{2I,1} = 0,$ $z_{2I,2} = 0,$ $z_{2I,3} = 0,$ $\eta_{4I} = 2$	AXI
2.20	UAs	0	134.481 ( $P_C 4_2/nnm$ )	$c2 = 1$	2.4 ( $P\bar{1}$ )	$z_{2I,1} = 0,$ $z_{2I,2} = 0,$ $z_{2I,3} = 0,$ $\eta_{4I} = 2$	AXI
2.20	UAs	4	134.481 ( $P_C 4_2/nnm$ )	$c2 = 1$	2.4 ( $P\bar{1}$ )	$z_{2I,1} = 0,$ $z_{2I,2} = 0,$ $z_{2I,3} = 0,$ $\eta_{4I} = 2$	AXI

2.20	UAs	6	134.481 ( $P_C4_2/nnm$ )	$c2 = 1$	2.4 ( $P\bar{1}$ )	$z_{2I,1} = 0,$ $z_{2I,2} = 0,$ $z_{2I,3} = 0,$ $\eta_{4I} = 2$	AXI
2.6	Nd <sub>2</sub> CuO <sub>4</sub>	0	134.481 ( $P_C4_2/nnm$ )	$c2 = 1$	2.4 ( $P\bar{1}$ )	$z_{2I,1} = 0,$ $z_{2I,2} = 0,$ $z_{2I,3} = 0,$ $\eta_{4I} = 2$	AXI
1.146	LaCrAsO	0	138.528 ( $P_c4_2/ncm$ )	$c2 = 1$	2.4 ( $P\bar{1}$ )	$z_{2I,1} = 0,$ $z_{2I,2} = 0,$ $z_{2I,3} = 0,$ $\eta_{4I} = 2$	AXI
1.146	LaCrAsO	1	138.528 ( $P_c4_2/ncm$ )	$c2 = 1$	2.4 ( $P\bar{1}$ )	$z_{2I,1} = 0,$ $z_{2I,2} = 0,$ $z_{2I,3} = 0,$ $\eta_{4I} = 2$	AXI
1.146	LaCrAsO	2	138.528 ( $P_c4_2/ncm$ )	$c2 = 1$	2.4 ( $P\bar{1}$ )	$z_{2I,1} = 0,$ $z_{2I,2} = 0,$ $z_{2I,3} = 0,$ $\eta_{4I} = 2$	AXI
1.146	LaCrAsO	3	138.528 ( $P_c4_2/ncm$ )	$c2 = 1$	2.4 ( $P\bar{1}$ )	$z_{2I,1} = 0,$ $z_{2I,2} = 0,$ $z_{2I,3} = 0,$ $\eta_{4I} = 2$	AXI
1.146	LaCrAsO	4	138.528 ( $P_c4_2/ncm$ )	$c2 = 1$	2.4 ( $P\bar{1}$ )	$z_{2I,1} = 0,$ $z_{2I,2} = 0,$ $z_{2I,3} = 0,$ $\eta_{4I} = 2$	AXI
0.228	TbCo <sub>2</sub>	0	166.101 ( $R\bar{3}m'$ )	$c2 = 1, c4 = 1$	2.4 ( $P\bar{1}$ )	$z_{2I,1} = 0,$ $z_{2I,2} = 0,$ $z_{2I,3} = 0,$ $\eta_{4I} = 3$	SISM
0.228	TbCo <sub>2</sub>	4	166.101 ( $R\bar{3}m'$ )	$c2 = 1, c4 = 3$	2.4 ( $P\bar{1}$ )	$z_{2I,1} = 0,$ $z_{2I,2} = 0,$ $z_{2I,3} = 0,$ $\eta_{4I} = 1$	SISM
0.228	TbCo <sub>2</sub>	6	166.101 ( $R\bar{3}m'$ )	$c2 = 1, c4 = 1$	2.4 ( $P\bar{1}$ )	$z_{2I,1} = 0,$ $z_{2I,2} = 0,$ $z_{2I,3} = 0,$ $\eta_{4I} = 3$	SISM
0.150	NiS <sub>2</sub>	0	205.33 ( $Pa\bar{3}$ )	$c2 = 1$	2.4 ( $P\bar{1}$ )	$z_{2I,1} = 0,$ $z_{2I,2} = 0,$ $z_{2I,3} = 0,$ $\eta_{4I} = 2$	AXI/3D QAHI
3.12	NpSb	0	224.113 ( $Pn\bar{3}m'$ )	$c2 = 1$	2.4 ( $P\bar{1}$ )	$z_{2I,1} = 0,$ $z_{2I,2} = 0,$ $z_{2I,3} = 0,$ $\eta_{4I} = 2$	AXI
3.12	NpSb	2	224.113 ( $Pn\bar{3}m'$ )	$c2 = 1$	2.4 ( $P\bar{1}$ )	$z_{2I,1} = 0,$ $z_{2I,2} = 0,$ $z_{2I,3} = 0,$ $\eta_{4I} = 2$	AXI
3.12	NpSb	4	224.113 ( $Pn\bar{3}m'$ )	$c2 = 1$	2.4 ( $P\bar{1}$ )	$z_{2I,1} = 0,$ $z_{2I,2} = 0,$ $z_{2I,3} = 0,$ $\eta_{4I} = 2$	AXI

3.12	NpSb	6	224.113 ( $Pn\bar{3}m'$ )	$c2 = 1$	2.4 ( $P\bar{1}$ )	$z_{2I,1} = 0,$ $z_{2I,2} = 0,$ $z_{2I,3} = 0,$ $\eta_{4I} = 2$	AXI
3.7	NpBi	0	224.113 ( $Pn\bar{3}m'$ )	$c2 = 1$	2.4 ( $P\bar{1}$ )	$z_{2I,1} = 0,$ $z_{2I,2} = 0,$ $z_{2I,3} = 0,$ $\eta_{4I} = 2$	AXI
3.7	NpBi	2	224.113 ( $Pn\bar{3}m'$ )	$c2 = 1$	2.4 ( $P\bar{1}$ )	$z_{2I,1} = 0,$ $z_{2I,2} = 0,$ $z_{2I,3} = 0,$ $\eta_{4I} = 2$	AXI
3.7	NpBi	4	224.113 ( $Pn\bar{3}m'$ )	$c2 = 1$	2.4 ( $P\bar{1}$ )	$z_{2I,1} = 0,$ $z_{2I,2} = 0,$ $z_{2I,3} = 0,$ $\eta_{4I} = 2$	AXI
3.7	NpBi	6	224.113 ( $Pn\bar{3}m'$ )	$c2 = 1$	2.4 ( $P\bar{1}$ )	$z_{2I,1} = 0,$ $z_{2I,2} = 0,$ $z_{2I,3} = 0,$ $\eta_{4I} = 2$	AXI
3.10	NpSe	0	228.139 ( $F_Sd\bar{3}c$ )	$c2 = 1$	2.4 ( $P\bar{1}$ )	$z_{2I,1} = 0,$ $z_{2I,2} = 0,$ $z_{2I,3} = 0,$ $\eta_{4I} = 2$	AXI
3.11	NpTe	0	228.139 ( $F_Sd\bar{3}c$ )	$c2 = 1$	2.4 ( $P\bar{1}$ )	$z_{2I,1} = 0,$ $z_{2I,2} = 0,$ $z_{2I,3} = 0,$ $\eta_{4I} = 2$	AXI
1.223	Tm <sub>2</sub> CoGa <sub>8</sub>	0	65.489 ( $C_ammm$ )	$c2 = 0, c4 = 1$	47.249 ( $Pmmm$ )	$z_{2w,1} = 0,$ $z_{2w,2} = 0,$ $z_{2w,3} = 1,$ $z_4 = 3$	AXI/MTCI
1.254	UNiGa <sub>5</sub>	2	140.550 ( $I_c4/mcm$ )	$c4 = 3$	47.249 ( $Pmmm$ )	$z_{2w,1} = 0,$ $z_{2w,2} = 0,$ $z_{2w,3} = 0,$ $z_4 = 3$	AXI
1.254	UNiGa <sub>5</sub>	4	140.550 ( $I_c4/mcm$ )	$c4 = 3$	47.249 ( $Pmmm$ )	$z_{2w,1} = 0,$ $z_{2w,2} = 0,$ $z_{2w,3} = 0,$ $z_4 = 3$	AXI
0.81	U <sub>2</sub> Pd <sub>2</sub> Sn	0	127.394 ( $P4'/m'bm'$ )	$c2 = 1$	81.33 ( $P\bar{4}$ )	$\delta_{2S} = 1,$ $z_2 = 1,$ $z_{4S} = 0$	SISM*
0.81	U <sub>2</sub> Pd <sub>2</sub> Sn	2	127.394 ( $P4'/m'bm'$ )	$c2 = 1$	81.33 ( $P\bar{4}$ )	$\delta_{2S} = 1,$ $z_2 = 1,$ $z_{4S} = 0$	SISM*
0.81	U <sub>2</sub> Pd <sub>2</sub> Sn	4	127.394 ( $P4'/m'bm'$ )	$c2 = 1$	81.33 ( $P\bar{4}$ )	$\delta_{2S} = 1,$ $z_2 = 1,$ $z_{4S} = 0$	SISM*
0.81	U <sub>2</sub> Pd <sub>2</sub> Sn	6	127.394 ( $P4'/m'bm'$ )	$c2 = 1$	81.33 ( $P\bar{4}$ )	$\delta_{2S} = 1,$ $z_2 = 1,$ $z_{4S} = 0$	SISM*
0.186	CeMnAsO	2	129.416 ( $P4'/n'm'm$ )	$c2 = 1$	81.33 ( $P\bar{4}$ )	$\delta_{2S} = 1,$ $z_2 = 1,$ $z_{4S} = 0$	SISM*
0.186	CeMnAsO	4	129.416 ( $P4'/n'm'm$ )	$c2 = 1$	81.33 ( $P\bar{4}$ )	$\delta_{2S} = 1,$ $z_2 = 1,$ $z_{4S} = 0$	SISM*

0.186	CeMnAsO	6	129.416 ( $P4'/n'm'm$ )	$c2 = 1$	81.33 ( $P\bar{4}$ )	$\delta_{2S} = 1,$ $z_2 = 1,$ $z_{4S} = 0$	SISM*
0.126	NpCo2	4	141.556 ( $I4'_1/a'm'd$ )	$c2 = 1$	81.33 ( $P\bar{4}$ )	$\delta_{2S} = 0,$ $z_2 = 0,$ $z_{4S} = 2$	3D QAH
1.251	NdCo2P2	6	124.360 ( $P_c4/mcc$ )	$c4 = 3$	83.43 ( $P4/m$ )	$z_{4m,\pi}^+ = 0,$ $z_{4m,\pi}^- = 0,$ $\delta_{4m} = 3$	AXI/MTCI
1.255	UPtGa5	0	124.360 ( $P_c4/mcc$ )	$c4 = 3$	83.43 ( $P4/m$ )	$z_{4m,\pi}^+ = 0,$ $z_{4m,\pi}^- = 0,$ $\delta_{4m} = 3$	AXI/MTCI
1.208	UAs	6	128.410 ( $P_I4/mnc$ )	$c4 = 3$	83.43 ( $P4/m$ )	$z_{4m,\pi}^+ = 0,$ $z_{4m,\pi}^- = 0,$ $\delta_{4m} = 3$	AXI/MTCI
0.51	Ho2Ru2O7	0	141.557 ( $I4_1/am'd'$ )	$c2_1 = 1, c2_2 = 1$	88.81 ( $I4_1/a$ )	$\eta'_{2I} = 1,$ $z_2 = 0$	3D QAH
0.117	LuFeO3	0	185.201 ( $P6_3c'm'$ )	$c3 = 1$	143.1 ( $P3$ )	$z_{3R} = 2$	3D QAH

\* Compatible with SISM

### Appendix I: Compatibility-relations along high-symmetry paths of the symmetry enforced semimetals

In TABLE XI, we check all the compatibility relations between maximal  $k$  vectors for the magnetic ESs in TABLE VII-VIII. Once band structures break the compatibility relations between two maximal  $k$  vectors, band crossings occur and form nodal points/nodal-lines.

TABLE XI: Compatibility-relations of the magnetic ESs. For each material, the first line lists BCSID, chemical formula, MSG and the value of U in LDA+U calculations. The 1st-3rd coloumns are two maximal  $k$  vectors ( $k_1$  and  $k_2$ ) and the intermediate path between them. The 4th coloumn identifies whether compatibility-relations between  $k_1$  and  $k_2$  are satisfied. If the answer is 'no', there have symmetry enforced band crossings between  $k_1$  and  $k_2$ . The 5th coloumn gives the location of band crossings. 'Line' stands for the band crossings are protected by (screw-)rotational symmetries and there are isolated degenerate points on the line. 'Plane' stands for the band crossings are protected by (glide-)mirror symmetries and the crossing points form nodal-lines on the plane. The coordinates of  $k$  vectors are written in the reciprocal conventional lattice, which are provided in the *CoRepresentation* subsection of BCS website.

BCSID: 0.165; Formula: SrMn(VO4)(OH); MSG: 4.7 ( $P2_1$ ); U= 0				
maximal $k_1$	intermediate path	maximal $k_2$	satisfied?	Line/Plane
$\Gamma:(0,0,0)$	LD:(0,v,0)	Z:(0,1/2,0)	no	Line
A:(1/2,0,1/2)	U:(1/2,v,1/2)	E:(1/2,1/2,1/2)	yes	Line
B:(0,0,1/2)	V:(0,v,1/2)	D:(0,1/2,1/2)	yes	Line
C:(1/2,1/2,0)	W:(1/2,v,0)	Y:(1/2,0,0)	yes	Line

BCSID: 1.22; Formula: DyCu2Si2; MSG: 12.63 ( $C_{2/m}$ ); U= 6eV				
maximal $k_1$	intermediate path	maximal $k_2$	satisfied?	Line/Plane
A:(0,0,1/2)	U:(0,v,1/2)	M:(0,1,1/2)	no	Line

BCSID: 0.105; Formula: ErVO3; MSG: 14.75 ( $P2_1/c$ ); U= 0				
maximal $k_1$	intermediate path	maximal $k_2$	satisfied?	Line/Plane
$\Gamma:(0,0,0)$	LD:(0,v,0)	Z:(0,1/2,0)	yes	Line
A:(1/2,0,1/2)	U:(1/2,v,1/2)	E:(1/2,1/2,1/2)	yes	Line
B:(0,0,1/2)	V:(0,v,1/2)	D:(0,1/2,1/2)	yes	Line
C:(1/2,1/2,0)	W:(1/2,v,0)	Y:(1/2,0,0)	no	Line
$\Gamma:(0,0,0)$	F:(u,0,w)	A:(1/2,0,1/2)	yes	Plane
$\Gamma:(0,0,0)$	F:(u,0,w)	B:(0,0,1/2)	yes	Plane

$\Gamma:(0,0,0)$	$F:(u,0,w)$	$Y:(1/2,0,0)$	no	Plane
$A:(1/2,0,1/2)$	$F:(u,0,w)$	$B:(0,0,1/2)$	yes	Plane
$A:(1/2,0,1/2)$	$F:(u,0,w)$	$Y:(1/2,0,0)$	no	Plane
$B:(0,0,1/2)$	$F:(u,0,w)$	$Y:(1/2,0,0)$	no	Plane
$C:(1/2,1/2,0)$	$G:(u,1/2,w)$	$D:(0,1/2,1/2)$	yes	Plane
$C:(1/2,1/2,0)$	$G:(u,1/2,w)$	$E:(1/2,1/2,1/2)$	yes	Plane
$C:(1/2,1/2,0)$	$G:(u,1/2,w)$	$Z:(0,1/2,0)$	yes	Plane
$D:(0,1/2,1/2)$	$G:(u,1/2,w)$	$E:(1/2,1/2,1/2)$	yes	Plane
$D:(0,1/2,1/2)$	$G:(u,1/2,w)$	$Z:(0,1/2,0)$	yes	Plane
$E:(1/2,1/2,1/2)$	$G:(u,1/2,w)$	$Z:(0,1/2,0)$	yes	Plane

BCSID: 1.263; Formula: Ca3Ru2O7; MSG: 33.154 ( $P_{Cna21}$ ); U= 0				
maximal $k_1$	intermediate path	maximal $k_2$	satisfied?	Line/Plane
$\Gamma:(0,0,0)$	$SM:(u,0,0)$	$X:(1/2,0,0)$	yes	Line
$\Gamma:(0,0,0)$	$DT:(0,v,0)$	$Y:(0,1/2,0)$	yes	Line
$R:(1/2,1/2,1/2)$	$E:(u,1/2,1/2)$	$T:(0,1/2,1/2)$	yes	Line
$S:(1/2,1/2,0)$	$D:(1/2,v,0)$	$X:(1/2,0,0)$	yes	Line
$S:(1/2,1/2,0)$	$C:(u,1/2,0)$	$Y:(0,1/2,0)$	yes	Line
$T:(0,1/2,1/2)$	$H:(0,1/2,w)$	$Y:(0,1/2,0)$	yes	Line
$U:(1/2,0,1/2)$	$G:(1/2,0,w)$	$X:(1/2,0,0)$	no	Line
$U:(1/2,0,1/2)$	$A:(u,0,1/2)$	$Z:(0,0,1/2)$	yes	Line
$\Gamma:(0,0,0)$	$K:(0,v,w)$	$T:(0,1/2,1/2)$	yes	Plane
$\Gamma:(0,0,0)$	$M:(u,0,w)$	$U:(1/2,0,1/2)$	yes	Plane
$\Gamma:(0,0,0)$	$M:(u,0,w)$	$X:(1/2,0,0)$	yes	Plane
$\Gamma:(0,0,0)$	$K:(0,v,w)$	$Y:(0,1/2,0)$	yes	Plane
$\Gamma:(0,0,0)$	$K:(0,v,w)$	$Z:(0,0,1/2)$	yes	Plane
$\Gamma:(0,0,0)$	$M:(u,0,w)$	$Z:(0,0,1/2)$	yes	Plane
$R:(1/2,1/2,1/2)$	$L:(1/2,v,w)$	$S:(1/2,1/2,0)$	yes	Plane
$R:(1/2,1/2,1/2)$	$N:(u,1/2,w)$	$S:(1/2,1/2,0)$	yes	Plane
$R:(1/2,1/2,1/2)$	$N:(u,1/2,w)$	$T:(0,1/2,1/2)$	yes	Plane
$R:(1/2,1/2,1/2)$	$L:(1/2,v,w)$	$U:(1/2,0,1/2)$	yes	Plane
$R:(1/2,1/2,1/2)$	$L:(1/2,v,w)$	$X:(1/2,0,0)$	yes	Plane
$R:(1/2,1/2,1/2)$	$N:(u,1/2,w)$	$Y:(0,1/2,0)$	yes	Plane
$S:(1/2,1/2,0)$	$N:(u,1/2,w)$	$T:(0,1/2,1/2)$	yes	Plane
$S:(1/2,1/2,0)$	$L:(1/2,v,w)$	$U:(1/2,0,1/2)$	yes	Plane
$S:(1/2,1/2,0)$	$L:(1/2,v,w)$	$X:(1/2,0,0)$	yes	Plane
$S:(1/2,1/2,0)$	$N:(u,1/2,w)$	$Y:(0,1/2,0)$	yes	Plane
$T:(0,1/2,1/2)$	$K:(0,v,w)$	$Y:(0,1/2,0)$	yes	Plane
$T:(0,1/2,1/2)$	$N:(u,1/2,w)$	$Y:(0,1/2,0)$	yes	Plane
$T:(0,1/2,1/2)$	$K:(0,v,w)$	$Z:(0,0,1/2)$	yes	Plane
$U:(1/2,0,1/2)$	$L:(1/2,v,w)$	$X:(1/2,0,0)$	yes	Plane
$U:(1/2,0,1/2)$	$M:(u,0,w)$	$X:(1/2,0,0)$	yes	Plane
$U:(1/2,0,1/2)$	$M:(u,0,w)$	$Z:(0,0,1/2)$	yes	Plane
$X:(1/2,0,0)$	$M:(u,0,w)$	$Z:(0,0,1/2)$	yes	Plane
$Y:(0,1/2,0)$	$K:(0,v,w)$	$Z:(0,0,1/2)$	yes	Plane

BCSID: 1.263; Formula: Ca3Ru2O7; MSG: 33.154 ( $P_{Cna21}$ ); U= 1eV				
maximal $k_1$	intermediate path	maximal $k_2$	satisfied?	Line/Plane
$\Gamma:(0,0,0)$	$SM:(u,0,0)$	$X:(1/2,0,0)$	yes	Line
$\Gamma:(0,0,0)$	$DT:(0,v,0)$	$Y:(0,1/2,0)$	yes	Line
$R:(1/2,1/2,1/2)$	$E:(u,1/2,1/2)$	$T:(0,1/2,1/2)$	yes	Line

S:(1/2,1/2,0)	D:(1/2,v,0)	X:(1/2,0,0)	yes	Line
S:(1/2,1/2,0)	C:(u,1/2,0)	Y:(0,1/2,0)	yes	Line
T:(0,1/2,1/2)	H:(0,1/2,w)	Y:(0,1/2,0)	yes	Line
U:(1/2,0,1/2)	G:(1/2,0,w)	X:(1/2,0,0)	no	Line
U:(1/2,0,1/2)	A:(u,0,1/2)	Z:(0,0,1/2)	yes	Line
$\Gamma$ :(0,0,0)	K:(0,v,w)	T:(0,1/2,1/2)	yes	Plane
$\Gamma$ :(0,0,0)	M:(u,0,w)	U:(1/2,0,1/2)	yes	Plane
$\Gamma$ :(0,0,0)	M:(u,0,w)	X:(1/2,0,0)	yes	Plane
$\Gamma$ :(0,0,0)	K:(0,v,w)	Y:(0,1/2,0)	yes	Plane
$\Gamma$ :(0,0,0)	K:(0,v,w)	Z:(0,0,1/2)	yes	Plane
$\Gamma$ :(0,0,0)	M:(u,0,w)	Z:(0,0,1/2)	yes	Plane
R:(1/2,1/2,1/2)	L:(1/2,v,w)	S:(1/2,1/2,0)	yes	Plane
R:(1/2,1/2,1/2)	N:(u,1/2,w)	S:(1/2,1/2,0)	yes	Plane
R:(1/2,1/2,1/2)	N:(u,1/2,w)	T:(0,1/2,1/2)	yes	Plane
R:(1/2,1/2,1/2)	L:(1/2,v,w)	U:(1/2,0,1/2)	yes	Plane
R:(1/2,1/2,1/2)	L:(1/2,v,w)	X:(1/2,0,0)	yes	Plane
R:(1/2,1/2,1/2)	N:(u,1/2,w)	Y:(0,1/2,0)	yes	Plane
S:(1/2,1/2,0)	N:(u,1/2,w)	T:(0,1/2,1/2)	yes	Plane
S:(1/2,1/2,0)	L:(1/2,v,w)	U:(1/2,0,1/2)	yes	Plane
S:(1/2,1/2,0)	L:(1/2,v,w)	X:(1/2,0,0)	yes	Plane
S:(1/2,1/2,0)	N:(u,1/2,w)	Y:(0,1/2,0)	yes	Plane
T:(0,1/2,1/2)	K:(0,v,w)	Y:(0,1/2,0)	yes	Plane
T:(0,1/2,1/2)	N:(u,1/2,w)	Y:(0,1/2,0)	yes	Plane
T:(0,1/2,1/2)	K:(0,v,w)	Z:(0,0,1/2)	yes	Plane
U:(1/2,0,1/2)	L:(1/2,v,w)	X:(1/2,0,0)	yes	Plane
U:(1/2,0,1/2)	M:(u,0,w)	X:(1/2,0,0)	yes	Plane
U:(1/2,0,1/2)	M:(u,0,w)	Z:(0,0,1/2)	yes	Plane
X:(1/2,0,0)	M:(u,0,w)	Z:(0,0,1/2)	yes	Plane
Y:(0,1/2,0)	K:(0,v,w)	Z:(0,0,1/2)	yes	Plane

BCSID: 1.43; Formula: PrNiO3; MSG: 36.178 ( $C_a mc_2$ ); U= 4eV				
maximal $k_1$	intermediate path	maximal $k_2$	satisfied?	Line/Plane
$\Gamma$ :(0,0,0)	DT:(0,v,0)	Y:(0,1,0)	yes	Line
$\Gamma$ :(0,0,0)	SM:(u,0,0)	Y:(1,0,0)	yes	Line
R:(1/2,1/2,1/2)	D:(1/2,1/2,w)	S:(1/2,1/2,0)	no	Line
T:(0,1,1/2)	B:(0,v,1/2)	Z:(0,0,1/2)	yes	Line
$\Gamma$ :(0,0,0)	K:(0,v,w)	T:(0,1,1/2)	yes	Plane
$\Gamma$ :(0,0,0)	M:(u,0,w)	T:(1,0,1/2)	yes	Plane
$\Gamma$ :(0,0,0)	K:(0,v,w)	Y:(0,1,0)	yes	Plane
$\Gamma$ :(0,0,0)	M:(u,0,w)	Y:(1,0,0)	yes	Plane
$\Gamma$ :(0,0,0)	K:(0,v,w)	Z:(0,0,1/2)	yes	Plane
$\Gamma$ :(0,0,0)	M:(u,0,w)	Z:(0,0,1/2)	yes	Plane
$\Gamma$ :(0,1,1/2)	K:(0,v,w)	Y:(0,1,0)	yes	Plane
T:(1,0,1/2)	M:(u,0,w)	Y:(1,0,0)	yes	Plane
T:(0,1,1/2)	K:(0,v,w)	Z:(0,0,1/2)	yes	Plane
T:(1,0,1/2)	M:(u,0,w)	Z:(0,0,1/2)	yes	Plane
Y:(0,1,0)	K:(0,v,w)	Z:(0,0,1/2)	yes	Plane
Y:(1,0,0)	M:(u,0,w)	Z:(0,0,1/2)	yes	Plane

BCSID: 0.26; Formula: TmAgGe; MSG: 38.191 ( $Am'm'2$ ); U= 0				
maximal $k_1$	intermediate path	maximal $k_2$	satisfied?	Line/Plane

$\Gamma:(0,0,0)$	SM:(0,0,w)	Y:(0,0,1)	no	Line
T:(1/2,0,-1)	A:(1/2,0,w)	Z:(1/2,0,0)	yes	Line

BCSID: 2.12; Formula: TbMg; MSG: 49.270 ( $Pc'cm'$ ); U= 0				
maximal $k_1$	intermediate path	maximal $k_2$	satisfied?	Line/Plane
$\Gamma:(0,0,0)$	SM:(u,0,0)	X:(1/2,0,0)	no	Line
$\Gamma:(0,0,0)$	DT:(0,v,0)	Y:(0,1/2,0)	yes	Line
$\Gamma:(0,0,0)$	LD:(0,0,w)	Z:(0,0,1/2)	no	Line
R:(1/2,1/2,1/2)	Q:(1/2,1/2,w)	S:(1/2,1/2,0)	yes	Line
R:(1/2,1/2,1/2)	P:(1/2,v,1/2)	U:(1/2,0,1/2)	yes	Line
S:(1/2,1/2,0)	D:(1/2,v,0)	X:(1/2,0,0)	yes	Line
S:(1/2,1/2,0)	C:(u,1/2,0)	Y:(0,1/2,0)	yes	Line
T:(0,1/2,1/2)	H:(0,1/2,w)	Y:(0,1/2,0)	yes	Line
T:(0,1/2,1/2)	B:(0,v,1/2)	Z:(0,0,1/2)	yes	Line
U:(1/2,0,1/2)	G:(1/2,0,w)	X:(1/2,0,0)	yes	Line
$\Gamma:(0,0,0)$	M:(u,0,w)	U:(1/2,0,1/2)	no	Plane
$\Gamma:(0,0,0)$	M:(u,0,w)	X:(1/2,0,0)	no	Plane
$\Gamma:(0,0,0)$	M:(u,0,w)	Z:(0,0,1/2)	no	Plane
R:(1/2,1/2,1/2)	N:(u,1/2,w)	S:(1/2,1/2,0)	yes	Plane
R:(1/2,1/2,1/2)	N:(u,1/2,w)	T:(0,1/2,1/2)	yes	Plane
R:(1/2,1/2,1/2)	N:(u,1/2,w)	Y:(0,1/2,0)	yes	Plane
S:(1/2,1/2,0)	N:(u,1/2,w)	T:(0,1/2,1/2)	yes	Plane
S:(1/2,1/2,0)	N:(u,1/2,w)	Y:(0,1/2,0)	yes	Plane
T:(0,1/2,1/2)	N:(u,1/2,w)	Y:(0,1/2,0)	yes	Plane
U:(1/2,0,1/2)	M:(u,0,w)	X:(1/2,0,0)	yes	Plane
U:(1/2,0,1/2)	M:(u,0,w)	Z:(0,0,1/2)	yes	Plane
X:(1/2,0,0)	M:(u,0,w)	Z:(0,0,1/2)	yes	Plane

BCSID: 2.12; Formula: TbMg; MSG: 49.270 ( $Pc'cm'$ ); U= 2eV				
maximal $k_1$	intermediate path	maximal $k_2$	satisfied?	Line/Plane
$\Gamma:(0,0,0)$	SM:(u,0,0)	X:(1/2,0,0)	no	Line
$\Gamma:(0,0,0)$	DT:(0,v,0)	Y:(0,1/2,0)	yes	Line
$\Gamma:(0,0,0)$	LD:(0,0,w)	Z:(0,0,1/2)	no	Line
R:(1/2,1/2,1/2)	Q:(1/2,1/2,w)	S:(1/2,1/2,0)	yes	Line
R:(1/2,1/2,1/2)	P:(1/2,v,1/2)	U:(1/2,0,1/2)	yes	Line
S:(1/2,1/2,0)	D:(1/2,v,0)	X:(1/2,0,0)	yes	Line
S:(1/2,1/2,0)	C:(u,1/2,0)	Y:(0,1/2,0)	yes	Line
T:(0,1/2,1/2)	H:(0,1/2,w)	Y:(0,1/2,0)	yes	Line
T:(0,1/2,1/2)	B:(0,v,1/2)	Z:(0,0,1/2)	yes	Line
U:(1/2,0,1/2)	G:(1/2,0,w)	X:(1/2,0,0)	yes	Line
$\Gamma:(0,0,0)$	M:(u,0,w)	U:(1/2,0,1/2)	no	Plane
$\Gamma:(0,0,0)$	M:(u,0,w)	X:(1/2,0,0)	no	Plane
$\Gamma:(0,0,0)$	M:(u,0,w)	Z:(0,0,1/2)	no	Plane
R:(1/2,1/2,1/2)	N:(u,1/2,w)	S:(1/2,1/2,0)	yes	Plane
R:(1/2,1/2,1/2)	N:(u,1/2,w)	T:(0,1/2,1/2)	yes	Plane
R:(1/2,1/2,1/2)	N:(u,1/2,w)	Y:(0,1/2,0)	yes	Plane
S:(1/2,1/2,0)	N:(u,1/2,w)	T:(0,1/2,1/2)	yes	Plane
S:(1/2,1/2,0)	N:(u,1/2,w)	Y:(0,1/2,0)	yes	Plane
T:(0,1/2,1/2)	N:(u,1/2,w)	Y:(0,1/2,0)	yes	Plane
U:(1/2,0,1/2)	M:(u,0,w)	X:(1/2,0,0)	yes	Plane
U:(1/2,0,1/2)	M:(u,0,w)	Z:(0,0,1/2)	yes	Plane

X:(1/2,0,0)	M:(u,0,w)	Z:(0,0,1/2)	yes	Plane
BCSID: 2.12; Formula: TbMg; MSG: 49.270 ( $Pc'cm'$ ); U= 4eV				
maximal $k_1$	intermediate path	maximal $k_2$	satisfied?	Line/Plane
$\Gamma:(0,0,0)$	SM:(u,0,0)	X:(1/2,0,0)	yes	Line
$\Gamma:(0,0,0)$	DT:(0,v,0)	Y:(0,1/2,0)	yes	Line
$\Gamma:(0,0,0)$	LD:(0,0,w)	Z:(0,0,1/2)	yes	Line
R:(1/2,1/2,1/2)	Q:(1/2,1/2,w)	S:(1/2,1/2,0)	no	Line
R:(1/2,1/2,1/2)	P:(1/2,v,1/2)	U:(1/2,0,1/2)	yes	Line
S:(1/2,1/2,0)	D:(1/2,v,0)	X:(1/2,0,0)	yes	Line
S:(1/2,1/2,0)	C:(u,1/2,0)	Y:(0,1/2,0)	no	Line
T:(0,1/2,1/2)	H:(0,1/2,w)	Y:(0,1/2,0)	yes	Line
T:(0,1/2,1/2)	B:(0,v,1/2)	Z:(0,0,1/2)	yes	Line
U:(1/2,0,1/2)	G:(1/2,0,w)	X:(1/2,0,0)	yes	Line
$\Gamma:(0,0,0)$	M:(u,0,w)	U:(1/2,0,1/2)	yes	Plane
$\Gamma:(0,0,0)$	M:(u,0,w)	X:(1/2,0,0)	yes	Plane
$\Gamma:(0,0,0)$	M:(u,0,w)	Z:(0,0,1/2)	yes	Plane
R:(1/2,1/2,1/2)	N:(u,1/2,w)	S:(1/2,1/2,0)	no	Plane
R:(1/2,1/2,1/2)	N:(u,1/2,w)	T:(0,1/2,1/2)	yes	Plane
R:(1/2,1/2,1/2)	N:(u,1/2,w)	Y:(0,1/2,0)	yes	Plane
S:(1/2,1/2,0)	N:(u,1/2,w)	T:(0,1/2,1/2)	no	Plane
S:(1/2,1/2,0)	N:(u,1/2,w)	Y:(0,1/2,0)	no	Plane
T:(0,1/2,1/2)	N:(u,1/2,w)	Y:(0,1/2,0)	yes	Plane
U:(1/2,0,1/2)	M:(u,0,w)	X:(1/2,0,0)	yes	Plane
U:(1/2,0,1/2)	M:(u,0,w)	Z:(0,0,1/2)	yes	Plane
X:(1/2,0,0)	M:(u,0,w)	Z:(0,0,1/2)	yes	Plane
BCSID: 2.12; Formula: TbMg; MSG: 49.270 ( $Pc'cm'$ ); U= 6eV				
maximal $k_1$	intermediate path	maximal $k_2$	satisfied?	Line/Plane
$\Gamma:(0,0,0)$	SM:(u,0,0)	X:(1/2,0,0)	no	Line
$\Gamma:(0,0,0)$	DT:(0,v,0)	Y:(0,1/2,0)	yes	Line
$\Gamma:(0,0,0)$	LD:(0,0,w)	Z:(0,0,1/2)	yes	Line
R:(1/2,1/2,1/2)	Q:(1/2,1/2,w)	S:(1/2,1/2,0)	yes	Line
R:(1/2,1/2,1/2)	P:(1/2,v,1/2)	U:(1/2,0,1/2)	yes	Line
S:(1/2,1/2,0)	D:(1/2,v,0)	X:(1/2,0,0)	no	Line
S:(1/2,1/2,0)	C:(u,1/2,0)	Y:(0,1/2,0)	yes	Line
T:(0,1/2,1/2)	H:(0,1/2,w)	Y:(0,1/2,0)	yes	Line
T:(0,1/2,1/2)	B:(0,v,1/2)	Z:(0,0,1/2)	yes	Line
U:(1/2,0,1/2)	G:(1/2,0,w)	X:(1/2,0,0)	no	Line
$\Gamma:(0,0,0)$	M:(u,0,w)	U:(1/2,0,1/2)	yes	Plane
$\Gamma:(0,0,0)$	M:(u,0,w)	X:(1/2,0,0)	no	Plane
$\Gamma:(0,0,0)$	M:(u,0,w)	Z:(0,0,1/2)	yes	Plane
R:(1/2,1/2,1/2)	N:(u,1/2,w)	S:(1/2,1/2,0)	yes	Plane
R:(1/2,1/2,1/2)	N:(u,1/2,w)	T:(0,1/2,1/2)	yes	Plane
R:(1/2,1/2,1/2)	N:(u,1/2,w)	Y:(0,1/2,0)	yes	Plane
S:(1/2,1/2,0)	N:(u,1/2,w)	T:(0,1/2,1/2)	yes	Plane
S:(1/2,1/2,0)	N:(u,1/2,w)	Y:(0,1/2,0)	yes	Plane
T:(0,1/2,1/2)	N:(u,1/2,w)	Y:(0,1/2,0)	yes	Plane
U:(1/2,0,1/2)	M:(u,0,w)	X:(1/2,0,0)	no	Plane
U:(1/2,0,1/2)	M:(u,0,w)	Z:(0,0,1/2)	yes	Plane
X:(1/2,0,0)	M:(u,0,w)	Z:(0,0,1/2)	no	Plane

BCSID: 1.139; Formula: Ho2RhIn8; MSG: 49.273 ( $P_c ccm$ ); U= 0				
maximal $k_1$	intermediate path	maximal $k_2$	satisfied?	Line/Plane
R:(1/2,1/2,1/2)	E:(u,1/2,1/2)	T:(0,1/2,1/2)	no	Line
R:(1/2,1/2,1/2)	P:(1/2,v,1/2)	U:(1/2,0,1/2)	no	Line
T:(0,1/2,1/2)	B:(0,v,1/2)	Z:(0,0,1/2)	no	Line
U:(1/2,0,1/2)	A:(u,0,1/2)	Z:(0,0,1/2)	no	Line
R:(1/2,1/2,1/2)	W:(u,v,1/2)	T:(0,1/2,1/2)	no	Plane
R:(1/2,1/2,1/2)	W:(u,v,1/2)	U:(1/2,0,1/2)	no	Plane
R:(1/2,1/2,1/2)	W:(u,v,1/2)	Z:(0,0,1/2)	yes	Plane
T:(0,1/2,1/2)	W:(u,v,1/2)	U:(1/2,0,1/2)	yes	Plane
T:(0,1/2,1/2)	W:(u,v,1/2)	Z:(0,0,1/2)	no	Plane
U:(1/2,0,1/2)	W:(u,v,1/2)	Z:(0,0,1/2)	no	Plane

BCSID: 2.11; Formula: TbMg; MSG: 51.295 ( $Pmm'a'$ ); U= 0				
maximal $k_1$	intermediate path	maximal $k_2$	satisfied?	Line/Plane
$\Gamma:(0,0,0)$	SM:(u,0,0)	X:(1/2,0,0)	no	Line
$\Gamma:(0,0,0)$	DT:(0,v,0)	Y:(0,1/2,0)	yes	Line
$\Gamma:(0,0,0)$	LD:(0,0,w)	Z:(0,0,1/2)	yes	Line
R:(1/2,1/2,1/2)	E:(u,1/2,1/2)	T:(0,1/2,1/2)	no	Line
R:(1/2,1/2,1/2)	P:(1/2,v,1/2)	U:(1/2,0,1/2)	yes	Line
S:(1/2,1/2,0)	D:(1/2,v,0)	X:(1/2,0,0)	yes	Line
S:(1/2,1/2,0)	C:(u,1/2,0)	Y:(0,1/2,0)	yes	Line
T:(0,1/2,1/2)	H:(0,1/2,w)	Y:(0,1/2,0)	no	Line
T:(0,1/2,1/2)	B:(0,v,1/2)	Z:(0,0,1/2)	no	Line
U:(1/2,0,1/2)	A:(u,0,1/2)	Z:(0,0,1/2)	yes	Line
$\Gamma:(0,0,0)$	K:(0,v,w)	T:(0,1/2,1/2)	no	Plane
$\Gamma:(0,0,0)$	K:(0,v,w)	Y:(0,1/2,0)	yes	Plane
$\Gamma:(0,0,0)$	K:(0,v,w)	Z:(0,0,1/2)	yes	Plane
R:(1/2,1/2,1/2)	L:(1/2,v,w)	S:(1/2,1/2,0)	yes	Plane
R:(1/2,1/2,1/2)	L:(1/2,v,w)	U:(1/2,0,1/2)	yes	Plane
R:(1/2,1/2,1/2)	L:(1/2,v,w)	X:(1/2,0,0)	yes	Plane
S:(1/2,1/2,0)	L:(1/2,v,w)	U:(1/2,0,1/2)	yes	Plane
S:(1/2,1/2,0)	L:(1/2,v,w)	X:(1/2,0,0)	yes	Plane
T:(0,1/2,1/2)	K:(0,v,w)	Y:(0,1/2,0)	no	Plane
T:(0,1/2,1/2)	K:(0,v,w)	Z:(0,0,1/2)	no	Plane
U:(1/2,0,1/2)	L:(1/2,v,w)	X:(1/2,0,0)	yes	Plane
Y:(0,1/2,0)	K:(0,v,w)	Z:(0,0,1/2)	yes	Plane

BCSID: 2.11; Formula: TbMg; MSG: 51.295 ( $Pmm'a'$ ); U= 2eV				
maximal $k_1$	intermediate path	maximal $k_2$	satisfied?	Line/Plane
$\Gamma:(0,0,0)$	SM:(u,0,0)	X:(1/2,0,0)	no	Line
$\Gamma:(0,0,0)$	DT:(0,v,0)	Y:(0,1/2,0)	yes	Line
$\Gamma:(0,0,0)$	LD:(0,0,w)	Z:(0,0,1/2)	yes	Line
R:(1/2,1/2,1/2)	E:(u,1/2,1/2)	T:(0,1/2,1/2)	yes	Line
R:(1/2,1/2,1/2)	P:(1/2,v,1/2)	U:(1/2,0,1/2)	yes	Line
S:(1/2,1/2,0)	D:(1/2,v,0)	X:(1/2,0,0)	yes	Line
S:(1/2,1/2,0)	C:(u,1/2,0)	Y:(0,1/2,0)	yes	Line
T:(0,1/2,1/2)	H:(0,1/2,w)	Y:(0,1/2,0)	no	Line
T:(0,1/2,1/2)	B:(0,v,1/2)	Z:(0,0,1/2)	no	Line
U:(1/2,0,1/2)	A:(u,0,1/2)	Z:(0,0,1/2)	yes	Line

$\Gamma:(0,0,0)$	K:(0,v,w)	T:(0,1/2,1/2)	no	Plane
$\Gamma:(0,0,0)$	K:(0,v,w)	Y:(0,1/2,0)	yes	Plane
$\Gamma:(0,0,0)$	K:(0,v,w)	Z:(0,0,1/2)	yes	Plane
R:(1/2,1/2,1/2)	L:(1/2,v,w)	S:(1/2,1/2,0)	yes	Plane
R:(1/2,1/2,1/2)	L:(1/2,v,w)	U:(1/2,0,1/2)	yes	Plane
R:(1/2,1/2,1/2)	L:(1/2,v,w)	X:(1/2,0,0)	yes	Plane
S:(1/2,1/2,0)	L:(1/2,v,w)	U:(1/2,0,1/2)	yes	Plane
S:(1/2,1/2,0)	L:(1/2,v,w)	X:(1/2,0,0)	yes	Plane
T:(0,1/2,1/2)	K:(0,v,w)	Y:(0,1/2,0)	no	Plane
T:(0,1/2,1/2)	K:(0,v,w)	Z:(0,0,1/2)	no	Plane
U:(1/2,0,1/2)	L:(1/2,v,w)	X:(1/2,0,0)	yes	Plane
Y:(0,1/2,0)	K:(0,v,w)	Z:(0,0,1/2)	yes	Plane

BCSID: 2.11; Formula: TbMg; MSG: 51.295 ( $Pmm'm'$ ); U= 4eV				
maximal $k_1$	intermediate path	maximal $k_2$	satisfied?	Line/Plane
$\Gamma:(0,0,0)$	SM:(u,0,0)	X:(1/2,0,0)	yes	Line
$\Gamma:(0,0,0)$	DT:(0,v,0)	Y:(0,1/2,0)	yes	Line
$\Gamma:(0,0,0)$	LD:(0,0,w)	Z:(0,0,1/2)	yes	Line
R:(1/2,1/2,1/2)	E:(u,1/2,1/2)	T:(0,1/2,1/2)	yes	Line
R:(1/2,1/2,1/2)	P:(1/2,v,1/2)	U:(1/2,0,1/2)	yes	Line
S:(1/2,1/2,0)	D:(1/2,v,0)	X:(1/2,0,0)	yes	Line
S:(1/2,1/2,0)	C:(u,1/2,0)	Y:(0,1/2,0)	yes	Line
T:(0,1/2,1/2)	H:(0,1/2,w)	Y:(0,1/2,0)	no	Line
T:(0,1/2,1/2)	B:(0,v,1/2)	Z:(0,0,1/2)	no	Line
U:(1/2,0,1/2)	A:(u,0,1/2)	Z:(0,0,1/2)	yes	Line
$\Gamma:(0,0,0)$	K:(0,v,w)	T:(0,1/2,1/2)	no	Plane
$\Gamma:(0,0,0)$	K:(0,v,w)	Y:(0,1/2,0)	yes	Plane
$\Gamma:(0,0,0)$	K:(0,v,w)	Z:(0,0,1/2)	yes	Plane
R:(1/2,1/2,1/2)	L:(1/2,v,w)	S:(1/2,1/2,0)	yes	Plane
R:(1/2,1/2,1/2)	L:(1/2,v,w)	U:(1/2,0,1/2)	yes	Plane
R:(1/2,1/2,1/2)	L:(1/2,v,w)	X:(1/2,0,0)	yes	Plane
S:(1/2,1/2,0)	L:(1/2,v,w)	U:(1/2,0,1/2)	yes	Plane
S:(1/2,1/2,0)	L:(1/2,v,w)	X:(1/2,0,0)	yes	Plane
T:(0,1/2,1/2)	K:(0,v,w)	Y:(0,1/2,0)	no	Plane
T:(0,1/2,1/2)	K:(0,v,w)	Z:(0,0,1/2)	no	Plane
U:(1/2,0,1/2)	L:(1/2,v,w)	X:(1/2,0,0)	yes	Plane
Y:(0,1/2,0)	K:(0,v,w)	Z:(0,0,1/2)	yes	Plane

BCSID: 2.11; Formula: TbMg; MSG: 51.295 ( $Pmm'm'$ ); U= 6eV				
maximal $k_1$	intermediate path	maximal $k_2$	satisfied?	Line/Plane
$\Gamma:(0,0,0)$	SM:(u,0,0)	X:(1/2,0,0)	yes	Line
$\Gamma:(0,0,0)$	DT:(0,v,0)	Y:(0,1/2,0)	yes	Line
$\Gamma:(0,0,0)$	LD:(0,0,w)	Z:(0,0,1/2)	yes	Line
R:(1/2,1/2,1/2)	E:(u,1/2,1/2)	T:(0,1/2,1/2)	yes	Line
R:(1/2,1/2,1/2)	P:(1/2,v,1/2)	U:(1/2,0,1/2)	yes	Line
S:(1/2,1/2,0)	D:(1/2,v,0)	X:(1/2,0,0)	yes	Line
S:(1/2,1/2,0)	C:(u,1/2,0)	Y:(0,1/2,0)	yes	Line
T:(0,1/2,1/2)	H:(0,1/2,w)	Y:(0,1/2,0)	no	Line
T:(0,1/2,1/2)	B:(0,v,1/2)	Z:(0,0,1/2)	no	Line
U:(1/2,0,1/2)	A:(u,0,1/2)	Z:(0,0,1/2)	yes	Line
$\Gamma:(0,0,0)$	K:(0,v,w)	T:(0,1/2,1/2)	no	Plane

$\Gamma:(0,0,0)$	$K:(0,v,w)$	$Y:(0,1/2,0)$	yes	Plane
$\Gamma:(0,0,0)$	$K:(0,v,w)$	$Z:(0,0,1/2)$	yes	Plane
$R:(1/2,1/2,1/2)$	$L:(1/2,v,w)$	$S:(1/2,1/2,0)$	yes	Plane
$R:(1/2,1/2,1/2)$	$L:(1/2,v,w)$	$U:(1/2,0,1/2)$	yes	Plane
$R:(1/2,1/2,1/2)$	$L:(1/2,v,w)$	$X:(1/2,0,0)$	yes	Plane
$S:(1/2,1/2,0)$	$L:(1/2,v,w)$	$U:(1/2,0,1/2)$	yes	Plane
$S:(1/2,1/2,0)$	$L:(1/2,v,w)$	$X:(1/2,0,0)$	yes	Plane
$T:(0,1/2,1/2)$	$K:(0,v,w)$	$Y:(0,1/2,0)$	no	Plane
$T:(0,1/2,1/2)$	$K:(0,v,w)$	$Z:(0,0,1/2)$	no	Plane
$U:(1/2,0,1/2)$	$L:(1/2,v,w)$	$X:(1/2,0,0)$	yes	Plane
$Y:(0,1/2,0)$	$K:(0,v,w)$	$Z:(0,0,1/2)$	yes	Plane

BCSID: 1.222; Formula: Er2CoGa8; MSG: 51.298 ( $P_{amma}$ ); U= 0				
maximal $k_1$	intermediate path	maximal $k_2$	satisfied?	Line/Plane
$R:(1/2,1/2,1/2)$	$P:(1/2,v,1/2)$	$U:(1/2,0,1/2)$	yes	Line
$S:(1/2,1/2,0)$	$D:(1/2,v,0)$	$X:(1/2,0,0)$	no	Line

BCSID: 1.222; Formula: Er2CoGa8; MSG: 51.298 ( $P_{amma}$ ); U= 2eV				
maximal $k_1$	intermediate path	maximal $k_2$	satisfied?	Line/Plane
$R:(1/2,1/2,1/2)$	$P:(1/2,v,1/2)$	$U:(1/2,0,1/2)$	no	Line
$S:(1/2,1/2,0)$	$D:(1/2,v,0)$	$X:(1/2,0,0)$	no	Line

BCSID: 1.3; Formula: Sr2IrO4; MSG: 54.352 ( $P_{icca}$ ); U= 1eV				
maximal $k_1$	intermediate path	maximal $k_2$	satisfied?	Line/Plane
$R:(1/2,1/2,1/2)$	$E:(u,1/2,1/2)$	$T:(0,1/2,1/2)$	yes	Line
$S:(1/2,1/2,0)$	$D:(1/2,v,0)$	$X:(1/2,0,0)$	yes	Line
$T:(0,1/2,1/2)$	$B:(0,v,1/2)$	$Z:(0,0,1/2)$	no	Line
$U:(1/2,0,1/2)$	$A:(u,0,1/2)$	$Z:(0,0,1/2)$	no	Line
$R:(1/2,1/2,1/2)$	$N:(u,1/2,w)$	$S:(1/2,1/2,0)$	yes	Plane
$R:(1/2,1/2,1/2)$	$N:(u,1/2,w)$	$T:(0,1/2,1/2)$	yes	Plane
$R:(1/2,1/2,1/2)$	$W:(u,v,1/2)$	$T:(0,1/2,1/2)$	yes	Plane
$R:(1/2,1/2,1/2)$	$W:(u,v,1/2)$	$U:(1/2,0,1/2)$	yes	Plane
$R:(1/2,1/2,1/2)$	$N:(u,1/2,w)$	$Y:(0,1/2,0)$	yes	Plane
$R:(1/2,1/2,1/2)$	$W:(u,v,1/2)$	$Z:(0,0,1/2)$	no	Plane
$S:(1/2,1/2,0)$	$N:(u,1/2,w)$	$T:(0,1/2,1/2)$	yes	Plane
$S:(1/2,1/2,0)$	$N:(u,1/2,w)$	$Y:(0,1/2,0)$	yes	Plane
$T:(0,1/2,1/2)$	$W:(u,v,1/2)$	$U:(1/2,0,1/2)$	yes	Plane
$T:(0,1/2,1/2)$	$N:(u,1/2,w)$	$Y:(0,1/2,0)$	yes	Plane
$T:(0,1/2,1/2)$	$W:(u,v,1/2)$	$Z:(0,0,1/2)$	no	Plane
$U:(1/2,0,1/2)$	$W:(u,v,1/2)$	$Z:(0,0,1/2)$	no	Plane

BCSID: 0.85; Formula: KCo4(PO4)3; MSG: 58.398 ( $Pnn'm'$ ); U= 0				
maximal $k_1$	intermediate path	maximal $k_2$	satisfied?	Line/Plane
$\Gamma:(0,0,0)$	$SM:(u,0,0)$	$X:(1/2,0,0)$	yes	Line
$\Gamma:(0,0,0)$	$DT:(0,v,0)$	$Y:(0,1/2,0)$	yes	Line
$\Gamma:(0,0,0)$	$LD:(0,0,w)$	$Z:(0,0,1/2)$	yes	Line
$R:(1/2,1/2,1/2)$	$P:(1/2,v,1/2)$	$U:(1/2,0,1/2)$	yes	Line
$U:(1/2,0,1/2)$	$G:(1/2,0,w)$	$X:(1/2,0,0)$	yes	Line
$U:(1/2,0,1/2)$	$A:(u,0,1/2)$	$Z:(0,0,1/2)$	no	Line
$\Gamma:(0,0,0)$	$K:(0,v,w)$	$T:(0,1/2,1/2)$	yes	Plane
$\Gamma:(0,0,0)$	$K:(0,v,w)$	$Y:(0,1/2,0)$	yes	Plane

$\Gamma:(0,0,0)$	$K:(0,v,w)$	$Z:(0,0,1/2)$	yes	Plane
$R:(1/2,1/2,1/2)$	$L:(1/2,v,w)$	$S:(1/2,1/2,0)$	yes	Plane
$R:(1/2,1/2,1/2)$	$L:(1/2,v,w)$	$U:(1/2,0,1/2)$	yes	Plane
$R:(1/2,1/2,1/2)$	$L:(1/2,v,w)$	$X:(1/2,0,0)$	yes	Plane
$S:(1/2,1/2,0)$	$L:(1/2,v,w)$	$U:(1/2,0,1/2)$	yes	Plane
$S:(1/2,1/2,0)$	$L:(1/2,v,w)$	$X:(1/2,0,0)$	yes	Plane
$T:(0,1/2,1/2)$	$K:(0,v,w)$	$Y:(0,1/2,0)$	yes	Plane
$T:(0,1/2,1/2)$	$K:(0,v,w)$	$Z:(0,0,1/2)$	yes	Plane
$U:(1/2,0,1/2)$	$L:(1/2,v,w)$	$X:(1/2,0,0)$	yes	Plane
$Y:(0,1/2,0)$	$K:(0,v,w)$	$Z:(0,0,1/2)$	yes	Plane

BCSID: 0.187; Formula: CeMnAsO; MSG: 59.407 ( $Pm'mn$ ); U= 0				
maximal $k_1$	intermediate path	maximal $k_2$	satisfied?	Line/Plane
$R:(1/2,1/2,1/2)$	$Q:(1/2,1/2,w)$	$S:(1/2,1/2,0)$	yes	Line
$R:(1/2,1/2,1/2)$	$E:(u,1/2,1/2)$	$T:(0,1/2,1/2)$	no	Line
$S:(1/2,1/2,0)$	$C:(u,1/2,0)$	$Y:(0,1/2,0)$	no	Line
$T:(0,1/2,1/2)$	$H:(0,1/2,w)$	$Y:(0,1/2,0)$	yes	Line
$R:(1/2,1/2,1/2)$	$N:(u,1/2,w)$	$S:(1/2,1/2,0)$	yes	Plane
$R:(1/2,1/2,1/2)$	$N:(u,1/2,w)$	$T:(0,1/2,1/2)$	no	Plane
$R:(1/2,1/2,1/2)$	$N:(u,1/2,w)$	$Y:(0,1/2,0)$	no	Plane
$S:(1/2,1/2,0)$	$N:(u,1/2,w)$	$T:(0,1/2,1/2)$	no	Plane
$S:(1/2,1/2,0)$	$N:(u,1/2,w)$	$Y:(0,1/2,0)$	no	Plane
$T:(0,1/2,1/2)$	$N:(u,1/2,w)$	$Y:(0,1/2,0)$	yes	Plane

BCSID: 1.88; Formula: Mn5Si3; MSG: 60.431 ( $Pcbcn$ ); U= 1eV				
maximal $k_1$	intermediate path	maximal $k_2$	satisfied?	Line/Plane
$R:(1/2,1/2,1/2)$	$Q:(1/2,1/2,w)$	$S:(1/2,1/2,0)$	no	Line
$R:(1/2,1/2,1/2)$	$P:(1/2,v,1/2)$	$U:(1/2,0,1/2)$	yes	Line
$S:(1/2,1/2,0)$	$D:(1/2,v,0)$	$X:(1/2,0,0)$	yes	Line
$S:(1/2,1/2,0)$	$C:(u,1/2,0)$	$Y:(0,1/2,0)$	no	Line
$T:(0,1/2,1/2)$	$H:(0,1/2,w)$	$Y:(0,1/2,0)$	yes	Line
$U:(1/2,0,1/2)$	$A:(u,0,1/2)$	$Z:(0,0,1/2)$	yes	Line
$R:(1/2,1/2,1/2)$	$N:(u,1/2,w)$	$S:(1/2,1/2,0)$	no	Plane
$R:(1/2,1/2,1/2)$	$N:(u,1/2,w)$	$T:(0,1/2,1/2)$	yes	Plane
$R:(1/2,1/2,1/2)$	$W:(u,v,1/2)$	$T:(0,1/2,1/2)$	yes	Plane
$R:(1/2,1/2,1/2)$	$W:(u,v,1/2)$	$U:(1/2,0,1/2)$	yes	Plane
$R:(1/2,1/2,1/2)$	$N:(u,1/2,w)$	$Y:(0,1/2,0)$	yes	Plane
$R:(1/2,1/2,1/2)$	$W:(u,v,1/2)$	$Z:(0,0,1/2)$	yes	Plane
$S:(1/2,1/2,0)$	$N:(u,1/2,w)$	$T:(0,1/2,1/2)$	no	Plane
$S:(1/2,1/2,0)$	$N:(u,1/2,w)$	$Y:(0,1/2,0)$	no	Plane
$T:(0,1/2,1/2)$	$W:(u,v,1/2)$	$U:(1/2,0,1/2)$	yes	Plane
$T:(0,1/2,1/2)$	$N:(u,1/2,w)$	$Y:(0,1/2,0)$	yes	Plane
$T:(0,1/2,1/2)$	$W:(u,v,1/2)$	$Z:(0,0,1/2)$	yes	Plane
$U:(1/2,0,1/2)$	$W:(u,v,1/2)$	$Z:(0,0,1/2)$	yes	Plane

BCSID: 2.1; Formula: EuFe2As2; MSG: 61.439 ( $Pcbca$ ); U= 1eV				
maximal $k_1$	intermediate path	maximal $k_2$	satisfied?	Line/Plane
$R:(1/2,1/2,1/2)$	$Q:(1/2,1/2,w)$	$S:(1/2,1/2,0)$	yes	Line
$R:(1/2,1/2,1/2)$	$E:(u,1/2,1/2)$	$T:(0,1/2,1/2)$	yes	Line
$R:(1/2,1/2,1/2)$	$P:(1/2,v,1/2)$	$U:(1/2,0,1/2)$	yes	Line
$S:(1/2,1/2,0)$	$D:(1/2,v,0)$	$X:(1/2,0,0)$	yes	Line

T:(0,1/2,1/2)	H:(0,1/2,w)	Y:(0,1/2,0)	no	Line
U:(1/2,0,1/2)	A:(u,0,1/2)	Z:(0,0,1/2)	yes	Line
R:(1/2,1/2,1/2)	W:(u,v,1/2)	T:(0,1/2,1/2)	yes	Plane
R:(1/2,1/2,1/2)	W:(u,v,1/2)	U:(1/2,0,1/2)	yes	Plane
R:(1/2,1/2,1/2)	W:(u,v,1/2)	Z:(0,0,1/2)	yes	Plane
T:(0,1/2,1/2)	W:(u,v,1/2)	U:(1/2,0,1/2)	yes	Plane
T:(0,1/2,1/2)	W:(u,v,1/2)	Z:(0,0,1/2)	yes	Plane
U:(1/2,0,1/2)	W:(u,v,1/2)	Z:(0,0,1/2)	yes	Plane

BCSID: 0.218; Formula: Co2SiO4; MSG: 62.441 ( <i>Pnma</i> ); U = 0				
maximal $k_1$	intermediate path	maximal $k_2$	satisfied?	Line/Plane
R:(1/2,1/2,1/2)	Q:(1/2,1/2,w)	S:(1/2,1/2,0)	yes	Line
S:(1/2,1/2,0)	D:(1/2,v,0)	X:(1/2,0,0)	no	Line
T:(0,1/2,1/2)	H:(0,1/2,w)	Y:(0,1/2,0)	yes	Line
T:(0,1/2,1/2)	B:(0,v,1/2)	Z:(0,0,1/2)	yes	Line
$\Gamma$ :(0,0,0)	V:(u,v,0)	S:(1/2,1/2,0)	yes	Plane
$\Gamma$ :(0,0,0)	K:(0,v,w)	T:(0,1/2,1/2)	yes	Plane
$\Gamma$ :(0,0,0)	M:(u,0,w)	U:(1/2,0,1/2)	yes	Plane
$\Gamma$ :(0,0,0)	M:(u,0,w)	X:(1/2,0,0)	yes	Plane
$\Gamma$ :(0,0,0)	V:(u,v,0)	X:(1/2,0,0)	yes	Plane
$\Gamma$ :(0,0,0)	K:(0,v,w)	Y:(0,1/2,0)	yes	Plane
$\Gamma$ :(0,0,0)	V:(u,v,0)	Y:(0,1/2,0)	yes	Plane
$\Gamma$ :(0,0,0)	K:(0,v,w)	Z:(0,0,1/2)	yes	Plane
$\Gamma$ :(0,0,0)	M:(u,0,w)	Z:(0,0,1/2)	yes	Plane
R:(1/2,1/2,1/2)	L:(1/2,v,w)	S:(1/2,1/2,0)	yes	Plane
R:(1/2,1/2,1/2)	N:(u,1/2,w)	S:(1/2,1/2,0)	yes	Plane
R:(1/2,1/2,1/2)	N:(u,1/2,w)	T:(0,1/2,1/2)	yes	Plane
R:(1/2,1/2,1/2)	W:(u,v,1/2)	T:(0,1/2,1/2)	yes	Plane
R:(1/2,1/2,1/2)	L:(1/2,v,w)	U:(1/2,0,1/2)	yes	Plane
R:(1/2,1/2,1/2)	W:(u,v,1/2)	U:(1/2,0,1/2)	yes	Plane
R:(1/2,1/2,1/2)	L:(1/2,v,w)	X:(1/2,0,0)	yes	Plane
R:(1/2,1/2,1/2)	N:(u,1/2,w)	Y:(0,1/2,0)	yes	Plane
R:(1/2,1/2,1/2)	W:(u,v,1/2)	Z:(0,0,1/2)	yes	Plane
S:(1/2,1/2,0)	N:(u,1/2,w)	T:(0,1/2,1/2)	yes	Plane
S:(1/2,1/2,0)	L:(1/2,v,w)	U:(1/2,0,1/2)	yes	Plane
S:(1/2,1/2,0)	L:(1/2,v,w)	X:(1/2,0,0)	yes	Plane
S:(1/2,1/2,0)	V:(u,v,0)	X:(1/2,0,0)	yes	Plane
S:(1/2,1/2,0)	N:(u,1/2,w)	Y:(0,1/2,0)	yes	Plane
S:(1/2,1/2,0)	V:(u,v,0)	Y:(0,1/2,0)	yes	Plane
T:(0,1/2,1/2)	W:(u,v,1/2)	U:(1/2,0,1/2)	yes	Plane
T:(0,1/2,1/2)	K:(0,v,w)	Y:(0,1/2,0)	yes	Plane
T:(0,1/2,1/2)	N:(u,1/2,w)	Y:(0,1/2,0)	yes	Plane
T:(0,1/2,1/2)	K:(0,v,w)	Z:(0,0,1/2)	yes	Plane
T:(0,1/2,1/2)	W:(u,v,1/2)	Z:(0,0,1/2)	yes	Plane
U:(1/2,0,1/2)	L:(1/2,v,w)	X:(1/2,0,0)	yes	Plane
U:(1/2,0,1/2)	M:(u,0,w)	X:(1/2,0,0)	yes	Plane
U:(1/2,0,1/2)	M:(u,0,w)	Z:(0,0,1/2)	yes	Plane
U:(1/2,0,1/2)	W:(u,v,1/2)	Z:(0,0,1/2)	yes	Plane
X:(1/2,0,0)	V:(u,v,0)	Y:(0,1/2,0)	yes	Plane
X:(1/2,0,0)	M:(u,0,w)	Z:(0,0,1/2)	yes	Plane
Y:(0,1/2,0)	K:(0,v,w)	Z:(0,0,1/2)	yes	Plane

BCSID: 0.219; Formula: Co2SiO4; MSG: 62.441 ( <i>Pnma</i> ); U= 0				
maximal $k_1$	intermediate path	maximal $k_2$	satisfied?	Line/Plane
R:(1/2,1/2,1/2)	Q:(1/2,1/2,w)	S:(1/2,1/2,0)	yes	Line
S:(1/2,1/2,0)	D:(1/2,v,0)	X:(1/2,0,0)	no	Line
T:(0,1/2,1/2)	H:(0,1/2,w)	Y:(0,1/2,0)	yes	Line
T:(0,1/2,1/2)	B:(0,v,1/2)	Z:(0,0,1/2)	yes	Line
$\Gamma$ :(0,0,0)	V:(u,v,0)	S:(1/2,1/2,0)	yes	Plane
$\Gamma$ :(0,0,0)	K:(0,v,w)	T:(0,1/2,1/2)	yes	Plane
$\Gamma$ :(0,0,0)	M:(u,0,w)	U:(1/2,0,1/2)	yes	Plane
$\Gamma$ :(0,0,0)	M:(u,0,w)	X:(1/2,0,0)	yes	Plane
$\Gamma$ :(0,0,0)	V:(u,v,0)	X:(1/2,0,0)	yes	Plane
$\Gamma$ :(0,0,0)	K:(0,v,w)	Y:(0,1/2,0)	yes	Plane
$\Gamma$ :(0,0,0)	V:(u,v,0)	Y:(0,1/2,0)	yes	Plane
$\Gamma$ :(0,0,0)	K:(0,v,w)	Z:(0,0,1/2)	yes	Plane
$\Gamma$ :(0,0,0)	M:(u,0,w)	Z:(0,0,1/2)	yes	Plane
R:(1/2,1/2,1/2)	L:(1/2,v,w)	S:(1/2,1/2,0)	yes	Plane
R:(1/2,1/2,1/2)	N:(u,1/2,w)	S:(1/2,1/2,0)	yes	Plane
R:(1/2,1/2,1/2)	N:(u,1/2,w)	T:(0,1/2,1/2)	yes	Plane
R:(1/2,1/2,1/2)	W:(u,v,1/2)	T:(0,1/2,1/2)	yes	Plane
R:(1/2,1/2,1/2)	L:(1/2,v,w)	U:(1/2,0,1/2)	yes	Plane
R:(1/2,1/2,1/2)	W:(u,v,1/2)	U:(1/2,0,1/2)	yes	Plane
R:(1/2,1/2,1/2)	L:(1/2,v,w)	X:(1/2,0,0)	yes	Plane
R:(1/2,1/2,1/2)	N:(u,1/2,w)	Y:(0,1/2,0)	yes	Plane
R:(1/2,1/2,1/2)	W:(u,v,1/2)	Z:(0,0,1/2)	yes	Plane
S:(1/2,1/2,0)	N:(u,1/2,w)	T:(0,1/2,1/2)	yes	Plane
S:(1/2,1/2,0)	L:(1/2,v,w)	U:(1/2,0,1/2)	yes	Plane
S:(1/2,1/2,0)	L:(1/2,v,w)	X:(1/2,0,0)	yes	Plane
S:(1/2,1/2,0)	V:(u,v,0)	X:(1/2,0,0)	yes	Plane
S:(1/2,1/2,0)	N:(u,1/2,w)	Y:(0,1/2,0)	yes	Plane
S:(1/2,1/2,0)	V:(u,v,0)	Y:(0,1/2,0)	yes	Plane
T:(0,1/2,1/2)	W:(u,v,1/2)	U:(1/2,0,1/2)	yes	Plane
T:(0,1/2,1/2)	K:(0,v,w)	Y:(0,1/2,0)	yes	Plane
T:(0,1/2,1/2)	N:(u,1/2,w)	Y:(0,1/2,0)	yes	Plane
T:(0,1/2,1/2)	K:(0,v,w)	Z:(0,0,1/2)	yes	Plane
T:(0,1/2,1/2)	W:(u,v,1/2)	Z:(0,0,1/2)	yes	Plane
U:(1/2,0,1/2)	L:(1/2,v,w)	X:(1/2,0,0)	yes	Plane
U:(1/2,0,1/2)	M:(u,0,w)	X:(1/2,0,0)	yes	Plane
U:(1/2,0,1/2)	M:(u,0,w)	Z:(0,0,1/2)	yes	Plane
U:(1/2,0,1/2)	W:(u,v,1/2)	Z:(0,0,1/2)	yes	Plane
X:(1/2,0,0)	V:(u,v,0)	Y:(0,1/2,0)	yes	Plane
X:(1/2,0,0)	M:(u,0,w)	Z:(0,0,1/2)	yes	Plane
Y:(0,1/2,0)	K:(0,v,w)	Z:(0,0,1/2)	yes	Plane

BCSID: 0.219; Formula: Co2SiO4; MSG: 62.441 ( <i>Pnma</i> ); U= 1eV				
maximal $k_1$	intermediate path	maximal $k_2$	satisfied?	Line/Plane
R:(1/2,1/2,1/2)	Q:(1/2,1/2,w)	S:(1/2,1/2,0)	yes	Line
S:(1/2,1/2,0)	D:(1/2,v,0)	X:(1/2,0,0)	no	Line
T:(0,1/2,1/2)	H:(0,1/2,w)	Y:(0,1/2,0)	yes	Line
T:(0,1/2,1/2)	B:(0,v,1/2)	Z:(0,0,1/2)	yes	Line
$\Gamma$ :(0,0,0)	V:(u,v,0)	S:(1/2,1/2,0)	yes	Plane

$\Gamma:(0,0,0)$	$K:(0,v,w)$	$T:(0,1/2,1/2)$	yes	Plane
$\Gamma:(0,0,0)$	$M:(u,0,w)$	$U:(1/2,0,1/2)$	yes	Plane
$\Gamma:(0,0,0)$	$M:(u,0,w)$	$X:(1/2,0,0)$	yes	Plane
$\Gamma:(0,0,0)$	$V:(u,v,0)$	$X:(1/2,0,0)$	yes	Plane
$\Gamma:(0,0,0)$	$K:(0,v,w)$	$Y:(0,1/2,0)$	yes	Plane
$\Gamma:(0,0,0)$	$V:(u,v,0)$	$Y:(0,1/2,0)$	yes	Plane
$\Gamma:(0,0,0)$	$K:(0,v,w)$	$Z:(0,0,1/2)$	yes	Plane
$\Gamma:(0,0,0)$	$M:(u,0,w)$	$Z:(0,0,1/2)$	yes	Plane
$R:(1/2,1/2,1/2)$	$L:(1/2,v,w)$	$S:(1/2,1/2,0)$	yes	Plane
$R:(1/2,1/2,1/2)$	$N:(u,1/2,w)$	$S:(1/2,1/2,0)$	yes	Plane
$R:(1/2,1/2,1/2)$	$N:(u,1/2,w)$	$T:(0,1/2,1/2)$	yes	Plane
$R:(1/2,1/2,1/2)$	$W:(u,v,1/2)$	$T:(0,1/2,1/2)$	yes	Plane
$R:(1/2,1/2,1/2)$	$L:(1/2,v,w)$	$U:(1/2,0,1/2)$	yes	Plane
$R:(1/2,1/2,1/2)$	$W:(u,v,1/2)$	$U:(1/2,0,1/2)$	yes	Plane
$R:(1/2,1/2,1/2)$	$L:(1/2,v,w)$	$X:(1/2,0,0)$	yes	Plane
$R:(1/2,1/2,1/2)$	$N:(u,1/2,w)$	$Y:(0,1/2,0)$	yes	Plane
$R:(1/2,1/2,1/2)$	$W:(u,v,1/2)$	$Z:(0,0,1/2)$	yes	Plane
$S:(1/2,1/2,0)$	$N:(u,1/2,w)$	$T:(0,1/2,1/2)$	yes	Plane
$S:(1/2,1/2,0)$	$L:(1/2,v,w)$	$U:(1/2,0,1/2)$	yes	Plane
$S:(1/2,1/2,0)$	$L:(1/2,v,w)$	$X:(1/2,0,0)$	yes	Plane
$S:(1/2,1/2,0)$	$V:(u,v,0)$	$X:(1/2,0,0)$	yes	Plane
$S:(1/2,1/2,0)$	$N:(u,1/2,w)$	$Y:(0,1/2,0)$	yes	Plane
$S:(1/2,1/2,0)$	$V:(u,v,0)$	$Y:(0,1/2,0)$	yes	Plane
$T:(0,1/2,1/2)$	$W:(u,v,1/2)$	$U:(1/2,0,1/2)$	yes	Plane
$T:(0,1/2,1/2)$	$K:(0,v,w)$	$Y:(0,1/2,0)$	yes	Plane
$T:(0,1/2,1/2)$	$N:(u,1/2,w)$	$Y:(0,1/2,0)$	yes	Plane
$T:(0,1/2,1/2)$	$K:(0,v,w)$	$Z:(0,0,1/2)$	yes	Plane
$T:(0,1/2,1/2)$	$W:(u,v,1/2)$	$Z:(0,0,1/2)$	yes	Plane
$U:(1/2,0,1/2)$	$L:(1/2,v,w)$	$X:(1/2,0,0)$	yes	Plane
$U:(1/2,0,1/2)$	$M:(u,0,w)$	$X:(1/2,0,0)$	yes	Plane
$U:(1/2,0,1/2)$	$M:(u,0,w)$	$Z:(0,0,1/2)$	yes	Plane
$U:(1/2,0,1/2)$	$W:(u,v,1/2)$	$Z:(0,0,1/2)$	yes	Plane
$X:(1/2,0,0)$	$V:(u,v,0)$	$Y:(0,1/2,0)$	yes	Plane
$X:(1/2,0,0)$	$M:(u,0,w)$	$Z:(0,0,1/2)$	yes	Plane
$Y:(0,1/2,0)$	$K:(0,v,w)$	$Z:(0,0,1/2)$	yes	Plane

BCSID: 0.221; Formula: Fe2SiO4; MSG: 62.441 (*Pnma*); U= 0

maximal $k_1$	intermediate path	maximal $k_2$	satisfied?	Line/Plane
$R:(1/2,1/2,1/2)$	$Q:(1/2,1/2,w)$	$S:(1/2,1/2,0)$	yes	Line
$S:(1/2,1/2,0)$	$D:(1/2,v,0)$	$X:(1/2,0,0)$	no	Line
$T:(0,1/2,1/2)$	$H:(0,1/2,w)$	$Y:(0,1/2,0)$	yes	Line
$T:(0,1/2,1/2)$	$B:(0,v,1/2)$	$Z:(0,0,1/2)$	no	Line
$\Gamma:(0,0,0)$	$V:(u,v,0)$	$S:(1/2,1/2,0)$	yes	Plane
$\Gamma:(0,0,0)$	$K:(0,v,w)$	$T:(0,1/2,1/2)$	yes	Plane
$\Gamma:(0,0,0)$	$M:(u,0,w)$	$U:(1/2,0,1/2)$	yes	Plane
$\Gamma:(0,0,0)$	$M:(u,0,w)$	$X:(1/2,0,0)$	yes	Plane
$\Gamma:(0,0,0)$	$V:(u,v,0)$	$X:(1/2,0,0)$	yes	Plane
$\Gamma:(0,0,0)$	$K:(0,v,w)$	$Y:(0,1/2,0)$	yes	Plane
$\Gamma:(0,0,0)$	$V:(u,v,0)$	$Y:(0,1/2,0)$	yes	Plane
$\Gamma:(0,0,0)$	$K:(0,v,w)$	$Z:(0,0,1/2)$	yes	Plane
$\Gamma:(0,0,0)$	$M:(u,0,w)$	$Z:(0,0,1/2)$	yes	Plane

R:(1/2,1/2,1/2)	L:(1/2,v,w)	S:(1/2,1/2,0)	yes	Plane
R:(1/2,1/2,1/2)	N:(u,1/2,w)	S:(1/2,1/2,0)	yes	Plane
R:(1/2,1/2,1/2)	N:(u,1/2,w)	T:(0,1/2,1/2)	yes	Plane
R:(1/2,1/2,1/2)	W:(u,v,1/2)	T:(0,1/2,1/2)	yes	Plane
R:(1/2,1/2,1/2)	L:(1/2,v,w)	U:(1/2,0,1/2)	yes	Plane
R:(1/2,1/2,1/2)	W:(u,v,1/2)	U:(1/2,0,1/2)	yes	Plane
R:(1/2,1/2,1/2)	L:(1/2,v,w)	X:(1/2,0,0)	yes	Plane
R:(1/2,1/2,1/2)	N:(u,1/2,w)	Y:(0,1/2,0)	yes	Plane
R:(1/2,1/2,1/2)	W:(u,v,1/2)	Z:(0,0,1/2)	yes	Plane
S:(1/2,1/2,0)	N:(u,1/2,w)	T:(0,1/2,1/2)	yes	Plane
S:(1/2,1/2,0)	L:(1/2,v,w)	U:(1/2,0,1/2)	yes	Plane
S:(1/2,1/2,0)	L:(1/2,v,w)	X:(1/2,0,0)	yes	Plane
S:(1/2,1/2,0)	V:(u,v,0)	X:(1/2,0,0)	yes	Plane
S:(1/2,1/2,0)	N:(u,1/2,w)	Y:(0,1/2,0)	yes	Plane
S:(1/2,1/2,0)	V:(u,v,0)	Y:(0,1/2,0)	yes	Plane
T:(0,1/2,1/2)	W:(u,v,1/2)	U:(1/2,0,1/2)	yes	Plane
T:(0,1/2,1/2)	K:(0,v,w)	Y:(0,1/2,0)	yes	Plane
T:(0,1/2,1/2)	N:(u,1/2,w)	Y:(0,1/2,0)	yes	Plane
T:(0,1/2,1/2)	K:(0,v,w)	Z:(0,0,1/2)	yes	Plane
T:(0,1/2,1/2)	W:(u,v,1/2)	Z:(0,0,1/2)	yes	Plane
U:(1/2,0,1/2)	L:(1/2,v,w)	X:(1/2,0,0)	yes	Plane
U:(1/2,0,1/2)	M:(u,0,w)	X:(1/2,0,0)	yes	Plane
U:(1/2,0,1/2)	M:(u,0,w)	Z:(0,0,1/2)	yes	Plane
U:(1/2,0,1/2)	W:(u,v,1/2)	Z:(0,0,1/2)	yes	Plane
X:(1/2,0,0)	V:(u,v,0)	Y:(0,1/2,0)	yes	Plane
X:(1/2,0,0)	M:(u,0,w)	Z:(0,0,1/2)	yes	Plane
Y:(0,1/2,0)	K:(0,v,w)	Z:(0,0,1/2)	yes	Plane

BCSID: 0.185; Formula: Nd5Ge4; MSG: 62.447 ( $Pnm'a'$ ); U= 0				
maximal $k_1$	intermediate path	maximal $k_2$	satisfied?	Line/Plane
$\Gamma:(0,0,0)$	SM:(u,0,0)	X:(1/2,0,0)	no	Line
$\Gamma:(0,0,0)$	DT:(0,v,0)	Y:(0,1/2,0)	yes	Line
$\Gamma:(0,0,0)$	LD:(0,0,w)	Z:(0,0,1/2)	yes	Line
R:(1/2,1/2,1/2)	Q:(1/2,1/2,w)	S:(1/2,1/2,0)	yes	Line
R:(1/2,1/2,1/2)	E:(u,1/2,1/2)	T:(0,1/2,1/2)	yes	Line
S:(1/2,1/2,0)	D:(1/2,v,0)	X:(1/2,0,0)	yes	Line
$\Gamma:(0,0,0)$	K:(0,v,w)	T:(0,1/2,1/2)	yes	Plane
$\Gamma:(0,0,0)$	K:(0,v,w)	Y:(0,1/2,0)	yes	Plane
$\Gamma:(0,0,0)$	K:(0,v,w)	Z:(0,0,1/2)	yes	Plane
R:(1/2,1/2,1/2)	L:(1/2,v,w)	S:(1/2,1/2,0)	yes	Plane
R:(1/2,1/2,1/2)	L:(1/2,v,w)	U:(1/2,0,1/2)	yes	Plane
R:(1/2,1/2,1/2)	L:(1/2,v,w)	X:(1/2,0,0)	yes	Plane
S:(1/2,1/2,0)	L:(1/2,v,w)	U:(1/2,0,1/2)	yes	Plane
S:(1/2,1/2,0)	L:(1/2,v,w)	X:(1/2,0,0)	yes	Plane
T:(0,1/2,1/2)	K:(0,v,w)	Y:(0,1/2,0)	yes	Plane
T:(0,1/2,1/2)	K:(0,v,w)	Z:(0,0,1/2)	yes	Plane
U:(1/2,0,1/2)	L:(1/2,v,w)	X:(1/2,0,0)	yes	Plane
Y:(0,1/2,0)	K:(0,v,w)	Z:(0,0,1/2)	yes	Plane

BCSID: 1.131; Formula: Fe2As; MSG: 62.450 ( $P_anma$ ); U= 2eV				
maximal $k_1$	intermediate path	maximal $k_2$	satisfied?	Line/Plane

R:(1/2,1/2,1/2)	Q:(1/2,1/2,w)	S:(1/2,1/2,0)	yes	Line
S:(1/2,1/2,0)	D:(1/2,v,0)	X:(1/2,0,0)	no	Line
T:(0,1/2,1/2)	H:(0,1/2,w)	Y:(0,1/2,0)	yes	Line
T:(0,1/2,1/2)	B:(0,v,1/2)	Z:(0,0,1/2)	yes	Line
R:(1/2,1/2,1/2)	N:(u,1/2,w)	S:(1/2,1/2,0)	yes	Plane
R:(1/2,1/2,1/2)	N:(u,1/2,w)	T:(0,1/2,1/2)	yes	Plane
R:(1/2,1/2,1/2)	W:(u,v,1/2)	T:(0,1/2,1/2)	yes	Plane
R:(1/2,1/2,1/2)	W:(u,v,1/2)	U:(1/2,0,1/2)	yes	Plane
R:(1/2,1/2,1/2)	N:(u,1/2,w)	Y:(0,1/2,0)	yes	Plane
R:(1/2,1/2,1/2)	W:(u,v,1/2)	Z:(0,0,1/2)	yes	Plane
S:(1/2,1/2,0)	N:(u,1/2,w)	T:(0,1/2,1/2)	yes	Plane
S:(1/2,1/2,0)	N:(u,1/2,w)	Y:(0,1/2,0)	yes	Plane
T:(0,1/2,1/2)	W:(u,v,1/2)	U:(1/2,0,1/2)	yes	Plane
T:(0,1/2,1/2)	N:(u,1/2,w)	Y:(0,1/2,0)	yes	Plane
T:(0,1/2,1/2)	W:(u,v,1/2)	Z:(0,0,1/2)	yes	Plane
U:(1/2,0,1/2)	W:(u,v,1/2)	Z:(0,0,1/2)	yes	Plane

BCSID: 1.132; Formula: Mn2As; MSG: 62.450 ( $P_{anma}$ ); U= 0				
maximal $k_1$	intermediate path	maximal $k_2$	satisfied?	Line/Plane
R:(1/2,1/2,1/2)	Q:(1/2,1/2,w)	S:(1/2,1/2,0)	yes	Line
S:(1/2,1/2,0)	D:(1/2,v,0)	X:(1/2,0,0)	no	Line
T:(0,1/2,1/2)	H:(0,1/2,w)	Y:(0,1/2,0)	yes	Line
T:(0,1/2,1/2)	B:(0,v,1/2)	Z:(0,0,1/2)	yes	Line
R:(1/2,1/2,1/2)	N:(u,1/2,w)	S:(1/2,1/2,0)	yes	Plane
R:(1/2,1/2,1/2)	N:(u,1/2,w)	T:(0,1/2,1/2)	yes	Plane
R:(1/2,1/2,1/2)	W:(u,v,1/2)	T:(0,1/2,1/2)	yes	Plane
R:(1/2,1/2,1/2)	W:(u,v,1/2)	U:(1/2,0,1/2)	yes	Plane
R:(1/2,1/2,1/2)	N:(u,1/2,w)	Y:(0,1/2,0)	yes	Plane
R:(1/2,1/2,1/2)	W:(u,v,1/2)	Z:(0,0,1/2)	yes	Plane
S:(1/2,1/2,0)	N:(u,1/2,w)	T:(0,1/2,1/2)	yes	Plane
S:(1/2,1/2,0)	N:(u,1/2,w)	Y:(0,1/2,0)	yes	Plane
T:(0,1/2,1/2)	W:(u,v,1/2)	U:(1/2,0,1/2)	yes	Plane
T:(0,1/2,1/2)	N:(u,1/2,w)	Y:(0,1/2,0)	yes	Plane
T:(0,1/2,1/2)	W:(u,v,1/2)	Z:(0,0,1/2)	yes	Plane
U:(1/2,0,1/2)	W:(u,v,1/2)	Z:(0,0,1/2)	yes	Plane

BCSID: 1.132; Formula: Mn2As; MSG: 62.450 ( $P_{anma}$ ); U= 1eV				
maximal $k_1$	intermediate path	maximal $k_2$	satisfied?	Line/Plane
R:(1/2,1/2,1/2)	Q:(1/2,1/2,w)	S:(1/2,1/2,0)	yes	Line
S:(1/2,1/2,0)	D:(1/2,v,0)	X:(1/2,0,0)	no	Line
T:(0,1/2,1/2)	H:(0,1/2,w)	Y:(0,1/2,0)	yes	Line
T:(0,1/2,1/2)	B:(0,v,1/2)	Z:(0,0,1/2)	yes	Line
R:(1/2,1/2,1/2)	N:(u,1/2,w)	S:(1/2,1/2,0)	yes	Plane
R:(1/2,1/2,1/2)	N:(u,1/2,w)	T:(0,1/2,1/2)	yes	Plane
R:(1/2,1/2,1/2)	W:(u,v,1/2)	T:(0,1/2,1/2)	yes	Plane
R:(1/2,1/2,1/2)	W:(u,v,1/2)	U:(1/2,0,1/2)	yes	Plane
R:(1/2,1/2,1/2)	N:(u,1/2,w)	Y:(0,1/2,0)	yes	Plane
R:(1/2,1/2,1/2)	W:(u,v,1/2)	Z:(0,0,1/2)	yes	Plane
S:(1/2,1/2,0)	N:(u,1/2,w)	T:(0,1/2,1/2)	yes	Plane
S:(1/2,1/2,0)	N:(u,1/2,w)	Y:(0,1/2,0)	yes	Plane
T:(0,1/2,1/2)	W:(u,v,1/2)	U:(1/2,0,1/2)	yes	Plane
T:(0,1/2,1/2)	N:(u,1/2,w)	Y:(0,1/2,0)	yes	Plane
T:(0,1/2,1/2)	W:(u,v,1/2)	Z:(0,0,1/2)	yes	Plane
U:(1/2,0,1/2)	W:(u,v,1/2)	Z:(0,0,1/2)	yes	Plane

T:(0,1/2,1/2)	N:(u,1/2,w)	Y:(0,1/2,0)	yes	Plane
T:(0,1/2,1/2)	W:(u,v,1/2)	Z:(0,0,1/2)	yes	Plane
U:(1/2,0,1/2)	W:(u,v,1/2)	Z:(0,0,1/2)	yes	Plane

BCSID: 1.132; Formula: Mn2As; MSG: 62.450 ( $P_{anma}$ ); U= 2eV				
maximal $k_1$	intermediate path	maximal $k_2$	satisfied?	Line/Plane
R:(1/2,1/2,1/2)	Q:(1/2,1/2,w)	S:(1/2,1/2,0)	yes	Line
S:(1/2,1/2,0)	D:(1/2,v,0)	X:(1/2,0,0)	no	Line
T:(0,1/2,1/2)	H:(0,1/2,w)	Y:(0,1/2,0)	yes	Line
T:(0,1/2,1/2)	B:(0,v,1/2)	Z:(0,0,1/2)	yes	Line
R:(1/2,1/2,1/2)	N:(u,1/2,w)	S:(1/2,1/2,0)	yes	Plane
R:(1/2,1/2,1/2)	N:(u,1/2,w)	T:(0,1/2,1/2)	yes	Plane
R:(1/2,1/2,1/2)	W:(u,v,1/2)	T:(0,1/2,1/2)	yes	Plane
R:(1/2,1/2,1/2)	W:(u,v,1/2)	U:(1/2,0,1/2)	yes	Plane
R:(1/2,1/2,1/2)	N:(u,1/2,w)	Y:(0,1/2,0)	yes	Plane
R:(1/2,1/2,1/2)	W:(u,v,1/2)	Z:(0,0,1/2)	yes	Plane
S:(1/2,1/2,0)	N:(u,1/2,w)	T:(0,1/2,1/2)	yes	Plane
S:(1/2,1/2,0)	N:(u,1/2,w)	Y:(0,1/2,0)	yes	Plane
T:(0,1/2,1/2)	W:(u,v,1/2)	U:(1/2,0,1/2)	yes	Plane
T:(0,1/2,1/2)	N:(u,1/2,w)	Y:(0,1/2,0)	yes	Plane
T:(0,1/2,1/2)	W:(u,v,1/2)	Z:(0,0,1/2)	yes	Plane
U:(1/2,0,1/2)	W:(u,v,1/2)	Z:(0,0,1/2)	yes	Plane

BCSID: 1.132; Formula: Mn2As; MSG: 62.450 ( $P_{anma}$ ); U= 3eV				
maximal $k_1$	intermediate path	maximal $k_2$	satisfied?	Line/Plane
R:(1/2,1/2,1/2)	Q:(1/2,1/2,w)	S:(1/2,1/2,0)	yes	Line
S:(1/2,1/2,0)	D:(1/2,v,0)	X:(1/2,0,0)	no	Line
T:(0,1/2,1/2)	H:(0,1/2,w)	Y:(0,1/2,0)	yes	Line
T:(0,1/2,1/2)	B:(0,v,1/2)	Z:(0,0,1/2)	yes	Line
R:(1/2,1/2,1/2)	N:(u,1/2,w)	S:(1/2,1/2,0)	yes	Plane
R:(1/2,1/2,1/2)	N:(u,1/2,w)	T:(0,1/2,1/2)	yes	Plane
R:(1/2,1/2,1/2)	W:(u,v,1/2)	T:(0,1/2,1/2)	yes	Plane
R:(1/2,1/2,1/2)	W:(u,v,1/2)	U:(1/2,0,1/2)	yes	Plane
R:(1/2,1/2,1/2)	N:(u,1/2,w)	Y:(0,1/2,0)	yes	Plane
R:(1/2,1/2,1/2)	W:(u,v,1/2)	Z:(0,0,1/2)	yes	Plane
S:(1/2,1/2,0)	N:(u,1/2,w)	T:(0,1/2,1/2)	yes	Plane
S:(1/2,1/2,0)	N:(u,1/2,w)	Y:(0,1/2,0)	yes	Plane
T:(0,1/2,1/2)	W:(u,v,1/2)	U:(1/2,0,1/2)	yes	Plane
T:(0,1/2,1/2)	N:(u,1/2,w)	Y:(0,1/2,0)	yes	Plane
T:(0,1/2,1/2)	W:(u,v,1/2)	Z:(0,0,1/2)	yes	Plane
U:(1/2,0,1/2)	W:(u,v,1/2)	Z:(0,0,1/2)	yes	Plane

BCSID: 1.179; Formula: NdCoAsO; MSG: 62.450 ( $P_{anma}$ ); U= 4eV				
maximal $k_1$	intermediate path	maximal $k_2$	satisfied?	Line/Plane
R:(1/2,1/2,1/2)	Q:(1/2,1/2,w)	S:(1/2,1/2,0)	yes	Line
S:(1/2,1/2,0)	D:(1/2,v,0)	X:(1/2,0,0)	no	Line
T:(0,1/2,1/2)	H:(0,1/2,w)	Y:(0,1/2,0)	yes	Line
T:(0,1/2,1/2)	B:(0,v,1/2)	Z:(0,0,1/2)	yes	Line
R:(1/2,1/2,1/2)	N:(u,1/2,w)	S:(1/2,1/2,0)	yes	Plane
R:(1/2,1/2,1/2)	N:(u,1/2,w)	T:(0,1/2,1/2)	yes	Plane
R:(1/2,1/2,1/2)	W:(u,v,1/2)	T:(0,1/2,1/2)	yes	Plane

R:(1/2,1/2,1/2)	W:(u,v,1/2)	U:(1/2,0,1/2)	yes	Plane
R:(1/2,1/2,1/2)	N:(u,1/2,w)	Y:(0,1/2,0)	yes	Plane
R:(1/2,1/2,1/2)	W:(u,v,1/2)	Z:(0,0,1/2)	yes	Plane
S:(1/2,1/2,0)	N:(u,1/2,w)	T:(0,1/2,1/2)	yes	Plane
S:(1/2,1/2,0)	N:(u,1/2,w)	Y:(0,1/2,0)	yes	Plane
T:(0,1/2,1/2)	W:(u,v,1/2)	U:(1/2,0,1/2)	yes	Plane
T:(0,1/2,1/2)	N:(u,1/2,w)	Y:(0,1/2,0)	yes	Plane
T:(0,1/2,1/2)	W:(u,v,1/2)	Z:(0,0,1/2)	yes	Plane
U:(1/2,0,1/2)	W:(u,v,1/2)	Z:(0,0,1/2)	yes	Plane

BCSID: 1.179; Formula: NdCoAsO; MSG: 62.450 ( $P_a nma$ ); U= 6eV				
maximal $k_1$	intermediate path	maximal $k_2$	satisfied?	Line/Plane
R:(1/2,1/2,1/2)	Q:(1/2,1/2,w)	S:(1/2,1/2,0)	yes	Line
S:(1/2,1/2,0)	D:(1/2,v,0)	X:(1/2,0,0)	no	Line
T:(0,1/2,1/2)	H:(0,1/2,w)	Y:(0,1/2,0)	yes	Line
T:(0,1/2,1/2)	B:(0,v,1/2)	Z:(0,0,1/2)	yes	Line
R:(1/2,1/2,1/2)	N:(u,1/2,w)	S:(1/2,1/2,0)	yes	Plane
R:(1/2,1/2,1/2)	N:(u,1/2,w)	T:(0,1/2,1/2)	yes	Plane
R:(1/2,1/2,1/2)	W:(u,v,1/2)	T:(0,1/2,1/2)	yes	Plane
R:(1/2,1/2,1/2)	W:(u,v,1/2)	U:(1/2,0,1/2)	yes	Plane
R:(1/2,1/2,1/2)	N:(u,1/2,w)	Y:(0,1/2,0)	yes	Plane
R:(1/2,1/2,1/2)	W:(u,v,1/2)	Z:(0,0,1/2)	yes	Plane
S:(1/2,1/2,0)	N:(u,1/2,w)	T:(0,1/2,1/2)	yes	Plane
S:(1/2,1/2,0)	N:(u,1/2,w)	Y:(0,1/2,0)	yes	Plane
T:(0,1/2,1/2)	W:(u,v,1/2)	U:(1/2,0,1/2)	yes	Plane
T:(0,1/2,1/2)	N:(u,1/2,w)	Y:(0,1/2,0)	yes	Plane
T:(0,1/2,1/2)	W:(u,v,1/2)	Z:(0,0,1/2)	yes	Plane
U:(1/2,0,1/2)	W:(u,v,1/2)	Z:(0,0,1/2)	yes	Plane

BCSID: 0.149; Formula: Nd <sub>3</sub> Ru <sub>4</sub> Al <sub>12</sub> ; MSG: 63.462 ( $Cm'c'm$ ); U= 2eV				
maximal $k_1$	intermediate path	maximal $k_2$	satisfied?	Line/Plane
$\Gamma:(0,0,0)$	DT:(0,v,0)	Y:(0,1,0)	yes	Line
$\Gamma:(0,0,0)$	SM:(u,0,0)	Y:(1,0,0)	yes	Line
$\Gamma:(0,0,0)$	LD:(0,0,w)	Z:(0,0,1/2)	no	Line
T:(1,0,1/2)	H:(1,0,w)	Y:(1,0,0)	yes	Line
T:(1,0,1/2)	A:(u,0,1/2)	Z:(0,0,1/2)	yes	Line
R:(1/2,1/2,-1/2)	D:(1/2,1/2,w)	S:(1/2,1/2,0)	yes	Line
RA:(1/2,-1/2,-1/2)	DA:(1/2,-1/2,w)	SA:(1/2,-1/2,0)	yes	Line
$\Gamma:(0,0,0)$	P:(u,v,0)	Y:(0,1,0)	yes	Plane
$\Gamma:(0,0,0)$	P:(u,v,0)	S:(1/2,1/2,0)	yes	Plane
$\Gamma:(0,0,0)$	P:(u,v,0)	SA:(-1/2,1/2,0)	yes	Plane
T:(1,0,1/2)	Q:(u,v,1/2)	Z:(0,0,1/2)	yes	Plane
T:(1,0,1/2)	Q:(u,v,1/2)	R:(1/2,1/2,1/2)	yes	Plane
T:(1,0,1/2)	Q:(u,v,1/2)	RA:(1/2,-1/2,1/2)	yes	Plane
Y:(1,0,0)	P:(u,v,0)	S:(1/2,1/2,0)	yes	Plane
Y:(1,0,0)	P:(u,v,0)	SA:(1/2,-1/2,0)	yes	Plane
Z:(0,0,1/2)	Q:(u,v,1/2)	R:(1/2,1/2,1/2)	yes	Plane
Z:(0,0,1/2)	Q:(u,v,1/2)	RA:(-1/2,1/2,1/2)	yes	Plane
R:(1/2,1/2,1/2)	Q:(u,v,1/2)	RA:(-1/2,1/2,1/2)	yes	Plane
S:(1/2,1/2,0)	P:(u,v,0)	SA:(-1/2,1/2,0)	yes	Plane

BCSID: 0.149; Formula: Nd <sub>3</sub> Ru <sub>4</sub> Al <sub>12</sub> ; MSG: 63.462 ( $Cm'c'm$ ); U= 6eV				
maximal $k_1$	intermediate path	maximal $k_2$	satisfied?	Line/Plane
$\Gamma:(0,0,0)$	DT:(0,v,0)	Y:(0,1,0)	yes	Line
$\Gamma:(0,0,0)$	SM:(u,0,0)	Y:(1,0,0)	yes	Line
$\Gamma:(0,0,0)$	LD:(0,0,w)	Z:(0,0,1/2)	no	Line
T:(1,0,1/2)	H:(1,0,w)	Y:(1,0,0)	yes	Line
T:(1,0,1/2)	A:(u,0,1/2)	Z:(0,0,1/2)	yes	Line
R:(1/2,1/2,-1/2)	D:(1/2,1/2,w)	S:(1/2,1/2,0)	yes	Line
RA:(1/2,-1/2,-1/2)	DA:(1/2,-1/2,w)	SA:(1/2,-1/2,0)	yes	Line
$\Gamma:(0,0,0)$	P:(u,v,0)	Y:(0,1,0)	yes	Plane
$\Gamma:(0,0,0)$	P:(u,v,0)	S:(1/2,1/2,0)	yes	Plane
$\Gamma:(0,0,0)$	P:(u,v,0)	SA:(-1/2,1/2,0)	yes	Plane
T:(1,0,1/2)	Q:(u,v,1/2)	Z:(0,0,1/2)	yes	Plane
T:(1,0,1/2)	Q:(u,v,1/2)	R:(1/2,1/2,1/2)	yes	Plane
T:(1,0,1/2)	Q:(u,v,1/2)	RA:(1/2,-1/2,1/2)	yes	Plane
Y:(1,0,0)	P:(u,v,0)	S:(1/2,1/2,0)	yes	Plane
Y:(1,0,0)	P:(u,v,0)	SA:(1/2,-1/2,0)	yes	Plane
Z:(0,0,1/2)	Q:(u,v,1/2)	R:(1/2,1/2,1/2)	yes	Plane
Z:(0,0,1/2)	Q:(u,v,1/2)	RA:(-1/2,1/2,1/2)	yes	Plane
R:(1/2,1/2,1/2)	Q:(u,v,1/2)	RA:(-1/2,1/2,1/2)	yes	Plane
S:(1/2,1/2,0)	P:(u,v,0)	SA:(-1/2,1/2,0)	yes	Plane

BCSID: 0.173; Formula: Pr <sub>3</sub> Ru <sub>4</sub> Al <sub>12</sub> ; MSG: 63.462 ( $Cm'c'm$ ); U= 2eV				
maximal $k_1$	intermediate path	maximal $k_2$	satisfied?	Line/Plane
$\Gamma:(0,0,0)$	DT:(0,v,0)	Y:(0,1,0)	yes	Line
$\Gamma:(0,0,0)$	SM:(u,0,0)	Y:(1,0,0)	yes	Line
$\Gamma:(0,0,0)$	LD:(0,0,w)	Z:(0,0,1/2)	no	Line
T:(1,0,1/2)	H:(1,0,w)	Y:(1,0,0)	yes	Line
T:(1,0,1/2)	A:(u,0,1/2)	Z:(0,0,1/2)	yes	Line
R:(1/2,1/2,-1/2)	D:(1/2,1/2,w)	S:(1/2,1/2,0)	yes	Line
RA:(1/2,-1/2,-1/2)	DA:(1/2,-1/2,w)	SA:(1/2,-1/2,0)	yes	Line
$\Gamma:(0,0,0)$	P:(u,v,0)	Y:(0,1,0)	yes	Plane
$\Gamma:(0,0,0)$	P:(u,v,0)	S:(1/2,1/2,0)	yes	Plane
$\Gamma:(0,0,0)$	P:(u,v,0)	SA:(-1/2,1/2,0)	yes	Plane
T:(1,0,1/2)	Q:(u,v,1/2)	Z:(0,0,1/2)	yes	Plane
T:(1,0,1/2)	Q:(u,v,1/2)	R:(1/2,1/2,1/2)	yes	Plane
T:(1,0,1/2)	Q:(u,v,1/2)	RA:(1/2,-1/2,1/2)	yes	Plane
Y:(1,0,0)	P:(u,v,0)	S:(1/2,1/2,0)	yes	Plane
Y:(1,0,0)	P:(u,v,0)	SA:(1/2,-1/2,0)	yes	Plane
Z:(0,0,1/2)	Q:(u,v,1/2)	R:(1/2,1/2,1/2)	yes	Plane
Z:(0,0,1/2)	Q:(u,v,1/2)	RA:(-1/2,1/2,1/2)	yes	Plane
R:(1/2,1/2,1/2)	Q:(u,v,1/2)	RA:(-1/2,1/2,1/2)	yes	Plane
S:(1/2,1/2,0)	P:(u,v,0)	SA:(-1/2,1/2,0)	yes	Plane

BCSID: 0.173; Formula: Pr <sub>3</sub> Ru <sub>4</sub> Al <sub>12</sub> ; MSG: 63.462 ( $Cm'c'm$ ); U= 4eV				
maximal $k_1$	intermediate path	maximal $k_2$	satisfied?	Line/Plane
$\Gamma:(0,0,0)$	DT:(0,v,0)	Y:(0,1,0)	yes	Line
$\Gamma:(0,0,0)$	SM:(u,0,0)	Y:(1,0,0)	yes	Line
$\Gamma:(0,0,0)$	LD:(0,0,w)	Z:(0,0,1/2)	no	Line
T:(1,0,1/2)	H:(1,0,w)	Y:(1,0,0)	yes	Line
T:(1,0,1/2)	A:(u,0,1/2)	Z:(0,0,1/2)	yes	Line

R:(1/2,1/2,-1/2)	D:(1/2,1/2,w)	S:(1/2,1/2,0)	yes	Line
RA:(1/2,-1/2,-1/2)	DA:(1/2,-1/2,w)	SA:(1/2,-1/2,0)	yes	Line
$\Gamma:(0,0,0)$	P:(u,v,0)	Y:(0,1,0)	yes	Plane
$\Gamma:(0,0,0)$	P:(u,v,0)	S:(1/2,1/2,0)	yes	Plane
$\Gamma:(0,0,0)$	P:(u,v,0)	SA:(-1/2,1/2,0)	yes	Plane
T:(1,0,1/2)	Q:(u,v,1/2)	Z:(0,0,1/2)	yes	Plane
T:(1,0,1/2)	Q:(u,v,1/2)	R:(1/2,1/2,1/2)	yes	Plane
T:(1,0,1/2)	Q:(u,v,1/2)	RA:(1/2,-1/2,1/2)	yes	Plane
Y:(1,0,0)	P:(u,v,0)	S:(1/2,1/2,0)	yes	Plane
Y:(1,0,0)	P:(u,v,0)	SA:(1/2,-1/2,0)	yes	Plane
Z:(0,0,1/2)	Q:(u,v,1/2)	R:(1/2,1/2,1/2)	yes	Plane
Z:(0,0,1/2)	Q:(u,v,1/2)	RA:(-1/2,1/2,1/2)	yes	Plane
R:(1/2,1/2,1/2)	Q:(u,v,1/2)	RA:(-1/2,1/2,1/2)	yes	Plane
S:(1/2,1/2,0)	P:(u,v,0)	SA:(-1/2,1/2,0)	yes	Plane

BCSID: 0.173; Formula: Pr3Ru4Al12; MSG: 63.462 ( $Cm'c'm$ ); U= 6eV				
maximal $k_1$	intermediate path	maximal $k_2$	satisfied?	Line/Plane
$\Gamma:(0,0,0)$	DT:(0,v,0)	Y:(0,1,0)	yes	Line
$\Gamma:(0,0,0)$	SM:(u,0,0)	Y:(1,0,0)	yes	Line
$\Gamma:(0,0,0)$	LD:(0,0,w)	Z:(0,0,1/2)	no	Line
T:(1,0,1/2)	H:(1,0,w)	Y:(1,0,0)	yes	Line
T:(1,0,1/2)	A:(u,0,1/2)	Z:(0,0,1/2)	yes	Line
R:(1/2,1/2,-1/2)	D:(1/2,1/2,w)	S:(1/2,1/2,0)	yes	Line
RA:(1/2,-1/2,-1/2)	DA:(1/2,-1/2,w)	SA:(1/2,-1/2,0)	yes	Line
$\Gamma:(0,0,0)$	P:(u,v,0)	Y:(0,1,0)	yes	Plane
$\Gamma:(0,0,0)$	P:(u,v,0)	S:(1/2,1/2,0)	yes	Plane
$\Gamma:(0,0,0)$	P:(u,v,0)	SA:(-1/2,1/2,0)	yes	Plane
T:(1,0,1/2)	Q:(u,v,1/2)	Z:(0,0,1/2)	yes	Plane
T:(1,0,1/2)	Q:(u,v,1/2)	R:(1/2,1/2,1/2)	yes	Plane
T:(1,0,1/2)	Q:(u,v,1/2)	RA:(1/2,-1/2,1/2)	yes	Plane
Y:(1,0,0)	P:(u,v,0)	S:(1/2,1/2,0)	yes	Plane
Y:(1,0,0)	P:(u,v,0)	SA:(1/2,-1/2,0)	yes	Plane
Z:(0,0,1/2)	Q:(u,v,1/2)	R:(1/2,1/2,1/2)	yes	Plane
Z:(0,0,1/2)	Q:(u,v,1/2)	RA:(-1/2,1/2,1/2)	yes	Plane
R:(1/2,1/2,1/2)	Q:(u,v,1/2)	RA:(-1/2,1/2,1/2)	yes	Plane
S:(1/2,1/2,0)	P:(u,v,0)	SA:(-1/2,1/2,0)	yes	Plane

BCSID: 0.199; Formula: Mn3Sn; MSG: 63.463 ( $Cmc'm'$ ); U= 0				
maximal $k_1$	intermediate path	maximal $k_2$	satisfied?	Line/Plane
$\Gamma:(0,0,0)$	DT:(0,v,0)	Y:(0,1,0)	yes	Line
$\Gamma:(0,0,0)$	SM:(u,0,0)	Y:(1,0,0)	no	Line
$\Gamma:(0,0,0)$	LD:(0,0,w)	Z:(0,0,1/2)	no	Line
T:(1,0,1/2)	H:(1,0,w)	Y:(1,0,0)	no	Line
T:(0,1,1/2)	B:(0,v,1/2)	Z:(0,0,1/2)	no	Line
$\Gamma:(0,0,0)$	K:(0,v,w)	T:(0,1,1/2)	no	Plane
$\Gamma:(0,0,0)$	K:(0,v,w)	Y:(0,1,0)	yes	Plane
$\Gamma:(0,0,0)$	K:(0,v,w)	Z:(0,0,1/2)	no	Plane
T:(0,1,1/2)	K:(0,v,w)	Y:(0,1,0)	no	Plane
T:(0,1,1/2)	K:(0,v,w)	Z:(0,0,1/2)	no	Plane
Y:(0,1,0)	K:(0,v,w)	Z:(0,0,1/2)	no	Plane

BCSID: 3.3; Formula: Ho2RhIn8; MSG: 63.464 ( $Cm'cm'$ ); U= 0				
maximal $k_1$	intermediate path	maximal $k_2$	satisfied?	Line/Plane
$\Gamma:(0,0,0)$	DT:(0,v,0)	Y:(0,1,0)	no	Line
$\Gamma:(0,0,0)$	SM:(u,0,0)	Y:(1,0,0)	yes	Line
$\Gamma:(0,0,0)$	LD:(0,0,w)	Z:(0,0,1/2)	yes	Line
T:(1,0,1/2)	H:(1,0,w)	Y:(1,0,0)	yes	Line
$\Gamma:(0,0,0)$	M:(u,0,w)	T:(1,0,1/2)	yes	Plane
$\Gamma:(0,0,0)$	M:(u,0,w)	Y:(1,0,0)	yes	Plane
$\Gamma:(0,0,0)$	M:(u,0,w)	Z:(0,0,1/2)	yes	Plane
T:(1,0,1/2)	M:(u,0,w)	Y:(1,0,0)	yes	Plane
T:(1,0,1/2)	M:(u,0,w)	Z:(0,0,1/2)	yes	Plane
Y:(1,0,0)	M:(u,0,w)	Z:(0,0,1/2)	yes	Plane

BCSID: 3.3; Formula: Ho2RhIn8; MSG: 63.464 ( $Cm'cm'$ ); U= 1eV				
maximal $k_1$	intermediate path	maximal $k_2$	satisfied?	Line/Plane
$\Gamma:(0,0,0)$	DT:(0,v,0)	Y:(0,1,0)	yes	Line
$\Gamma:(0,0,0)$	SM:(u,0,0)	Y:(1,0,0)	no	Line
$\Gamma:(0,0,0)$	LD:(0,0,w)	Z:(0,0,1/2)	yes	Line
T:(1,0,1/2)	H:(1,0,w)	Y:(1,0,0)	no	Line
$\Gamma:(0,0,0)$	M:(u,0,w)	T:(1,0,1/2)	yes	Plane
$\Gamma:(0,0,0)$	M:(u,0,w)	Y:(1,0,0)	no	Plane
$\Gamma:(0,0,0)$	M:(u,0,w)	Z:(0,0,1/2)	yes	Plane
T:(1,0,1/2)	M:(u,0,w)	Y:(1,0,0)	no	Plane
T:(1,0,1/2)	M:(u,0,w)	Z:(0,0,1/2)	yes	Plane
Y:(1,0,0)	M:(u,0,w)	Z:(0,0,1/2)	no	Plane

BCSID: 3.3; Formula: Ho2RhIn8; MSG: 63.464 ( $Cm'cm'$ ); U= 2eV				
maximal $k_1$	intermediate path	maximal $k_2$	satisfied?	Line/Plane
$\Gamma:(0,0,0)$	DT:(0,v,0)	Y:(0,1,0)	yes	Line
$\Gamma:(0,0,0)$	SM:(u,0,0)	Y:(1,0,0)	no	Line
$\Gamma:(0,0,0)$	LD:(0,0,w)	Z:(0,0,1/2)	yes	Line
T:(1,0,1/2)	H:(1,0,w)	Y:(1,0,0)	no	Line
$\Gamma:(0,0,0)$	M:(u,0,w)	T:(1,0,1/2)	yes	Plane
$\Gamma:(0,0,0)$	M:(u,0,w)	Y:(1,0,0)	no	Plane
$\Gamma:(0,0,0)$	M:(u,0,w)	Z:(0,0,1/2)	yes	Plane
T:(1,0,1/2)	M:(u,0,w)	Y:(1,0,0)	no	Plane
T:(1,0,1/2)	M:(u,0,w)	Z:(0,0,1/2)	yes	Plane
Y:(1,0,0)	M:(u,0,w)	Z:(0,0,1/2)	no	Plane

BCSID: 1.262; Formula: NpRhGa5; MSG: 63.466 ( $C_{cmcm}$ ); U= 4eV				
maximal $k_1$	intermediate path	maximal $k_2$	satisfied?	Line/Plane
T:(1,0,1/2)	A:(u,0,1/2)	Z:(0,0,1/2)	no	Line

BCSID: 1.145; Formula: Mn3Ni20P6; MSG: 64.480 ( $C_{Amca}$ ); U= 0				
maximal $k_1$	intermediate path	maximal $k_2$	satisfied?	Line/Plane
T:(1,0,1/2)	A:(u,0,1/2)	Z:(0,0,1/2)	no	Line

BCSID: 1.188; Formula: CeRh2Si2; MSG: 64.480 ( $C_{Amca}$ ); U= 4eV				
maximal $k_1$	intermediate path	maximal $k_2$	satisfied?	Line/Plane
T:(1,0,1/2)	A:(u,0,1/2)	Z:(0,0,1/2)	no	Line

BCSID: 2.15; Formula: Mn3Ni20P6; MSG: 65.486 ( $Cmm'm'$ ); U= 1eV				
maximal $k_1$	intermediate path	maximal $k_2$	satisfied?	Line/Plane
$\Gamma:(0,0,0)$	DT:(0,v,0)	Y:(0,1,0)	yes	Line
$\Gamma:(0,0,0)$	SM:(u,0,0)	Y:(1,0,0)	no	Line
$\Gamma:(0,0,0)$	LD:(0,0,w)	Z:(0,0,1/2)	yes	Line
T:(1,0,1/2)	H:(1,0,w)	Y:(1,0,0)	no	Line
T:(1,0,1/2)	A:(u,0,1/2)	Z:(0,0,1/2)	no	Line
T:(0,1,1/2)	B:(0,v,1/2)	Z:(0,0,1/2)	no	Line
$\Gamma:(0,0,0)$	K:(0,v,w)	T:(0,1,1/2)	no	Plane
$\Gamma:(0,0,0)$	K:(0,v,w)	Y:(0,1,0)	yes	Plane
$\Gamma:(0,0,0)$	K:(0,v,w)	Z:(0,0,1/2)	yes	Plane
T:(0,1,1/2)	K:(0,v,w)	Y:(0,1,0)	no	Plane
T:(0,1,1/2)	K:(0,v,w)	Z:(0,0,1/2)	no	Plane
Y:(0,1,0)	K:(0,v,w)	Z:(0,0,1/2)	yes	Plane

BCSID: 2.15; Formula: Mn3Ni20P6; MSG: 65.486 ( $Cmm'm'$ ); U= 2eV				
maximal $k_1$	intermediate path	maximal $k_2$	satisfied?	Line/Plane
$\Gamma:(0,0,0)$	DT:(0,v,0)	Y:(0,1,0)	yes	Line
$\Gamma:(0,0,0)$	SM:(u,0,0)	Y:(1,0,0)	no	Line
$\Gamma:(0,0,0)$	LD:(0,0,w)	Z:(0,0,1/2)	yes	Line
T:(1,0,1/2)	H:(1,0,w)	Y:(1,0,0)	yes	Line
T:(1,0,1/2)	A:(u,0,1/2)	Z:(0,0,1/2)	yes	Line
T:(0,1,1/2)	B:(0,v,1/2)	Z:(0,0,1/2)	yes	Line
$\Gamma:(0,0,0)$	K:(0,v,w)	T:(0,1,1/2)	yes	Plane
$\Gamma:(0,0,0)$	K:(0,v,w)	Y:(0,1,0)	yes	Plane
$\Gamma:(0,0,0)$	K:(0,v,w)	Z:(0,0,1/2)	yes	Plane
T:(0,1,1/2)	K:(0,v,w)	Y:(0,1,0)	yes	Plane
T:(0,1,1/2)	K:(0,v,w)	Z:(0,0,1/2)	yes	Plane
Y:(0,1,0)	K:(0,v,w)	Z:(0,0,1/2)	yes	Plane

BCSID: 2.15; Formula: Mn3Ni20P6; MSG: 65.486 ( $Cmm'm'$ ); U= 4eV				
maximal $k_1$	intermediate path	maximal $k_2$	satisfied?	Line/Plane
$\Gamma:(0,0,0)$	DT:(0,v,0)	Y:(0,1,0)	yes	Line
$\Gamma:(0,0,0)$	SM:(u,0,0)	Y:(1,0,0)	no	Line
$\Gamma:(0,0,0)$	LD:(0,0,w)	Z:(0,0,1/2)	yes	Line
T:(1,0,1/2)	H:(1,0,w)	Y:(1,0,0)	yes	Line
T:(1,0,1/2)	A:(u,0,1/2)	Z:(0,0,1/2)	yes	Line
T:(0,1,1/2)	B:(0,v,1/2)	Z:(0,0,1/2)	yes	Line
$\Gamma:(0,0,0)$	K:(0,v,w)	T:(0,1,1/2)	yes	Plane
$\Gamma:(0,0,0)$	K:(0,v,w)	Y:(0,1,0)	yes	Plane
$\Gamma:(0,0,0)$	K:(0,v,w)	Z:(0,0,1/2)	yes	Plane
T:(0,1,1/2)	K:(0,v,w)	Y:(0,1,0)	yes	Plane
T:(0,1,1/2)	K:(0,v,w)	Z:(0,0,1/2)	yes	Plane
Y:(0,1,0)	K:(0,v,w)	Z:(0,0,1/2)	yes	Plane

BCSID: 1.223; Formula: Tm2CoGa8; MSG: 65.489 ( $C_ammm$ ); U= 2eV				
maximal $k_1$	intermediate path	maximal $k_2$	satisfied?	Line/Plane
R:(1/2,1/2,1/2)	D:(1/2,1/2,w)	S:(1/2,1/2,0)	no	Line

BCSID: 1.223; Formula: Tm2CoGa8; MSG: 65.489 ( $C_ammm$ ); U= 4eV				
maximal $k_1$	intermediate path	maximal $k_2$	satisfied?	Line/Plane

R:(1/2,1/2,1/2)	D:(1/2,1/2,w)	S:(1/2,1/2,0)	no	Line
BCSID: 0.4; Formula: NiCr <sub>2</sub> O <sub>4</sub> ; MSG: 70.530 ( $Fd'd'd$ ); U= 0				
maximal $k_1$	intermediate path	maximal $k_2$	satisfied?	Line/Plane
$\Gamma:(0,0,0)$	SM:(u,0,0)	T:(1,0,0)	yes	Line
$\Gamma:(0,0,0)$	DT:(0,v,0)	Y:(0,1,0)	yes	Line
$\Gamma:(0,0,0)$	LD:(0,0,w)	Z:(0,0,1)	no	Line
T:(0,1,1)	H:(0,1,w)	Y:(0,1,0)	yes	Line
$\Gamma:(0,0,0)$	M:(u,v,0)	T:(1,0,0)	yes	Plane
$\Gamma:(0,0,0)$	M:(u,v,0)	Y:(0,1,0)	yes	Plane
$\Gamma:(0,0,0)$	M:(u,v,0)	Z:(1,1,0)	yes	Plane
T:(1,0,0)	M:(u,v,0)	Y:(0,1,0)	yes	Plane
T:(1,0,0)	M:(u,v,0)	Z:(1,1,0)	yes	Plane
Y:(0,1,0)	M:(u,v,0)	Z:(1,1,0)	yes	Plane
BCSID: 1.0.12; Formula: UAu <sub>2</sub> Si <sub>2</sub> ; MSG: 71.536 ( $Im'm'm$ ); U= 0				
maximal $k_1$	intermediate path	maximal $k_2$	satisfied?	Line/Plane
$\Gamma:(0,0,0)$	DT:(0,v,0)	X:(0,1,0)	no	Line
$\Gamma:(0,0,0)$	LD:(0,0,w)	X:(0,0,1)	no	Line
$\Gamma:(0,0,0)$	SM:(u,0,0)	X:(1,0,0)	no	Line
W:(1/2,1/2,1/2)	P:(1/2,1/2,w)	T:(1/2,1/2,0)	yes	Line
W:(1/2,1/2,1/2)	P:(1/2,1/2,w)	TA:(1/2,1/2,1)	yes	Line
T:(1/2,1/2,2)	P:(1/2,1/2,w)	TA:(1/2,1/2,1)	yes	Line
$\Gamma:(0,0,0)$	C:(u,v,0)	X:(0,1,0)	no	Plane
$\Gamma:(0,0,0)$	C:(u,v,0)	T:(1/2,1/2,0)	no	Plane
$\Gamma:(0,0,0)$	C:(u,v,0)	TA:(-1/2,1/2,0)	no	Plane
X:(2,1,0)	C:(u,v,0)	T:(3/2,3/2,0)	no	Plane
X:(2,1,0)	C:(u,v,0)	TA:(3/2,1/2,0)	no	Plane
T:(3/2,-1/2,0)	C:(u,v,0)	TA:(1/2,-1/2,0)	yes	Plane
BCSID: 1.0.12; Formula: UAu <sub>2</sub> Si <sub>2</sub> ; MSG: 71.536 ( $Im'm'm$ ); U= 2eV				
maximal $k_1$	intermediate path	maximal $k_2$	satisfied?	Line/Plane
$\Gamma:(0,0,0)$	DT:(0,v,0)	X:(0,1,0)	no	Line
$\Gamma:(0,0,0)$	LD:(0,0,w)	X:(0,0,1)	yes	Line
$\Gamma:(0,0,0)$	SM:(u,0,0)	X:(1,0,0)	no	Line
W:(1/2,1/2,1/2)	P:(1/2,1/2,w)	T:(1/2,1/2,0)	yes	Line
W:(1/2,1/2,1/2)	P:(1/2,1/2,w)	TA:(1/2,1/2,1)	yes	Line
T:(1/2,1/2,2)	P:(1/2,1/2,w)	TA:(1/2,1/2,1)	yes	Line
$\Gamma:(0,0,0)$	C:(u,v,0)	X:(0,1,0)	no	Plane
$\Gamma:(0,0,0)$	C:(u,v,0)	T:(1/2,1/2,0)	no	Plane
$\Gamma:(0,0,0)$	C:(u,v,0)	TA:(-1/2,1/2,0)	no	Plane
X:(2,1,0)	C:(u,v,0)	T:(3/2,3/2,0)	yes	Plane
X:(2,1,0)	C:(u,v,0)	TA:(3/2,1/2,0)	yes	Plane
T:(3/2,-1/2,0)	C:(u,v,0)	TA:(1/2,-1/2,0)	yes	Plane
BCSID: 1.0.12; Formula: UAu <sub>2</sub> Si <sub>2</sub> ; MSG: 71.536 ( $Im'm'm$ ); U= 6eV				
maximal $k_1$	intermediate path	maximal $k_2$	satisfied?	Line/Plane
$\Gamma:(0,0,0)$	DT:(0,v,0)	X:(0,1,0)	no	Line
$\Gamma:(0,0,0)$	LD:(0,0,w)	X:(0,0,1)	yes	Line
$\Gamma:(0,0,0)$	SM:(u,0,0)	X:(1,0,0)	no	Line

W:(1/2,1/2,1/2)	P:(1/2,1/2,w)	T:(1/2,1/2,0)	yes	Line
W:(1/2,1/2,1/2)	P:(1/2,1/2,w)	TA:(1/2,1/2,1)	yes	Line
T:(1/2,1/2,2)	P:(1/2,1/2,w)	TA:(1/2,1/2,1)	yes	Line
$\Gamma:(0,0,0)$	C:(u,v,0)	X:(0,1,0)	no	Plane
$\Gamma:(0,0,0)$	C:(u,v,0)	T:(1/2,1/2,0)	no	Plane
$\Gamma:(0,0,0)$	C:(u,v,0)	TA:(-1/2,1/2,0)	no	Plane
X:(2,1,0)	C:(u,v,0)	T:(3/2,3/2,0)	yes	Plane
X:(2,1,0)	C:(u,v,0)	TA:(3/2,1/2,0)	yes	Plane
T:(3/2,-1/2,0)	C:(u,v,0)	TA:(1/2,-1/2,0)	yes	Plane

BCSID: 2.28; Formula: NpNiGa5; MSG: 74.559 ( $Imm'a'$ ); U= 0				
maximal $k_1$	intermediate path	maximal $k_2$	satisfied?	Line/Plane
$\Gamma:(0,0,0)$	DT:(0,v,0)	X:(0,1,0)	yes	Line
$\Gamma:(0,0,0)$	LD:(0,0,w)	X:(0,0,1)	yes	Line
$\Gamma:(0,0,0)$	SM:(u,0,0)	X:(1,0,0)	no	Line
W:(1/2,1/2,1/2)	D:(u,1/2,1/2)	S:(0,1/2,1/2)	yes	Line
W:(1/2,1/2,1/2)	D:(u,1/2,1/2)	SA:(1,1/2,1/2)	yes	Line
S:(0,1/2,1/2)	D:(u,1/2,1/2)	SA:(1,1/2,1/2)	yes	Line
$\Gamma:(0,0,0)$	A:(0,v,w)	X:(0,0,1)	yes	Plane
$\Gamma:(0,0,0)$	A:(0,v,w)	S:(0,1/2,1/2)	yes	Plane
$\Gamma:(0,0,0)$	A:(0,v,w)	SA:(0,-1/2,1/2)	yes	Plane
X:(0,2,1)	A:(0,v,w)	S:(0,3/2,3/2)	yes	Plane
X:(0,2,1)	A:(0,v,w)	SA:(0,3/2,1/2)	yes	Plane
S:(0,1/2,1/2)	A:(0,v,w)	SA:(0,-1/2,1/2)	yes	Plane

BCSID: 2.28; Formula: NpNiGa5; MSG: 74.559 ( $Imm'a'$ ); U= 2eV				
maximal $k_1$	intermediate path	maximal $k_2$	satisfied?	Line/Plane
$\Gamma:(0,0,0)$	DT:(0,v,0)	X:(0,1,0)	no	Line
$\Gamma:(0,0,0)$	LD:(0,0,w)	X:(0,0,1)	no	Line
$\Gamma:(0,0,0)$	SM:(u,0,0)	X:(1,0,0)	yes	Line
W:(1/2,1/2,1/2)	D:(u,1/2,1/2)	S:(0,1/2,1/2)	yes	Line
W:(1/2,1/2,1/2)	D:(u,1/2,1/2)	SA:(1,1/2,1/2)	yes	Line
S:(0,1/2,1/2)	D:(u,1/2,1/2)	SA:(1,1/2,1/2)	yes	Line
$\Gamma:(0,0,0)$	A:(0,v,w)	X:(0,0,1)	no	Plane
$\Gamma:(0,0,0)$	A:(0,v,w)	S:(0,1/2,1/2)	no	Plane
$\Gamma:(0,0,0)$	A:(0,v,w)	SA:(0,-1/2,1/2)	no	Plane
X:(0,2,1)	A:(0,v,w)	S:(0,3/2,3/2)	yes	Plane
X:(0,2,1)	A:(0,v,w)	SA:(0,3/2,1/2)	yes	Plane
S:(0,1/2,1/2)	A:(0,v,w)	SA:(0,-1/2,1/2)	yes	Plane

BCSID: 2.28; Formula: NpNiGa5; MSG: 74.559 ( $Imm'a'$ ); U= 6eV				
maximal $k_1$	intermediate path	maximal $k_2$	satisfied?	Line/Plane
$\Gamma:(0,0,0)$	DT:(0,v,0)	X:(0,1,0)	no	Line
$\Gamma:(0,0,0)$	LD:(0,0,w)	X:(0,0,1)	no	Line
$\Gamma:(0,0,0)$	SM:(u,0,0)	X:(1,0,0)	yes	Line
W:(1/2,1/2,1/2)	D:(u,1/2,1/2)	S:(0,1/2,1/2)	yes	Line
W:(1/2,1/2,1/2)	D:(u,1/2,1/2)	SA:(1,1/2,1/2)	yes	Line
S:(0,1/2,1/2)	D:(u,1/2,1/2)	SA:(1,1/2,1/2)	yes	Line
$\Gamma:(0,0,0)$	A:(0,v,w)	X:(0,0,1)	no	Plane
$\Gamma:(0,0,0)$	A:(0,v,w)	S:(0,1/2,1/2)	no	Plane
$\Gamma:(0,0,0)$	A:(0,v,w)	SA:(0,-1/2,1/2)	no	Plane

X:(0,2,1)	A:(0,v,w)	S:(0,3/2,3/2)	yes	Plane
X:(0,2,1)	A:(0,v,w)	SA:(0,3/2,1/2)	yes	Plane
S:(0,1/2,1/2)	A:(0,v,w)	SA:(0,-1/2,1/2)	yes	Plane

BCSID: 2.5; Formula: Mn <sub>3</sub> CuN; MSG: 85.59 ( <i>P</i> 4/ <i>n</i> ); U= 0				
maximal <i>k</i> <sub>1</sub>	intermediate path	maximal <i>k</i> <sub>2</sub>	satisfied?	Line/Plane
$\Gamma:(0,0,0)$	SM:(u,u,0)	M:(1/2,1/2,0)	yes	Line
$\Gamma:(0,0,0)$	DT:(0,v,0)	X:(0,1/2,0)	yes	Line
$\Gamma:(0,0,0)$	LD:(0,0,w)	Z:(0,0,1/2)	no	Line
A:(1/2,1/2,1/2)	V:(1/2,1/2,w)	M:(1/2,1/2,0)	yes	Line
A:(1/2,1/2,1/2)	T:(u,1/2,1/2)	R:(0,1/2,1/2)	yes	Line
A:(1/2,1/2,1/2)	S:(u,u,1/2)	Z:(0,0,1/2)	yes	Line
M:(1/2,1/2,0)	Y:(u,1/2,0)	X:(0,1/2,0)	yes	Line
R:(0,1/2,1/2)	W:(0,1/2,w)	X:(0,1/2,0)	yes	Line
R:(0,1/2,1/2)	U:(0,v,1/2)	Z:(0,0,1/2)	yes	Line
$\Gamma:(0,0,0)$	D:(u,v,0)	M:(1/2,1/2,0)	yes	Plane
$\Gamma:(0,0,0)$	D:(u,v,0)	X:(0,1/2,0)	yes	Plane
A:(1/2,1/2,1/2)	E:(u,v,1/2)	R:(0,1/2,1/2)	yes	Plane
A:(1/2,1/2,1/2)	E:(u,v,1/2)	Z:(0,0,1/2)	yes	Plane
M:(1/2,1/2,0)	D:(u,v,0)	X:(0,1/2,0)	yes	Plane
R:(0,1/2,1/2)	E:(u,v,1/2)	Z:(0,0,1/2)	yes	Plane

BCSID: 2.5; Formula: Mn <sub>3</sub> CuN; MSG: 85.59 ( <i>P</i> 4/ <i>n</i> ); U= 1eV				
maximal <i>k</i> <sub>1</sub>	intermediate path	maximal <i>k</i> <sub>2</sub>	satisfied?	Line/Plane
$\Gamma:(0,0,0)$	SM:(u,u,0)	M:(1/2,1/2,0)	yes	Line
$\Gamma:(0,0,0)$	DT:(0,v,0)	X:(0,1/2,0)	yes	Line
$\Gamma:(0,0,0)$	LD:(0,0,w)	Z:(0,0,1/2)	no	Line
A:(1/2,1/2,1/2)	V:(1/2,1/2,w)	M:(1/2,1/2,0)	yes	Line
A:(1/2,1/2,1/2)	T:(u,1/2,1/2)	R:(0,1/2,1/2)	yes	Line
A:(1/2,1/2,1/2)	S:(u,u,1/2)	Z:(0,0,1/2)	yes	Line
M:(1/2,1/2,0)	Y:(u,1/2,0)	X:(0,1/2,0)	yes	Line
R:(0,1/2,1/2)	W:(0,1/2,w)	X:(0,1/2,0)	yes	Line
R:(0,1/2,1/2)	U:(0,v,1/2)	Z:(0,0,1/2)	yes	Line
$\Gamma:(0,0,0)$	D:(u,v,0)	M:(1/2,1/2,0)	yes	Plane
$\Gamma:(0,0,0)$	D:(u,v,0)	X:(0,1/2,0)	yes	Plane
A:(1/2,1/2,1/2)	E:(u,v,1/2)	R:(0,1/2,1/2)	yes	Plane
A:(1/2,1/2,1/2)	E:(u,v,1/2)	Z:(0,0,1/2)	yes	Plane
M:(1/2,1/2,0)	D:(u,v,0)	X:(0,1/2,0)	yes	Plane
R:(0,1/2,1/2)	E:(u,v,1/2)	Z:(0,0,1/2)	yes	Plane

BCSID: 2.5; Formula: Mn <sub>3</sub> CuN; MSG: 85.59 ( <i>P</i> 4/ <i>n</i> ); U= 2eV				
maximal <i>k</i> <sub>1</sub>	intermediate path	maximal <i>k</i> <sub>2</sub>	satisfied?	Line/Plane
$\Gamma:(0,0,0)$	SM:(u,u,0)	M:(1/2,1/2,0)	yes	Line
$\Gamma:(0,0,0)$	DT:(0,v,0)	X:(0,1/2,0)	yes	Line
$\Gamma:(0,0,0)$	LD:(0,0,w)	Z:(0,0,1/2)	no	Line
A:(1/2,1/2,1/2)	V:(1/2,1/2,w)	M:(1/2,1/2,0)	yes	Line
A:(1/2,1/2,1/2)	T:(u,1/2,1/2)	R:(0,1/2,1/2)	yes	Line
A:(1/2,1/2,1/2)	S:(u,u,1/2)	Z:(0,0,1/2)	yes	Line
M:(1/2,1/2,0)	Y:(u,1/2,0)	X:(0,1/2,0)	yes	Line
R:(0,1/2,1/2)	W:(0,1/2,w)	X:(0,1/2,0)	yes	Line
R:(0,1/2,1/2)	U:(0,v,1/2)	Z:(0,0,1/2)	yes	Line

$\Gamma:(0,0,0)$	D:(u,v,0)	M:(1/2,1/2,0)	yes	Plane
$\Gamma:(0,0,0)$	D:(u,v,0)	X:(0,1/2,0)	yes	Plane
A:(1/2,1/2,1/2)	E:(u,v,1/2)	R:(0,1/2,1/2)	yes	Plane
A:(1/2,1/2,1/2)	E:(u,v,1/2)	Z:(0,0,1/2)	yes	Plane
M:(1/2,1/2,0)	D:(u,v,0)	X:(0,1/2,0)	yes	Plane
R:(0,1/2,1/2)	E:(u,v,1/2)	Z:(0,0,1/2)	yes	Plane

BCSID: 2.5; Formula: Mn <sub>3</sub> CuN; MSG: 85.59 ( $P4/n$ ); U= 3eV				
maximal $k_1$	intermediate path	maximal $k_2$	satisfied?	Line/Plane
$\Gamma:(0,0,0)$	SM:(u,u,0)	M:(1/2,1/2,0)	yes	Line
$\Gamma:(0,0,0)$	DT:(0,v,0)	X:(0,1/2,0)	yes	Line
$\Gamma:(0,0,0)$	LD:(0,0,w)	Z:(0,0,1/2)	no	Line
A:(1/2,1/2,1/2)	V:(1/2,1/2,w)	M:(1/2,1/2,0)	yes	Line
A:(1/2,1/2,1/2)	T:(u,1/2,1/2)	R:(0,1/2,1/2)	yes	Line
A:(1/2,1/2,1/2)	S:(u,u,1/2)	Z:(0,0,1/2)	yes	Line
M:(1/2,1/2,0)	Y:(u,1/2,0)	X:(0,1/2,0)	yes	Line
R:(0,1/2,1/2)	W:(0,1/2,w)	X:(0,1/2,0)	yes	Line
R:(0,1/2,1/2)	U:(0,v,1/2)	Z:(0,0,1/2)	yes	Line
$\Gamma:(0,0,0)$	D:(u,v,0)	M:(1/2,1/2,0)	yes	Plane
$\Gamma:(0,0,0)$	D:(u,v,0)	X:(0,1/2,0)	yes	Plane
A:(1/2,1/2,1/2)	E:(u,v,1/2)	R:(0,1/2,1/2)	yes	Plane
A:(1/2,1/2,1/2)	E:(u,v,1/2)	Z:(0,0,1/2)	yes	Plane
M:(1/2,1/2,0)	D:(u,v,0)	X:(0,1/2,0)	yes	Plane
R:(0,1/2,1/2)	E:(u,v,1/2)	Z:(0,0,1/2)	yes	Plane

BCSID: 2.5; Formula: Mn <sub>3</sub> CuN; MSG: 85.59 ( $P4/n$ ); U= 4eV				
maximal $k_1$	intermediate path	maximal $k_2$	satisfied?	Line/Plane
$\Gamma:(0,0,0)$	SM:(u,u,0)	M:(1/2,1/2,0)	yes	Line
$\Gamma:(0,0,0)$	DT:(0,v,0)	X:(0,1/2,0)	yes	Line
$\Gamma:(0,0,0)$	LD:(0,0,w)	Z:(0,0,1/2)	no	Line
A:(1/2,1/2,1/2)	V:(1/2,1/2,w)	M:(1/2,1/2,0)	no	Line
A:(1/2,1/2,1/2)	T:(u,1/2,1/2)	R:(0,1/2,1/2)	yes	Line
A:(1/2,1/2,1/2)	S:(u,u,1/2)	Z:(0,0,1/2)	yes	Line
M:(1/2,1/2,0)	Y:(u,1/2,0)	X:(0,1/2,0)	yes	Line
R:(0,1/2,1/2)	W:(0,1/2,w)	X:(0,1/2,0)	yes	Line
R:(0,1/2,1/2)	U:(0,v,1/2)	Z:(0,0,1/2)	yes	Line
$\Gamma:(0,0,0)$	D:(u,v,0)	M:(1/2,1/2,0)	yes	Plane
$\Gamma:(0,0,0)$	D:(u,v,0)	X:(0,1/2,0)	yes	Plane
A:(1/2,1/2,1/2)	E:(u,v,1/2)	R:(0,1/2,1/2)	yes	Plane
A:(1/2,1/2,1/2)	E:(u,v,1/2)	Z:(0,0,1/2)	yes	Plane
M:(1/2,1/2,0)	D:(u,v,0)	X:(0,1/2,0)	yes	Plane
R:(0,1/2,1/2)	E:(u,v,1/2)	Z:(0,0,1/2)	yes	Plane

BCSID: 0.207; Formula: TlFe <sub>1.6</sub> Se <sub>2</sub> ; MSG: 87.75 ( $I4/m$ ); U= 1eV				
maximal $k_1$	intermediate path	maximal $k_2$	satisfied?	Line/Plane
$\Gamma:(0,0,0)$	LD:(0,0,w)	M:(0,0,1)	yes	Line
$\Gamma:(0,0,0)$	SM:(u,0,0)	M:(1,0,0)	no	Line
$\Gamma:(0,0,0)$	DT:(u,u,0)	X:(1/2,1/2,0)	no	Line
M:(1,0,0)	Y:(u,1-u,0)	X:(1/2,1/2,0)	yes	Line
P:(1/2,1/2,1/2)	W:(1/2,1/2,w)	X:(1/2,1/2,0)	yes	Line
$\Gamma:(0,0,0)$	C:(u,v,0)	M:(0,1,0)	no	Plane

$\Gamma:(0,0,0)$	$C:(u,v,0)$	$X:(1/2,1/2,0)$	no	Plane
$M:(2,1,0)$	$C:(u,v,0)$	$X:(3/2,3/2,0)$	yes	Plane

BCSID: 0.207; Formula: TlFe1.6Se2; MSG: 87.75 ( $I4/m$ ); U= 2eV				
maximal $k_1$	intermediate path	maximal $k_2$	satisfied?	Line/Plane
$\Gamma:(0,0,0)$	$LD:(0,0,w)$	$M:(0,0,1)$	yes	Line
$\Gamma:(0,0,0)$	$SM:(u,0,0)$	$M:(1,0,0)$	yes	Line
$\Gamma:(0,0,0)$	$DT:(u,u,0)$	$X:(1/2,1/2,0)$	no	Line
$M:(1,0,0)$	$Y:(u,1-u,0)$	$X:(1/2,1/2,0)$	no	Line
$P:(1/2,1/2,1/2)$	$W:(1/2,1/2,w)$	$X:(1/2,1/2,0)$	yes	Line
$\Gamma:(0,0,0)$	$C:(u,v,0)$	$M:(0,1,0)$	yes	Plane
$\Gamma:(0,0,0)$	$C:(u,v,0)$	$X:(1/2,1/2,0)$	no	Plane
$M:(2,1,0)$	$C:(u,v,0)$	$X:(3/2,3/2,0)$	no	Plane

BCSID: 0.207; Formula: TlFe1.6Se2; MSG: 87.75 ( $I4/m$ ); U= 3eV				
maximal $k_1$	intermediate path	maximal $k_2$	satisfied?	Line/Plane
$\Gamma:(0,0,0)$	$LD:(0,0,w)$	$M:(0,0,1)$	yes	Line
$\Gamma:(0,0,0)$	$SM:(u,0,0)$	$M:(1,0,0)$	no	Line
$\Gamma:(0,0,0)$	$DT:(u,u,0)$	$X:(1/2,1/2,0)$	no	Line
$M:(1,0,0)$	$Y:(u,1-u,0)$	$X:(1/2,1/2,0)$	yes	Line
$P:(1/2,1/2,1/2)$	$W:(1/2,1/2,w)$	$X:(1/2,1/2,0)$	yes	Line
$\Gamma:(0,0,0)$	$C:(u,v,0)$	$M:(0,1,0)$	no	Plane
$\Gamma:(0,0,0)$	$C:(u,v,0)$	$X:(1/2,1/2,0)$	no	Plane
$M:(2,1,0)$	$C:(u,v,0)$	$X:(3/2,3/2,0)$	yes	Plane

BCSID: 0.64; Formula: MnV2O4; MSG: 88.81 ( $I4_1/a$ ); U= 0				
maximal $k_1$	intermediate path	maximal $k_2$	satisfied?	Line/Plane
$\Gamma:(0,0,0)$	$LD:(0,0,w)$	$M:(0,0,1)$	no	Line
$\Gamma:(0,0,0)$	$SM:(u,0,0)$	$M:(1,0,0)$	yes	Line
$\Gamma:(0,0,0)$	$DT:(u,u,0)$	$X:(1/2,1/2,0)$	yes	Line
$M:(1,0,0)$	$Y:(u,1-u,0)$	$X:(1/2,1/2,0)$	yes	Line
$P:(1/2,1/2,1/2)$	$W:(1/2,1/2,w)$	$X:(1/2,1/2,0)$	yes	Line
$\Gamma:(0,0,0)$	$C:(u,v,0)$	$M:(0,1,0)$	yes	Plane
$\Gamma:(0,0,0)$	$C:(u,v,0)$	$X:(1/2,1/2,0)$	yes	Plane
$M:(2,1,0)$	$C:(u,v,0)$	$X:(3/2,3/2,0)$	yes	Plane

BCSID: 1.0.11; Formula: CeCoGe3; MSG: 107.231 ( $I4m'm'$ ); U= 4eV				
maximal $k_1$	intermediate path	maximal $k_2$	satisfied?	Line/Plane
$\Gamma:(0,0,0)$	$LD:(0,0,w)$	$M:(0,0,1)$	no	Line
$P:(1/2,1/2,1/2)$	$W:(1/2,1/2,w)$	$X:(1/2,1/2,0)$	yes	Line

BCSID: 1.85; Formula: alpha-Mn; MSG: 114.282 ( $P_I - 42_1 c$ ); U= 0				
maximal $k_1$	intermediate path	maximal $k_2$	satisfied?	Line/Plane
$\Gamma:(0,0,0)$	$SM:(u,u,0)$	$M:(1/2,1/2,0)$	yes	Line
$\Gamma:(0,0,0)$	$DT:(0,v,0)$	$X:(0,1/2,0)$	yes	Line
$M:(1/2,1/2,0)$	$Y:(u,1/2,0)$	$X:(0,1/2,0)$	yes	Line
$R:(0,1/2,1/2)$	$W:(0,1/2,w)$	$X:(0,1/2,0)$	no	Line
$\Gamma:(0,0,0)$	$C:(u,u,w)$	$A:(1/2,1/2,1/2)$	yes	Plane
$\Gamma:(0,0,0)$	$C:(u,u,w)$	$M:(1/2,1/2,0)$	yes	Plane
$\Gamma:(0,0,0)$	$C:(u,u,w)$	$Z:(0,0,1/2)$	yes	Plane
$A:(1/2,1/2,1/2)$	$C:(u,u,w)$	$M:(1/2,1/2,0)$	yes	Plane

A:(1/2,1/2,1/2)	C:(u,u,w)	Z:(0,0,1/2)	yes	Plane
M:(1/2,1/2,0)	C:(u,u,w)	Z:(0,0,1/2)	yes	Plane

BCSID: 2.26; Formula: PrCo2P2; MSG: 123.345 ( $P4/mm'm'$ ); U= 0				
maximal $k_1$	intermediate path	maximal $k_2$	satisfied?	Line/Plane
$\Gamma:(0,0,0)$	SM:(u,u,0)	M:(1/2,1/2,0)	no	Line
$\Gamma:(0,0,0)$	DT:(0,v,0)	X:(0,1/2,0)	no	Line
$\Gamma:(0,0,0)$	LD:(0,0,w)	Z:(0,0,1/2)	yes	Line
A:(1/2,1/2,1/2)	V:(1/2,1/2,w)	M:(1/2,1/2,0)	no	Line
A:(1/2,1/2,1/2)	T:(u,1/2,1/2)	R:(0,1/2,1/2)	yes	Line
A:(1/2,1/2,1/2)	S:(u,u,1/2)	Z:(0,0,1/2)	yes	Line
M:(1/2,1/2,0)	Y:(u,1/2,0)	X:(0,1/2,0)	no	Line
R:(0,1/2,1/2)	W:(0,1/2,w)	X:(0,1/2,0)	yes	Line
R:(0,1/2,1/2)	U:(0,v,1/2)	Z:(0,0,1/2)	yes	Line
$\Gamma:(0,0,0)$	D:(u,v,0)	M:(1/2,1/2,0)	no	Plane
$\Gamma:(0,0,0)$	D:(u,v,0)	X:(0,1/2,0)	no	Plane
A:(1/2,1/2,1/2)	E:(u,v,1/2)	R:(0,1/2,1/2)	yes	Plane
A:(1/2,1/2,1/2)	E:(u,v,1/2)	Z:(0,0,1/2)	yes	Plane
M:(1/2,1/2,0)	D:(u,v,0)	X:(0,1/2,0)	no	Plane
R:(0,1/2,1/2)	E:(u,v,1/2)	Z:(0,0,1/2)	yes	Plane

BCSID: 2.26; Formula: PrCo2P2; MSG: 123.345 ( $P4/mm'm'$ ); U= 2eV				
maximal $k_1$	intermediate path	maximal $k_2$	satisfied?	Line/Plane
$\Gamma:(0,0,0)$	SM:(u,u,0)	M:(1/2,1/2,0)	yes	Line
$\Gamma:(0,0,0)$	DT:(0,v,0)	X:(0,1/2,0)	yes	Line
$\Gamma:(0,0,0)$	LD:(0,0,w)	Z:(0,0,1/2)	yes	Line
A:(1/2,1/2,1/2)	V:(1/2,1/2,w)	M:(1/2,1/2,0)	yes	Line
A:(1/2,1/2,1/2)	T:(u,1/2,1/2)	R:(0,1/2,1/2)	no	Line
A:(1/2,1/2,1/2)	S:(u,u,1/2)	Z:(0,0,1/2)	yes	Line
M:(1/2,1/2,0)	Y:(u,1/2,0)	X:(0,1/2,0)	yes	Line
R:(0,1/2,1/2)	W:(0,1/2,w)	X:(0,1/2,0)	yes	Line
R:(0,1/2,1/2)	U:(0,v,1/2)	Z:(0,0,1/2)	no	Line
$\Gamma:(0,0,0)$	D:(u,v,0)	M:(1/2,1/2,0)	yes	Plane
$\Gamma:(0,0,0)$	D:(u,v,0)	X:(0,1/2,0)	yes	Plane
A:(1/2,1/2,1/2)	E:(u,v,1/2)	R:(0,1/2,1/2)	no	Plane
A:(1/2,1/2,1/2)	E:(u,v,1/2)	Z:(0,0,1/2)	yes	Plane
M:(1/2,1/2,0)	D:(u,v,0)	X:(0,1/2,0)	yes	Plane
R:(0,1/2,1/2)	E:(u,v,1/2)	Z:(0,0,1/2)	no	Plane

BCSID: 2.26; Formula: PrCo2P2; MSG: 123.345 ( $P4/mm'm'$ ); U= 4eV				
maximal $k_1$	intermediate path	maximal $k_2$	satisfied?	Line/Plane
$\Gamma:(0,0,0)$	SM:(u,u,0)	M:(1/2,1/2,0)	yes	Line
$\Gamma:(0,0,0)$	DT:(0,v,0)	X:(0,1/2,0)	no	Line
$\Gamma:(0,0,0)$	LD:(0,0,w)	Z:(0,0,1/2)	yes	Line
A:(1/2,1/2,1/2)	V:(1/2,1/2,w)	M:(1/2,1/2,0)	yes	Line
A:(1/2,1/2,1/2)	T:(u,1/2,1/2)	R:(0,1/2,1/2)	no	Line
A:(1/2,1/2,1/2)	S:(u,u,1/2)	Z:(0,0,1/2)	no	Line
M:(1/2,1/2,0)	Y:(u,1/2,0)	X:(0,1/2,0)	no	Line
R:(0,1/2,1/2)	W:(0,1/2,w)	X:(0,1/2,0)	no	Line
R:(0,1/2,1/2)	U:(0,v,1/2)	Z:(0,0,1/2)	no	Line
$\Gamma:(0,0,0)$	D:(u,v,0)	M:(1/2,1/2,0)	yes	Plane

$\Gamma:(0,0,0)$	D:(u,v,0)	X:(0,1/2,0)	no	Plane
A:(1/2,1/2,1/2)	E:(u,v,1/2)	R:(0,1/2,1/2)	no	Plane
A:(1/2,1/2,1/2)	E:(u,v,1/2)	Z:(0,0,1/2)	no	Plane
M:(1/2,1/2,0)	D:(u,v,0)	X:(0,1/2,0)	no	Plane
R:(0,1/2,1/2)	E:(u,v,1/2)	Z:(0,0,1/2)	no	Plane

BCSID: 2.26; Formula: PrCo2P2; MSG: 123.345 ( $P4/mm'm'$ ); U= 6eV				
maximal $k_1$	intermediate path	maximal $k_2$	satisfied?	Line/Plane
$\Gamma:(0,0,0)$	SM:(u,u,0)	M:(1/2,1/2,0)	no	Line
$\Gamma:(0,0,0)$	DT:(0,v,0)	X:(0,1/2,0)	no	Line
$\Gamma:(0,0,0)$	LD:(0,0,w)	Z:(0,0,1/2)	no	Line
A:(1/2,1/2,1/2)	V:(1/2,1/2,w)	M:(1/2,1/2,0)	yes	Line
A:(1/2,1/2,1/2)	T:(u,1/2,1/2)	R:(0,1/2,1/2)	no	Line
A:(1/2,1/2,1/2)	S:(u,u,1/2)	Z:(0,0,1/2)	yes	Line
M:(1/2,1/2,0)	Y:(u,1/2,0)	X:(0,1/2,0)	yes	Line
R:(0,1/2,1/2)	W:(0,1/2,w)	X:(0,1/2,0)	yes	Line
R:(0,1/2,1/2)	U:(0,v,1/2)	Z:(0,0,1/2)	no	Line
$\Gamma:(0,0,0)$	D:(u,v,0)	M:(1/2,1/2,0)	no	Plane
$\Gamma:(0,0,0)$	D:(u,v,0)	X:(0,1/2,0)	no	Plane
A:(1/2,1/2,1/2)	E:(u,v,1/2)	R:(0,1/2,1/2)	no	Plane
A:(1/2,1/2,1/2)	E:(u,v,1/2)	Z:(0,0,1/2)	yes	Plane
M:(1/2,1/2,0)	D:(u,v,0)	X:(0,1/2,0)	yes	Plane
R:(0,1/2,1/2)	E:(u,v,1/2)	Z:(0,0,1/2)	no	Plane

BCSID: 1.162; Formula: NdMg; MSG: 124.360 ( $P_c4/mcc$ ); U= 0				
maximal $k_1$	intermediate path	maximal $k_2$	satisfied?	Line/Plane
$\Gamma:(0,0,0)$	LD:(0,0,w)	Z:(0,0,1/2)	yes	Line
A:(1/2,1/2,1/2)	V:(1/2,1/2,w)	M:(1/2,1/2,0)	yes	Line
A:(1/2,1/2,1/2)	T:(u,1/2,1/2)	R:(0,1/2,1/2)	no	Line
A:(1/2,1/2,1/2)	S:(u,u,1/2)	Z:(0,0,1/2)	no	Line
R:(0,1/2,1/2)	U:(0,v,1/2)	Z:(0,0,1/2)	yes	Line
A:(1/2,1/2,1/2)	E:(u,v,1/2)	R:(0,1/2,1/2)	no	Plane
A:(1/2,1/2,1/2)	E:(u,v,1/2)	Z:(0,0,1/2)	no	Plane
R:(0,1/2,1/2)	E:(u,v,1/2)	Z:(0,0,1/2)	yes	Plane

BCSID: 1.162; Formula: NdMg; MSG: 124.360 ( $P_c4/mcc$ ); U= 2eV				
maximal $k_1$	intermediate path	maximal $k_2$	satisfied?	Line/Plane
$\Gamma:(0,0,0)$	LD:(0,0,w)	Z:(0,0,1/2)	yes	Line
A:(1/2,1/2,1/2)	V:(1/2,1/2,w)	M:(1/2,1/2,0)	no	Line
A:(1/2,1/2,1/2)	T:(u,1/2,1/2)	R:(0,1/2,1/2)	yes	Line
A:(1/2,1/2,1/2)	S:(u,u,1/2)	Z:(0,0,1/2)	yes	Line
R:(0,1/2,1/2)	U:(0,v,1/2)	Z:(0,0,1/2)	yes	Line
A:(1/2,1/2,1/2)	E:(u,v,1/2)	R:(0,1/2,1/2)	yes	Plane
A:(1/2,1/2,1/2)	E:(u,v,1/2)	Z:(0,0,1/2)	yes	Plane
R:(0,1/2,1/2)	E:(u,v,1/2)	Z:(0,0,1/2)	yes	Plane

BCSID: 1.162; Formula: NdMg; MSG: 124.360 ( $P_c4/mcc$ ); U= 6eV				
maximal $k_1$	intermediate path	maximal $k_2$	satisfied?	Line/Plane
$\Gamma:(0,0,0)$	LD:(0,0,w)	Z:(0,0,1/2)	yes	Line
A:(1/2,1/2,1/2)	V:(1/2,1/2,w)	M:(1/2,1/2,0)	yes	Line
A:(1/2,1/2,1/2)	T:(u,1/2,1/2)	R:(0,1/2,1/2)	no	Line

A:(1/2,1/2,1/2)	S:(u,u,1/2)	Z:(0,0,1/2)	no	Line
R:(0,1/2,1/2)	U:(0,v,1/2)	Z:(0,0,1/2)	yes	Line
A:(1/2,1/2,1/2)	E:(u,v,1/2)	R:(0,1/2,1/2)	no	Plane
A:(1/2,1/2,1/2)	E:(u,v,1/2)	Z:(0,0,1/2)	no	Plane
R:(0,1/2,1/2)	E:(u,v,1/2)	Z:(0,0,1/2)	yes	Plane

BCSID: 1.251; Formula: NdCo2P2; MSG: 124.360 ( $P_c4/mcc$ ); U= 0				
maximal $k_1$	intermediate path	maximal $k_2$	satisfied?	Line/Plane
$\Gamma:(0,0,0)$	LD:(0,0,w)	Z:(0,0,1/2)	no	Line
A:(1/2,1/2,1/2)	V:(1/2,1/2,w)	M:(1/2,1/2,0)	yes	Line
A:(1/2,1/2,1/2)	T:(u,1/2,1/2)	R:(0,1/2,1/2)	yes	Line
A:(1/2,1/2,1/2)	S:(u,u,1/2)	Z:(0,0,1/2)	no	Line
R:(0,1/2,1/2)	U:(0,v,1/2)	Z:(0,0,1/2)	no	Line
A:(1/2,1/2,1/2)	E:(u,v,1/2)	R:(0,1/2,1/2)	yes	Plane
A:(1/2,1/2,1/2)	E:(u,v,1/2)	Z:(0,0,1/2)	no	Plane
R:(0,1/2,1/2)	E:(u,v,1/2)	Z:(0,0,1/2)	no	Plane

BCSID: 1.251; Formula: NdCo2P2; MSG: 124.360 ( $P_c4/mcc$ ); U= 2eV				
maximal $k_1$	intermediate path	maximal $k_2$	satisfied?	Line/Plane
$\Gamma:(0,0,0)$	LD:(0,0,w)	Z:(0,0,1/2)	yes	Line
A:(1/2,1/2,1/2)	V:(1/2,1/2,w)	M:(1/2,1/2,0)	yes	Line
A:(1/2,1/2,1/2)	T:(u,1/2,1/2)	R:(0,1/2,1/2)	no	Line
A:(1/2,1/2,1/2)	S:(u,u,1/2)	Z:(0,0,1/2)	no	Line
R:(0,1/2,1/2)	U:(0,v,1/2)	Z:(0,0,1/2)	yes	Line
A:(1/2,1/2,1/2)	E:(u,v,1/2)	R:(0,1/2,1/2)	no	Plane
A:(1/2,1/2,1/2)	E:(u,v,1/2)	Z:(0,0,1/2)	no	Plane
R:(0,1/2,1/2)	E:(u,v,1/2)	Z:(0,0,1/2)	yes	Plane

BCSID: 1.251; Formula: NdCo2P2; MSG: 124.360 ( $P_c4/mcc$ ); U= 4eV				
maximal $k_1$	intermediate path	maximal $k_2$	satisfied?	Line/Plane
$\Gamma:(0,0,0)$	LD:(0,0,w)	Z:(0,0,1/2)	no	Line
A:(1/2,1/2,1/2)	V:(1/2,1/2,w)	M:(1/2,1/2,0)	yes	Line
A:(1/2,1/2,1/2)	T:(u,1/2,1/2)	R:(0,1/2,1/2)	yes	Line
A:(1/2,1/2,1/2)	S:(u,u,1/2)	Z:(0,0,1/2)	yes	Line
R:(0,1/2,1/2)	U:(0,v,1/2)	Z:(0,0,1/2)	yes	Line
A:(1/2,1/2,1/2)	E:(u,v,1/2)	R:(0,1/2,1/2)	yes	Plane
A:(1/2,1/2,1/2)	E:(u,v,1/2)	Z:(0,0,1/2)	yes	Plane
R:(0,1/2,1/2)	E:(u,v,1/2)	Z:(0,0,1/2)	yes	Plane

BCSID: 1.255; Formula: UPtGa5; MSG: 124.360 ( $P_c4/mcc$ ); U= 2eV				
maximal $k_1$	intermediate path	maximal $k_2$	satisfied?	Line/Plane
$\Gamma:(0,0,0)$	LD:(0,0,w)	Z:(0,0,1/2)	no	Line
A:(1/2,1/2,1/2)	V:(1/2,1/2,w)	M:(1/2,1/2,0)	yes	Line
A:(1/2,1/2,1/2)	T:(u,1/2,1/2)	R:(0,1/2,1/2)	yes	Line
A:(1/2,1/2,1/2)	S:(u,u,1/2)	Z:(0,0,1/2)	yes	Line
R:(0,1/2,1/2)	U:(0,v,1/2)	Z:(0,0,1/2)	yes	Line
A:(1/2,1/2,1/2)	E:(u,v,1/2)	R:(0,1/2,1/2)	yes	Plane
A:(1/2,1/2,1/2)	E:(u,v,1/2)	Z:(0,0,1/2)	yes	Plane
R:(0,1/2,1/2)	E:(u,v,1/2)	Z:(0,0,1/2)	yes	Plane

BCSID: 1.255; Formula: UPtGa5; MSG: 124.360 ( $P_c4/mcc$ ); U= 4eV				
--	--	--	--	--

maximal $k_1$	intermediate path	maximal $k_2$	satisfied?	Line/Plane
$\Gamma:(0,0,0)$	LD:(0,0,w)	Z:(0,0,1/2)	no	Line
A:(1/2,1/2,1/2)	V:(1/2,1/2,w)	M:(1/2,1/2,0)	yes	Line
A:(1/2,1/2,1/2)	T:(u,1/2,1/2)	R:(0,1/2,1/2)	yes	Line
A:(1/2,1/2,1/2)	S:(u,u,1/2)	Z:(0,0,1/2)	yes	Line
R:(0,1/2,1/2)	U:(0,v,1/2)	Z:(0,0,1/2)	yes	Line
A:(1/2,1/2,1/2)	E:(u,v,1/2)	R:(0,1/2,1/2)	yes	Plane
A:(1/2,1/2,1/2)	E:(u,v,1/2)	Z:(0,0,1/2)	yes	Plane
R:(0,1/2,1/2)	E:(u,v,1/2)	Z:(0,0,1/2)	yes	Plane

BCSID: 1.255; Formula: UPtGa5; MSG: 124.360 ( $P_c4/mcc$ ); U= 6eV				
maximal $k_1$	intermediate path	maximal $k_2$	satisfied?	Line/Plane
$\Gamma:(0,0,0)$	LD:(0,0,w)	Z:(0,0,1/2)	no	Line
A:(1/2,1/2,1/2)	V:(1/2,1/2,w)	M:(1/2,1/2,0)	no	Line
A:(1/2,1/2,1/2)	T:(u,1/2,1/2)	R:(0,1/2,1/2)	yes	Line
A:(1/2,1/2,1/2)	S:(u,u,1/2)	Z:(0,0,1/2)	yes	Line
R:(0,1/2,1/2)	U:(0,v,1/2)	Z:(0,0,1/2)	yes	Line
A:(1/2,1/2,1/2)	E:(u,v,1/2)	R:(0,1/2,1/2)	yes	Plane
A:(1/2,1/2,1/2)	E:(u,v,1/2)	Z:(0,0,1/2)	yes	Plane
R:(0,1/2,1/2)	E:(u,v,1/2)	Z:(0,0,1/2)	yes	Plane

BCSID: 1.261; Formula: NpRhGa5; MSG: 124.360 ( $P_c4/mcc$ ); U= 0				
maximal $k_1$	intermediate path	maximal $k_2$	satisfied?	Line/Plane
$\Gamma:(0,0,0)$	LD:(0,0,w)	Z:(0,0,1/2)	no	Line
A:(1/2,1/2,1/2)	V:(1/2,1/2,w)	M:(1/2,1/2,0)	yes	Line
A:(1/2,1/2,1/2)	T:(u,1/2,1/2)	R:(0,1/2,1/2)	yes	Line
A:(1/2,1/2,1/2)	S:(u,u,1/2)	Z:(0,0,1/2)	yes	Line
R:(0,1/2,1/2)	U:(0,v,1/2)	Z:(0,0,1/2)	yes	Line
A:(1/2,1/2,1/2)	E:(u,v,1/2)	R:(0,1/2,1/2)	yes	Plane
A:(1/2,1/2,1/2)	E:(u,v,1/2)	Z:(0,0,1/2)	yes	Plane
R:(0,1/2,1/2)	E:(u,v,1/2)	Z:(0,0,1/2)	yes	Plane

BCSID: 1.261; Formula: NpRhGa5; MSG: 124.360 ( $P_c4/mcc$ ); U= 2eV				
maximal $k_1$	intermediate path	maximal $k_2$	satisfied?	Line/Plane
$\Gamma:(0,0,0)$	LD:(0,0,w)	Z:(0,0,1/2)	no	Line
A:(1/2,1/2,1/2)	V:(1/2,1/2,w)	M:(1/2,1/2,0)	no	Line
A:(1/2,1/2,1/2)	T:(u,1/2,1/2)	R:(0,1/2,1/2)	no	Line
A:(1/2,1/2,1/2)	S:(u,u,1/2)	Z:(0,0,1/2)	yes	Line
R:(0,1/2,1/2)	U:(0,v,1/2)	Z:(0,0,1/2)	no	Line
A:(1/2,1/2,1/2)	E:(u,v,1/2)	R:(0,1/2,1/2)	no	Plane
A:(1/2,1/2,1/2)	E:(u,v,1/2)	Z:(0,0,1/2)	yes	Plane
R:(0,1/2,1/2)	E:(u,v,1/2)	Z:(0,0,1/2)	no	Plane

BCSID: 1.261; Formula: NpRhGa5; MSG: 124.360 ( $P_c4/mcc$ ); U= 4eV				
maximal $k_1$	intermediate path	maximal $k_2$	satisfied?	Line/Plane
$\Gamma:(0,0,0)$	LD:(0,0,w)	Z:(0,0,1/2)	yes	Line
A:(1/2,1/2,1/2)	V:(1/2,1/2,w)	M:(1/2,1/2,0)	no	Line
A:(1/2,1/2,1/2)	T:(u,1/2,1/2)	R:(0,1/2,1/2)	no	Line
A:(1/2,1/2,1/2)	S:(u,u,1/2)	Z:(0,0,1/2)	no	Line
R:(0,1/2,1/2)	U:(0,v,1/2)	Z:(0,0,1/2)	yes	Line
A:(1/2,1/2,1/2)	E:(u,v,1/2)	R:(0,1/2,1/2)	no	Plane

A:(1/2,1/2,1/2)	E:(u,v,1/2)	Z:(0,0,1/2)	no	Plane
R:(0,1/2,1/2)	E:(u,v,1/2)	Z:(0,0,1/2)	yes	Plane

BCSID: 1.261; Formula: NpRhGa5; MSG: 124.360 ( $P_c4/mcc$ ); U= 6eV				
maximal $k_1$	intermediate path	maximal $k_2$	satisfied?	Line/Plane
$\Gamma:(0,0,0)$	LD:(0,0,w)	Z:(0,0,1/2)	no	Line
A:(1/2,1/2,1/2)	V:(1/2,1/2,w)	M:(1/2,1/2,0)	no	Line
A:(1/2,1/2,1/2)	T:(u,1/2,1/2)	R:(0,1/2,1/2)	no	Line
A:(1/2,1/2,1/2)	S:(u,u,1/2)	Z:(0,0,1/2)	yes	Line
R:(0,1/2,1/2)	U:(0,v,1/2)	Z:(0,0,1/2)	no	Line
A:(1/2,1/2,1/2)	E:(u,v,1/2)	R:(0,1/2,1/2)	no	Plane
A:(1/2,1/2,1/2)	E:(u,v,1/2)	Z:(0,0,1/2)	yes	Plane
R:(0,1/2,1/2)	E:(u,v,1/2)	Z:(0,0,1/2)	no	Plane

BCSID: 2.14; Formula: NdMg; MSG: 125.373 ( $P_C4/nbm$ ); U= 0				
maximal $k_1$	intermediate path	maximal $k_2$	satisfied?	Line/Plane
$\Gamma:(0,0,0)$	LD:(0,0,w)	Z:(0,0,1/2)	no	Line
A:(1/2,1/2,1/2)	T:(u,1/2,1/2)	R:(0,1/2,1/2)	yes	Line
M:(1/2,1/2,0)	Y:(u,1/2,0)	X:(0,1/2,0)	yes	Line
R:(0,1/2,1/2)	W:(0,1/2,w)	X:(0,1/2,0)	yes	Line
A:(1/2,1/2,1/2)	F:(u,1/2,w)	M:(1/2,1/2,0)	yes	Plane
A:(1/2,1/2,1/2)	F:(u,1/2,w)	R:(0,1/2,1/2)	yes	Plane
A:(1/2,1/2,1/2)	F:(u,1/2,w)	X:(0,1/2,0)	yes	Plane
M:(1/2,1/2,0)	F:(u,1/2,w)	R:(0,1/2,1/2)	yes	Plane
M:(1/2,1/2,0)	F:(u,1/2,w)	X:(0,1/2,0)	yes	Plane
R:(0,1/2,1/2)	F:(u,1/2,w)	X:(0,1/2,0)	yes	Plane

BCSID: 2.14; Formula: NdMg; MSG: 125.373 ( $P_C4/nbm$ ); U= 2eV				
maximal $k_1$	intermediate path	maximal $k_2$	satisfied?	Line/Plane
$\Gamma:(0,0,0)$	LD:(0,0,w)	Z:(0,0,1/2)	no	Line
A:(1/2,1/2,1/2)	T:(u,1/2,1/2)	R:(0,1/2,1/2)	yes	Line
M:(1/2,1/2,0)	Y:(u,1/2,0)	X:(0,1/2,0)	yes	Line
R:(0,1/2,1/2)	W:(0,1/2,w)	X:(0,1/2,0)	yes	Line
A:(1/2,1/2,1/2)	F:(u,1/2,w)	M:(1/2,1/2,0)	yes	Plane
A:(1/2,1/2,1/2)	F:(u,1/2,w)	R:(0,1/2,1/2)	yes	Plane
A:(1/2,1/2,1/2)	F:(u,1/2,w)	X:(0,1/2,0)	yes	Plane
M:(1/2,1/2,0)	F:(u,1/2,w)	R:(0,1/2,1/2)	yes	Plane
M:(1/2,1/2,0)	F:(u,1/2,w)	X:(0,1/2,0)	yes	Plane
R:(0,1/2,1/2)	F:(u,1/2,w)	X:(0,1/2,0)	yes	Plane

BCSID: 2.14; Formula: NdMg; MSG: 125.373 ( $P_C4/nbm$ ); U= 4eV				
maximal $k_1$	intermediate path	maximal $k_2$	satisfied?	Line/Plane
$\Gamma:(0,0,0)$	LD:(0,0,w)	Z:(0,0,1/2)	no	Line
A:(1/2,1/2,1/2)	T:(u,1/2,1/2)	R:(0,1/2,1/2)	yes	Line
M:(1/2,1/2,0)	Y:(u,1/2,0)	X:(0,1/2,0)	yes	Line
R:(0,1/2,1/2)	W:(0,1/2,w)	X:(0,1/2,0)	yes	Line
A:(1/2,1/2,1/2)	F:(u,1/2,w)	M:(1/2,1/2,0)	yes	Plane
A:(1/2,1/2,1/2)	F:(u,1/2,w)	R:(0,1/2,1/2)	yes	Plane
A:(1/2,1/2,1/2)	F:(u,1/2,w)	X:(0,1/2,0)	yes	Plane
M:(1/2,1/2,0)	F:(u,1/2,w)	R:(0,1/2,1/2)	yes	Plane
M:(1/2,1/2,0)	F:(u,1/2,w)	X:(0,1/2,0)	yes	Plane

R:(0,1/2,1/2)	F:(u,1/2,w)	X:(0,1/2,0)	yes	Plane
BCSID: 2.14; Formula: NdMg; MSG: 125.373 ( $P_C4/nbm$ ); U= 6eV				
maximal $k_1$	intermediate path	maximal $k_2$	satisfied?	Line/Plane
$\Gamma:(0,0,0)$	LD:(0,0,w)	Z:(0,0,1/2)	no	Line
A:(1/2,1/2,1/2)	T:(u,1/2,1/2)	R:(0,1/2,1/2)	yes	Line
M:(1/2,1/2,0)	Y:(u,1/2,0)	X:(0,1/2,0)	yes	Line
R:(0,1/2,1/2)	W:(0,1/2,w)	X:(0,1/2,0)	yes	Line
A:(1/2,1/2,1/2)	F:(u,1/2,w)	M:(1/2,1/2,0)	yes	Plane
A:(1/2,1/2,1/2)	F:(u,1/2,w)	R:(0,1/2,1/2)	yes	Plane
A:(1/2,1/2,1/2)	F:(u,1/2,w)	X:(0,1/2,0)	yes	Plane
M:(1/2,1/2,0)	F:(u,1/2,w)	R:(0,1/2,1/2)	yes	Plane
M:(1/2,1/2,0)	F:(u,1/2,w)	X:(0,1/2,0)	yes	Plane
R:(0,1/2,1/2)	F:(u,1/2,w)	X:(0,1/2,0)	yes	Plane
BCSID: 1.253; Formula: CeCo2P2; MSG: 126.386 ( $P_I4/nnc$ ); U= 0				
maximal $k_1$	intermediate path	maximal $k_2$	satisfied?	Line/Plane
$\Gamma:(0,0,0)$	LD:(0,0,w)	Z:(0,0,1/2)	no	Line
A:(1/2,1/2,1/2)	S:(u,u,1/2)	Z:(0,0,1/2)	yes	Line
M:(1/2,1/2,0)	Y:(u,1/2,0)	X:(0,1/2,0)	yes	Line
R:(0,1/2,1/2)	W:(0,1/2,w)	X:(0,1/2,0)	yes	Line
R:(0,1/2,1/2)	U:(0,v,1/2)	Z:(0,0,1/2)	yes	Line
A:(1/2,1/2,1/2)	F:(u,1/2,w)	M:(1/2,1/2,0)	yes	Plane
A:(1/2,1/2,1/2)	E:(u,v,1/2)	R:(0,1/2,1/2)	yes	Plane
A:(1/2,1/2,1/2)	F:(u,1/2,w)	R:(0,1/2,1/2)	yes	Plane
A:(1/2,1/2,1/2)	F:(u,1/2,w)	X:(0,1/2,0)	yes	Plane
A:(1/2,1/2,1/2)	E:(u,v,1/2)	Z:(0,0,1/2)	yes	Plane
M:(1/2,1/2,0)	F:(u,1/2,w)	R:(0,1/2,1/2)	yes	Plane
M:(1/2,1/2,0)	F:(u,1/2,w)	X:(0,1/2,0)	yes	Plane
R:(0,1/2,1/2)	F:(u,1/2,w)	X:(0,1/2,0)	yes	Plane
R:(0,1/2,1/2)	E:(u,v,1/2)	Z:(0,0,1/2)	yes	Plane
BCSID: 1.253; Formula: CeCo2P2; MSG: 126.386 ( $P_I4/nnc$ ); U= 2eV				
maximal $k_1$	intermediate path	maximal $k_2$	satisfied?	Line/Plane
$\Gamma:(0,0,0)$	LD:(0,0,w)	Z:(0,0,1/2)	no	Line
A:(1/2,1/2,1/2)	S:(u,u,1/2)	Z:(0,0,1/2)	yes	Line
M:(1/2,1/2,0)	Y:(u,1/2,0)	X:(0,1/2,0)	yes	Line
R:(0,1/2,1/2)	W:(0,1/2,w)	X:(0,1/2,0)	yes	Line
R:(0,1/2,1/2)	U:(0,v,1/2)	Z:(0,0,1/2)	yes	Line
A:(1/2,1/2,1/2)	F:(u,1/2,w)	M:(1/2,1/2,0)	yes	Plane
A:(1/2,1/2,1/2)	E:(u,v,1/2)	R:(0,1/2,1/2)	yes	Plane
A:(1/2,1/2,1/2)	F:(u,1/2,w)	R:(0,1/2,1/2)	yes	Plane
A:(1/2,1/2,1/2)	F:(u,1/2,w)	X:(0,1/2,0)	yes	Plane
A:(1/2,1/2,1/2)	E:(u,v,1/2)	Z:(0,0,1/2)	yes	Plane
M:(1/2,1/2,0)	F:(u,1/2,w)	R:(0,1/2,1/2)	yes	Plane
M:(1/2,1/2,0)	F:(u,1/2,w)	X:(0,1/2,0)	yes	Plane
R:(0,1/2,1/2)	F:(u,1/2,w)	X:(0,1/2,0)	yes	Plane
R:(0,1/2,1/2)	E:(u,v,1/2)	Z:(0,0,1/2)	yes	Plane
BCSID: 1.253; Formula: CeCo2P2; MSG: 126.386 ( $P_I4/nnc$ ); U= 4eV				
maximal $k_1$	intermediate path	maximal $k_2$	satisfied?	Line/Plane

$\Gamma:(0,0,0)$	LD:(0,0,w)	Z:(0,0,1/2)	yes	Line
A:(1/2,1/2,1/2)	S:(u,u,1/2)	Z:(0,0,1/2)	no	Line
M:(1/2,1/2,0)	Y:(u,1/2,0)	X:(0,1/2,0)	yes	Line
R:(0,1/2,1/2)	W:(0,1/2,w)	X:(0,1/2,0)	yes	Line
R:(0,1/2,1/2)	U:(0,v,1/2)	Z:(0,0,1/2)	no	Line
A:(1/2,1/2,1/2)	F:(u,1/2,w)	M:(1/2,1/2,0)	yes	Plane
A:(1/2,1/2,1/2)	E:(u,v,1/2)	R:(0,1/2,1/2)	yes	Plane
A:(1/2,1/2,1/2)	F:(u,1/2,w)	R:(0,1/2,1/2)	yes	Plane
A:(1/2,1/2,1/2)	F:(u,1/2,w)	X:(0,1/2,0)	yes	Plane
A:(1/2,1/2,1/2)	E:(u,v,1/2)	Z:(0,0,1/2)	no	Plane
M:(1/2,1/2,0)	F:(u,1/2,w)	R:(0,1/2,1/2)	yes	Plane
M:(1/2,1/2,0)	F:(u,1/2,w)	X:(0,1/2,0)	yes	Plane
R:(0,1/2,1/2)	F:(u,1/2,w)	X:(0,1/2,0)	yes	Plane
R:(0,1/2,1/2)	E:(u,v,1/2)	Z:(0,0,1/2)	no	Plane

BCSID: 1.253; Formula: CeCo2P2; MSG: 126.386 ( $P_I4/nnc$ ); U= 6eV				
maximal $k_1$	intermediate path	maximal $k_2$	satisfied?	Line/Plane
$\Gamma:(0,0,0)$	LD:(0,0,w)	Z:(0,0,1/2)	yes	Line
A:(1/2,1/2,1/2)	S:(u,u,1/2)	Z:(0,0,1/2)	no	Line
M:(1/2,1/2,0)	Y:(u,1/2,0)	X:(0,1/2,0)	yes	Line
R:(0,1/2,1/2)	W:(0,1/2,w)	X:(0,1/2,0)	yes	Line
R:(0,1/2,1/2)	U:(0,v,1/2)	Z:(0,0,1/2)	no	Line
A:(1/2,1/2,1/2)	F:(u,1/2,w)	M:(1/2,1/2,0)	yes	Plane
A:(1/2,1/2,1/2)	E:(u,v,1/2)	R:(0,1/2,1/2)	yes	Plane
A:(1/2,1/2,1/2)	F:(u,1/2,w)	R:(0,1/2,1/2)	yes	Plane
A:(1/2,1/2,1/2)	F:(u,1/2,w)	X:(0,1/2,0)	yes	Plane
A:(1/2,1/2,1/2)	E:(u,v,1/2)	Z:(0,0,1/2)	no	Plane
M:(1/2,1/2,0)	F:(u,1/2,w)	R:(0,1/2,1/2)	yes	Plane
M:(1/2,1/2,0)	F:(u,1/2,w)	X:(0,1/2,0)	yes	Plane
R:(0,1/2,1/2)	F:(u,1/2,w)	X:(0,1/2,0)	yes	Plane
R:(0,1/2,1/2)	E:(u,v,1/2)	Z:(0,0,1/2)	no	Plane

BCSID: 1.81; Formula: GdIn3; MSG: 127.397 ( $P_C4/mbm$ ); U= 0				
maximal $k_1$	intermediate path	maximal $k_2$	satisfied?	Line/Plane
$\Gamma:(0,0,0)$	LD:(0,0,w)	Z:(0,0,1/2)	no	Line
A:(1/2,1/2,1/2)	V:(1/2,1/2,w)	M:(1/2,1/2,0)	no	Line
R:(0,1/2,1/2)	W:(0,1/2,w)	X:(0,1/2,0)	yes	Line

BCSID: 1.81; Formula: GdIn3; MSG: 127.397 ( $P_C4/mbm$ ); U= 2eV				
maximal $k_1$	intermediate path	maximal $k_2$	satisfied?	Line/Plane
$\Gamma:(0,0,0)$	LD:(0,0,w)	Z:(0,0,1/2)	no	Line
A:(1/2,1/2,1/2)	V:(1/2,1/2,w)	M:(1/2,1/2,0)	yes	Line
R:(0,1/2,1/2)	W:(0,1/2,w)	X:(0,1/2,0)	yes	Line

BCSID: 1.81; Formula: GdIn3; MSG: 127.397 ( $P_C4/mbm$ ); U= 4eV				
maximal $k_1$	intermediate path	maximal $k_2$	satisfied?	Line/Plane
$\Gamma:(0,0,0)$	LD:(0,0,w)	Z:(0,0,1/2)	no	Line
A:(1/2,1/2,1/2)	V:(1/2,1/2,w)	M:(1/2,1/2,0)	no	Line
R:(0,1/2,1/2)	W:(0,1/2,w)	X:(0,1/2,0)	yes	Line

BCSID: 1.81; Formula: GdIn3; MSG: 127.397 ( $P_{C4}/mbm$ ); U= 6eV				
maximal $k_1$	intermediate path	maximal $k_2$	satisfied?	Line/Plane
$\Gamma:(0,0,0)$	LD:(0,0,w)	Z:(0,0,1/2)	no	Line
A:(1/2,1/2,1/2)	V:(1/2,1/2,w)	M:(1/2,1/2,0)	yes	Line
R:(0,1/2,1/2)	W:(0,1/2,w)	X:(0,1/2,0)	yes	Line

BCSID: 1.102; Formula: U2Ni2In; MSG: 128.408 ( $P_{c4}/mnc$ ); U= 0				
maximal $k_1$	intermediate path	maximal $k_2$	satisfied?	Line/Plane
$\Gamma:(0,0,0)$	LD:(0,0,w)	Z:(0,0,1/2)	no	Line
A:(1/2,1/2,1/2)	T:(u,1/2,1/2)	R:(0,1/2,1/2)	no	Line
A:(1/2,1/2,1/2)	S:(u,u,1/2)	Z:(0,0,1/2)	no	Line
R:(0,1/2,1/2)	W:(0,1/2,w)	X:(0,1/2,0)	yes	Line
R:(0,1/2,1/2)	U:(0,v,1/2)	Z:(0,0,1/2)	yes	Line
A:(1/2,1/2,1/2)	F:(u,1/2,w)	M:(1/2,1/2,0)	yes	Plane
A:(1/2,1/2,1/2)	E:(u,v,1/2)	R:(0,1/2,1/2)	no	Plane
A:(1/2,1/2,1/2)	F:(u,1/2,w)	R:(0,1/2,1/2)	yes	Plane
A:(1/2,1/2,1/2)	F:(u,1/2,w)	X:(0,1/2,0)	yes	Plane
A:(1/2,1/2,1/2)	E:(u,v,1/2)	Z:(0,0,1/2)	no	Plane
M:(1/2,1/2,0)	F:(u,1/2,w)	R:(0,1/2,1/2)	yes	Plane
M:(1/2,1/2,0)	F:(u,1/2,w)	X:(0,1/2,0)	yes	Plane
R:(0,1/2,1/2)	F:(u,1/2,w)	X:(0,1/2,0)	yes	Plane
R:(0,1/2,1/2)	E:(u,v,1/2)	Z:(0,0,1/2)	yes	Plane

BCSID: 1.102; Formula: U2Ni2In; MSG: 128.408 ( $P_{c4}/mnc$ ); U= 2eV				
maximal $k_1$	intermediate path	maximal $k_2$	satisfied?	Line/Plane
$\Gamma:(0,0,0)$	LD:(0,0,w)	Z:(0,0,1/2)	yes	Line
A:(1/2,1/2,1/2)	T:(u,1/2,1/2)	R:(0,1/2,1/2)	no	Line
A:(1/2,1/2,1/2)	S:(u,u,1/2)	Z:(0,0,1/2)	no	Line
R:(0,1/2,1/2)	W:(0,1/2,w)	X:(0,1/2,0)	yes	Line
R:(0,1/2,1/2)	U:(0,v,1/2)	Z:(0,0,1/2)	yes	Line
A:(1/2,1/2,1/2)	F:(u,1/2,w)	M:(1/2,1/2,0)	yes	Plane
A:(1/2,1/2,1/2)	E:(u,v,1/2)	R:(0,1/2,1/2)	no	Plane
A:(1/2,1/2,1/2)	F:(u,1/2,w)	R:(0,1/2,1/2)	yes	Plane
A:(1/2,1/2,1/2)	F:(u,1/2,w)	X:(0,1/2,0)	yes	Plane
A:(1/2,1/2,1/2)	E:(u,v,1/2)	Z:(0,0,1/2)	no	Plane
M:(1/2,1/2,0)	F:(u,1/2,w)	R:(0,1/2,1/2)	yes	Plane
M:(1/2,1/2,0)	F:(u,1/2,w)	X:(0,1/2,0)	yes	Plane
R:(0,1/2,1/2)	F:(u,1/2,w)	X:(0,1/2,0)	yes	Plane
R:(0,1/2,1/2)	E:(u,v,1/2)	Z:(0,0,1/2)	yes	Plane

BCSID: 1.102; Formula: U2Ni2In; MSG: 128.408 ( $P_{c4}/mnc$ ); U= 4eV				
maximal $k_1$	intermediate path	maximal $k_2$	satisfied?	Line/Plane
$\Gamma:(0,0,0)$	LD:(0,0,w)	Z:(0,0,1/2)	yes	Line
A:(1/2,1/2,1/2)	T:(u,1/2,1/2)	R:(0,1/2,1/2)	yes	Line
A:(1/2,1/2,1/2)	S:(u,u,1/2)	Z:(0,0,1/2)	no	Line
R:(0,1/2,1/2)	W:(0,1/2,w)	X:(0,1/2,0)	yes	Line
R:(0,1/2,1/2)	U:(0,v,1/2)	Z:(0,0,1/2)	no	Line
A:(1/2,1/2,1/2)	F:(u,1/2,w)	M:(1/2,1/2,0)	yes	Plane
A:(1/2,1/2,1/2)	E:(u,v,1/2)	R:(0,1/2,1/2)	yes	Plane
A:(1/2,1/2,1/2)	F:(u,1/2,w)	R:(0,1/2,1/2)	yes	Plane
A:(1/2,1/2,1/2)	F:(u,1/2,w)	X:(0,1/2,0)	yes	Plane

A:(1/2,1/2,1/2)	E:(u,v,1/2)	Z:(0,0,1/2)	no	Plane
M:(1/2,1/2,0)	F:(u,1/2,w)	R:(0,1/2,1/2)	yes	Plane
M:(1/2,1/2,0)	F:(u,1/2,w)	X:(0,1/2,0)	yes	Plane
R:(0,1/2,1/2)	F:(u,1/2,w)	X:(0,1/2,0)	yes	Plane
R:(0,1/2,1/2)	E:(u,v,1/2)	Z:(0,0,1/2)	no	Plane

BCSID: 1.102; Formula: U2Ni2In; MSG: 128.408 ( $P_{c4}/mnc$ ); U= 6eV				
maximal $k_1$	intermediate path	maximal $k_2$	satisfied?	Line/Plane
$\Gamma:(0,0,0)$	LD:(0,0,w)	Z:(0,0,1/2)	no	Line
A:(1/2,1/2,1/2)	T:(u,1/2,1/2)	R:(0,1/2,1/2)	no	Line
A:(1/2,1/2,1/2)	S:(u,u,1/2)	Z:(0,0,1/2)	no	Line
R:(0,1/2,1/2)	W:(0,1/2,w)	X:(0,1/2,0)	no	Line
R:(0,1/2,1/2)	U:(0,v,1/2)	Z:(0,0,1/2)	yes	Line
A:(1/2,1/2,1/2)	F:(u,1/2,w)	M:(1/2,1/2,0)	yes	Plane
A:(1/2,1/2,1/2)	E:(u,v,1/2)	R:(0,1/2,1/2)	no	Plane
A:(1/2,1/2,1/2)	F:(u,1/2,w)	R:(0,1/2,1/2)	no	Plane
A:(1/2,1/2,1/2)	F:(u,1/2,w)	X:(0,1/2,0)	yes	Plane
A:(1/2,1/2,1/2)	E:(u,v,1/2)	Z:(0,0,1/2)	no	Plane
M:(1/2,1/2,0)	F:(u,1/2,w)	R:(0,1/2,1/2)	no	Plane
M:(1/2,1/2,0)	F:(u,1/2,w)	X:(0,1/2,0)	yes	Plane
R:(0,1/2,1/2)	F:(u,1/2,w)	X:(0,1/2,0)	no	Plane
R:(0,1/2,1/2)	E:(u,v,1/2)	Z:(0,0,1/2)	yes	Plane

BCSID: 1.160; Formula: UP; MSG: 128.410 ( $P_{I4}/mnc$ ); U= 0				
maximal $k_1$	intermediate path	maximal $k_2$	satisfied?	Line/Plane
$\Gamma:(0,0,0)$	LD:(0,0,w)	Z:(0,0,1/2)	yes	Line
A:(1/2,1/2,1/2)	V:(1/2,1/2,w)	M:(1/2,1/2,0)	yes	Line
A:(1/2,1/2,1/2)	T:(u,1/2,1/2)	R:(0,1/2,1/2)	no	Line
A:(1/2,1/2,1/2)	S:(u,u,1/2)	Z:(0,0,1/2)	no	Line
R:(0,1/2,1/2)	W:(0,1/2,w)	X:(0,1/2,0)	no	Line
R:(0,1/2,1/2)	U:(0,v,1/2)	Z:(0,0,1/2)	yes	Line
A:(1/2,1/2,1/2)	E:(u,v,1/2)	R:(0,1/2,1/2)	no	Plane
A:(1/2,1/2,1/2)	E:(u,v,1/2)	Z:(0,0,1/2)	no	Plane
R:(0,1/2,1/2)	E:(u,v,1/2)	Z:(0,0,1/2)	yes	Plane

BCSID: 1.160; Formula: UP; MSG: 128.410 ( $P_{I4}/mnc$ ); U= 2eV				
maximal $k_1$	intermediate path	maximal $k_2$	satisfied?	Line/Plane
$\Gamma:(0,0,0)$	LD:(0,0,w)	Z:(0,0,1/2)	no	Line
A:(1/2,1/2,1/2)	V:(1/2,1/2,w)	M:(1/2,1/2,0)	no	Line
A:(1/2,1/2,1/2)	T:(u,1/2,1/2)	R:(0,1/2,1/2)	yes	Line
A:(1/2,1/2,1/2)	S:(u,u,1/2)	Z:(0,0,1/2)	no	Line
R:(0,1/2,1/2)	W:(0,1/2,w)	X:(0,1/2,0)	yes	Line
R:(0,1/2,1/2)	U:(0,v,1/2)	Z:(0,0,1/2)	no	Line
A:(1/2,1/2,1/2)	E:(u,v,1/2)	R:(0,1/2,1/2)	yes	Plane
A:(1/2,1/2,1/2)	E:(u,v,1/2)	Z:(0,0,1/2)	no	Plane
R:(0,1/2,1/2)	E:(u,v,1/2)	Z:(0,0,1/2)	no	Plane

BCSID: 1.160; Formula: UP; MSG: 128.410 ( $P_{I4}/mnc$ ); U= 4eV				
maximal $k_1$	intermediate path	maximal $k_2$	satisfied?	Line/Plane
$\Gamma:(0,0,0)$	LD:(0,0,w)	Z:(0,0,1/2)	yes	Line
A:(1/2,1/2,1/2)	V:(1/2,1/2,w)	M:(1/2,1/2,0)	no	Line

A:(1/2,1/2,1/2)	T:(u,1/2,1/2)	R:(0,1/2,1/2)	yes	Line
A:(1/2,1/2,1/2)	S:(u,u,1/2)	Z:(0,0,1/2)	yes	Line
R:(0,1/2,1/2)	W:(0,1/2,w)	X:(0,1/2,0)	yes	Line
R:(0,1/2,1/2)	U:(0,v,1/2)	Z:(0,0,1/2)	yes	Line
A:(1/2,1/2,1/2)	E:(u,v,1/2)	R:(0,1/2,1/2)	yes	Plane
A:(1/2,1/2,1/2)	E:(u,v,1/2)	Z:(0,0,1/2)	yes	Plane
R:(0,1/2,1/2)	E:(u,v,1/2)	Z:(0,0,1/2)	yes	Plane

BCSID: 1.160; Formula: UP; MSG: 128.410 ( $P_{I4}/mnc$ ); U= 6eV				
maximal $k_1$	intermediate path	maximal $k_2$	satisfied?	Line/Plane
$\Gamma:(0,0,0)$	LD:(0,0,w)	Z:(0,0,1/2)	no	Line
A:(1/2,1/2,1/2)	V:(1/2,1/2,w)	M:(1/2,1/2,0)	yes	Line
A:(1/2,1/2,1/2)	T:(u,1/2,1/2)	R:(0,1/2,1/2)	no	Line
A:(1/2,1/2,1/2)	S:(u,u,1/2)	Z:(0,0,1/2)	no	Line
R:(0,1/2,1/2)	W:(0,1/2,w)	X:(0,1/2,0)	yes	Line
R:(0,1/2,1/2)	U:(0,v,1/2)	Z:(0,0,1/2)	yes	Line
A:(1/2,1/2,1/2)	E:(u,v,1/2)	R:(0,1/2,1/2)	no	Plane
A:(1/2,1/2,1/2)	E:(u,v,1/2)	Z:(0,0,1/2)	no	Plane
R:(0,1/2,1/2)	E:(u,v,1/2)	Z:(0,0,1/2)	yes	Plane

BCSID: 1.187; Formula: TbRh2Si2; MSG: 128.410 ( $P_{I4}/mnc$ ); U= 0				
maximal $k_1$	intermediate path	maximal $k_2$	satisfied?	Line/Plane
$\Gamma:(0,0,0)$	LD:(0,0,w)	Z:(0,0,1/2)	no	Line
A:(1/2,1/2,1/2)	V:(1/2,1/2,w)	M:(1/2,1/2,0)	yes	Line
A:(1/2,1/2,1/2)	T:(u,1/2,1/2)	R:(0,1/2,1/2)	yes	Line
A:(1/2,1/2,1/2)	S:(u,u,1/2)	Z:(0,0,1/2)	yes	Line
R:(0,1/2,1/2)	W:(0,1/2,w)	X:(0,1/2,0)	no	Line
R:(0,1/2,1/2)	U:(0,v,1/2)	Z:(0,0,1/2)	yes	Line
A:(1/2,1/2,1/2)	E:(u,v,1/2)	R:(0,1/2,1/2)	yes	Plane
A:(1/2,1/2,1/2)	E:(u,v,1/2)	Z:(0,0,1/2)	yes	Plane
R:(0,1/2,1/2)	E:(u,v,1/2)	Z:(0,0,1/2)	yes	Plane

BCSID: 1.187; Formula: TbRh2Si2; MSG: 128.410 ( $P_{I4}/mnc$ ); U= 2eV				
maximal $k_1$	intermediate path	maximal $k_2$	satisfied?	Line/Plane
$\Gamma:(0,0,0)$	LD:(0,0,w)	Z:(0,0,1/2)	no	Line
A:(1/2,1/2,1/2)	V:(1/2,1/2,w)	M:(1/2,1/2,0)	yes	Line
A:(1/2,1/2,1/2)	T:(u,1/2,1/2)	R:(0,1/2,1/2)	yes	Line
A:(1/2,1/2,1/2)	S:(u,u,1/2)	Z:(0,0,1/2)	yes	Line
R:(0,1/2,1/2)	W:(0,1/2,w)	X:(0,1/2,0)	yes	Line
R:(0,1/2,1/2)	U:(0,v,1/2)	Z:(0,0,1/2)	yes	Line
A:(1/2,1/2,1/2)	E:(u,v,1/2)	R:(0,1/2,1/2)	yes	Plane
A:(1/2,1/2,1/2)	E:(u,v,1/2)	Z:(0,0,1/2)	yes	Plane
R:(0,1/2,1/2)	E:(u,v,1/2)	Z:(0,0,1/2)	yes	Plane

BCSID: 1.187; Formula: TbRh2Si2; MSG: 128.410 ( $P_{I4}/mnc$ ); U= 4eV				
maximal $k_1$	intermediate path	maximal $k_2$	satisfied?	Line/Plane
$\Gamma:(0,0,0)$	LD:(0,0,w)	Z:(0,0,1/2)	no	Line
A:(1/2,1/2,1/2)	V:(1/2,1/2,w)	M:(1/2,1/2,0)	yes	Line
A:(1/2,1/2,1/2)	T:(u,1/2,1/2)	R:(0,1/2,1/2)	no	Line
A:(1/2,1/2,1/2)	S:(u,u,1/2)	Z:(0,0,1/2)	no	Line
R:(0,1/2,1/2)	W:(0,1/2,w)	X:(0,1/2,0)	yes	Line

R:(0,1/2,1/2)	U:(0,v,1/2)	Z:(0,0,1/2)	yes	Line
A:(1/2,1/2,1/2)	E:(u,v,1/2)	R:(0,1/2,1/2)	no	Plane
A:(1/2,1/2,1/2)	E:(u,v,1/2)	Z:(0,0,1/2)	no	Plane
R:(0,1/2,1/2)	E:(u,v,1/2)	Z:(0,0,1/2)	yes	Plane

BCSID: 1.187; Formula: TbRh2Si2; MSG: 128.410 ( $P_{I4}/mnc$ ); U= 6eV				
maximal $k_1$	intermediate path	maximal $k_2$	satisfied?	Line/Plane
$\Gamma:(0,0,0)$	LD:(0,0,w)	Z:(0,0,1/2)	no	Line
A:(1/2,1/2,1/2)	V:(1/2,1/2,w)	M:(1/2,1/2,0)	yes	Line
A:(1/2,1/2,1/2)	T:(u,1/2,1/2)	R:(0,1/2,1/2)	no	Line
A:(1/2,1/2,1/2)	S:(u,u,1/2)	Z:(0,0,1/2)	no	Line
R:(0,1/2,1/2)	W:(0,1/2,w)	X:(0,1/2,0)	yes	Line
R:(0,1/2,1/2)	U:(0,v,1/2)	Z:(0,0,1/2)	yes	Line
A:(1/2,1/2,1/2)	E:(u,v,1/2)	R:(0,1/2,1/2)	no	Plane
A:(1/2,1/2,1/2)	E:(u,v,1/2)	Z:(0,0,1/2)	no	Plane
R:(0,1/2,1/2)	E:(u,v,1/2)	Z:(0,0,1/2)	yes	Plane

BCSID: 1.208; Formula: UAs; MSG: 128.410 ( $P_{I4}/mnc$ ); U= 0				
maximal $k_1$	intermediate path	maximal $k_2$	satisfied?	Line/Plane
$\Gamma:(0,0,0)$	LD:(0,0,w)	Z:(0,0,1/2)	yes	Line
A:(1/2,1/2,1/2)	V:(1/2,1/2,w)	M:(1/2,1/2,0)	yes	Line
A:(1/2,1/2,1/2)	T:(u,1/2,1/2)	R:(0,1/2,1/2)	no	Line
A:(1/2,1/2,1/2)	S:(u,u,1/2)	Z:(0,0,1/2)	no	Line
R:(0,1/2,1/2)	W:(0,1/2,w)	X:(0,1/2,0)	no	Line
R:(0,1/2,1/2)	U:(0,v,1/2)	Z:(0,0,1/2)	yes	Line
A:(1/2,1/2,1/2)	E:(u,v,1/2)	R:(0,1/2,1/2)	no	Plane
A:(1/2,1/2,1/2)	E:(u,v,1/2)	Z:(0,0,1/2)	no	Plane
R:(0,1/2,1/2)	E:(u,v,1/2)	Z:(0,0,1/2)	yes	Plane

BCSID: 1.208; Formula: UAs; MSG: 128.410 ( $P_{I4}/mnc$ ); U= 2eV				
maximal $k_1$	intermediate path	maximal $k_2$	satisfied?	Line/Plane
$\Gamma:(0,0,0)$	LD:(0,0,w)	Z:(0,0,1/2)	yes	Line
A:(1/2,1/2,1/2)	V:(1/2,1/2,w)	M:(1/2,1/2,0)	no	Line
A:(1/2,1/2,1/2)	T:(u,1/2,1/2)	R:(0,1/2,1/2)	yes	Line
A:(1/2,1/2,1/2)	S:(u,u,1/2)	Z:(0,0,1/2)	yes	Line
R:(0,1/2,1/2)	W:(0,1/2,w)	X:(0,1/2,0)	yes	Line
R:(0,1/2,1/2)	U:(0,v,1/2)	Z:(0,0,1/2)	yes	Line
A:(1/2,1/2,1/2)	E:(u,v,1/2)	R:(0,1/2,1/2)	yes	Plane
A:(1/2,1/2,1/2)	E:(u,v,1/2)	Z:(0,0,1/2)	yes	Plane
R:(0,1/2,1/2)	E:(u,v,1/2)	Z:(0,0,1/2)	yes	Plane

BCSID: 1.208; Formula: UAs; MSG: 128.410 ( $P_{I4}/mnc$ ); U= 4eV				
maximal $k_1$	intermediate path	maximal $k_2$	satisfied?	Line/Plane
$\Gamma:(0,0,0)$	LD:(0,0,w)	Z:(0,0,1/2)	yes	Line
A:(1/2,1/2,1/2)	V:(1/2,1/2,w)	M:(1/2,1/2,0)	no	Line
A:(1/2,1/2,1/2)	T:(u,1/2,1/2)	R:(0,1/2,1/2)	yes	Line
A:(1/2,1/2,1/2)	S:(u,u,1/2)	Z:(0,0,1/2)	yes	Line
R:(0,1/2,1/2)	W:(0,1/2,w)	X:(0,1/2,0)	yes	Line
R:(0,1/2,1/2)	U:(0,v,1/2)	Z:(0,0,1/2)	yes	Line
A:(1/2,1/2,1/2)	E:(u,v,1/2)	R:(0,1/2,1/2)	yes	Plane
A:(1/2,1/2,1/2)	E:(u,v,1/2)	Z:(0,0,1/2)	yes	Plane

R:(0,1/2,1/2)	E:(u,v,1/2)	Z:(0,0,1/2)	yes	Plane
BCSID: 1.21; Formula: DyCo <sub>2</sub> Si <sub>2</sub> ; MSG: 128.410 ( $P_I4/mnc$ ); U= 2eV				
maximal $k_1$	intermediate path	maximal $k_2$	satisfied?	Line/Plane
$\Gamma:(0,0,0)$	LD:(0,0,w)	Z:(0,0,1/2)	no	Line
A:(1/2,1/2,1/2)	V:(1/2,1/2,w)	M:(1/2,1/2,0)	yes	Line
A:(1/2,1/2,1/2)	T:(u,1/2,1/2)	R:(0,1/2,1/2)	yes	Line
A:(1/2,1/2,1/2)	S:(u,u,1/2)	Z:(0,0,1/2)	yes	Line
R:(0,1/2,1/2)	W:(0,1/2,w)	X:(0,1/2,0)	yes	Line
R:(0,1/2,1/2)	U:(0,v,1/2)	Z:(0,0,1/2)	yes	Line
A:(1/2,1/2,1/2)	E:(u,v,1/2)	R:(0,1/2,1/2)	yes	Plane
A:(1/2,1/2,1/2)	E:(u,v,1/2)	Z:(0,0,1/2)	yes	Plane
R:(0,1/2,1/2)	E:(u,v,1/2)	Z:(0,0,1/2)	yes	Plane
BCSID: 1.21; Formula: DyCo <sub>2</sub> Si <sub>2</sub> ; MSG: 128.410 ( $P_I4/mnc$ ); U= 4eV				
maximal $k_1$	intermediate path	maximal $k_2$	satisfied?	Line/Plane
$\Gamma:(0,0,0)$	LD:(0,0,w)	Z:(0,0,1/2)	no	Line
A:(1/2,1/2,1/2)	V:(1/2,1/2,w)	M:(1/2,1/2,0)	yes	Line
A:(1/2,1/2,1/2)	T:(u,1/2,1/2)	R:(0,1/2,1/2)	yes	Line
A:(1/2,1/2,1/2)	S:(u,u,1/2)	Z:(0,0,1/2)	yes	Line
R:(0,1/2,1/2)	W:(0,1/2,w)	X:(0,1/2,0)	yes	Line
R:(0,1/2,1/2)	U:(0,v,1/2)	Z:(0,0,1/2)	yes	Line
A:(1/2,1/2,1/2)	E:(u,v,1/2)	R:(0,1/2,1/2)	yes	Plane
A:(1/2,1/2,1/2)	E:(u,v,1/2)	Z:(0,0,1/2)	yes	Plane
R:(0,1/2,1/2)	E:(u,v,1/2)	Z:(0,0,1/2)	yes	Plane
BCSID: 1.215; Formula: UP2; MSG: 130.432 ( $P_c4/ncc$ ); U= 0				
maximal $k_1$	intermediate path	maximal $k_2$	satisfied?	Line/Plane
$\Gamma:(0,0,0)$	LD:(0,0,w)	Z:(0,0,1/2)	yes	Line
A:(1/2,1/2,1/2)	S:(u,u,1/2)	Z:(0,0,1/2)	no	Line
M:(1/2,1/2,0)	Y:(u,1/2,0)	X:(0,1/2,0)	yes	Line
R:(0,1/2,1/2)	U:(0,v,1/2)	Z:(0,0,1/2)	no	Line
A:(1/2,1/2,1/2)	F:(u,1/2,w)	M:(1/2,1/2,0)	yes	Plane
A:(1/2,1/2,1/2)	E:(u,v,1/2)	R:(0,1/2,1/2)	yes	Plane
A:(1/2,1/2,1/2)	F:(u,1/2,w)	R:(0,1/2,1/2)	yes	Plane
A:(1/2,1/2,1/2)	F:(u,1/2,w)	X:(0,1/2,0)	yes	Plane
A:(1/2,1/2,1/2)	E:(u,v,1/2)	Z:(0,0,1/2)	no	Plane
M:(1/2,1/2,0)	F:(u,1/2,w)	R:(0,1/2,1/2)	yes	Plane
M:(1/2,1/2,0)	F:(u,1/2,w)	X:(0,1/2,0)	yes	Plane
R:(0,1/2,1/2)	F:(u,1/2,w)	X:(0,1/2,0)	yes	Plane
R:(0,1/2,1/2)	E:(u,v,1/2)	Z:(0,0,1/2)	no	Plane
BCSID: 1.215; Formula: UP2; MSG: 130.432 ( $P_c4/ncc$ ); U= 2eV				
maximal $k_1$	intermediate path	maximal $k_2$	satisfied?	Line/Plane
$\Gamma:(0,0,0)$	LD:(0,0,w)	Z:(0,0,1/2)	no	Line
A:(1/2,1/2,1/2)	S:(u,u,1/2)	Z:(0,0,1/2)	yes	Line
M:(1/2,1/2,0)	Y:(u,1/2,0)	X:(0,1/2,0)	yes	Line
R:(0,1/2,1/2)	U:(0,v,1/2)	Z:(0,0,1/2)	yes	Line
A:(1/2,1/2,1/2)	F:(u,1/2,w)	M:(1/2,1/2,0)	yes	Plane
A:(1/2,1/2,1/2)	E:(u,v,1/2)	R:(0,1/2,1/2)	yes	Plane
A:(1/2,1/2,1/2)	F:(u,1/2,w)	R:(0,1/2,1/2)	yes	Plane

A:(1/2,1/2,1/2)	F:(u,1/2,w)	X:(0,1/2,0)	yes	Plane
A:(1/2,1/2,1/2)	E:(u,v,1/2)	Z:(0,0,1/2)	yes	Plane
M:(1/2,1/2,0)	F:(u,1/2,w)	R:(0,1/2,1/2)	yes	Plane
M:(1/2,1/2,0)	F:(u,1/2,w)	X:(0,1/2,0)	yes	Plane
R:(0,1/2,1/2)	F:(u,1/2,w)	X:(0,1/2,0)	yes	Plane
R:(0,1/2,1/2)	E:(u,v,1/2)	Z:(0,0,1/2)	yes	Plane

BCSID: 1.215; Formula: UP2; MSG: 130.432 ( $P_{c4}/ncc$ ); U= 4eV				
maximal $k_1$	intermediate path	maximal $k_2$	satisfied?	Line/Plane
$\Gamma:(0,0,0)$	LD:(0,0,w)	Z:(0,0,1/2)	yes	Line
A:(1/2,1/2,1/2)	S:(u,v,1/2)	Z:(0,0,1/2)	no	Line
M:(1/2,1/2,0)	Y:(u,1/2,0)	X:(0,1/2,0)	yes	Line
R:(0,1/2,1/2)	U:(0,v,1/2)	Z:(0,0,1/2)	no	Line
A:(1/2,1/2,1/2)	F:(u,1/2,w)	M:(1/2,1/2,0)	yes	Plane
A:(1/2,1/2,1/2)	E:(u,v,1/2)	R:(0,1/2,1/2)	yes	Plane
A:(1/2,1/2,1/2)	F:(u,1/2,w)	R:(0,1/2,1/2)	yes	Plane
A:(1/2,1/2,1/2)	F:(u,1/2,w)	X:(0,1/2,0)	yes	Plane
A:(1/2,1/2,1/2)	E:(u,v,1/2)	Z:(0,0,1/2)	no	Plane
M:(1/2,1/2,0)	F:(u,1/2,w)	R:(0,1/2,1/2)	yes	Plane
M:(1/2,1/2,0)	F:(u,1/2,w)	X:(0,1/2,0)	yes	Plane
R:(0,1/2,1/2)	F:(u,1/2,w)	X:(0,1/2,0)	yes	Plane
R:(0,1/2,1/2)	E:(u,v,1/2)	Z:(0,0,1/2)	no	Plane

BCSID: 1.215; Formula: UP2; MSG: 130.432 ( $P_{c4}/ncc$ ); U= 6eV				
maximal $k_1$	intermediate path	maximal $k_2$	satisfied?	Line/Plane
$\Gamma:(0,0,0)$	LD:(0,0,w)	Z:(0,0,1/2)	yes	Line
A:(1/2,1/2,1/2)	S:(u,v,1/2)	Z:(0,0,1/2)	no	Line
M:(1/2,1/2,0)	Y:(u,1/2,0)	X:(0,1/2,0)	yes	Line
R:(0,1/2,1/2)	U:(0,v,1/2)	Z:(0,0,1/2)	no	Line
A:(1/2,1/2,1/2)	F:(u,1/2,w)	M:(1/2,1/2,0)	yes	Plane
A:(1/2,1/2,1/2)	E:(u,v,1/2)	R:(0,1/2,1/2)	yes	Plane
A:(1/2,1/2,1/2)	F:(u,1/2,w)	R:(0,1/2,1/2)	yes	Plane
A:(1/2,1/2,1/2)	F:(u,1/2,w)	X:(0,1/2,0)	yes	Plane
A:(1/2,1/2,1/2)	E:(u,v,1/2)	Z:(0,0,1/2)	no	Plane
M:(1/2,1/2,0)	F:(u,1/2,w)	R:(0,1/2,1/2)	yes	Plane
M:(1/2,1/2,0)	F:(u,1/2,w)	X:(0,1/2,0)	yes	Plane
R:(0,1/2,1/2)	F:(u,1/2,w)	X:(0,1/2,0)	yes	Plane
R:(0,1/2,1/2)	E:(u,v,1/2)	Z:(0,0,1/2)	no	Plane

BCSID: 2.20; Formula: UAs; MSG: 134.481 ( $P_{C42}/nnm$ ); U= 2eV				
maximal $k_1$	intermediate path	maximal $k_2$	satisfied?	Line/Plane
$\Gamma:(0,0,0)$	LD:(0,0,w)	Z:(0,0,1/2)	yes	Line
M:(1/2,1/2,0)	Y:(u,1/2,0)	X:(0,1/2,0)	no	Line
R:(0,1/2,1/2)	W:(0,1/2,w)	X:(0,1/2,0)	no	Line
R:(0,1/2,1/2)	U:(0,v,1/2)	Z:(0,0,1/2)	yes	Line
A:(1/2,1/2,1/2)	F:(u,1/2,w)	M:(1/2,1/2,0)	yes	Plane
A:(1/2,1/2,1/2)	F:(u,1/2,w)	R:(0,1/2,1/2)	yes	Plane
A:(1/2,1/2,1/2)	F:(u,1/2,w)	X:(0,1/2,0)	no	Plane
M:(1/2,1/2,0)	F:(u,1/2,w)	R:(0,1/2,1/2)	yes	Plane
M:(1/2,1/2,0)	F:(u,1/2,w)	X:(0,1/2,0)	no	Plane
R:(0,1/2,1/2)	F:(u,1/2,w)	X:(0,1/2,0)	no	Plane

BCSID: 1.103; Formula: U2Rh2Sn; MSG: 135.492 ( $P_c4_2/mbc$ ); U= 0				
maximal $k_1$	intermediate path	maximal $k_2$	satisfied?	Line/Plane
$\Gamma:(0,0,0)$	LD:(0,0,w)	Z:(0,0,1/2)	no	Line
A:(1/2,1/2,1/2)	S:(u,u,1/2)	Z:(0,0,1/2)	yes	Line
R:(0,1/2,1/2)	W:(0,1/2,w)	X:(0,1/2,0)	yes	Line
A:(1/2,1/2,1/2)	F:(u,1/2,w)	M:(1/2,1/2,0)	yes	Plane
A:(1/2,1/2,1/2)	E:(u,v,1/2)	R:(0,1/2,1/2)	yes	Plane
A:(1/2,1/2,1/2)	F:(u,1/2,w)	R:(0,1/2,1/2)	yes	Plane
A:(1/2,1/2,1/2)	F:(u,1/2,w)	X:(0,1/2,0)	yes	Plane
A:(1/2,1/2,1/2)	E:(u,v,1/2)	Z:(0,0,1/2)	yes	Plane
M:(1/2,1/2,0)	F:(u,1/2,w)	R:(0,1/2,1/2)	yes	Plane
M:(1/2,1/2,0)	F:(u,1/2,w)	X:(0,1/2,0)	yes	Plane
R:(0,1/2,1/2)	F:(u,1/2,w)	X:(0,1/2,0)	yes	Plane
R:(0,1/2,1/2)	E:(u,v,1/2)	Z:(0,0,1/2)	yes	Plane

BCSID: 1.103; Formula: U2Rh2Sn; MSG: 135.492 ( $P_c4_2/mbc$ ); U= 2eV				
maximal $k_1$	intermediate path	maximal $k_2$	satisfied?	Line/Plane
$\Gamma:(0,0,0)$	LD:(0,0,w)	Z:(0,0,1/2)	no	Line
A:(1/2,1/2,1/2)	S:(u,u,1/2)	Z:(0,0,1/2)	yes	Line
R:(0,1/2,1/2)	W:(0,1/2,w)	X:(0,1/2,0)	yes	Line
A:(1/2,1/2,1/2)	F:(u,1/2,w)	M:(1/2,1/2,0)	yes	Plane
A:(1/2,1/2,1/2)	E:(u,v,1/2)	R:(0,1/2,1/2)	yes	Plane
A:(1/2,1/2,1/2)	F:(u,1/2,w)	R:(0,1/2,1/2)	yes	Plane
A:(1/2,1/2,1/2)	F:(u,1/2,w)	X:(0,1/2,0)	yes	Plane
A:(1/2,1/2,1/2)	E:(u,v,1/2)	Z:(0,0,1/2)	yes	Plane
M:(1/2,1/2,0)	F:(u,1/2,w)	R:(0,1/2,1/2)	yes	Plane
M:(1/2,1/2,0)	F:(u,1/2,w)	X:(0,1/2,0)	yes	Plane
R:(0,1/2,1/2)	F:(u,1/2,w)	X:(0,1/2,0)	yes	Plane
R:(0,1/2,1/2)	E:(u,v,1/2)	Z:(0,0,1/2)	yes	Plane

BCSID: 1.103; Formula: U2Rh2Sn; MSG: 135.492 ( $P_c4_2/mbc$ ); U= 4eV				
maximal $k_1$	intermediate path	maximal $k_2$	satisfied?	Line/Plane
$\Gamma:(0,0,0)$	LD:(0,0,w)	Z:(0,0,1/2)	no	Line
A:(1/2,1/2,1/2)	S:(u,u,1/2)	Z:(0,0,1/2)	yes	Line
R:(0,1/2,1/2)	W:(0,1/2,w)	X:(0,1/2,0)	yes	Line
A:(1/2,1/2,1/2)	F:(u,1/2,w)	M:(1/2,1/2,0)	yes	Plane
A:(1/2,1/2,1/2)	E:(u,v,1/2)	R:(0,1/2,1/2)	yes	Plane
A:(1/2,1/2,1/2)	F:(u,1/2,w)	R:(0,1/2,1/2)	yes	Plane
A:(1/2,1/2,1/2)	F:(u,1/2,w)	X:(0,1/2,0)	yes	Plane
A:(1/2,1/2,1/2)	E:(u,v,1/2)	Z:(0,0,1/2)	yes	Plane
M:(1/2,1/2,0)	F:(u,1/2,w)	R:(0,1/2,1/2)	yes	Plane
M:(1/2,1/2,0)	F:(u,1/2,w)	X:(0,1/2,0)	yes	Plane
R:(0,1/2,1/2)	F:(u,1/2,w)	X:(0,1/2,0)	yes	Plane
R:(0,1/2,1/2)	E:(u,v,1/2)	Z:(0,0,1/2)	yes	Plane

BCSID: 1.103; Formula: U2Rh2Sn; MSG: 135.492 ( $P_c4_2/mbc$ ); U= 6eV				
maximal $k_1$	intermediate path	maximal $k_2$	satisfied?	Line/Plane
$\Gamma:(0,0,0)$	LD:(0,0,w)	Z:(0,0,1/2)	no	Line
A:(1/2,1/2,1/2)	S:(u,u,1/2)	Z:(0,0,1/2)	yes	Line
R:(0,1/2,1/2)	W:(0,1/2,w)	X:(0,1/2,0)	yes	Line

A:(1/2,1/2,1/2)	F:(u,1/2,w)	M:(1/2,1/2,0)	yes	Plane
A:(1/2,1/2,1/2)	E:(u,v,1/2)	R:(0,1/2,1/2)	yes	Plane
A:(1/2,1/2,1/2)	F:(u,1/2,w)	R:(0,1/2,1/2)	yes	Plane
A:(1/2,1/2,1/2)	F:(u,1/2,w)	X:(0,1/2,0)	yes	Plane
A:(1/2,1/2,1/2)	E:(u,v,1/2)	Z:(0,0,1/2)	yes	Plane
M:(1/2,1/2,0)	F:(u,1/2,w)	R:(0,1/2,1/2)	yes	Plane
M:(1/2,1/2,0)	F:(u,1/2,w)	X:(0,1/2,0)	yes	Plane
R:(0,1/2,1/2)	F:(u,1/2,w)	X:(0,1/2,0)	yes	Plane
R:(0,1/2,1/2)	E:(u,v,1/2)	Z:(0,0,1/2)	yes	Plane

BCSID: 1.207; Formula: U2Rh2Sn; MSG: 135.492 ( $P_c4_2/mbc$ ); U = 0				
maximal $k_1$	intermediate path	maximal $k_2$	satisfied?	Line/Plane
$\Gamma:(0,0,0)$	LD:(0,0,w)	Z:(0,0,1/2)	no	Line
A:(1/2,1/2,1/2)	S:(u,u,1/2)	Z:(0,0,1/2)	yes	Line
R:(0,1/2,1/2)	W:(0,1/2,w)	X:(0,1/2,0)	yes	Line
A:(1/2,1/2,1/2)	F:(u,1/2,w)	M:(1/2,1/2,0)	yes	Plane
A:(1/2,1/2,1/2)	E:(u,v,1/2)	R:(0,1/2,1/2)	yes	Plane
A:(1/2,1/2,1/2)	F:(u,1/2,w)	R:(0,1/2,1/2)	yes	Plane
A:(1/2,1/2,1/2)	F:(u,1/2,w)	X:(0,1/2,0)	yes	Plane
A:(1/2,1/2,1/2)	E:(u,v,1/2)	Z:(0,0,1/2)	yes	Plane
M:(1/2,1/2,0)	F:(u,1/2,w)	R:(0,1/2,1/2)	yes	Plane
M:(1/2,1/2,0)	F:(u,1/2,w)	X:(0,1/2,0)	yes	Plane
R:(0,1/2,1/2)	F:(u,1/2,w)	X:(0,1/2,0)	yes	Plane
R:(0,1/2,1/2)	E:(u,v,1/2)	Z:(0,0,1/2)	yes	Plane

BCSID: 1.207; Formula: U2Rh2Sn; MSG: 135.492 ( $P_c4_2/mbc$ ); U = 2eV				
maximal $k_1$	intermediate path	maximal $k_2$	satisfied?	Line/Plane
$\Gamma:(0,0,0)$	LD:(0,0,w)	Z:(0,0,1/2)	no	Line
A:(1/2,1/2,1/2)	S:(u,u,1/2)	Z:(0,0,1/2)	yes	Line
R:(0,1/2,1/2)	W:(0,1/2,w)	X:(0,1/2,0)	yes	Line
A:(1/2,1/2,1/2)	F:(u,1/2,w)	M:(1/2,1/2,0)	yes	Plane
A:(1/2,1/2,1/2)	E:(u,v,1/2)	R:(0,1/2,1/2)	yes	Plane
A:(1/2,1/2,1/2)	F:(u,1/2,w)	R:(0,1/2,1/2)	yes	Plane
A:(1/2,1/2,1/2)	F:(u,1/2,w)	X:(0,1/2,0)	yes	Plane
A:(1/2,1/2,1/2)	E:(u,v,1/2)	Z:(0,0,1/2)	yes	Plane
M:(1/2,1/2,0)	F:(u,1/2,w)	R:(0,1/2,1/2)	yes	Plane
M:(1/2,1/2,0)	F:(u,1/2,w)	X:(0,1/2,0)	yes	Plane
R:(0,1/2,1/2)	F:(u,1/2,w)	X:(0,1/2,0)	yes	Plane
R:(0,1/2,1/2)	E:(u,v,1/2)	Z:(0,0,1/2)	yes	Plane

BCSID: 1.207; Formula: U2Rh2Sn; MSG: 135.492 ( $P_c4_2/mbc$ ); U = 4eV				
maximal $k_1$	intermediate path	maximal $k_2$	satisfied?	Line/Plane
$\Gamma:(0,0,0)$	LD:(0,0,w)	Z:(0,0,1/2)	no	Line
A:(1/2,1/2,1/2)	S:(u,u,1/2)	Z:(0,0,1/2)	yes	Line
R:(0,1/2,1/2)	W:(0,1/2,w)	X:(0,1/2,0)	yes	Line
A:(1/2,1/2,1/2)	F:(u,1/2,w)	M:(1/2,1/2,0)	yes	Plane
A:(1/2,1/2,1/2)	E:(u,v,1/2)	R:(0,1/2,1/2)	yes	Plane
A:(1/2,1/2,1/2)	F:(u,1/2,w)	R:(0,1/2,1/2)	yes	Plane
A:(1/2,1/2,1/2)	F:(u,1/2,w)	X:(0,1/2,0)	yes	Plane
A:(1/2,1/2,1/2)	E:(u,v,1/2)	Z:(0,0,1/2)	yes	Plane
M:(1/2,1/2,0)	F:(u,1/2,w)	R:(0,1/2,1/2)	yes	Plane

M:(1/2,1/2,0)	F:(u,1/2,w)	X:(0,1/2,0)	yes	Plane
R:(0,1/2,1/2)	F:(u,1/2,w)	X:(0,1/2,0)	yes	Plane
R:(0,1/2,1/2)	E:(u,v,1/2)	Z:(0,0,1/2)	yes	Plane

BCSID: 1.207; Formula: U2Rh2Sn; MSG: 135.492 ( $P_c4_2/mbc$ ); U= 6eV				
maximal $k_1$	intermediate path	maximal $k_2$	satisfied?	Line/Plane
$\Gamma:(0,0,0)$	LD:(0,0,w)	Z:(0,0,1/2)	no	Line
A:(1/2,1/2,1/2)	S:(u,u,1/2)	Z:(0,0,1/2)	yes	Line
R:(0,1/2,1/2)	W:(0,1/2,w)	X:(0,1/2,0)	yes	Line
A:(1/2,1/2,1/2)	F:(u,1/2,w)	M:(1/2,1/2,0)	yes	Plane
A:(1/2,1/2,1/2)	E:(u,v,1/2)	R:(0,1/2,1/2)	yes	Plane
A:(1/2,1/2,1/2)	F:(u,1/2,w)	R:(0,1/2,1/2)	yes	Plane
A:(1/2,1/2,1/2)	F:(u,1/2,w)	X:(0,1/2,0)	yes	Plane
A:(1/2,1/2,1/2)	E:(u,v,1/2)	Z:(0,0,1/2)	yes	Plane
M:(1/2,1/2,0)	F:(u,1/2,w)	R:(0,1/2,1/2)	yes	Plane
M:(1/2,1/2,0)	F:(u,1/2,w)	X:(0,1/2,0)	yes	Plane
R:(0,1/2,1/2)	F:(u,1/2,w)	X:(0,1/2,0)	yes	Plane
R:(0,1/2,1/2)	E:(u,v,1/2)	Z:(0,0,1/2)	yes	Plane

BCSID: 2.19; Formula: Mn3ZnC; MSG: 139.537 ( $I4/mm'm'$ ); U= 0				
maximal $k_1$	intermediate path	maximal $k_2$	satisfied?	Line/Plane
$\Gamma:(0,0,0)$	LD:(0,0,w)	M:(0,0,1)	no	Line
$\Gamma:(0,0,0)$	SM:(u,0,0)	M:(1,0,0)	no	Line
$\Gamma:(0,0,0)$	DT:(u,u,0)	X:(1/2,1/2,0)	no	Line
M:(1,0,0)	Y:(u,1-u,0)	X:(1/2,1/2,0)	no	Line
P:(1/2,1/2,1/2)	W:(1/2,1/2,w)	X:(1/2,1/2,0)	yes	Line
$\Gamma:(0,0,0)$	C:(u,v,0)	M:(0,1,0)	no	Plane
$\Gamma:(0,0,0)$	C:(u,v,0)	X:(1/2,1/2,0)	no	Plane
M:(2,1,0)	C:(u,v,0)	X:(3/2,3/2,0)	no	Plane

BCSID: 2.19; Formula: Mn3ZnC; MSG: 139.537 ( $I4/mm'm'$ ); U= 2eV				
maximal $k_1$	intermediate path	maximal $k_2$	satisfied?	Line/Plane
$\Gamma:(0,0,0)$	LD:(0,0,w)	M:(0,0,1)	no	Line
$\Gamma:(0,0,0)$	SM:(u,0,0)	M:(1,0,0)	no	Line
$\Gamma:(0,0,0)$	DT:(u,u,0)	X:(1/2,1/2,0)	no	Line
M:(1,0,0)	Y:(u,1-u,0)	X:(1/2,1/2,0)	yes	Line
P:(1/2,1/2,1/2)	W:(1/2,1/2,w)	X:(1/2,1/2,0)	yes	Line
$\Gamma:(0,0,0)$	C:(u,v,0)	M:(0,1,0)	no	Plane
$\Gamma:(0,0,0)$	C:(u,v,0)	X:(1/2,1/2,0)	no	Plane
M:(2,1,0)	C:(u,v,0)	X:(3/2,3/2,0)	yes	Plane

BCSID: 2.19; Formula: Mn3ZnC; MSG: 139.537 ( $I4/mm'm'$ ); U= 3eV				
maximal $k_1$	intermediate path	maximal $k_2$	satisfied?	Line/Plane
$\Gamma:(0,0,0)$	LD:(0,0,w)	M:(0,0,1)	no	Line
$\Gamma:(0,0,0)$	SM:(u,0,0)	M:(1,0,0)	no	Line
$\Gamma:(0,0,0)$	DT:(u,u,0)	X:(1/2,1/2,0)	no	Line
M:(1,0,0)	Y:(u,1-u,0)	X:(1/2,1/2,0)	yes	Line
P:(1/2,1/2,1/2)	W:(1/2,1/2,w)	X:(1/2,1/2,0)	yes	Line
$\Gamma:(0,0,0)$	C:(u,v,0)	M:(0,1,0)	no	Plane
$\Gamma:(0,0,0)$	C:(u,v,0)	X:(1/2,1/2,0)	no	Plane
M:(2,1,0)	C:(u,v,0)	X:(3/2,3/2,0)	yes	Plane

BCSID: 2.19; Formula: Mn3ZnC; MSG: 139.537 ( $I_4/mm'm'$ ); U= 4eV				
maximal $k_1$	intermediate path	maximal $k_2$	satisfied?	Line/Plane
$\Gamma:(0,0,0)$	LD:(0,0,w)	M:(0,0,1)	no	Line
$\Gamma:(0,0,0)$	SM:(u,0,0)	M:(1,0,0)	no	Line
$\Gamma:(0,0,0)$	DT:(u,u,0)	X:(1/2,1/2,0)	no	Line
M:(1,0,0)	Y:(u,1-u,0)	X:(1/2,1/2,0)	yes	Line
P:(1/2,1/2,1/2)	W:(1/2,1/2,w)	X:(1/2,1/2,0)	yes	Line
$\Gamma:(0,0,0)$	C:(u,v,0)	M:(0,1,0)	no	Plane
$\Gamma:(0,0,0)$	C:(u,v,0)	X:(1/2,1/2,0)	no	Plane
M:(2,1,0)	C:(u,v,0)	X:(3/2,3/2,0)	yes	Plane
BCSID: 1.80; Formula: DyCo2Ga8; MSG: 140.550 ( $I_c4/mcm$ ); U= 2eV				
maximal $k_1$	intermediate path	maximal $k_2$	satisfied?	Line/Plane
$\Gamma:(0,0,0)$	LD:(0,0,w)	M:(0,0,1)	no	Line
BCSID: 1.80; Formula: DyCo2Ga8; MSG: 140.550 ( $I_c4/mcm$ ); U= 4eV				
maximal $k_1$	intermediate path	maximal $k_2$	satisfied?	Line/Plane
$\Gamma:(0,0,0)$	LD:(0,0,w)	M:(0,0,1)	no	Line
BCSID: 1.80; Formula: DyCo2Ga8; MSG: 140.550 ( $I_c4/mcm$ ); U= 6eV				
maximal $k_1$	intermediate path	maximal $k_2$	satisfied?	Line/Plane
$\Gamma:(0,0,0)$	LD:(0,0,w)	M:(0,0,1)	no	Line
BCSID: 1.82; Formula: Nd2RhIn8; MSG: 140.550 ( $I_c4/mcm$ ); U= 4eV				
maximal $k_1$	intermediate path	maximal $k_2$	satisfied?	Line/Plane
$\Gamma:(0,0,0)$	LD:(0,0,w)	M:(0,0,1)	no	Line
BCSID: 1.82; Formula: Nd2RhIn8; MSG: 140.550 ( $I_c4/mcm$ ); U= 6eV				
maximal $k_1$	intermediate path	maximal $k_2$	satisfied?	Line/Plane
$\Gamma:(0,0,0)$	LD:(0,0,w)	M:(0,0,1)	no	Line
BCSID: 1.87; Formula: TbCo2Ga8; MSG: 140.550 ( $I_c4/mcm$ ); U= 2eV				
maximal $k_1$	intermediate path	maximal $k_2$	satisfied?	Line/Plane
$\Gamma:(0,0,0)$	LD:(0,0,w)	M:(0,0,1)	no	Line
BCSID: 1.87; Formula: TbCo2Ga8; MSG: 140.550 ( $I_c4/mcm$ ); U= 4eV				
maximal $k_1$	intermediate path	maximal $k_2$	satisfied?	Line/Plane
$\Gamma:(0,0,0)$	LD:(0,0,w)	M:(0,0,1)	no	Line
BCSID: 0.151; Formula: Tm2Mn2O7; MSG: 141.557 ( $I4_1/am'd'$ ); U= 0				
maximal $k_1$	intermediate path	maximal $k_2$	satisfied?	Line/Plane
$\Gamma:(0,0,0)$	LD:(0,0,w)	M:(0,0,1)	no	Line
$\Gamma:(0,0,0)$	SM:(u,0,0)	M:(1,0,0)	no	Line
$\Gamma:(0,0,0)$	DT:(u,u,0)	X:(1/2,1/2,0)	no	Line
P:(1/2,1/2,1/2)	W:(1/2,1/2,w)	X:(1/2,1/2,0)	yes	Line
$\Gamma:(0,0,0)$	C:(u,v,0)	M:(0,1,0)	no	Plane
$\Gamma:(0,0,0)$	C:(u,v,0)	X:(1/2,1/2,0)	no	Plane
M:(2,1,0)	C:(u,v,0)	X:(3/2,3/2,0)	yes	Plane

BCSID: 0.158; Formula: Yb2Ti2O7; MSG: 141.557 ( $I4_1/am'd'$ ); U= 1eV

maximal $k_1$	intermediate path	maximal $k_2$	satisfied?	Line/Plane
$\Gamma:(0,0,0)$	LD:(0,0,w)	M:(0,0,1)	no	Line
$\Gamma:(0,0,0)$	SM:(u,0,0)	M:(1,0,0)	yes	Line
$\Gamma:(0,0,0)$	DT:(u,u,0)	X:(1/2,1/2,0)	yes	Line
P:(1/2,1/2,1/2)	W:(1/2,1/2,w)	X:(1/2,1/2,0)	yes	Line
$\Gamma:(0,0,0)$	C:(u,v,0)	M:(0,1,0)	yes	Plane
$\Gamma:(0,0,0)$	C:(u,v,0)	X:(1/2,1/2,0)	yes	Plane
M:(2,1,0)	C:(u,v,0)	X:(3/2,3/2,0)	yes	Plane

BCSID: 0.227; Formula: NdCo2; MSG: 141.557 ( $I4_1/am'd'$ ); U= 0				
maximal $k_1$	intermediate path	maximal $k_2$	satisfied?	Line/Plane
$\Gamma:(0,0,0)$	LD:(0,0,w)	M:(0,0,1)	no	Line
$\Gamma:(0,0,0)$	SM:(u,0,0)	M:(1,0,0)	yes	Line
$\Gamma:(0,0,0)$	DT:(u,u,0)	X:(1/2,1/2,0)	yes	Line
P:(1/2,1/2,1/2)	W:(1/2,1/2,w)	X:(1/2,1/2,0)	yes	Line
$\Gamma:(0,0,0)$	C:(u,v,0)	M:(0,1,0)	yes	Plane
$\Gamma:(0,0,0)$	C:(u,v,0)	X:(1/2,1/2,0)	yes	Plane
M:(2,1,0)	C:(u,v,0)	X:(3/2,3/2,0)	yes	Plane

BCSID: 0.227; Formula: NdCo2; MSG: 141.557 ( $I4_1/am'd'$ ); U= 2eV				
maximal $k_1$	intermediate path	maximal $k_2$	satisfied?	Line/Plane
$\Gamma:(0,0,0)$	LD:(0,0,w)	M:(0,0,1)	no	Line
$\Gamma:(0,0,0)$	SM:(u,0,0)	M:(1,0,0)	yes	Line
$\Gamma:(0,0,0)$	DT:(u,u,0)	X:(1/2,1/2,0)	yes	Line
P:(1/2,1/2,1/2)	W:(1/2,1/2,w)	X:(1/2,1/2,0)	yes	Line
$\Gamma:(0,0,0)$	C:(u,v,0)	M:(0,1,0)	yes	Plane
$\Gamma:(0,0,0)$	C:(u,v,0)	X:(1/2,1/2,0)	yes	Plane
M:(2,1,0)	C:(u,v,0)	X:(3/2,3/2,0)	yes	Plane

BCSID: 0.227; Formula: NdCo2; MSG: 141.557 ( $I4_1/am'd'$ ); U= 4eV				
maximal $k_1$	intermediate path	maximal $k_2$	satisfied?	Line/Plane
$\Gamma:(0,0,0)$	LD:(0,0,w)	M:(0,0,1)	no	Line
$\Gamma:(0,0,0)$	SM:(u,0,0)	M:(1,0,0)	yes	Line
$\Gamma:(0,0,0)$	DT:(u,u,0)	X:(1/2,1/2,0)	yes	Line
P:(1/2,1/2,1/2)	W:(1/2,1/2,w)	X:(1/2,1/2,0)	yes	Line
$\Gamma:(0,0,0)$	C:(u,v,0)	M:(0,1,0)	yes	Plane
$\Gamma:(0,0,0)$	C:(u,v,0)	X:(1/2,1/2,0)	yes	Plane
M:(2,1,0)	C:(u,v,0)	X:(3/2,3/2,0)	yes	Plane

BCSID: 0.227; Formula: NdCo2; MSG: 141.557 ( $I4_1/am'd'$ ); U= 6eV				
maximal $k_1$	intermediate path	maximal $k_2$	satisfied?	Line/Plane
$\Gamma:(0,0,0)$	LD:(0,0,w)	M:(0,0,1)	no	Line
$\Gamma:(0,0,0)$	SM:(u,0,0)	M:(1,0,0)	no	Line
$\Gamma:(0,0,0)$	DT:(u,u,0)	X:(1/2,1/2,0)	no	Line
P:(1/2,1/2,1/2)	W:(1/2,1/2,w)	X:(1/2,1/2,0)	yes	Line
$\Gamma:(0,0,0)$	C:(u,v,0)	M:(0,1,0)	no	Plane
$\Gamma:(0,0,0)$	C:(u,v,0)	X:(1/2,1/2,0)	no	Plane
M:(2,1,0)	C:(u,v,0)	X:(3/2,3/2,0)	yes	Plane

BCSID: 0.48; Formula: Tb2Sn2O7; MSG: 141.557 ( $I4_1/am'd'$ ); U= 0				
---	--	--	--	--

maximal $k_1$	intermediate path	maximal $k_2$	satisfied?	Line/Plane
$\Gamma:(0,0,0)$	LD:(0,0,w)	M:(0,0,1)	yes	Line
$\Gamma:(0,0,0)$	SM:(u,0,0)	M:(1,0,0)	yes	Line
$\Gamma:(0,0,0)$	DT:(u,u,0)	X:(1/2,1/2,0)	yes	Line
P:(1/2,1/2,1/2)	W:(1/2,1/2,w)	X:(1/2,1/2,0)	no	Line
$\Gamma:(0,0,0)$	C:(u,v,0)	M:(0,1,0)	yes	Plane
$\Gamma:(0,0,0)$	C:(u,v,0)	X:(1/2,1/2,0)	yes	Plane
M:(2,1,0)	C:(u,v,0)	X:(3/2,3/2,0)	yes	Plane

BCSID: 0.49; Formula: Ho2Ru2O7; MSG: 141.557 ( $I4_1/am'd'$ ); U= 0				
maximal $k_1$	intermediate path	maximal $k_2$	satisfied?	Line/Plane
$\Gamma:(0,0,0)$	LD:(0,0,w)	M:(0,0,1)	no	Line
$\Gamma:(0,0,0)$	SM:(u,0,0)	M:(1,0,0)	no	Line
$\Gamma:(0,0,0)$	DT:(u,u,0)	X:(1/2,1/2,0)	no	Line
P:(1/2,1/2,1/2)	W:(1/2,1/2,w)	X:(1/2,1/2,0)	yes	Line
$\Gamma:(0,0,0)$	C:(u,v,0)	M:(0,1,0)	no	Plane
$\Gamma:(0,0,0)$	C:(u,v,0)	X:(1/2,1/2,0)	no	Plane
M:(2,1,0)	C:(u,v,0)	X:(3/2,3/2,0)	yes	Plane

BCSID: 0.51; Formula: Ho2Ru2O7; MSG: 141.557 ( $I4_1/am'd'$ ); U= 6eV				
maximal $k_1$	intermediate path	maximal $k_2$	satisfied?	Line/Plane
$\Gamma:(0,0,0)$	LD:(0,0,w)	M:(0,0,1)	no	Line
$\Gamma:(0,0,0)$	SM:(u,0,0)	M:(1,0,0)	no	Line
$\Gamma:(0,0,0)$	DT:(u,u,0)	X:(1/2,1/2,0)	no	Line
P:(1/2,1/2,1/2)	W:(1/2,1/2,w)	X:(1/2,1/2,0)	yes	Line
$\Gamma:(0,0,0)$	C:(u,v,0)	M:(0,1,0)	no	Plane
$\Gamma:(0,0,0)$	C:(u,v,0)	X:(1/2,1/2,0)	no	Plane
M:(2,1,0)	C:(u,v,0)	X:(3/2,3/2,0)	yes	Plane

BCSID: 0.125; Formula: MnGeO3; MSG: 148.19 ( $R - 3'$ ); U= 3eV				
maximal $k_1$	intermediate path	maximal $k_2$	satisfied?	Line/Plane
$\Gamma:(0,0,0)$	LD:(0,0,w)	T:(0,0,3/2)	no	Line

BCSID: 0.125; Formula: MnGeO3; MSG: 148.19 ( $R - 3'$ ); U= 4eV				
maximal $k_1$	intermediate path	maximal $k_2$	satisfied?	Line/Plane
$\Gamma:(0,0,0)$	LD:(0,0,w)	T:(0,0,3/2)	no	Line

BCSID: 1.161; Formula: PrFe3(BO3)4; MSG: 155.48 ( $R_I32$ ); U= 4eV				
maximal $k_1$	intermediate path	maximal $k_2$	satisfied?	Line/Plane
$\Gamma:(0,0,0)$	SM:(u,-2*u,0)	F:(-1/2,1,0)	yes	Line
$\Gamma:(0,0,0)$	LD:(0,0,w)	T:(0,0,3/2)	no	Line
L:(1/2,1/2,3/2)	Y:(u,u,3/2)	T:(0,0,3/2)	yes	Line

BCSID: 0.169; Formula: U3As4; MSG: 161.71 ( $R3c'$ ); U= 0				
maximal $k_1$	intermediate path	maximal $k_2$	satisfied?	Line/Plane
$\Gamma:(0,0,0)$	LD:(0,0,w)	T:(0,0,3/2)	no	Line

BCSID: 0.169; Formula: U3As4; MSG: 161.71 ( $R3c'$ ); U= 2eV				
maximal $k_1$	intermediate path	maximal $k_2$	satisfied?	Line/Plane
$\Gamma:(0,0,0)$	LD:(0,0,w)	T:(0,0,3/2)	no	Line

BCSID: 0.170; Formula: U3P4; MSG: 161.71 ( $R3c'$ ); U= 0				
maximal $k_1$	intermediate path	maximal $k_2$	satisfied?	Line/Plane
$\Gamma:(0,0,0)$	LD:(0,0,w)	T:(0,0,3/2)	no	Line
BCSID: 0.170; Formula: U3P4; MSG: 161.71 ( $R3c'$ ); U= 2eV				
maximal $k_1$	intermediate path	maximal $k_2$	satisfied?	Line/Plane
$\Gamma:(0,0,0)$	LD:(0,0,w)	T:(0,0,3/2)	no	Line
BCSID: 1.0.5; Formula: Sr3CoIrO6; MSG: 165.95 ( $P - 3c'1$ ); U= 0				
maximal $k_1$	intermediate path	maximal $k_2$	satisfied?	Line/Plane
$\Gamma:(0,0,0)$	DT:(0,0,w)	A:(0,0,1/2)	no	Line
H:(1/3,1/3,1/2)	P:(1/3,1/3,w)	K:(1/3,1/3,0)	yes	Line
BCSID: 0.177; Formula: Mn3GaN; MSG: 166.97 ( $R - 3m$ ); U= 0				
maximal $k_1$	intermediate path	maximal $k_2$	satisfied?	Line/Plane
$\Gamma:(0,0,0)$	SM:(u,-2*u,0)	F:(-1/2,1,0)	no	Line
$\Gamma:(0,0,0)$	LD:(0,0,w)	T:(0,0,3/2)	yes	Line
L:(1/2,1/2,3/2)	Y:(u,u,3/2)	T:(0,0,3/2)	yes	Line
$\Gamma:(0,0,0)$	C:(u,-u,w)	F:(1/2,-1/2,1)	no	Plane
$\Gamma:(0,0,0)$	C:(u,-u,w)	L:(-1/2,1/2,1/2)	yes	Plane
$\Gamma:(0,0,0)$	C:(u,-u,w)	T:(0,0,3/2)	yes	Plane
F:(0,1/2,1)	C:(0,u,w)	L:(0,-1/2,1/2)	no	Plane
F:(0,1/2,1)	C:(0,u,w)	T:(0,1,1/2)	no	Plane
L:(-1/2,1/2,1/2)	C:(u,-u,w)	T:(0,0,3/2)	yes	Plane
BCSID: 0.177; Formula: Mn3GaN; MSG: 166.97 ( $R - 3m$ ); U= 2eV				
maximal $k_1$	intermediate path	maximal $k_2$	satisfied?	Line/Plane
$\Gamma:(0,0,0)$	SM:(u,-2*u,0)	F:(-1/2,1,0)	no	Line
$\Gamma:(0,0,0)$	LD:(0,0,w)	T:(0,0,3/2)	no	Line
L:(1/2,1/2,3/2)	Y:(u,u,3/2)	T:(0,0,3/2)	yes	Line
$\Gamma:(0,0,0)$	C:(u,-u,w)	F:(1/2,-1/2,1)	no	Plane
$\Gamma:(0,0,0)$	C:(u,-u,w)	L:(-1/2,1/2,1/2)	no	Plane
$\Gamma:(0,0,0)$	C:(u,-u,w)	T:(0,0,3/2)	no	Plane
F:(0,1/2,1)	C:(0,u,w)	L:(0,-1/2,1/2)	yes	Plane
F:(0,1/2,1)	C:(0,u,w)	T:(0,1,1/2)	yes	Plane
L:(-1/2,1/2,1/2)	C:(u,-u,w)	T:(0,0,3/2)	yes	Plane
BCSID: 0.108; Formula: Mn3Ir; MSG: 166.101 ( $R - 3m'$ ); U= 0				
maximal $k_1$	intermediate path	maximal $k_2$	satisfied?	Line/Plane
$\Gamma:(0,0,0)$	LD:(0,0,w)	T:(0,0,3/2)	no	Line
BCSID: 0.108; Formula: Mn3Ir; MSG: 166.101 ( $R - 3m'$ ); U= 1eV				
maximal $k_1$	intermediate path	maximal $k_2$	satisfied?	Line/Plane
$\Gamma:(0,0,0)$	LD:(0,0,w)	T:(0,0,3/2)	no	Line
BCSID: 0.108; Formula: Mn3Ir; MSG: 166.101 ( $R - 3m'$ ); U= 2eV				
maximal $k_1$	intermediate path	maximal $k_2$	satisfied?	Line/Plane
$\Gamma:(0,0,0)$	LD:(0,0,w)	T:(0,0,3/2)	no	Line
BCSID: 0.108; Formula: Mn3Ir; MSG: 166.101 ( $R - 3m'$ ); U= 3eV				
maximal $k_1$	intermediate path	maximal $k_2$	satisfied?	Line/Plane

$\Gamma:(0,0,0)$	LD:(0,0,w)	T:(0,0,3/2)	no	Line
BCSID: 0.108; Formula: Mn3Ir; MSG: 166.101 ( $R - 3m'$ ); U= 4eV				
maximal $k_1$	intermediate path	maximal $k_2$	satisfied?	Line/Plane
$\Gamma:(0,0,0)$	LD:(0,0,w)	T:(0,0,3/2)	no	Line
BCSID: 0.109; Formula: Mn3Pt; MSG: 166.101 ( $R - 3m'$ ); U= 0				
maximal $k_1$	intermediate path	maximal $k_2$	satisfied?	Line/Plane
$\Gamma:(0,0,0)$	LD:(0,0,w)	T:(0,0,3/2)	no	Line
BCSID: 0.109; Formula: Mn3Pt; MSG: 166.101 ( $R - 3m'$ ); U= 2eV				
maximal $k_1$	intermediate path	maximal $k_2$	satisfied?	Line/Plane
$\Gamma:(0,0,0)$	LD:(0,0,w)	T:(0,0,3/2)	no	Line
BCSID: 0.109; Formula: Mn3Pt; MSG: 166.101 ( $R - 3m'$ ); U= 3eV				
maximal $k_1$	intermediate path	maximal $k_2$	satisfied?	Line/Plane
$\Gamma:(0,0,0)$	LD:(0,0,w)	T:(0,0,3/2)	no	Line
BCSID: 0.109; Formula: Mn3Pt; MSG: 166.101 ( $R - 3m'$ ); U= 4eV				
maximal $k_1$	intermediate path	maximal $k_2$	satisfied?	Line/Plane
$\Gamma:(0,0,0)$	LD:(0,0,w)	T:(0,0,3/2)	no	Line
BCSID: 0.228; Formula: TbCo2; MSG: 166.101 ( $R - 3m'$ ); U= 2eV				
maximal $k_1$	intermediate path	maximal $k_2$	satisfied?	Line/Plane
$\Gamma:(0,0,0)$	LD:(0,0,w)	T:(0,0,3/2)	no	Line
BCSID: 0.77; Formula: Tb2Ti2O7; MSG: 166.101 ( $R - 3m'$ ); U= 0				
maximal $k_1$	intermediate path	maximal $k_2$	satisfied?	Line/Plane
$\Gamma:(0,0,0)$	LD:(0,0,w)	T:(0,0,3/2)	no	Line
BCSID: 1.153; Formula: Mn3GaC; MSG: 167.108 ( $R_I - 3c$ ); U= 0				
maximal $k_1$	intermediate path	maximal $k_2$	satisfied?	Line/Plane
$\Gamma:(0,0,0)$	LD:(0,0,w)	T:(0,0,3/2)	no	Line
BCSID: 0.33; Formula: HoMnO3; MSG: 185.197 ( $P6_3cm$ ); U= 4eV				
maximal $k_1$	intermediate path	maximal $k_2$	satisfied?	Line/Plane
$\Gamma:(0,0,0)$	DT:(0,0,w)	A:(0,0,1/2)	no	Line
$\Gamma:(0,0,0)$	LD:(u,u,0)	K:(1/3,1/3,0)	yes	Line
$\Gamma:(0,0,0)$	LD:(u,u,0)	M:(1/2,1/2,0)	yes	Line
$\Gamma:(0,0,0)$	SM:(u,0,0)	M:(1/2,0,0)	yes	Line
A:(0,0,1/2)	Q:(u,u,1/2)	H:(1/3,1/3,1/2)	yes	Line
A:(0,0,1/2)	Q:(u,u,1/2)	L:(1/2,1/2,1/2)	yes	Line
A:(0,0,1/2)	R:(u,0,1/2)	L:(1/2,0,1/2)	yes	Line
H:(1/3,1/3,1/2)	P:(1/3,1/3,w)	K:(1/3,1/3,0)	yes	Line
H:(1/3,1/3,1/2)	Q:(u,u,1/2)	L:(1/2,1/2,1/2)	yes	Line
K:(1/3,1/3,0)	LD:(u,u,0)	M:(1/2,1/2,0)	yes	Line
$\Gamma:(0,0,0)$	C:(u,u,w)	A:(0,0,1/2)	yes	Plane
$\Gamma:(0,0,0)$	D:(u,0,w)	A:(0,0,1/2)	yes	Plane
$\Gamma:(0,0,0)$	C:(u,u,w)	H:(1/3,1/3,1/2)	yes	Plane
$\Gamma:(0,0,0)$	C:(u,u,w)	K:(1/3,1/3,0)	yes	Plane
$\Gamma:(0,0,0)$	C:(u,u,w)	L:(1/2,1/2,1/2)	yes	Plane

$\Gamma:(0,0,0)$	D:(u,0,w)	L:(1/2,0,1/2)	yes	Plane
$\Gamma:(0,0,0)$	C:(u,u,w)	M:(1/2,1/2,0)	yes	Plane
$\Gamma:(0,0,0)$	D:(u,0,w)	M:(1/2,0,0)	yes	Plane
A:(0,0,1/2)	C:(u,u,w)	H:(1/3,1/3,1/2)	yes	Plane
A:(0,0,1/2)	C:(u,u,w)	K:(1/3,1/3,0)	yes	Plane
A:(0,0,1/2)	C:(u,u,w)	L:(1/2,1/2,1/2)	yes	Plane
A:(0,0,1/2)	D:(u,0,w)	L:(1/2,0,1/2)	yes	Plane
A:(0,0,1/2)	C:(u,u,w)	M:(1/2,1/2,0)	yes	Plane
A:(0,0,1/2)	D:(u,0,w)	M:(1/2,0,0)	yes	Plane
H:(1/3,1/3,1/2)	C:(u,u,w)	K:(1/3,1/3,0)	yes	Plane
H:(1/3,1/3,1/2)	C:(u,u,w)	K:(2/3,2/3,0)	yes	Plane
H:(1/3,1/3,1/2)	C:(u,u,w)	L:(1/2,1/2,1/2)	yes	Plane
H:(1/3,1/3,1/2)	C:(u,u,w)	M:(1/2,1/2,0)	yes	Plane
K:(1/3,1/3,0)	C:(u,u,w)	L:(1/2,1/2,1/2)	yes	Plane
K:(1/3,1/3,0)	C:(u,u,w)	M:(1/2,1/2,0)	yes	Plane
L:(1/2,-1,1/2)	C:(u,-2*u,w)	M:(1/2,-1,0)	yes	Plane
L:(1/2,0,1/2)	D:(u,0,w)	M:(1/2,0,0)	yes	Plane

BCSID: 1.110; Formula: ScMn6Ge6; MSG: 192.252 ( $P_c6/mcc$ ); U = 0				
maximal $k_1$	intermediate path	maximal $k_2$	satisfied?	Line/Plane
$\Gamma:(0,0,0)$	DT:(0,0,w)	A:(0,0,1/2)	yes	Line
A:(0,0,1/2)	Q:(u,u,1/2)	H:(1/3,1/3,1/2)	no	Line
A:(0,0,1/2)	Q:(u,u,1/2)	L:(1/2,1/2,1/2)	yes	Line
A:(0,0,1/2)	R:(u,0,1/2)	L:(1/2,0,1/2)	yes	Line
H:(1/3,1/3,1/2)	P:(1/3,1/3,w)	K:(1/3,1/3,0)	yes	Line
H:(1/3,1/3,1/2)	Q:(u,u,1/2)	L:(1/2,1/2,1/2)	no	Line
A:(0,0,1/2)	E:(u,v,1/2)	H:(1/3,1/3,1/2)	no	Plane
A:(0,0,1/2)	E:(u,v,1/2)	L:(1/2,0,1/2)	yes	Plane
H:(1/3,1/3,1/2)	E:(u,v,1/2)	L:(1/2,0,1/2)	no	Plane

BCSID: 1.225; Formula: ScMn6Ge6; MSG: 192.252 ( $P_c6/mcc$ ); U = 0				
maximal $k_1$	intermediate path	maximal $k_2$	satisfied?	Line/Plane
$\Gamma:(0,0,0)$	DT:(0,0,w)	A:(0,0,1/2)	yes	Line
A:(0,0,1/2)	Q:(u,u,1/2)	H:(1/3,1/3,1/2)	no	Line
A:(0,0,1/2)	Q:(u,u,1/2)	L:(1/2,1/2,1/2)	yes	Line
A:(0,0,1/2)	R:(u,0,1/2)	L:(1/2,0,1/2)	yes	Line
H:(1/3,1/3,1/2)	P:(1/3,1/3,w)	K:(1/3,1/3,0)	yes	Line
H:(1/3,1/3,1/2)	Q:(u,u,1/2)	L:(1/2,1/2,1/2)	no	Line
A:(0,0,1/2)	E:(u,v,1/2)	H:(1/3,1/3,1/2)	no	Plane
A:(0,0,1/2)	E:(u,v,1/2)	L:(1/2,0,1/2)	yes	Plane
H:(1/3,1/3,1/2)	E:(u,v,1/2)	L:(1/2,0,1/2)	no	Plane

BCSID: 1.225; Formula: ScMn6Ge6; MSG: 192.252 ( $P_c6/mcc$ ); U = 1eV				
maximal $k_1$	intermediate path	maximal $k_2$	satisfied?	Line/Plane
$\Gamma:(0,0,0)$	DT:(0,0,w)	A:(0,0,1/2)	yes	Line
A:(0,0,1/2)	Q:(u,u,1/2)	H:(1/3,1/3,1/2)	no	Line
A:(0,0,1/2)	Q:(u,u,1/2)	L:(1/2,1/2,1/2)	yes	Line
A:(0,0,1/2)	R:(u,0,1/2)	L:(1/2,0,1/2)	yes	Line
H:(1/3,1/3,1/2)	P:(1/3,1/3,w)	K:(1/3,1/3,0)	yes	Line
H:(1/3,1/3,1/2)	Q:(u,u,1/2)	L:(1/2,1/2,1/2)	no	Line
A:(0,0,1/2)	E:(u,v,1/2)	H:(1/3,1/3,1/2)	no	Plane

A:(0,0,1/2)	E:(u,v,1/2)	L:(1/2,0,1/2)	yes	Plane
H:(1/3,1/3,1/2)	E:(u,v,1/2)	L:(1/2,0,1/2)	no	Plane

BCSID: 1.225; Formula: ScMn6Ge6; MSG: 192.252 ( $P_c6/mcc$ ); U= 2eV				
maximal $k_1$	intermediate path	maximal $k_2$	satisfied?	Line/Plane
$\Gamma:(0,0,0)$	DT:(0,0,w)	A:(0,0,1/2)	yes	Line
A:(0,0,1/2)	Q:(u,u,1/2)	H:(1/3,1/3,1/2)	no	Line
A:(0,0,1/2)	Q:(u,u,1/2)	L:(1/2,1/2,1/2)	no	Line
A:(0,0,1/2)	R:(u,0,1/2)	L:(1/2,0,1/2)	no	Line
H:(1/3,1/3,1/2)	P:(1/3,1/3,w)	K:(1/3,1/3,0)	yes	Line
H:(1/3,1/3,1/2)	Q:(u,u,1/2)	L:(1/2,1/2,1/2)	no	Line
A:(0,0,1/2)	E:(u,v,1/2)	H:(1/3,1/3,1/2)	no	Plane
A:(0,0,1/2)	E:(u,v,1/2)	L:(1/2,0,1/2)	no	Plane
H:(1/3,1/3,1/2)	E:(u,v,1/2)	L:(1/2,0,1/2)	no	Plane

BCSID: 1.225; Formula: ScMn6Ge6; MSG: 192.252 ( $P_c6/mcc$ ); U= 3eV				
maximal $k_1$	intermediate path	maximal $k_2$	satisfied?	Line/Plane
$\Gamma:(0,0,0)$	DT:(0,0,w)	A:(0,0,1/2)	no	Line
A:(0,0,1/2)	Q:(u,u,1/2)	H:(1/3,1/3,1/2)	no	Line
A:(0,0,1/2)	Q:(u,u,1/2)	L:(1/2,1/2,1/2)	yes	Line
A:(0,0,1/2)	R:(u,0,1/2)	L:(1/2,0,1/2)	yes	Line
H:(1/3,1/3,1/2)	P:(1/3,1/3,w)	K:(1/3,1/3,0)	no	Line
H:(1/3,1/3,1/2)	Q:(u,u,1/2)	L:(1/2,1/2,1/2)	no	Line
A:(0,0,1/2)	E:(u,v,1/2)	H:(1/3,1/3,1/2)	no	Plane
A:(0,0,1/2)	E:(u,v,1/2)	L:(1/2,0,1/2)	yes	Plane
H:(1/3,1/3,1/2)	E:(u,v,1/2)	L:(1/2,0,1/2)	no	Plane

BCSID: 0.118; Formula: Ba5Co5ClO13; MSG: 194.268 ( $P6'_3/m'm'c$ ); U= 4eV				
maximal $k_1$	intermediate path	maximal $k_2$	satisfied?	Line/Plane
$\Gamma:(0,0,0)$	DT:(0,0,w)	A:(0,0,1/2)	yes	Line
$\Gamma:(0,0,0)$	LD:(u,u,0)	K:(1/3,1/3,0)	yes	Line
$\Gamma:(0,0,0)$	LD:(u,u,0)	M:(1/2,1/2,0)	yes	Line
$\Gamma:(0,0,0)$	SM:(u,0,0)	M:(1/2,0,0)	no	Line
H:(1/3,1/3,1/2)	P:(1/3,1/3,w)	K:(1/3,1/3,0)	yes	Line
K:(1/3,1/3,0)	LD:(u,u,0)	M:(1/2,1/2,0)	yes	Line
L:(1/2,0,1/2)	U:(1/2,0,w)	M:(1/2,0,0)	yes	Line
$\Gamma:(0,0,0)$	C:(u,u,w)	A:(0,0,1/2)	yes	Plane
$\Gamma:(0,0,0)$	C:(u,u,w)	H:(1/3,1/3,1/2)	yes	Plane
$\Gamma:(0,0,0)$	C:(u,u,w)	K:(1/3,1/3,0)	yes	Plane
$\Gamma:(0,0,0)$	C:(u,u,w)	L:(1/2,1/2,1/2)	yes	Plane
$\Gamma:(0,0,0)$	C:(u,u,w)	M:(1/2,1/2,0)	yes	Plane
A:(0,0,1/2)	C:(u,u,w)	H:(1/3,1/3,1/2)	yes	Plane
A:(0,0,1/2)	C:(u,u,w)	K:(1/3,1/3,0)	yes	Plane
A:(0,0,1/2)	C:(u,u,w)	L:(1/2,1/2,1/2)	yes	Plane
A:(0,0,1/2)	C:(u,u,w)	M:(1/2,1/2,0)	yes	Plane
H:(1/3,1/3,1/2)	C:(u,u,w)	K:(1/3,1/3,0)	yes	Plane
H:(1/3,1/3,1/2)	C:(u,u,w)	L:(1/2,1/2,1/2)	yes	Plane
H:(1/3,1/3,1/2)	C:(u,u,w)	M:(1/2,1/2,0)	yes	Plane
K:(1/3,1/3,0)	C:(u,u,w)	L:(1/2,1/2,1/2)	yes	Plane
K:(1/3,1/3,0)	C:(u,u,w)	M:(1/2,1/2,0)	yes	Plane
L:(1/2,-1,1/2)	C:(u,-2*u,w)	M:(1/2,-1,0)	yes	Plane

BCSID: 3.8; Formula: NdZn; MSG: 222.103 ( $P_I n - 3n$ ); U= 2eV				
maximal $k_1$	intermediate path	maximal $k_2$	satisfied?	Line/Plane
$\Gamma:(0,0,0)$	LD:(u,u,u)	R:(1/2,1/2,1/2)	yes	Line
$\Gamma:(0,0,0)$	DT:(0,v,0)	X:(0,1/2,0)	no	Line
M:(1/2,1/2,0)	Z:(u,1/2,0)	X:(0,1/2,0)	no	Line
R:(1/2,1/2,1/2)	S:(u,1/2,u)	X:(0,1/2,0)	no	Line
M:(1/2,1/2,0)	B:(u,1/2,w)	R:(1/2,1/2,1/2)	yes	Plane
M:(1/2,1/2,0)	B:(u,1/2,w)	X:(0,1/2,0)	no	Plane
R:(1/2,1/2,1/2)	B:(u,1/2,w)	X:(0,1/2,0)	no	Plane

BCSID: 3.8; Formula: NdZn; MSG: 222.103 ( $P_I n - 3n$ ); U= 4eV				
maximal $k_1$	intermediate path	maximal $k_2$	satisfied?	Line/Plane
$\Gamma:(0,0,0)$	LD:(u,u,u)	R:(1/2,1/2,1/2)	yes	Line
$\Gamma:(0,0,0)$	DT:(0,v,0)	X:(0,1/2,0)	no	Line
M:(1/2,1/2,0)	Z:(u,1/2,0)	X:(0,1/2,0)	yes	Line
R:(1/2,1/2,1/2)	S:(u,1/2,u)	X:(0,1/2,0)	yes	Line
M:(1/2,1/2,0)	B:(u,1/2,w)	R:(1/2,1/2,1/2)	yes	Plane
M:(1/2,1/2,0)	B:(u,1/2,w)	X:(0,1/2,0)	yes	Plane
R:(1/2,1/2,1/2)	B:(u,1/2,w)	X:(0,1/2,0)	yes	Plane

BCSID: 3.2; Formula: UO2; MSG: 224.113 ( $Pn - 3m'$ ); U= 0				
maximal $k_1$	intermediate path	maximal $k_2$	satisfied?	Line/Plane
$\Gamma:(0,0,0)$	SM:(u,u,0)	M:(1/2,1/2,0)	yes	Line
$\Gamma:(0,0,0)$	LD:(u,u,u)	R:(1/2,1/2,1/2)	no	Line
M:(1/2,1/2,0)	Z:(u,1/2,0)	X:(0,1/2,0)	yes	Line
M:(-1/2,1/2,0)	ZA:(-1/2,-u,0)	X:(-1/2,0,0)	yes	Line
R:(1/2,1/2,1/2)	S:(u,1/2,u)	X:(0,1/2,0)	yes	Line
$\Gamma:(0,0,0)$	A:(u,v,0)	M:(1/2,1/2,0)	yes	Plane
$\Gamma:(0,0,0)$	A:(u,v,0)	X:(0,1/2,0)	yes	Plane
M:(1/2,1/2,0)	B:(u,1/2,w)	R:(1/2,1/2,1/2)	yes	Plane
M:(1/2,1/2,0)	A:(u,v,0)	X:(0,1/2,0)	yes	Plane
M:(1/2,1/2,0)	B:(u,1/2,w)	X:(0,1/2,0)	yes	Plane
R:(1/2,1/2,1/2)	B:(u,1/2,w)	X:(0,1/2,0)	yes	Plane

BCSID: 3.9; Formula: NpS; MSG: 228.139 ( $F_{Sd} - 3c$ ); U= 0				
maximal $k_1$	intermediate path	maximal $k_2$	satisfied?	Line/Plane
$\Gamma:(0,0,0)$	LD:(u,u,u)	L:(1/2,1/2,1/2)	no	Line
$\Gamma:(0,0,0)$	DT:(0,v,0)	X:(0,1,0)	yes	Line
W:(1/2,1,0)	V:(u,1,0)	X:(0,1,0)	yes	Line

BCSID: 0.127; Formula: Dy3Al5O12; MSG: 230.148 ( $Ia - 3d'$ ); U= 0				
maximal $k_1$	intermediate path	maximal $k_2$	satisfied?	Line/Plane
$\Gamma:(0,0,0)$	LD:(u,u,u)	H:(1,1,1)	no	Line
$\Gamma:(0,0,0)$	SM:(u,u,0)	N:(1/2,1/2,0)	yes	Line
$\Gamma:(0,0,0)$	LD:(u,u,u)	P:(1/2,1/2,1/2)	no	Line
H:(1,1,1)	LD:(u,u,u)	P:(1/2,1/2,1/2)	no	Line
N:(1/2,1/2,0)	D:(1/2,1/2,w)	P:(1/2,1/2,1/2)	yes	Line
$\Gamma:(0,0,0)$	A:(u,v,0)	H:(0,1,0)	yes	Plane
$\Gamma:(0,0,0)$	A:(u,v,0)	N:(1/2,1/2,0)	yes	Plane
H:(2,1,0)	A:(u,v,0)	N:(3/2,3/2,0)	yes	Plane

## Appendix J: Detailed discussion of the ideal magnetic TI and SMs

### 1. Higher-order topology of the ideal Axion insulator NpBi

The crystal structure of NpBi adopts a face-centered cubic lattice with space group  $Fm\bar{3}m$ (No. 225) in the high temperature paramagnetic phase. Below 192.5 K, it undergoes a phase transition to the antiferromagnetic phase and the magnetic unit cell adopts simple cubic lattice with MSG 224.113( $Pn\bar{3}m'$ ), as shown in FIG. 32(a). The generators of this MSG include two-fold screw rotation along the [100] direction  $\tilde{C}_{2x} = \{C_{2x}|(0, 0.5, 0.5)\}$ , three-fold rotation along the [111] direction  $C_{3xyz}$ , inversion  $I$  and an anti-unitary symmetry  $C_{2\bar{x}z} \cdot T$  ( $C_{2\bar{x}z}$  is the two-fold rotation along the  $[\bar{1}10]$  direction and  $T$  is the time reversal symmetry). We use the experimental lattice constant  $a = 6.37$  Å and the magnetic momentum of Np is initialized as  $2.42\mu_B$  along the (111) direction in our first-principle calculations. In order to consider the interaction of the 5f electron on Np, we apply the LDA+U calculation with  $U=0, 2, 4, 6$  eV. We find that the band structures at the four US have the same topology. In the main text, we have calculated the parity-based stable topological indices and find  $Z_4 = 2$ , which corresponds to the axion insulator phase. Here we only chose  $U = 2$  eV to analyze the material's topological surface states. It has been proved in Ref. [43] that the  $C_2 \cdot T$  symmetry protects the gapless surface states of axion insulators, on the plane perpendicular to the two-fold rotation axis. Such an axion insulator also exhibits chiral hinge states [61–65, 102] between the two gapped surfaces related by  $C_2 \cdot T$  symmetry.

There are three equivalent first Miller planes,  $\langle\bar{1}10\rangle$ ,  $\langle0\bar{1}1\rangle$  and  $\langle10\bar{1}\rangle$  that preserve  $C_2 \cdot T$  symmetry. We perform the surface states calculations on the  $\langle\bar{1}10\rangle$  plane where the  $C_2 \cdot T$  symmetry is preserved. As shown in FIG. 32(e), the surface Dirac cone emerges and strictly on the  $\tilde{\Gamma}\tilde{X}$  path constrained by the glide mirror symmetry  $\tilde{M}_z = \{M_z|(0.5, 0.5, 0)\}$ . For the  $\langle001\rangle$  surface plane, it has no  $C_2 \cdot T$  symmetry and the surface states are fully gaped as shown in FIG. 32(f). Considering the  $I$  and  $C_{3xyz}$  symmetries, the chiral flow of charge on the hinges of a cubic NpBi sample is schematically shown in FIG. 32(d).

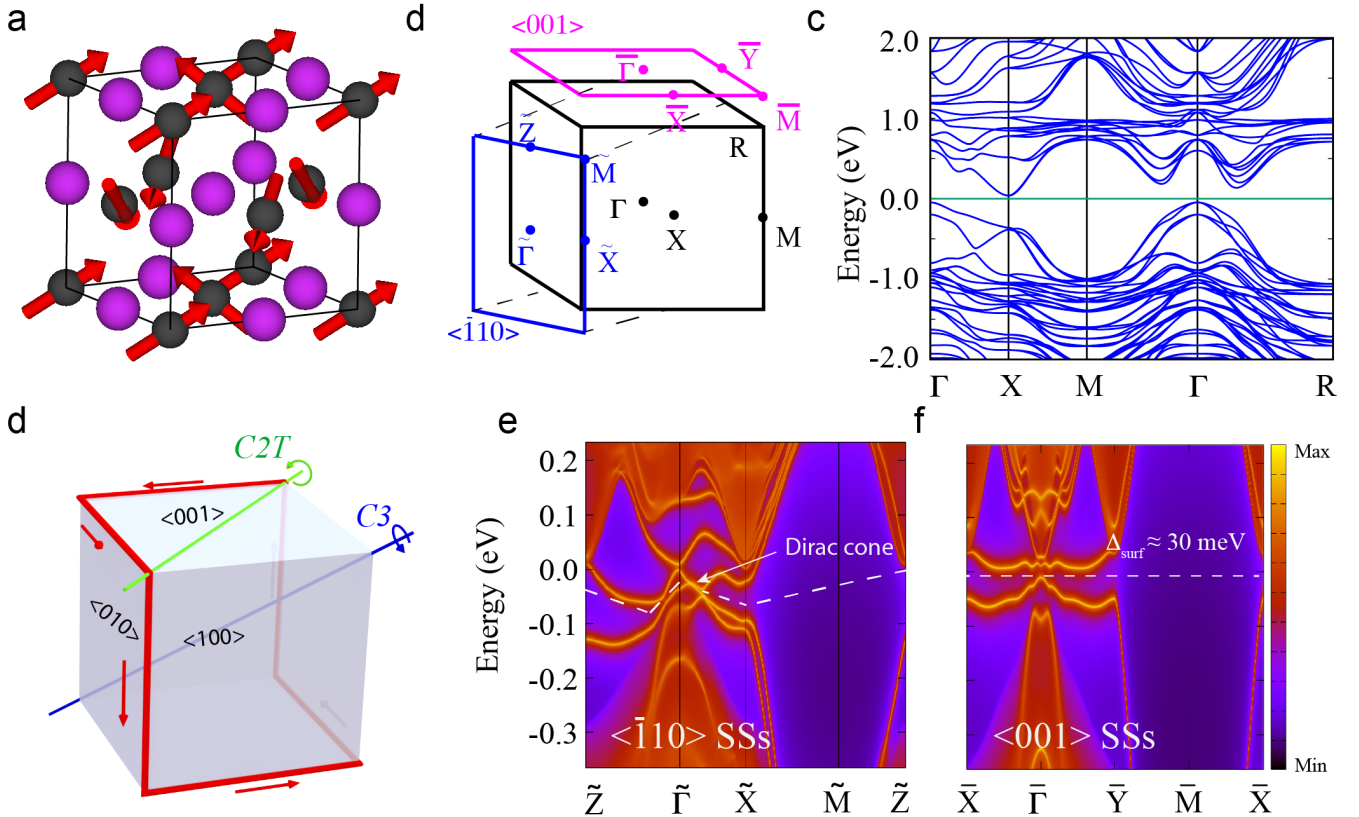


FIG. 32. (a) The crystal and magnetic structures of NpBi with MSG 224.113( $Pn\bar{3}m'$ ). (b) 3D bulk BZ and the projected 2D surface BZ on the  $\langle001\rangle$ (blue) and  $\langle\bar{1}10\rangle$ (pink) surfaces. (c) Electronic band structures of NpBi along the high symmetry paths in BZ with the interaction parameter  $U = 2$  eV. (d) Schematic of the chiral flow of charge on the hinge of NpBi. The 1D chiral modes (red) on the six hinges are related to each other by  $I$  and  $C_{3xyz}$  symmetries. (e) Surface states calculation on the  $C_{2\bar{x}y} \cdot T$  symmetric  $\langle\bar{1}10\rangle$  surface plane. The Dirac cone surface states is along the path  $\tilde{\Gamma}\tilde{X}$  constrained by the glide mirror symmetry  $\tilde{M}_z = \{M_z|(0.5, 0.5, 0)\}$  and the dashed line indicates the "curved Fermi level", the band number below which equals that of electrons. (f) The surface states of  $\langle001\rangle$  surface plane have a full gap in the whole BZ.

$\Lambda_\alpha$	MLCG	Irreps	$\{C_{4z}^+   (0.5, 0, 0)\}$	$I$	$\{M_z   (0.5, 0.5, 0)\}$	$\{M_y   (0.5, 0, 0.5)\}$
$\Gamma$	$4/mmm1'$	$\bar{\Gamma}_6(2)$	$-\sqrt{2}$	2	0	0
		$\bar{\Gamma}_9(2)$	$\sqrt{2}$	-2	0	0
$Z$	$4/mmm1'$	$\bar{Z}_5(2)$	$-\sqrt{2}$	0	$-2i$	0
		$\bar{Z}_7(2)$	$-\sqrt{2}$	0	$2i$	0

TABLE XII. Character table of the irreducible co-representations  $\bar{\Gamma}_6$ ,  $\bar{\Gamma}_9$ ,  $\bar{Z}_5$  and  $\bar{Z}_7$  of MSG 126.386( $P_I4/nnc$ ) at  $\Gamma$  and  $Z$  points, respectively. The first two columns are the momenta and their magnetic little co-group(MLCG); the third column is the irreps of the MLCG; the 4th-7th columns are the characters of the symmetry generators of the unitary subgroup. The  $\bar{\Gamma}_6$  and  $\bar{\Gamma}_9$  irreps have different eigenvalues of  $C_{4z}$  and  $I$ , and  $\bar{Z}_5$  and  $\bar{Z}_7$  irreps have different eigenvalues of  $M_z$ .

## 2. Topological phase diagram of the ideal antiferromagnetic nodal-line semimetal $\text{CeCo}_2\text{P}_2$

The space group(SG) of  $\text{CeCo}_2\text{P}_2$  in the paramagnetic phase is  $I4/mmm$ . The antiferromagnetic phase transition occurs at 440 K below which the magnetic structure, as shown in FIG. 33(a), is characterized by the MSG 126.386( $P_I4/nnc$ ). The generators of this MSG include inversion  $I$ , four-fold rotation  $C_{4z} = \{C_{4z}|(0.5, 0, 0)\}$ , two-fold rotation  $C_{2x} = \{C_{2x}|(0, 0.5, 0.5)\}$  and  $C_{2xy} = \{C_{2xy}|(0, 0, 0.5)\}$ , and the anti-unitary translation  $T\tau(\tau = (0.5, 0.5, 0.5))$ .

Considering that the correlation effect of the  $f$  electron on Ce is very strong, we take the Coulomb interaction strength of the  $4f$  electron in the range  $0 \sim 6$  eV. For convenience, we set  $U=2$  eV for the  $3d$  electron of the Co atom. As shown in the phase diagram Table VIII,  $\text{CeCo}_2\text{P}_2$  is ES for all  $U$  values. But we find that there is a topological phase transition between DSM and NLSM around  $U = 3.85$  eV.

The band structures along  $\Gamma - Z - R$  path have been plotted in the FIG. 33(c), with the Coulomb interaction  $U = 0, 2, 3.5, 4$  and  $6$  eV. When  $U < 3.85$  eV, both the band inversion between the highest occupied valence bands(HOVB) and the lowest unoccupied conduction bands(LUCB) occurs around  $\Gamma$  point. The irreps of HOVB and LUCB are  $\bar{\Gamma}_6$  and  $\bar{\Gamma}_9$ , which have different  $C_{4z}$  eigenvalues (See the characters in Table XII). Thus the band inversion between them creates two crossing points protected by  $C_{4z}$  on the  $k_x = k_y = 0$  line. As the Dirac points are symmetry protected on the  $k_x = k_y = 0$  line with co-little group  $4/mmm1'$ ,  $\text{CeCo}_2\text{P}_2$  is also a higher-order topological SM. [41] With  $U > 3.85$  eV, the band inversion around  $\Gamma$  point is removed and the two Dirac points annihilate each other. However, a new band inversion between HOVB and LUCB appears around  $Z$  point. As the irreps of the two bands at  $Z$  point are  $\bar{Z}_5$  and  $\bar{Z}_7$ , which have different  $M_z$  eigenvalues, the band crossing between them form a nodal line on the  $M_z$  invariant  $k_z = \pi$  plane. We also find that for  $U$  equal to the critical point of 3.85 eV, band inversions occur both around  $\Gamma$  and  $Z$  points. So the Dirac points and nodal line coexist at the critical point  $U = 3.85$  eV.

When we take the Coulomb interaction of  $f$  electron on Ce to be 6 eV and  $d$  electron interaction on Co to be 2 eV, the calculated magnetic moments on Co is  $0.94\mu_B$ , which matches the experimental magnetic moments. Then the band structure in FIG. 33(d) has a clean Fermi surface and forms an ideal antiferromagnetic NLSM. The surface states on the  $\langle 001 \rangle$  surface plane are calculated with the Wannier tight-binding Hamiltonian. As shown in the FIG. 33(b), there are two branches of surface states connecting to the nodal points near the Fermi level; These are distinguishable from the bulk states and can be observed by the ARPES/STM experiments.

## 3. Topological phase diagram of the antiferromagnetic Dirac semimetal $\text{MnGeO}_3$

$\text{MnGeO}_3$  with ilmenite structure was reported to be an antiferromagnet with Néel temperature  $T_N = 120K$ . The magnetic moment on the divalent cation  $\text{Mn}^{2+}$  is about  $5\mu_B$ , which is realized by the fully polarized high-spin configuration. It has a hexagonal lattice with SG  $R\bar{3}$  and MSG 148.19( $R\bar{3}'$ ) in the paramagnetic and antiferromagnetic phase, respectively. The MSG have two symmetry generators, three-fold rotation  $C_{3z}$  and the combination of inversion and time reversal symmetries  $P \cdot T$ . The experimental lattice constants  $a = 5.012$  Å and  $b = 14.2986$  Å are used in the first principle calculations. Because of the absence of time reversal symmetry, a new situation not possible in the time reversal invariant space groups arises in the MSG 148.19( $R\bar{3}'$ ). In this situation, all the  $k$  points on the  $C_{3z}$  rotational axis are maximal  $k$  points. If the eigenvalues of  $C_{3z}$  between any two points on the axis are changed, the system is predicted to be an ES.

We take the Coulomb interaction strength of  $3d$  electron of Mn from 0 to 4 eV and plot the band structures along the  $C_{3z}$  symmetric path  $\bar{F} - \Gamma - F$ , as shown in the FIG. 34, where the green and red lines represent the bands that have different eigenvalues of  $C_{3z}$  symmetry. The little co-group(LCG) of the momenta along  $\Gamma F$  path is  $\bar{3}'$ , which have two irreducible co-representations  $\bar{\Gamma}_5\bar{\Gamma}_6$  with  $C_3 = e^{\pm i\pi/3}$  doublet and  $\bar{\Gamma}_4\bar{\Gamma}_4$  with  $C_3 = -1, -1$  doublet, where the two doublets are stabilized by the  $P \cdot T$  symmetry. Without taking into account the correlation effect, the bands H1 with irrep  $\bar{\Gamma}_5\bar{\Gamma}_6$  and L1 with irrep  $\bar{\Gamma}_4\bar{\Gamma}_4$  have an anti-crossing between the  $\bar{F}$  and  $\Gamma$  points, which generate two Dirac points (DPs). Upon adding  $U$ , the second highest occupied band H2 moves up and there exist 2 pairs of DPs with  $U = 2$  eV, as shown in FIG. 34(c). With increasing  $U$  to 3 and 4 eV, one out of the two pairs DPs annihilates, leaving one pair of DPs locating on the two sides of  $\Gamma$  point. In the FIG. 2(c)-(d) of the main text, we have calculated the surface states with  $U = 4$ eV, on the  $\langle 010 \rangle$  surface plane. The surface states connecting to the Dirac cone on  $\Gamma F$  path can be distinguished from the bulk states.

In symmorphic groups, Dirac nodes always appear in pairs. Since the irrep of one band is changed when it traverses though a symmetry protected DP, there must be even number of DPs for the irrep to go back to itself after a period of the BZ. It indicates that the crystalline Nielsen-Ninomiya theorem, which guarantees the doubling of the number of Dirac nodes in a crystal is still valid for the Dirac fermions in magnetic crystals.

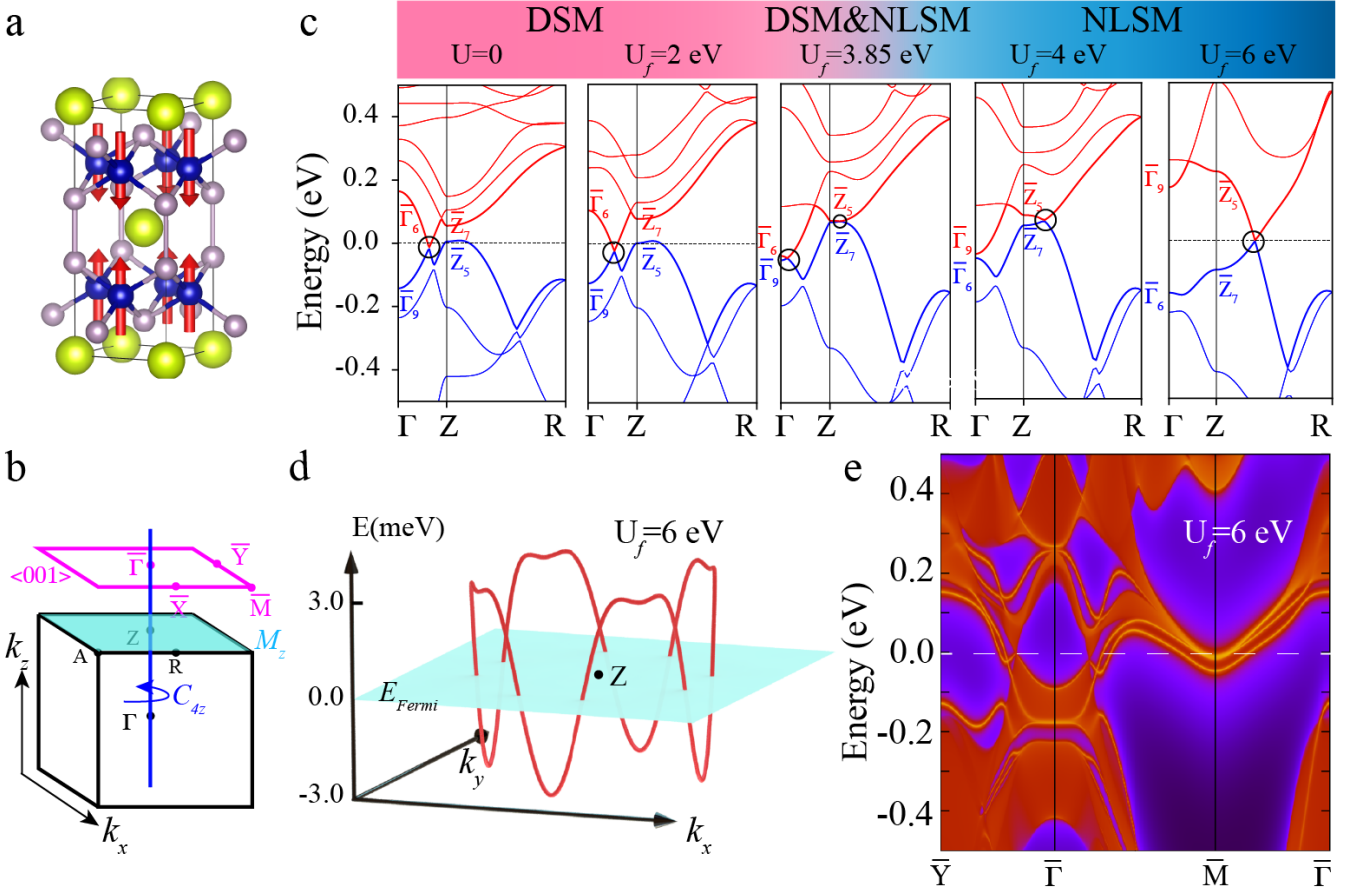


FIG. 33. (a) The crystal and magnetic structures of the antiferromagnetic CeCo<sub>2</sub>P<sub>2</sub> with MSG 126.386( $Pt4/nnc$ ). (b) The 3D BZ with high symmetry momenta and the surface BZ projected on the <001> surface plane. The  $C_{4z}$  rotation axis along  $\Gamma Z$  and the  $M_z$  plane  $k_z = \pi$  are represented by the blue line and green plane, respectively. (c) The topological phase diagrams of CeCo<sub>2</sub>P<sub>2</sub> with different Coulomb interaction strength applied. The irreps of the HOVB and LUCB are blue-colored and red-colored at both  $\Gamma$  and  $Z$  points. The topology with  $U \leq 3$  eV belongs to DSM and is transformed to NLSM once  $U \geq 4$  eV. All of the nodal points along the high symmetry path are indicated by the black circles. (d) The energy dispersion of the nodal line on the  $k_z = \pi$  plane, which is protected by  $M_z$  symmetry. (e) The drumhead-like surface states that connect the nodal line on the <001> surface. The Hubbard  $U$  of  $f$  electron on Ce is equal to 6 eV in (d) and (e).

#### 4. Weyl nodes, Nodal-lines and Anomalous Hall effect in Mn<sub>3</sub>ZnC

Mn<sub>3</sub>ZnC adopts a cubic lattice with anti-perovskite structure in the paramagnetic phase and undergoes a phase transition to ferromagnetic phase with Currie temperature  $T_c = 470K$ . At 215 K, there is a second order phase transition from ferromagnetic to non-collinear ferrimagnetic phase accompanied with a structural transformation from cubic lattice to a body-centered tetragonal lattice, as shown in FIG. 35. In this article, we focus on the low-temperature non-collinear ferrimagnetic phase of Mn<sub>3</sub>ZnC.

The MSG of ferrimagnetic Mn<sub>3</sub>ZnC is MSG 139.537( $I_4/mm'm'$ ), which is generated by the four-fold rotational symmetry along [001] direction  $C_{4z}$ , inversion symmetry  $I$  and the anti-unitary symmetry  $C_{2x} \cdot T$  ( $C_{2x}$  is the two-fold rotational symmetry along [100] direction and  $T$  is time reversal symmetry). There are two non-equivalent Mn atoms occupy the Wyckoff position 4c(0,1/2,0) and 8f(1/4,1/4,1/4), respectively. The Mn atoms on 4c site form the non-collinear antiferromagnetic structure with ferromagnetic canting along [001] direction. While the Mn atoms on 8f site are ferromagnetically polarized along [001] direction. In the *ab initio* calculations, non-collinear ferrimagnetic Mn<sub>3</sub>ZnC is diagnosed as ES for all  $U$  values (i.e.  $U = 0, 1, 2, 3, 4$  eV for 3d electron on Mn). Considering the strong correlations on 3d electron, we take  $U = 4$ eV and explain the band structure's topology in detail.

When  $U = 4$ eV, compatibility-relations of the band representations are not satisfied along  $\Gamma X$  and  $\Gamma T$  paths. So there have symmetry enforced band crossings between the HOVB and LUCB along  $\Gamma X$  and  $\Gamma T$ . In FIG. 35c, we plot the band structures along  $T - \Gamma - X$  and  $S_0\Gamma$  near the Fermi level. The irreps of HOVB and LUCB have been indicated by different colors. (See TABLE XIII for the characters of the irreps.) Along  $\Gamma T$  path, one can easily find two crossing points, WP3 and WP4, between the HOVB and LUCB, which have different  $C_{4z}$  eigenvalues. So WP3 and WP4 are  $C_{4z}$  protected Weyl points (WPs). On the  $\Gamma X$  and  $S_0\Gamma$  paths, there are many band crossings, which have different  $M_z$  eigenvalues. So these crossing points on the  $k_z = 0$  plane form the Nodal-lines (NLs) protected by mirror symmetry,  $M_z$ . Using WannierTools package, we find 10 pairs of WPs and 5 NLs in the first BZ. The positions of them are plotted in the BZ, as shown in FIG. 35. The 10 pairs of WPs can be classified to four non-equivalent types, among which WP3 and WP4 are

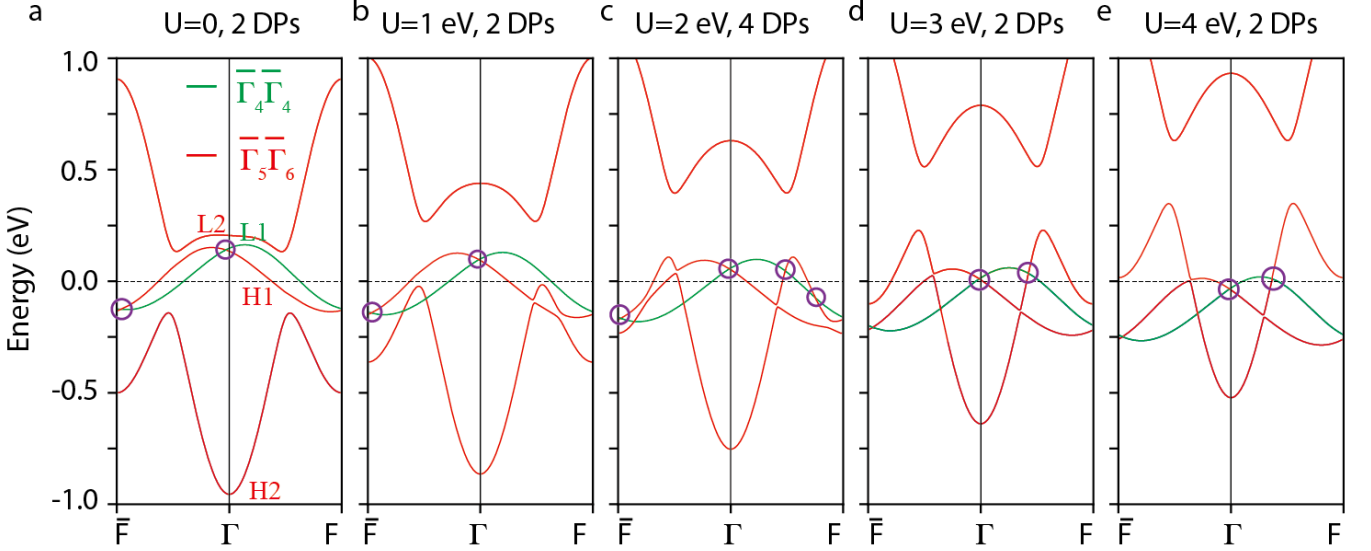


FIG. 34. The band structures and topologies evolution of MnGeO<sub>3</sub> (MSG  $R\bar{3}'$ ) with the Hubbard  $U$  parameter increasing from 0 to 4 eV. The  $(N_e - 1)$ th to  $(N_e + 2)$ th bands are plotted, with  $N_e$  being the number of electrons per unit cell. All of the points on the  $\bar{F} - \Gamma - F$  path respect the same LCG  $\bar{3}'$ , which have two different 2-dimensional irreps named as  $\bar{\Gamma}_4\bar{\Gamma}_4$  and  $\bar{\Gamma}_5\bar{\Gamma}_6$ . The three lines H1, H2 and L2 have the same  $\bar{\Gamma}_5\bar{\Gamma}_6$  representation and are red-colored; the line L1 is the  $\bar{\Gamma}_4\bar{\Gamma}_4$  representation and is blue-colored. (a) For  $U = 0$ , L1 and H1 have an anti-crossing along the  $\bar{F}\Gamma$  path and generate two DPs. (b)-(e) With increasing the Coulomb interaction, the lines L2 and H2 move to higher energy and much more crossing generate between H2 and the branch of (L1, H1). The DPs formed by the HOVB and LUCB are indicated by the purple circles.

symmetry enforced WPs, WP1 and WP2 are generated by accidental band crossings. WPs in each type are related by  $C_{4z}$  and  $M_z$  symmetries. Using Wilson loop method [?], we have identified the chiralities of the WPs, as shown in FIG. 35e. We tabulated the exact positions and chiralities of them in TABLE XIV. The 5 NLs are classified to two types. The first type (NL1) is symmetry enforced and localized around the  $\Gamma$  point. The other four NLs (NL2) are generated by accidental band crossings near  $S_0\Gamma$  path and they are related by  $C_{4z}$  symmetry.

In time reversal breaking (TRB) systems, nonzero Berry curvatures of occupied Bloch states contribute the intrinsic anomalous Hall conductivities (AHC). In non-collinear ferrimagnetic Mn<sub>3</sub>ZnC, the Berry curvatures of bands near the WPs and NLs are very large, which will contribute giant AHC. We calculate the AHC of ferrimagnetic Mn<sub>3</sub>ZnC by the sum of Berry curvatures over all occupied bands,

$$\sigma_{xy} = -\frac{2\pi e^2}{h} \int_{BZ} \frac{d^3\vec{k}}{(2\pi)^3} \sum_n f_n(\vec{k}) \Omega_n^z(\vec{k}) \quad (J1)$$

where  $f_n(\vec{k})$  is the Fermi-Dirac distribution function, and  $n$  is the index of the occupied bands. The Berry curvature is arisen from Kubo-formula derivation,

$$\Omega_n^z(\vec{k}) = -2\text{Im} \sum_{m \neq n} \frac{\langle \Psi_{n\vec{k}} | v_x | \Psi_{m\vec{k}} \rangle \langle \Psi_{m\vec{k}} | v_y | \Psi_{n\vec{k}} \rangle}{(E_m(\vec{k}) - E_n(\vec{k}))^2} \quad (J2)$$

where  $v_x(y)$  is the velocity operator. We calculate the intrinsic AHC with a  $101 \times 101 \times 101$   $k$ -point grid in the first BZ based on the Wannier tight-binding Hamiltonian.

In FIG. 35f, we plot the energy dependence of intrinsic AHC near the Fermi level. On the Fermi level, the AHC is about  $-123 \Omega^{-1} \cdot cm^{-1}$ , which can be observed in transport experiments.

$\Lambda_\alpha$	MLCG	Irreps	$C_{4z}^+$	$\Lambda_\alpha$	MLCG	Irreps	$M_z$
LD(0,0,w)	42'2'	$\overline{LD}_5$	$\frac{-1+i}{\sqrt{2}}$	DT(u,u,0)	$m'm2'$	$\overline{DT}_3$	-i
		$\overline{LD}_6$	$\frac{1-i}{\sqrt{2}}$			$\overline{DT}_4$	i
		$\overline{LD}_7$	$\frac{-1-i}{\sqrt{2}}$	SM(u,0,0)	$m'm2'$	$\overline{SM}_3$	-i
		$\overline{LD}_8$	$\frac{1+i}{\sqrt{2}}$			$\overline{SM}_4$	i

TABLE XIII. Character table of the irreducible co-representations of MSG  $P14/nnc$  at  $LD(0,0,w)$ ,  $DT(u,u,0)$  and  $SM(u,0,0)$  points. The first two(5th-6th) columns are the momenta and their magnetic little co-groups(MLCG); the third(7th) column are the irreps of the MLCG; the 4th(8th) columns are the characters of the symmetry generators of the unitary subgroup.

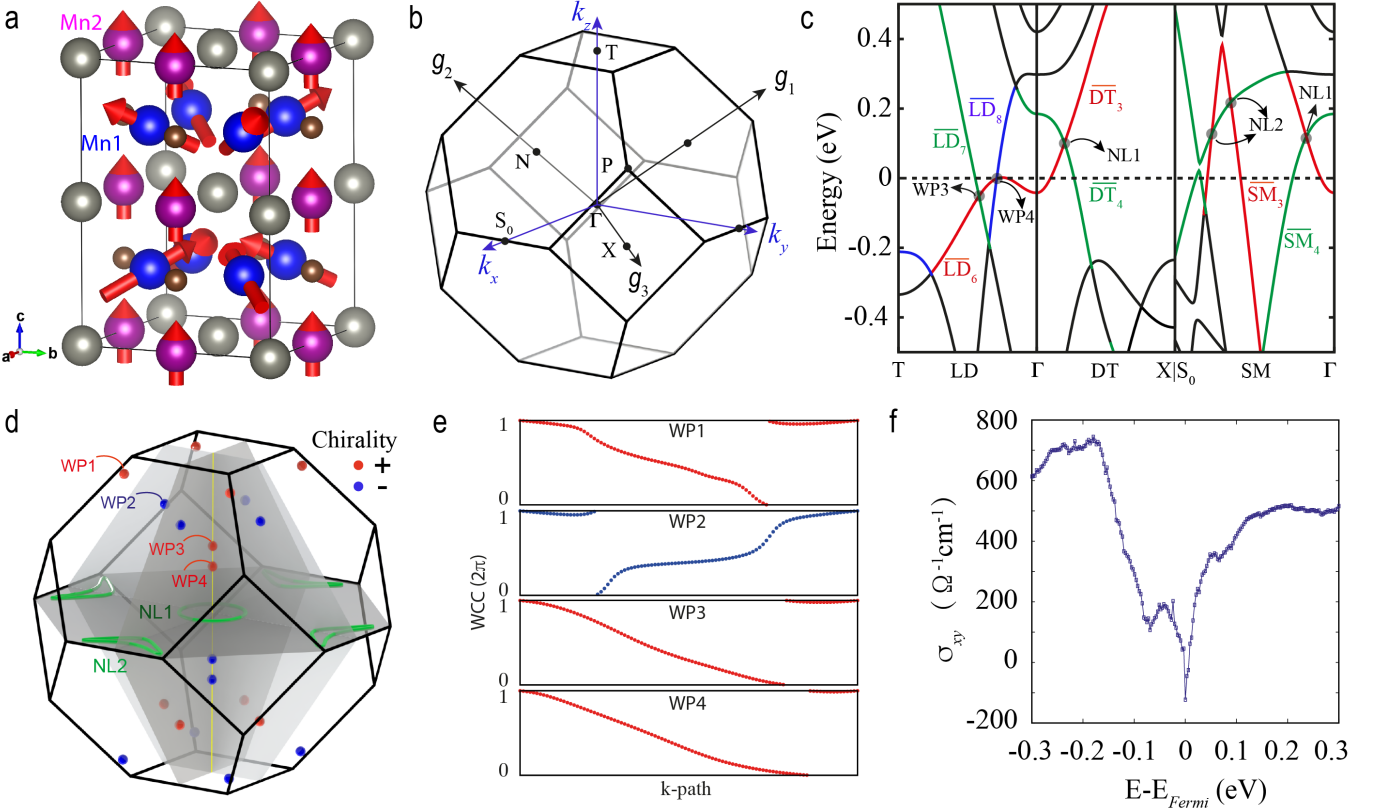


FIG. 35. Weyl nodes and Nodal-lines in ferrimagnetic  $\text{Mn}_3\text{ZnC}$  ( $\text{MSG } I_4/mm'm'$ ) with  $U = 4\text{eV}$ . (a) The magnetic crystal structure and (b) the corresponding Brillouin zone (BZ) of non-collinear ferrimagnetic  $\text{Mn}_3\text{ZnC}$ . (c) Band structures along the high-symmetry paths  $T - \Gamma - X$  and  $S_0\Gamma$ . The irreps of HOVB and LUCB are tagged by different colors. Band crossings on  $TT$  path form the two WPs, WP3 and WP4. Band crossings on the  $k_z = 0$  plane generate 5 NLs, which are protected by  $M_z$  symmetry. (d) Locations of WPs and NLs in the first BZ. The red(blue) balls stand for WPs with chirality +1(-1). (e) The evolution of Wannier charge centers (WCCs) on the manifold that enclosing WP1, WP2, WP3 and WP4, respectively. (f) Energy dependence of the intrinsic AHC in the non-collinear ferrimagnetic  $\text{Mn}_3\text{ZnC}$ . The Fermi energy is set to 0.

### Appendix K: Fragile bands in the magnetic materials

In Table XV, we tabulate all of the magnetic materials that have fragile bands below the Fermi level. For the materials having more than one fragile branch, we provide the irreducible co-representations at high symmetry momenta of the fragile branches closest to the Fermi level.

TABLE XV: The fragile occupied bands in magnetic materials. In the first four columns the chemical formulae (Formula), the material identification number on BCSMD (BCSID), the magnetic space group number (MSG) and the Coulomb interaction strength (U) are tabulated. The fifth column gives the number of fragile branches (NF) in the band structure of the corresponding material. In the sixth and seventh columns, the band indices (Bands) and the irreducible representations (Irreps) at high symmetry momenta of the fragile branch closest to the Fermi level are tabulated.

Formula	BCSID	MSG	U(eV)	NF	Bands	Irreps
CeCoGe3	1.0.11	107.231	4	1	-83~81	$\bar{\Gamma}_6 + \bar{\Gamma}_8 + \bar{M}_6 + \bar{M}_8 + \bar{N}_2 + \bar{P}_4 + \bar{X}_4$
alpha-Mn	1.85	114.282	0	5	-43~40	$\bar{A}_6 + \bar{A}_7 + \bar{\Gamma}_6 + \bar{M}_7 + \bar{R}_2\bar{R}_4 + \bar{R}_3\bar{R}_5 + \bar{X}_2 + \bar{X}_3 + \bar{X}_4 + \bar{X}_5 + \bar{Z}_6 + \bar{Z}_7$
PrCo <sub>2</sub> P <sub>2</sub>	2.26	123.345	0	1	-115~108	$\bar{A}_{10} + \bar{A}_{11} + \bar{A}_{12} + \bar{A}_5 + \bar{A}_6 + \bar{A}_7 + \bar{A}_8 + \bar{A}_9 + \bar{\Gamma}_{10} + \bar{\Gamma}_{12} + \bar{\Gamma}_6 + \bar{\Gamma}_8 + \bar{M}_{11} + \bar{M}_5 + \bar{M}_6 + \bar{M}_7 + \bar{M}_8 + \bar{M}_9 + \bar{R}_3 + \bar{R}_4 + \bar{R}_5 + \bar{R}_6 + \bar{X}_3 + \bar{X}_4 + \bar{X}_5 + \bar{X}_6 + \bar{Z}_{10} + \bar{Z}_{12} + \bar{Z}_6 + \bar{Z}_8$
NdCo <sub>2</sub> P <sub>2</sub>	1.251	124.360	0	2	-119~112	$\bar{A}_5 + \bar{A}_6 + \bar{A}_7 + \bar{A}_8 + \bar{\Gamma}_7 + \bar{\Gamma}_9 + \bar{M}_6 + \bar{M}_7 + \bar{M}_8 + \bar{R}_3 + \bar{R}_4 + \bar{X}_5 + \bar{X}_6 + \bar{Z}_6 + \bar{Z}_8$
NdCo <sub>2</sub> P <sub>2</sub>	1.251	124.360	4	1	-119~112	$\bar{A}_5 + \bar{A}_6 + \bar{A}_7 + \bar{A}_8 + \bar{\Gamma}_7 + \bar{\Gamma}_9 + \bar{M}_6 + \bar{M}_7 + \bar{M}_8 + \bar{R}_3 + \bar{R}_4 + \bar{X}_5 + \bar{X}_6 + \bar{Z}_6 + \bar{Z}_8$

WPs	Position ( $k_x, k_y, k_z$ ) $(\text{\AA}^{-1})$	Chirality	$E - E_{Fermi}$ (eV)
WP1	( 0.3101, 0.3101, 0.7154)	+1	-0.0767
	( -0.3101, -0.3101, 0.7154)	+1	-0.0767
	( -0.3101, 0.3101, 0.7154)	+1	-0.0767
	( 0.3101, -0.3101, 0.7154)	+1	-0.0767
	( 0.3101, 0.3101, -0.7154)	-1	-0.0767
	( -0.3101, -0.3101, -0.7154)	-1	-0.0767
	( -0.3101, 0.3101, -0.7154)	-1	-0.0767
	( 0.3101, -0.3101, -0.7154)	-1	-0.0767
WP2	( 0.0, -0.2798, 0.5009)	-1	-0.2310
	( 0.0, 0.2798, 0.5009)	-1	-0.2310
	( 0.2798, 0.0, 0.5009)	-1	-0.2310
	( -0.2798, 0.0, 0.5009)	-1	-0.2310
	( 0.0, 0.2798, -0.5009)	+1	-0.2310
	( 0.0, -0.2798, -0.5009)	+1	-0.2310
	( -0.2798, 0.0, -0.5009)	+1	-0.2310
	( 0.2798, 0.0, -0.5009)	+1	-0.2310
WP3	( 0.0, 0.0, 0.3343)	+1	-0.14
	( 0.0, 0.0, -0.3343)	-1	-0.14
WP4	( 0.0, 0.0, 0.2320)	+1	-0.0901
	( 0.0, 0.0, -0.2320)	-1	-0.0901

TABLE XIV. The 10 pairs of WPs in the first BZ. The first column is the type of WPs. In each type, the WPs are related by  $C_{4z}$  and  $M_z$  symmetries. The second column is the position of each WP in the cartesian coordinate system of BZ. The 4th-5th columns are the chirality and energy related to the Fermi level of each WP.

UPtGa5	1.255	124.360	6	1	-37~~-30	$\bar{A}_5 + \bar{A}_7 + \bar{\Gamma}_7 + \bar{\Gamma}_8 + \bar{\Gamma}_9 + \bar{M}_6 + \bar{M}_8 + \bar{R}_3 + \bar{R}_4 + \bar{X}_5 + \bar{X}_6 + \bar{Z}_5 + \bar{Z}_6 + \bar{Z}_7 + \bar{Z}_8$
NpRhGa5	1.261	124.360	0	4	-69~~-66	$\bar{A}_5 + \bar{A}_7 + \bar{\Gamma}_6 + \bar{M}_6 + \bar{R}_3 + \bar{R}_4 + \bar{X}_6 + \bar{Z}_5 + \bar{Z}_7$
NpRhGa5	1.261	124.360	4	1	-167~~-164	$\bar{A}_5 + \bar{A}_8 + \bar{\Gamma}_8 + \bar{\Gamma}_9 + \bar{M}_8 + \bar{M}_9 + \bar{R}_3 + \bar{R}_4 + \bar{X}_6 + \bar{Z}_6 + \bar{Z}_7$
Fe4Si2Sn7O16	1.197	12.63	1	1	-163~~-160	$\bar{A}_3\bar{A}_5 + \bar{A}_4\bar{A}_6 + \bar{\Gamma}_3\bar{\Gamma}_4 + \bar{L}_2\bar{L}_3 + \bar{M}_3\bar{M}_5 + \bar{M}_4\bar{M}_6 + \bar{V}_3\bar{V}_3 + \bar{Y}_5\bar{Y}_6$
MnBr2	1.239	12.63	2	1	-11~~-8	$\bar{A}_3\bar{A}_5 + \bar{A}_4\bar{A}_6 + \bar{\Gamma}_5\bar{\Gamma}_6 + \bar{L}_2\bar{L}_3 + \bar{M}_3\bar{M}_5 + \bar{M}_4\bar{M}_6 + \bar{V}_3\bar{V}_3 + \bar{Y}_3\bar{Y}_4$
Li2MnO3	1.97	12.63	0	2	-119~~-116	$\bar{A}_3\bar{A}_5 + \bar{A}_4\bar{A}_6 + \bar{\Gamma}_5\bar{\Gamma}_6 + \bar{L}_2\bar{L}_3 + \bar{M}_3\bar{M}_5 + \bar{M}_4\bar{M}_6 + \bar{V}_3\bar{V}_3 + \bar{Y}_3\bar{Y}_4$
U2Ni2In	1.102	128.408	0	4	-155~~-140	$\bar{A}_5\bar{A}_6 + \bar{A}_7\bar{A}_8 + \bar{\Gamma}_6 + \bar{\Gamma}_7 + \bar{M}_6\bar{M}_7 + \bar{R}_2\bar{R}_7 + \bar{R}_3\bar{R}_6 + \bar{R}_4\bar{R}_9 + \bar{R}_5\bar{R}_8 + \bar{X}_3\bar{X}_4 + \bar{Z}_5 + \bar{Z}_6 + \bar{Z}_7 + \bar{Z}_8$
U2Ni2In	1.102	128.408	2	2	-155~~-140	$\bar{A}_5\bar{A}_6 + \bar{A}_7\bar{A}_8 + \bar{\Gamma}_6 + \bar{\Gamma}_7 + \bar{M}_6\bar{M}_7 + \bar{R}_2\bar{R}_7 + \bar{R}_3\bar{R}_6 + \bar{R}_4\bar{R}_9 + \bar{R}_5\bar{R}_8 + \bar{X}_3\bar{X}_4 + \bar{Z}_5 + \bar{Z}_6 + \bar{Z}_7 + \bar{Z}_8$
U2Ni2In	1.102	128.408	4	2	-155~~-140	$\bar{A}_5\bar{A}_6 + \bar{A}_7\bar{A}_8 + \bar{\Gamma}_6 + \bar{\Gamma}_7 + \bar{M}_6\bar{M}_7 + \bar{R}_2\bar{R}_7 + \bar{R}_3\bar{R}_6 + \bar{R}_4\bar{R}_9 + \bar{R}_5\bar{R}_8 + \bar{X}_3\bar{X}_4 + \bar{Z}_5 + \bar{Z}_6 + \bar{Z}_7 + \bar{Z}_8$
U2Ni2In	1.102	128.408	6	2	-171~~-164	$\bar{A}_5\bar{A}_6 + \bar{A}_7\bar{A}_8 + \bar{\Gamma}_6 + \bar{\Gamma}_7 + \bar{M}_6\bar{M}_7 + \bar{R}_2\bar{R}_7 + \bar{R}_3\bar{R}_6 + \bar{R}_4\bar{R}_9 + \bar{R}_5\bar{R}_8 + \bar{X}_3\bar{X}_4 + \bar{Z}_5 + \bar{Z}_6 + \bar{Z}_7 + \bar{Z}_8$
TbRh2Si2	1.187	128.410	0	1	-65~~-62	$\bar{A}_5 + \bar{A}_7 + \bar{\Gamma}_7 + \bar{M}_6 + \bar{M}_7 + \bar{R}_2\bar{R}_4 + \bar{R}_3\bar{R}_5 + \bar{X}_3 + \bar{X}_4 + \bar{Z}_6 + \bar{Z}_8$
TbRh2Si2	1.187	128.410	4	1	-69~~-66	$\bar{A}_5 + \bar{A}_7 + \bar{\Gamma}_9 + \bar{M}_8 + \bar{M}_9 + \bar{R}_2\bar{R}_4 + \bar{R}_3\bar{R}_5 + \bar{X}_3 + \bar{X}_4 + \bar{Z}_6 + \bar{Z}_8$
TbRh2Si2	1.187	128.410	6	1	-51~~-48	$\bar{A}_5 + \bar{A}_7 + \bar{\Gamma}_7 + \bar{M}_6 + \bar{M}_7 + \bar{R}_2\bar{R}_4 + \bar{R}_3\bar{R}_5 + \bar{X}_3 + \bar{X}_4 + \bar{Z}_6 + \bar{Z}_8$
DyCo2Si2	1.21	128.410	0	2	-63~~-58	$\bar{A}_6 + \bar{A}_7 + \bar{A}_8 + \bar{\Gamma}_8 + \bar{\Gamma}_9 + \bar{M}_8 + \bar{M}_9 + \bar{R}_6\bar{R}_8 + \bar{R}_7\bar{R}_9 + \bar{X}_3 + \bar{X}_4 + \bar{Z}_5 + \bar{Z}_7 + \bar{Z}_8$
DyCo2Si2	1.21	128.410	2	1	-59~~-52	$\bar{A}_5 + \bar{A}_6 + \bar{A}_7 + \bar{A}_8 + \bar{\Gamma}_7 + \bar{\Gamma}_8 + \bar{\Gamma}_9 + \bar{M}_6 + \bar{M}_7 + \bar{M}_8 + \bar{M}_9 + \bar{R}_2\bar{R}_4 + \bar{R}_3\bar{R}_5 + \bar{R}_6\bar{R}_8 + \bar{R}_7\bar{R}_9 + \bar{X}_3 + \bar{X}_4 + \bar{Z}_5 + \bar{Z}_6 + \bar{Z}_7 + \bar{Z}_8$
DyCo2Si2	1.21	128.410	4	3	-9~~-6	$\bar{A}_6 + \bar{A}_7 + \bar{A}_8 + \bar{\Gamma}_6 + \bar{\Gamma}_7 + \bar{M}_7 + \bar{M}_9 + \bar{R}_6\bar{R}_8 + \bar{R}_7\bar{R}_9 + \bar{X}_3 + \bar{X}_4 + \bar{Z}_6 + \bar{Z}_7 + \bar{Z}_8$
CeMnAsO	0.186	129.416	0	9	-1~~0	$\bar{A}_7 + \bar{\Gamma}_7 + \bar{M}_6 + \bar{R}_2\bar{R}_4 + \bar{X}_2\bar{X}_4 + \bar{Z}_6$
CeMnAsO	0.186	129.416	3	6	-9~~-8	$\bar{A}_6 + \bar{\Gamma}_6 + \bar{M}_7 + \bar{R}_2\bar{R}_4 + \bar{X}_2\bar{X}_4 + \bar{Z}_7$
CeMnAsO	0.186	129.416	4	6	-1~~0	$\bar{A}_7 + \bar{\Gamma}_7 + \bar{M}_7 + \bar{R}_3\bar{R}_5 + \bar{X}_3\bar{X}_5 + \bar{Z}_7$
CaMnBi2	0.72	129.416	0	4	-7~~-6	$\bar{A}_6 + \bar{\Gamma}_6 + \bar{M}_6 + \bar{R}_3\bar{R}_5 + \bar{X}_3\bar{X}_5 + \bar{Z}_6$

CaMnBi2	0.72	129.416	1	4	-7~6	$\bar{A}_6 + \bar{\Gamma}_6 + \bar{M}_6 + \bar{R}_3\bar{R}_5 + \bar{X}_3\bar{X}_5 + \bar{Z}_6$
CaMnBi2	0.72	129.416	2	8	-1~0	$\bar{A}_7 + \bar{\Gamma}_6 + \bar{M}_6 + \bar{R}_3\bar{R}_5 + \bar{X}_3\bar{X}_5 + \bar{Z}_7$
CaMnBi2	0.72	129.416	3	5	-1~0	$\bar{A}_7 + \bar{\Gamma}_6 + \bar{M}_6 + \bar{R}_3\bar{R}_5 + \bar{X}_3\bar{X}_5 + \bar{Z}_7$
CaMnBi2	0.72	129.416	4	5	-1~0	$\bar{A}_7 + \bar{\Gamma}_6 + \bar{M}_6 + \bar{R}_3\bar{R}_5 + \bar{X}_3\bar{X}_5 + \bar{Z}_7$
UPt2Si2	0.194	129.419	0	6	-19~18	$\bar{A}_7 + \bar{\Gamma}_6 + \bar{M}_7 + \bar{R}_2\bar{R}_4$
UPt2Si2	0.194	129.419	2	5	-39~38	$\bar{A}_7 + \bar{\Gamma}_7 + \bar{M}_7 + \bar{R}_3\bar{R}_5$
UPt2Si2	0.194	129.419	4	9	-13~12	$\bar{A}_7 + \bar{\Gamma}_7 + \bar{M}_7 + \bar{R}_3\bar{R}_5$
UPt2Si2	0.194	129.419	6	8	-31~28	$\bar{A}_6 + \bar{A}_7 + \bar{\Gamma}_7 + \bar{M}_6 + \bar{M}_7 + \bar{R}_3\bar{R}_5 + \bar{X}_3\bar{X}_5 + \bar{Z}_7$
Nd2CuO4	2.6	134.481	2	1	-71~56	$\bar{A}_6\bar{A}_7 + \bar{\Gamma}_6 + \bar{\Gamma}_7 + \bar{G}_8 + \bar{\Gamma}_9 + \bar{M}_5 + \bar{R}_3\bar{R}_4 + \bar{X}_3 + \bar{X}_4 + \bar{Z}_5$
UNiGa5	1.254	140.550	6	2	-43~40	$\bar{G}_8 + \bar{\Gamma}_9 + \bar{M}_6 + \bar{M}_7 + \bar{N}_2 + \bar{P}_7 + \bar{X}_5 + \bar{X}_6$
Nd2RhIn8	1.82	140.550	4	1	-97~90	$\bar{G}_6 + \bar{\Gamma}_7 + \bar{\Gamma}_8 + \bar{M}_6 + \bar{M}_7 + \bar{N}_2 + \bar{P}_6 + \bar{P}_7 + \bar{X}_5 + \bar{X}_6$
TbCo2Ga8	1.87	140.550	2	1	-63~60	$\bar{G}_8 + \bar{\Gamma}_9 + \bar{M}_6 + \bar{M}_7 + \bar{N}_2 + \bar{P}_6 + \bar{X}_5 + \bar{X}_6$
Er2Ru2O7	0.154	141.554	0	1	-115~112	$\bar{Z}_3 + \bar{Z}_4 + \bar{L}_3 + \bar{H}_2\bar{H}_4 + \bar{H}_3 + \bar{H}_5 + \bar{Y}_3 + \bar{Y}_4 + \bar{T}_3 + \bar{T}_4 + \bar{\Gamma}_5 + \bar{\Gamma}_6$
Er2Ru2O7	0.154	141.554	2	1	-103~100	$\bar{Z}_3 + \bar{Z}_4 + \bar{L}_3 + \bar{H}_2\bar{H}_4 + \bar{H}_3 + \bar{H}_5 + \bar{Y}_3 + \bar{Y}_4 + \bar{T}_3 + \bar{T}_4 + \bar{\Gamma}_5 + \bar{\Gamma}_6$
Er2Ru2O7	0.154	141.554	4	1	-87~84	$\bar{Z}_3 + \bar{Z}_4 + \bar{L}_3 + \bar{H}_2\bar{H}_4 + \bar{H}_3 + \bar{H}_5 + \bar{Y}_3 + \bar{Y}_4 + \bar{T}_3 + \bar{T}_4 + \bar{\Gamma}_5 + \bar{\Gamma}_6$
Gd2Sn2O7	0.47	141.555	2	3	-99~96	$\bar{X}_5\bar{X}_6 + \bar{R}_3 + \bar{R}_4 + \bar{S}_3 + \bar{S}_4 + \bar{W}_2\bar{W}_4 + \bar{W}_3 + \bar{W}_5 + \bar{T}_2 + \bar{\Gamma}_5 + \bar{\Gamma}_6$
Gd2Sn2O7	0.47	141.555	4	1	-139~136	$\bar{X}_5\bar{X}_6 + \bar{R}_5 + \bar{R}_6 + \bar{S}_5 + \bar{S}_6 + \bar{W}_2\bar{W}_4 + \bar{W}_3 + \bar{W}_5 + \bar{T}_2 + \bar{\Gamma}_5 + \bar{\Gamma}_6$
Gd2Sn2O7	0.47	141.555	6	1	-139~136	$\bar{X}_5\bar{X}_6 + \bar{R}_5 + \bar{R}_6 + \bar{S}_5 + \bar{S}_6 + \bar{W}_2\bar{W}_4 + \bar{W}_3 + \bar{W}_5 + \bar{T}_2 + \bar{\Gamma}_5 + \bar{\Gamma}_6$
Tm2Mn2O7	0.151	141.557	0	1	-25~12	$\bar{\Gamma}_{10} + \bar{\Gamma}_{11} + \bar{\Gamma}_{12} + \bar{\Gamma}_5 + \bar{\Gamma}_6 + \bar{\Gamma}_7 + \bar{\Gamma}_8 + \bar{\Gamma}_9 + \bar{M}_3 + \bar{M}_4 + \bar{N}_2 + \bar{N}_3 + \bar{P}_5 + \bar{P}_6 + \bar{P}_7 + \bar{P}_8 + \bar{X}_2$
Tb2Sn2O7	0.48	141.557	2	1	-119~116	$\bar{\Gamma}_{11} + \bar{\Gamma}_6 + \bar{\Gamma}_8 + \bar{\Gamma}_9 + \bar{M}_3 + \bar{M}_4 + \bar{N}_2 + \bar{P}_5 + \bar{P}_6 + \bar{P}_7 + \bar{X}_2$
Tb2Sn2O7	0.48	141.557	4	1	-119~116	$\bar{\Gamma}_{11} + \bar{\Gamma}_6 + \bar{\Gamma}_8 + \bar{\Gamma}_9 + \bar{M}_3 + \bar{M}_4 + \bar{N}_2 + \bar{P}_5 + \bar{P}_6 + \bar{P}_7 + \bar{X}_2$
Ho2Ru2O7	0.51	141.557	0	2	-19~16	$\bar{\Gamma}_5 + \bar{\Gamma}_6 + \bar{\Gamma}_7 + \bar{\Gamma}_8 + \bar{M}_3 + \bar{M}_4 + \bar{N}_2 + \bar{N}_3 + \bar{P}_5 + \bar{P}_7 + \bar{X}_2$
Li2Mn(SO4)2	0.122	14.75	0	1	-121~118	$\bar{A}_2 + \bar{B}_2 + \bar{C}_2 + \bar{D}_3 + \bar{D}_4 + \bar{E}_3 + \bar{E}_4 + \bar{\Gamma}_5 + \bar{\Gamma}_6 + \bar{Y}_3 + \bar{Y}_4 + \bar{Z}_2$
Li2Mn(SO4)2	0.122	14.75	1	2	-101~98	$\bar{A}_2 + \bar{B}_2 + \bar{C}_2 + \bar{D}_5 + \bar{D}_6 + \bar{E}_3 + \bar{E}_4 + \bar{\Gamma}_5 + \bar{\Gamma}_6 + \bar{Y}_5 + \bar{Y}_6 + \bar{Z}_2$
Li2Mn(SO4)2	0.122	14.75	2	1	-121~118	$\bar{A}_2 + \bar{B}_2 + \bar{C}_2 + \bar{D}_3 + \bar{D}_4 + \bar{E}_3 + \bar{E}_4 + \bar{\Gamma}_5 + \bar{\Gamma}_6 + \bar{Y}_3 + \bar{Y}_4 + \bar{Z}_2$
Li2Mn(SO4)2	0.122	14.75	3	1	-121~118	$\bar{A}_2 + \bar{B}_2 + \bar{C}_2 + \bar{D}_3 + \bar{D}_4 + \bar{E}_3 + \bar{E}_4 + \bar{\Gamma}_5 + \bar{\Gamma}_6 + \bar{Y}_3 + \bar{Y}_4 + \bar{Z}_2$
Li2Co(SO4)2	0.121	14.79	0	2	-109~106	$\bar{U}_2\bar{U}_3 + \bar{Z}_2\bar{Z}_3 + \bar{V}_2\bar{V}_3 + \bar{T}_3\bar{T}_3 + \bar{R}_2\bar{R}_2 + \bar{X}_3 + \bar{Y}_2\bar{Y}_3 + \bar{\Gamma}_3$
Li2Co(SO4)2	0.121	14.79	1	1	-125~122	$\bar{U}_2\bar{U}_3 + \bar{Z}_2\bar{Z}_3 + \bar{V}_2\bar{V}_3 + \bar{T}_3\bar{T}_3 + \bar{R}_2\bar{R}_2 + \bar{X}_2 + \bar{Y}_2\bar{Y}_3 + \bar{\Gamma}_2$
Li2Co(SO4)2	0.121	14.79	3	1	-125~122	$\bar{U}_2\bar{U}_3 + \bar{Z}_2\bar{Z}_3 + \bar{V}_2\bar{V}_3 + \bar{T}_3\bar{T}_3 + \bar{R}_2\bar{R}_2 + \bar{X}_2 + \bar{Y}_2\bar{Y}_3 + \bar{\Gamma}_2$
Li2Co(SO4)2	0.121	14.79	4	1	-125~122	$\bar{U}_2\bar{U}_3 + \bar{Z}_2\bar{Z}_3 + \bar{V}_2\bar{V}_3 + \bar{T}_3\bar{T}_3 + \bar{R}_2\bar{R}_2 + \bar{X}_2 + \bar{Y}_2\bar{Y}_3 + \bar{\Gamma}_2$
NiN2O6	0.78	148.17	0	1	-87~86	$\bar{F}_2 + \bar{\Gamma}_5 + \bar{\Gamma}_6 + \bar{L}_3 + \bar{T}_8 + \bar{T}_9$
NiN2O6	0.78	148.17	2	1	-153~151	$\bar{F}_2 + \bar{F}_3 + \bar{\Gamma}_7 + \bar{\Gamma}_8 + \bar{\Gamma}_9 + \bar{L}_2 + \bar{T}_5 + \bar{T}_6 + \bar{T}_7$
NiN2O6	0.78	148.17	3	1	-153~151	$\bar{F}_2 + \bar{F}_3 + \bar{\Gamma}_7 + \bar{\Gamma}_8 + \bar{\Gamma}_9 + \bar{L}_2 + \bar{T}_5 + \bar{T}_6 + \bar{T}_7$
NiCO3	0.113	15.85	1	1	-23~20	$\bar{A}_2 + \bar{\Gamma}_5 + \bar{\Gamma}_6 + \bar{L}_3 + \bar{M}_2 + \bar{V}_2 + \bar{V}_3 + \bar{Y}_5 + \bar{Y}_6$
CoCO3	0.114	15.85	2	1	-27~22	$\bar{A}_2 + \bar{\Gamma}_3 + \bar{\Gamma}_4 + \bar{\Gamma}_5 + \bar{\Gamma}_6 + \bar{L}_2 + \bar{M}_2 + \bar{V}_2 + \bar{V}_3 + \bar{Y}_3 + \bar{Y}_4$
CoCO3	0.114	15.85	3	1	-11~8	$\bar{A}_2 + \bar{\Gamma}_5 + \bar{\Gamma}_6 + \bar{L}_3 + \bar{M}_2 + \bar{V}_2 + \bar{V}_3 + \bar{Y}_5 + \bar{Y}_6$
CoCO3	0.114	15.85	4	1	-11~8	$\bar{A}_2 + \bar{\Gamma}_5 + \bar{\Gamma}_6 + \bar{L}_3 + \bar{M}_2 + \bar{V}_2 + \bar{V}_3 + \bar{Y}_5 + \bar{Y}_6$
MnCO3	0.115	15.85	0	1	-19~16	$\bar{A}_2 + \bar{\Gamma}_3 + \bar{\Gamma}_4 + \bar{L}_2 + \bar{M}_2 + \bar{V}_2 + \bar{V}_3 + \bar{Y}_3 + \bar{Y}_4$
MnCO3	0.115	15.85	1	1	-13~10	$\bar{A}_2 + \bar{\Gamma}_5 + \bar{\Gamma}_6 + \bar{L}_3 + \bar{M}_2 + \bar{V}_2 + \bar{V}_3 + \bar{Y}_5 + \bar{Y}_6$
MnCO3	0.115	15.85	4	1	-9~6	$\bar{A}_2 + \bar{\Gamma}_5 + \bar{\Gamma}_6 + \bar{L}_3 + \bar{M}_2 + \bar{V}_2 + \bar{V}_3 + \bar{Y}_5 + \bar{Y}_6$
FeBO3	0.112	15.89	1	1	-19~16	$\bar{Z}_2\bar{Z}_3 + \bar{U}_3 + \bar{T}_2 + \bar{R}_2\bar{R}_3 + \bar{X}_2 + \bar{X}_3 + \bar{Y}_2 + \bar{Y}_3 + \bar{V}_3 + \bar{\Gamma}_3$
FeBO3	0.112	15.89	2	1	-19~16	$\bar{Z}_2\bar{Z}_3 + \bar{U}_3 + \bar{T}_2 + \bar{R}_2\bar{R}_3 + \bar{X}_2 + \bar{X}_3 + \bar{Y}_2 + \bar{Y}_3 + \bar{V}_3 + \bar{\Gamma}_3$
FeBO3	0.112	15.89	3	1	-3~0	$\bar{Z}_2\bar{Z}_3 + \bar{U}_2 + \bar{T}_3 + \bar{R}_2\bar{R}_3 + \bar{X}_2 + \bar{X}_3 + \bar{Y}_2 + \bar{Y}_3 + \bar{V}_2 + \bar{\Gamma}_2$
FeBO3	0.112	15.89	4	3	-3~0	$\bar{Z}_2\bar{Z}_3 + \bar{U}_2 + \bar{T}_3 + \bar{R}_2\bar{R}_3 + \bar{X}_2 + \bar{X}_3 + \bar{Y}_2 + \bar{Y}_3 + \bar{V}_2 + \bar{\Gamma}_2$
Pr3Ru4Al12	0.174	15.89	0	1	-145~140	$\bar{Z}_2\bar{Z}_3 + \bar{U}_2 + \bar{U}_3 + \bar{T}_2 + \bar{T}_3 + \bar{R}_2\bar{R}_3 + \bar{X}_2 + \bar{Y}_2 + \bar{V}_2 + \bar{\Gamma}_2 + \bar{\Gamma}_3$
Fe2O3-alpha	0.65	15.89	0	1	-23~20	$\bar{Z}_2\bar{Z}_3 + \bar{U}_3 + \bar{T}_2 + \bar{R}_2\bar{R}_3 + \bar{X}_2 + \bar{X}_3 + \bar{Y}_2 + \bar{Y}_3 + \bar{V}_2 + \bar{\Gamma}_2$
Yb2O2Se	1.214	15.90	2	1	-103~100	$\bar{A}_2 + \bar{\Gamma}_5\bar{\Gamma}_6 + \bar{L}_2\bar{L}_3 + \bar{M}_2 + \bar{V}_2\bar{V}_3 + \bar{Y}_3\bar{Y}_4$
CoBr2	1.245	15.90	0	1	-11~8	$\bar{A}_2 + \bar{\Gamma}_5\bar{\Gamma}_6 + \bar{L}_2\bar{L}_3 + \bar{M}_2 + \bar{V}_2\bar{V}_3 + \bar{Y}_3\bar{Y}_4$
CoBr2	1.245	15.90	1	1	-7~4	$\bar{A}_2 + \bar{\Gamma}_5\bar{\Gamma}_6 + \bar{L}_2\bar{L}_3 + \bar{M}_2 + \bar{V}_2\bar{V}_3 + \bar{Y}_3\bar{Y}_4$
CoBr2	1.245	15.90	2	1	-7~4	$\bar{A}_2 + \bar{\Gamma}_5\bar{\Gamma}_6 + \bar{L}_2\bar{L}_3 + \bar{M}_2 + \bar{V}_2\bar{V}_3 + \bar{Y}_3\bar{Y}_4$
CoBr2	1.245	15.90	3	1	-27~24	$\bar{A}_2 + \bar{\Gamma}_3\bar{\Gamma}_4 + \bar{L}_2\bar{L}_3 + \bar{M}_2 + \bar{V}_3\bar{V}_3 + \bar{Y}_5\bar{Y}_6$
CoCl2	1.246	15.90	0	1	-33~30	$\bar{A}_2 + \bar{\Gamma}_3\bar{\Gamma}_4 + \bar{L}_2\bar{L}_3 + \bar{M}_2 + \bar{V}_3\bar{V}_3 + \bar{Y}_5\bar{Y}_6$

CoCl2	1.246	15.90	1	1	-11~ -8	$\bar{A}_2 + \bar{\Gamma}_5 \bar{\Gamma}_6 + \bar{L}_2 \bar{L}_3 + \bar{M}_2 + \bar{V}_2 \bar{V}_2 + \bar{Y}_3 \bar{Y}_4$
CoCl2	1.246	15.90	3	1	-7~ -4	$\bar{A}_2 + \bar{\Gamma}_5 \bar{\Gamma}_6 + \bar{L}_2 \bar{L}_3 + \bar{M}_2 + \bar{V}_2 \bar{V}_2 + \bar{Y}_3 \bar{Y}_4$
NiCl2	1.247	15.90	0	1	-35~ -32	$\bar{A}_2 + \bar{\Gamma}_3 \bar{\Gamma}_4 + \bar{L}_2 \bar{L}_3 + \bar{M}_2 + \bar{V}_3 \bar{V}_3 + \bar{Y}_5 \bar{Y}_6$
NiCl2	1.247	15.90	1	1	-35~ -32	$\bar{A}_2 + \bar{\Gamma}_3 \bar{\Gamma}_4 + \bar{L}_2 \bar{L}_3 + \bar{M}_2 + \bar{V}_3 \bar{V}_3 + \bar{Y}_5 \bar{Y}_6$
NiCl2	1.247	15.90	2	1	-7~ -4	$\bar{A}_2 + \bar{\Gamma}_5 \bar{\Gamma}_6 + \bar{L}_2 \bar{L}_3 + \bar{M}_2 + \bar{V}_2 \bar{V}_2 + \bar{Y}_3 \bar{Y}_4$
NiBr2	1.248	15.90	0	1	-35~ -32	$\bar{A}_2 + \bar{\Gamma}_3 \bar{\Gamma}_4 + \bar{L}_2 \bar{L}_3 + \bar{M}_2 + \bar{V}_3 \bar{V}_3 + \bar{Y}_5 \bar{Y}_6$
NiBr2	1.248	15.90	1	2	-7~ -4	$\bar{A}_2 + \bar{\Gamma}_5 \bar{\Gamma}_6 + \bar{L}_2 \bar{L}_3 + \bar{M}_2 + \bar{V}_2 \bar{V}_2 + \bar{Y}_3 \bar{Y}_4$
NiBr2	1.248	15.90	2	1	-7~ -4	$\bar{A}_2 + \bar{\Gamma}_5 \bar{\Gamma}_6 + \bar{L}_2 \bar{L}_3 + \bar{M}_2 + \bar{V}_2 \bar{V}_2 + \bar{Y}_3 \bar{Y}_4$
NiBr2	1.248	15.90	3	1	-7~ -4	$\bar{A}_2 + \bar{\Gamma}_5 \bar{\Gamma}_6 + \bar{L}_2 \bar{L}_3 + \bar{M}_2 + \bar{V}_2 \bar{V}_2 + \bar{Y}_3 \bar{Y}_4$
Ag2NiO2	1.49	15.90	1	1	-87~ -84	$\bar{A}_2 + \bar{\Gamma}_5 \bar{\Gamma}_6 + \bar{L}_2 \bar{L}_3 + \bar{M}_2 + \bar{V}_3 \bar{V}_3 + \bar{Y}_3 \bar{Y}_4$
Ag2NiO2	1.49	15.90	2	1	-29~ -26	$\bar{A}_2 + \bar{\Gamma}_5 \bar{\Gamma}_6 + \bar{L}_2 \bar{L}_3 + \bar{M}_2 + \bar{V}_2 \bar{V}_2 + \bar{Y}_3 \bar{Y}_4$
Sr2CoOsO6	1.72	15.90	0	5	-69~ -66	$\bar{A}_2 + \bar{\Gamma}_3 \bar{\Gamma}_4 + \bar{L}_2 \bar{L}_3 + \bar{M}_2 + \bar{V}_2 \bar{V}_2 + \bar{Y}_5 \bar{Y}_6$
Sr2CoOsO6	1.72	15.90	1	5	-69~ -66	$\bar{A}_2 + \bar{\Gamma}_3 \bar{\Gamma}_4 + \bar{L}_2 \bar{L}_3 + \bar{M}_2 + \bar{V}_2 \bar{V}_2 + \bar{Y}_5 \bar{Y}_6$
Sr2CoOsO6	1.72	15.90	2	4	-97~ -94	$\bar{A}_2 + \bar{\Gamma}_5 \bar{\Gamma}_6 + \bar{L}_2 \bar{L}_3 + \bar{M}_2 + \bar{V}_3 \bar{V}_3 + \bar{Y}_3 \bar{Y}_4$
Sr2CoOsO6	1.72	15.90	3	6	-65~ -62	$\bar{A}_2 + \bar{\Gamma}_3 \bar{\Gamma}_4 + \bar{L}_2 \bar{L}_3 + \bar{M}_2 + \bar{V}_3 \bar{V}_3 + \bar{Y}_5 \bar{Y}_6$
Sr2CoOsO6	1.72	15.90	4	5	-65~ -62	$\bar{A}_2 + \bar{\Gamma}_3 \bar{\Gamma}_4 + \bar{L}_2 \bar{L}_3 + \bar{M}_2 + \bar{V}_2 \bar{V}_2 + \bar{Y}_5 \bar{Y}_6$
VCl2	1.237	159.64	1	2	-115~ -114	$\bar{A}_4 + \bar{A}_5 + \bar{\Gamma}_4 \bar{\Gamma}_5 + \bar{H} A_6 + \bar{K} A_6 + \bar{L}_3 + \bar{L}_4 + \bar{M}_3 \bar{M}_4$
VCl2	1.237	159.64	2	2	-115~ -114	$\bar{A}_4 + \bar{A}_5 + \bar{\Gamma}_4 \bar{\Gamma}_5 + \bar{H} A_6 + \bar{K} A_6 + \bar{L}_3 + \bar{L}_4 + \bar{M}_3 \bar{M}_4$
VCl2	1.237	159.64	3	2	-115~ -114	$\bar{A}_4 + \bar{A}_5 + \bar{\Gamma}_4 \bar{\Gamma}_5 + \bar{H} A_6 + \bar{K} A_6 + \bar{L}_3 + \bar{L}_4 + \bar{M}_3 \bar{M}_4$
VCl2	1.237	159.64	4	2	-115~ -114	$\bar{A}_4 + \bar{A}_5 + \bar{\Gamma}_4 \bar{\Gamma}_5 + \bar{H} A_6 + \bar{K} A_6 + \bar{L}_3 + \bar{L}_4 + \bar{M}_3 \bar{M}_4$
SrRu2O6	1.186	162.78	0	3	-31~ -24	$\bar{A}_4 \bar{A}_6 + \bar{A}_5 \bar{A}_7 + \bar{A}_8 \bar{A}_9 + \bar{\Gamma}_4 \bar{\Gamma}_5 + \bar{\Gamma}_8 + \bar{H}_4 \bar{H}_5 + \bar{H}_6 + \bar{K}_4 \bar{K}_5 + \bar{K}_6 + \bar{L}_3 \bar{L}_5 + \bar{L}_4 \bar{L}_6 + \bar{M}_3 \bar{M}_4 + \bar{M}_5 \bar{M}_6$
SrRu2O6	1.186	162.78	1	3	-31~ -24	$\bar{A}_4 \bar{A}_6 + \bar{A}_5 \bar{A}_7 + \bar{A}_8 \bar{A}_9 + \bar{\Gamma}_4 \bar{\Gamma}_5 + \bar{\Gamma}_8 + \bar{H}_4 \bar{H}_5 + \bar{H}_6 + \bar{K}_4 \bar{K}_5 + \bar{K}_6 + \bar{L}_3 \bar{L}_5 + \bar{L}_4 \bar{L}_6 + \bar{M}_3 \bar{M}_4 + \bar{M}_5 \bar{M}_6$
SrRu2O6	1.186	162.78	2	3	-31~ -24	$\bar{A}_4 \bar{A}_6 + \bar{A}_5 \bar{A}_7 + \bar{A}_8 \bar{A}_9 + \bar{\Gamma}_4 \bar{\Gamma}_5 + \bar{\Gamma}_8 + \bar{H}_4 \bar{H}_5 + \bar{H}_6 + \bar{K}_4 \bar{K}_5 + \bar{K}_6 + \bar{L}_3 \bar{L}_5 + \bar{L}_4 \bar{L}_6 + \bar{M}_3 \bar{M}_4 + \bar{M}_5 \bar{M}_6$
SrRu2O6	1.186	162.78	3	3	-31~ -24	$\bar{A}_4 \bar{A}_6 + \bar{A}_5 \bar{A}_7 + \bar{A}_8 \bar{A}_9 + \bar{\Gamma}_4 \bar{\Gamma}_5 + \bar{\Gamma}_8 + \bar{H}_4 \bar{H}_5 + \bar{H}_6 + \bar{K}_4 \bar{K}_5 + \bar{K}_6 + \bar{L}_3 \bar{L}_5 + \bar{L}_4 \bar{L}_6 + \bar{M}_3 \bar{M}_4 + \bar{M}_5 \bar{M}_6$
SrRu2O6	1.186	162.78	4	3	-31~ -20	$\bar{A}_4 \bar{A}_6 + \bar{A}_5 \bar{A}_7 + \bar{A}_8 \bar{A}_9 + \bar{\Gamma}_4 \bar{\Gamma}_5 + \bar{\Gamma}_8 + \bar{\Gamma}_9 + \bar{H}_4 \bar{H}_5 + \bar{H}_6 + \bar{K}_4 \bar{K}_5 + \bar{K}_6 + \bar{L}_3 \bar{L}_5 + \bar{L}_4 \bar{L}_6 + \bar{M}_3 \bar{M}_4 + \bar{M}_5 \bar{M}_6$
FeBr2	1.242	165.96	0	5	-3~ -2	$\bar{A}_4 + \bar{\Gamma}_4 \bar{\Gamma}_5 + \bar{H}_6 + \bar{K}_6 + \bar{L}_2 + \bar{M}_3 \bar{M}_4$
FeBr2	1.242	165.96	1	5	-3~ -2	$\bar{A}_4 + \bar{\Gamma}_4 \bar{\Gamma}_5 + \bar{H}_6 + \bar{K}_6 + \bar{L}_2 + \bar{M}_3 \bar{M}_4$
FeBr2	1.242	165.96	2	7	-3~ -2	$\bar{A}_4 + \bar{\Gamma}_4 \bar{\Gamma}_5 + \bar{H}_6 + \bar{K}_6 + \bar{L}_2 + \bar{M}_3 \bar{M}_4$
FeBr2	1.242	165.96	3	7	-3~ -2	$\bar{A}_4 + \bar{\Gamma}_4 \bar{\Gamma}_5 + \bar{H}_6 + \bar{K}_6 + \bar{L}_2 + \bar{M}_3 \bar{M}_4$
FeBr2	1.242	165.96	4	7	-11~ -4	$\bar{A}_4 + \bar{A}_6 + \bar{\Gamma}_4 \bar{\Gamma}_5 + \bar{G}_6 \bar{G}_7 + \bar{\Gamma}_9 + \bar{H}_4 \bar{H}_5 + \bar{H}_6 + \bar{K}_4 \bar{K}_5 + \bar{K}_6 + \bar{L}_2 + \bar{M}_3 \bar{M}_4 + \bar{M}_5 \bar{M}_6$
Mn3Ir	0.108	166.101	3	1	-15~ -11	$\bar{F}_2 + \bar{F}_3 + \bar{\Gamma}_4 + \bar{\Gamma}_5 + \bar{\Gamma}_6 + \bar{L}_2 + \bar{L}_3 + \bar{T}_4 + \bar{T}_5 + \bar{T}_6$
Mn3Pt	0.109	166.101	1	1	-6~ -4	$\bar{F}_2 + \bar{F}_3 + \bar{\Gamma}_4 + \bar{\Gamma}_5 + \bar{\Gamma}_6 + \bar{L}_3 + \bar{T}_4 + \bar{T}_8 + \bar{T}_9$
Nd3Sb3Mg2O14	0.167	166.101	0	5	-4~ -3	$\bar{F}_3 + \bar{\Gamma}_8 + \bar{\Gamma}_9 + \bar{L}_3 + \bar{T}_8 + \bar{T}_9$
Nd3Sb3Mg2O14	0.167	166.101	2	4	-1~ 0	$\bar{F}_3 + \bar{\Gamma}_7 + \bar{\Gamma}_8 + \bar{L}_3 + \bar{T}_7 + \bar{T}_8$
TbCo2	0.228	166.101	0	2	-57~ -56	$\bar{F}_2 + \bar{\Gamma}_5 + \bar{\Gamma}_6 + \bar{L}_2 + \bar{T}_5 + \bar{T}_6$
TbCo2	0.228	166.101	2	1	-36~ -35	$\bar{F}_2 + \bar{\Gamma}_5 + \bar{\Gamma}_6 + \bar{L}_2 + \bar{T}_5 + \bar{T}_6$
Tb2Ti2O7	0.77	166.101	6	7	-14~ -10	$\bar{F}_2 + \bar{F}_3 + \bar{\Gamma}_7 + \bar{\Gamma}_8 + \bar{\Gamma}_9 + \bar{L}_2 + \bar{L}_3 + \bar{T}_4 + \bar{T}_5 + \bar{T}_8 + \bar{T}_9$
Gd2Ti2O7	1.56	166.102	0	3	-121~ -118	$\bar{F}_3 \bar{F}_4 + \bar{\Gamma}_9 + \bar{L}_3 \bar{L}_5 + \bar{L}_4 \bar{L}_6 + \bar{T}_8 \bar{T}_9$
Gd2Ti2O7	1.56	166.102	4	1	-197~ -194	$\bar{F}_3 \bar{F}_4 + \bar{\Gamma}_9 + \bar{L}_3 \bar{L}_5 + \bar{L}_4 \bar{L}_6 + \bar{T}_8 \bar{T}_9$
Gd2Ti2O7	1.56	166.102	6	1	-197~ -194	$\bar{F}_3 \bar{F}_4 + \bar{\Gamma}_9 + \bar{L}_3 \bar{L}_5 + \bar{L}_4 \bar{L}_6 + \bar{T}_8 \bar{T}_9$
Mn3Cu0.5Ge0.5N	0.74	166.97	0	2	-12~ -11	$\bar{F}_5 + \bar{F}_6 + \bar{\Gamma}_8 + \bar{L}_5 + \bar{L}_6 + \bar{T}_8$
FeCO3	0.116	167.103	1	1	-13~ -10	$\bar{F}_3 + \bar{F}_4 + \bar{\Gamma}_6 + \bar{\Gamma}_7 + \bar{\Gamma}_9 + \bar{L}_2 + \bar{T}_4 + \bar{T}_5$
FeCO3	0.116	167.103	3	1	-25~ -22	$\bar{F}_5 + \bar{F}_6 + \bar{\Gamma}_4 + \bar{\Gamma}_5 + \bar{\Gamma}_8 + \bar{L}_2 + \bar{T}_4 + \bar{T}_5$
AgFe3(SO4)2(OD)6	1.129	167.108	0	4	-55~ -50	$\bar{F}_3 \bar{F}_4 + \bar{\Gamma}_6 \bar{\Gamma}_7 + \bar{\Gamma}_8 + \bar{\Gamma}_9 + \bar{L}_2 + \bar{T}_4 + \bar{T}_5 + \bar{T}_6$
AgFe3(SO4)2(OD)6	1.129	167.108	1	4	-65~ -62	$\bar{F}_5 \bar{F}_6 + \bar{\Gamma}_4 \bar{\Gamma}_5 + \bar{\Gamma}_8 + \bar{L}_2 + \bar{T}_4 + \bar{T}_5$
AgFe3(SO4)2(OD)6	1.129	167.108	2	2	-143~ -140	$\bar{F}_5 \bar{F}_6 + \bar{\Gamma}_8 + \bar{L}_2 + \bar{T}_5 + \bar{T}_6$
AgFe3(SO4)2(OD)6	1.129	167.108	3	1	-241~ -238	$\bar{F}_5 \bar{F}_6 + \bar{\Gamma}_8 + \bar{L}_2 + \bar{T}_5 + \bar{T}_6$
AgFe3(SO4)2(OD)6	1.129	167.108	4	1	-241~ -238	$\bar{F}_5 \bar{F}_6 + \bar{\Gamma}_8 + \bar{L}_2 + \bar{T}_5 + \bar{T}_6$

Mn3GaC	1.153	167.108	0	1	-29~24	$\bar{F}_5\bar{F}_6 + \bar{\Gamma}_4\bar{\Gamma}_5 + \bar{\Gamma}_8 + \bar{\Gamma}_9 + \bar{L}_2 + \bar{T}_4 + \bar{T}_6$
Mn3GaC	1.153	167.108	1	1	-3~0	$\bar{F}_5\bar{F}_6 + \bar{\Gamma}_4\bar{\Gamma}_5 + \bar{\Gamma}_8 + \bar{L}_2 + \bar{T}_4 + \bar{T}_6$
Mn3GaC	1.153	167.108	2	1	-47~44	$\bar{F}_5\bar{F}_6 + \bar{\Gamma}_4\bar{\Gamma}_5 + \bar{\Gamma}_8 + \bar{L}_2 + \bar{T}_4 + \bar{T}_6$
Mn3GaC	1.153	167.108	3	2	-23~20	$\bar{F}_5\bar{F}_6 + \bar{\Gamma}_4\bar{\Gamma}_5 + \bar{\Gamma}_8 + \bar{L}_2 + \bar{T}_4 + \bar{T}_6$
Mn3GaC	1.153	167.108	4	1	-29~26	$\bar{F}_5\bar{F}_6 + \bar{\Gamma}_4\bar{\Gamma}_5 + \bar{\Gamma}_8 + \bar{L}_2 + \bar{T}_4 + \bar{T}_6$
FeCl2	1.241	167.108	0	2	-9~6	$\bar{F}_3\bar{F}_4 + \bar{\Gamma}_6\bar{\Gamma}_7 + \bar{\Gamma}_9 + \bar{L}_2 + \bar{T}_4 + \bar{T}_6$
FeCl2	1.241	167.108	1	1	-9~6	$\bar{F}_3\bar{F}_4 + \bar{\Gamma}_6\bar{\Gamma}_7 + \bar{\Gamma}_9 + \bar{L}_2 + \bar{T}_4 + \bar{T}_6$
YMnO3	0.44	173.131	4	1	-199~196	$\bar{A}_5\bar{A}_6 + \bar{\Gamma}_5\bar{\Gamma}_6 + \bar{H}_4\bar{H}_4 + \bar{H}A_4\bar{H}A_4 + \bar{K}_4 + \bar{K}A_4 + \bar{L}_2\bar{L}_2 + \bar{M}_2$
HoMnO3	0.32	185.197	6	8	-15~14	$\bar{A}_7 + \bar{\Gamma}_7 + \bar{H}_6 + \bar{K}_6$
HoMnO3	0.33	185.197	4	8	-21~20	$\bar{A}_7 + \bar{\Gamma}_7 + \bar{H}_6 + \bar{K}_6$
YMnO3	0.6	185.197	3	1	-95~92	$\bar{A}_7 + \bar{\Gamma}_7 + \bar{H}_4 + \bar{H}_5 + \bar{H}_6 + \bar{K}_4 + \bar{K}_5 + \bar{K}_6 + \bar{L}_5 + \bar{M}_5$
LuFeO3	0.117	185.201	2	1	-181~178	$\bar{A}_{10}\bar{A}_9 + \bar{A}_{11}\bar{A}_{12} + \bar{\Gamma}_{10} + \bar{\Gamma}_{11} + \bar{\Gamma}_{12} + \bar{\Gamma}_9 + \bar{H}_4\bar{H}_4 + \bar{K}_4 + \bar{L}_3\bar{L}_4 + \bar{M}_3 + \bar{M}_4$
LuFeO3	0.117	185.201	3	1	-181~178	$\bar{A}_{10}\bar{A}_9 + \bar{A}_{11}\bar{A}_{12} + \bar{\Gamma}_{10} + \bar{\Gamma}_{11} + \bar{\Gamma}_{12} + \bar{\Gamma}_9 + \bar{H}_4\bar{H}_4 + \bar{K}_4 + \bar{L}_3\bar{L}_4 + \bar{M}_3 + \bar{M}_4$
LuFeO3	0.117	185.201	4	1	-181~178	$\bar{A}_{10}\bar{A}_9 + \bar{A}_{11}\bar{A}_{12} + \bar{\Gamma}_{10} + \bar{\Gamma}_{11} + \bar{\Gamma}_{12} + \bar{\Gamma}_9 + \bar{H}_4\bar{H}_4 + \bar{K}_4 + \bar{L}_3\bar{L}_4 + \bar{M}_3 + \bar{M}_4$
ScMnO3	0.7	185.201	0	1	-199~196	$\bar{A}_{10}\bar{A}_9 + \bar{A}_{11}\bar{A}_{12} + \bar{\Gamma}_{10} + \bar{\Gamma}_{11} + \bar{\Gamma}_{12} + \bar{\Gamma}_9 + \bar{H}_4\bar{H}_4 + \bar{K}_4 + \bar{L}_3\bar{L}_4 + \bar{M}_3 + \bar{M}_4$
ScMn6Ge6	1.110	192.252	0	3	-167~164	$\bar{A}_{11} + \bar{A}_8 + \bar{\Gamma}_{11} + \bar{\Gamma}_9 + \bar{H}_4\bar{H}_5 + \bar{H}_9 + \bar{K}_7 + \bar{K}_8 + \bar{L}_3 + \bar{L}_4 + \bar{M}_5 + \bar{M}_6$
ScMn6Ge6	1.110	192.252	4	3	-189~186	$\bar{A}_{12} + \bar{A}_8 + \bar{\Gamma}_{11} + \bar{\Gamma}_8 + \bar{H}_4\bar{H}_5 + \bar{H}_6\bar{H}_7 + \bar{K}_7 + \bar{L}_3 + \bar{L}_4 + \bar{M}_5 + \bar{M}_6$
ScMn6Ge6	1.225	192.252	0	6	-31~22	$\bar{A}_{10} + \bar{A}_{11} + \bar{A}_7 + \bar{A}_8 + \bar{\Gamma}_{12} + \bar{\Gamma}_7 + \bar{\Gamma}_8 + \bar{\Gamma}_9 + \bar{H}_4\bar{H}_5 + \bar{H}_6\bar{H}_7 + \bar{H}_8 + \bar{H}_9 + \bar{K}_7 + \bar{K}_8 + \bar{K}_9 + \bar{L}_3 + \bar{L}_4 + \bar{M}_5 + \bar{M}_6$
ScMn6Ge6	1.225	192.252	1	3	-281~278	$\bar{A}_{11} + \bar{A}_9 + \bar{\Gamma}_{12} + \bar{\Gamma}_9 + \bar{H}_4\bar{H}_5 + \bar{H}_6\bar{H}_7 + \bar{K}_7 + \bar{L}_3 + \bar{L}_4 + \bar{M}_5 + \bar{M}_6$
ScMn6Ge6	1.225	192.252	2	4	-163~152	$\bar{A}_{10} + \bar{A}_{11} + \bar{A}_{12} + \bar{A}_7 + \bar{A}_8 + \bar{\Gamma}_{10} + \bar{\Gamma}_{11} + \bar{\Gamma}_7 + \bar{\Gamma}_8 + \bar{\Gamma}_9 + \bar{H}_4\bar{H}_5 + \bar{H}_6\bar{H}_7 + \bar{H}_8 + \bar{H}_9 + \bar{K}_7 + \bar{K}_8 + \bar{K}_9 + \bar{L}_3 + \bar{L}_4 + \bar{M}_5 + \bar{M}_6$
ScMn6Ge6	1.225	192.252	3	2	-281~278	$\bar{A}_{11} + \bar{A}_9 + \bar{\Gamma}_{12} + \bar{\Gamma}_9 + \bar{H}_4\bar{H}_5 + \bar{H}_6\bar{H}_7 + \bar{K}_7 + \bar{L}_3 + \bar{L}_4 + \bar{M}_5 + \bar{M}_6$
ScMn6Ge6	1.225	192.252	4	2	-281~278	$\bar{A}_{11} + \bar{A}_9 + \bar{\Gamma}_{12} + \bar{\Gamma}_9 + \bar{H}_4\bar{H}_5 + \bar{H}_6\bar{H}_7 + \bar{K}_7 + \bar{L}_3 + \bar{L}_4 + \bar{M}_5 + \bar{M}_6$
Ba5Co5ClO13	0.118	194.268	1	28	-13~10	$\bar{A}_5 + \bar{\Gamma}_8 + \bar{\Gamma}_9 + \bar{H}_4\bar{H}_5 + \bar{H}_6 + \bar{K}_4 + \bar{K}_5 + \bar{K}_6 + \bar{L}_2 + \bar{M}_3 + \bar{M}_4 + \bar{M}_5 + \bar{M}_6$
Ba5Co5ClO13	0.118	194.268	2	21	-11~10	$\bar{A}_4 + \bar{\Gamma}_6 + \bar{\Gamma}_7 + \bar{H}_6 + \bar{K}_6 + \bar{L}_2 + \bar{M}_5 + \bar{M}_6$
Ba5Co5ClO13	0.118	194.268	3	29	-3~2	$\bar{A}_4 + \bar{\Gamma}_4 + \bar{\Gamma}_5 + \bar{H}_6 + \bar{K}_6 + \bar{L}_2 + \bar{M}_3 + \bar{M}_4$
Ba5Co5ClO13	0.118	194.268	4	27	-5~4	$\bar{A}_4 + \bar{\Gamma}_6 + \bar{\Gamma}_7 + \bar{H}_6 + \bar{K}_6 + \bar{L}_2 + \bar{M}_5 + \bar{M}_6$
Na3Co(CO3)2Cl	0.70	203.26	1	2	-83~80	$\bar{\Gamma}_8 + \bar{L}_6 + \bar{L}_8 + \bar{L}_9 + \bar{W}_2 + \bar{W}_3 + \bar{W}_4 + \bar{W}_5 + \bar{X}_3 + \bar{X}_4$
Na3Co(CO3)2Cl	0.70	203.26	2	1	-15~8	$\bar{\Gamma}_5 + \bar{\Gamma}_7 + \bar{\Gamma}_9 + \bar{L}_4 + \bar{L}_5 + \bar{L}_6 + \bar{L}_7 + \bar{L}_8 + \bar{L}_9 + \bar{W}_2 + \bar{W}_3 + \bar{W}_4 + \bar{W}_5 + \bar{X}_3 + \bar{X}_4$
Na3Co(CO3)2Cl	0.70	203.26	3	4	-11~8	$\bar{\Gamma}_7 + \bar{\Gamma}_9 + \bar{L}_4 + \bar{L}_5 + \bar{L}_7 + \bar{L}_9 + \bar{W}_2 + \bar{W}_3 + \bar{W}_4 + \bar{W}_5 + \bar{X}_3 + \bar{X}_4$
NiS2	0.150	205.33	0	1	-63~52	$\bar{\Gamma}_{10} + \bar{\Gamma}_5 + \bar{\Gamma}_9 + \bar{M}_3 + \bar{M}_4 + \bar{R}_{10} + \bar{R}_{11} + \bar{R}_4 + \bar{R}_8 + \bar{R}_9 + \bar{X}_3 + \bar{X}_4$
NiS2	0.150	205.33	1	1	-63~52	$\bar{\Gamma}_{10} + \bar{\Gamma}_5 + \bar{\Gamma}_9 + \bar{M}_3 + \bar{M}_4 + \bar{R}_{10} + \bar{R}_{11} + \bar{R}_4 + \bar{R}_8 + \bar{R}_9 + \bar{X}_3 + \bar{X}_4$
Gd2Ti2O7	3.16	216.77	0	6	-115~112	$\bar{\Gamma}_6 + \bar{\Gamma}_7 + \bar{L}_6\bar{L}_6 + \bar{W}_5\bar{W}_6 + \bar{W}_7\bar{W}_8 + \bar{X}_6 + \bar{X}_7$
NdZn	3.8	222.103	2	1	-59~28	$\bar{\Gamma}_{10} + \bar{\Gamma}_{11} + \bar{\Gamma}_6 + \bar{\Gamma}_8 + \bar{\Gamma}_9 + \bar{M}_5 + \bar{R}_5 + \bar{R}_6 + \bar{R}_7 + \bar{X}_5 + \bar{X}_6 + \bar{X}_7 + \bar{X}_8$
USb	3.12	224.113	4	1	-11~0	$\bar{\Gamma}_{10} + \bar{\Gamma}_5 + \bar{\Gamma}_8 + \bar{\Gamma}_9 + \bar{M}_3 + \bar{M}_4 + \bar{R}_{10} + \bar{R}_7 + \bar{R}_8 + \bar{R}_9 + \bar{X}_3 + \bar{X}_4$
Cd2Os2O7	0.2	227.131	1	3	-23~12	$\bar{\Gamma}_{10} + \bar{\Gamma}_5 + \bar{\Gamma}_6 + \bar{\Gamma}_7 + \bar{\Gamma}_8 + \bar{\Gamma}_9 + \bar{L}_4 + \bar{L}_5 + \bar{L}_6 + \bar{W}_2 + \bar{W}_3\bar{W}_5 + \bar{W}_4 + \bar{X}_3 + \bar{X}_4$
Cd2Os2O7	0.2	227.131	2	1	-23~12	$\bar{\Gamma}_{10} + \bar{\Gamma}_5 + \bar{\Gamma}_6 + \bar{\Gamma}_7 + \bar{\Gamma}_8 + \bar{\Gamma}_9 + \bar{L}_4 + \bar{L}_5 + \bar{L}_6 + \bar{W}_2 + \bar{W}_3\bar{W}_5 + \bar{W}_4 + \bar{X}_3 + \bar{X}_4$
NpSe	3.10	228.139	0	2	-35~8	$\bar{\Gamma}_{11} + \bar{\Gamma}_6 + \bar{\Gamma}_8 + \bar{\Gamma}_9 + \bar{L}_4 + \bar{L}_5 + \bar{L}_6 + \bar{W}_3\bar{W}_4 + \bar{W}_5\bar{W}_6 + \bar{W}_7 + \bar{X}_5$
NpSe	3.10	228.139	2	1	-67~52	$\bar{\Gamma}_{10} + \bar{\Gamma}_{11} + \bar{\Gamma}_8 + \bar{\Gamma}_9 + \bar{L}_4 + \bar{L}_5 + \bar{L}_6 + \bar{W}_3\bar{W}_4 + \bar{W}_5\bar{W}_6 + \bar{W}_7 + \bar{X}_5$
NpTe	3.11	228.139	0	1	-115~108	$\bar{\Gamma}_{11} + \bar{L}_4 + \bar{L}_6 + \bar{W}_3\bar{W}_4 + \bar{W}_5\bar{W}_6 + \bar{W}_7 + \bar{X}_5$
NpTe	3.11	228.139	2	1	-31~12	$\bar{\Gamma}_{11} + \bar{\Gamma}_6 + \bar{\Gamma}_8 + \bar{\Gamma}_9 + \bar{L}_4 + \bar{L}_5 + \bar{L}_6 + \bar{W}_3\bar{W}_4 + \bar{W}_5\bar{W}_6 + \bar{W}_7 + \bar{X}_5$
NpTe	3.11	228.139	6	1	-67~60	$\bar{\Gamma}_{11} + \bar{\Gamma}_8 + \bar{\Gamma}_9 + \bar{L}_4 + \bar{L}_5 + \bar{L}_6 + \bar{W}_5\bar{W}_6 + \bar{W}_7 + \bar{X}_5$
NpS	3.9	228.139	0	1	-35~8	$\bar{\Gamma}_{11} + \bar{\Gamma}_6 + \bar{\Gamma}_8 + \bar{\Gamma}_9 + \bar{L}_4 + \bar{L}_5 + \bar{L}_6 + \bar{W}_3\bar{W}_4 + \bar{W}_5\bar{W}_6 + \bar{W}_7 + \bar{X}_5$
Fe2O3-alpha	0.66	2.4	0	1	-53~50	$\bar{\Gamma}_3 + \bar{R}_2 + \bar{T}_2 + \bar{U}_2 + \bar{U}_3 + \bar{V}_2 + \bar{V}_3 + \bar{X}_2 + \bar{Y}_2 + \bar{Y}_3 + \bar{Z}_2 + \bar{Z}_3$
NiS2	1.167	2.7	3	1	-101~98	$\bar{\Gamma}_2\bar{\Gamma}_2 + \bar{R}_2\bar{R}_3 + \bar{T}_2\bar{T}_3 + \bar{U}_2\bar{U}_3 + \bar{V}_3\bar{V}_3 + \bar{X}_2\bar{X}_2 + \bar{Y}_2\bar{Y}_2 + \bar{Z}_2\bar{Z}_3$

NiS2	1.167	2.7	4	1	-109~~-106	$\bar{\Gamma}_2\bar{\Gamma}_2 + \bar{R}_2\bar{R}_3 + \bar{T}_2\bar{T}_3 + \bar{U}_2\bar{U}_3 + \bar{V}_3\bar{V}_3 + \bar{X}_2\bar{X}_2 + \bar{Y}_2\bar{Y}_2 + \bar{Z}_2\bar{Z}_3$
FePSe3	1.210	2.7	1	1	-75~~-72	$\bar{\Gamma}_2\bar{\Gamma}_2 + \bar{R}_2\bar{R}_3 + \bar{T}_2\bar{T}_3 + \bar{U}_2\bar{U}_3 + \bar{V}_3\bar{V}_3 + \bar{X}_3\bar{X}_3 + \bar{Y}_3\bar{Y}_3 + \bar{Z}_2\bar{Z}_3$
CrCl3	1.244	2.7	0	3	-15~~-12	$\bar{\Gamma}_2\bar{\Gamma}_2 + \bar{R}_2\bar{R}_3 + \bar{T}_2\bar{T}_3 + \bar{U}_2\bar{U}_3 + \bar{V}_3\bar{V}_3 + \bar{X}_3\bar{X}_3 + \bar{Y}_3\bar{Y}_3 + \bar{Z}_2\bar{Z}_3$
CrCl3	1.244	2.7	1	2	-87~~-84	$\bar{\Gamma}_2\bar{\Gamma}_2 + \bar{R}_2\bar{R}_3 + \bar{T}_2\bar{T}_3 + \bar{U}_2\bar{U}_3 + \bar{V}_3\bar{V}_3 + \bar{X}_3\bar{X}_3 + \bar{Y}_3\bar{Y}_3 + \bar{Z}_2\bar{Z}_3$
CrCl3	1.244	2.7	2	2	-87~~-84	$\bar{\Gamma}_2\bar{\Gamma}_2 + \bar{R}_2\bar{R}_3 + \bar{T}_2\bar{T}_3 + \bar{U}_2\bar{U}_3 + \bar{V}_3\bar{V}_3 + \bar{X}_3\bar{X}_3 + \bar{Y}_3\bar{Y}_3 + \bar{Z}_2\bar{Z}_3$
CrCl3	1.244	2.7	3	3	-87~~-84	$\bar{\Gamma}_2\bar{\Gamma}_2 + \bar{R}_2\bar{R}_3 + \bar{T}_2\bar{T}_3 + \bar{U}_2\bar{U}_3 + \bar{V}_3\bar{V}_3 + \bar{X}_3\bar{X}_3 + \bar{Y}_3\bar{Y}_3 + \bar{Z}_2\bar{Z}_3$
CrCl3	1.244	2.7	4	4	-43~~-40	$\bar{\Gamma}_3\bar{\Gamma}_3 + \bar{R}_2\bar{R}_3 + \bar{T}_2\bar{T}_3 + \bar{U}_2\bar{U}_3 + \bar{V}_2\bar{V}_2 + \bar{X}_2\bar{X}_2 + \bar{Y}_2\bar{Y}_2 + \bar{Z}_2\bar{Z}_3$
BaNi2V2O8	1.256	2.7	0	2	-39~~-36	$\bar{\Gamma}_2\bar{\Gamma}_2 + \bar{R}_2\bar{R}_3 + \bar{T}_2\bar{T}_3 + \bar{U}_2\bar{U}_3 + \bar{V}_3\bar{V}_3 + \bar{X}_3\bar{X}_3 + \bar{Y}_3\bar{Y}_3 + \bar{Z}_2\bar{Z}_3$
BaNi2V2O8	1.256	2.7	1	4	-39~~-36	$\bar{\Gamma}_2\bar{\Gamma}_2 + \bar{R}_2\bar{R}_3 + \bar{T}_2\bar{T}_3 + \bar{U}_2\bar{U}_3 + \bar{V}_3\bar{V}_3 + \bar{X}_3\bar{X}_3 + \bar{Y}_3\bar{Y}_3 + \bar{Z}_2\bar{Z}_3$
BaNi2V2O8	1.256	2.7	2	5	-63~~-60	$\bar{\Gamma}_2\bar{\Gamma}_2 + \bar{R}_2\bar{R}_3 + \bar{T}_2\bar{T}_3 + \bar{U}_2\bar{U}_3 + \bar{V}_3\bar{V}_3 + \bar{X}_3\bar{X}_3 + \bar{Y}_3\bar{Y}_3 + \bar{Z}_2\bar{Z}_3$
BaNi2V2O8	1.256	2.7	3	2	-63~~-60	$\bar{\Gamma}_2\bar{\Gamma}_2 + \bar{R}_2\bar{R}_3 + \bar{T}_2\bar{T}_3 + \bar{U}_2\bar{U}_3 + \bar{V}_3\bar{V}_3 + \bar{X}_3\bar{X}_3 + \bar{Y}_3\bar{Y}_3 + \bar{Z}_2\bar{Z}_3$
BaNi2V2O8	1.256	2.7	4	2	-15~~-12	$\bar{\Gamma}_2\bar{\Gamma}_2 + \bar{R}_2\bar{R}_3 + \bar{T}_2\bar{T}_3 + \bar{U}_2\bar{U}_3 + \bar{V}_3\bar{V}_3 + \bar{X}_3\bar{X}_3 + \bar{Y}_3\bar{Y}_3 + \bar{Z}_2\bar{Z}_3$
Ho2RhIn8	1.139	49.273	0	1	-97~~-94	$\bar{\Gamma}_5 + \bar{R}_3 + \bar{R}_4 + \bar{S}_6 + \bar{T}_3 + \bar{T}_4 + \bar{U}_3 + \bar{U}_4 + \bar{X}_5 + \bar{Y}_5 + \bar{Z}_3 + \bar{Z}_4$
Er2CoGa8	1.222	51.298	0	1	-109~~-106	$\bar{\Gamma}_6 + \bar{R}_3 + \bar{R}_4 + \bar{S}_3 + \bar{S}_4 + \bar{T}_5 + \bar{U}_3 + \bar{U}_4 + \bar{X}_3 + \bar{X}_4 + \bar{Y}_5 + \bar{Z}_5$
Er2CoGa8	1.222	51.298	2	1	-109~~-106	$\bar{\Gamma}_6 + \bar{R}_3 + \bar{R}_4 + \bar{S}_3 + \bar{S}_4 + \bar{T}_5 + \bar{U}_3 + \bar{U}_4 + \bar{X}_3 + \bar{X}_4 + \bar{Y}_5 + \bar{Z}_5$
PrAg	1.150	53.334	0	1	-7~~-4	$\bar{\Gamma}_6 + \bar{R}_6\bar{R}_7 + \bar{R}_8\bar{R}_9 + \bar{S}_3 + \bar{S}_4 + \bar{T}_3 + \bar{T}_4 + \bar{U}_2\bar{U}_3 + \bar{U}_4\bar{U}_5 + \bar{X}_3 + \bar{X}_4 + \bar{Y}_6 + \bar{Z}_3 + \bar{Z}_4$
YMn3Al4O12	1.158	58.404	3	2	-151~~-148	$\bar{\Gamma}_5 + \bar{R}_3 + \bar{R}_4 + \bar{S}_6 + \bar{T}_6\bar{T}_8 + \bar{T}_7\bar{T}_9 + \bar{U}_6\bar{U}_8 + \bar{U}_7\bar{U}_9 + \bar{X}_3 + \bar{X}_4 + \bar{Y}_3 + \bar{Y}_4 + \bar{Z}_3 + \bar{Z}_4$
YMn3Al4O12	1.158	58.404	4	2	-151~~-148	$\bar{\Gamma}_5 + \bar{R}_3 + \bar{R}_4 + \bar{S}_6 + \bar{T}_6\bar{T}_8 + \bar{T}_7\bar{T}_9 + \bar{U}_6\bar{U}_8 + \bar{U}_7\bar{U}_9 + \bar{X}_3 + \bar{X}_4 + \bar{Y}_3 + \bar{Y}_4 + \bar{Z}_3 + \bar{Z}_4$
Nd3Ru4Al12	0.149	63.462	6	1	-93~~-90	$\bar{C}_2 + \bar{D}_2 + \bar{Y}_5 + \bar{Y}_6 + \bar{B}_5 + \bar{B}_6 + \bar{E}_2 + \bar{A}_5 + \bar{A}_6 + \bar{\Gamma}_3 + \bar{\Gamma}_4 + \bar{Z}_2$
Pr3Ru4Al12	0.173	63.462	2	2	-51~~-48	$\bar{C}_2 + \bar{D}_2 + \bar{Y}_5 + \bar{Y}_6 + \bar{B}_5 + \bar{B}_6 + \bar{E}_2 + \bar{A}_5 + \bar{A}_6 + \bar{\Gamma}_3 + \bar{\Gamma}_4 + \bar{Z}_2$
Pr3Ru4Al12	0.173	63.462	4	1	-143~~-140	$\bar{C}_2 + \bar{D}_2 + \bar{Y}_5 + \bar{Y}_6 + \bar{B}_5 + \bar{B}_6 + \bar{E}_2 + \bar{A}_5 + \bar{A}_6 + \bar{\Gamma}_3 + \bar{\Gamma}_4 + \bar{Z}_2$
Pr3Ru4Al12	0.173	63.462	6	1	-143~~-140	$\bar{C}_2 + \bar{D}_2 + \bar{Y}_5 + \bar{Y}_6 + \bar{B}_5 + \bar{B}_6 + \bar{E}_2 + \bar{A}_5 + \bar{A}_6 + \bar{\Gamma}_3 + \bar{\Gamma}_4 + \bar{Z}_2$
Mn3Ni20P6	1.145	64.480	0	1	-361~~-358	$\bar{\Gamma}_6 + \bar{R}_3\bar{R}_4 + \bar{S}_2 + \bar{T}_3 + \bar{T}_4 + \bar{Y}_5 + \bar{Z}_3 + \bar{Z}_4$
Mn3Ni20P6	1.145	64.480	4	1	-5~~-0	$\bar{\Gamma}_6 + \bar{R}_5\bar{R}_6 + \bar{S}_2 + \bar{T}_3 + \bar{T}_4 + \bar{Y}_5 + \bar{Y}_6 + \bar{Z}_3 + \bar{Z}_4$
CeRh2Si2	1.188	64.480	0	2	-7~~-4	$\bar{\Gamma}_5 + \bar{R}_3\bar{R}_4 + \bar{S}_2 + \bar{T}_3 + \bar{T}_4 + \bar{Y}_6 + \bar{Z}_3 + \bar{Z}_4$
CeRh2Si2	1.188	64.480	2	1	-11~~-8	$\bar{\Gamma}_5 + \bar{R}_5\bar{R}_6 + \bar{S}_2 + \bar{T}_3 + \bar{T}_4 + \bar{Y}_6 + \bar{Z}_3 + \bar{Z}_4$
CeRh2Si2	1.188	64.480	4	1	-11~~-8	$\bar{\Gamma}_5 + \bar{R}_5\bar{R}_6 + \bar{S}_2 + \bar{T}_3 + \bar{T}_4 + \bar{Y}_6 + \bar{Z}_3 + \bar{Z}_4$
CaFe2As2	1.52	64.480	2	1	-43~~-40	$\bar{\Gamma}_6 + \bar{R}_5\bar{R}_6 + \bar{S}_2 + \bar{T}_3 + \bar{T}_4 + \bar{Y}_5 + \bar{Z}_3 + \bar{Z}_4$
CaFe2As2	1.52	64.480	3	1	-43~~-40	$\bar{\Gamma}_6 + \bar{R}_5\bar{R}_6 + \bar{S}_2 + \bar{T}_3 + \bar{T}_4 + \bar{Y}_5 + \bar{Z}_3 + \bar{Z}_4$
CaFe2As2	1.52	64.480	4	1	-43~~-40	$\bar{\Gamma}_6 + \bar{R}_5\bar{R}_6 + \bar{S}_2 + \bar{T}_3 + \bar{T}_4 + \bar{Y}_5 + \bar{Z}_3 + \bar{Z}_4$
Mn3Ni20P6	2.15	65.486	1	1	-831~~-830	$\bar{L}_2 + \bar{V}_3 + \bar{M}_3 + \bar{M}_4 + \bar{A}_5 + \bar{A}_6 + \bar{\Gamma}_5 + \bar{\Gamma}_6 + \bar{Y}_3 + \bar{Y}_4$
Gd2CuO4	1.104	66.500	0	3	-17~~-14	$\bar{\Gamma}_5 + \bar{R}_3\bar{R}_3 + \bar{R}_4\bar{R}_4 + \bar{S}_3\bar{S}_5 + \bar{S}_4\bar{S}_6 + \bar{T}_3 + \bar{T}_4 + \bar{Y}_5 + \bar{Z}_3 + \bar{Z}_4$
Gd2CuO4	1.104	66.500	1	1	-5~~-2	$\bar{\Gamma}_6 + \bar{R}_3\bar{R}_3 + \bar{R}_4\bar{R}_4 + \bar{S}_3\bar{S}_5 + \bar{S}_4\bar{S}_6 + \bar{T}_3 + \bar{T}_4 + \bar{Y}_6 + \bar{Z}_3 + \bar{Z}_4$
NiCr2O4	0.4	70.530	4	1	-59~~-50	$\bar{V}_2 + \bar{V}_3 + \bar{M}_2 + \bar{A}_2 + \bar{Y}_3\bar{Y}_5 + \bar{Y}_4\bar{Y}_6 + \bar{G}_3 + \bar{G}_4 + \bar{G}_5 + \bar{G}_6 + \bar{L}_2 + \bar{L}_3$
NpNiGa5	2.28	74.559	2	1	-67~~-64	$\bar{L}_2 + \bar{L}_3 + \bar{A}_5 + \bar{A}_6 + \bar{M}_3 + \bar{M}_4 + \bar{V}_2\bar{V}_3 + \bar{U}_3\bar{U}_4 + \bar{Y}_5 + \bar{Y}_6 + \bar{G}_5 + \bar{G}_6$
Sr2FeOsO6	1.47	83.50	0	1	-87~~-84	$\bar{A}_{11}\bar{A}_6 + \bar{A}_8\bar{A}_9 + \bar{G}_6\bar{G}_8 + \bar{M}_5\bar{M}_8 + \bar{M}_6\bar{M}_7 + \bar{R}_5\bar{R}_5 + \bar{R}_6\bar{R}_6 + \bar{X}_3\bar{X}_5 + \bar{X}_4\bar{X}_6 + \bar{Z}_{10}\bar{Z}_8 + \bar{Z}_{12}\bar{Z}_6$
Ba2CoO2Ag2Se2	2.24	86.73	0	1	-179~~-172	$\bar{A}_{10}\bar{A}_{11} + \bar{A}_{12}\bar{A}_9 + \bar{G}_{10}\bar{G}_{12} + \bar{G}_5\bar{G}_7 + \bar{M}_3\bar{M}_4 + \bar{R}_2 + \bar{X}_2 + \bar{Z}_3\bar{Z}_4$
Ba2CoO2Ag2Se2	2.24	86.73	1	1	-179~~-172	$\bar{A}_{10}\bar{A}_{11} + \bar{A}_{12}\bar{A}_9 + \bar{G}_{10}\bar{G}_{12} + \bar{G}_5\bar{G}_7 + \bar{M}_3\bar{M}_4 + \bar{R}_2 + \bar{X}_2 + \bar{Z}_3\bar{Z}_4$
Ba2CoO2Ag2Se2	2.24	86.73	3	2	-95~~-88	$\bar{A}_5\bar{A}_8 + \bar{A}_6\bar{A}_7 + \bar{G}_{10}\bar{G}_{12} + \bar{G}_5\bar{G}_7 + \bar{M}_3\bar{M}_4 + \bar{R}_2 + \bar{X}_2 + \bar{Z}_3\bar{Z}_4$
Ba2CoO2Ag2Se2	2.24	86.73	4	1	-111~~-104	$\bar{A}_5\bar{A}_8 + \bar{A}_6\bar{A}_7 + \bar{G}_{11}\bar{G}_9 + \bar{G}_6\bar{G}_8 + \bar{M}_3\bar{M}_4 + \bar{R}_2 + \bar{X}_2 + \bar{Z}_3\bar{Z}_4$

#### Appendix L: Magnetic moments for each materials with different Coulomb interactions

The experimental and calculated magnetic moments on the nonequivalent magnetic atoms of each material have been listed below. As it only consider the moments that contributed by spin component in the VASP, it may have an estimate for those materials that have large orbital magnetic moments. For all of the magnetic materials, we define the average error of the calculated magnetic moments as  $\frac{1}{N} \sum_{i=1}^N \frac{|M_i^{Exp} - M_i^T|}{M_i^{Exp}} \times 100\%$ , where  $N$  is the number of nonequivalent magnetic atoms,  $M^{Exp}$  is the experimental magnetic moments and  $M^T$  is the calculated magnetic moments. We label the magnetic moments that are closest to the experimental value by red color and

Average error	0~10%	10%~30%	30%~50%	>50%	Total
Count	139	117	68	79	403

TABLE XVI. Statistics of the materials with the average error of calculated magnetic moments margin in 0 ~ 10%, 10% ~ 30%, 30% ~ 50% and >50%.

tabulate the number of materials with the error margin in 0 10%, 10% 30%, 30% 50% and >50% in Table XVI.

TABLE XVII: Magnetic moments of the magnetic materials with 3d/4d electrons. The first four column give the chemical formulae (Formula), BCSID, MSG for each materials. The 5th to 11th column give the magnetic moments of each nonequivalent magnetic atom, including the experimental (Exp.) magnetic moments and the calculated magnetic moments with Coulomb interaction  $U = 0, 1, 2, 3, 4$  eV. The calculated magnetic moments closest to the experimental value are tagged by red color.

No.	Formula	BCSID	MSG	Magnetic moments ( $\mu_B$ )							
				Mag.	Ele.	Exp.	U=0	U=1 eV	U=2 eV	U=3 eV	U=4 eV
1	BiCrO <sub>3</sub>	0.139	2.4	Cr	<b>2.62</b>	2.66	2.73	2.79	2.84	2.88	
				Error(%)		<b>1.527</b>	4.198	6.489	8.397	9.924	
2	Cr <sub>2</sub> S <sub>3</sub>	0.5	2.4	Cr	<b>1.2</b>	2.65	2.81	2.9	2.99	3.07	
				Error(%)		<b>120.833</b>	134.167	141.667	149.167	155.833	
3	Fe <sub>2</sub> O <sub>3</sub> -alpha	0.66	2.4	Fe	<b>4.22</b>	3.56	3.8	3.94	4.05	4.13	
				Error(%)		15.64	9.953	6.635	4.028	<b>2.133</b>	
4	CaMnGe <sub>2</sub> O <sub>6</sub>	0.155	2.6	Mn	<b>4.19</b>	4.44	4.49	4.54	4.57	4.61	
				Error(%)		<b>5.967</b>	7.16	8.353	9.069	10.024	
5	MnPSe <sub>3</sub>	0.180	2.6	Mn	<b>4.74</b>	4.19	4.3	4.38	4.45	4.51	
				Error(%)		11.603	9.283	7.595	6.118	<b>4.852</b>	
6	BaNi <sub>2</sub> P <sub>2</sub> O <sub>8</sub>	0.215	2.6	Ni	<b>2.0</b>	1.57	1.63	1.67	1.7	1.73	
				Error(%)		21.5	18.5	16.5	15.0	<b>13.5</b>	
7	NiSb <sub>2</sub> O <sub>6</sub>	1.113	2.7	Ni	<b>1.56</b>	1.53	1.61	1.65	1.69	1.72	
				Error(%)		<b>1.923</b>	3.205	5.769	8.333	10.256	
8	LiFeSO <sub>4</sub> F	1.155	2.7	Fe	<b>3.78</b>	3.61	3.64	3.68	3.71	3.74	
				Error(%)		4.497	3.704	2.646	1.852	<b>1.058</b>	
9	Li <sub>2</sub> Ni(WO <sub>4</sub> ) <sub>2</sub>	1.159	2.7	Ni	<b>1.94</b>	1.56	1.61	1.65	1.68	1.71	
				Error(%)		19.588	17.01	14.948	13.402	<b>11.856</b>	
10	La <sub>2</sub> LiOsO <sub>6</sub>	1.166	2.7	Os	<b>1.8</b>	1.71	1.84	1.96	2.1	2.24	
				Error(%)		5.0	<b>2.222</b>	8.889	16.667	24.444	
11	NiS <sub>2</sub>	1.167	2.7	Ni	<b>1.27</b>	0.02	1.1	1.23	1.32	1.41	
				Ni	<b>0.66</b>	0.02	1.11	1.24	1.33	1.41	
				Ni	<b>1.27</b>	0.02	1.11	1.23	1.33	1.41	
				Error(%)		97.939	<b>31.388</b>	31.393	36.725	45.229	
12	Sr <sub>2</sub> CuWO <sub>6</sub>	1.177	2.7	Cu	<b>0.57</b>	0.52	0.59	0.59	0.6	0.59	
				Error(%)		8.772	<b>3.509</b>	3.509	5.263	3.509	
13	Na <sub>3</sub> Co <sub>2</sub> SbO <sub>6</sub>	1.180	2.7	Co	<b>1.79</b>	2.55	2.58	2.63	2.69	2.73	
				Error(%)		<b>42.458</b>	44.134	46.927	50.279	52.514	
14	TlMnO <sub>3</sub>	1.182	2.7	Mn	<b>3.71</b>	3.52	3.62	3.7	3.77	3.83	
				Error(%)		5.121	2.426	<b>0.27</b>	1.617	3.235	
15	YCr(BO <sub>3</sub> ) <sub>2</sub>	1.190	2.7	Cr	<b>2.47</b>	2.83	2.84	2.88	2.9	2.93	
				Error(%)		<b>14.575</b>	14.98	16.599	17.409	18.623	
16	CrTe <sub>3</sub>	1.193	2.7	Cr	<b>1.98</b>	3.45	-	3.13	3.28	3.42	
				Error(%)		74.242	-	<b>58.081</b>	65.657	72.727	
17	FePSe <sub>3</sub>	1.210	2.7	Fe	<b>4.9</b>	3.31	3.39	3.44	3.51	3.57	
				Error(%)		32.449	30.816	29.796	28.367	<b>27.143</b>	
18	CuF <sub>2</sub>	1.219	2.7	Cu	<b>0.73</b>	0.62	0.65	0.65	0.65	0.65	
				Error(%)		15.068	<b>10.959</b>	10.959	10.959	10.959	
19	BaMoP <sub>2</sub> O <sub>8</sub>	1.229	2.7	Mo	<b>1.12</b>	-	1.72	1.77	1.81	1.85	

				Error(%)	-	<b>53.571</b>	58.036	61.607	65.179
20	FeI2	1.240	2.7	Fe	<b>3.7</b>	3.38	3.43	3.5	3.56
				Error(%)		8.649	7.297	5.405	3.784
21	CrCl3	1.244	2.7	Cr	<b>3.0</b>	2.88	2.9	2.95	3.0
				Error(%)		4.0	3.333	1.667	<b>0.0</b>
22	BaNi2V2O8	1.256	2.7	Ni	<b>1.55</b>	1.43	1.54	1.6	1.65
				Error(%)		7.742	<b>0.645</b>	3.226	6.452
23	BaNi2As2O8	1.257	2.7	Ni	<b>2.0</b>	1.55	1.61	1.65	1.69
				Error(%)		22.5	19.5	17.5	<b>15.5</b>
24	NaMnGe2O6	1.260	2.7	Mn	<b>1.83</b>	3.59	3.65	3.71	3.76
				Error(%)		<b>96.175</b>	99.454	102.732	105.464
25	CuMnO2	1.57	2.7	Mn	<b>3.04</b>	3.55	3.64	3.72	3.79
				Error(%)		<b>16.776</b>	19.737	22.368	24.671
26	Sc2NiMnO6	2.18	2.7	Mn	<b>1.66</b>	-	2.75	2.84	2.93
				Ni	<b>1.49</b>	-	1.5	1.56	1.61
				Error(%)		-	<b>33.167</b>	37.891	42.28
27	YBaFe4O7	1.124	4.10	Fe	<b>2.63</b>	-	3.61	3.72	3.61
				Fe	<b>3.11</b>	-	3.61	3.63	3.92
				Fe	<b>2.58</b>	-	3.34	3.41	3.48
				Fe	<b>2.39</b>	-	3.59	3.7	3.7
				Error(%)		-	<b>33.251</b>	36.287	38.251
28	Lu2MnCoO6	1.32	4.10	Co	<b>2.56</b>	2.36	2.46	2.52	2.58
				Error(%)		7.813	3.906	1.563	<b>0.781</b>
29	Cs2CoCl4	1.51	4.10	Co	<b>1.65</b>	2.42	2.49	2.54	2.6
				Error(%)		<b>46.667</b>	50.909	53.939	57.576
30	BaNiF4	1.64	4.10	Ni	<b>2.0</b>	1.56	1.65	1.7	1.73
				Error(%)		22.0	17.5	15.0	13.5
31	Ca2Cr2O5	1.227	4.12	Cr	<b>1.71</b>	2.71	2.82	2.78	2.89
				Error(%)		<b>58.48</b>	64.912	62.573	69.006
32	SrMn(VO4)(OH)	0.165	4.7	Mn	<b>3.32</b>	3.63	3.87	4.06	4.2
				Error(%)		<b>9.337</b>	16.566	22.289	26.506
33	LiFeP2O7	0.83	4.7	Fe	<b>4.62</b>	4.08	4.15	4.2	4.26
				Error(%)		11.688	10.173	9.091	<b>7.792</b>
34	Cu2MnSnS4	1.100	5.16	Mn	<b>4.28</b>	4.16	4.26	4.35	4.42
				Error(%)		2.804	<b>0.467</b>	1.636	3.271
35	YFe3(BO3)4	1.90	5.16	Fe	<b>3.95</b>	4.01	4.1	4.16	4.22
				Error(%)		<b>1.519</b>	3.797	5.316	6.835
36	Na2MnF5	1.55	7.29	Mn	<b>3.3</b>	3.62	3.66	3.7	3.75
				Error(%)		<b>9.697</b>	10.909	12.121	13.636
37	BiMn2O5	1.75	8.36	Mn	<b>2.14</b>	-	2.66	2.77	2.87
				Mn	<b>2.15</b>	-	2.66	2.77	2.87
				Mn	<b>2.85</b>	-	3.52	3.62	3.7
				Mn	<b>2.82</b>	-	3.54	3.64	3.72
				Mn	<b>2.84</b>	-	3.52	3.62	3.7
				Mn	<b>2.81</b>	-	3.54	3.64	3.72
				Error(%)		-	<b>24.497</b>	28.562	32.0
38	MnTiO3	0.50	9.39	Mn	<b>3.9</b>	4.35	4.43	4.49	4.54
				Error(%)		<b>11.538</b>	13.59	15.128	16.41
39	CuMnSb	1.232	9.40	Mn	<b>3.84</b>	3.72	3.94	4.13	4.27
				Error(%)		3.125	<b>2.604</b>	7.552	11.198
40	La2O2Fe2OSe2	1.58	9.40	Fe	<b>2.83</b>	3.29	3.37	3.45	3.51
				Error(%)		<b>16.254</b>	19.081	21.908	24.028

41	BaFe2Se3	1.120	9.41	Fe	<b>2.8</b>	-	3.06	3.2	3.3	-
				Error(%)	-		<b>9.286</b>	14.286	17.857	-
42	Li2CoSiO4	1.79	9.41	Co	<b>2.92</b>	2.51	2.57	2.62	2.67	2.71
				Error(%)		14.041	11.986	10.274	8.562	<b>7.192</b>
43	RuCl3	1.228	10.49	Ru	<b>0.44</b>	0.66	0.66	0.22	0.58	0.43
				Error(%)		50.0	50.0	50.0	31.818	<b>2.273</b>
44	AgMnVO4	1.116	11.55	Mn	<b>4.0</b>	4.41	4.48	4.53	4.57	4.61
				Error(%)		<b>10.25</b>	12.0	13.25	14.25	15.25
45	Co2C10O8H2	1.134	11.57	Co	<b>2.98</b>	2.6	2.65	2.69	2.73	2.77
				Error(%)		12.752	11.074	9.732	8.389	<b>7.047</b>
46	NiPS3	1.230	11.57	Ni	<b>1.0</b>	1.13	1.27	1.36	1.43	1.49
				Error(%)		<b>13.0</b>	27.0	36.0	43.0	49.0
47	CoPS3	1.264	11.57	Co	<b>3.36</b>	2.24	2.36	2.44	2.51	2.57
				Error(%)		33.333	29.762	27.381	25.298	<b>23.512</b>
48	MnPS3	0.163	12.60	Mn	<b>4.43</b>	4.25	4.34	4.41	4.47	4.25
				Error(%)		4.063	2.032	<b>0.451</b>	0.903	4.063
49	CaMn2Sb2	0.92	12.60	Mn	<b>2.8</b>	3.83	4.04	4.2	4.32	4.41
				Error(%)		<b>36.786</b>	44.286	50.0	54.286	57.5
50	Ag2CrO2	1.0.1	12.60	Cr	<b>2.9</b>	2.59	2.73	2.82	2.88	-
				Error(%)		10.69	5.862	2.759	<b>0.69</b>	-
51	Mn3Ge	0.203	12.62	Mn	<b>1.7</b>	2.78	3.24	3.58	3.82	4.01
				Error(%)		<b>63.529</b>	90.588	110.588	124.706	135.882
52	FeI2	1.0.13	12.62	Fe	<b>1.0</b>	3.39	3.45	3.51	3.57	3.62
				Error(%)		<b>239.0</b>	245.0	251.0	257.0	262.0
53	CoV2O6	1.0.6	12.62	Co	<b>4.4</b>	2.53	2.59	2.65	2.7	2.74
				Error(%)		42.5	41.136	39.773	38.636	<b>37.727</b>
54	LuFe2O4	1.0.7	12.62	Fe	<b>4.5</b>	3.65	3.7	3.77	-	3.9
				Error(%)		18.889	17.778	16.222	-	<b>13.333</b>
55	FeI2	3.14	12.62	Fe	<b>1.0</b>	3.4	3.41	3.5	3.56	-
				Error(%)		<b>240.0</b>	241.0	250.0	256.0	-
56	FePS3	1.183	12.63	Fe	<b>4.52</b>	3.22	3.32	3.4	3.47	3.53
				Error(%)		28.761	26.549	24.779	23.23	<b>21.903</b>
57	Fe4Si2Sn7O16	1.197	12.63	Fe	<b>2.52</b>	3.6	3.63	3.66	3.7	3.73
				Error(%)		<b>42.857</b>	44.048	45.238	46.825	48.016
58	MnBr2	1.239	12.63	Mn	<b>1.0</b>	4.42	4.48	4.52	4.57	4.6
				Error(%)		<b>342.0</b>	348.0	352.0	357.0	360.0
59	Li2MnO3	1.97	12.63	Mn	<b>2.35</b>	2.68	2.74	2.82	2.9	2.99
				Error(%)		<b>14.043</b>	16.596	20.0	23.404	27.234
60	Sr2F2Fe2OS2	2.2	12.64	Fe	<b>3.3</b>	0.1	0.09	0.08	0.07	0.06
				Error(%)		<b>96.97</b>	97.273	97.576	97.879	98.182
61	NiWO4	1.194	13.70	Ni	<b>2.25</b>	1.5	1.56	1.62	1.56	1.7
				Error(%)		33.333	30.667	28.0	30.667	<b>24.444</b>
62	Ca4IrO6	1.114	13.74	Ir	<b>0.42</b>	0.3	0.39	0.44	0.33	0.52
				Error(%)		28.571	7.143	<b>4.762</b>	21.429	23.81
63	NaFeSO4F	1.121	13.74	Fe	<b>3.85</b>	3.59	3.63	3.67	3.7	3.73
				Error(%)		6.753	5.714	4.675	3.896	<b>3.117</b>
64	NaCoSO4F	1.126	13.74	Co	<b>4.06</b>	2.61	2.67	2.71	2.75	2.79
				Error(%)		35.714	34.236	33.251	32.266	<b>31.281</b>
65	Mn2GeO4	0.103	14.75	Mn	<b>3.4</b>	2.95	2.87	2.92	2.98	4.2
				Mn	<b>2.96</b>	2.92	2.86	2.91	2.97	3.06
				Mn	<b>4.47</b>	3.97	4.22	4.33	4.41	4.45
				Error(%)		8.591	8.186	6.313	<b>4.678</b>	9.118

66	Li <sub>2</sub> Mn(SO <sub>4</sub> ) <sub>2</sub>	0.122	14.75	Mn	<b>4.59</b>	4.52	4.56	4.6	4.63	4.65
				Error(%)		1.525	0.654	<b>0.218</b>	0.871	1.307
67	La <sub>2</sub> LiRuO <sub>6</sub>	0.148	14.75	Ru	<b>2.2</b>	1.84	1.92	2.0	2.07	2.15
				Error(%)		16.364	12.727	9.091	5.909	<b>2.273</b>
68	Ca <sub>2</sub> MnReO <sub>6</sub>	0.204	14.75	Mn	<b>4.34</b>	4.16	-	-	4.47	-
				Re	<b>0.22</b>	0.41	-	-	0.7	-
				Error(%)		<b>45.256</b>	-	-	110.589	-
69	LiCrGe <sub>2</sub> O <sub>6</sub>	0.217	14.77	Cr	<b>2.33</b>	2.77	2.8	2.84	2.87	2.9
				Error(%)		<b>18.884</b>	20.172	21.888	23.176	24.464
70	LiFePO <sub>4</sub>	0.152	14.78	Fe	<b>4.09</b>	3.55	3.6	3.64	3.68	3.71
				Error(%)		13.203	11.98	11.002	10.024	<b>9.291</b>
71	LiFeSi <sub>2</sub> O <sub>6</sub>	0.28	14.78	Fe	<b>4.68</b>	4.06	4.12	4.17	4.23	4.28
				Error(%)		13.248	11.966	10.897	9.615	<b>8.547</b>
72	Li <sub>2</sub> Co(SO <sub>4</sub> ) <sub>2</sub>	0.121	14.79	Co	<b>3.33</b>	2.63	2.68	2.72	2.76	2.79
				Error(%)		21.021	19.52	18.318	17.117	<b>16.216</b>
73	Y <sub>2</sub> MnCoO <sub>6</sub>	0.164	14.79	Co	<b>2.92</b>	2.46	2.5	2.56	2.6	2.65
				Error(%)		15.753	14.384	12.329	10.959	<b>9.247</b>
74	CuSb <sub>2</sub> O <sub>6</sub>	1.133	14.80	Cu	<b>0.51</b>	-	0.66	0.7	0.73	0.76
				Error(%)		-	<b>29.412</b>	37.255	43.137	49.02
75	Li <sub>2</sub> Fe(SO <sub>4</sub> ) <sub>2</sub>	1.147	14.80	Fe	<b>3.22</b>	3.6	3.63	3.66	-	3.73
				Error(%)		<b>11.801</b>	12.733	13.665	-	15.839
76	MnV <sub>2</sub> O <sub>6</sub>	1.196	14.80	Mn	<b>3.75</b>	4.08	4.2	4.3	4.38	4.46
				Error(%)		<b>8.8</b>	12.0	14.667	16.8	18.933
77	Sc <sub>2</sub> NiMnO <sub>6</sub>	1.199	14.80	Mn	<b>1.66</b>	2.61	2.74	2.97	3.15	3.18
				Error(%)		<b>57.229</b>	65.06	78.916	89.759	91.566
78	Cr <sub>2</sub> ReO <sub>6</sub>	1.201	14.80	Cr	<b>1.62</b>	0.97	1.87	-	2.63	-
				Re	<b>0.26</b>	0.09	0.23	-	0.47	-
				Error(%)		52.754	<b>13.485</b>	-	71.558	-
79	LiFeGe <sub>2</sub> O <sub>6</sub>	1.39	14.80	Fe	<b>4.27</b>	3.99	4.07	4.13	4.19	4.25
				Error(%)		6.557	4.684	3.279	1.874	<b>0.468</b>
80	CuO	1.62	14.80	Cu	<b>0.65</b>	-	0.49	0.55	0.59	0.63
				Error(%)		-	24.615	15.385	9.231	<b>3.077</b>
81	MnPb <sub>4</sub> Sb <sub>6</sub> S <sub>14</sub>	1.63	14.80	Mn	<b>3.2</b>	-	-	4.39	4.45	4.51
				Error(%)		-	-	<b>37.187</b>	39.063	40.937
82	NiTa <sub>2</sub> O <sub>6</sub>	1.112	14.82	Ni	<b>1.93</b>	1.55	1.61	1.65	-	-
				Error(%)		19.689	16.58	<b>14.508</b>	-	-
83	NaFePO <sub>4</sub>	1.117	14.82	Fe	<b>3.89</b>	3.58	3.62	3.66	3.69	3.72
				Error(%)		7.969	6.941	5.913	5.141	<b>4.37</b>
84	Ni <sub>2</sub> SiO <sub>4</sub>	1.203	14.82	Ni	<b>1.41</b>	1.52	1.59	1.63	1.67	1.7
				Error(%)		<b>7.801</b>	12.766	15.603	18.44	20.567
85	Ni <sub>2</sub> SiO <sub>4</sub>	1.204	14.82	Ni	<b>2.03</b>	1.53	1.6	1.64	1.67	1.71
				Ni	<b>2.08</b>	1.54	1.62	1.67	1.7	1.74
				Error(%)		25.296	21.649	19.462	18.002	<b>16.055</b>
86	CsFe <sub>2</sub> Se <sub>3</sub>	1.26	14.82	Fe	<b>1.77</b>	2.81	3.07	3.25	3.37	3.48
				Error(%)		<b>58.757</b>	73.446	83.616	90.395	96.61
87	NaFeSi <sub>2</sub> O <sub>6</sub>	1.154	14.84	Fe	<b>1.73</b>	4.06	4.12	4.18	4.23	4.28
				Error(%)		<b>134.682</b>	138.15	141.618	144.509	147.399
88	CaCoGe <sub>2</sub> O <sub>6</sub>	1.169	14.84	Co	<b>2.93</b>	2.59	2.63	2.67	2.71	2.76
				Error(%)		11.604	10.239	8.874	7.509	<b>5.802</b>
89	CuSe <sub>2</sub> O <sub>5</sub>	1.2	14.84	Cu	<b>0.52</b>	-	0.58	0.61	0.64	0.67
				Error(%)		-	<b>11.538</b>	17.308	23.077	28.846
90	Ca <sub>3</sub> Co <sub>2</sub> O <sub>6</sub>	1.60	14.84	Co	<b>1.0</b>	0.13	2.73	2.86	2.93	3.01

				Error(%)		<b>87.0</b>	173.0	186.0	193.0	201.0
91	Ba3LaRu2O9	1.94	14.84	Ru	<b>1.43</b>	0.98	1.72	1.8	1.86	1.92
				Error(%)		31.469	<b>20.28</b>	25.874	30.07	34.266
92	NiCO3	0.113	15.85	Ni	<b>1.73</b>	1.54	1.62	1.66	1.7	1.73
				Error(%)		10.983	6.358	4.046	1.734	<b>0.0</b>
93	CoCO3	0.114	15.85	Co	<b>1.73</b>	2.57	2.63	2.68	2.72	2.76
				Error(%)		<b>48.555</b>	52.023	54.913	57.225	59.538
94	MnCO3	0.115	15.85	Mn	<b>1.73</b>	4.49	4.54	4.58	4.61	4.64
				Error(%)		<b>159.538</b>	162.428	164.74	166.474	168.208
95	BiCrO3	0.138	15.85	Cr	<b>2.04</b>	2.66	2.73	2.8	2.84	2.89
				Error(%)		<b>30.392</b>	33.824	37.255	39.216	41.667
96	Sr2CoOsO6	0.210	15.85	Co	<b>1.57</b>	2.61	2.69	2.77	2.92	2.98
				Os	<b>0.7</b>	0.71	1.08	0.17	1.65	0.3
				Error(%)		<b>33.835</b>	62.812	76.074	110.851	73.475
97	Cr2O3	0.110	15.87	Cr	<b>1.0</b>	2.66	2.74	2.8	2.85	2.89
				Error(%)		<b>166.0</b>	174.0	180.0	185.0	189.0
98	Co3TeO6	0.145	15.87	Co	<b>1.03</b>	0.87	0.94	2.65	2.7	2.74
				Co	<b>2.73</b>	0.79	2.54	2.61	2.67	2.72
				Co	<b>2.84</b>	0.71	2.52	2.59	2.65	2.7
				Co	<b>1.1</b>	1.02	0.4	2.62	2.67	2.72
				Co	<b>2.85</b>	2.33	2.44	2.52	2.59	2.65
				Error(%)		<b>37.423</b>	<b>20.998</b>	64.048	64.575	65.122
99	CaMnGe2O6	0.156	15.87	Mn	<b>4.17</b>	4.46	4.51	4.55	4.58	4.62
				Error(%)		<b>6.954</b>	8.153	9.113	9.832	10.791
100	Co4Nb2O9	0.196	15.88	Co	<b>3.5</b>	2.49	2.45	2.62	2.67	2.71
				Co	<b>2.6</b>	2.46	0.84	2.63	2.67	2.73
				Error(%)		17.121	48.846	<b>13.148</b>	13.203	13.786
101	Co4Nb2O9	0.197	15.88	Co	<b>2.32</b>	2.44	2.55	2.63	2.67	2.73
				Co	<b>2.52</b>	2.39	2.54	2.61	2.66	2.71
				Error(%)		<b>5.165</b>	5.354	8.467	10.321	12.606
102	FeBO3	0.112	15.89	Fe	<b>4.7</b>	3.92	4.04	4.12	4.19	4.25
				Error(%)		16.596	14.043	12.34	10.851	<b>9.574</b>
103	FeSO4F	0.128	15.89	Fe	<b>4.32</b>	4.05	4.12	4.18	4.24	4.3
				Error(%)		6.25	4.63	3.241	1.852	<b>0.463</b>
104	Mn3Ti2Te6	0.176	15.89	Mn	<b>4.2</b>	4.2	4.3	4.39	4.46	4.52
				Error(%)		<b>0.0</b>	2.381	4.524	6.19	7.619
105	Ca3LiOsO6	0.3	15.89	Os	<b>2.2</b>	1.69	1.83	1.96	2.09	2.23
				Error(%)		23.182	16.818	10.909	5.0	<b>1.364</b>
106	Fe2O3-alpha	0.65	15.89	Fe	<b>4.12</b>	3.58	3.81	3.95	4.05	4.13
				Error(%)		13.107	7.524	4.126	1.699	<b>0.243</b>
107	Sr2CuTeO6	1.168	15.90	Cu	<b>0.69</b>	-	0.62	0.65	0.69	0.72
				Error(%)		-	10.145	5.797	<b>0.0</b>	4.348
108	CoV2O6-alpha	1.17	15.90	Co	<b>5.08</b>	2.51	2.59	2.65	2.7	2.74
				Error(%)		50.591	49.016	47.835	46.85	<b>46.063</b>
109	FeI2	1.209	15.90	Fe	<b>3.7</b>	3.37	3.43	3.49	3.56	3.61
				Error(%)		8.919	7.297	5.676	3.784	<b>2.432</b>
110	CoBr2	1.245	15.90	Co	<b>2.77</b>	2.42	2.49	2.55	2.6	2.65
				Error(%)		12.635	10.108	7.942	6.137	<b>4.332</b>
111	CoCl2	1.246	15.90	Co	<b>3.0</b>	2.48	2.55	2.59	2.64	2.68
				Error(%)		17.333	15.0	13.667	12.0	<b>10.667</b>
112	NiCl2	1.247	15.90	Ni	<b>2.11</b>	1.43	1.5	1.54	1.59	1.63
				Error(%)		32.227	28.91	27.014	24.645	<b>22.749</b>

113	NiBr2	1.248	15.90	Ni	<b>2.0</b>	1.35	1.42	1.47	1.53	1.58
				Error(%)		32.5	29.0	26.5	23.5	<b>21.0</b>
114	MnO	1.31	15.90	Mn	<b>5.66</b>	4.33	4.41	4.47	4.52	4.57
				Error(%)		23.498	22.085	21.025	20.141	<b>19.258</b>
115	Ag2NiO2	1.49	15.90	Ni	<b>0.66</b>	0.53	0.66	0.9	1.09	1.25
				Ni	<b>0.33</b>	0.54	0.87	0.98	1.08	1.22
				Error(%)		<b>41.666</b>	81.818	116.667	146.212	179.545
116	NiO	1.6	15.90	Ni	<b>2.45</b>	1.34	1.44	1.52	1.58	1.63
				Error(%)		45.306	41.224	37.959	35.51	<b>33.469</b>
117	CoO	1.69	15.90	Co	<b>3.98</b>	2.4	-	2.55	2.63	2.69
				Error(%)		39.698	-	35.93	33.92	<b>32.412</b>
118	CoV2O6	1.70	15.90	Co	<b>3.98</b>	2.53	2.59	2.65	2.7	2.74
				Error(%)		36.432	34.925	33.417	32.161	<b>31.156</b>
119	VOCl	1.37	15.91	V	<b>1.3</b>	1.74	1.8	1.84	1.87	1.89
				Error(%)		<b>33.846</b>	38.462	41.538	43.846	45.385
120	AgNiO2	1.50	18.22	Ni	<b>1.55</b>	1.31	1.42	1.54	1.6	-
				Error(%)		15.484	8.387	<b>0.645</b>	3.226	-
121	FePO4	0.17	19.25	Fe	<b>4.16</b>	3.97	4.06	4.13	4.19	4.25
				Error(%)		4.567	2.404	<b>0.721</b>	0.721	2.163
122	Cu3Mo2O9	0.129	19.27	Cu	<b>0.99</b>	0.37	0.03	0.45	0.45	0.45
				Error(%)		62.626	96.97	<b>54.545</b>	54.545	54.545
123	CoNb2O6	1.224	19.28	Co	<b>3.05</b>	2.55	2.61	2.66	2.71	2.75
				Error(%)		16.393	14.426	12.787	11.148	<b>9.836</b>
124	CsNiCl3	1.0.4	20.34	Ni	<b>0.6</b>	1.42	1.5	1.55	1.59	1.64
				Ni	<b>0.4</b>	1.42	1.5	1.55	1.59	1.64
				Error(%)		<b>195.833</b>	212.5	222.917	231.25	241.667
125	MgV2O4	1.138	20.37	V	<b>0.47</b>	1.6	1.71	1.78	1.84	1.88
				Error(%)		<b>240.426</b>	263.83	278.723	291.489	300.0
126	FeSb2O4	0.97	26.66	Fe	<b>3.68</b>	3.56	3.56	3.61	3.65	3.68
				Error(%)		3.261	3.261	1.902	0.815	<b>0.0</b>
127	Cu3Mo2O9	0.130	26.68	Cu	<b>0.09</b>	-	0.02	0.6	0.65	0.69
				Cu	<b>0.62</b>	-	0.01	0.66	0.68	0.71
				Error(%)		-	<b>88.083</b>	286.559	315.95	340.591
128	Ni3B7O13Cl	0.133	29.101	Ni	<b>1.65</b>	1.6	1.63	1.67	1.71	1.75
				Ni	<b>0.79</b>	1.58	1.63	1.67	1.71	1.74
				Error(%)		<b>51.515</b>	53.771	56.302	60.046	63.157
129	Ni3B7O13Br	0.135	29.101	Ni	<b>3.56</b>	1.54	1.62	1.66	1.7	1.74
				Ni	<b>1.33</b>	1.5	1.61	1.65	1.69	1.73
				Ni	<b>1.4</b>	1.51	1.61	1.66	1.7	1.73
				Error(%)		<b>25.794</b>	30.183	32.0	33.582	34.923
130	MnS2	1.18	29.105	Mn	<b>0.5</b>	0.22	1.44	1.1	2.9	1.54
				Error(%)		<b>56.0</b>	188.0	120.0	480.0	208.0
131	SrCo2V2O8	1.71	29.110	Co	<b>2.25</b>	-	-	2.63	2.68	2.73
				Error(%)		-	-	<b>16.889</b>	19.111	21.333
132	LuMnO3	1.101	31.129	Mn	<b>3.37</b>	3.44	3.55	3.63	3.7	3.76
				Error(%)		<b>2.077</b>	5.341	7.715	9.792	11.573
133	GaFeO3	0.38	33.147	Ga	<b>4.7</b>	0.02	0.02	0.02	0.01	0.01
				Fe	<b>3.9</b>	3.72	3.89	4.0	4.09	4.16
				Fe	<b>4.5</b>	3.73	3.89	4.0	4.09	4.16
				Error(%)		40.433	37.795	<b>37.75</b>	37.923	38.003
134	CaBaCo4O7	0.46	33.147	Co	<b>2.83</b>	-	2.7	2.81	2.9	2.98
				Co	<b>2.04</b>	-	2.32	2.43	2.52	2.6

				Co	<b>2.05</b>	-	2.27	2.38	2.48	2.57
				Co	<b>2.44</b>	-	2.71	2.82	2.91	2.99
				Error(%)		-	<b>10.028</b>	12.873	16.56	20.164
135	GeV4S8	1.86	33.149	V	<b>0.7</b>	0.75	1.11	1.52	1.82	2.0
				V	<b>0.13</b>	0.21	0.22	0.5	0.12	0.12
				Error(%)		<b>34.34</b>	63.901	200.879	83.846	96.703
136	Ca3Ru2O7	1.263	33.154	Ru	<b>1.59</b>	1.37	1.4	1.44	1.51	1.57
				Error(%)		13.836	11.95	9.434	5.031	<b>1.258</b>
137	Ba2CoGe2O7	0.56	35.167	Co	<b>2.9</b>	2.53	2.59	2.64	2.68	2.73
				Error(%)		12.759	10.69	8.966	7.586	<b>5.862</b>
138	Ca3Mn2O7	0.23	36.174	Mn	<b>2.67</b>	2.55	2.64	2.74	2.83	2.93
				Error(%)		4.494	<b>1.124</b>	2.622	5.993	9.738
139	CsCoBr3	1.03	36.174	Co	<b>3.02</b>	2.38	2.47	2.54	2.6	2.65
				Error(%)		21.192	18.212	15.894	13.907	<b>12.252</b>
140	BaCuF4	0.191	36.176	Cu	<b>0.83</b>	-	0.7	0.74	0.77	0.79
				Error(%)		-	15.663	10.843	7.229	<b>4.819</b>
141	BiMn2O5	1.74	36.178	Mn	<b>2.51</b>	2.58	2.67	2.78	2.87	2.98
				Mn	<b>3.22</b>	3.4	3.52	3.62	3.7	3.77
				Error(%)		<b>4.189</b>	7.845	11.589	14.624	17.903
142	NiTa2O6	1.172	41.217	Ni	<b>1.6</b>	1.53	1.6	1.64	1.68	1.72
				Error(%)		4.375	<b>0.0</b>	2.5	5.0	7.5
143	Cu2V2O7	0.137	43.227	Cu	<b>0.93</b>	0.54	0.55	0.55	0.55	0.55
				Error(%)		41.935	<b>40.86</b>	40.86	40.86	40.86
144	SrMn2V2O8	0.62	45.237	Mn	<b>3.99</b>	4.28	4.37	4.44	4.5	4.28
				Error(%)		<b>7.268</b>	9.524	11.278	12.782	7.268
145	La2NiO4	1.42	53.335	Ni	<b>1.6</b>	1.24	1.42	1.5	1.56	1.61
				Error(%)		22.5	11.25	6.25	2.5	<b>0.625</b>
146	Sr2IrO4	1.3	54.352	Ir	<b>0.24</b>	0.0	0.0	0.14	0.09	0.19
				Error(%)		100.0	100.0	41.667	62.5	<b>20.833</b>
147	BaCo2V2O8	1.30	54.352	Co	<b>2.27</b>	-	-	2.63	-	2.73
				Error(%)		-	-	<b>15.859</b>	-	20.264
148	Sr2IrO4	1.77	54.352	Ir	<b>0.21</b>	0.0	0.03	0.14	0.16	0.18
				Error(%)		100.0	85.714	33.333	23.81	<b>14.286</b>
149	La2NiO4	0.45	56.369	Ni	<b>1.68</b>	1.28	1.44	1.51	1.57	1.62
				Error(%)		23.81	14.286	10.119	6.548	<b>3.571</b>
150	Cu3Bi(SeO3)2O2Br	1.122	56.373	Cu	<b>0.92</b>	-	0.62	0.64	0.67	0.7
				Cu	<b>0.9</b>	-	0.62	0.64	0.66	0.69
				Error(%)		-	31.86	29.661	26.92	<b>23.624</b>
151	Cu3Y(SeO3)2O2Cl	1.123	56.373	Cu	<b>0.41</b>	-	0.64	0.66	0.68	0.7
				Cu	<b>1.04</b>	-	0.62	0.64	0.66	0.68
				Error(%)		-	<b>48.241</b>	49.719	51.196	52.674
152	La2CuO4	1.23	56.374	Cu	<b>0.17</b>	-	0.42	0.5	0.56	0.6
				Error(%)		-	<b>147.059</b>	194.118	229.412	252.941
153	Li2VOSiO4	1.9	57.389	V	<b>0.63</b>	0.95	0.97	0.99	1.01	1.03
				Error(%)		<b>50.794</b>	53.968	57.143	60.317	63.492
154	Cr2TeO6	0.143	58.395	Cr	<b>2.45</b>	2.67	2.74	2.8	2.84	2.88
				Error(%)		<b>8.98</b>	11.837	14.286	15.918	17.551
155	Cr2WO6	0.144	58.395	Cr	<b>2.14</b>	2.66	2.75	2.75	2.75	2.75
				Error(%)		<b>24.299</b>	28.505	28.505	28.505	28.505
156	Cr2WO6	0.75	58.395	Cr	<b>1.0</b>	2.66	2.75	2.81	2.75	2.75
				Error(%)		<b>166.0</b>	175.0	181.0	175.0	175.0
157	Cr2TeO6	0.76	58.395	Cr	<b>1.0</b>	2.68	2.74	2.8	2.84	2.88

				Error(%)		168.0	174.0	180.0	184.0	188.0
158	Mn(N(CN2))2	0.131	58.398	Mn	<b>5.01</b>	4.42	4.48	4.52	4.56	4.6
				Error(%)		11.776	10.579	9.78	8.982	<b>8.184</b>
159	NiF2	0.36	58.398	Ni	<b>2.0</b>	1.61	1.69	1.73	1.76	1.78
				Error(%)		19.5	15.5	13.5	12.0	<b>11.0</b>
160	KCo4(PO4)3	0.85	58.398	Co	<b>2.16</b>	2.53	2.59	2.66	2.7	2.74
				Co	<b>3.18</b>	2.64	2.67	2.7	2.73	2.76
				Co	<b>3.14</b>	2.45	2.5	2.57	2.64	2.69
				Error(%)		18.695	18.776	18.798	18.358	<b>18.131</b>
161	LuFe4Ge2	0.140	58.399	Fe	<b>0.45</b>	1.83	2.27	2.54	2.73	2.79
				Error(%)		<b>306.667</b>	404.444	464.444	506.667	520.0
162	YFe4Ge2	0.27	58.399	Fe	<b>0.64</b>	1.94	2.31	2.56	2.75	2.83
				Error(%)		<b>203.125</b>	260.938	300.0	329.687	342.188
163	YMn3Al4O12	1.158	58.404	Mn	<b>2.92</b>	3.65	3.71	3.77	3.82	3.88
				Error(%)		<b>25.0</b>	27.055	29.11	30.822	32.877
164	CuMnAs	0.222	59.407	Mn	<b>3.6</b>	3.54	3.83	4.05	4.21	4.34
				Error(%)		<b>1.667</b>	6.389	12.5	16.944	20.556
165	CaCo2P2	1.252	59.416	Co	<b>0.32</b>	0.49	0.57	0.64	0.71	0.79
				Error(%)		<b>53.125</b>	78.125	100.0	121.875	146.875
166	CoSe2O5	0.119	60.419	Co	<b>3.2</b>	2.57	2.63	2.68	2.72	2.76
				Error(%)		19.688	17.813	16.25	15.0	<b>13.75</b>
167	CoSe2O5	0.161	60.419	Co	<b>3.0</b>	-	-	2.68	-	2.68
				Error(%)		-	-	<b>10.667</b>	-	10.667
168	Mn5Si3	1.88	60.431	Mn	<b>1.89</b>	2.54	3.1	3.48	3.72	3.91
				Error(%)		<b>34.392</b>	64.021	84.127	96.825	106.878
169	Mn2O3-alpha	0.40	61.433	Mn	<b>3.05</b>	3.42	3.55	3.64	3.72	3.78
				Mn	<b>3.47</b>	3.52	3.62	3.7	3.77	3.83
				Mn	<b>3.49</b>	3.52	3.61	3.69	3.76	3.82
				Mn	<b>3.27</b>	3.48	3.59	3.67	3.75	3.82
				Mn	<b>4.19</b>	3.48	3.58	3.66	3.74	3.8
				Error(%)		<b>7.559</b>	9.701	11.317	12.753	13.979
170	Mn2O3-alpha	0.41	61.433	Mn	<b>2.69</b>	-	3.54	3.63	3.71	3.77
				Mn	<b>3.1</b>	-	3.63	3.71	3.77	3.83
				Mn	<b>3.01</b>	-	3.61	3.69	3.76	3.82
				Mn	<b>2.92</b>	-	3.59	3.67	3.75	3.82
				Mn	<b>3.54</b>	-	3.58	3.67	3.74	3.8
				Error(%)		-	<b>18.541</b>	21.313	23.705	25.755
171	Li2Ni(SO4)2	0.71	61.437	Ni	<b>2.15</b>	-	-	1.38	1.46	1.53
				Error(%)		-	-	35.814	32.093	<b>28.837</b>
172	EuFe2As2	2.1	61.439	Eu	<b>6.8</b>	6.73	6.77	6.9	6.9	6.9
				Fe	<b>0.98</b>	0.0	2.38	2.69	2.88	3.01
				Error(%)		<b>50.515</b>	71.65	87.98	97.674	104.306
173	Mn2GeO4	0.102	62.441	Mn	<b>4.09</b>	4.44	4.5	4.54	4.58	4.61
				Mn	<b>4.9</b>	4.45	4.5	4.55	4.59	4.62
				Error(%)		<b>8.871</b>	9.094	9.072	9.153	9.214
174	NH4Fe2O6	0.168	62.441	Fe	<b>4.13</b>	3.99	4.1	4.19	4.28	4.34
				Fe	<b>3.12</b>	3.77	3.77	3.75	3.73	3.74
				Error(%)		12.112	<b>10.78</b>	10.822	11.592	12.478
175	RbFe2F6	0.192	62.441	Fe	<b>3.99</b>	3.79	3.79	3.77	3.73	3.75
				Fe	<b>4.29</b>	3.99	4.1	4.19	4.28	4.34
				Error(%)		6.003	4.72	3.923	<b>3.375</b>	3.591
176	Co2SiO4	0.218	62.441	Co	<b>3.88</b>	2.44	2.6	2.65	2.7	2.74

				Co	<b>3.64</b>	2.53	2.63	2.68	2.72	2.76
				Error(%)		33.804	30.369	29.038	27.843	<b>26.779</b>
177	Co2SiO4	0.219	62.441	Co	<b>3.87</b>	2.44	2.57	2.65	2.7	2.73
				Co	<b>3.35</b>	2.53	2.58	2.65	2.72	2.76
				Error(%)		30.714	28.289	26.21	24.519	<b>23.535</b>
178	Fe2SiO4	0.221	62.441	Fe	<b>4.44</b>	3.49	3.58	3.62	3.67	3.7
				Fe	<b>4.4</b>	3.57	3.59	3.63	3.67	3.7
				Error(%)		20.13	18.89	17.984	16.966	<b>16.288</b>
179	Rb2Fe2O(AsO4)2	0.90	62.441	Fe	<b>3.64</b>	3.89	4.0	4.09	4.16	4.22
				Fe	<b>3.19</b>	3.75	3.97	4.06	4.15	4.21
				Error(%)		<b>12.211</b>	17.171	19.817	22.19	23.954
180	CoSO4	0.96	62.441	Co	<b>3.22</b>	2.61	2.67	2.71	2.75	2.78
				Error(%)		18.944	17.081	15.839	14.596	<b>13.665</b>
181	KCrF4	0.182	62.443	Cr	<b>2.11</b>	2.78	-	-	-	-
				Cr	<b>1.91</b>	2.78	-	-	-	-
				Cr	<b>2.19</b>	2.77	-	-	-	-
				Error(%)		<b>34.596</b>	-	-	-	-
182	LiNiPO4	0.88	62.444	Ni	<b>2.22</b>	1.56	1.64	1.68	1.71	1.74
				Error(%)		29.73	26.126	24.324	22.973	<b>21.622</b>
183	LiCoPO4	0.193	62.445	Co	<b>1.0</b>	2.54	2.62	2.67	2.71	2.75
				Error(%)		<b>154.0</b>	162.0	167.0	171.0	175.0
184	SrEr2O4	0.216	62.445	Er	<b>4.5</b>	2.74	-	2.81	-	2.85
				Error(%)		39.111	-	37.556	-	<b>36.667</b>
185	KMn4(PO4)3	0.86	62.445	Mn	<b>4.43</b>	4.5	4.55	4.58	4.62	4.5
				Mn	<b>4.21</b>	4.46	4.51	4.55	4.59	4.46
				Mn	<b>4.57</b>	4.49	4.53	4.57	4.6	4.49
				Error(%)		<b>3.09</b>	3.57	3.821	4.658	3.09
186	NaFePO4	0.87	62.445	Fe	<b>4.55</b>	3.56	3.61	3.65	3.68	3.72
				Error(%)		21.758	20.659	19.78	19.121	<b>18.242</b>
187	LiFePO4	0.95	62.445	Fe	<b>4.19</b>	3.55	3.6	3.64	3.68	3.71
				Error(%)		15.274	14.081	13.126	12.172	<b>11.456</b>
188	Mn2GeO4	0.101	62.446	Mn	<b>3.03</b>	4.45	4.5	4.54	4.58	4.61
				Mn	<b>4.5</b>	4.44	4.5	4.55	4.59	4.62
				Error(%)		<b>24.099</b>	24.257	25.473	26.578	27.406
				Mn	<b>3.85</b>	4.44	4.5	4.54	4.58	4.62
189	Mn2SiO4	0.220	62.446	Mn	<b>4.68</b>	4.46	4.51	4.56	4.6	4.63
				Error(%)		<b>10.012</b>	10.258	10.243	10.336	10.534
				Mn	<b>3.87</b>	3.55	3.63	3.71	3.77	3.83
190	LaMnO3	0.1	62.448	Error(%)		8.269	6.202	4.134	2.584	<b>1.034</b>
				Os	<b>1.0</b>	0.97	1.37	1.65	1.88	2.08
191	NaOsO3	0.25	62.448	Error(%)		<b>3.0</b>	37.0	65.0	88.0	108.0
				Fe	<b>3.1</b>	3.88	4.01	4.09	4.16	4.22
192	Rb2Fe2O(AsO4)2	0.91	62.448	Fe	<b>3.09</b>	3.74	3.94	4.06	4.14	4.21
				Error(%)		<b>23.099</b>	28.431	31.664	34.087	36.188
				Mn	<b>3.9</b>	4.5	4.54	4.58	4.61	4.64
193	LiMnPO4	0.24	62.449	Error(%)		<b>15.385</b>	16.41	17.436	18.205	18.974
				Cr	<b>0.4</b>	0.01	1.76	0.01	0.6	0.05
194	Cr2As	1.130	62.450	Cr	<b>1.34</b>	2.1	2.63	0.25	0.57	1.05
				Error(%)		77.108	218.134	89.422	<b>53.731</b>	54.571
				Fe	<b>0.95</b>	1.27	2.09	2.48	2.72	2.89
195	Fe2As	1.131	62.450	Fe	<b>1.52</b>	2.34	2.61	2.82	3.04	3.07
				Error(%)		<b>43.816</b>	95.855	123.289	143.158	153.092

196	Mn2As	1.132	62.450	Mn	<b>3.7</b>	2.03	2.59	3.35	3.53	3.68
				Mn	<b>3.5</b>	3.52	3.8	4.04	4.2	4.32
				Error(%)		22.854	19.286	12.444	12.297	<b>11.984</b>
197	CrN	1.28	62.450	Cr	<b>2.4</b>	2.46	2.65	2.76	2.83	2.89
				Error(%)		<b>2.5</b>	10.417	15.0	17.917	20.417
198	Mn3O4	1.1	62.452	Mn	<b>3.49</b>	3.56	3.7	3.85	3.83	3.9
				Error(%)		<b>2.006</b>	6.017	10.315	9.742	11.748
199	Sr2Mn3Sb2O2	2.27	63.459	Mn	<b>4.2</b>	3.96	4.26	4.37	4.44	4.5
				Mn	<b>3.5</b>	3.7	3.97	4.15	4.28	4.37
				Error(%)		<b>5.714</b>	7.428	11.31	14.0	16.0
200	Mn3Sn	0.199	63.463	Mn	<b>3.0</b>	3.34	3.48	3.74	3.92	4.07
				Error(%)		<b>11.333</b>	16.0	24.667	30.667	35.667
201	Mn3Sn	0.200	63.464	Mn	<b>3.0</b>	3.16	3.51	3.77	3.97	4.13
				Error(%)		<b>5.333</b>	17.0	25.667	32.333	37.667
202	CaIrO3	0.79	63.464	Ir	<b>1.0</b>	0.23	0.43	0.52	0.55	-
				Error(%)		77.0	57.0	48.0	<b>45.0</b>	-
203	Gd2CuO4	0.82	64.476	Cu	<b>1.02</b>	-	0.25	0.42	0.48	0.53
				Error(%)		-	75.49	58.824	52.941	<b>48.039</b>
204	Mn3Ni20P6	1.145	64.480	Mn	<b>2.4</b>	3.71	3.93	4.11	4.25	4.36
				Error(%)		<b>54.583</b>	63.75	71.25	77.083	81.667
205	BaFe2As2	1.16	64.480	Fe	<b>0.87</b>	2.02	2.55	2.8	2.97	3.09
				Error(%)		<b>132.184</b>	193.103	221.839	241.379	255.172
206	K2NiF4	1.249	64.480	Ni	<b>1.0</b>	1.55	1.65	1.69	1.73	1.76
				Error(%)		<b>55.0</b>	65.0	69.0	73.0	76.0
207	CaFe2As2	1.52	64.480	Fe	<b>0.8</b>	1.83	2.35	2.67	2.86	3.0
				Error(%)		<b>128.75</b>	193.75	233.75	257.5	275.0
208	Mn3Ni20P6	2.15	65.486	Mn	<b>2.2</b>	-	-	-	-	4.36
				Mn	<b>2.7</b>	-	-	-	-	4.47
				Error(%)		-	-	-	-	<b>81.869</b>
209	Gd2CuO4	1.104	66.500	Cu	<b>1.41</b>	-	0.04	0.39	0.48	0.53
				Error(%)		-	97.163	72.34	65.957	<b>62.411</b>
210	SrFeO2	1.65	69.526	Fe	<b>3.1</b>	3.35	3.43	3.51	3.56	3.61
				Error(%)		<b>8.065</b>	10.645	13.226	14.839	16.452
211	NiCr2O4	0.4	70.530	Ni	<b>1.64</b>	0.66	0.43	1.54	1.62	1.67
				Cr	<b>1.4</b>	2.6	2.75	2.84	2.89	2.93
				Error(%)		72.735	85.104	54.478	<b>53.824</b>	55.558
212	LaFeAsO	1.125	73.553	Fe	<b>0.63</b>	1.91	2.46	2.74	2.93	3.07
				Error(%)		<b>203.175</b>	290.476	334.921	365.079	387.302
213	YbCo2Si2	1.176	73.553	Yb	<b>1.41</b>	0.0	0.0	0.0	3.65	-
				Error(%)		<b>100.0</b>	100.0	100.0	158.865	-
214	Sr2FeOsO6	1.47	83.50	Fe	<b>1.83</b>	3.82	3.96	4.05	4.13	4.2
				Os	<b>0.48</b>	1.36	1.64	1.83	1.99	2.15
				Error(%)		<b>146.039</b>	179.03	201.281	220.134	238.712
215	Mn3CuN	2.5	85.59	Mn	<b>2.86</b>	2.81	3.2	3.48	3.68	3.9
				Mn	<b>0.65</b>	3.13	3.43	3.63	3.78	3.95
				Error(%)		<b>191.643</b>	219.79	240.07	255.105	272.028
216	Sr2CoO2Ag2Se2	2.23	86.73	Co	<b>3.77</b>	2.21	2.45	2.52	2.58	2.63
				Error(%)		41.379	35.013	33.156	31.565	<b>30.239</b>
217	Ba2CoO2Ag2Se2	2.24	86.73	Co	<b>3.97</b>	2.38	2.47	2.54	2.61	2.66
				Error(%)		40.05	37.783	36.02	34.257	<b>32.997</b>
218	MnV2O4	0.64	88.81	Mn	<b>4.2</b>	4.2	4.33	4.42	4.49	4.55
				V	<b>1.3</b>	1.66	1.73	1.78	1.82	1.86

				Error(%)		13.846	18.086	21.081	23.452	25.705
219	FeTa2O6	2.22	88.86	Fe	<b>3.69</b>	3.55	3.58	3.62	3.66	3.69
				Error(%)		3.794	2.981	1.897	0.813	<b>0.0</b>
220	Ba(TiO)Cu4(PO4)4	1.235	94.132	Cu	<b>0.8</b>	-	0.65	0.68	0.7	0.72
				Error(%)		-	18.75	15.0	12.5	<b>10.0</b>
221	ZnV2O4	1.24	96.150	V	<b>0.65</b>	1.57	1.66	1.81	1.86	1.89
				Error(%)		<b>141.538</b>	155.385	178.462	186.154	190.769
222	MgCr2O4	3.4	111.255	Cr	<b>0.69</b>	0.01	2.88	2.98	3.07	3.17
				Error(%)		<b>98.551</b>	317.391	331.884	344.928	359.42
223	alpha-Mn	1.85	114.282	Mn	<b>2.83</b>	0.01	3.52	3.81	4.0	-
				Mn	<b>1.83</b>	0.05	0.34	0.11	0.22	-
				Mn	<b>0.74</b>	0.84	0.11	0.05	0.21	-
				Mn	<b>0.48</b>	0.26	0.13	0.07	0.08	-
				Mn	<b>0.59</b>	0.24	1.18	0.2	0.08	-
				Mn	<b>0.66</b>	0.18	0.25	0.17	0.11	-
				Error(%)		<b>64.718</b>	70.997	74.604	75.675	-
224	GeCu2O4	1.185	122.338	Cu	<b>0.89</b>	-	0.62	0.65	0.68	0.7
				Error(%)		-	30.337	26.966	23.596	<b>21.348</b>
225	CaMnBi2	0.72	129.416	Mn	<b>3.73</b>	3.87	4.08	4.23	4.35	4.45
				Error(%)		<b>3.753</b>	9.383	13.405	16.622	19.303
226	Mn3Pt	1.143	132.456	Mn	<b>3.4</b>	3.04	3.56	3.98	4.18	4.31
				Error(%)		10.588	<b>4.706</b>	17.059	22.941	26.765
227	MnF2	0.15	136.499	Mn	<b>4.6</b>	4.54	4.58	4.61	4.64	4.67
				Error(%)		1.304	0.435	<b>0.217</b>	0.87	1.522
228	CoF2	0.178	136.499	Co	<b>2.6</b>	2.64	2.69	2.73	2.77	2.8
				Error(%)		<b>1.538</b>	3.462	5.0	6.538	7.692
229	Fe2TeO6	0.142	136.503	Fe	<b>4.19</b>	3.8	3.97	4.08	4.15	4.22
				Error(%)		9.308	5.251	2.625	0.955	<b>0.716</b>
230	LaCrAsO	1.146	138.528	Cr	<b>1.57</b>	2.63	3.05	3.35	3.56	3.71
				Error(%)		<b>67.516</b>	94.268	113.376	126.752	136.306
231	BaMn2As2	0.18	139.536	Mn	<b>3.88</b>	3.68	3.93	4.11	4.24	4.35
				Error(%)		5.155	<b>1.289</b>	5.928	9.278	12.113
232	Sr2Mn3As2O2	0.212	139.536	Mn	<b>3.4</b>	3.56	3.83	4.04	4.21	4.31
				Error(%)		<b>4.706</b>	12.647	18.824	23.824	26.765
233	SrMnBi2	0.73	139.536	Mn	<b>3.75</b>	3.98	4.16	4.29	4.4	4.48
				Error(%)		<b>6.133</b>	10.933	14.4	17.333	19.467
234	BaMn2Bi2	0.89	139.536	Mn	<b>3.83</b>	3.97	4.15	4.29	4.39	4.48
				Error(%)		<b>3.655</b>	8.355	12.01	14.621	16.971
235	Mn3ZnC	2.19	139.537	Mn	<b>2.73</b>	2.58	3.0	3.28	3.5	3.67
				Mn	<b>1.6</b>	2.48	3.08	3.43	3.63	3.78
				Error(%)		<b>30.247</b>	51.195	67.261	77.54	85.341
236	KNiF3	1.250	140.550	Ni	<b>2.22</b>	1.52	1.64	1.69	1.73	1.76
				Error(%)		31.532	26.126	23.874	22.072	<b>20.721</b>
237	CoAl2O4	0.58	141.556	Co	<b>1.9</b>	2.53	2.59	2.64	2.69	2.73
				Error(%)		<b>33.158</b>	36.316	38.947	41.579	43.684
238	Ca2MnO4	0.211	142.568	Mn	<b>2.4</b>	2.54	2.63	2.72	2.82	2.91
				Error(%)		<b>5.833</b>	9.583	13.333	17.5	21.25
239	LaMn3Cr4O12	1.156	146.12	Mn	<b>3.39</b>	3.64	3.7	3.76	3.82	3.87
				Cr	<b>2.89</b>	2.57	2.67	2.75	2.81	2.85
				Error(%)		9.223	8.378	7.879	<b>7.726</b>	7.772
240	Ni3TeO6	1.165	146.12	Ni	<b>2.03</b>	1.48	1.57	1.62	1.66	1.7
				Error(%)		27.094	22.66	20.197	18.227	<b>16.256</b>

241	NiN <sub>2</sub> O <sub>6</sub>	0.78	148.17	Ni	<b>1.34</b>	1.56	1.62	1.66	1.7	1.73
				Ni	<b>1.33</b>	1.56	1.62	1.66	1.7	1.73
				Error(%)		<b>16.856</b>	21.35	24.346	27.343	29.59
242	MnGeO <sub>3</sub>	0.125	148.19	Mn	<b>4.6</b>	3.55	3.78	3.98	4.13	4.27
				Error(%)		22.826	17.826	13.478	10.217	<b>7.174</b>
243	MnTiO <sub>3</sub>	0.19	148.19	Mn	<b>4.55</b>	4.36	4.43	4.5	4.55	4.59
				Error(%)		4.176	2.637	1.099	<b>0.0</b>	0.879
244	Ba <sub>3</sub> MnNb <sub>2</sub> O <sub>9</sub>	1.0.8	157.53	Mn	<b>4.91</b>	4.34	4.41	4.47	4.52	4.56
				Error(%)		11.609	10.183	8.961	7.943	<b>7.128</b>
245	Ba <sub>3</sub> Nb <sub>2</sub> NiO <sub>9</sub>	1.13	159.64	Ni	<b>1.47</b>	1.58	1.62	1.66	1.7	1.73
				Error(%)		<b>7.483</b>	10.204	12.925	15.646	17.687
246	VCl <sub>2</sub>	1.237	159.64	V	<b>0.93</b>	2.51	2.58	2.63	2.67	2.51
				Error(%)		<b>169.892</b>	177.419	182.796	187.097	169.892
247	VBr <sub>2</sub>	1.238	159.64	V	<b>2.48</b>	2.53	2.59	2.64	2.68	2.53
				Error(%)		<b>2.016</b>	4.435	6.452	8.065	2.016
248	PbNiO <sub>3</sub>	0.21	161.69	Ni	<b>1.69</b>	-	1.53	1.59	-	1.68
				Error(%)		-	9.467	5.917	-	<b>0.592</b>
249	CuMnSb	1.233	161.72	Mn	<b>2.94</b>	3.76	3.97	4.13	4.26	4.24
				Error(%)		<b>27.891</b>	35.034	40.476	44.898	44.218
250	CuMnSb	1.265	161.72	Mn	<b>3.9</b>	3.75	3.96	4.13	4.26	4.36
				Error(%)		3.846	<b>1.538</b>	5.897	9.231	11.795
251	SrRu <sub>2</sub> O <sub>6</sub>	1.186	162.78	Ru	<b>1.3</b>	1.43	1.69	1.85	1.98	2.09
				Error(%)		<b>10.0</b>	30.0	42.308	52.308	60.769
252	Co <sub>4</sub> Nb <sub>2</sub> O <sub>9</sub>	0.111	165.94	Co	<b>3.0</b>	2.41	2.56	2.62	2.67	2.72
				Error(%)		19.667	14.667	12.667	11.0	<b>9.333</b>
253	Sr <sub>3</sub> NiIrO <sub>6</sub>	1.0.10	165.95	Ir	<b>0.5</b>	0.15	0.05	0.14	0.2	0.26
				Ir	<b>0.25</b>	0.14	0.05	0.14	0.2	0.26
				Ni	<b>1.5</b>	1.4	1.5	1.57	1.63	1.68
				Ni	<b>0.75</b>	1.4	1.5	1.57	1.63	1.68
				Error(%)		51.834	67.5	57.5	51.5	<b>47.0</b>
254	Sr <sub>3</sub> CoIrO <sub>6</sub>	1.0.5	165.95	Co	<b>3.6</b>	2.53	2.57	2.61	2.65	2.7
				Co	<b>1.8</b>	2.53	2.57	2.61	2.66	2.7
				Ir	<b>0.6</b>	0.38	0.17	0.01	0.1	0.18
				Ir	<b>0.3</b>	0.38	0.17	0.01	0.1	0.18
				Error(%)		<b>33.404</b>	46.597	66.875	56.041	46.25
255	FeBr <sub>2</sub>	1.242	165.96	Fe	<b>3.9</b>	3.48	3.52	3.57	3.61	3.65
				Error(%)		10.769	9.744	8.462	7.436	<b>6.41</b>
256	Mn <sub>3</sub> Ir	0.108	166.101	Mn	<b>2.45</b>	2.87	3.34	3.69	3.94	4.13
				Error(%)		<b>17.143</b>	36.327	50.612	60.816	68.571
257	Mn <sub>3</sub> Pt	0.109	166.101	Mn	<b>2.94</b>	3.07	3.49	3.77	3.99	4.18
				Error(%)		<b>4.422</b>	18.707	28.231	35.714	42.177
258	Mn <sub>3</sub> GaN	0.177	166.97	Mn	<b>1.17</b>	2.57	3.01	3.3	3.51	3.72
				Error(%)		<b>119.658</b>	157.265	182.051	200.0	217.949
259	FeCO <sub>3</sub>	0.116	167.103	Fe	<b>1.0</b>	3.57	3.61	3.65	3.68	3.72
				Error(%)		<b>257.0</b>	261.0	265.0	268.0	272.0
260	Cr <sub>2</sub> O <sub>3</sub>	0.59	167.106	Cr	<b>2.48</b>	2.67	2.75	2.81	2.86	2.9
				Error(%)		<b>7.661</b>	10.887	13.306	15.323	16.935
261	Mn <sub>3</sub> GaC	1.153	167.108	Mn	<b>1.82</b>	1.78	2.78	3.24	3.46	3.64
				Error(%)		<b>2.198</b>	52.747	78.022	90.11	100.0
262	FeCl <sub>2</sub>	1.241	167.108	Fe	<b>4.5</b>	3.52	3.56	3.6	3.59	3.67
				Error(%)		21.778	20.889	20.0	20.222	<b>18.444</b>
263	ScMnO <sub>3</sub>	0.8	173.129	Mn	<b>3.54</b>	3.4	3.49	3.58	3.66	3.73

				Error(%)		3.955	1.412	<b>1.13</b>	3.39	5.367
264	YMnO <sub>3</sub>	0.44	173.131	Mn	<b>3.14</b>	3.51	3.59	3.67	3.74	3.8
				Error(%)		<b>11.783</b>	14.331	16.879	19.108	21.019
265	YMnO <sub>3</sub>	0.6	185.197	Mn	<b>2.91</b>	3.47	3.56	3.64	3.72	3.78
				Error(%)		<b>19.244</b>	22.337	25.086	27.835	29.897
266	LuFeO <sub>3</sub>	0.117	185.201	Fe	<b>2.9</b>	3.58	3.85	3.97	4.06	4.14
				Error(%)		<b>23.448</b>	32.759	36.897	40.0	42.759
267	ScMnO <sub>3</sub>	0.7	185.201	Mn	<b>3.03</b>	3.4	3.49	3.58	3.66	3.73
				Error(%)		<b>12.211</b>	15.182	18.152	20.792	23.102
268	CsFeCl <sub>3</sub>	1.0.14	189.223	Fe	<b>3.16</b>	3.5	3.5	3.58	3.63	3.66
				Error(%)		<b>10.759</b>	10.759	13.291	14.873	15.823
269	ScMn <sub>6</sub> Ge <sub>6</sub>	1.110	192.252	Mn	<b>1.96</b>	2.08	2.41	2.76	3.5	3.82
				Error(%)		<b>6.122</b>	22.959	40.816	78.571	94.898
270	ScMn <sub>6</sub> Ge <sub>6</sub>	1.225	192.252	Mn	<b>2.08</b>	2.04	2.39	2.73	3.48	3.83
				Error(%)		<b>1.923</b>	14.904	31.25	67.308	84.135
271	CsCoCl <sub>3</sub>	1.0.9	193.259	Co	<b>2.8</b>	2.43	2.53	2.58	2.63	2.68
				Co	<b>2.66</b>	2.43	2.54	2.58	2.63	2.68
				Error(%)		10.93	7.077	5.433	3.6	<b>2.519</b>
272	Ba <sub>5</sub> Co <sub>5</sub> ClO <sub>13</sub>	0.118	194.268	Co	<b>0.61</b>	0.64	0.53	0.42	0.31	0.27
				Co	<b>2.21</b>	2.48	2.62	2.71	2.82	2.88
				Co	<b>0.35</b>	0.39	0.36	0.44	0.46	0.97
				Error(%)		<b>9.521</b>	11.508	26.495	36.07	87.733
273	Na <sub>3</sub> Co(CO <sub>3</sub> ) <sub>2</sub> Cl	0.70	203.26	Co	<b>1.73</b>	2.6	2.65	2.7	2.74	2.77
				Error(%)		<b>50.289</b>	53.179	56.069	58.382	60.116
274	NiS <sub>2</sub>	0.150	205.33	Ni	<b>0.99</b>	0.59	1.09	1.24	1.37	1.45
				Error(%)		40.404	<b>10.101</b>	25.253	38.384	46.465
275	MnTe <sub>2</sub>	0.20	205.33	Mn	<b>4.28</b>	4.06	4.22	4.33	4.41	4.48
				Error(%)		5.14	1.402	<b>1.168</b>	3.037	4.673
276	Cd <sub>2</sub> Os <sub>2</sub> O <sub>7</sub>	0.2	227.131	Os	<b>1.04</b>	0.73	1.31	1.66	1.92	2.14
				Error(%)		29.808	<b>25.962</b>	59.615	84.615	105.769

TABLE XVIII: Magnetic moments of the magnetic materials with *4f/5f* electron. The first four column give the chemical formulae (Formula), BCSID, MSG for each materials. The 5th to 10th column give the magnetic moments of each nonequivalent magnetic atom, including the experimental (Exp.) magnetic moments and the calculated magnetic moments with Coulomb interaction  $U = 0, 2, 4, 6$  eV for *4f/5f* electron. If the materials have transition metal elements at the same time, we take the Coulomb interactions of *3d/4d* electron as 2 eV. The calculated magnetic moments closest to the experimental value are labeled by red color.

No.	Formula	BCSID	MSG	Magnetic moments ( $\mu_B$ )					
				Mag. Ele.	Exp.	U=0	U=2 eV	U=4 eV	U=6 eV
277	HoCr(BO <sub>3</sub> ) <sub>2</sub>	1.191	2.7	Cr	<b>3.07</b>	2.84	-	2.82	-
				Error(%)		<b>7.492</b>	-	8.143	-
278	Dy <sub>2</sub> Fe <sub>2</sub> Si <sub>2</sub> C	1.206	2.7	Dy	<b>12.11</b>	4.81	4.87	4.99	5.14
				Error(%)		60.281	59.785	58.794	<b>57.556</b>
279	Tm <sub>2</sub> BaNiO <sub>5</sub>	1.218	2.7	Tm	<b>3.33</b>	1.45	1.73	1.8	1.83
				Ni	<b>1.15</b>	0.01	1.37	1.41	1.71
				Error(%)		77.793	<b>33.589</b>	34.277	46.871
280	Nd <sub>2</sub> NaOsO <sub>6</sub>	1.38	2.7	Nd	<b>1.61</b>	-	-	2.94	-
				Os	<b>0.9</b>	-	-	1.79	-
				Error(%)		-	-	<b>90.748</b>	-
281	U <sub>3</sub> Al <sub>2</sub> Si <sub>3</sub>	0.37	5.15	U	<b>0.16</b>	0.1	1.69	0.56	1.61
				U	<b>1.29</b>	1.81	1.94	1.52	2.53
				Error(%)		<b>38.905</b>	503.319	133.915	501.187

282	GdBiPt	1.111	9.40	Gd	<b>6.61</b>	6.87	6.98	7.03	7.06
				Error(%)		<b>3.933</b>	5.598	6.354	6.808
283	ErVO3	0.104	11.54	V	<b>1.19</b>	0.05	0.01	0.59	0.5
				Error(%)		95.798	99.16	<b>50.42</b>	57.983
284	DyVO3	0.106	11.54	Dy	<b>7.76</b>	-	4.79	4.91	4.99
				V	<b>1.45</b>	-	1.81	1.77	0.42
				Error(%)		-	31.551	<b>29.397</b>	53.365
285	Tb2Fe2Si2C	1.171	12.63	Tb	<b>8.0</b>	5.88	5.97	6.01	-
				Error(%)		26.5	25.375	<b>24.875</b>	-
286	DyCu2Si2	1.22	12.63	Dy	<b>8.3</b>	4.31	4.56	4.85	4.94
				Error(%)		48.072	45.06	41.566	<b>40.482</b>
287	CeMnAsO	0.188	13.67	Ce	<b>0.76</b>	0.64	0.3	0.36	-
				Mn	<b>3.32</b>	3.47	4.0	4.28	-
				Error(%)		<b>10.154</b>	40.504	40.774	-
288	PrMgPb	1.140	13.73	Pr	<b>1.8</b>	2.15	2.0	2.26	2.28
				Error(%)		19.444	<b>11.111</b>	25.556	26.667
289	NdMgPb	1.141	13.73	Pr	<b>3.38</b>	2.13	2.01	1.86	1.82
				Error(%)		<b>36.982</b>	40.533	44.97	46.154
290	Ho2O2Se	1.213	13.73	Ho	<b>9.3</b>	3.68	3.79	3.87	3.93
				Error(%)		60.43	59.247	58.387	<b>57.742</b>
291	ErVO3	0.105	14.75	Er	<b>8.2</b>	2.47	2.78	2.82	2.87
				V	<b>1.47</b>	0.15	1.7	0.18	0.3
				Error(%)		79.837	<b>40.872</b>	76.683	72.296
292	Nd2NaRuO6	0.39	14.75	Nd	<b>2.25</b>	2.93	2.92	2.93	2.94
				Ru	<b>1.62</b>	1.57	0.76	2.04	2.04
				Error(%)		<b>16.654</b>	41.432	28.074	28.296
293	TbOOH	2.21	14.78	Tb	<b>8.02</b>	5.79	5.88	5.94	-
				Error(%)		27.805	26.683	<b>25.935</b>	-
294	SrHo2O4	2.8	14.78	Ho	<b>6.08</b>	3.75	-	3.9	3.97
				Ho	<b>7.74</b>	3.54	-	3.89	3.96
				Error(%)		46.293	-	42.799	<b>41.771</b>
295	BaNd2O4	1.95	14.80	Nd	<b>2.64</b>	-	-	-	2.94
				Error(%)		-	-	-	<b>11.364</b>
296	LiErF4	1.35	14.84	Er	<b>2.2</b>	2.8	2.83	2.9	2.92
				Error(%)		<b>27.273</b>	28.636	31.818	32.727
297	Pr3Ru4Al12	0.174	15.89	Pr	<b>3.2</b>	1.96	2.06	2.18	1.71
				Pr	<b>1.39</b>	1.95	2.04	2.04	1.01
				Error(%)		39.519	41.194	39.318	<b>36.95</b>
298	NdCo2	0.226	15.89	Nd	<b>2.8</b>	3.5	0.44	0.97	3.17
				Co	<b>0.74</b>	1.3	0.4	1.3	1.32
				Error(%)		50.338	65.116	70.517	<b>45.796</b>
299	HoP	2.10	15.89	Ho	<b>8.8</b>	3.5	3.61	3.77	3.88
				Error(%)		60.227	58.977	57.159	<b>55.909</b>
300	Ho2BaNiO5	1.14	15.90	Ho	<b>9.06</b>	3.65	3.85	3.92	3.99
				Ni	<b>1.39</b>	0.05	1.42	1.43	1.43
				Error(%)		78.058	29.832	29.805	<b>29.419</b>
301	Er2BaNiO5	1.15	15.90	Ho	<b>7.89</b>	3.65	3.82	3.92	3.99
				Ni	<b>1.54</b>	0.06	0.18	1.43	1.43
				Error(%)		74.921	69.948	28.729	<b>28.286</b>
302	Dy2O2S	1.211	15.90	Dy	<b>7.2</b>	4.85	4.85	4.89	-
				Error(%)		32.639	32.639	<b>32.083</b>	-
303	Dy2O2Se	1.212	15.90	Dy	<b>9.0</b>	4.84	4.85	4.89	4.96

				Error(%)		46.222	46.111	45.667	44.889
304	Nd2BaNiO5	1.216	15.90	Nd	<b>2.65</b>	2.91	2.92	2.96	2.96
				Ni	<b>1.58</b>	0.14	0.23	1.55	1.55
				Error(%)		50.476	47.816	6.798	6.798
305	Tb2BaNiO5	1.217	15.90	Ni	<b>2.02</b>	-	0.17	0.31	0.04
				Tb	<b>8.03</b>	-	6.01	6.05	6.15
				Error(%)		-	58.37	<b>54.656</b>	60.716
306	Dy2BaNiO5	1.36	15.90	Dy	<b>7.7</b>	4.63	4.84	4.91	5.01
				Ni	<b>1.35</b>	0.15	1.55	0.04	0.04
				Error(%)		64.379	<b>25.978</b>	66.636	65.987
307	Er2BaNiO5	1.53	15.90	Er	<b>7.24</b>	2.66	2.82	2.84	-
				Ni	<b>1.39</b>	1.27	1.43	0.02	-
				Error(%)		35.947	<b>31.964</b>	79.668	-
308	HoMnO3	1.20	31.129	Mn	<b>3.87</b>	0.0	-	-	-
				Error(%)		<b>100.0</b>	-	-	-
309	ErAuGe	1.33	33.154	Er	<b>8.8</b>	2.52	2.69	2.71	2.88
				Error(%)		71.364	69.432	69.205	<b>67.273</b>
310	PrNiO3	1.43	36.178	Ni	<b>0.93</b>	-	0.89	0.79	0.9
				Error(%)		-	4.301	15.054	<b>3.226</b>
311	TmAgGe	0.26	38.191	Tm	<b>6.44</b>	1.49	1.6	1.55	1.51
				Error(%)		76.863	<b>75.155</b>	75.932	76.553
312	TbMg	2.12	49.270	Tb	<b>7.34</b>	5.9	5.86	6.06	6.18
				Error(%)		19.619	20.163	17.439	<b>15.804</b>
313	Ho2RhIn8	1.139	49.273	Ho	<b>6.9</b>	3.61	3.66	3.76	3.94
				Error(%)		47.681	46.957	45.507	<b>42.899</b>
314	TbMg	2.11	51.295	Tb	<b>7.34</b>	5.92	6.06	6.16	6.18
				Error(%)		19.346	17.439	16.076	<b>15.804</b>
315	Er2CoGa8	1.222	51.298	Er	<b>4.71</b>	2.46	2.69	2.81	2.91
				Error(%)		47.771	42.887	40.34	<b>38.217</b>
316	PrAg	1.150	53.334	Pr	<b>2.12</b>	2.11	2.13	2.1	2.36
				Error(%)		<b>0.472</b>	0.472	0.943	11.321
317	DyB4	0.22	55.355	Dy	<b>9.8</b>	4.72	4.81	4.86	4.98
				Error(%)		51.837	50.918	50.408	<b>49.184</b>
318	Gd2CuO4	1.105	56.374	Cu	<b>1.22</b>	-	0.45	0.56	-
				Error(%)		-	63.115	<b>54.098</b>	-
319	CeRu2Al10	1.8	57.391	Ce	<b>0.34</b>	-	0.02	0.17	0.22
				Error(%)		-	94.118	50.0	<b>35.294</b>
320	CeMnAsO	0.187	59.407	Ce	<b>0.7</b>	-	0.77	0.44	0.05
				Mn	<b>3.3</b>	-	4.01	4.03	4.03
				Error(%)		-	<b>15.758</b>	29.632	57.49
321	EuZrO3	0.146	62.444	Eu	<b>7.3</b>	6.73	6.82	6.88	6.92
				Error(%)		7.808	6.575	5.753	<b>5.205</b>
322	Nd5Ge4	0.185	62.447	Nd	<b>1.85</b>	3.24	3.15	-	3.14
				Nd	<b>3.17</b>	3.15	3.05	-	3.03
				Nd	<b>2.75</b>	3.21	3.08	-	3.03
				Error(%)		30.831	28.685	-	<b>28.109</b>
323	EuZrO3	0.147	62.449	Eu	<b>6.4</b>	6.75	6.82	6.88	6.92
				Error(%)		<b>5.469</b>	6.562	7.5	8.125
324	DyCoO3	0.159	62.449	Dy	<b>9.08</b>	4.83	4.86	4.93	5.0
				Error(%)		46.806	46.476	45.705	<b>44.934</b>
325	DyScO3	0.171	62.449	Dy	<b>9.47</b>	4.8	4.86	4.92	5.0

				Error(%)		49.314	48.68	48.046	47.202
326	NdCoAsO	1.179	62.450	Nd	<b>1.39</b>	3.04	2.93	2.95	2.95
				Co	<b>0.32</b>	0.48	0.56	0.57	0.56
				Error(%)		<b>84.353</b>	92.896	95.177	93.615
327	U3Ru4Al12	0.12	63.461	U	<b>2.5</b>	1.49	-	1.63	1.43
				Error(%)		40.4	-	<b>34.8</b>	42.8
				Nd	<b>0.95</b>	0.07	0.23	0.07	-
328	Nd3Ru4Al12	0.149	63.462	Nd	<b>2.66</b>	3.21	3.11	3.07	-
				Error(%)		56.654	<b>46.354</b>	54.023	-
				Pr	<b>3.1</b>	1.85	2.04	2.04	2.03
329	Pr3Ru4Al12	0.173	63.462	Pr	<b>1.4</b>	0.07	0.1	2.04	1.03
				Error(%)		67.661	63.526	39.954	<b>30.472</b>
				Ho	<b>7.5</b>	3.41	3.55	-	-
330	Ho2RhIn8	3.3	63.464	Error(%)		54.533	<b>52.667</b>	-	-
				U	<b>1.41</b>	1.44	1.74	1.69	1.3
				Error(%)		<b>2.128</b>	23.404	19.858	7.801
331	U2Ni2Sn	1.200	63.466	Np	<b>0.89</b>	2.86	3.39	3.59	3.73
				Error(%)		<b>221.348</b>	280.899	303.371	319.101
				Er	<b>7.71</b>	-	2.7	2.78	2.91
332	NpRhGa5	1.262	63.466	Error(%)		-	64.981	63.943	<b>62.257</b>
				Ce	<b>0.28</b>	0.57	-	-	-
				Error(%)		<b>103.571</b>	-	-	-
333	CeRh2Si2	1.188	64.480	Ce	<b>1.5</b>	0.22	0.87	0.94	0.15
				Error(%)		85.333	42.0	<b>37.333</b>	90.0
				Tb	<b>9.45</b>	5.81	5.92	5.99	-
334	TbGe2	0.141	65.483	Tb	<b>7.55</b>	5.69	5.73	5.98	-
				Error(%)		31.577	30.73	<b>28.704</b>	-
				Tm	<b>2.35</b>	1.23	1.4	1.48	1.78
335	Tm2CoGa8	1.223	65.489	Error(%)		47.66	40.426	37.021	<b>24.255</b>
				Pr	<b>0.08</b>	-	1.85	0.16	1.95
				Cu	<b>0.4</b>	-	0.04	0.02	0.37
336	Pr2CuO4	1.106	66.500	Error(%)		-	1151.25	<b>97.5</b>	1172.5
				Ce	<b>1.39</b>	0.66	0.89	0.02	0.03
				Error(%)		52.518	<b>35.971</b>	98.561	97.842
337	CeMgPb	1.142	67.510	Eu	<b>6.93</b>	-	-	6.87	-
				Error(%)		-	-	<b>0.866</b>	-
				U	<b>0.9</b>	0.36	2.32	2.51	2.65
338	UAu2Si2	1.0.12	71.536	Error(%)		<b>60.0</b>	157.778	178.889	194.444
				Np	<b>0.84</b>	0.18	3.45	3.59	3.74
				Error(%)		<b>78.571</b>	310.714	327.381	345.238
339	KTb3F12	1.59	84.58	Tb	<b>6.95</b>	6.23	6.41	6.63	-
				Error(%)		10.36	7.77	<b>4.604</b>	-
				Ho	<b>9.06</b>	3.75	3.84	3.88	3.94
340	Ho2Ge2O7	0.107	92.111	Error(%)		58.609	57.616	57.174	<b>56.512</b>
				Nd	<b>2.39</b>	3.32	3.31	3.25	-
				Nd	<b>2.47</b>	3.22	3.17	3.12	-
341	Nd5Si4	0.184	92.114	Nd	<b>2.79</b>	3.29	3.21	3.16	-
				Error(%)		29.066	27.296	<b>25.187</b>	-
				Ce	<b>0.36</b>	0.07	0.46	0.06	-
342	CeCoGe3	1.0.11	107.231	Error(%)		80.556	<b>27.778</b>	83.333	-
				Pr	<b>3.08</b>	1.76	1.76	1.97	1.96
				Co	<b>0.9</b>	0.73	0.88	0.86	0.87
343	PrCo2P2	2.26	123.345						

				Error(%)		30.873	22.54	20.241	19.849
348	NdMg	1.162	124.360	Nd	<b>2.6</b>	3.42	3.49	3.26	3.13
				Error(%)		31.538	34.231	25.385	20.385
349	NdCo2P2	1.251	124.360	Nd	<b>0.74</b>	0.71	2.99	2.96	0.38
				Co	<b>0.64</b>	0.75	0.91	0.01	0.87
				Error(%)		10.621	173.121	199.219	42.293
350	UPtGa5	1.255	124.360	U	<b>0.32</b>	0.94	1.67	2.35	1.57
				Error(%)		193.75	421.875	634.375	390.625
				Np	<b>0.32</b>	0.05	3.39	0.35	2.79
351	NpRhGa5	1.261	124.360	Error(%)		84.375	959.375	9.375	771.875
				Mn	<b>4.61</b>	4.41	4.42	4.43	4.45
352	CeMn2Ge4O12	0.189	125.367	Error(%)		4.338	4.121	3.905	3.471
				Nd	<b>2.56</b>	3.41	3.28	3.2	3.16
353	NdMg	2.14	125.373	Error(%)		33.203	28.125	25.0	23.438
				Co	<b>0.94</b>	0.78	0.96	0.95	0.93
354	CeCo2P2	1.253	126.386	Error(%)		17.021	2.128	1.064	1.064
				U	<b>1.4</b>	1.53	1.55	2.39	2.54
				Error(%)		9.286	10.714	70.714	81.429
355	U2Pd2In	0.80	127.394	U	<b>1.9</b>	1.59	1.5	2.44	2.57
				Error(%)		16.316	21.053	28.421	35.263
				Gd	<b>7.14</b>	6.84	6.93	6.99	7.04
356	GdB4	0.9	127.395	Error(%)		4.202	2.941	2.101	1.401
				Gd	<b>1.0</b>	0.36	0.09	1.32	1.13
				Error(%)		64.0	91.0	32.0	13.0
357	GdIn3	1.81	127.397	U	<b>0.59</b>	1.43	1.5	1.67	2.56
				Ni	<b>0.37</b>	0.01	0.01	0.01	0.0
				Error(%)		119.835	125.768	140.174	216.949
358	U2Ni2In	1.102	128.408	U	<b>1.7</b>	1.58	1.64	1.77	1.4
				Error(%)		7.059	3.529	4.118	17.647
359	UP	1.160	128.410	Tb	<b>8.5</b>	6.07	5.93	6.0	6.04
				Error(%)		28.588	30.235	29.412	28.941
360	TbRh2Si2	1.187	128.410	U	<b>1.9</b>	1.79	1.85	2.09	2.29
				Error(%)		5.789	2.632	10.0	20.526
361	UAs	1.208	128.410	Dy	<b>9.5</b>	4.83	4.87	4.9	4.95
				Error(%)		49.158	48.737	48.421	47.895
362	DyCo2Si2	1.21	128.410	Mn	<b>2.78</b>	-	3.98	3.99	3.99
				Error(%)		-	43.165	43.525	43.525
363	CeMnAsO	0.186	129.416	U	<b>1.67</b>	1.54	1.78	1.72	1.55
				Error(%)		7.784	6.587	2.994	7.186
364	UPt2Si2	0.194	129.419	U	<b>1.0</b>	1.05	1.26	1.4	1.46
				Error(%)		5.0	26.0	40.0	46.0
365	UP2	1.215	130.432	Ce	<b>0.38</b>	0.44	0.88	0.08	0.13
				Error(%)		15.789	131.579	78.947	65.789
366	CeSbTe	1.271	130.432	U	<b>1.91</b>	1.62	1.91	2.19	2.34
				Error(%)		15.183	0.0	14.66	22.513
367	UAs	2.20	134.481	U	<b>2.26</b>	1.74	2.07	2.26	2.43
				Error(%)		23.009	8.407	0.0	7.522
368	Nd2CuO4	2.6	134.481	Cu	<b>1.0</b>	-	0.3	0.36	0.27
				Error(%)		-	70.0	64.0	73.0
369	U2Rh2Sn	1.103	135.492	U	<b>0.53</b>	1.17	1.42	1.58	1.53
				Error(%)		120.755	167.925	198.113	188.679
370	U2Rh2Sn	1.207	135.492	U	<b>0.5</b>	1.1	1.4	1.57	1.57

				Rh	<b>0.06</b>	0.0	0.01	0.01	0.01
				Error(%)		<b>110.0</b>	131.667	148.667	148.667
373	UNiGa5	1.254	140.550	U	<b>0.75</b>	0.0	2.17	2.31	2.58
				Error(%)		<b>100.0</b>	189.333	208.0	244.0
374	Nd2RhIn8	1.82	140.550	Nd	<b>2.53</b>	3.5	3.3	3.14	3.03
				Error(%)		38.34	30.435	24.111	<b>19.763</b>
375	TbCo2Ga8	1.87	140.550	Tb	<b>9.6</b>	5.54	5.85	5.98	6.05
				Error(%)		42.292	39.063	37.708	<b>36.979</b>
376	Er2Ru2O7	0.154	141.554	Er	<b>4.5</b>	2.55	2.79	2.84	2.87
				Ru	<b>2.0</b>	0.13	1.22	1.24	0.02
				Error(%)		68.417	38.5	<b>37.444</b>	67.611
377	Er2Ti2O7	0.29	141.554	Er	<b>3.25</b>	2.74	2.8	2.84	2.91
				Error(%)		15.692	13.846	12.615	<b>10.462</b>
378	Gd2Sn2O7	0.47	141.555	Gd	<b>6.08</b>	6.83	6.89	6.95	7.0
				Error(%)		<b>12.336</b>	13.322	14.309	15.132
379	NpCo2	0.126	141.556	Np	<b>0.5</b>	0.0	0.08	0.03	0.02
				Error(%)		100.0	<b>84.0</b>	94.0	96.0
380	GdVO4	0.198	141.556	Gd	<b>7.0</b>	6.83	6.89	6.93	6.97
				Error(%)		2.429	1.571	1.0	<b>0.429</b>
381	Tm2Mn2O7	0.151	141.557	Mn	<b>1.85</b>	-	-	-	2.93
				Tm	<b>2.31</b>	-	-	-	1.8
				Error(%)		-	-	-	<b>40.228</b>
382	Yb2Sn2O7	0.157	141.557	Yb	<b>1.05</b>	-	0.61	0.68	0.75
				Error(%)		-	41.905	35.238	<b>28.571</b>
383	NdCo2	0.227	141.557	Nd	<b>2.43</b>	0.09	0.21	3.12	2.68
				Co	<b>0.59</b>	0.24	1.18	1.7	1.07
				Error(%)		77.809	95.679	108.266	<b>45.822</b>
384	Tb2Sn2O7	0.48	141.557	Tb	<b>5.87</b>	5.8	5.87	5.94	6.02
				Error(%)		1.193	<b>0.0</b>	1.193	2.555
385	Ho2Ru2O7	0.49	141.557	Ru	<b>1.2</b>	1.27	1.57	0.97	0.08
				Error(%)		<b>5.833</b>	30.833	19.167	93.333
386	Ho2Ru2O7	0.51	141.557	Ho	<b>6.3</b>	3.67	3.84	3.9	3.97
				Ru	<b>1.8</b>	0.46	1.57	1.63	1.81
				Error(%)		58.095	25.913	23.77	<b>18.77</b>
387	PrFe3(BO3)4	1.161	155.48	Pr	<b>0.79</b>	-	-	2.58	-
				Fe	<b>4.32</b>	-	-	3.94	-
				Error(%)		-	-	<b>117.689</b>	-
388	U3As4	0.169	161.71	U	<b>1.9</b>	1.69	1.73	1.59	1.54
				Error(%)		11.053	<b>8.947</b>	16.316	18.947
389	U3P4	0.170	161.71	U	<b>1.48</b>	1.62	1.66	1.49	1.5
				Error(%)		9.459	12.162	<b>0.676</b>	1.351
390	Nd3Sb3Mg2O14	0.167	166.101	Nd	<b>1.79</b>	2.95	2.95	2.95	2.95
				Error(%)		<b>64.804</b>	64.804	64.804	64.804
391	TbCo2	0.228	166.101	Tb	<b>8.3</b>	0.29	5.89	6.01	5.24
				Co	<b>1.3</b>	0.03	0.06	0.37	1.41
				Co	<b>1.19</b>	0.04	0.06	0.37	1.49
				Error(%)		96.946	73.127	56.012	<b>23.513</b>
392	Tb2Ti2O7	0.77	166.101	Tb	<b>5.54</b>	-	-	-	6.06
				Tb	<b>3.54</b>	-	-	-	6.06
				Error(%)		-	-	-	<b>40.286</b>
393	TbMg3	1.189	167.108	Tb	<b>9.6</b>	5.89	-	6.08	-
				Error(%)		38.646	-	<b>36.667</b>	-

394	HoMnO <sub>3</sub>	0.32	185.197	Mn	<b>2.98</b>	3.48	0.03	0.55	-
				Error(%)		16.779	98.993	81.544	-
395	HoMnO <sub>3</sub>	0.33	185.197	Ho	<b>2.87</b>	0.09	2.31	3.9	-
				Mn	<b>3.05</b>	0.05	0.07	0.05	-
				Error(%)		97.612	58.608	67.124	-
396	NdZn	3.8	222.103	Nd	<b>2.51</b>	3.37	3.33	3.17	3.14
				Error(%)		34.263	32.669	26.295	25.1
397	NpSb	3.12	224.113	Np	<b>2.86</b>	3.46	3.61	3.71	3.79
				Error(%)		20.979	26.224	29.72	32.517
398	UO <sub>2</sub>	3.2	224.113	U	<b>1.73</b>	0.96	1.49	1.53	1.56
				Error(%)		44.509	13.873	11.561	9.827
399	NpBi	3.7	224.113	Np	<b>2.42</b>	3.59	3.69	3.76	3.83
				Error(%)		48.347	52.479	55.372	58.264
400	NpSe	3.10	228.139	Np	<b>1.3</b>	3.42	3.64	3.77	3.86
				Error(%)		163.077	180.0	190.0	196.923
401	NpTe	3.11	228.139	Np	<b>1.4</b>	3.69	3.76	3.85	3.92
				Error(%)		163.571	168.571	175.0	180.0
402	NpS	3.9	228.139	Np	<b>0.69</b>	3.22	3.51	3.69	3.81
				Error(%)		366.667	408.696	434.783	452.174
403	DyCu	3.6	229.143	Dy	<b>8.63</b>	4.4	4.41	4.65	5.04
				Error(%)		49.015	48.899	46.118	41.599

### 1. Ferro(Ferri)magnetic materials

Among the 403 materials, there have 51 magnetic materials with net moments/ferromagnetic canting. All of them are tabulated in Table XIX with the BCSID, chemical formula and the MSG. All of the MSGs of them are Type-I/Type-III MSG, which are compatible with ferro(ferri)magnets.

TABLE XIX: Magnetic materials with non-zero net moments or ferromagnetic canting.

BCSID	Formula	MSG	BCSID	Formula	MSG	BCSID	Formula	MSG
0.26	TmAgGe	38.191	0.36	NiF2	58.398	0.37	U3Al2Si3	5.15
0.48	Tb2Sn2O7	141.557	0.49	Ho2Ru2O7	141.557	0.64	MnV2O4	88.81
0.77	Tb2Ti2O7	166.101	0.78	NiN2O6	148.17	0.85	KCo4(PO4)3	58.398
0.91	Rb2Fe2O(AsO4)2	62.448	0.121	Li2Co(SO4)2	14.79	0.122	Li2Mn(SO4)2	14.75
0.149	Nd3Ru4Al12	63.462	0.151	Tm2Mn2O7	141.557	0.157	Yb2Sn2O7	141.557
0.165	SrMn(VO4)(OH)	4.7	0.169	U3As4	161.71	0.170	U3P4	161.71
0.173	Pr3Ru4Al12	63.462	0.174	Pr3Ru4Al12	15.89	0.176	Mn3Ti2Te6	15.89
0.184	Nd5Si4	92.114	0.185	Nd5Ge4	62.447	0.191	BaCuF4	36.176
0.203	Mn3Ge	12.62	0.220	Mn2SiO4	62.446	0.226	NdCo2	15.89
0.227	NdCo2	141.557	0.228	TbCo2	166.101	1.0.11	CeCoGe3	107.231
1.0.12	UAu2Si2	71.536	1.0.13	FeI2	12.62	2.5	Mn3CuN	85.59
2.10	HoP	15.89	2.11	TbMg	51.295	2.12	TbMg	49.270
2.19	Mn3ZnC	139.537	2.28	NpNiGa5	74.559	3.3	Ho2RhIn8	63.464

### Appendix M: Band structures and detailed information

We list the band structures for all of the 403 magnetic materials in the following tables, with the energy range set between  $-1.0 \sim 1.0$  eV relative to the Fermi level. Apart from the crystal and band structures for each material, the tables also include the material identification number on BCSMD (BCSID), chemical formula (Formula), the ICSD number if available, the magnetic space group (MSG) and stable topological classification of the MSG (T.C.). For the magnetic TIs diagnosed by MTQC, see H for the stable topological indices and the physical interpretations of them. For the magnetic ESs diagnosed by MTQC, see I for the high-symmetry  $k$  paths that break compatibility relations.

BCSID	Formula	ICSD	MSG	T.C.	
0.139	BiCrO <sub>3</sub>	174406	$2.4(P1)$	$\mathbb{Z}_2\mathbb{Z}_2\mathbb{Z}_2\mathbb{Z}_4$	
Topology	 U=0 , LCEBR	 U=1eV , LCEBR	 U=2eV , LCEBR	 U=3eV , LCEBR	 U=4eV , LCEBR

TABLE XX. Topology phase diagram of BiCrO<sub>3</sub>.

BCSID	Formula	ICSD	MSG	T.C.	
0.5	Cr <sub>2</sub> S <sub>3</sub>	626604	$2.4(P1)$	$\mathbb{Z}_2\mathbb{Z}_2\mathbb{Z}_2\mathbb{Z}_4$	
Topology	 U=0 , LCEBR	 U=1eV , LCEBR	 U=2eV , LCEBR	 U=3eV , LCEBR	 U=4eV , LCEBR

TABLE XXI. Topology phase diagram of Cr<sub>2</sub>S<sub>3</sub>.

BCSID	Formula	ICSD	MSG	T.C.	
0.66	Fe <sub>2</sub> O <sub>3</sub> -alpha	*	$2.4(P1)$	$\mathbb{Z}_2\mathbb{Z}_2\mathbb{Z}_2\mathbb{Z}_4$	
Topology	 U=0 , LCEBR	 U=1eV , LCEBR	 U=2eV , LCEBR	 U=3eV , LCEBR	 U=4eV , LCEBR

TABLE XXII. Topology phase diagram of Fe<sub>2</sub>O<sub>3</sub>-alpha.

BCSID	Formula	ICSD	MSG	T.C.	
0.155	CaMnGe <sub>2</sub> O <sub>6</sub>	*	$2.6(P1')$	w/o	
Topology	 U=0 , LCEBR	 U=1eV , LCEBR	 U=2eV , LCEBR	 U=3eV , LCEBR	 U=4eV , LCEBR

TABLE XXIII. Topology phase diagram of CaMnGe<sub>2</sub>O<sub>6</sub>.

BCSID	Formula	ICSD	MSG	T.C.	
0.180	MnPSe <sub>3</sub>	54140	2.6( $P1'$ )	w/o	
Topology	 U=0 , LCEBR	 U=1eV , LCEBR	 U=2eV , LCEBR	 U=3eV , LCEBR	 U=4eV , LCEBR

TABLE XXIV. Topology phase diagram of MnPSe<sub>3</sub>.

BCSID	Formula	ICSD	MSG	T.C.	
0.215	BaNi <sub>2</sub> P <sub>2</sub> O <sub>8</sub>	411629	2.6( $P1'$ )	w/o	
Topology	 U=0 , LCEBR	 U=1eV , LCEBR	 U=2eV , LCEBR	 U=3eV , LCEBR	 U=4eV , LCEBR

TABLE XXV. Topology phase diagram of BaNi<sub>2</sub>P<sub>2</sub>O<sub>8</sub>.

BCSID	Formula	ICSD	MSG	T.C.	
1.113	NiSb <sub>2</sub> O <sub>6</sub>	80802	2.7( $P_S1$ )	$\mathbb{Z}_2$	
Topology	 U=0 , LCEBR	 U=1eV , LCEBR	 U=2eV , LCEBR	 U=3eV , LCEBR	 U=4eV , LCEBR

TABLE XXVI. Topology phase diagram of NiSb<sub>2</sub>O<sub>6</sub>.

BCSID	Formula	ICSD	MSG	T.C.	
1.155	LiFeSO <sub>4</sub> F	182944	2.7( $P_S1$ )	$\mathbb{Z}_2$	
Topology	 U=0 , LCEBR	 U=1eV , LCEBR	 U=2eV , LCEBR	 U=3eV , LCEBR	 U=4eV , LCEBR

TABLE XXVII. Topology phase diagram of LiFeSO<sub>4</sub>F.

BCSID	Formula	ICSD	MSG	T.C.	
1.159	$\text{Li}_2\text{Ni}(\text{WO}_4)_2$	92853	$2.7(P_S1)$	$\mathbb{Z}_2$	
Topology	 $U=0, \text{LCEBR}$				

TABLE XXVIII. Topology phase diagram of  $\text{Li}_2\text{Ni}(\text{WO}_4)_2$ .

BCSID	Formula	ICSD	MSG	T.C.	
1.166	$\text{La}_2\text{LiOsO}_6$	*	$2.7(P_S1)$	$\mathbb{Z}_2$	
Topology	 $U=0, \text{LCEBR}$				

TABLE XXIX. Topology phase diagram of  $\text{La}_2\text{LiOsO}_6$ .

BCSID	Formula	ICSD	MSG	T.C.	
1.167	$\text{NiS}_2$	76684	$2.7(P_S1)$	$\mathbb{Z}_2$	
Topology	 $U=0, \text{LCEBR}$				

TABLE XXX. Topology phase diagram of  $\text{NiS}_2$ .

BCSID	Formula	ICSD	MSG	T.C.	
1.177	$\text{Sr}_2\text{CuWO}_6$	193615	$2.7(P_S1)$	$\mathbb{Z}_2$	
Topology	 $U=0, \text{LCEBR}$				

TABLE XXXI. Topology phase diagram of  $\text{Sr}_2\text{CuWO}_6$ .

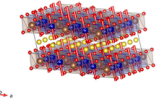
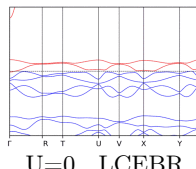
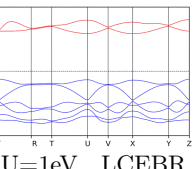
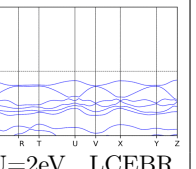
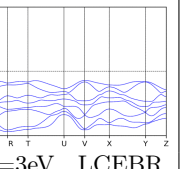
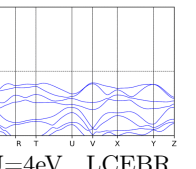
BCSID	Formula	ICSD	MSG	T.C.	
1.180	Na <sub>3</sub> Co <sub>2</sub> SbO <sub>6</sub>	245538	2.7( $P_S1$ )	$\mathbb{Z}_2$	
Topology	 U=0 , LCEBR	 U=1eV , LCEBR	 U=2eV , LCEBR	 U=3eV , LCEBR	 U=4eV , LCEBR

TABLE XXXII. Topology phase diagram of Na<sub>3</sub>Co<sub>2</sub>SbO<sub>6</sub>.

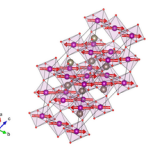
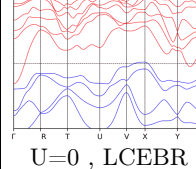
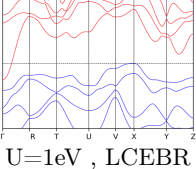
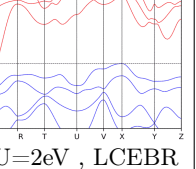
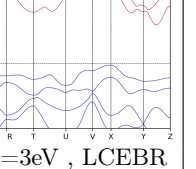
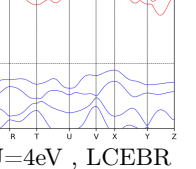
BCSID	Formula	ICSD	MSG	T.C.	
1.182	TlMnO <sub>3</sub>	*	2.7( $P_S1$ )	$\mathbb{Z}_2$	
Topology	 U=0 , LCEBR	 U=1eV , LCEBR	 U=2eV , LCEBR	 U=3eV , LCEBR	 U=4eV , LCEBR

TABLE XXXIII. Topology phase diagram of TlMnO<sub>3</sub>.

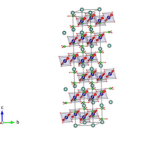
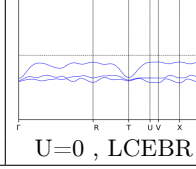
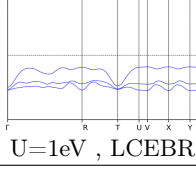
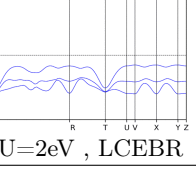
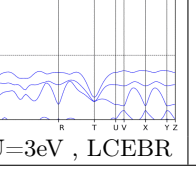
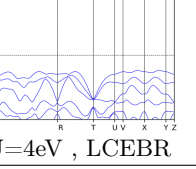
BCSID	Formula	ICSD	MSG	T.C.	
1.190	YCr(BO <sub>3</sub> ) <sub>2</sub>	189501	2.7( $P_S1$ )	$\mathbb{Z}_2$	
Topology	 U=0 , LCEBR	 U=1eV , LCEBR	 U=2eV , LCEBR	 U=3eV , LCEBR	 U=4eV , LCEBR

TABLE XXXIV. Topology phase diagram of YCr(BO<sub>3</sub>)<sub>2</sub>.

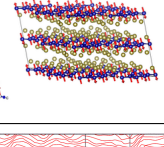
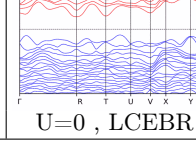
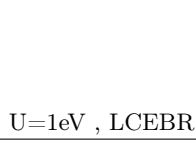
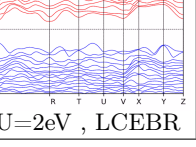
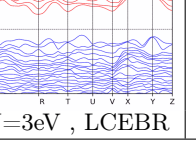
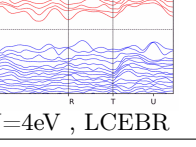
BCSID	Formula	ICSD	MSG	T.C.		
1.193	CrTe <sub>3</sub>	*	2.7( $P_S1$ )	$\mathbb{Z}_2$		
Topology	 U=0 , LCEBR		 U=1eV , LCEBR	 U=2eV , LCEBR	 U=3eV , LCEBR	 U=4eV , LCEBR

TABLE XXXV. Topology phase diagram of CrTe<sub>3</sub>.

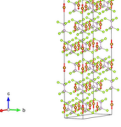
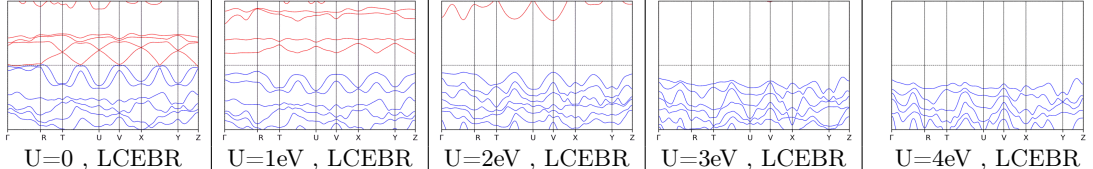
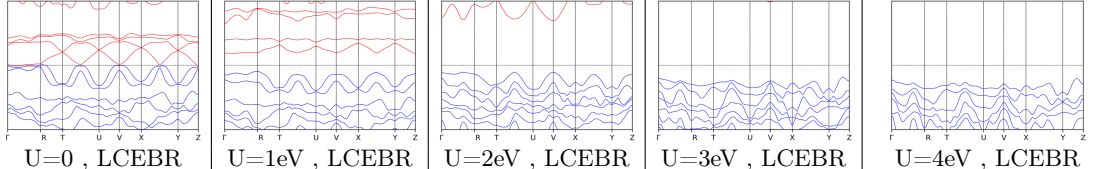
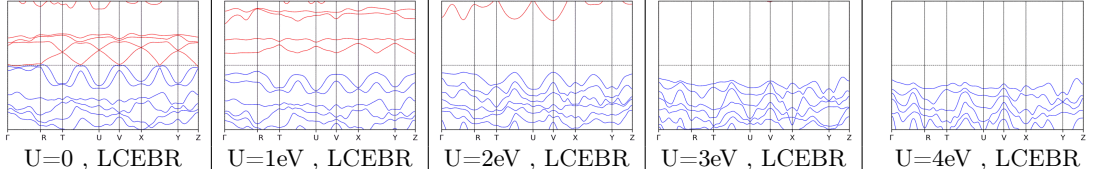
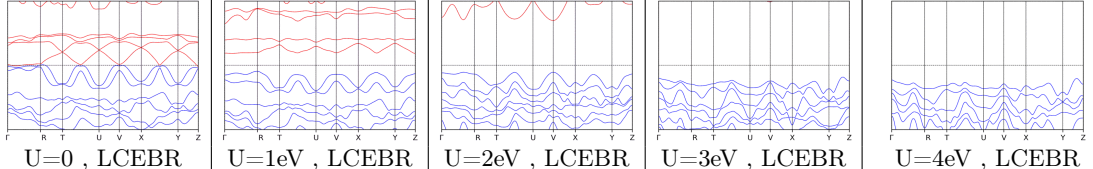
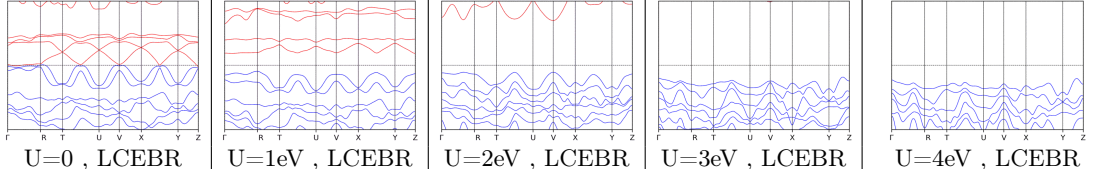
BCSID	Formula	ICSD	MSG	T.C.	
1.210	FePSe <sub>3</sub>	54141	2.7( $P_S1$ )	$\mathbb{Z}_2$	
Topology					

TABLE XXXVI. Topology phase diagram of FePSe<sub>3</sub>.

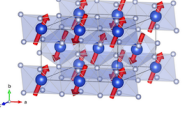
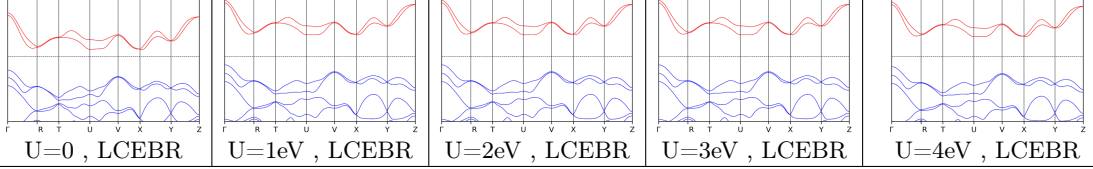
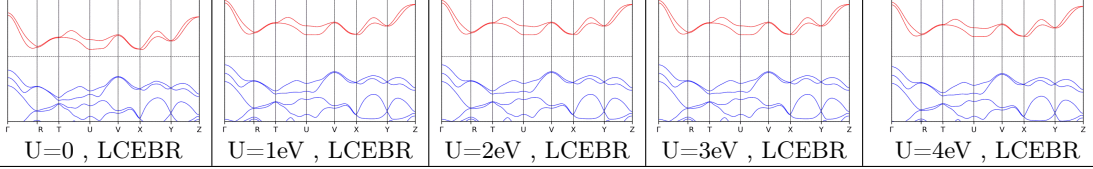
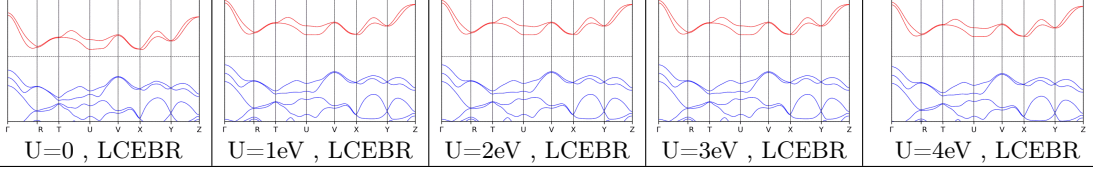
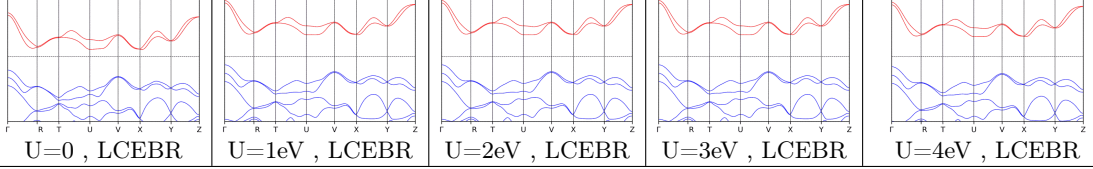
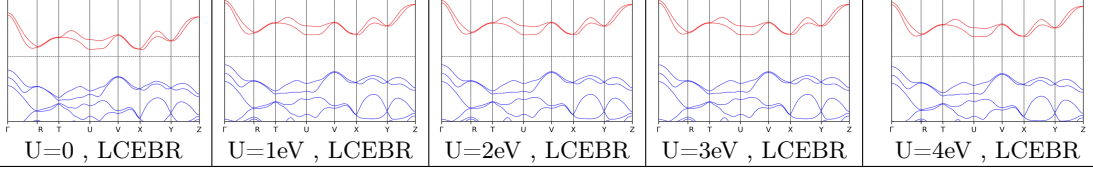
BCSID	Formula	ICSD	MSG	T.C.	
1.219	CuF <sub>2</sub>	9790	2.7( $P_S1$ )	$\mathbb{Z}_2$	
Topology					

TABLE XXXVII. Topology phase diagram of CuF<sub>2</sub>.

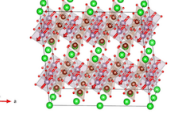
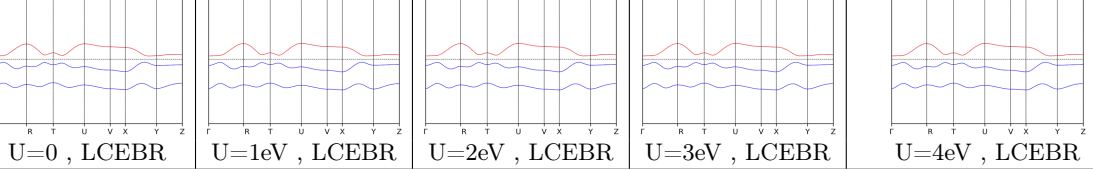
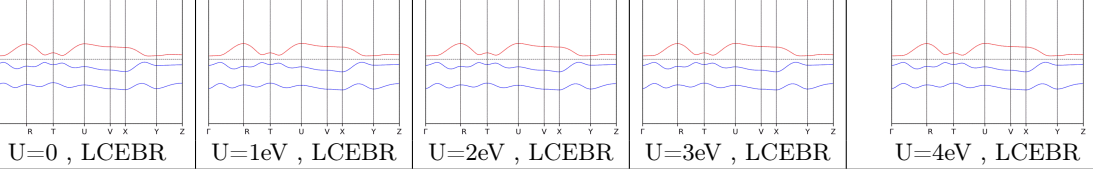
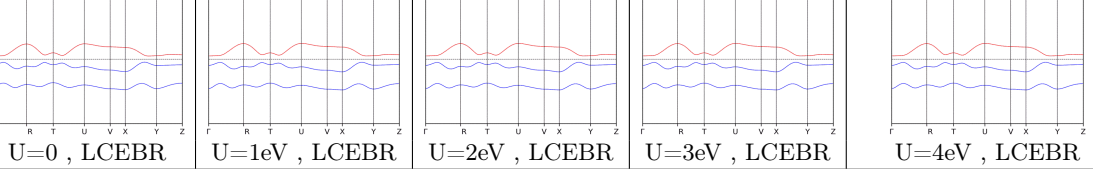
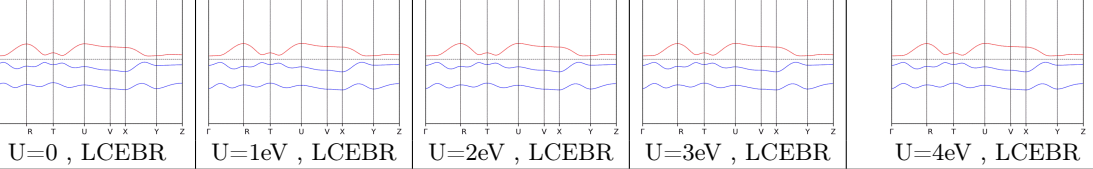
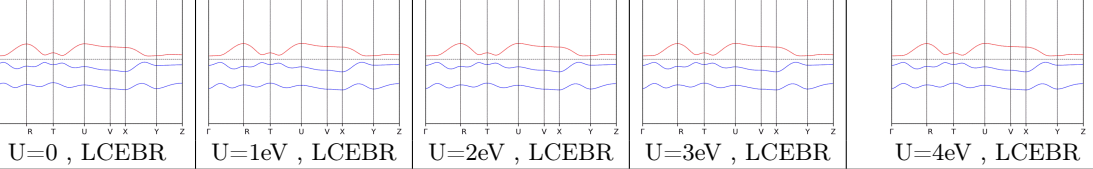
BCSID	Formula	ICSD	MSG	T.C.	
1.229	BaMoP <sub>2</sub> O <sub>8</sub>	79507	2.7( $P_S1$ )	$\mathbb{Z}_2$	
Topology					

TABLE XXXVIII. Topology phase diagram of BaMoP<sub>2</sub>O<sub>8</sub>.

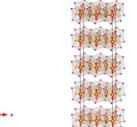
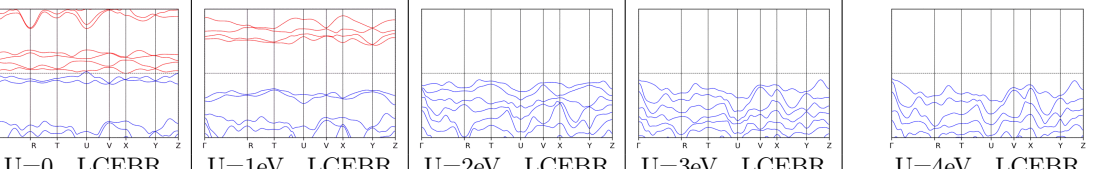
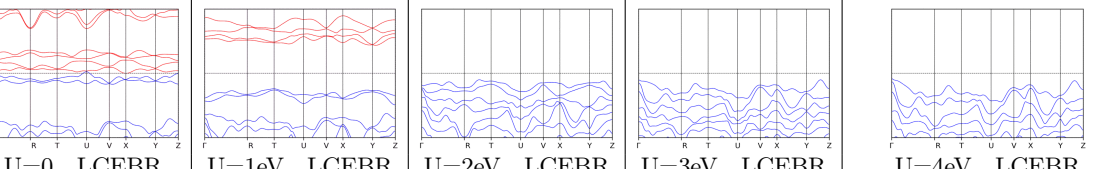
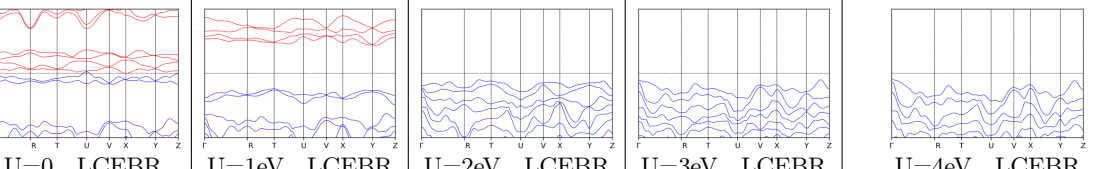
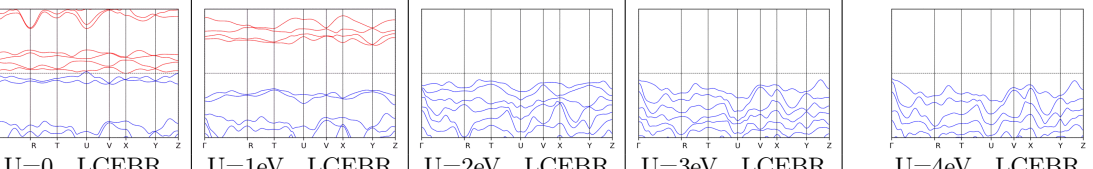
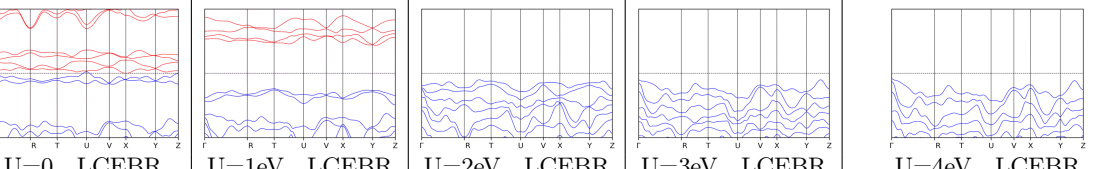
BCSID	Formula	ICSD	MSG	T.C.	
1.240	FeI <sub>2</sub>	52369	2.7( $P_S1$ )	$\mathbb{Z}_2$	
Topology					

TABLE XXXIX. Topology phase diagram of FeI<sub>2</sub>.

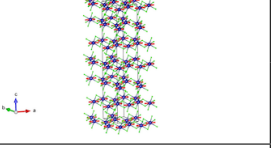
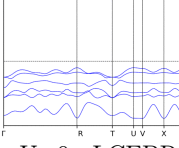
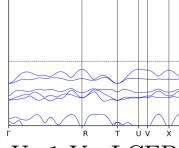
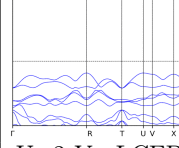
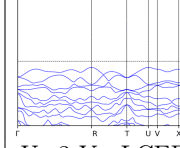
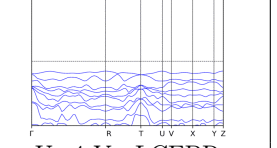
BCSID	Formula	ICSD	MSG	T.C.	
1.244	CrCl <sub>3</sub>	22081	2.7( $P_S1$ )	$\mathbb{Z}_2$	
Topology	 U=0 , LCEBR	 U=1eV , LCEBR	 U=2eV , LCEBR	 U=3eV , LCEBR	 U=4eV , LCEBR

TABLE XL. Topology phase diagram of CrCl<sub>3</sub>.

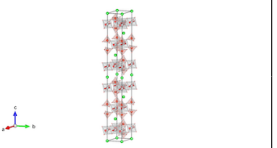
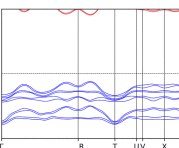
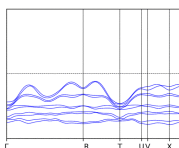
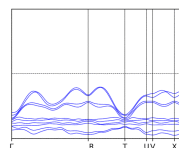
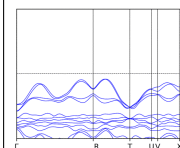
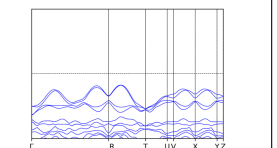
BCSID	Formula	ICSD	MSG	T.C.	
1.256	BaNi <sub>2</sub> V <sub>2</sub> O <sub>8</sub>	96087	2.7( $P_S1$ )	$\mathbb{Z}_2$	
Topology	 U=0 , LCEBR	 U=1eV , LCEBR	 U=2eV , LCEBR	 U=3eV , LCEBR	 U=4eV , LCEBR

TABLE XLI. Topology phase diagram of BaNi<sub>2</sub>V<sub>2</sub>O<sub>8</sub>.

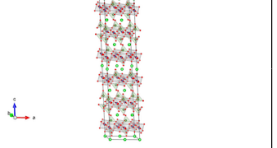
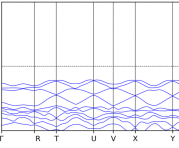
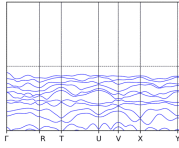
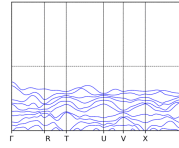
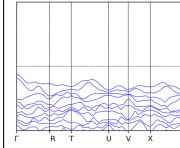
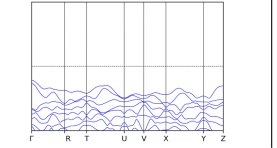
BCSID	Formula	ICSD	MSG	T.C.	
1.257	BaNi <sub>2</sub> As <sub>2</sub> O <sub>8</sub>	27014	2.7( $P_S1$ )	$\mathbb{Z}_2$	
Topology	 U=0 , LCEBR	 U=1eV , LCEBR	 U=2eV , LCEBR	 U=3eV , LCEBR	 U=4eV , LCEBR

TABLE XLII. Topology phase diagram of BaNi<sub>2</sub>As<sub>2</sub>O<sub>8</sub>.

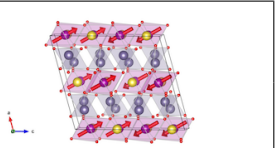
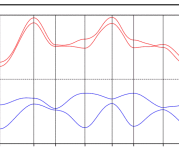
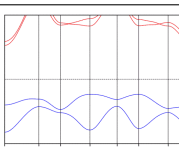
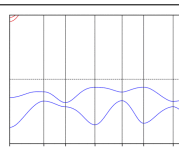
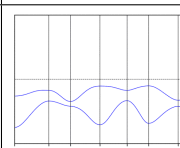
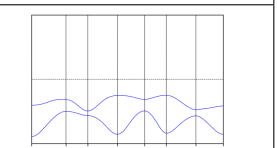
BCSID	Formula	ICSD	MSG	T.C.	
1.260	NaMnGe <sub>2</sub> O <sub>6</sub>	237747	2.7( $P_S1$ )	$\mathbb{Z}_2$	
Topology	 U=0 , LCEBR	 U=1eV , LCEBR	 U=2eV , LCEBR	 U=3eV , LCEBR	 U=4eV , LCEBR

TABLE XLIII. Topology phase diagram of NaMnGe<sub>2</sub>O<sub>6</sub>.

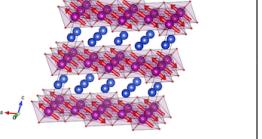
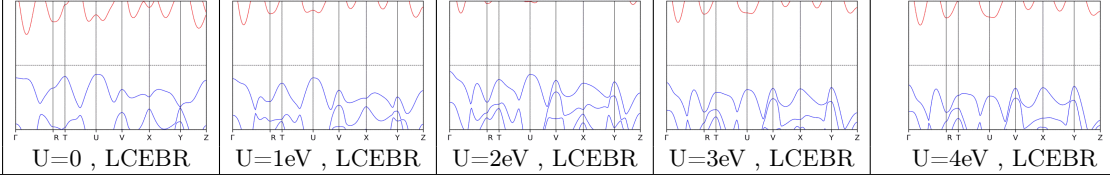
BCSID	Formula	ICSD	MSG	T.C.	
1.57	CuMnO <sub>2</sub>	*	2.7( $P_S1$ )	$\mathbb{Z}_2$	
Topology	 U=0 , LCEBR    U=1eV , LCEBR    U=2eV , LCEBR    U=3eV , LCEBR    U=4eV , LCEBR				

TABLE XLIV. Topology phase diagram of CuMnO<sub>2</sub>.

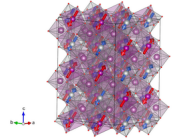
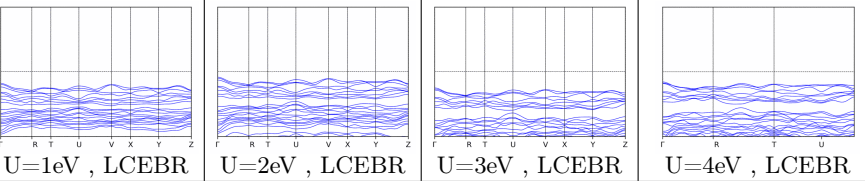
BCSID	Formula	ICSD	MSG	T.C.	
2.18	Sc <sub>2</sub> NiMnO <sub>6</sub>	251833	2.7( $P_S1$ )	$\mathbb{Z}_2$	
Topology	 U=0 , LCEBR    U=1eV , LCEBR    U=2eV , LCEBR    U=3eV , LCEBR    U=4eV , LCEBR				

TABLE XLV. Topology phase diagram of Sc<sub>2</sub>NiMnO<sub>6</sub>.

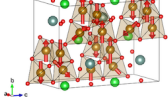
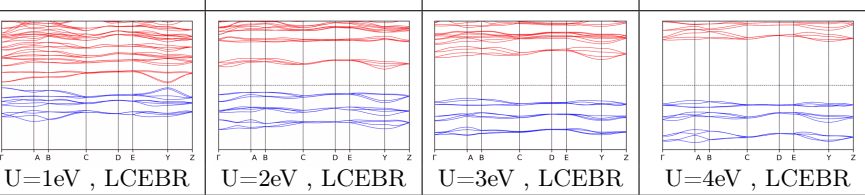
BCSID	Formula	ICSD	MSG	T.C.	
1.124	YBaFe <sub>4</sub> O <sub>7</sub>	*	4.10( $P_a2_1$ )	w/o	
Topology	 U=0 , LCEBR    U=1eV , LCEBR    U=2eV , LCEBR    U=3eV , LCEBR    U=4eV , LCEBR				

TABLE XLVI. Topology phase diagram of YBaFe<sub>4</sub>O<sub>7</sub>.

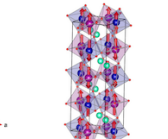
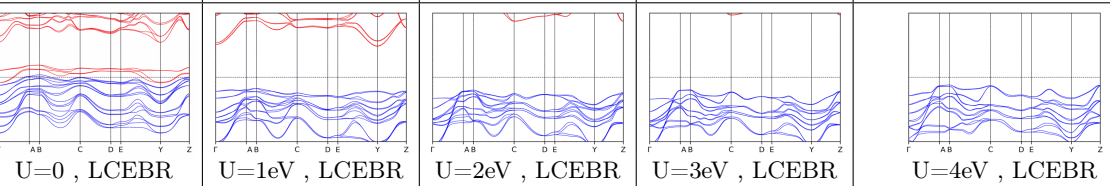
BCSID	Formula	ICSD	MSG	T.C.	
1.32	Lu <sub>2</sub> MnCoO <sub>6</sub>	*	4.10( $P_a2_1$ )	w/o	
Topology	 U=0 , LCEBR    U=1eV , LCEBR    U=2eV , LCEBR    U=3eV , LCEBR    U=4eV , LCEBR				

TABLE XLVII. Topology phase diagram of Lu<sub>2</sub>MnCoO<sub>6</sub>.

BCSID	Formula	ICSD	MSG	T.C.	
1.51	Cs <sub>2</sub> CoCl <sub>4</sub>	62548	4.10( $P_a2_1$ )	w/o	
Topology	 U=0 , LCEBR	 U=1eV , LCEBR	 U=2eV , LCEBR	 U=3eV , LCEBR	 U=4eV , LCEBR

TABLE XLVIII. Topology phase diagram of Cs<sub>2</sub>CoCl<sub>4</sub>.

BCSID	Formula	ICSD	MSG	T.C.	
1.64	BaNiF <sub>4</sub>	23141	4.10( $P_a2_1$ )	w/o	
Topology	 U=0 , LCEBR	 U=1eV , LCEBR	 U=2eV , LCEBR	 U=3eV , LCEBR	 U=4eV , LCEBR

TABLE XLIX. Topology phase diagram of BaNiF<sub>4</sub>.

BCSID	Formula	ICSD	MSG	T.C.	
1.227	Ca <sub>2</sub> Cr <sub>2</sub> O <sub>5</sub>	238797	4.12( $P_C2_1$ )	w/o	
Topology	 U=0 , LCEBR	 U=1eV , TBD	 U=2eV , TBD	 U=3eV , TBD	 U=4eV , LCEBR

TABLE L. Topology phase diagram of Ca<sub>2</sub>Cr<sub>2</sub>O<sub>5</sub>.

BCSID	Formula	ICSD	MSG	T.C.	
0.165	SrMn(VO <sub>4</sub> )(OH)	*	4.7( $P2_1$ )	w/o	
Topology	 U=0 , ES	 U=1eV , LCEBR	 U=2eV , LCEBR	 U=3eV , LCEBR	 U=4eV , LCEBR

TABLE LI. Topology phase diagram of SrMn(VO<sub>4</sub>)(OH).

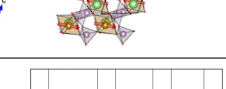
BCSID	Formula	ICSD	MSG	T.C.	
0.83	LiFeP2O7	95751	4.7( $P2_1$ )	w/o	
Topology					
	U=0 , LCEBR	U=1eV , LCEBR	U=2eV , LCEBR	U=3eV , LCEBR	U=4eV , LCEBR

TABLE LII. Topology phase diagram of LiFeP<sub>2</sub>O<sub>7</sub>.

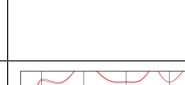
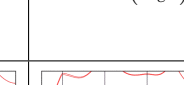
BCSID	Formula	ICSD	MSG	T.C.	
1.100	Cu <sub>2</sub> MnSnS <sub>4</sub>	56601	5.16( $C_c2$ )	w/o	
Topology					
	U=0 , LCEBR	U=1eV , LCEBR	U=2eV , LCEBR	U=3eV , LCEBR	U=4eV , LCEBR

TABLE LIII. Topology phase diagram of Cu<sub>2</sub>MnSnS<sub>4</sub>.

BCSID	Formula	ICSD	MSG	T.C.	
1.90	YFe <sub>3</sub> (BO <sub>3</sub> ) <sub>4</sub>	*	5.16( $C_c2$ )	w/o	
Topology					U=0 , LCEBR      U=1eV , TBD      U=2eV , LCEBR      U=3eV , TBD      U=4eV , LCEBR

TABLE LIV. Topology phase diagram of YFe<sub>3</sub>(BO<sub>3</sub>)<sub>4</sub>.

BCSID	Formula	ICSD	MSG	T.C.	
1.55	Na <sub>2</sub> MnF <sub>5</sub>	*	7.29( $P_b$ c)	w/o	
Topology	 U=0 , LCEBR	 U=1eV , LCEBR	 U=2eV , LCEBR	 U=3eV , LCEBR	 U=4eV , LCEBR

TABLE LV. Topology phase diagram of Na<sub>2</sub>MnF<sub>5</sub>.

BCSID	Formula	ICSD	MSG	T.C.		
1.75	BiMn <sub>2</sub> O <sub>5</sub>	*	8.36( $C_a m$ )	w/o		
Topology						
	U=0 , LCEBR	U=1eV , LCEBR	U=2eV , LCEBR	U=3eV , LCEBR	U=4eV , LCEBR	

TABLE LVI. Topology phase diagram of BiMn<sub>2</sub>O<sub>5</sub>.

BCSID	Formula	ICSD	MSG	T.C.		
0.50	MnTiO <sub>3</sub>	*	9.39( $Cc'$ )	w/o		
Topology						
	U=0 , LCEBR	U=1eV , LCEBR	U=2eV , LCEBR	U=3eV , LCEBR	U=4eV , LCEBR	

TABLE LVII. Topology phase diagram of MnTiO<sub>3</sub>.

BCSID	Formula	ICSD	MSG	T.C.		
1.232	CuMnSb	628385	9.40( $C_c c$ )	w/o		
Topology						
	U=0 , LCEBR	U=1eV , LCEBR	U=2eV , LCEBR	U=3eV , LCEBR	U=4eV , LCEBR	

TABLE LVIII. Topology phase diagram of CuMnSb.

BCSID	Formula	ICSD	MSG	T.C.		
1.58	La <sub>2</sub> O <sub>2</sub> Fe <sub>2</sub> OSe <sub>2</sub>	*	9.40( $C_c c$ )	w/o		
Topology						
	U=0 , LCEBR	U=1eV , LCEBR	U=2eV , LCEBR	U=3eV , LCEBR	U=4eV , LCEBR	

TABLE LIX. Topology phase diagram of La<sub>2</sub>O<sub>2</sub>Fe<sub>2</sub>OSe<sub>2</sub>.

BCSID	Formula	ICSD	MSG	T.C.	
1.120	BaFe <sub>2</sub> Se <sub>3</sub>	424315	9.41( $C_{ac}$ )	w/o	
Topology			    		
	U=0 , LCEBR	U=1eV , LCEBR	U=2eV , LCEBR	U=3eV , LCEBR	U=4eV , LCEBR

TABLE LX. Topology phase diagram of BaFe<sub>2</sub>Se<sub>3</sub>.

BCSID	Formula	ICSD	MSG	T.C.	
1.79	Li <sub>2</sub> CoSiO <sub>4</sub>	245536	9.41( $C_{ac}$ )	w/o	
Topology			    		
	U=0 , LCEBR	U=1eV , LCEBR	U=2eV , LCEBR	U=3eV , LCEBR	U=4eV , LCEBR

TABLE LXI. Topology phase diagram of Li<sub>2</sub>CoSiO<sub>4</sub>.

BCSID	Formula	ICSD	MSG	T.C.	
1.228	RuCl <sub>3</sub>	*	10.49( $P_C 2/m$ )	$\mathbb{Z}_2$	
Topology			    		
	U=0 , TBD	U=1eV , TBD	U=2eV , TBD	U=3eV , LCEBR	U=4eV , TBD

TABLE LXII. Topology phase diagram of RuCl<sub>3</sub>.

BCSID	Formula	ICSD	MSG	T.C.	
1.116	AgMnVO <sub>4</sub>	246202	11.55( $P_a 2_1/m$ )	$\mathbb{Z}_2$	
Topology			    		
	U=0 , LCEBR	U=1eV , LCEBR	U=2eV , LCEBR	U=3eV , LCEBR	U=4eV , LCEBR

TABLE LXIII. Topology phase diagram of AgMnVO<sub>4</sub>.

BCSID	Formula	ICSD	MSG	T.C.	
1.134	Co <sub>2</sub> C <sub>10</sub> O <sub>8</sub> H <sub>2</sub>	*	11.57( $P_C 2_1/m$ )	$\mathbb{Z}_2$	
Topology	 U=0 , LCEBR				

TABLE LXIV. Topology phase diagram of Co<sub>2</sub>C<sub>10</sub>O<sub>8</sub>H<sub>2</sub>.

BCSID	Formula	ICSD	MSG	T.C.	
1.230	NiPS3	646133	11.57( $P_C 2_1/m$ )	$\mathbb{Z}_2$	
Topology	 U=0 , LCEBR				

TABLE LXV. Topology phase diagram of NiPS3.

BCSID	Formula	ICSD	MSG	T.C.	
1.264	CoPS3	*	11.57( $P_C 2_1/m$ )	$\mathbb{Z}_2$	
Topology	 U=0 , TI				

TABLE LXVI. Topology phase diagram of CoPS3.

BCSID	Formula	ICSD	MSG	T.C.	
0.163	MnPS3	61391	12.60( $C2'/m$ )	w/o	
Topology	 U=0 , LCEBR				

TABLE LXVII. Topology phase diagram of MnPS3.

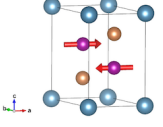
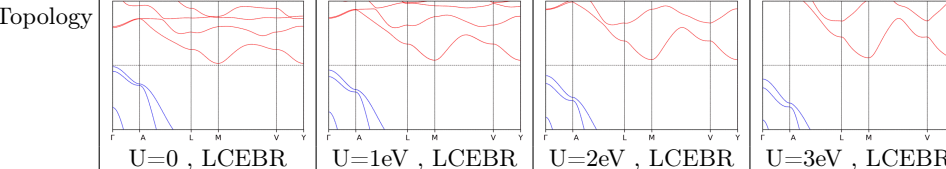
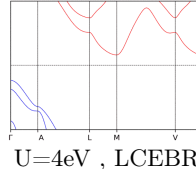
BCSID	Formula	ICSD	MSG	T.C.	
0.92	CaMn <sub>2</sub> Sb <sub>2</sub>	163778	$12.60(C2'/m)$	w/o	
Topology					

TABLE LXVIII. Topology phase diagram of CaMn<sub>2</sub>Sb<sub>2</sub>.

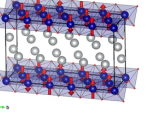
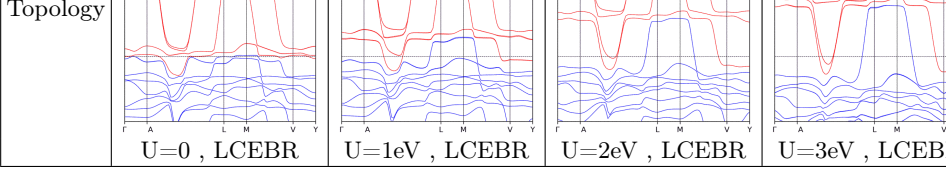
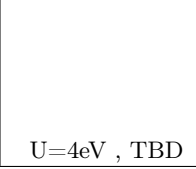
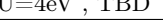
BCSID	Formula	ICSD	MSG	T.C.	
1.0.1	Ag <sub>2</sub> CrO <sub>2</sub>	*	$12.60(C2'/m)$	w/o	
Topology					

TABLE LXIX. Topology phase diagram of Ag<sub>2</sub>CrO<sub>2</sub>.

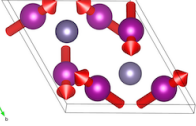
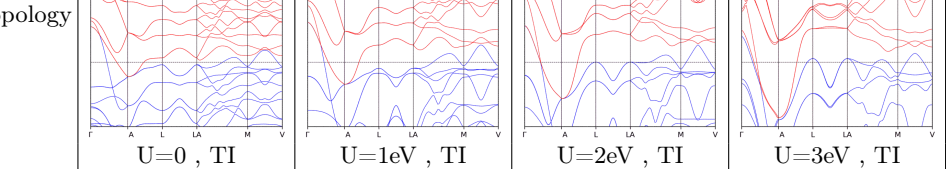
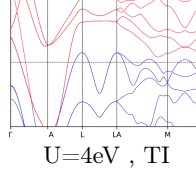
BCSID	Formula	ICSD	MSG	T.C.	
0.203	Mn <sub>3</sub> Ge	603343	$12.62(C2'/m')$	$\mathbb{Z}_2\mathbb{Z}_2\mathbb{Z}_4$	
Topology					

TABLE LXX. Topology phase diagram of Mn<sub>3</sub>Ge.

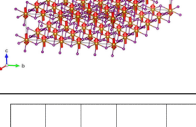
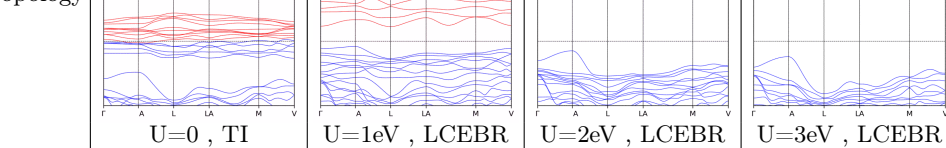
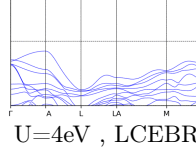
BCSID	Formula	ICSD	MSG	T.C.	
1.0.13	FeI <sub>2</sub>	52369	$12.62(C2'/m')$	$\mathbb{Z}_2\mathbb{Z}_2\mathbb{Z}_4$	
Topology					

TABLE LXXI. Topology phase diagram of FeI<sub>2</sub>.

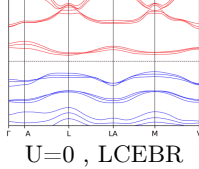
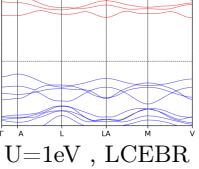
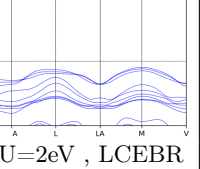
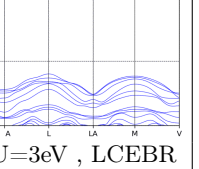
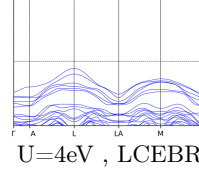
BCSID	Formula	ICSD	MSG	T.C.	
1.0.6	CoV <sub>2</sub> O <sub>6</sub>	263002	$12.62(C2'/m')$	$\mathbb{Z}_2\mathbb{Z}_2\mathbb{Z}_4$	
Topology					

TABLE LXXII. Topology phase diagram of CoV<sub>2</sub>O<sub>6</sub>.

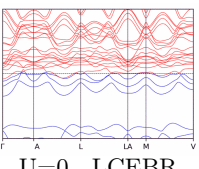
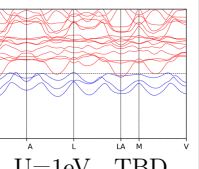
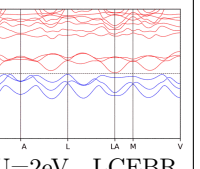
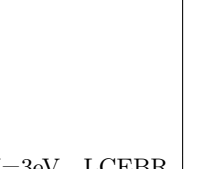
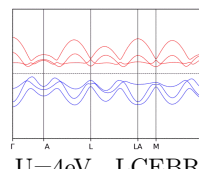
BCSID	Formula	ICSD	MSG	T.C.	
1.0.7	LuFe <sub>2</sub> O <sub>4</sub>	68481	$12.62(C2'/m')$	$\mathbb{Z}_2\mathbb{Z}_2\mathbb{Z}_4$	
Topology					

TABLE LXXIII. Topology phase diagram of LuFe<sub>2</sub>O<sub>4</sub>.

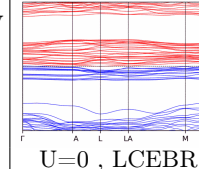
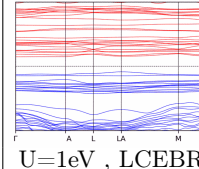
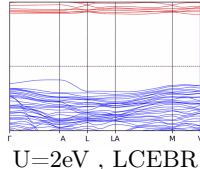
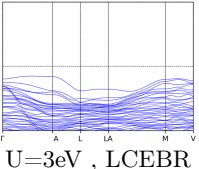
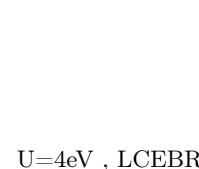
BCSID	Formula	ICSD	MSG	T.C.	
3.14	FeI <sub>2</sub>	52369	$12.62(C2'/m')$	$\mathbb{Z}_2\mathbb{Z}_2\mathbb{Z}_4$	
Topology					

TABLE LXXIV. Topology phase diagram of FeI<sub>2</sub>.

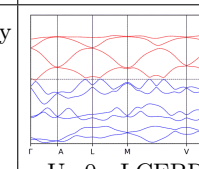
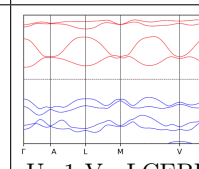
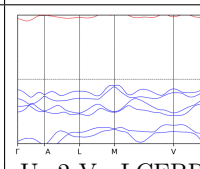
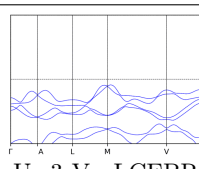
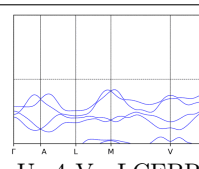
BCSID	Formula	ICSD	MSG	T.C.	
1.183	FePS <sub>3</sub>	*	$12.63(C_c2/m)$	$\mathbb{Z}_2$	
Topology					

TABLE LXXV. Topology phase diagram of FePS<sub>3</sub>.

BCSID	Formula	ICSD	MSG	T.C.	
1.197	Fe4Si2Sn7O16	407506	$12.63(C_c2/m)$	$\mathbb{Z}_2$	
Topology	 $U=0, \text{LCEBR}$	 $U=1\text{eV}, \text{LCEBR}$	 $U=2\text{eV}, \text{LCEBR}$	 $U=3\text{eV}, \text{LCEBR}$	 $U=4\text{eV}, \text{LCEBR}$

TABLE LXXVI. Topology phase diagram of Fe4Si2Sn7O16.

BCSID	Formula	ICSD	MSG	T.C.	
1.239	MnBr2	60250	$12.63(C_c2/m)$	$\mathbb{Z}_2$	
Topology	 $U=0, \text{LCEBR}$	 $U=1\text{eV}, \text{LCEBR}$	 $U=2\text{eV}, \text{LCEBR}$	 $U=3\text{eV}, \text{LCEBR}$	 $U=4\text{eV}, \text{LCEBR}$

TABLE LXXVII. Topology phase diagram of MnBr2.

BCSID	Formula	ICSD	MSG	T.C.	
1.97	Li2MnO3	187499	$12.63(C_c2/m)$	$\mathbb{Z}_2$	
Topology	 $U=0, \text{LCEBR}$	 $U=1\text{eV}, \text{LCEBR}$	 $U=2\text{eV}, \text{LCEBR}$	 $U=3\text{eV}, \text{LCEBR}$	 $U=4\text{eV}, \text{LCEBR}$

TABLE LXXVIII. Topology phase diagram of Li2MnO3.

BCSID	Formula	ICSD	MSG	T.C.	
2.2	Sr2F2Fe2OS2	*	$12.64(C_a2/m)$	$\mathbb{Z}_2$	
Topology	 $U=0, \text{LCEBR}$	 $U=1\text{eV}, \text{LCEBR}$	 $U=2\text{eV}, \text{LCEBR}$	 $U=3\text{eV}, \text{LCEBR}$	 $U=4\text{eV}, \text{LCEBR}$

TABLE LXXIX. Topology phase diagram of Sr2F2Fe2OS2.

BCSID	Formula	ICSD	MSG	T.C.	
1.194	NiWO <sub>4</sub>	15852	13.70( $P_a2/c$ )	$\mathbb{Z}_2$	
Topology	 U=0 , LCEBR	 U=1eV , LCEBR	 U=2eV , LCEBR	 U=3eV , LCEBR	 U=4eV , LCEBR

TABLE LXXX. Topology phase diagram of NiWO<sub>4</sub>.

BCSID	Formula	ICSD	MSG	T.C.	
1.114	Ca <sub>4</sub> IrO <sub>6</sub>	280873	13.74( $P_C2/c$ )	$\mathbb{Z}_2$	
Topology	 U=0 , LCEBR	 U=1eV , LCEBR	 U=2eV , LCEBR	 U=3eV , LCEBR	 U=4eV , LCEBR

TABLE LXXXI. Topology phase diagram of Ca<sub>4</sub>IrO<sub>6</sub>.

BCSID	Formula	ICSD	MSG	T.C.	
1.121	NaFeSO <sub>4</sub> F	290051	13.74( $P_C2/c$ )	$\mathbb{Z}_2$	
Topology	 U=0 , LCEBR	 U=1eV , LCEBR	 U=2eV , LCEBR	 U=3eV , LCEBR	 U=4eV , LCEBR

TABLE LXXXII. Topology phase diagram of NaFeSO<sub>4</sub>F.

BCSID	Formula	ICSD	MSG	T.C.	
1.126	NaCoSO <sub>4</sub> F	290052	13.74( $P_C2/c$ )	$\mathbb{Z}_2$	
Topology	 U=0 , LCEBR	 U=1eV , LCEBR	 U=2eV , LCEBR	 U=3eV , LCEBR	 U=4eV , LCEBR

TABLE LXXXIII. Topology phase diagram of NaCoSO<sub>4</sub>F.

BCSID	Formula	ICSD	MSG	T.C.	
0.103	Mn <sub>2</sub> GeO <sub>4</sub>	*	14.75( $P2_1/c$ )	$\mathbb{Z}_2$	
Topology	 U=0 , LCEBR	 U=1eV , LCEBR	 U=2eV , LCEBR	 U=3eV , LCEBR	 U=4eV , LCEBR

TABLE LXXXIV. Topology phase diagram of Mn<sub>2</sub>GeO<sub>4</sub>.

BCSID	Formula	ICSD	MSG	T.C.	
0.122	Li <sub>2</sub> Mn(SO <sub>4</sub> ) <sub>2</sub>	290292	14.75( $P2_1/c$ )	$\mathbb{Z}_2$	
Topology	 U=0 , LCEBR	 U=1eV , LCEBR	 U=2eV , LCEBR	 U=3eV , LCEBR	 U=4eV , LCEBR

TABLE LXXXV. Topology phase diagram of Li<sub>2</sub>Mn(SO<sub>4</sub>)<sub>2</sub>.

BCSID	Formula	ICSD	MSG	T.C.	
0.148	La <sub>2</sub> LiRuO <sub>6</sub>	97488	14.75( $P2_1/c$ )	$\mathbb{Z}_2$	
Topology	 U=0 , LCEBR	 U=1eV , LCEBR	 U=2eV , LCEBR	 U=3eV , LCEBR	 U=4eV , LCEBR

TABLE LXXXVI. Topology phase diagram of La<sub>2</sub>LiRuO<sub>6</sub>.

BCSID	Formula	ICSD	MSG	T.C.	
0.204	Ca <sub>2</sub> MnReO <sub>6</sub>	*	14.75( $P2_1/c$ )	$\mathbb{Z}_2$	
Topology	 U=0 , LCEBR	 U=1eV , TBD	 U=2eV , TBD	 U=3eV , LCEBR	 U=4eV , LCEBR

TABLE LXXXVII. Topology phase diagram of Ca<sub>2</sub>MnReO<sub>6</sub>.

BCSID	Formula	ICSD	MSG	T.C.	
0.217	LiCrGe2O6	*	14.77( $P2_1/c$ )	w/o	
Topology	 $U=0$ , LCEBR	 $U=1\text{eV}$ , LCEBR	 $U=2\text{eV}$ , LCEBR	 $U=3\text{eV}$ , LCEBR	 $U=4\text{eV}$ , LCEBR

TABLE LXXXVIII. Topology phase diagram of LiCrGe2O6.

BCSID	Formula	ICSD	MSG	T.C.	
0.152	LiFePO4	*	14.78( $P2_1/c'$ )	w/o	
Topology	 $U=0$ , LCEBR	 $U=1\text{eV}$ , LCEBR	 $U=2\text{eV}$ , LCEBR	 $U=3\text{eV}$ , LCEBR	 $U=4\text{eV}$ , LCEBR

TABLE LXXXIX. Topology phase diagram of LiFePO4.

BCSID	Formula	ICSD	MSG	T.C.	
0.28	LiFeSi2O6	158579	14.78( $P2_1/c'$ )	w/o	
Topology	 $U=0$ , LCEBR	 $U=1\text{eV}$ , LCEBR	 $U=2\text{eV}$ , LCEBR	 $U=3\text{eV}$ , LCEBR	 $U=4\text{eV}$ , LCEBR

TABLE XC. Topology phase diagram of LiFeSi2O6.

BCSID	Formula	ICSD	MSG	T.C.	
0.121	Li <sub>2</sub> Co(SO <sub>4</sub> ) <sub>2</sub>	*	14.79( $P2_1/c'$ )	$\mathbb{Z}_2\mathbb{Z}_4$	
Topology	 $U=0$ , LCEBR	 $U=1\text{eV}$ , LCEBR	 $U=2\text{eV}$ , LCEBR	 $U=3\text{eV}$ , LCEBR	 $U=4\text{eV}$ , LCEBR

TABLE XCI. Topology phase diagram of Li<sub>2</sub>Co(SO<sub>4</sub>)<sub>2</sub>.

BCSID	Formula	ICSD	MSG	T.C.	
0.164	Y <sub>2</sub> MnCoO <sub>6</sub>	*	14.79( $P_2'_1/c'$ )	$\mathbb{Z}_2\mathbb{Z}_4$	
Topology	 U=0 , LCEBR	 U=1eV , LCEBR	 U=2eV , LCEBR	 U=3eV , LCEBR	 U=4eV , LCEBR

TABLE XCII. Topology phase diagram of Y<sub>2</sub>MnCoO<sub>6</sub>.

BCSID	Formula	ICSD	MSG	T.C.	
1.133	CuSb <sub>2</sub> O <sub>6</sub>	80576	14.80( $P_a2_1/c$ )	$\mathbb{Z}_2$	
Topology	 U=0 , LCEBR	 U=1eV , LCEBR	 U=2eV , LCEBR	 U=3eV , LCEBR	 U=4eV , LCEBR

TABLE XCIII. Topology phase diagram of CuSb<sub>2</sub>O<sub>6</sub>.

BCSID	Formula	ICSD	MSG	T.C.	
1.147	Li <sub>2</sub> Fe(SO <sub>4</sub> ) <sub>2</sub>	*	14.80( $P_a2_1/c$ )	$\mathbb{Z}_2$	
Topology	 U=0 , LCEBR	 U=1eV , LCEBR	 U=2eV , LCEBR	 U=3eV , LCEBR	 U=4eV , LCEBR

TABLE XCIV. Topology phase diagram of Li<sub>2</sub>Fe(SO<sub>4</sub>)<sub>2</sub>.

BCSID	Formula	ICSD	MSG	T.C.	
1.196	MnV <sub>2</sub> O <sub>6</sub>	*	14.80( $P_a2_1/c$ )	$\mathbb{Z}_2$	
Topology	 U=0 , LCEBR	 U=1eV , LCEBR	 U=2eV , LCEBR	 U=3eV , LCEBR	 U=4eV , LCEBR

TABLE XCV. Topology phase diagram of MnV<sub>2</sub>O<sub>6</sub>.

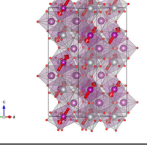
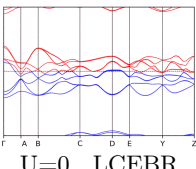
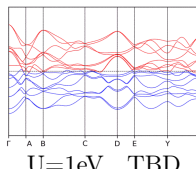
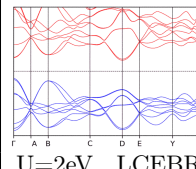
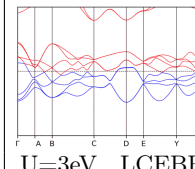
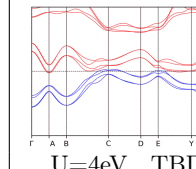
BCSID	Formula	ICSD	MSG	T.C.	
1.199	Sc <sub>2</sub> NiMnO <sub>6</sub>	251833	14.80( $P_a2_1/c$ )	$\mathbb{Z}_2$	
Topology	 U=0 , LCEBR	 U=1eV , TBD	 U=2eV , LCEBR	 U=3eV , LCEBR	 U=4eV , TBD

TABLE XCVI. Topology phase diagram of Sc<sub>2</sub>NiMnO<sub>6</sub>.

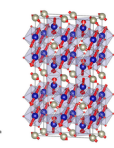
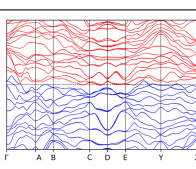
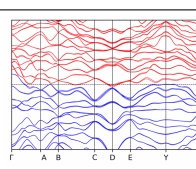
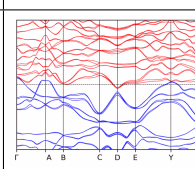
BCSID	Formula	ICSD	MSG	T.C.	
1.201	Cr <sub>2</sub> ReO <sub>6</sub>	*	14.80( $P_a2_1/c$ )	$\mathbb{Z}_2$	
Topology	 U=0 , TI	 U=1eV , LCEBR	 U=2eV , LCEBR	 U=3eV , TBD	 U=4eV , TBD

TABLE XCVII. Topology phase diagram of Cr<sub>2</sub>ReO<sub>6</sub>.

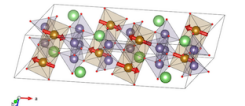
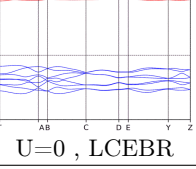
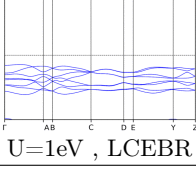
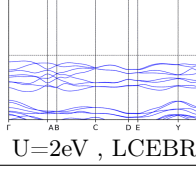
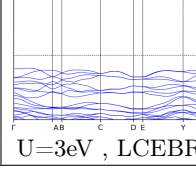
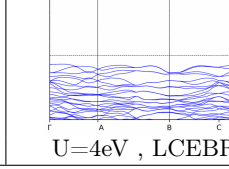
BCSID	Formula	ICSD	MSG	T.C.	
1.39	LiFeGe <sub>2</sub> O <sub>6</sub>	*	14.80( $P_a2_1/c$ )	$\mathbb{Z}_2$	
Topology	 U=0 , LCEBR	 U=1eV , LCEBR	 U=2eV , LCEBR	 U=3eV , LCEBR	 U=4eV , LCEBR

TABLE XCVIII. Topology phase diagram of LiFeGe<sub>2</sub>O<sub>6</sub>.

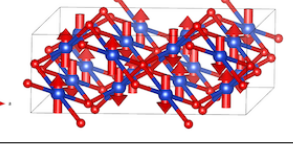
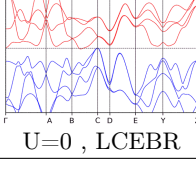
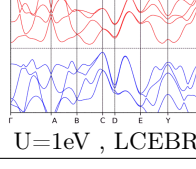
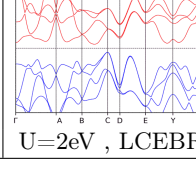
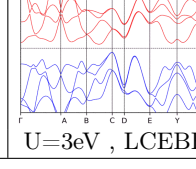
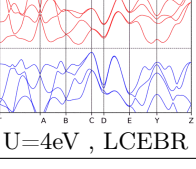
BCSID	Formula	ICSD	MSG	T.C.	
1.62	CuO	*	14.80( $P_a2_1/c$ )	$\mathbb{Z}_2$	
Topology	 U=0 , LCEBR	 U=1eV , LCEBR	 U=2eV , LCEBR	 U=3eV , LCEBR	 U=4eV , LCEBR

TABLE XCIX. Topology phase diagram of CuO.

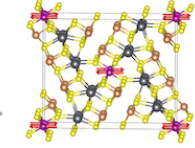
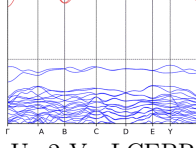
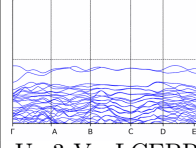
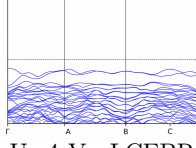
BCSID	Formula	ICSD	MSG	T.C.	
1.63	MnPb4Sb6S14	98581	$14.80(P_a2_1/c)$	$\mathbb{Z}_2$	
Topology	$U=0, \text{LCEBR}$	$U=1\text{eV}, \text{LCEBR}$	$U=2\text{eV}, \text{LCEBR}$	$U=3\text{eV}, \text{LCEBR}$	
					

TABLE C. Topology phase diagram of MnPb4Sb6S14.

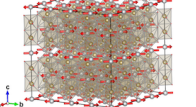
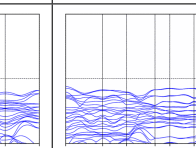
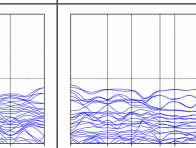
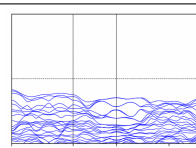
BCSID	Formula	ICSD	MSG	T.C.	
1.112	NiTa2O6	247807	$14.82(P_c2_1/c)$	$\mathbb{Z}_2$	
Topology	$U=0, \text{LCEBR}$	$U=1\text{eV}, \text{LCEBR}$	$U=2\text{eV}, \text{LCEBR}$	$U=3\text{eV}, \text{LCEBR}$	
					

TABLE CI. Topology phase diagram of NiTa2O6.

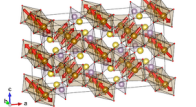
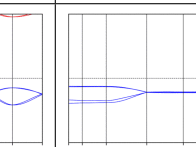
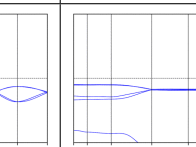
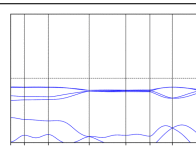
BCSID	Formula	ICSD	MSG	T.C.	
1.117	NaFePO4	85671	$14.82(P_c2_1/c)$	$\mathbb{Z}_2$	
Topology	$U=0, \text{LCEBR}$	$U=1\text{eV}, \text{LCEBR}$	$U=2\text{eV}, \text{LCEBR}$	$U=3\text{eV}, \text{LCEBR}$	
					

TABLE CII. Topology phase diagram of NaFePO4.

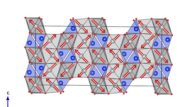
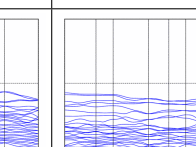
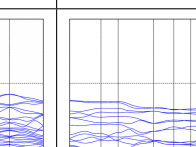
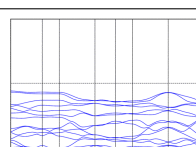
BCSID	Formula	ICSD	MSG	T.C.	
1.203	Ni2SiO4	35675	$14.82(P_c2_1/c)$	$\mathbb{Z}_2$	
Topology	$U=0, \text{LCEBR}$	$U=1\text{eV}, \text{LCEBR}$	$U=2\text{eV}, \text{LCEBR}$	$U=3\text{eV}, \text{LCEBR}$	
					

TABLE CIII. Topology phase diagram of Ni2SiO4.

BCSID	Formula	ICSD	MSG	T.C.	
1.204	Ni <sub>2</sub> SiO <sub>4</sub>	35675	$14.82(P_c2_1/c)$	$\mathbb{Z}_2$	
Topology	    	    	    	    	    

TABLE CIV. Topology phase diagram of Ni<sub>2</sub>SiO<sub>4</sub>.

BCSID	Formula	ICSD	MSG	T.C.	
1.26	CsFe <sub>2</sub> Se <sub>3</sub>	*	$14.82(P_c2_1/c)$	$\mathbb{Z}_2$	
Topology	    	    	    	    	    

TABLE CV. Topology phase diagram of CsFe<sub>2</sub>Se<sub>3</sub>.

BCSID	Formula	ICSD	MSG	T.C.	
1.154	NaFeSi <sub>2</sub> O <sub>6</sub>	*	$14.84(P_C2_1/c)$	$\mathbb{Z}_2$	
Topology	    	    	    	    	    

TABLE CVI. Topology phase diagram of NaFeSi<sub>2</sub>O<sub>6</sub>.

BCSID	Formula	ICSD	MSG	T.C.	
1.169	CaCoGe <sub>2</sub> O <sub>6</sub>	*	$14.84(P_C2_1/c)$	$\mathbb{Z}_2$	
Topology	    	    	    	    	    

TABLE CVII. Topology phase diagram of CaCoGe<sub>2</sub>O<sub>6</sub>.

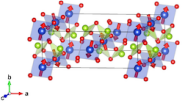
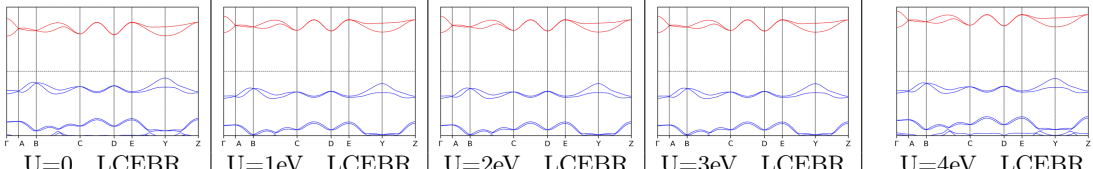
BCSID	Formula	ICSD	MSG	T.C.	
1.2	CuSe <sub>2</sub> O <sub>5</sub>	603	$14.84(P_C 2_1/c)$	$\mathbb{Z}_2$	
Topology					

TABLE CVIII. Topology phase diagram of CuSe<sub>2</sub>O<sub>5</sub>.

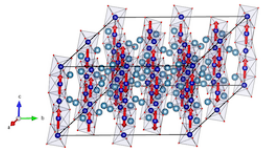
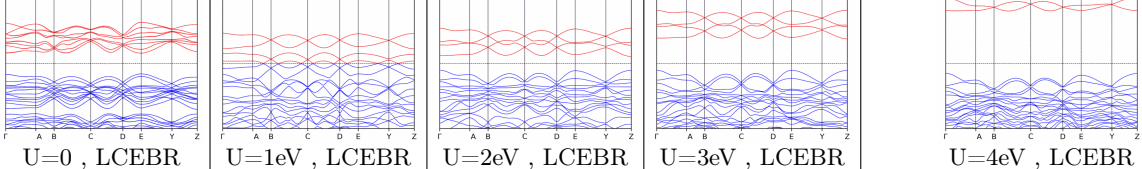
BCSID	Formula	ICSD	MSG	T.C.	
1.60	Ca <sub>3</sub> Co <sub>2</sub> O <sub>6</sub>	246282	$14.84(P_C 2_1/c)$	$\mathbb{Z}_2$	
Topology					

TABLE CIX. Topology phase diagram of Ca<sub>3</sub>Co<sub>2</sub>O<sub>6</sub>.

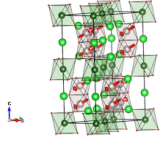
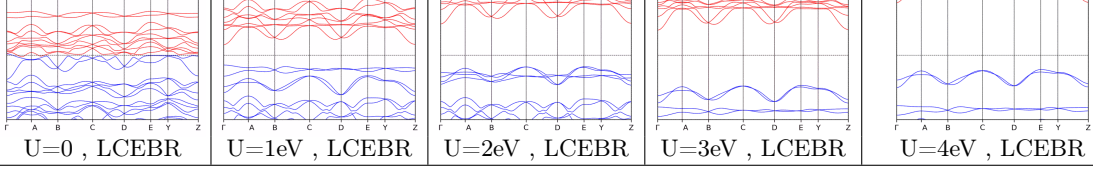
BCSID	Formula	ICSD	MSG	T.C.	
1.94	Ba <sub>3</sub> LaRu <sub>2</sub> O <sub>9</sub>	*	$14.84(P_C 2_1/c)$	$\mathbb{Z}_2$	
Topology					

TABLE CX. Topology phase diagram of Ba<sub>3</sub>LaRu<sub>2</sub>O<sub>9</sub>.

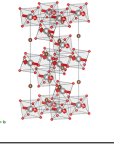
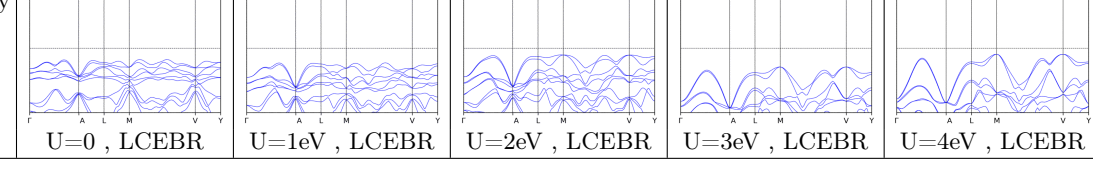
BCSID	Formula	ICSD	MSG	T.C.	
0.113	NiCO <sub>3</sub>	173985	$15.85(C2/c)$	$\mathbb{Z}_2 \mathbb{Z}_2$	
Topology					

TABLE CXI. Topology phase diagram of NiCO<sub>3</sub>.

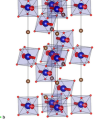
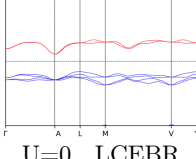
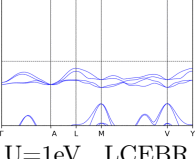
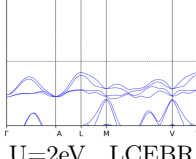
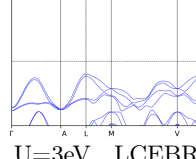
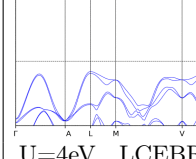
BCSID	Formula	ICSD	MSG	T.C.	
0.114	CoCO <sub>3</sub>	61066	15.85( $C2/c$ )	$\mathbb{Z}_2\mathbb{Z}_2$	
Topology	 U=0 , LCEBR	 U=1eV , LCEBR	 U=2eV , LCEBR	 U=3eV , LCEBR	 U=4eV , LCEBR

TABLE CXII. Topology phase diagram of CoCO<sub>3</sub>.

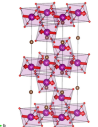
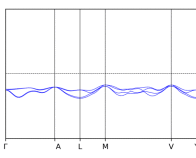
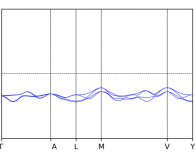
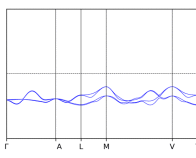
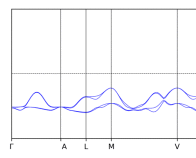
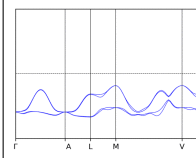
BCSID	Formula	ICSD	MSG	T.C.	
0.115	MnCO <sub>3</sub>	*	15.85( $C2/c$ )	$\mathbb{Z}_2\mathbb{Z}_2$	
Topology	 U=0 , LCEBR	 U=1eV , LCEBR	 U=2eV , LCEBR	 U=3eV , LCEBR	 U=4eV , LCEBR

TABLE CXIII. Topology phase diagram of MnCO<sub>3</sub>.

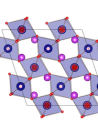
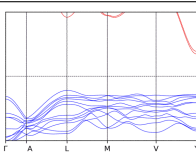
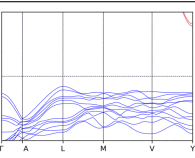
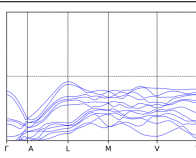
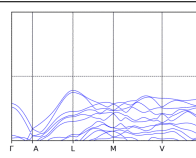
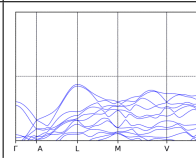
BCSID	Formula	ICSD	MSG	T.C.	
0.138	BiCrO <sub>3</sub>	174405	15.85( $C2/c$ )	$\mathbb{Z}_2\mathbb{Z}_2$	
Topology	 U=0 , LCEBR	 U=1eV , LCEBR	 U=2eV , LCEBR	 U=3eV , LCEBR	 U=4eV , LCEBR

TABLE CXIV. Topology phase diagram of BiCrO<sub>3</sub>.

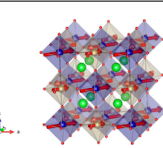
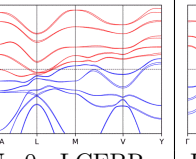
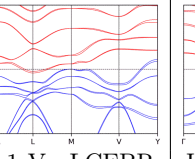
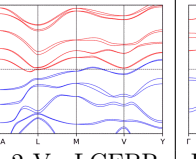
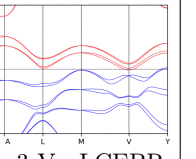
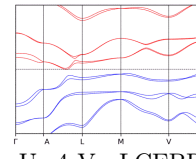
BCSID	Formula	ICSD	MSG	T.C.	
0.210	Sr <sub>2</sub> CoOsO <sub>6</sub>	*	15.85( $C2/c$ )	$\mathbb{Z}_2\mathbb{Z}_2$	
Topology	 U=0 , LCEBR	 U=1eV , LCEBR	 U=2eV , LCEBR	 U=3eV , LCEBR	 U=4eV , LCEBR

TABLE CXV. Topology phase diagram of Sr<sub>2</sub>CoOsO<sub>6</sub>.

BCSID	Formula	ICSD	MSG	T.C.	
0.110	Cr <sub>2</sub> O <sub>3</sub>	75577	$15.87(C2'/c)$	w/o	
Topology	 U=0 , LCEBR	 U=1eV , LCEBR	 U=2eV , LCEBR	 U=3eV , LCEBR	 U=4eV , LCEBR

TABLE CXVI. Topology phase diagram of Cr<sub>2</sub>O<sub>3</sub>.

BCSID	Formula	ICSD	MSG	T.C.	
0.145	Co <sub>3</sub> TeO <sub>6</sub>	183805	$15.87(C2'/c)$	w/o	
Topology	 U=0 , LCEBR	 U=1eV , LCEBR	 U=2eV , LCEBR	 U=3eV , LCEBR	 U=4eV , LCEBR

TABLE CXVII. Topology phase diagram of Co<sub>3</sub>TeO<sub>6</sub>.

BCSID	Formula	ICSD	MSG	T.C.	
0.156	CaMnGe <sub>2</sub> O <sub>6</sub>	*	$15.87(C2'/c)$	w/o	
Topology	 U=0 , LCEBR	 U=1eV , LCEBR	 U=2eV , LCEBR	 U=3eV , LCEBR	 U=4eV , LCEBR

TABLE CXVIII. Topology phase diagram of CaMnGe<sub>2</sub>O<sub>6</sub>.

BCSID	Formula	ICSD	MSG	T.C.	
0.196	Co <sub>4</sub> Nb <sub>2</sub> O <sub>9</sub>	172186	$15.88(C2/c')$	w/o	
Topology	 U=0 , TBD	 U=1eV , LCEBR	 U=2eV , LCEBR	 U=3eV , LCEBR	 U=4eV , LCEBR

TABLE CXIX. Topology phase diagram of Co<sub>4</sub>Nb<sub>2</sub>O<sub>9</sub>.

BCSID	Formula	ICSD	MSG	T.C.	
0.197	Co4Nb2O9	*	15.88( $C2/c'$ )	w/o	
Topology	 U=0 , LCEBR	 U=1eV , LCEBR	 U=2eV , LCEBR	 U=3eV , LCEBR	 U=4eV , LCEBR

TABLE CXX. Topology phase diagram of Co4Nb2O9.

BCSID	Formula	ICSD	MSG	T.C.	
0.112	FeBO3	34474	15.89( $C2'/c'$ )	$\mathbb{Z}_2\mathbb{Z}_4$	
Topology	 U=0 , LCEBR	 U=1eV , LCEBR	 U=2eV , LCEBR	 U=3eV , LCEBR	 U=4eV , LCEBR

TABLE CXXI. Topology phase diagram of FeBO3.

BCSID	Formula	ICSD	MSG	T.C.	
0.128	FeSO4F	182945	15.89( $C2'/c'$ )	$\mathbb{Z}_2\mathbb{Z}_4$	
Topology	 U=0 , LCEBR	 U=1eV , LCEBR	 U=2eV , LCEBR	 U=3eV , LCEBR	 U=4eV , LCEBR

TABLE CXXII. Topology phase diagram of FeSO4F.

BCSID	Formula	ICSD	MSG	T.C.	
0.176	Mn3Ti2Te6	41021	15.89( $C2'/c'$ )	$\mathbb{Z}_2\mathbb{Z}_4$	
Topology	 U=0 , LCEBR	 U=1eV , LCEBR	 U=2eV , LCEBR	 U=3eV , LCEBR	 U=4eV , LCEBR

TABLE CXXIII. Topology phase diagram of Mn3Ti2Te6.

BCSID	Formula	ICSD	MSG	T.C.	
0.3	Ca3LiOsO6	*	15.89( $C2'/c'$ )	$\mathbb{Z}_2\mathbb{Z}_4$	
Topology					

TABLE CXXIV. Topology phase diagram of Ca3LiOsO6.

BCSID	Formula	ICSD	MSG	T.C.	
0.65	Fe2O3-alpha	*	15.89( $C2'/c'$ )	$\mathbb{Z}_2\mathbb{Z}_4$	
Topology					

TABLE CXXV. Topology phase diagram of Fe2O3-alpha.

BCSID	Formula	ICSD	MSG	T.C.	
1.168	Sr2CuTeO6	*	15.90( $C_c2/c$ )	$\mathbb{Z}_2$	
Topology					

TABLE CXXVI. Topology phase diagram of Sr2CuTeO6.

BCSID	Formula	ICSD	MSG	T.C.	
1.17	CoV2O6-alpha	*	15.90( $C_c2/c$ )	$\mathbb{Z}_2$	
Topology					

TABLE CXXVII. Topology phase diagram of CoV2O6-alpha.

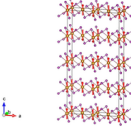
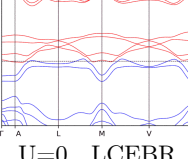
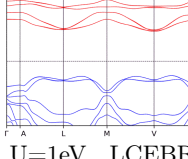
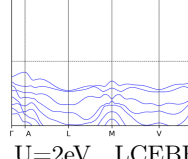
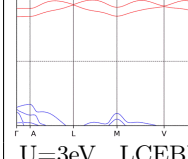
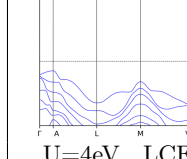
BCSID	Formula	ICSD	MSG	T.C.	
1.209	FeI <sub>2</sub>	52369	$15.90(C_c2/c)$	$\mathbb{Z}_2$	
Topology	 U=0 , LCEBR	 U=1eV , LCEBR	 U=2eV , LCEBR	 U=3eV , LCEBR	 U=4eV , LCEBR

TABLE CXXVIII. Topology phase diagram of FeI<sub>2</sub>.

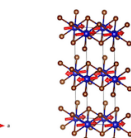
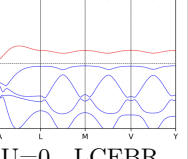
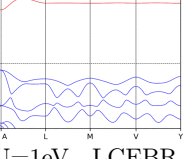
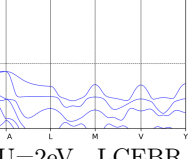
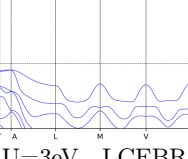
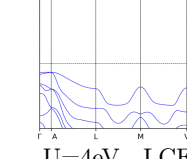
BCSID	Formula	ICSD	MSG	T.C.	
1.245	CoBr <sub>2</sub>	52364	$15.90(C_c2/c)$	$\mathbb{Z}_2$	
Topology	 U=0 , LCEBR	 U=1eV , LCEBR	 U=2eV , LCEBR	 U=3eV , LCEBR	 U=4eV , LCEBR

TABLE CXXIX. Topology phase diagram of CoBr<sub>2</sub>.

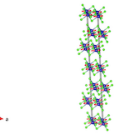
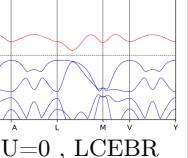
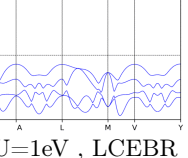
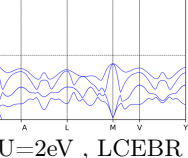
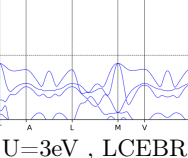
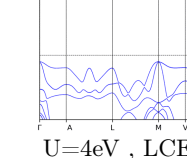
BCSID	Formula	ICSD	MSG	T.C.	
1.246	CoCl <sub>2</sub>	44398	$15.90(C_c2/c)$	$\mathbb{Z}_2$	
Topology	 U=0 , LCEBR	 U=1eV , LCEBR	 U=2eV , LCEBR	 U=3eV , LCEBR	 U=4eV , LCEBR

TABLE CXXX. Topology phase diagram of CoCl<sub>2</sub>.

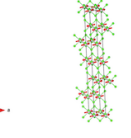
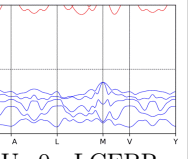
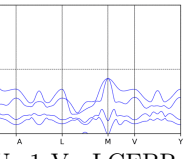
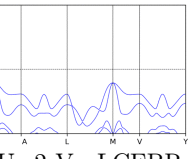
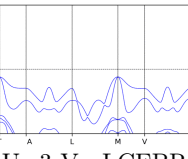
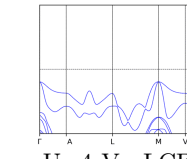
BCSID	Formula	ICSD	MSG	T.C.	
1.247	NiCl <sub>2</sub>	14208	$15.90(C_c2/c)$	$\mathbb{Z}_2$	
Topology	 U=0 , LCEBR	 U=1eV , LCEBR	 U=2eV , LCEBR	 U=3eV , LCEBR	 U=4eV , LCEBR

TABLE CXXXI. Topology phase diagram of NiCl<sub>2</sub>.

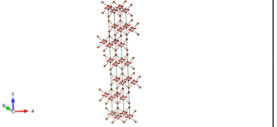
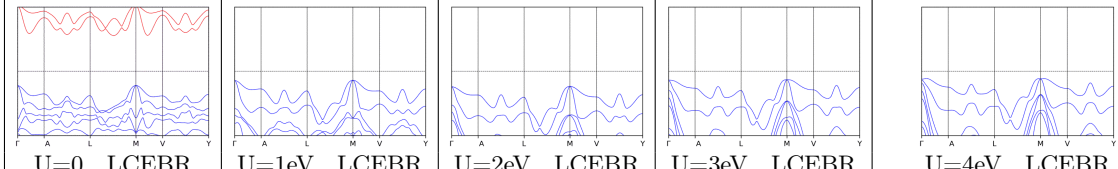
BCSID	Formula	ICSD	MSG	T.C.	
1.248	NiBr <sub>2</sub>	22106	15.90( $C_c2/c$ )	$\mathbb{Z}_2$	
Topology	 U=0 , LCEBR    U=1eV , LCEBR    U=2eV , LCEBR    U=3eV , LCEBR    U=4eV , LCEBR				

TABLE CXXXII. Topology phase diagram of NiBr<sub>2</sub>.

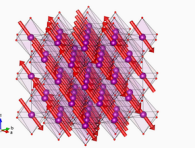
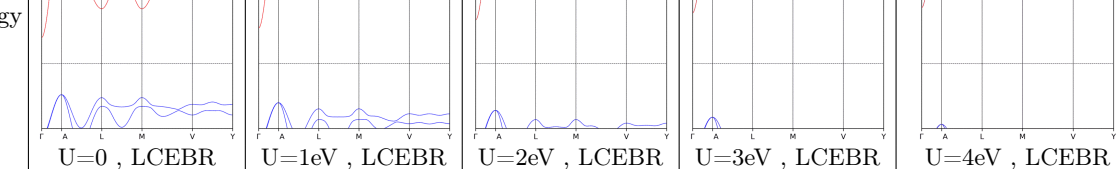
BCSID	Formula	ICSD	MSG	T.C.	
1.31	MnO	9864	15.90( $C_c2/c$ )	$\mathbb{Z}_2$	
Topology	 U=0 , LCEBR    U=1eV , LCEBR    U=2eV , LCEBR    U=3eV , LCEBR    U=4eV , LCEBR				

TABLE CXXXIII. Topology phase diagram of MnO.

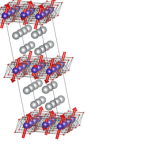
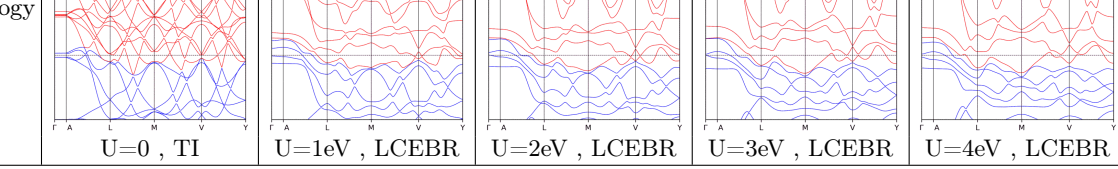
BCSID	Formula	ICSD	MSG	T.C.	
1.49	Ag <sub>2</sub> NiO <sub>2</sub>	*	15.90( $C_c2/c$ )	$\mathbb{Z}_2$	
Topology	 U=0 , TI    U=1eV , LCEBR    U=2eV , LCEBR    U=3eV , LCEBR    U=4eV , LCEBR				

TABLE CXXXIV. Topology phase diagram of Ag<sub>2</sub>NiO<sub>2</sub>.

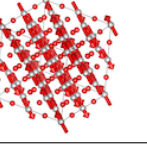
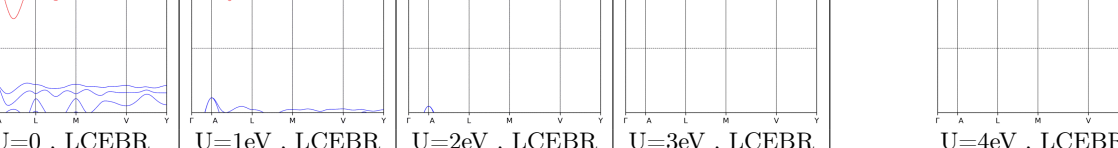
BCSID	Formula	ICSD	MSG	T.C.	
1.6	NiO	*	15.90( $C_c2/c$ )	$\mathbb{Z}_2$	
Topology	 U=0 , LCEBR    U=1eV , LCEBR    U=2eV , LCEBR    U=3eV , LCEBR    U=4eV , LCEBR				

TABLE CXXXV. Topology phase diagram of NiO.

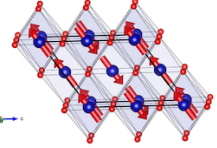
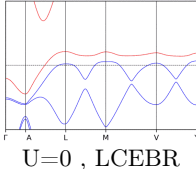
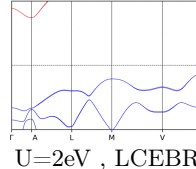
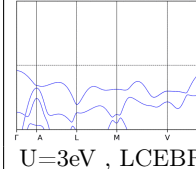
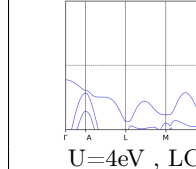
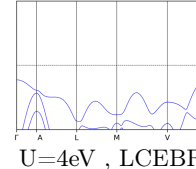
BCSID	Formula	ICSD	MSG	T.C.		
1.69	CoO	*	15.90( $C_c 2/c$ )	$\mathbb{Z}_2$		
Topology	 U=0 , LCEBR		 U=1eV , LCEBR	 U=2eV , LCEBR	 U=3eV , LCEBR	 U=4eV , LCEBR

TABLE CXXXVI. Topology phase diagram of CoO.

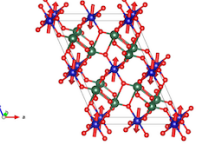
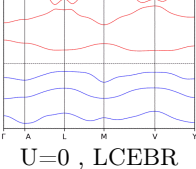
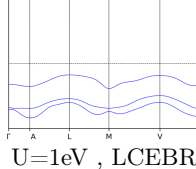
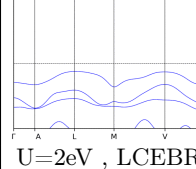
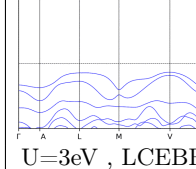
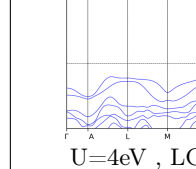
BCSID	Formula	ICSD	MSG	T.C.	
1.70	CoV2O6	263002	15.90( $C_c 2/c$ )	$\mathbb{Z}_2$	
Topology	 U=0 , LCEBR	 U=1eV , LCEBR	 U=2eV , LCEBR	 U=3eV , LCEBR	 U=4eV , LCEBR

TABLE CXXXVII. Topology phase diagram of CoV2O6.

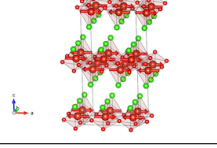
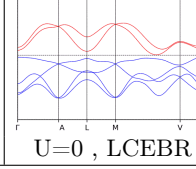
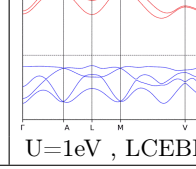
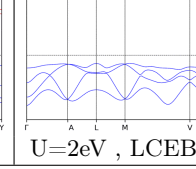
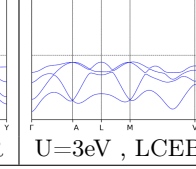
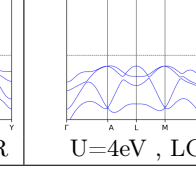
BCSID	Formula	ICSD	MSG	T.C.	
1.37	VOCl	*	15.91( $C_a 2/c$ )	$\mathbb{Z}_2$	
Topology	 U=0 , LCEBR	 U=1eV , LCEBR	 U=2eV , LCEBR	 U=3eV , LCEBR	 U=4eV , LCEBR

TABLE CXXXVIII. Topology phase diagram of VOCl.

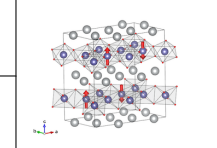
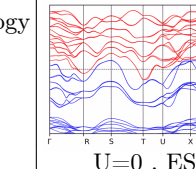
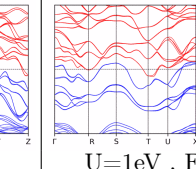
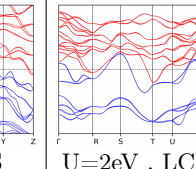
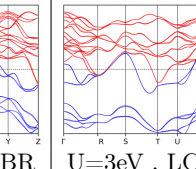
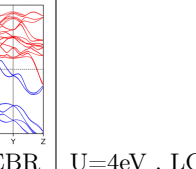
BCSID	Formula	ICSD	MSG	T.C.	
1.50	AgNiO2	*	18.22( $P_B 2_1 2_1 2$ )	w/o	
Topology	 U=0 , ES	 U=1eV , ES	 U=2eV , LCEBR	 U=3eV , LCEBR	 U=4eV , LCEBR

TABLE CXXXIX. Topology phase diagram of AgNiO2.

BCSID	Formula	ICSD	MSG	T.C.	
0.17	FePO4	*	19.25( $P2_12_12_1$ )	w/o	
Topology	 U=0 , LCEBR    U=1eV , LCEBR    U=2eV , LCEBR    U=3eV , LCEBR    U=4eV , LCEBR				

TABLE CXL. Topology phase diagram of FePO4.

BCSID	Formula	ICSD	MSG	T.C.	
0.129	Cu3Mo2O9	173779	19.27( $P2'_12'_12_1$ )	w/o	
Topology	 U=0 , LCEBR    U=1eV , LCEBR    U=2eV , LCEBR    U=3eV , LCEBR    U=4eV , LCEBR				

TABLE CXLI. Topology phase diagram of Cu3Mo2O9.

BCSID	Formula	ICSD	MSG	T.C.	
1.224	CoNb2O6	15854	19.28( $P_c2_12_12_1$ )	w/o	
Topology	 U=0 , LCEBR    U=1eV , LCEBR    U=2eV , LCEBR    U=3eV , LCEBR    U=4eV , LCEBR				

TABLE CXLII. Topology phase diagram of CoNb2O6.

BCSID	Formula	ICSD	MSG	T.C.	
1.0.4	CsNiCl3	59371	20.34( $C22'2'_1$ )	w/o	
Topology	 U=0 , LCEBR    U=1eV , LCEBR    U=2eV , LCEBR    U=3eV , LCEBR    U=4eV , LCEBR				

TABLE CXLIII. Topology phase diagram of CsNiCl3.

BCSID	Formula	ICSD	MSG	T.C.	
1.138	MgV <sub>2</sub> O <sub>4</sub>	*	20.37( <i>C</i> <sub>A</sub> 2221)	w/o	
Topology	 U=0 , LCEBR	 U=1eV , LCEBR	 U=2eV , LCEBR	 U=3eV , LCEBR	 U=4eV , LCEBR

TABLE CXLIV. Topology phase diagram of MgV<sub>2</sub>O<sub>4</sub>.

BCSID	Formula	ICSD	MSG	T.C.	
0.97	FeSb <sub>2</sub> O <sub>4</sub>	182798	26.66( <i>Pmc</i> 2 <sub>1</sub> )	w/o	
Topology	 U=0 , LCEBR	 U=1eV , LCEBR	 U=2eV , LCEBR	 U=3eV , LCEBR	 U=4eV , LCEBR

TABLE CXLV. Topology phase diagram of FeSb<sub>2</sub>O<sub>4</sub>.

BCSID	Formula	ICSD	MSG	T.C.		
0.130	Cu <sub>3</sub> Mo <sub>2</sub> O <sub>9</sub>	*	26.68( <i>Pm'</i> c21')	w/o		
Topology	 U=0 , LCEBR		 U=1eV , LCEBR	 U=2eV , LCEBR	 U=3eV , LCEBR	 U=4eV , LCEBR

TABLE CXLVI. Topology phase diagram of Cu<sub>3</sub>Mo<sub>2</sub>O<sub>9</sub>.

BCSID	Formula	ICSD	MSG	T.C.	
0.133	Ni <sub>3</sub> B <sub>7</sub> O <sub>13</sub> Cl	*	29.101( <i>Pc'</i> a2' <sub>1</sub> )	w/o	
Topology					
	U=0 , LCEBR	U=1eV , LCEBR	U=2eV , LCEBR	U=3eV , LCEBR	U=4eV , LCEBR

TABLE CXLVII. Topology phase diagram of Ni<sub>3</sub>B<sub>7</sub>O<sub>13</sub>Cl.

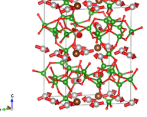
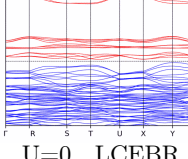
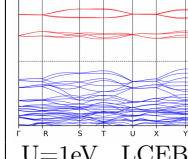
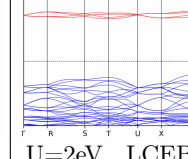
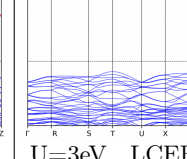
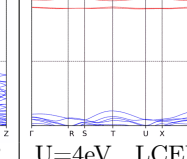
BCSID	Formula	ICSD	MSG	T.C.	
0.135	Ni3B7O13Br	79127	29.101( $Pc'a2_1'$ )	w/o	
Topology	 U=0 , LCEBR	 U=1eV , LCEBR	 U=2eV , LCEBR	 U=3eV , LCEBR	 U=4eV , LCEBR

TABLE CXLVIII. Topology phase diagram of Ni3B7O13Br.

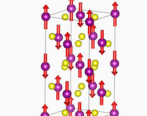
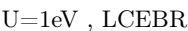
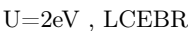
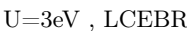
BCSID	Formula	ICSD	MSG	T.C.	
1.18	MnS2	36545	29.105( $P_bca2_1$ )	w/o	
Topology	 U=0 , LCEBR	 U=1eV , LCEBR	 U=2eV , LCEBR	 U=3eV , LCEBR	 U=4eV , LCEBR

TABLE CXLIX. Topology phase diagram of MnS2.

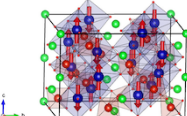
BCSID	Formula	ICSD	MSG	T.C.	
1.71	SrCo2V2O8	400765	29.110( $P_1ca2_1$ )	w/o	
Topology	 U=0 , LCEBR	 U=1eV , LCEBR	 U=2eV , LCEBR	 U=3eV , LCEBR	 U=4eV , LCEBR

TABLE CL. Topology phase diagram of SrCo2V2O8.

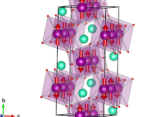
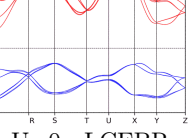
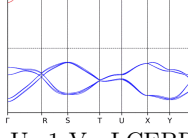
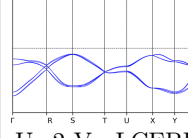
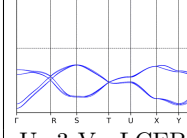
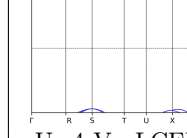
BCSID	Formula	ICSD	MSG	T.C.	
1.101	LuMnO3	*	31.129( $P_bmn2_1$ )	w/o	
Topology	 U=0 , LCEBR	 U=1eV , LCEBR	 U=2eV , LCEBR	 U=3eV , LCEBR	 U=4eV , LCEBR

TABLE CLI. Topology phase diagram of LuMnO3.

BCSID	Formula	ICSD	MSG	T.C.	
0.38	GaFeO <sub>3</sub>	151722	33.147( $Pna'2_1'$ )	w/o	
Topology	 U=0 , LCEBR	 U=1eV , LCEBR	 U=2eV , LCEBR	 U=3eV , LCEBR	 U=4eV , LCEBR

TABLE CLII. Topology phase diagram of GaFeO<sub>3</sub>.

BCSID	Formula	ICSD	MSG	T.C.	
0.46	CaBaCo <sub>4</sub> O <sub>7</sub>	*	33.147( $Pna'2_1'$ )	w/o	
Topology	 U=0 , LCEBR	 U=1eV , LCEBR	 U=2eV , LCEBR	 U=3eV , LCEBR	 U=4eV , LCEBR

TABLE CLIII. Topology phase diagram of CaBaCo<sub>4</sub>O<sub>7</sub>.

BCSID	Formula	ICSD	MSG	T.C.	
1.86	GeV4S8	*	33.149( $P_{ana}2_1$ )	w/o	
Topology	 U=0 , LCEBR	 U=1eV , LCEBR	 U=2eV , LCEBR	 U=3eV , LCEBR	 U=4eV , LCEBR

TABLE CLIV. Topology phase diagram of GeV4S8.

BCSID	Formula	ICSD	MSG	T.C.	
1.263	Ca <sub>3</sub> Ru <sub>2</sub> O <sub>7</sub>	153776	33.154( $P_Cna2_1$ )	w/o	
Topology	 U=0 , ES	 U=1eV , ES	 U=2eV , LCEBR	 U=3eV , LCEBR	 U=4eV , LCEBR

TABLE CLV. Topology phase diagram of Ca<sub>3</sub>Ru<sub>2</sub>O<sub>7</sub>.

BCSID	Formula	ICSD	MSG	T.C.	
0.56	Ba <sub>2</sub> CoGeO <sub>7</sub>	*	35.167( $Cm'm2'$ )	w/o	
Topology	 $U=0$ , LCEBR	 $U=1\text{eV}$ , LCEBR	 $U=2\text{eV}$ , LCEBR	 $U=3\text{eV}$ , LCEBR	 $U=4\text{eV}$ , LCEBR

TABLE CLVI. Topology phase diagram of Ba<sub>2</sub>CoGeO<sub>7</sub>.

BCSID	Formula	ICSD	MSG	T.C.	
0.23	Ca <sub>3</sub> Mn <sub>2</sub> O <sub>7</sub>	55666	36.174( $Cm'c2'_1$ )	w/o	
Topology	 $U=0$ , LCEBR	 $U=1\text{eV}$ , LCEBR	 $U=2\text{eV}$ , LCEBR	 $U=3\text{eV}$ , LCEBR	 $U=4\text{eV}$ , LCEBR

TABLE CLVII. Topology phase diagram of Ca<sub>3</sub>Mn<sub>2</sub>O<sub>7</sub>.

BCSID	Formula	ICSD	MSG	T.C.	
1.0.3	CsCoBr <sub>3</sub>	*	36.174( $Cm'c2'_1$ )	w/o	
Topology	 $U=0$ , LCEBR	 $U=1\text{eV}$ , LCEBR	 $U=2\text{eV}$ , LCEBR	 $U=3\text{eV}$ , LCEBR	 $U=4\text{eV}$ , LCEBR

TABLE CLVIII. Topology phase diagram of CsCoBr<sub>3</sub>.

BCSID	Formula	ICSD	MSG	T.C.	
0.191	BaCuF <sub>4</sub>	9930	36.176( $Cm'c'2_1$ )	w/o	
Topology	 $U=0$ , LCEBR	 $U=1\text{eV}$ , LCEBR	 $U=2\text{eV}$ , LCEBR	 $U=3\text{eV}$ , LCEBR	 $U=4\text{eV}$ , LCEBR

TABLE CLIX. Topology phase diagram of BaCuF<sub>4</sub>.

BCSID	Formula	ICSD	MSG	T.C.	
1.74	BiMn <sub>2</sub> O <sub>5</sub>	*	36.178( $C_a mc2_1$ )	w/o	
Topology	 U=0 , LCEBR	 U=1eV , LCEBR	 U=2eV , LCEBR	 U=3eV , LCEBR	 U=4eV , LCEBR

TABLE CLX. Topology phase diagram of BiMn<sub>2</sub>O<sub>5</sub>.

BCSID	Formula	ICSD	MSG	T.C.	
1.172	NiTa <sub>2</sub> O <sub>6</sub>	*	41.217( $A_bba2$ )	w/o	
Topology	 U=0 , LCEBR	 U=1eV , LCEBR	 U=2eV , LCEBR	 U=3eV , LCEBR	 U=4eV , LCEBR

TABLE CLXI. Topology phase diagram of NiTa<sub>2</sub>O<sub>6</sub>.

BCSID	Formula	ICSD	MSG	T.C.	
0.137	Cu <sub>2</sub> V <sub>2</sub> O <sub>7</sub>	*	43.227( $Fd'd'2$ )	w/o	
Topology	 U=0 , LCEBR	 U=1eV , LCEBR	 U=2eV , LCEBR	 U=3eV , LCEBR	 U=4eV , LCEBR

TABLE CLXII. Topology phase diagram of Cu<sub>2</sub>V<sub>2</sub>O<sub>7</sub>.

BCSID	Formula	ICSD	MSG	T.C.	
0.62	SrMn <sub>2</sub> V <sub>2</sub> O <sub>8</sub>	182224	45.237( $Ib'a2'$ )	w/o	
Topology	 U=0 , LCEBR	 U=1eV , LCEBR	 U=2eV , LCEBR	 U=3eV , LCEBR	 U=4eV , LCEBR

TABLE CLXIII. Topology phase diagram of SrMn<sub>2</sub>V<sub>2</sub>O<sub>8</sub>.

BCSID	Formula	ICSD	MSG	T.C.	
1.42	La <sub>2</sub> NiO <sub>4</sub>	69753	53.335( $P_C mna$ )	$\mathbb{Z}_2$	
Topology	 U=0 , LCEBR	 U=1eV , LCEBR	 U=2eV , LCEBR	 U=3eV , LCEBR	 U=4eV , LCEBR

TABLE CLXIV. Topology phase diagram of La<sub>2</sub>NiO<sub>4</sub>.

BCSID	Formula	ICSD	MSG	T.C.	
1.3	Sr <sub>2</sub> IrO <sub>4</sub>	78261	54.352( $P_{Icc}\bar{a}$ )	$\mathbb{Z}_2$	
Topology	 U=0 , LCEBR	 U=1eV , LCEBR	 U=2eV , LCEBR	 U=3eV , LCEBR	 U=4eV , LCEBR

TABLE CLXV. Topology phase diagram of Sr<sub>2</sub>IrO<sub>4</sub>.

BCSID	Formula	ICSD	MSG	T.C.	
1.30	BaCo <sub>2</sub> V <sub>2</sub> O <sub>8</sub>	*	54.352( $P_{Icc}\bar{a}$ )	$\mathbb{Z}_2$	
Topology	 U=0 , LCEBR	 U=1eV , LCEBR	 U=2eV , LCEBR	 U=3eV , LCEBR	 U=4eV , LCEBR

TABLE CLXVI. Topology phase diagram of BaCo<sub>2</sub>V<sub>2</sub>O<sub>8</sub>.

BCSID	Formula	ICSD	MSG	T.C.	
1.77	Sr <sub>2</sub> IrO <sub>4</sub>	78261	54.352( $P_{Icc}\bar{a}$ )	$\mathbb{Z}_2$	
Topology	 U=0 , LCEBR	 U=1eV , LCEBR	 U=2eV , LCEBR	 U=3eV , LCEBR	 U=4eV , LCEBR

TABLE CLXVII. Topology phase diagram of Sr<sub>2</sub>IrO<sub>4</sub>.

BCSID	Formula	ICSD	MSG	T.C.	
0.45	La <sub>2</sub> NiO <sub>4</sub>	69753	56.369( <i>Pcc'n</i> )	$\mathbb{Z}_2\mathbb{Z}_2$	
Topology					

TABLE CLXVIII. Topology phase diagram of La<sub>2</sub>NiO<sub>4</sub>.

BCSID	Formula	ICSD	MSG	T.C.	
1.122	Cu <sub>3</sub> Bi(SeO <sub>3</sub> ) <sub>2</sub> O <sub>2</sub> Br	280759	56.373( <i>Pccn</i> )	$\mathbb{Z}_2$	
Topology					

TABLE CLXIX. Topology phase diagram of Cu<sub>3</sub>Bi(SeO<sub>3</sub>)<sub>2</sub>O<sub>2</sub>Br.

BCSID	Formula	ICSD	MSG	T.C.	
1.123	Cu <sub>3</sub> Y(SeO <sub>3</sub> ) <sub>2</sub> O <sub>2</sub> Cl	*	56.373( <i>Pccn</i> )	$\mathbb{Z}_2$	
Topology					

TABLE CLXX. Topology phase diagram of Cu<sub>3</sub>Y(SeO<sub>3</sub>)<sub>2</sub>O<sub>2</sub>Cl.

BCSID	Formula	ICSD	MSG	T.C.	
1.23	La <sub>2</sub> CuO <sub>4</sub>	87969	56.374('Paccn')	$\mathbb{Z}_2$	
Topology					

TABLE CLXXI. Topology phase diagram of La<sub>2</sub>CuO<sub>4</sub>.

BCSID	Formula	ICSD	MSG	T.C.	
1.9	Li <sub>2</sub> VOSiO <sub>4</sub>	59359	57.389( $P_{Abcm}$ )	$\mathbb{Z}_2$	
Topology	 U=0 , LCEBR	 U=1eV , LCEBR	 U=2eV , LCEBR	 U=3eV , LCEBR	 U=4eV , LCEBR

TABLE CLXXII. Topology phase diagram of Li<sub>2</sub>VOSiO<sub>4</sub>.

BCSID	Formula	ICSD	MSG	T.C.	
0.143	Cr <sub>2</sub> TeO <sub>6</sub>	24794	58.395( $Pn'nm$ )	w/o	
Topology	 U=0 , LCEBR	 U=1eV , LCEBR	 U=2eV , LCEBR	 U=3eV , LCEBR	 U=4eV , LCEBR

TABLE CLXXIII. Topology phase diagram of Cr<sub>2</sub>TeO<sub>6</sub>.

BCSID	Formula	ICSD	MSG	T.C.	
0.144	Cr <sub>2</sub> WO <sub>6</sub>	24793	58.395( $Pn'nm$ )	w/o	
Topology	 U=0 , LCEBR	 U=1eV , LCEBR	 U=2eV , LCEBR	 U=3eV , LCEBR	 U=4eV , LCEBR

TABLE CLXXIV. Topology phase diagram of Cr<sub>2</sub>WO<sub>6</sub>.

BCSID	Formula	ICSD	MSG	T.C.	
0.75	Cr <sub>2</sub> WO <sub>6</sub>	24793	58.395( $Pn'nm$ )	w/o	
Topology	 U=0 , LCEBR	 U=1eV , LCEBR	 U=2eV , LCEBR	 U=3eV , LCEBR	 U=4eV , LCEBR

TABLE CLXXV. Topology phase diagram of Cr<sub>2</sub>WO<sub>6</sub>.

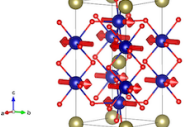
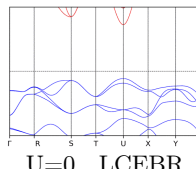
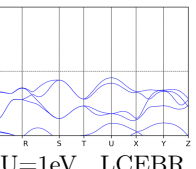
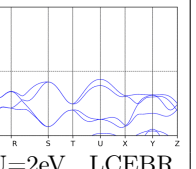
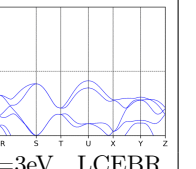
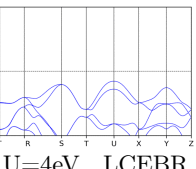
BCSID	Formula	ICSD	MSG	T.C.	
0.76	Cr <sub>2</sub> TeO <sub>6</sub>	24794	58.395( $Pn'n'm$ )	w/o	
Topology	 U=0 , LCEBR	 U=1eV , LCEBR	 U=2eV , LCEBR	 U=3eV , LCEBR	 U=4eV , LCEBR

TABLE CLXXVI. Topology phase diagram of Cr<sub>2</sub>TeO<sub>6</sub>.

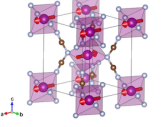
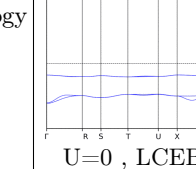
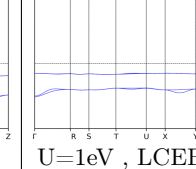
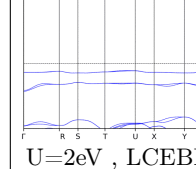
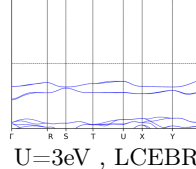
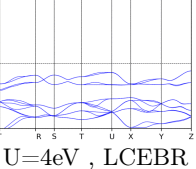
BCSID	Formula	ICSD	MSG	T.C.	
0.131	Mn(N(CN <sub>2</sub> )) <sub>2</sub>	*	58.398( $Pnn'm'$ )	$\mathbb{Z}_2$	
Topology	 U=0 , LCEBR	 U=1eV , LCEBR	 U=2eV , LCEBR	 U=3eV , LCEBR	 U=4eV , LCEBR

TABLE CLXXVII. Topology phase diagram of Mn(N(CN<sub>2</sub>))<sub>2</sub>.

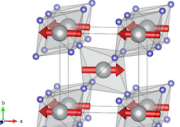
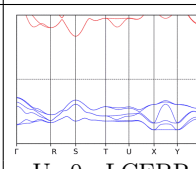
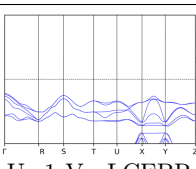
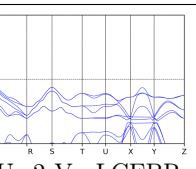
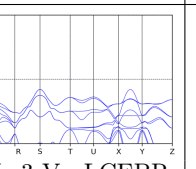
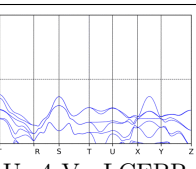
BCSID	Formula	ICSD	MSG	T.C.	
0.36	NiF <sub>2</sub>	*	58.398( $Pnn'm'$ )	$\mathbb{Z}_2$	
Topology	 U=0 , LCEBR	 U=1eV , LCEBR	 U=2eV , LCEBR	 U=3eV , LCEBR	 U=4eV , LCEBR

TABLE CLXXVIII. Topology phase diagram of NiF<sub>2</sub>.

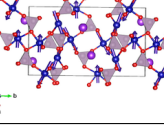
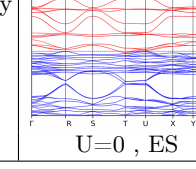
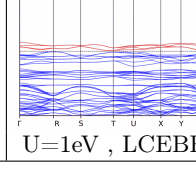
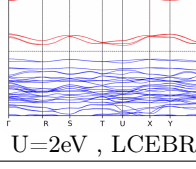
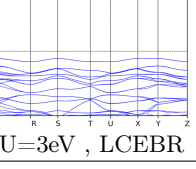
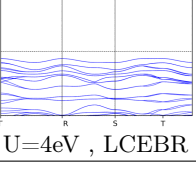
BCSID	Formula	ICSD	MSG	T.C.	
0.85	KCo <sub>4</sub> (PO <sub>4</sub> ) <sub>3</sub>	*	58.398( $Pnn'm'$ )	$\mathbb{Z}_2$	
Topology	 U=0 , ES	 U=1eV , LCEBR	 U=2eV , LCEBR	 U=3eV , LCEBR	 U=4eV , LCEBR

TABLE CLXXIX. Topology phase diagram of KCo<sub>4</sub>(PO<sub>4</sub>)<sub>3</sub>.

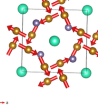
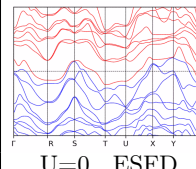
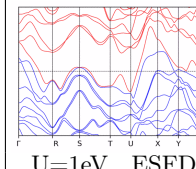
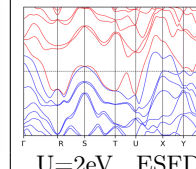
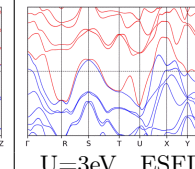
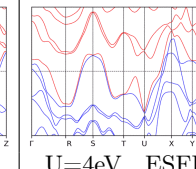
BCSID	Formula	ICSD	MSG	T.C.	
0.140	LuFe <sub>4</sub> Ge <sub>2</sub>	186047	58.399( $Pn'n'm'$ )	w/o	
Topology	 U=0 , ESFD	 U=1eV , ESFD	 U=2eV , ESFD	 U=3eV , ESFD	 U=4eV , ESFD

TABLE CLXXX. Topology phase diagram of LuFe<sub>4</sub>Ge<sub>2</sub>.

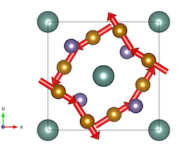
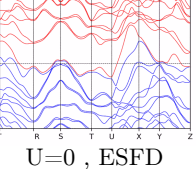
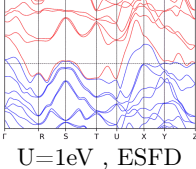
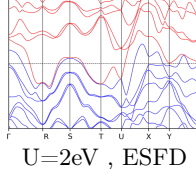
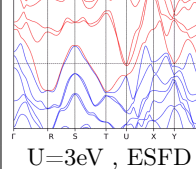
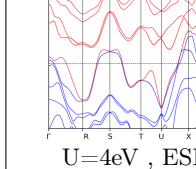
BCSID	Formula	ICSD	MSG	T.C.	
0.27	YFe <sub>4</sub> Ge <sub>2</sub>	*	58.399( $Pn'n'm'$ )	w/o	
Topology	 U=0 , ESFD	 U=1eV , ESFD	 U=2eV , ESFD	 U=3eV , ESFD	 U=4eV , ESFD

TABLE CLXXXI. Topology phase diagram of YFe<sub>4</sub>Ge<sub>2</sub>.

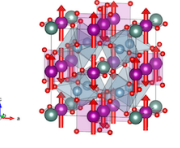
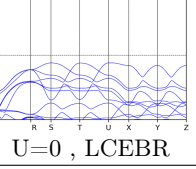
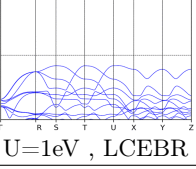
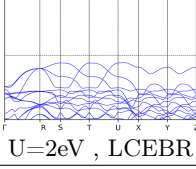
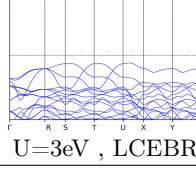
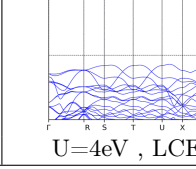
BCSID	Formula	ICSD	MSG	T.C.	
1.158	YMn <sub>3</sub> Al <sub>4</sub> O <sub>12</sub>	*	58.404( $P_{Innm}$ )	$\mathbb{Z}_2$	
Topology	 U=0 , LCEBR	 U=1eV , LCEBR	 U=2eV , LCEBR	 U=3eV , LCEBR	 U=4eV , LCEBR

TABLE CLXXXII. Topology phase diagram of YMn<sub>3</sub>Al<sub>4</sub>O<sub>12</sub>.

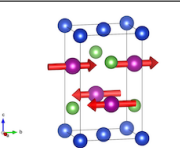
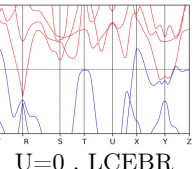
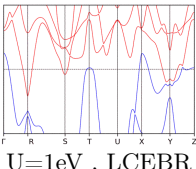
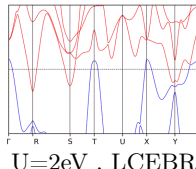
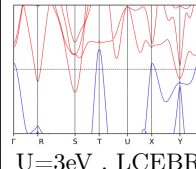
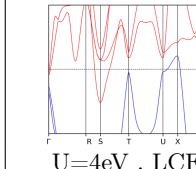
BCSID	Formula	ICSD	MSG	T.C.	
0.222	CuMnAs	423230	59.407( $Pm'mn$ )	w/o	
Topology	 U=0 , LCEBR	 U=1eV , LCEBR	 U=2eV , LCEBR	 U=3eV , LCEBR	 U=4eV , LCEBR

TABLE CLXXXIII. Topology phase diagram of CuMnAs.

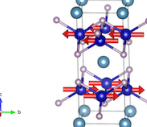
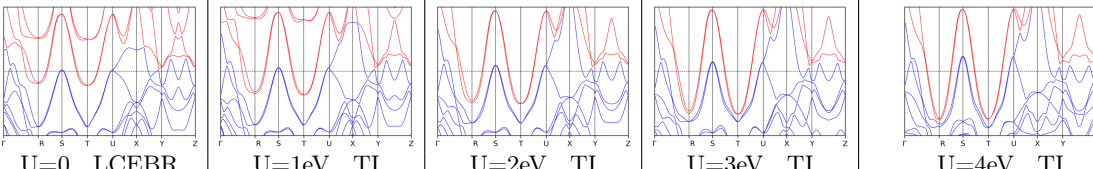
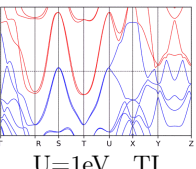
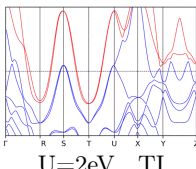
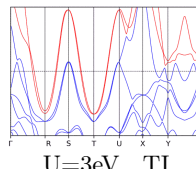
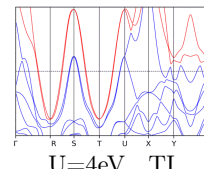
BCSID	Formula	ICSD	MSG	T.C.	
1.252	CaCo <sub>2</sub> P <sub>2</sub>	85892	59.416( $P_{Immn}$ )	$\mathbb{Z}_2$	
Topology					

TABLE CLXXXIV. Topology phase diagram of CaCo<sub>2</sub>P<sub>2</sub>.

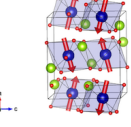
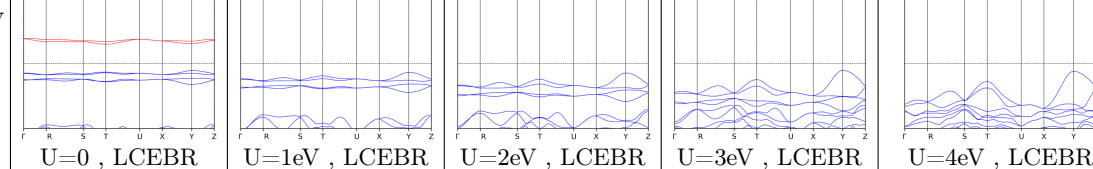
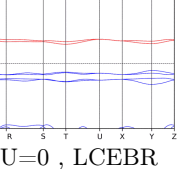
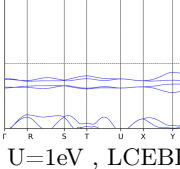
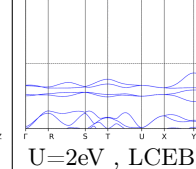
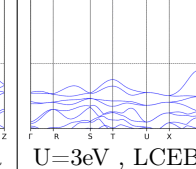
BCSID	Formula	ICSD	MSG	T.C.	
0.119	CoSe <sub>2</sub> O <sub>5</sub>	169716	60.419( $Pb'cn$ )	w/o	
Topology					

TABLE CLXXXV. Topology phase diagram of CoSe<sub>2</sub>O<sub>5</sub>.

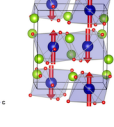
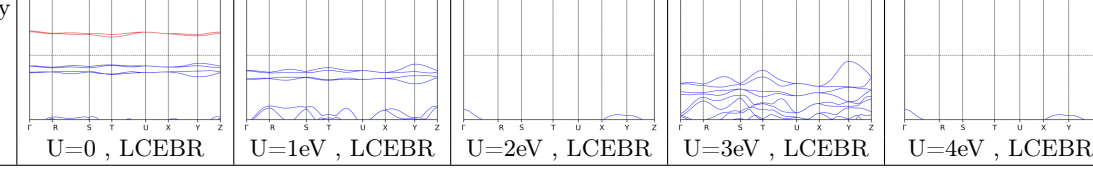
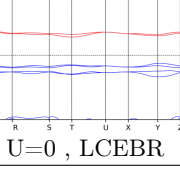
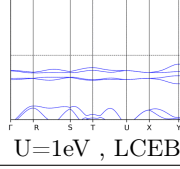
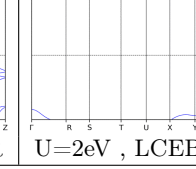
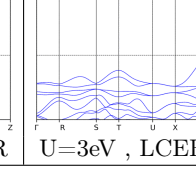
BCSID	Formula	ICSD	MSG	T.C.	
0.161	CoSe <sub>2</sub> O <sub>5</sub>	169716	60.419( $Pb'cn$ )	w/o	
Topology					

TABLE CLXXXVI. Topology phase diagram of CoSe<sub>2</sub>O<sub>5</sub>.

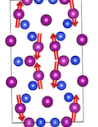
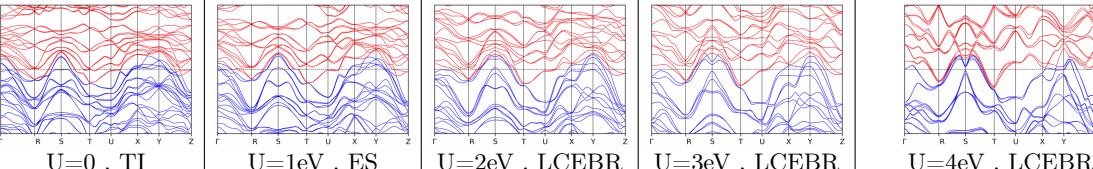
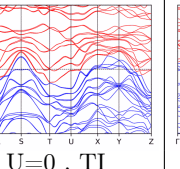
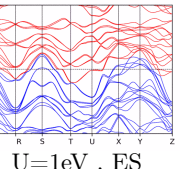
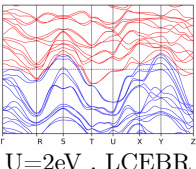
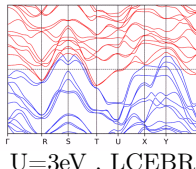
BCSID	Formula	ICSD	MSG	T.C.	
1.88	Mn <sub>5</sub> Si <sub>3</sub>	*	60.431( $P_Cbcn$ )	$\mathbb{Z}_2$	
Topology					

TABLE CLXXXVII. Topology phase diagram of Mn<sub>5</sub>Si<sub>3</sub>.

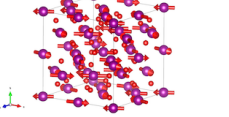
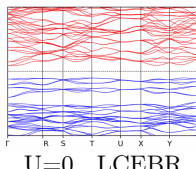
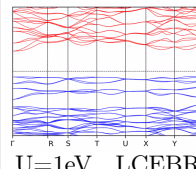
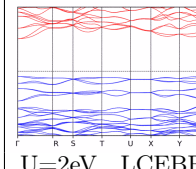
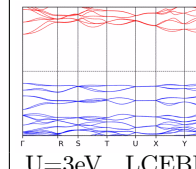
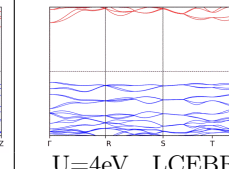
BCSID	Formula	ICSD	MSG	T.C.	
0.40	Mn2O3-alpha	*	61.433( $Pbca$ )	$\mathbb{Z}_2$	
Topology	 $U=0$ , LCEBR	 $U=1\text{eV}$ , LCEBR	 $U=2\text{eV}$ , LCEBR	 $U=3\text{eV}$ , LCEBR	 $U=4\text{eV}$ , LCEBR

TABLE CLXXXVIII. Topology phase diagram of Mn2O3-alpha.

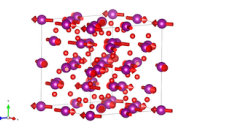
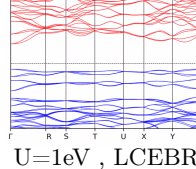
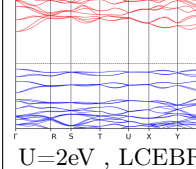
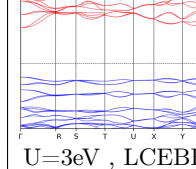
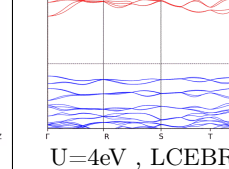
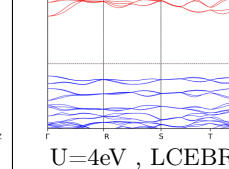
BCSID	Formula	ICSD	MSG	T.C.	
0.41	Mn2O3-alpha	*	61.433( $Pbca$ )	$\mathbb{Z}_2$	
Topology	 $U=0$ , LCEBR	 $U=1\text{eV}$ , LCEBR	 $U=2\text{eV}$ , LCEBR	 $U=3\text{eV}$ , LCEBR	 $U=4\text{eV}$ , LCEBR

TABLE CLXXXIX. Topology phase diagram of Mn2O3-alpha.

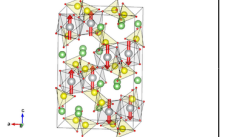
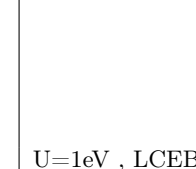
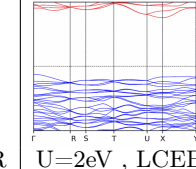
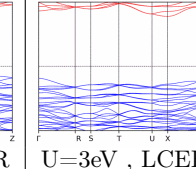
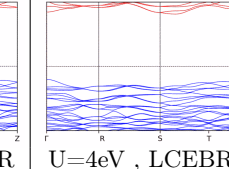
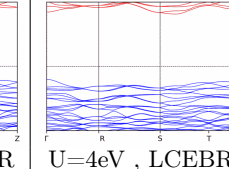
BCSID	Formula	ICSD	MSG	T.C.	
0.71	Li2Ni(SO4)2	*	61.437( $Pb'c'a'$ )	w/o	
Topology	 $U=0$ , LCEBR	 $U=1\text{eV}$ , LCEBR	 $U=2\text{eV}$ , LCEBR	 $U=3\text{eV}$ , LCEBR	 $U=4\text{eV}$ , LCEBR

TABLE CXC. Topology phase diagram of Li2Ni(SO4)2.

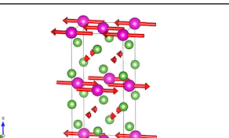
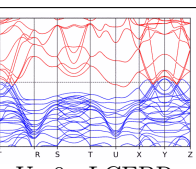
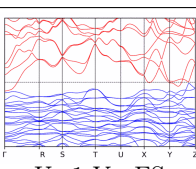
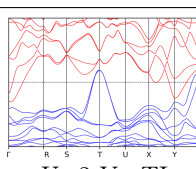
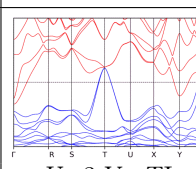
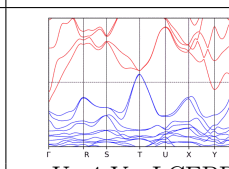
BCSID	Formula	ICSD	MSG	T.C.	
2.1	EuFe2As2	*	61.439( $P_Cbca$ )	$\mathbb{Z}_2$	
Topology	 $U=0$ , LCEBR	 $U=1\text{eV}$ , ES	 $U=2\text{eV}$ , TI	 $U=3\text{eV}$ , TI	 $U=4\text{eV}$ , LCEBR

TABLE CXCI. Topology phase diagram of EuFe2As2.

BCSID	Formula	ICSD	MSG	T.C.	
0.102	Mn <sub>2</sub> GeO <sub>4</sub>	*	62.441( <i>Pnma</i> )	$\mathbb{Z}_2$	
Topology	    				

TABLE CXCII. Topology phase diagram of Mn<sub>2</sub>GeO<sub>4</sub>.

BCSID	Formula	ICSD	MSG	T.C.	
0.168	NH <sub>4</sub> Fe <sub>2</sub> O <sub>6</sub>	*	62.441( <i>Pnma</i> )	$\mathbb{Z}_2$	
Topology	    				

TABLE CXCIII. Topology phase diagram of NH<sub>4</sub>Fe<sub>2</sub>O<sub>6</sub>.

BCSID	Formula	ICSD	MSG	T.C.	
0.192	RbFe <sub>2</sub> F <sub>6</sub>	186748	62.441( <i>Pnma</i> )	$\mathbb{Z}_2$	
Topology	    				

TABLE CXCIV. Topology phase diagram of RbFe<sub>2</sub>F<sub>6</sub>.

BCSID	Formula	ICSD	MSG	T.C.	
0.218	Co <sub>2</sub> SiO <sub>4</sub>	260092	62.441( <i>Pnma</i> )	$\mathbb{Z}_2$	
Topology	    				

TABLE CXCV. Topology phase diagram of Co<sub>2</sub>SiO<sub>4</sub>.

BCSID	Formula	ICSD	MSG	T.C.	
0.219	Co <sub>2</sub> SiO <sub>4</sub>	260092	62.441( <i>Pnma</i> )	$\mathbb{Z}_2$	
Topology	 U=0 , ES	 U=1eV , ES	 U=2eV , LCEBR	 U=3eV , LCEBR	 U=4eV , LCEBR

TABLE CXCVI. Topology phase diagram of Co<sub>2</sub>SiO<sub>4</sub>.

BCSID	Formula	ICSD	MSG	T.C.	
0.221	Fe <sub>2</sub> SiO <sub>4</sub>	26375	62.441( <i>Pnma</i> )	$\mathbb{Z}_2$	
Topology	 U=0 , ES	 U=1eV , LCEBR	 U=2eV , LCEBR	 U=3eV , LCEBR	 U=4eV , LCEBR

TABLE CXCVII. Topology phase diagram of Fe<sub>2</sub>SiO<sub>4</sub>.

BCSID	Formula	ICSD	MSG	T.C.	
0.90	Rb <sub>2</sub> Fe <sub>2</sub> O(AsO <sub>4</sub> ) <sub>2</sub>	*	62.441( <i>Pnma</i> )	$\mathbb{Z}_2$	
Topology	 U=0 , LCEBR	 U=1eV , LCEBR	 U=2eV , LCEBR	 U=3eV , LCEBR	 U=4eV , LCEBR

TABLE CXCVIII. Topology phase diagram of Rb<sub>2</sub>Fe<sub>2</sub>O(AsO<sub>4</sub>)<sub>2</sub>.

BCSID	Formula	ICSD	MSG	T.C.	
0.96	CoSO <sub>4</sub>	18175	62.441( <i>Pnma</i> )	$\mathbb{Z}_2$	
Topology	 U=0 , LCEBR	 U=1eV , LCEBR	 U=2eV , LCEBR	 U=3eV , LCEBR	 U=4eV , LCEBR

TABLE CXCIX. Topology phase diagram of CoSO<sub>4</sub>.

BCSID	Formula	ICSD	MSG	T.C.	
0.182	KCrF4	60896	$62.443(Pn'ma)$	w/o	
Topology	 U=0 , LCEBR				 U=4eV , LCEBR
		U=1eV , LCEBR	U=2eV , LCEBR	U=3eV , LCEBR	

TABLE CC. Topology phase diagram of KCrF4.

BCSID	Formula	ICSD	MSG	T.C.	
0.88	LiNiPO4	402760	$62.444(Pnm'a)$	w/o	
Topology	 U=0 , LCEBR	 U=1eV , LCEBR	 U=2eV , LCEBR	 U=3eV , LCEBR	 U=4eV , LCEBR

TABLE CCI. Topology phase diagram of LiNiPO4.

BCSID	Formula	ICSD	MSG	T.C.	
0.193	LiCoPO4	400625	$62.445(Pnma')$	w/o	
Topology	 U=0 , LCEBR	 U=1eV , LCEBR	 U=2eV , LCEBR	 U=3eV , LCEBR	 U=4eV , LCEBR

TABLE CCII. Topology phase diagram of LiCoPO4.

BCSID	Formula	ICSD	MSG	T.C.	
0.216	SrEr2O4	239309	$62.445(Pnmd')$	w/o	
Topology	 U=0 , LCEBR		 U=2eV , LCEBR		 U=4eV , LCEBR
		U=1eV , LCEBR		U=3eV , LCEBR	

TABLE CCIII. Topology phase diagram of SrEr2O4.

BCSID	Formula	ICSD	MSG	T.C.	
0.86	KMn <sub>4</sub> (PO <sub>4</sub> ) <sub>3</sub>	246135	62.445( <i>Pnma'</i> )	w/o	
Topology	 U=0 , LCEBR	 U=1eV , LCEBR	 U=2eV , LCEBR	 U=3eV , LCEBR	 U=4eV , LCEBR

TABLE CCIV. Topology phase diagram of KMn<sub>4</sub>(PO<sub>4</sub>)<sub>3</sub>.

BCSID	Formula	ICSD	MSG	T.C.	
0.87	NaFePO <sub>4</sub>	169118	62.445( <i>Pnma'</i> )	w/o	
Topology	 U=0 , LCEBR	 U=1eV , LCEBR	 U=2eV , LCEBR	 U=3eV , LCEBR	 U=4eV , LCEBR

TABLE CCV. Topology phase diagram of NaFePO<sub>4</sub>.

BCSID	Formula	ICSD	MSG	T.C.	
0.95	LiFePO <sub>4</sub>	*	62.445( <i>Pnma'</i> )	w/o	
Topology	 U=0 , LCEBR	 U=1eV , LCEBR	 U=2eV , LCEBR	 U=3eV , LCEBR	 U=4eV , LCEBR

TABLE CCVI. Topology phase diagram of LiFePO<sub>4</sub>.

BCSID	Formula	ICSD	MSG	T.C.	
0.101	Mn <sub>2</sub> GeO <sub>4</sub>	*	62.446( <i>Pn'm'a</i> )	$\mathbb{Z}_2$	
Topology	 U=0 , LCEBR	 U=1eV , LCEBR	 U=2eV , LCEBR	 U=3eV , LCEBR	 U=4eV , LCEBR

TABLE CCVII. Topology phase diagram of Mn<sub>2</sub>GeO<sub>4</sub>.

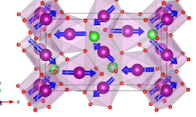
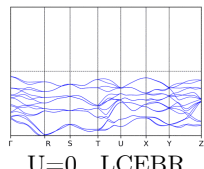
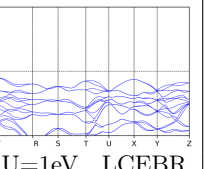
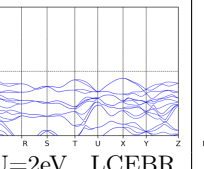
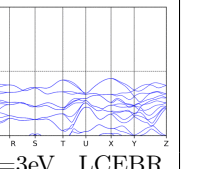
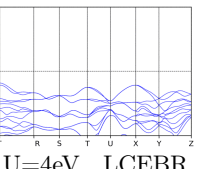
BCSID	Formula	ICSD	MSG	T.C.	
0.220	Mn <sub>2</sub> SiO <sub>4</sub>	88026	62.446( $Pn'm'a$ )	$\mathbb{Z}_2$	
Topology	 U=0 , LCEBR	 U=1eV , LCEBR	 U=2eV , LCEBR	 U=3eV , LCEBR	 U=4eV , LCEBR

TABLE CCVIII. Topology phase diagram of Mn<sub>2</sub>SiO<sub>4</sub>.

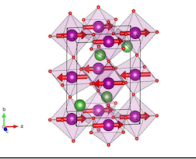
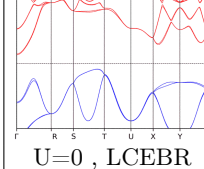
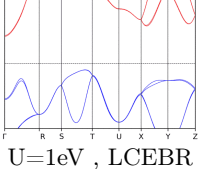
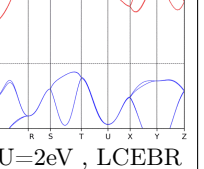
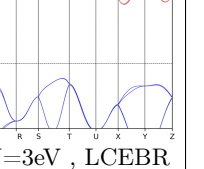
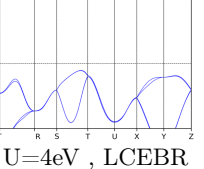
BCSID	Formula	ICSD	MSG	T.C.	
0.1	LaMnO <sub>3</sub>	*	62.448( $Pn'ma'$ )	$\mathbb{Z}_2$	
Topology	 U=0 , LCEBR	 U=1eV , LCEBR	 U=2eV , LCEBR	 U=3eV , LCEBR	 U=4eV , LCEBR

TABLE CCIX. Topology phase diagram of LaMnO<sub>3</sub>.

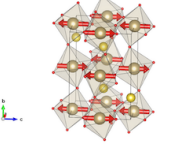
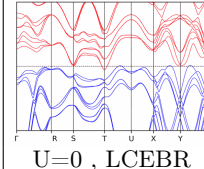
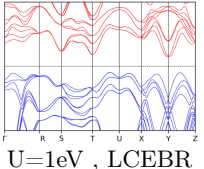
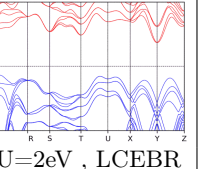
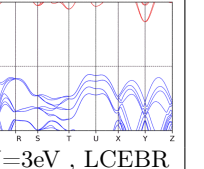
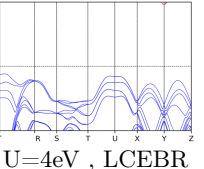
BCSID	Formula	ICSD	MSG	T.C.	
0.25	NaOsO <sub>3</sub>	*	62.448( $Pn'ma'$ )	$\mathbb{Z}_2$	
Topology	 U=0 , LCEBR	 U=1eV , LCEBR	 U=2eV , LCEBR	 U=3eV , LCEBR	 U=4eV , LCEBR

TABLE CCX. Topology phase diagram of NaOsO<sub>3</sub>.

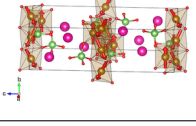
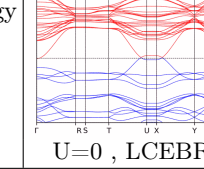
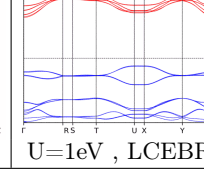
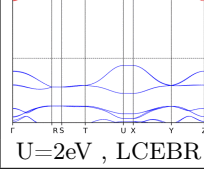
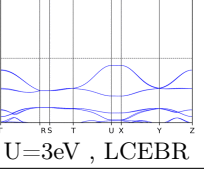
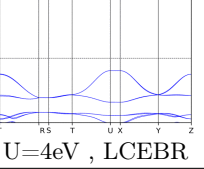
BCSID	Formula	ICSD	MSG	T.C.	
0.91	Rb <sub>2</sub> Fe <sub>2</sub> O(AsO <sub>4</sub> ) <sub>2</sub>	*	62.448( $Pn'ma'$ )	$\mathbb{Z}_2$	
Topology	 U=0 , LCEBR	 U=1eV , LCEBR	 U=2eV , LCEBR	 U=3eV , LCEBR	 U=4eV , LCEBR

TABLE CCXI. Topology phase diagram of Rb<sub>2</sub>Fe<sub>2</sub>O(AsO<sub>4</sub>)<sub>2</sub>.

BCSID	Formula	ICSD	MSG	T.C.	
0.24	LiMnPO <sub>4</sub>	25834	62.449( $Pn'm'a'$ )	w/o	
Topology	 U=0 , LCEBR	 U=1eV , LCEBR	 U=2eV , LCEBR	 U=3eV , LCEBR	 U=4eV , LCEBR

TABLE CCXII. Topology phase diagram of LiMnPO<sub>4</sub>.

BCSID	Formula	ICSD	MSG	T.C.	
1.130	Cr <sub>2</sub> As	42335	62.450( $P_anma$ )	$\mathbb{Z}_2$	
Topology	 U=0 , LCEBR	 U=1eV , TI	 U=2eV , LCEBR	 U=3eV , LCEBR	 U=4eV , LCEBR

TABLE CCXIII. Topology phase diagram of Cr<sub>2</sub>As.

BCSID	Formula	ICSD	MSG	T.C.	
1.131	Fe <sub>2</sub> As	42335	62.450( $P_anma$ )	$\mathbb{Z}_2$	
Topology	 U=0 , TI	 U=1eV , TI	 U=2eV , ES	 U=3eV , TI	 U=4eV , TI

TABLE CCXIV. Topology phase diagram of Fe<sub>2</sub>As.

BCSID	Formula	ICSD	MSG	T.C.	
1.132	Mn <sub>2</sub> As	164396	62.450( $P_anma$ )	$\mathbb{Z}_2$	
Topology	 U=0 , ES	 U=1eV , ES	 U=2eV , ES	 U=3eV , ES	 U=4eV , ES

TABLE CCXV. Topology phase diagram of Mn<sub>2</sub>As.

BCSID	Formula	ICSD	MSG	T.C.	
1.28	CrN	*	62.450( $P_{anma}$ )	$\mathbb{Z}_2$	
Topology	 U=0 , TI	 U=1eV , TI	 U=2eV , LCEBR	 U=3eV , LCEBR	 U=4eV , LCEBR

TABLE CCXVI. Topology phase diagram of CrN.

BCSID	Formula	ICSD	MSG	T.C.	
1.1	Mn <sub>3</sub> O <sub>4</sub>	*	62.452( $P_c nma$ )	$\mathbb{Z}_2$	
Topology	 U=0 , LCEBR	 U=1eV , TBD	 U=2eV , TBD	 U=3eV , LCEBR	 U=4eV , LCEBR

TABLE CCXVII. Topology phase diagram of Mn<sub>3</sub>O<sub>4</sub>.

BCSID	Formula	ICSD	MSG	T.C.	
2.27	Sr <sub>2</sub> Mn <sub>3</sub> Sb <sub>2</sub> O <sub>2</sub>	81792	63.459( $Cm'm'$ )	w/o	
Topology	 U=0 , LCEBR	 U=1eV , LCEBR	 U=2eV , LCEBR	 U=3eV , LCEBR	 U=4eV , LCEBR

TABLE CCXVIII. Topology phase diagram of Sr<sub>2</sub>Mn<sub>3</sub>Sb<sub>2</sub>O<sub>2</sub>.

BCSID	Formula	ICSD	MSG	T.C.	
0.199	Mn <sub>3</sub> Sn	643730	63.463( $Cmc'm'$ )	$\mathbb{Z}_2\mathbb{Z}_2$	
Topology	 U=0 , ES	 U=1eV , ES	 U=2eV , ES	 U=3eV , ES	 U=4eV , ES

TABLE CCXIX. Topology phase diagram of Mn<sub>3</sub>Sn.

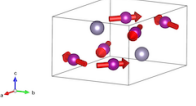
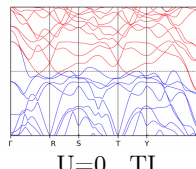
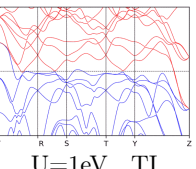
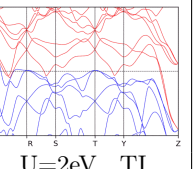
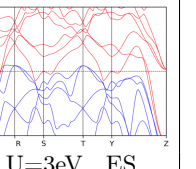
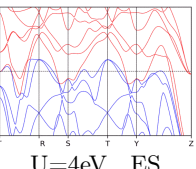
BCSID	Formula	ICSD	MSG	T.C.	
0.200	Mn <sub>3</sub> Sn	643730	$63.464(Cm'cm')$	$\mathbb{Z}_2\mathbb{Z}_2$	
Topology	 $U=0, \text{TI}$	 $U=1\text{eV}, \text{TI}$	 $U=2\text{eV}, \text{TI}$	 $U=3\text{eV}, \text{ES}$	 $U=4\text{eV}, \text{ES}$

TABLE CCXX. Topology phase diagram of Mn<sub>3</sub>Sn.

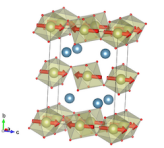
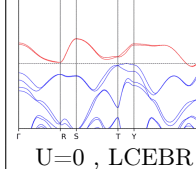
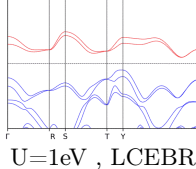
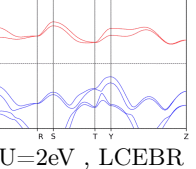
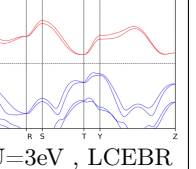
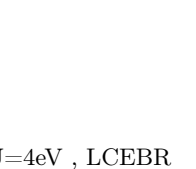
BCSID	Formula	ICSD	MSG	T.C.	
0.79	CaIrO <sub>3</sub>	160816	$63.464(Cm'cm')$	$\mathbb{Z}_2\mathbb{Z}_2$	
Topology	 $U=0, \text{LCEBR}$	 $U=1\text{eV}, \text{LCEBR}$	 $U=2\text{eV}, \text{LCEBR}$	 $U=3\text{eV}, \text{LCEBR}$	 $U=4\text{eV}, \text{LCEBR}$

TABLE CCXXI. Topology phase diagram of CaIrO<sub>3</sub>.

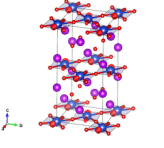
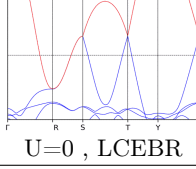
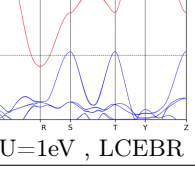
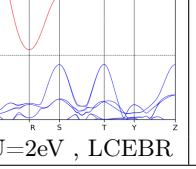
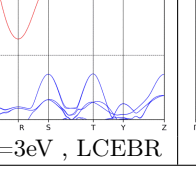
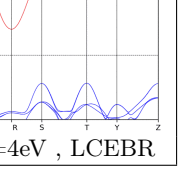
BCSID	Formula	ICSD	MSG	T.C.	
0.82	Gd <sub>2</sub> CuO <sub>4</sub>	75425	$64.476(Cm'ca')$	$\mathbb{Z}_2\mathbb{Z}_2$	
Topology	 $U=0, \text{LCEBR}$	 $U=1\text{eV}, \text{LCEBR}$	 $U=2\text{eV}, \text{LCEBR}$	 $U=3\text{eV}, \text{LCEBR}$	 $U=4\text{eV}, \text{LCEBR}$

TABLE CCXXII. Topology phase diagram of Gd<sub>2</sub>CuO<sub>4</sub>.

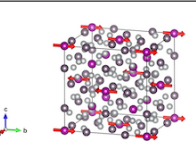
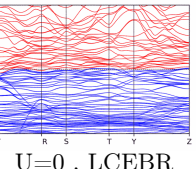
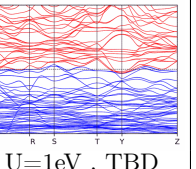
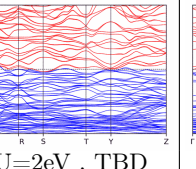
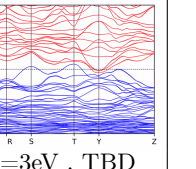
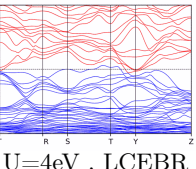
BCSID	Formula	ICSD	MSG	T.C.	
1.145	Mn <sub>3</sub> Ni <sub>20</sub> P <sub>6</sub>	72351	$64.480(C_A mca)$	$\mathbb{Z}_2$	
Topology	 $U=0, \text{LCEBR}$	 $U=1\text{eV}, \text{TBD}$	 $U=2\text{eV}, \text{TBD}$	 $U=3\text{eV}, \text{TBD}$	 $U=4\text{eV}, \text{LCEBR}$

TABLE CCXXIII. Topology phase diagram of Mn<sub>3</sub>Ni<sub>20</sub>P<sub>6</sub>.

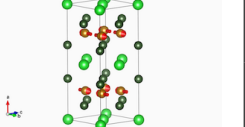
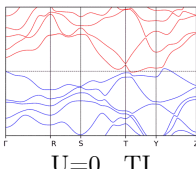
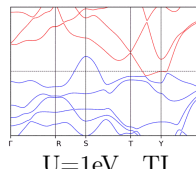
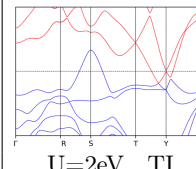
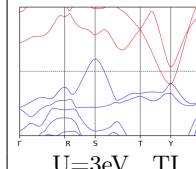
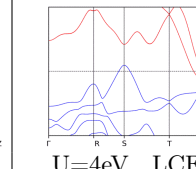
BCSID	Formula	ICSD	MSG	T.C.	
1.16	BaFe2As2	*	64.480( $C_A mca$ )	$\mathbb{Z}_2$	
Topology	 U=0 , TI	 U=1eV , TI	 U=2eV , TI	 U=3eV , TI	 U=4eV , LCEBR

TABLE CCXXIV. Topology phase diagram of BaFe2As2.

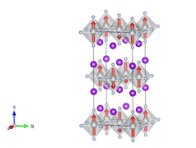
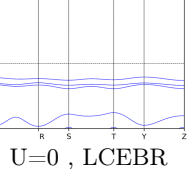
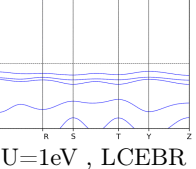
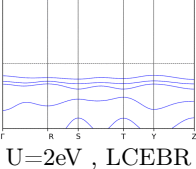
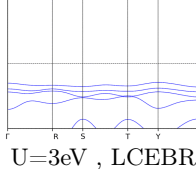
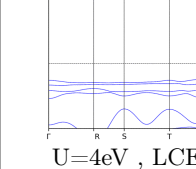
BCSID	Formula	ICSD	MSG	T.C.	
1.249	K2NiF4	33520	64.480( $C_A mca$ )	$\mathbb{Z}_2$	
Topology	 U=0 , LCEBR	 U=1eV , LCEBR	 U=2eV , LCEBR	 U=3eV , LCEBR	 U=4eV , LCEBR

TABLE CCXXV. Topology phase diagram of K2NiF4.

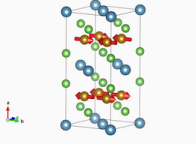
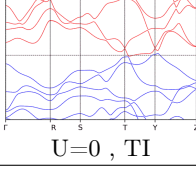
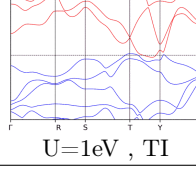
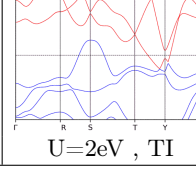
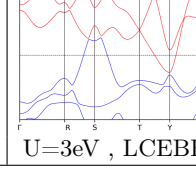
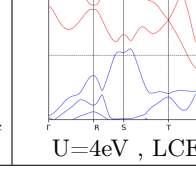
BCSID	Formula	ICSD	MSG	T.C.	
1.52	CaFe2As2	*	64.480( $C_A mca$ )	$\mathbb{Z}_2$	
Topology	 U=0 , TI	 U=1eV , TI	 U=2eV , TI	 U=3eV , LCEBR	 U=4eV , LCEBR

TABLE CCXXVI. Topology phase diagram of CaFe2As2.

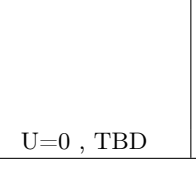
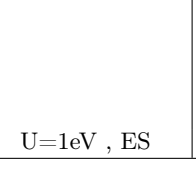
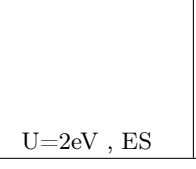
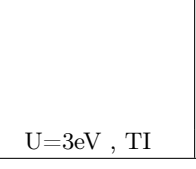
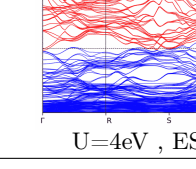
BCSID	Formula	ICSD	MSG	T.C.	
2.15	Mn3Ni20P6	72351	65.486( $Cmm'm'$ )	$\mathbb{Z}_2\mathbb{Z}_2$	
Topology	 U=0 , TBD	 U=1eV , ES	 U=2eV , ES	 U=3eV , TI	 U=4eV , ES

TABLE CCXXVII. Topology phase diagram of Mn3Ni20P6.

BCSID	Formula	ICSD	MSG	T.C.	
1.104	Gd <sub>2</sub> CuO <sub>4</sub>	65015	66.500( $C_{Accm}$ )	$\mathbb{Z}_2$	
Topology	 U=0 , LCEBR	 U=1eV , LCEBR	 U=2eV , LCEBR	 U=3eV , LCEBR	 U=4eV , LCEBR

TABLE CCXXVIII. Topology phase diagram of Gd<sub>2</sub>CuO<sub>4</sub>.

BCSID	Formula	ICSD	MSG	T.C.	
1.65	SrFeO <sub>2</sub>	*	69.526( $F_Smmm$ )	$\mathbb{Z}_4$	
Topology	 U=0 , LCEBR	 U=1eV , LCEBR	 U=2eV , LCEBR	 U=3eV , LCEBR	 U=4eV , LCEBR

TABLE CCXXIX. Topology phase diagram of SrFeO<sub>2</sub>.

BCSID	Formula	ICSD	MSG	T.C.	
0.4	NiCr <sub>2</sub> O <sub>4</sub>	280061	70.530( $Fd'd'd$ )	$\mathbb{Z}_2$	
Topology	 U=0 , ES	 U=1eV , LCEBR	 U=2eV , LCEBR	 U=3eV , LCEBR	 U=4eV , LCEBR

TABLE CCXXX. Topology phase diagram of NiCr<sub>2</sub>O<sub>4</sub>.

BCSID	Formula	ICSD	MSG	T.C.	
1.125	LaFeAsO	180434	73.553( $I_c bca$ )	$\mathbb{Z}_2$	
Topology	 U=0 , TI	 U=1eV , LCEBR	 U=2eV , LCEBR	 U=3eV , LCEBR	 U=4eV , LCEBR

TABLE CCXXXI. Topology phase diagram of LaFeAsO.

BCSID	Formula	ICSD	MSG	T.C.	
1.176	YbCo <sub>2</sub> Si <sub>2</sub>	625132	73.553( $I_c bca$ )	$\mathbb{Z}_2$	
Topology	 U=0 , LCEBR	 U=1eV , TI	 U=2eV , TI	 U=3eV , TI	 U=4eV , TI

TABLE CCXXXII. Topology phase diagram of YbCo<sub>2</sub>Si<sub>2</sub>.

BCSID	Formula	ICSD	MSG	T.C.	
1.47	Sr <sub>2</sub> FeOsO <sub>6</sub>	*	83.50( $P_I 4/m$ )	$\mathbb{Z}_4$	
Topology	 U=0 , LCEBR	 U=1eV , LCEBR	 U=2eV , LCEBR	 U=3eV , LCEBR	 U=4eV , LCEBR

TABLE CCXXXIII. Topology phase diagram of Sr<sub>2</sub>FeOsO<sub>6</sub>.

BCSID	Formula	ICSD	MSG	T.C.	
2.5	Mn <sub>3</sub> CuN	628356	85.59( $P4/n$ )	$\mathbb{Z}_2 \mathbb{Z}_4$	
Topology	 U=0 , ES	 U=1eV , ES	 U=2eV , ES	 U=3eV , ES	 U=4eV , ES

TABLE CCXXXIV. Topology phase diagram of Mn<sub>3</sub>CuN.

BCSID	Formula	ICSD	MSG	T.C.	
2.23	Sr <sub>2</sub> CoO <sub>2</sub> Ag <sub>2</sub> Se <sub>2</sub>	*	86.73( $P_C 4_2/n$ )	$\mathbb{Z}_2$	
Topology	 U=0 , LCEBR	 U=1eV , LCEBR	 U=2eV , LCEBR	 U=3eV , LCEBR	 U=4eV , LCEBR

TABLE CCXXXV. Topology phase diagram of Sr<sub>2</sub>CoO<sub>2</sub>Ag<sub>2</sub>Se<sub>2</sub>.

BCSID	Formula	ICSD	MSG	T.C.	
2.24	Ba <sub>2</sub> CoO <sub>2</sub> Ag <sub>2</sub> Se <sub>2</sub>	*	86.73( $P_C4_2/n$ )	$\mathbb{Z}_2$	
Topology		U=0 , LCEBR U=1eV , LCEBR U=2eV , LCEBR U=3eV , LCEBR U=4eV , LCEBR			

TABLE CCXXXVI. Topology phase diagram of Ba<sub>2</sub>CoO<sub>2</sub>Ag<sub>2</sub>Se<sub>2</sub>.

BCSID	Formula	ICSD	MSG	T.C.	
0.64	MnV <sub>2</sub> O <sub>4</sub>	*	88.81( $I4_1/a$ )	$\mathbb{Z}_2\mathbb{Z}_2$	
Topology		U=0 , ES U=1eV , LCEBR U=2eV , LCEBR U=3eV , LCEBR U=4eV , LCEBR			

TABLE CCXXXVII. Topology phase diagram of MnV<sub>2</sub>O<sub>4</sub>.

BCSID	Formula	ICSD	MSG	T.C.	
2.22	FeTa <sub>2</sub> O <sub>6</sub>	201754	88.86( $I_c4_1/a$ )	$\mathbb{Z}_2$	
Topology		U=0 , LCEBR U=1eV , LCEBR U=2eV , LCEBR U=3eV , LCEBR U=4eV , LCEBR			

TABLE CCXXXVIII. Topology phase diagram of FeTa<sub>2</sub>O<sub>6</sub>.

BCSID	Formula	ICSD	MSG	T.C.	
1.235	Ba(TiO)Cu <sub>4</sub> (PO <sub>4</sub> ) <sub>4</sub>	239146	94.132( $P_c4_22_12$ )	w/o	
Topology		U=0 , LCEBR U=1eV , LCEBR U=2eV , LCEBR U=3eV , LCEBR U=4eV , LCEBR			

TABLE CCXXXIX. Topology phase diagram of Ba(TiO)Cu<sub>4</sub>(PO<sub>4</sub>)<sub>4</sub>.

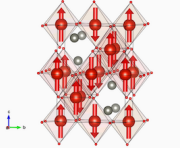
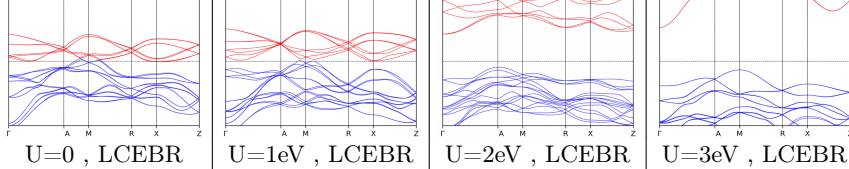
BCSID	Formula	ICSD	MSG	T.C.	
1.24	ZnV <sub>2</sub> O <sub>4</sub>	55443	96.150( $P_I4_32_12$ )	w/o	
Topology					

TABLE CCXL. Topology phase diagram of ZnV<sub>2</sub>O<sub>4</sub>.

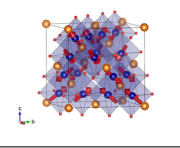
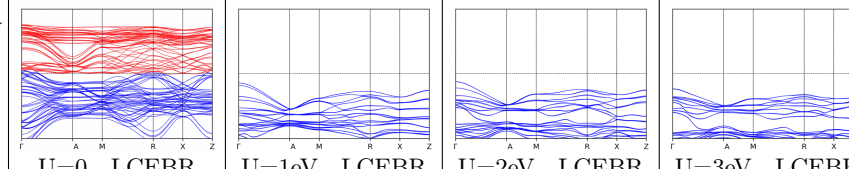
BCSID	Formula	ICSD	MSG	T.C.	
3.4	MgCr <sub>2</sub> O <sub>4</sub>	*	111.255( $P42'm'$ )	$\mathbb{Z}_2\mathbb{Z}_2\mathbb{Z}_4$	
Topology					

TABLE CCXLI. Topology phase diagram of MgCr<sub>2</sub>O<sub>4</sub>.

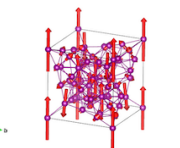
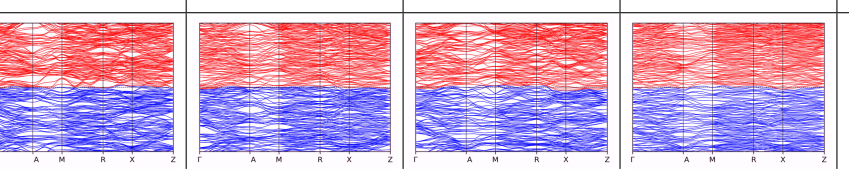
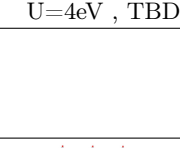
BCSID	Formula	ICSD	MSG	T.C.	
1.85	alpha-Mn	*	114.282( $P_I42_1c$ )	$\mathbb{Z}_2$	
Topology					

TABLE CCXLII. Topology phase diagram of alpha-Mn.

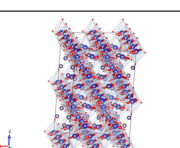
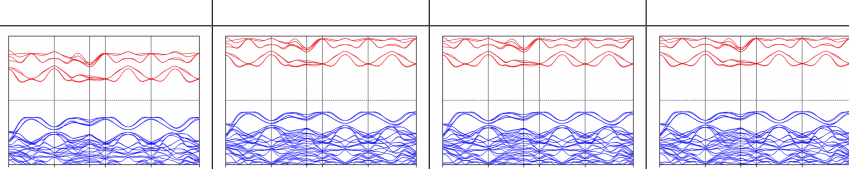
BCSID	Formula	ICSD	MSG	T.C.	
1.185	GeCu <sub>2</sub> O <sub>4</sub>	100796	122.338( $I_c42d$ )	$\mathbb{Z}_2$	
Topology					

TABLE CCXLIII. Topology phase diagram of GeCu<sub>2</sub>O<sub>4</sub>.

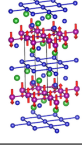
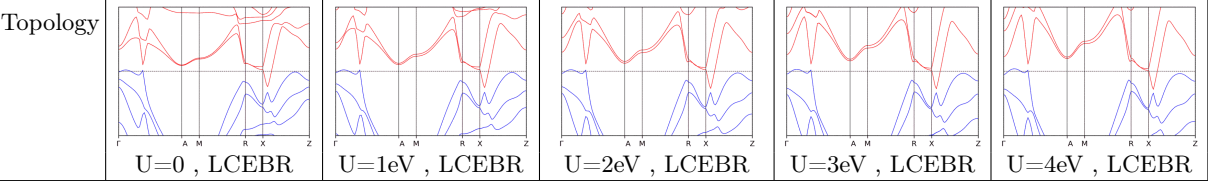
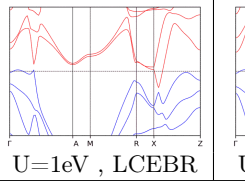
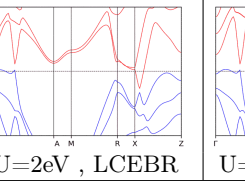
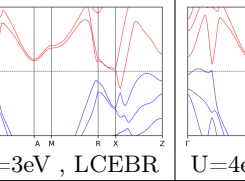
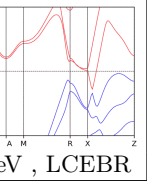
BCSID	Formula	ICSD	MSG	T.C.	
0.72	CaMnBi2	10454	$129.416(P4'/n'm'm)$	$\mathbb{Z}_2$	
Topology					

TABLE CCXLIV. Topology phase diagram of CaMnBi2.

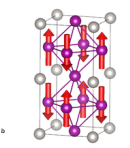
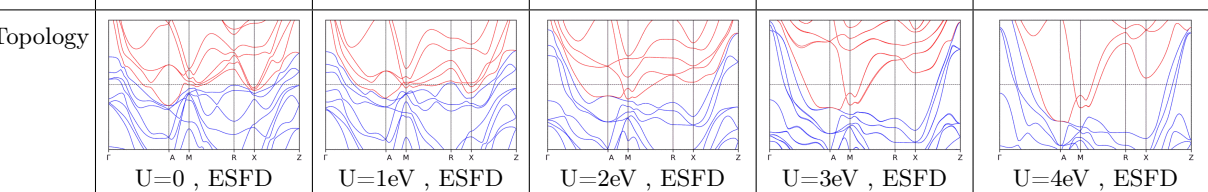
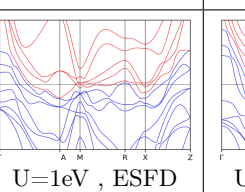
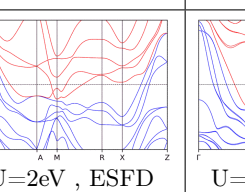
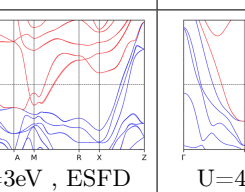
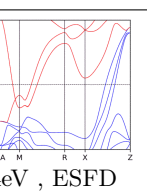
BCSID	Formula	ICSD	MSG	T.C.	
1.143	Mn3Pt	*	$132.456(P_c4_2/mcm)$	$\mathbb{Z}_4$	
Topology					

TABLE CCXLV. Topology phase diagram of Mn3Pt.

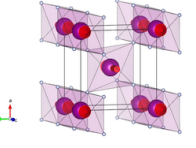
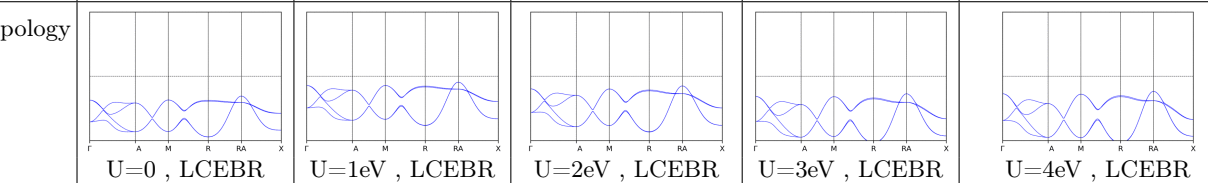
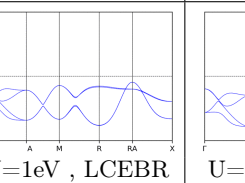
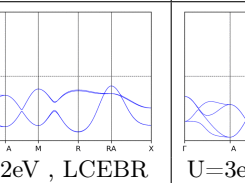
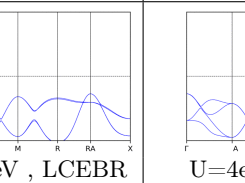
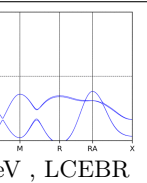
BCSID	Formula	ICSD	MSG	T.C.	
0.15	MnF2	68735	$136.499(P4'_2/mnm')$	$\mathbb{Z}_2$	
Topology					

TABLE CCXLVI. Topology phase diagram of MnF2.

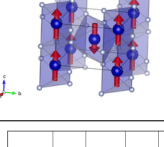
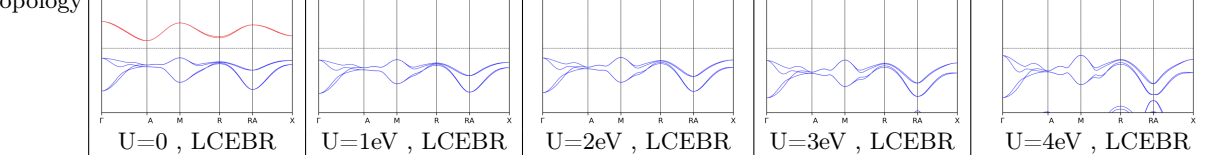
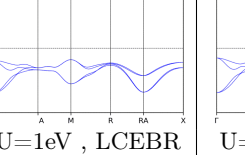
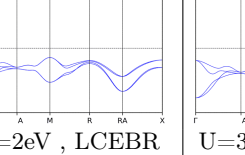
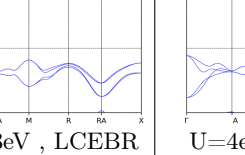
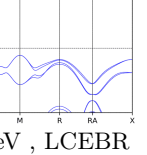
BCSID	Formula	ICSD	MSG	T.C.	
0.178	CoF2	98786	$136.499(P4'_2/mnm')$	$\mathbb{Z}_2$	
Topology					

TABLE CCXLVII. Topology phase diagram of CoF2.

BCSID	Formula	ICSD	MSG	T.C.	
0.142	Fe <sub>2</sub> TeO <sub>6</sub>	24795	136.503( $P4_2/m'm'm'$ )	w/o	
Topology	 U=0 , LCEBR      U=1eV , LCEBR      U=2eV , LCEBR      U=3eV , LCEBR      U=4eV , LCEBR				

TABLE CCXLVIII. Topology phase diagram of Fe<sub>2</sub>TeO<sub>6</sub>.

BCSID	Formula	ICSD	MSG	T.C.	
1.146	LaCrAsO	185855	138.528( $P_c4_2/ncm$ )	$\mathbb{Z}_2$	
Topology	 U=0 , TI      U=1eV , TI      U=2eV , TI      U=3eV , TI      U=4eV , TI				

TABLE CCXLIX. Topology phase diagram of LaCrAsO.

BCSID	Formula	ICSD	MSG	T.C.	
0.18	BaMn <sub>2</sub> As <sub>2</sub>	*	139.536( $I4'/m'm'm$ )	$\mathbb{Z}_2$	
Topology	 U=0 , LCEBR      U=1eV , LCEBR      U=2eV , LCEBR      U=3eV , LCEBR      U=4eV , LCEBR				

TABLE CCL. Topology phase diagram of BaMn<sub>2</sub>As<sub>2</sub>.

BCSID	Formula	ICSD	MSG	T.C.	
0.212	Sr <sub>2</sub> Mn <sub>3</sub> As <sub>2</sub> O <sub>2</sub>	81803	139.536( $I4'/m'm'm$ )	$\mathbb{Z}_2$	
Topology	 U=0 , ESFD      U=1eV , ESFD      U=2eV , ESFD      U=3eV , ESFD      U=4eV , ESFD				

TABLE CCLI. Topology phase diagram of Sr<sub>2</sub>Mn<sub>3</sub>As<sub>2</sub>O<sub>2</sub>.

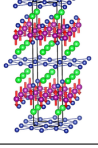
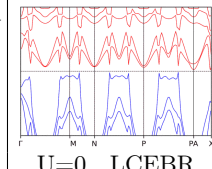
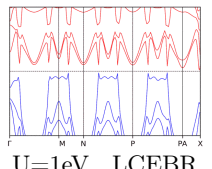
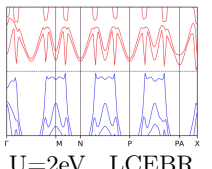
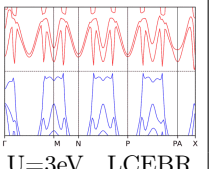
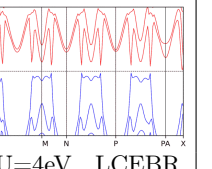
BCSID	Formula	ICSD	MSG	T.C.	
0.73	SrMnBi2	100025	$139.536(I4'/m'm'm)$	$\mathbb{Z}_2$	
Topology	 $U=0, \text{LCEBR}$	 $U=1\text{eV}, \text{LCEBR}$	 $U=2\text{eV}, \text{LCEBR}$	 $U=3\text{eV}, \text{LCEBR}$	 $U=4\text{eV}, \text{LCEBR}$

TABLE CCLII. Topology phase diagram of SrMnBi2.

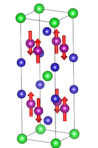
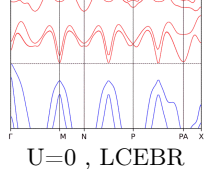
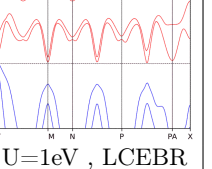
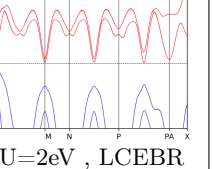
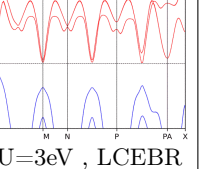
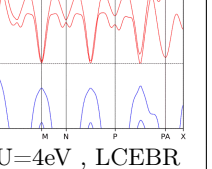
BCSID	Formula	ICSD	MSG	T.C.	
0.89	BaMn2Bi2	*	$139.536(I4'/m'm'm)$	$\mathbb{Z}_2$	
Topology	 $U=0, \text{LCEBR}$	 $U=1\text{eV}, \text{LCEBR}$	 $U=2\text{eV}, \text{LCEBR}$	 $U=3\text{eV}, \text{LCEBR}$	 $U=4\text{eV}, \text{LCEBR}$

TABLE CCLIII. Topology phase diagram of BaMn2Bi2.

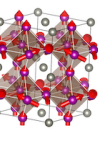
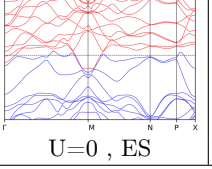
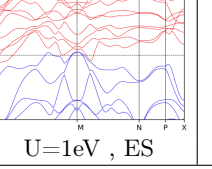
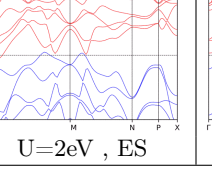
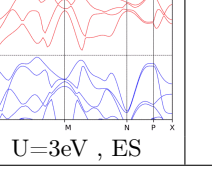
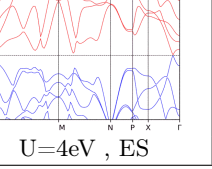
BCSID	Formula	ICSD	MSG	T.C.	
2.19	Mn <sub>3</sub> ZnC	618284	$139.537(I4/mm'm')$	$\mathbb{Z}_4\mathbb{Z}_4$	
Topology	 $U=0, \text{ES}$	 $U=1\text{eV}, \text{ES}$	 $U=2\text{eV}, \text{ES}$	 $U=3\text{eV}, \text{ES}$	 $U=4\text{eV}, \text{ES}$

TABLE CCLIV. Topology phase diagram of Mn<sub>3</sub>ZnC.

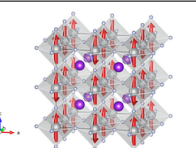
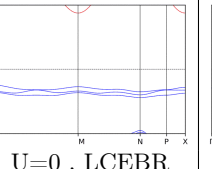
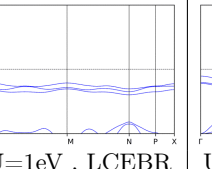
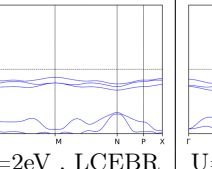
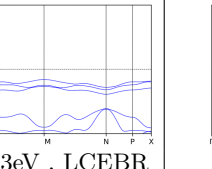
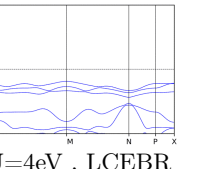
BCSID	Formula	ICSD	MSG	T.C.	
1.250	KNiF <sub>3</sub>	15426	$140.550(I_c4/mcm)$	$\mathbb{Z}_4$	
Topology	 $U=0, \text{LCEBR}$	 $U=1\text{eV}, \text{LCEBR}$	 $U=2\text{eV}, \text{LCEBR}$	 $U=3\text{eV}, \text{LCEBR}$	 $U=4\text{eV}, \text{LCEBR}$

TABLE CCLV. Topology phase diagram of KNiF3.

BCSID	Formula	ICSD	MSG	T.C.	
0.58	CoAl <sub>2</sub> O <sub>4</sub>	*	141.556( $I4'_1/a'm'd$ )	$\mathbb{Z}_2$	
Topology	    	    	    	    	    

TABLE CCLVI. Topology phase diagram of CoAl<sub>2</sub>O<sub>4</sub>.

BCSID	Formula	ICSD	MSG	T.C.	
0.211	Ca <sub>2</sub> MnO <sub>4</sub>	99523	142.568( $I4'_1/a'cd'$ )	$\mathbb{Z}_2$	
Topology	    	    	    	    	    

TABLE CCLVII. Topology phase diagram of Ca<sub>2</sub>MnO<sub>4</sub>.

BCSID	Formula	ICSD	MSG	T.C.	
1.156	LaMn <sub>3</sub> Cr <sub>4</sub> O <sub>12</sub>	*	146.12( $R_I3$ )	w/o	
Topology	    	    	    	    	    

TABLE CCLVIII. Topology phase diagram of LaMn<sub>3</sub>Cr<sub>4</sub>O<sub>12</sub>.

BCSID	Formula	ICSD	MSG	T.C.	
1.165	Ni <sub>3</sub> TeO <sub>6</sub>	240377	146.12( $R_I3$ )	w/o	
Topology	    	    	    	    	    

TABLE CCLIX. Topology phase diagram of Ni<sub>3</sub>TeO<sub>6</sub>.

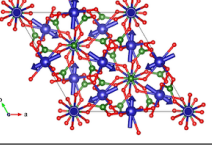
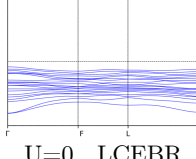
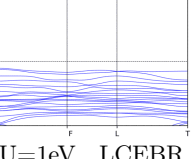
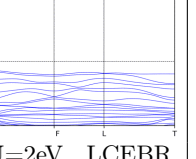
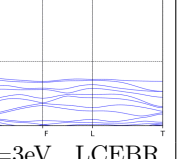
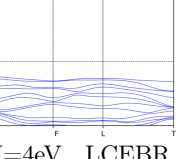
BCSID	Formula	ICSD	MSG	T.C.	
0.78	NiN <sub>2</sub> O <sub>6</sub>	*	148.17( <i>R</i> 3)	$\mathbb{Z}_2\mathbb{Z}_4$	
Topology	 U=0 , LCEBR	 U=1eV , LCEBR	 U=2eV , LCEBR	 U=3eV , LCEBR	 U=4eV , LCEBR

TABLE CCLX. Topology phase diagram of NiN<sub>2</sub>O<sub>6</sub>.

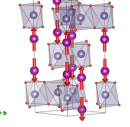
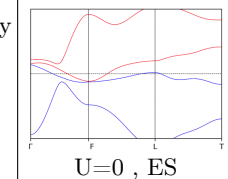
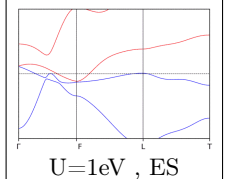
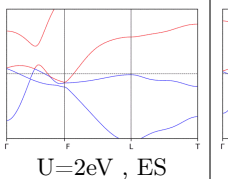
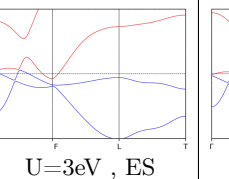
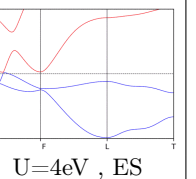
BCSID	Formula	ICSD	MSG	T.C.	
0.125	MnGeO <sub>3</sub>	174042	148.19( <i>R</i> 3')	w/o	
Topology	 U=0 , ES	 U=1eV , ES	 U=2eV , ES	 U=3eV , ES	 U=4eV , ES

TABLE CCLXI. Topology phase diagram of MnGeO<sub>3</sub>.

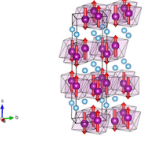
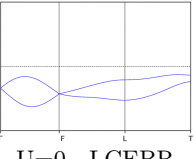
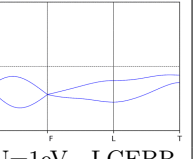
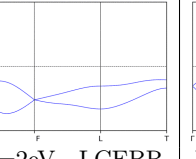
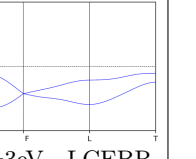
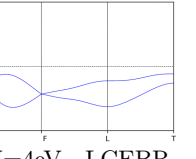
BCSID	Formula	ICSD	MSG	T.C.	
0.19	MnTiO <sub>3</sub>	171579	148.19( <i>R</i> 3')	w/o	
Topology	 U=0 , LCEBR	 U=1eV , LCEBR	 U=2eV , LCEBR	 U=3eV , LCEBR	 U=4eV , LCEBR

TABLE CCLXII. Topology phase diagram of MnTiO<sub>3</sub>.

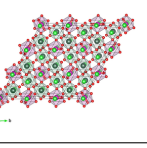
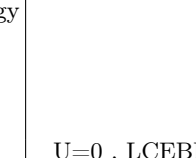
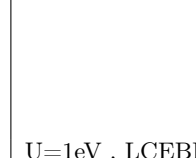
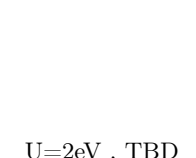
BCSID	Formula	ICSD	MSG	T.C.	
1.0.8	Ba <sub>3</sub> MnNb <sub>2</sub> O <sub>9</sub>	*	157.53( <i>P</i> 31 <i>m</i> )	w/o	
Topology	 U=0 , LCEBR	 U=1eV , LCEBR	 U=2eV , TBD	 U=3eV , LCEBR	 U=4eV , LCEBR

TABLE CCLXIII. Topology phase diagram of Ba<sub>3</sub>MnNb<sub>2</sub>O<sub>9</sub>.

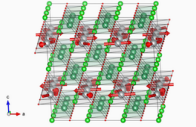
BCSID	Formula	ICSD	MSG	T.C.	
1.13	Ba3Nb2NiO9	240280	159.64( $P_c31c$ )	w/o	
Topology					 U=0 , LCEBR    U=1eV , TBD    U=2eV , LCEBR    U=3eV , LCEBR    U=4eV , TBD

TABLE CCLXIV. Topology phase diagram of Ba3Nb2NiO9.

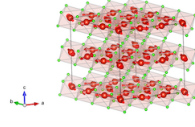
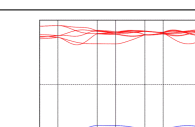
BCSID	Formula	ICSD	MSG	T.C.	
1.237	VCl2	246905	159.64( $P_c31c$ )	w/o	
Topology					 U=0 , LCEBR    U=1eV , LCEBR    U=2eV , LCEBR    U=3eV , LCEBR    U=4eV , LCEBR

TABLE CCLXV. Topology phase diagram of VCl2.

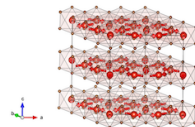
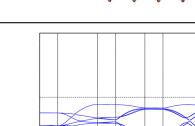
BCSID	Formula	ICSD	MSG	T.C.	
1.238	VBr2	246906	159.64( $P_c31c$ )	w/o	
Topology					 U=0 , LCEBR    U=1eV , LCEBR    U=2eV , LCEBR    U=3eV , LCEBR    U=4eV , LCEBR

TABLE CCLXVI. Topology phase diagram of VBr2.

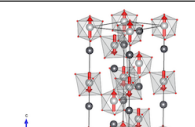
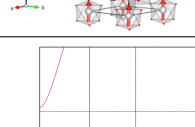
BCSID	Formula	ICSD	MSG	T.C.	
0.21	PbNiO3	*	161.69( $R3c$ )	w/o	
Topology					 U=0 , ESFD    U=1eV , ESFD    U=2eV , ESFD    U=3eV , LCEBR    U=4eV , LCEBR

TABLE CCLXVII. Topology phase diagram of PbNiO3.

BCSID	Formula	ICSD	MSG	T.C.	
1.233	CuMnSb	628385	$161.72(R_I3c)$	w/o	
Topology					

TABLE CCLXVIII. Topology phase diagram of CuMnSb.

BCSID	Formula	ICSD	MSG	T.C.	
1.265	CuMnSb	42978	$161.72(R_I3c)$	w/o	
Topology					

TABLE CCLXIX. Topology phase diagram of CuMnSb.

BCSID	Formula	ICSD	MSG	T.C.	
1.186	SrRu2O <sub>6</sub>	248351	$162.78(P_31m)$	$\mathbb{Z}_2$	
Topology					

TABLE CCLXX. Topology phase diagram of SrRu<sub>2</sub>O<sub>6</sub>.

BCSID	Formula	ICSD	MSG	T.C.	
0.111	Co <sub>4</sub> Nb <sub>2</sub> O <sub>9</sub>	172186	$165.94(P_3'c'1)$	w/o	
Topology					

TABLE CCLXXI. Topology phase diagram of Co<sub>4</sub>Nb<sub>2</sub>O<sub>9</sub>.

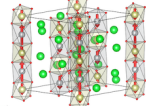
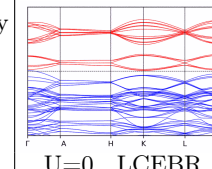
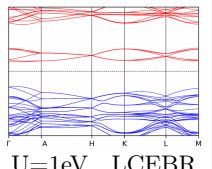
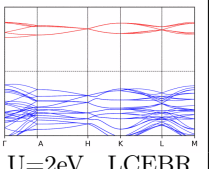
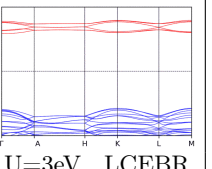
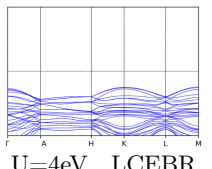
BCSID	Formula	ICSD	MSG	T.C.	
1.0.10	Sr <sub>3</sub> NiIrO <sub>6</sub>	80287	165.95( <i>P</i> 3 <i>c</i> '1)	$\mathbb{Z}_1\mathbb{Z}$	
Topology	 U=0 , LCEBR	 U=1eV , LCEBR	 U=2eV , LCEBR	 U=3eV , LCEBR	 U=4eV , LCEBR

TABLE CCLXXII. Topology phase diagram of Sr<sub>3</sub>NiIrO<sub>6</sub>.

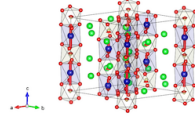
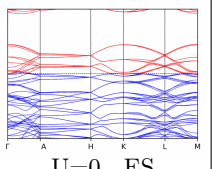
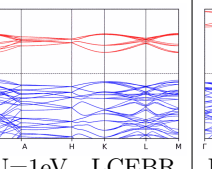
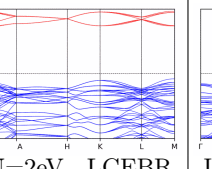
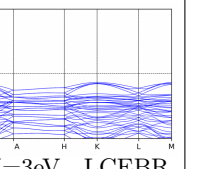
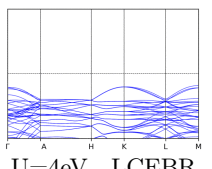
BCSID	Formula	ICSD	MSG	T.C.	
1.0.5	Sr <sub>3</sub> CoIrO <sub>6</sub>	*	165.95( <i>P</i> 3 <i>c</i> '1)	$\mathbb{Z}_1\mathbb{Z}$	
Topology	 U=0 , ES	 U=1eV , LCEBR	 U=2eV , LCEBR	 U=3eV , LCEBR	 U=4eV , LCEBR

TABLE CCLXXIII. Topology phase diagram of Sr<sub>3</sub>CoIrO<sub>6</sub>.

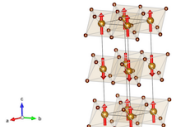
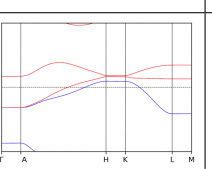
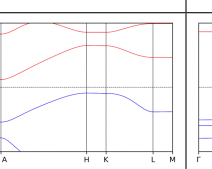
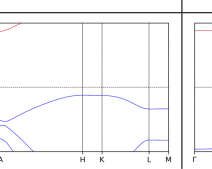
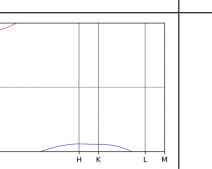
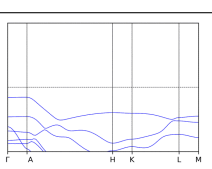
BCSID	Formula	ICSD	MSG	T.C.	
1.242	FeBr <sub>2</sub>	409571	165.96( <i>P</i> <sub>c</sub> 3 <i>c</i> 1)	$\mathbb{Z}_2$	
Topology	 U=0 , LCEBR	 U=1eV , LCEBR	 U=2eV , LCEBR	 U=3eV , LCEBR	 U=4eV , LCEBR

TABLE CCLXXIV. Topology phase diagram of FeBr<sub>2</sub>.

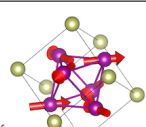
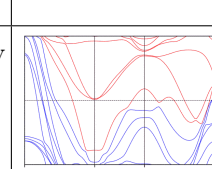
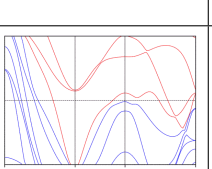
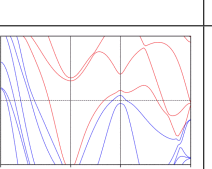
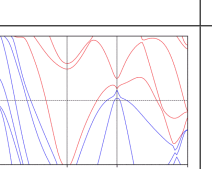
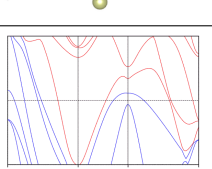
BCSID	Formula	ICSD	MSG	T.C.	
0.108	Mn <sub>3</sub> Ir	*	166.101( <i>R</i> 3 <i>m'</i> )	$\mathbb{Z}_2\mathbb{Z}_4$	
Topology	 U=0 , ES	 U=1eV , ES	 U=2eV , ES	 U=3eV , ES	 U=4eV , ES

TABLE CCLXXV. Topology phase diagram of Mn<sub>3</sub>Ir.

BCSID	Formula	ICSD	MSG	T.C.	
0.109	Mn3Pt	*	166.101( $R3m'$ )	$\mathbb{Z}_2\mathbb{Z}_4$	
Topology	 U=0 , ES	 U=1eV , ES	 U=2eV , ES	 U=3eV , ES	 U=4eV , ES

TABLE CCLXXVI. Topology phase diagram of Mn3Pt.

BCSID	Formula	ICSD	MSG	T.C.	
0.177	Mn3GaN	87399	166.97( $R3m$ )	$\mathbb{Z}_2$	
Topology	 U=0 , ES	 U=1eV , ES	 U=2eV , ES	 U=3eV , ES	 U=4eV , ESFD

TABLE CCLXXVII. Topology phase diagram of Mn3GaN.

BCSID	Formula	ICSD	MSG	T.C.	
0.116	FeCO <sub>3</sub>	100678	167.103( $R3c$ )	$\mathbb{Z}_2$	
Topology	 U=0 , LCEBR	 U=1eV , LCEBR	 U=2eV , LCEBR	 U=3eV , LCEBR	 U=4eV , LCEBR

TABLE CCLXXVIII. Topology phase diagram of FeCO<sub>3</sub>.

BCSID	Formula	ICSD	MSG	T.C.	
0.59	Cr <sub>2</sub> O <sub>3</sub>	*	167.106( $R3'c'$ )	w/o	
Topology	 U=0 , LCEBR	 U=1eV , LCEBR	 U=2eV , LCEBR	 U=3eV , LCEBR	 U=4eV , LCEBR

TABLE CCLXXIX. Topology phase diagram of Cr<sub>2</sub>O<sub>3</sub>.

BCSID	Formula	ICSD	MSG	T.C.	
1.153	Mn <sub>3</sub> GaC	23586	167.108( $R_I3c$ )	$\mathbb{Z}_2$	
Topology	 U=0 , ES				

TABLE CCLXXX. Topology phase diagram of Mn<sub>3</sub>GaC.

BCSID	Formula	ICSD	MSG	T.C.	
1.241	FeCl <sub>2</sub>	44397	167.108( $R_I3c$ )	$\mathbb{Z}_2$	
Topology	 U=0 , LCEBR	 U=1eV , LCEBR	 U=2eV , LCEBR	 U=3eV , LCEBR	 U=4eV , LCEBR

TABLE CCLXXXI. Topology phase diagram of FeCl<sub>2</sub>.

BCSID	Formula	ICSD	MSG	T.C.	
0.8	ScMnO <sub>3</sub>	50694	173.129( $P6_3$ )	$\mathbb{Z}_3$	
Topology	 U=0 , LCEBR	 U=1eV , LCEBR	 U=2eV , LCEBR	 U=3eV , LCEBR	 U=4eV , LCEBR

TABLE CCLXXXII. Topology phase diagram of ScMnO<sub>3</sub>.

BCSID	Formula	ICSD	MSG	T.C.	
0.44	YMnO <sub>3</sub>	*	173.131( $P6'_3$ )	w/o	
Topology	 U=0 , LCEBR	 U=1eV , LCEBR	 U=2eV , LCEBR	 U=3eV , LCEBR	 U=4eV , LCEBR

TABLE CCLXXXIII. Topology phase diagram of YMnO<sub>3</sub>.

BCSID	Formula	ICSD	MSG	T.C.	
0.6	YMnO <sub>3</sub>	*	185.197( $P6_3cm$ )	w/o	
Topology	    	    	    	    	    

TABLE CCLXXXIV. Topology phase diagram of YMnO<sub>3</sub>.

BCSID	Formula	ICSD	MSG	T.C.	
0.117	LuFeO <sub>3</sub>	183152	185.201( $P6_3c'm'$ )	$\mathbb{Z}_3$	
Topology	    	    	    	    	    

TABLE CCLXXXV. Topology phase diagram of LuFeO<sub>3</sub>.

BCSID	Formula	ICSD	MSG	T.C.	
0.7	ScMnO <sub>3</sub>	50694	185.201( $P6_3c'm'$ )	$\mathbb{Z}_3$	
Topology	    	    	    	    	    

TABLE CCLXXXVI. Topology phase diagram of ScMnO<sub>3</sub>.

BCSID	Formula	ICSD	MSG	T.C.	
1.0.14	CsFeCl <sub>3</sub>	300249	189.223( $P6'2'm$ )	w/o	
Topology	    	    	    	    	    

TABLE CCLXXXVII. Topology phase diagram of CsFeCl<sub>3</sub>.

BCSID	Formula	ICSD	MSG	T.C.	
1.110	ScMn6Ge6	*	192.252( $P_c6/mcc$ )	$\mathbb{Z}_6$	
Topology	 U=0 , ES	 U=1eV , ES	 U=2eV , ES	 U=3eV , ES	 U=4eV , ES

TABLE CCLXXXVIII. Topology phase diagram of ScMn6Ge6.

BCSID	Formula	ICSD	MSG	T.C.	
1.225	ScMn6Ge6	192907	192.252( $P_c6/mcc$ )	$\mathbb{Z}_6$	
Topology	 U=0 , ES	 U=1eV , ES	 U=2eV , ES	 U=3eV , ES	 U=4eV , ES

TABLE CCLXXXIX. Topology phase diagram of ScMn6Ge6.

BCSID	Formula	ICSD	MSG	T.C.	
1.0.9	CsCoCl <sub>3</sub>	27511	193.259( $P6'_3/m'cm'$ )	$\mathbb{Z}_2$	
Topology	 U=0 , LCEBR	 U=1eV , LCEBR	 U=2eV , LCEBR	 U=3eV , LCEBR	 U=4eV , LCEBR

TABLE CCXC. Topology phase diagram of CsCoCl<sub>3</sub>.

BCSID	Formula	ICSD	MSG	T.C.	
0.118	Ba <sub>5</sub> Co <sub>5</sub> ClO <sub>13</sub>	99371	194.268( $P6'_3/m'm'c$ )	$\mathbb{Z}_2$	
Topology	 U=0 , LCEBR	 U=1eV , LCEBR	 U=2eV , LCEBR	 U=3eV , LCEBR	 U=4eV , ES

TABLE CCXCI. Topology phase diagram of Ba<sub>5</sub>Co<sub>5</sub>ClO<sub>13</sub>.

BCSID	Formula	ICSD	MSG	T.C.	
0.70	Na <sub>3</sub> Co(CO <sub>3</sub> ) <sub>2</sub> Cl	262045	203.26( <i>Fd</i> 3)	$\mathbb{Z}_2$	
Topology	 U=0 , LCEBR	 U=1eV , LCEBR	 U=2eV , LCEBR	 U=3eV , LCEBR	 U=4eV , LCEBR

TABLE CCXCII. Topology phase diagram of Na<sub>3</sub>Co(CO<sub>3</sub>)<sub>2</sub>Cl.

BCSID	Formula	ICSD	MSG	T.C.	
0.150	NiS <sub>2</sub>	76684	205.33( <i>Pa</i> 3)	$\mathbb{Z}_2$	
Topology	 U=0 , TI	 U=1eV , LCEBR	 U=2eV , LCEBR	 U=3eV , LCEBR	 U=4eV , LCEBR

TABLE CCXCIII. Topology phase diagram of NiS<sub>2</sub>.

BCSID	Formula	ICSD	MSG	T.C.	
0.20	MnTe <sub>2</sub>	*	205.33( <i>Pa</i> 3)	$\mathbb{Z}_2$	
Topology	 U=0 , LCEBR	 U=1eV , LCEBR	 U=2eV , LCEBR	 U=3eV , LCEBR	 U=4eV , LCEBR

TABLE CCXCIV. Topology phase diagram of MnTe<sub>2</sub>.

BCSID	Formula	ICSD	MSG	T.C.	
0.2	Cd <sub>2</sub> O <sub>3</sub> S <sub>2</sub> O <sub>7</sub>	155771	227.131( <i>Fd</i> 3 <i>m'</i> )	$\mathbb{Z}_2$	
Topology	 U=0 , ES	 U=1eV , LCEBR	 U=2eV , LCEBR	 U=3eV , LCEBR	 U=4eV , LCEBR

TABLE CCXCV. Topology phase diagram of Cd<sub>2</sub>O<sub>3</sub>S<sub>2</sub>O<sub>7</sub>.

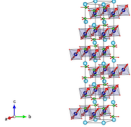
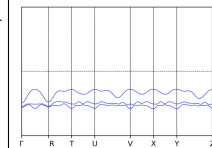
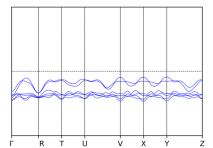
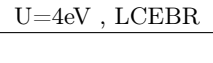
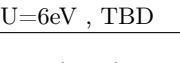
BCS ID	Formula	ICSD	MSG	T.C.	
1.191	HoCr(BO <sub>3</sub> ) <sub>2</sub>	189502	2.7( $P_S\bar{1}$ )	$\mathbb{Z}_2$	
Topology	 U=0 , LCEBR		 U=2eV , TBD	 U=4eV , LCEBR	 U=6eV , TBD

TABLE CCXCVI. Topology phase diagram of HoCr(BO<sub>3</sub>)<sub>2</sub>.

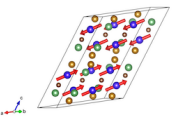
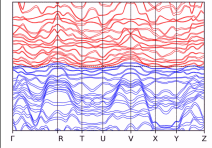
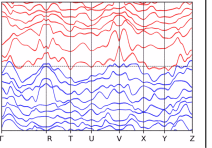
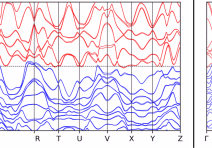
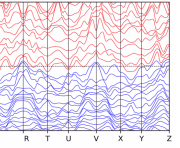
BCS ID	Formula	ICSD	MSG	T.C.	
1.206	Dy <sub>2</sub> Fe <sub>2</sub> Si <sub>2</sub> C	*	2.7( $P_S\bar{1}$ )	$\mathbb{Z}_2$	
Topology	 U=0 , TI	 U=2eV , TI	 U=4eV , TI	 U=6eV , TI	

TABLE CCXCVII. Topology phase diagram of Dy<sub>2</sub>Fe<sub>2</sub>Si<sub>2</sub>C.

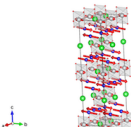
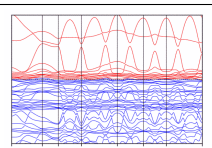
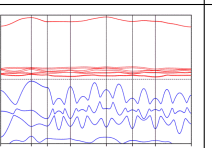
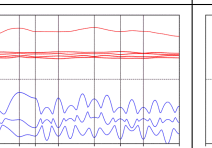
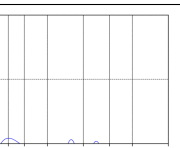
BCS ID	Formula	ICSD	MSG	T.C.	
1.218	Tm <sub>2</sub> BaNiO <sub>5</sub>	72631	2.7( $P_S\bar{1}$ )	$\mathbb{Z}_2$	
Topology	 U=0 , TBD	 U=2eV , TBD	 U=4eV , LCEBR	 U=6eV , LCEBR	

TABLE CCXCVIII. Topology phase diagram of Tm<sub>2</sub>BaNiO<sub>5</sub>.

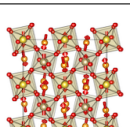
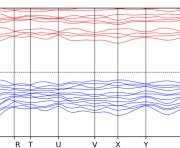
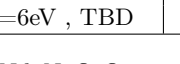
BCS ID	Formula	ICSD	MSG	T.C.	
1.38	Nd <sub>2</sub> NaOsO <sub>6</sub>	*	2.7( $P_S\bar{1}$ )	$\mathbb{Z}_2$	
Topology			 U=4eV , LCEBR	 U=6eV , TBD	
	U=0 , LCEBR	U=2eV , TBD			

TABLE CCXCIX. Topology phase diagram of Nd<sub>2</sub>NaOsO<sub>6</sub>.

BCS ID	Formula	ICSD	MSG	T.C.	
0.37	U <sub>3</sub> Al <sub>2</sub> Si <sub>3</sub>	*	5.15( $C2'$ )	w/o	
Topology	 U=0 , LCEBR	 U=2eV , LCEBR	 U=4eV , LCEBR	 U=6eV , LCEBR	

TABLE CCC. Topology phase diagram of U<sub>3</sub>Al<sub>2</sub>Si<sub>3</sub>.

BCS ID	Formula	ICSD	MSG	T.C.	
1.111	GdBiPt	58786	9.40( $C_{cc}$ )	w/o	
Topology	 U=0 , LCEBR	 U=2eV , LCEBR	 U=4eV , LCEBR	 U=6eV , LCEBR	

TABLE CCCI. Topology phase diagram of GdBiPt.

BCS ID	Formula	ICSD	MSG	T.C.	
0.104	ErVO <sub>3</sub>	185838	11.54( $P2'_1/m'$ )	$\mathbb{Z}_2\mathbb{Z}_2\mathbb{Z}_4$	
Topology	 U=0 , LCEBR	 U=2eV , TI	 U=4eV , LCEBR	 U=6eV , LCEBR	

TABLE CCCII. Topology phase diagram of ErVO<sub>3</sub>.

BCS ID	Formula	ICSD	MSG	T.C.	
0.106	DyVO <sub>3</sub>	40392	11.54( $P2'_1/m'$ )	$\mathbb{Z}_2\mathbb{Z}_2\mathbb{Z}_4$	
Topology	 U=0 , TI	 U=2eV , LCEBR	 U=4eV , LCEBR	 U=6eV , LCEBR	

TABLE CCCIII. Topology phase diagram of DyVO<sub>3</sub>.

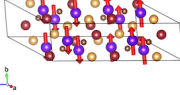
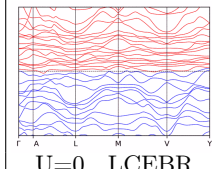
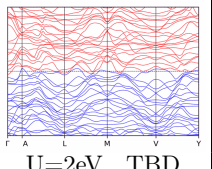
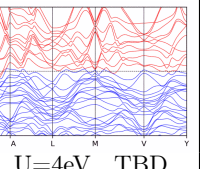
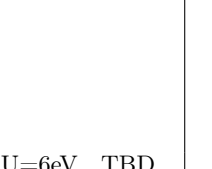
BCS ID	Formula	ICSD	MSG	T.C.	
1.171	Tb <sub>2</sub> Fe <sub>2</sub> Si <sub>2</sub> C	*	12.63( $C_c2/m$ )	$\mathbb{Z}_2$	
Topology	 U=0 , LCEBR	 U=2eV , TBD	 U=4eV , TBD	 U=6eV , TBD	

TABLE CCCIV. Topology phase diagram of Tb<sub>2</sub>Fe<sub>2</sub>Si<sub>2</sub>C.

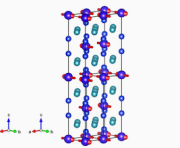
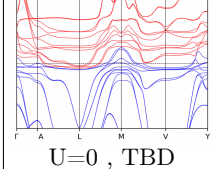
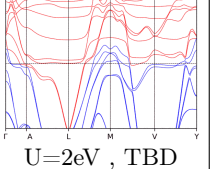
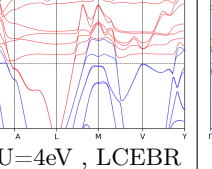
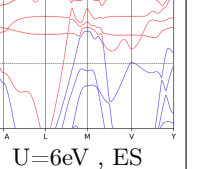
BCS ID	Formula	ICSD	MSG	T.C.	
1.22	DyCu <sub>2</sub> Si <sub>2</sub>	627185	12.63( $C_c2/m$ )	$\mathbb{Z}_2$	
Topology	 U=0 , TBD	 U=2eV , TBD	 U=4eV , LCEBR	 U=6eV , ES	

TABLE CCCV. Topology phase diagram of DyCu<sub>2</sub>Si<sub>2</sub>.

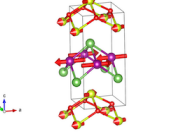
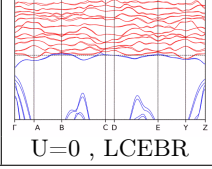
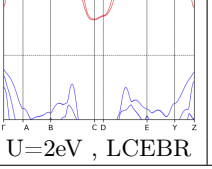
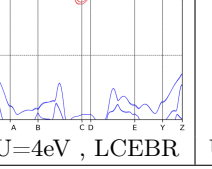
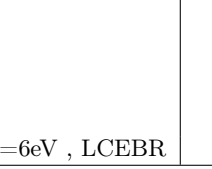
BCS ID	Formula	ICSD	MSG	T.C.	
0.188	CeMnAsO	195499	13.67( $P2'/c$ )	w/o	
Topology	 U=0 , LCEBR	 U=2eV , LCEBR	 U=4eV , LCEBR	 U=6eV , LCEBR	

TABLE CCCVI. Topology phase diagram of CeMnAsO.

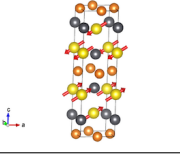
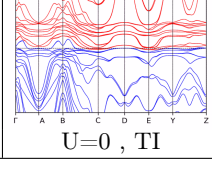
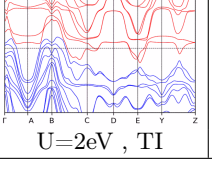
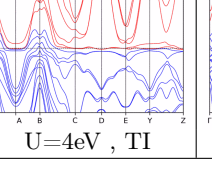
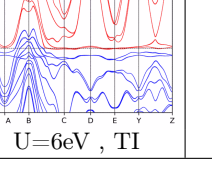
BCS ID	Formula	ICSD	MSG	T.C.	
1.140	PrMgPb	*	13.73( $P_A2/c$ )	$\mathbb{Z}_2$	
Topology	 U=0 , TI	 U=2eV , TI	 U=4eV , TI	 U=6eV , TI	

TABLE CCCVII. Topology phase diagram of PrMgPb.

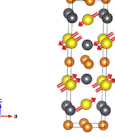
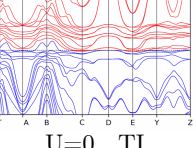
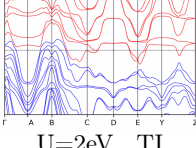
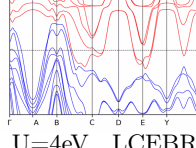
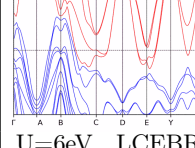
BCS ID	Formula	ICSD	MSG	T.C.	
1.141	NdMgPb	*	13.73( $P_A2/c$ )	$\mathbb{Z}_2$	
Topology	 $U=0, \text{TI}$  $U=2\text{eV}, \text{TI}$  $U=4\text{eV}, \text{LCEBR}$  $U=6\text{eV}, \text{LCEBR}$				

TABLE CCCVIII. Topology phase diagram of NdMgPb.

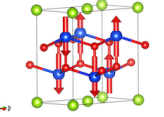
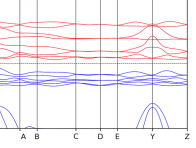
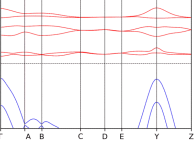
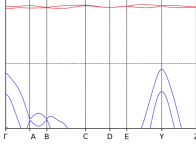
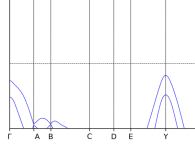
BCS ID	Formula	ICSD	MSG	T.C.	
1.213	Ho <sub>2</sub> O <sub>2</sub> Se	25809	13.73( $P_A2/c$ )	$\mathbb{Z}_2$	
Topology	 $U=0, \text{LCEBR}$  $U=2\text{eV}, \text{LCEBR}$  $U=4\text{eV}, \text{LCEBR}$  $U=6\text{eV}, \text{LCEBR}$				

TABLE CCCIX. Topology phase diagram of Ho<sub>2</sub>O<sub>2</sub>Se.

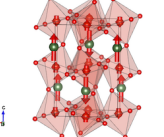
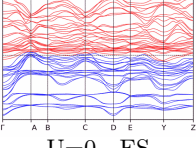
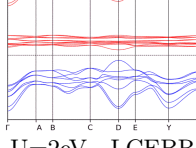
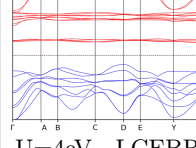
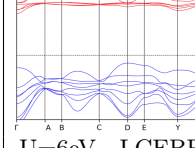
BCS ID	Formula	ICSD	MSG	T.C.	
0.105	ErVO <sub>3</sub>	185838	14.75( $P_2_1/c$ )	$\mathbb{Z}_2$	
Topology	 $U=0, \text{ES}$  $U=2\text{eV}, \text{LCEBR}$  $U=4\text{eV}, \text{LCEBR}$  $U=6\text{eV}, \text{LCEBR}$				

TABLE CCCX. Topology phase diagram of ErVO<sub>3</sub>.

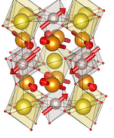
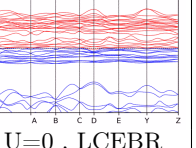
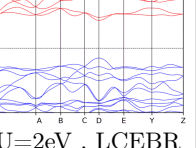
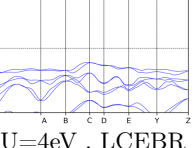
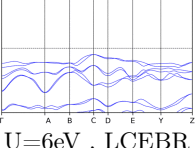
BCS ID	Formula	ICSD	MSG	T.C.	
0.39	Nd <sub>2</sub> NaRuO <sub>6</sub>	*	14.75( $P_2_1/c$ )	$\mathbb{Z}_2$	
Topology	 $U=0, \text{LCEBR}$  $U=2\text{eV}, \text{LCEBR}$  $U=4\text{eV}, \text{LCEBR}$  $U=6\text{eV}, \text{LCEBR}$				

TABLE CCCXI. Topology phase diagram of Nd<sub>2</sub>NaRuO<sub>6</sub>.

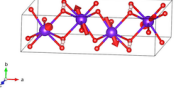
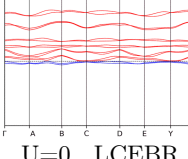
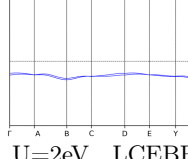
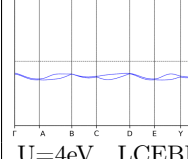
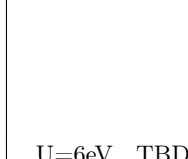
BCS ID	Formula	ICSD	MSG	T.C.	
2.21	TbOOH	6164	$14.78(P2_1/c')$	w/o	
Topology	 $U=0, \text{LCEBR}$	 $U=2\text{eV}, \text{LCEBR}$	 $U=4\text{eV}, \text{LCEBR}$		 $U=6\text{eV}, \text{TBD}$

TABLE CCCXII. Topology phase diagram of TbOOH.

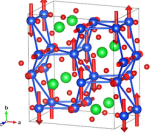
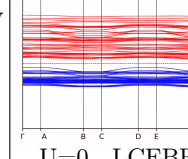
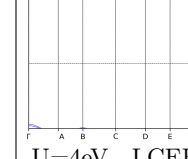
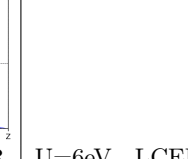
BCS ID	Formula	ICSD	MSG	T.C.	
2.8	SrHo2O4	246550	$14.78(P2_1/c')$	w/o	
Topology	 $U=0, \text{LCEBR}$	 $U=2\text{eV}, \text{LCEBR}$	 $U=4\text{eV}, \text{LCEBR}$		 $U=6\text{eV}, \text{LCEBR}$

TABLE CCCXIII. Topology phase diagram of SrHo2O4.

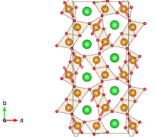
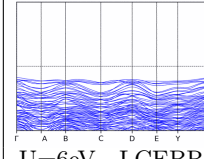
BCS ID	Formula	ICSD	MSG	T.C.	
1.95	BaNd2O4	78486	$14.80(P_a2_1/c)$	$\mathbb{Z}_2$	
Topology					 $U=6\text{eV}, \text{LCEBR}$

TABLE CCCXIV. Topology phase diagram of BaNd2O4.

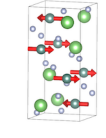
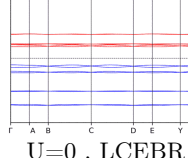
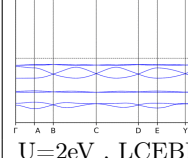
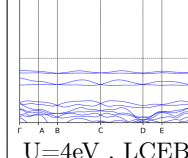
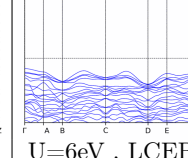
BCS ID	Formula	ICSD	MSG	T.C.	
1.35	LiErF4	*	$14.84(P_C2_1/c)$	$\mathbb{Z}_2$	
Topology	 $U=0, \text{LCEBR}$	 $U=2\text{eV}, \text{LCEBR}$	 $U=4\text{eV}, \text{LCEBR}$	 $U=6\text{eV}, \text{LCEBR}$	

TABLE CCCXV. Topology phase diagram of LiErF4.

BCS ID	Formula	ICSD	MSG	T.C.	
0.174	Pr <sub>3</sub> Ru <sub>4</sub> Al <sub>12</sub>	*	15.89( $C2'/c'$ )	$\mathbb{Z}_2\mathbb{Z}_4$	
Topology	 U=0 , TI      U=2eV , TI      U=4eV , TI      U=6eV , TI				

TABLE CCCXVI. Topology phase diagram of Pr<sub>3</sub>Ru<sub>4</sub>Al<sub>12</sub>.

BCS ID	Formula	ICSD	MSG	T.C.	
0.226	NdCo <sub>2</sub>	246554	15.89( $C2'/c'$ )	$\mathbb{Z}_2\mathbb{Z}_4$	
Topology	 U=0 , ES      U=2eV , TI      U=4eV , TI      U=6eV , TI				

TABLE CCCXVII. Topology phase diagram of NdCo<sub>2</sub>.

BCS ID	Formula	ICSD	MSG	T.C.	
2.10	HoP	*	15.89( $C2'/c'$ )	$\mathbb{Z}_2\mathbb{Z}_4$	
Topology	 U=0 , TI      U=2eV , TI      U=4eV , TI      U=6eV , TI				

TABLE CCCXVIII. Topology phase diagram of HoP.

BCS ID	Formula	ICSD	MSG	T.C.	
1.14	Ho <sub>2</sub> BaNiO <sub>5</sub>	67930	15.90( $C_c2/c$ )	$\mathbb{Z}_2$	
Topology	 U=0 , LCEBR      U=2eV , LCEBR      U=4eV , LCEBR      U=6eV , LCEBR				

TABLE CCCXIX. Topology phase diagram of Ho<sub>2</sub>BaNiO<sub>5</sub>.

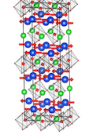
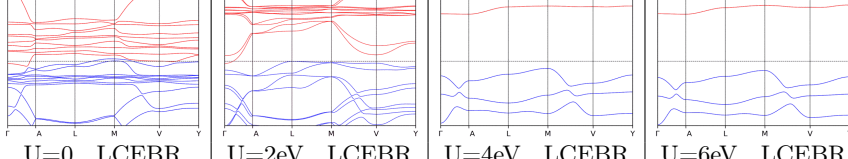
BCS ID	Formula	ICSD	MSG	T.C.	
1.15	Er <sub>2</sub> BaNiO <sub>5</sub>	72630	$15.90(C_c2/c)$	$\mathbb{Z}_2$	
Topology	 U=0 , LCEBR    U=2eV , LCEBR    U=4eV , LCEBR    U=6eV , LCEBR				

TABLE CCCXX. Topology phase diagram of Er<sub>2</sub>BaNiO<sub>5</sub>.

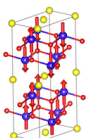
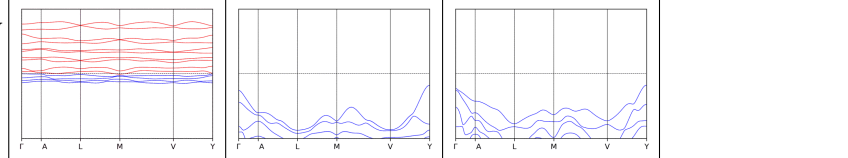
BCS ID	Formula	ICSD	MSG	T.C.	
1.211	Dy <sub>2</sub> O <sub>2</sub> S	*	$15.90(C_c2/c)$	$\mathbb{Z}_2$	
Topology	 U=0 , TI    U=2eV , LCEBR    U=4eV , LCEBR    U=6eV , LCEBR				

TABLE CCCXXI. Topology phase diagram of Dy<sub>2</sub>O<sub>2</sub>S.

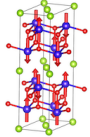
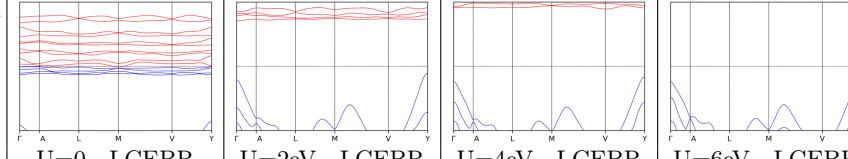
BCS ID	Formula	ICSD	MSG	T.C.	
1.212	Dy <sub>2</sub> O <sub>2</sub> Se	*	$15.90(C_c2/c)$	$\mathbb{Z}_2$	
Topology	 U=0 , LCEBR    U=2eV , LCEBR    U=4eV , LCEBR    U=6eV , LCEBR				

TABLE CCCXXII. Topology phase diagram of Dy<sub>2</sub>O<sub>2</sub>Se.

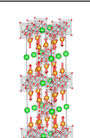
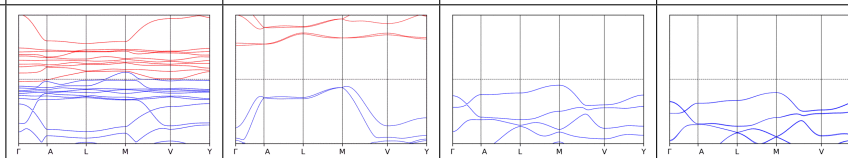
BCS ID	Formula	ICSD	MSG	T.C.	
1.216	Nd <sub>2</sub> BaNiO <sub>5</sub>	72626	$15.90(C_c2/c)$	$\mathbb{Z}_2$	
Topology	 U=0 , TI    U=2eV , LCEBR    U=4eV , LCEBR    U=6eV , LCEBR				

TABLE CCCXXIII. Topology phase diagram of Nd<sub>2</sub>BaNiO<sub>5</sub>.

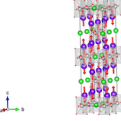
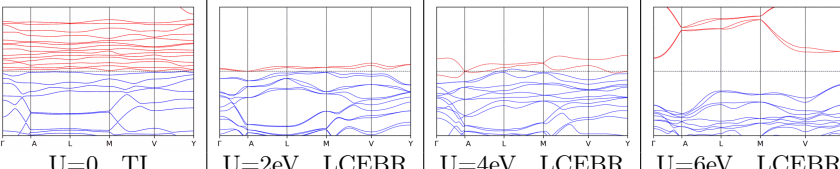
BCS ID	Formula	ICSD	MSG	T.C.	
1.217	Tb <sub>2</sub> BaNiO <sub>5</sub>	66078	15.90( $C_c2/c$ )	$\mathbb{Z}_2$	
Topology					

TABLE CCCXXIV. Topology phase diagram of Tb<sub>2</sub>BaNiO<sub>5</sub>.

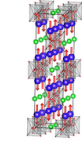
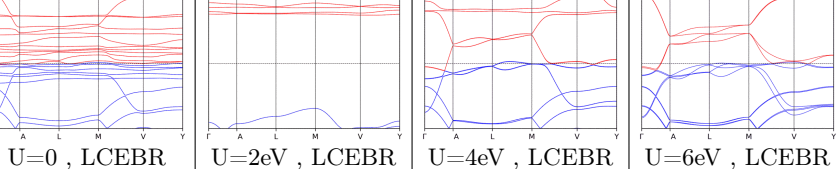
BCS ID	Formula	ICSD	MSG	T.C.	
1.36	Dy <sub>2</sub> BaNiO <sub>5</sub>	72627	15.90( $C_c2/c$ )	$\mathbb{Z}_2$	
Topology					

TABLE CCCXXV. Topology phase diagram of Dy<sub>2</sub>BaNiO<sub>5</sub>.

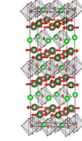
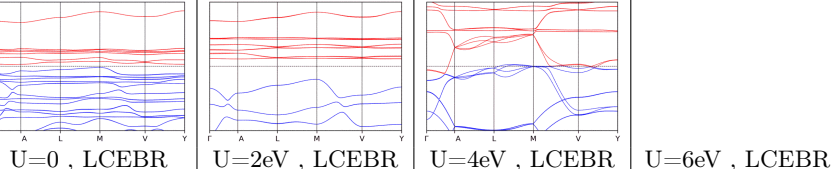
BCS ID	Formula	ICSD	MSG	T.C.	
1.53	Er <sub>2</sub> BaNiO <sub>5</sub>	72630	15.90( $C_c2/c$ )	$\mathbb{Z}_2$	
Topology					

TABLE CCCXXVI. Topology phase diagram of Er<sub>2</sub>BaNiO<sub>5</sub>.

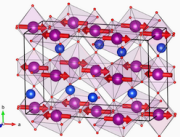
BCS ID	Formula	ICSD	MSG	T.C.	
1.20	HoMnO <sub>3</sub>	*	31.129( $P_bmn2_1$ )	w/o	
Topology					
	U=0 , LCEBR	U=2eV , TBD	U=4eV , TBD	U=6eV , TBD	

TABLE CCCXXVII. Topology phase diagram of HoMnO<sub>3</sub>.

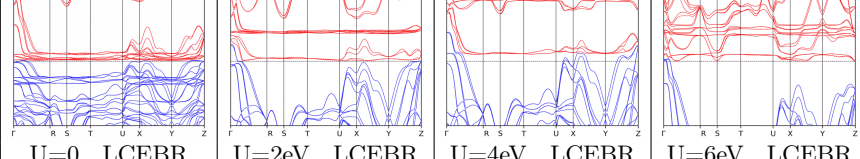
BCS ID	Formula	ICSD	MSG	T.C.	
1.33	ErAuGe	*	33.154( $P_{Cn}a2_1$ )	w/o	
Topology					

TABLE CCCXXVIII. Topology phase diagram of ErAuGe.

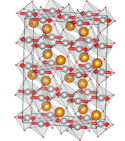
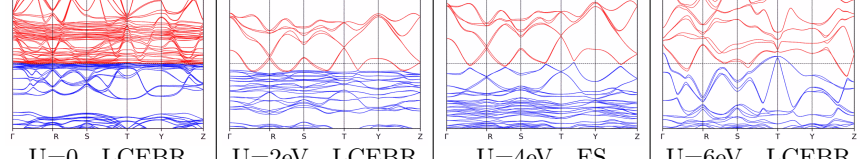
BCS ID	Formula	ICSD	MSG	T.C.	
1.43	PrNiO <sub>3</sub>	67718	36.178( $C_{am}c2_1$ )	w/o	
Topology					

TABLE CCCXXIX. Topology phase diagram of PrNiO<sub>3</sub>.

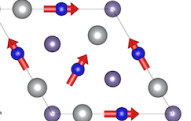
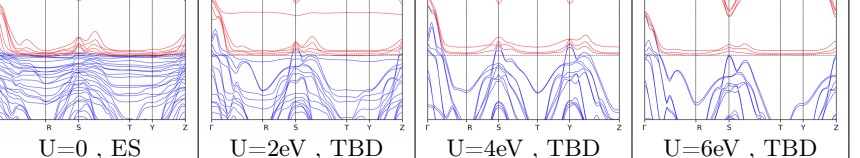
BCS ID	Formula	ICSD	MSG	T.C.	
0.26	TmAgGe	164587	38.191( $Am'm'2$ )	w/o	
Topology					

TABLE CCCXXX. Topology phase diagram of TmAgGe.

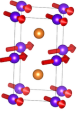
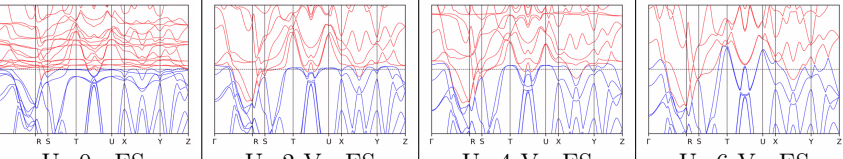
BCS ID	Formula	ICSD	MSG	T.C.	
2.12	TbMg	104880	49.270( $Pc'cm'$ )	$\mathbb{Z}_2\mathbb{Z}_2$	
Topology					

TABLE CCCXXXI. Topology phase diagram of TbMg.

BCS ID	Formula	ICSD	MSG	T.C.	
1.139	Ho <sub>2</sub> RhIn <sub>8</sub>	*	49.273( $P_{ccm}$ )	$\mathbb{Z}_2$	
Topology					

TABLE CCCXXXII. Topology phase diagram of Ho<sub>2</sub>RhIn<sub>8</sub>.

BCS ID	Formula	ICSD	MSG	T.C.	
2.11	TbMg	104880	51.295( $P_{mm'm'a'}$ )	$\mathbb{Z}_2$	
Topology					

TABLE CCCXXXIII. Topology phase diagram of TbMg.

BCS ID	Formula	ICSD	MSG	T.C.	
1.222	Er <sub>2</sub> CoGa <sub>8</sub>	169772	51.298( $P_a mma$ )	$\mathbb{Z}_2 \mathbb{Z}_2$	
Topology					

TABLE CCCXXXIV. Topology phase diagram of Er<sub>2</sub>CoGa<sub>8</sub>.

BCS ID	Formula	ICSD	MSG	T.C.	
1.150	PrAg	605674	53.334( $P_B mna$ )	$\mathbb{Z}_2$	
Topology					

TABLE CCCXXXV. Topology phase diagram of PrAg.

BCS ID	Formula	ICSD	MSG	T.C.	
0.22	DyB4	68651	55.355( $Pb'am$ )	w/o	
Topology					

TABLE CCCXXXVI. Topology phase diagram of DyB4.

BCS ID	Formula	ICSD	MSG	T.C.	
1.105	Gd <sub>2</sub> CuO <sub>4</sub>	75425	56.374('P <sub>Accn</sub> ')	$\mathbb{Z}_2$	
Topology					

TABLE CCCXXXVII. Topology phase diagram of Gd<sub>2</sub>CuO<sub>4</sub>.

BCS ID	Formula	ICSD	MSG	T.C.	
1.8	CeRu <sub>2</sub> Al <sub>10</sub>	59912	57.391( $Pbcm$ )	$\mathbb{Z}_2$	
Topology					

TABLE CCCXXXVIII. Topology phase diagram of CeRu<sub>2</sub>Al<sub>10</sub>.

BCS ID	Formula	ICSD	MSG	T.C.	
0.187	CeMnAsO	195499	59.407( $Pm'mn$ )	w/o	
Topology					

TABLE CCCXXXIX. Topology phase diagram of CeMnAsO.

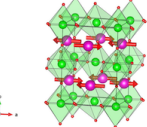
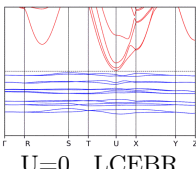
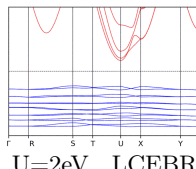
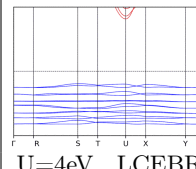
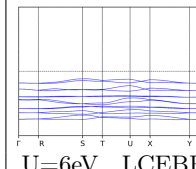
BCS ID	Formula	ICSD	MSG	T.C.	
0.146	EuZrO <sub>3</sub>	*	62.444( $Pnm'a$ )	w/o	
Topology	 U=0 , LCEBR	 U=2eV , LCEBR	 U=4eV , LCEBR	 U=6eV , LCEBR	

TABLE CCCXL. Topology phase diagram of EuZrO<sub>3</sub>.

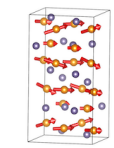
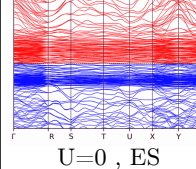
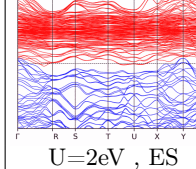
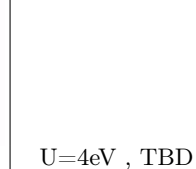
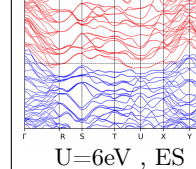
BCS ID	Formula	ICSD	MSG	T.C.	
0.185	Nd <sub>5</sub> Ge <sub>4</sub>	190405	62.447( $Pnm'a'$ )	$\mathbb{Z}_2$	
Topology	 U=0 , ES	 U=2eV , ES	 U=4eV , TBD	 U=6eV , ES	

TABLE CCCXLI. Topology phase diagram of Nd<sub>5</sub>Ge<sub>4</sub>.

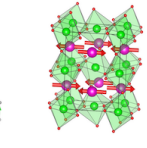
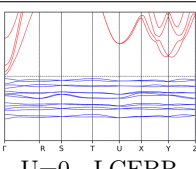
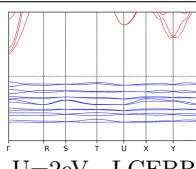
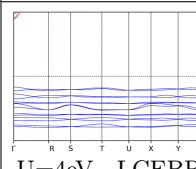
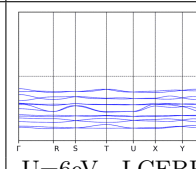
BCS ID	Formula	ICSD	MSG	T.C.	
0.147	EuZrO <sub>3</sub>	*	62.449( $Pn'm'a'$ )	w/o	
Topology	 U=0 , LCEBR	 U=2eV , LCEBR	 U=4eV , LCEBR	 U=6eV , LCEBR	

TABLE CCCXLII. Topology phase diagram of EuZrO<sub>3</sub>.

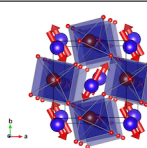
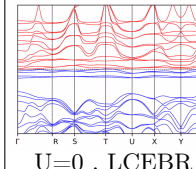
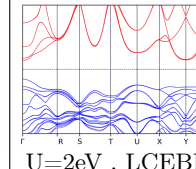
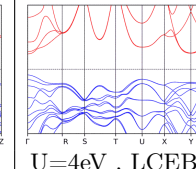
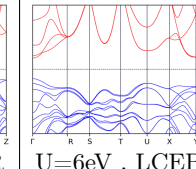
BCS ID	Formula	ICSD	MSG	T.C.	
0.159	DyCoO <sub>3</sub>	190949	62.449( $Pn'm'a'$ )	w/o	
Topology	 U=0 , LCEBR	 U=2eV , LCEBR	 U=4eV , LCEBR	 U=6eV , LCEBR	

TABLE CCCXLIII. Topology phase diagram of DyCoO<sub>3</sub>.

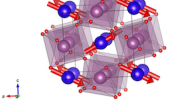
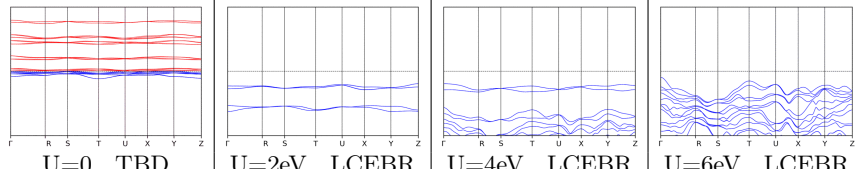
BCS ID	Formula	ICSD	MSG	T.C.	
0.171	DyScO <sub>3</sub>	99545	$62.449(Pn'm'a')$	w/o	
Topology	 U=0 , TBD    U=2eV , LCEBR    U=4eV , LCEBR    U=6eV , LCEBR				

TABLE CCCXLIV. Topology phase diagram of DyScO<sub>3</sub>.

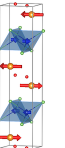
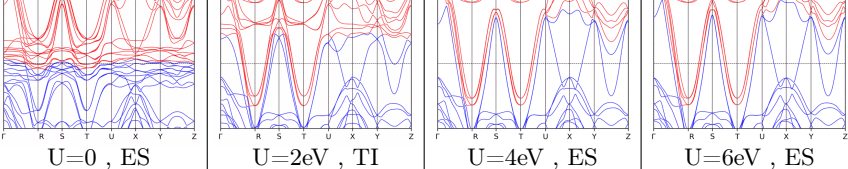
BCS ID	Formula	ICSD	MSG	T.C.	
1.179	NdCoAsO	180774	$62.450(P_anma)$	$\mathbb{Z}_2$	
Topology	 U=0 , ES    U=2eV , TI    U=4eV , ES    U=6eV , ES				

TABLE CCCXLV. Topology phase diagram of NdCoAsO.

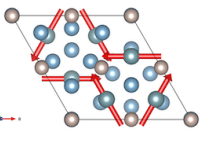
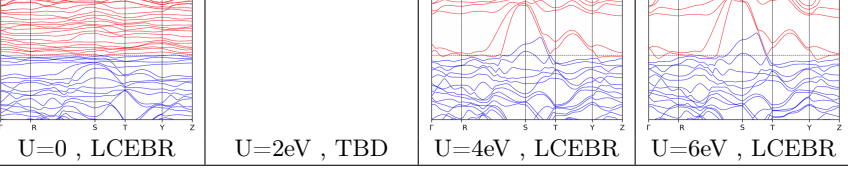
BCS ID	Formula	ICSD	MSG	T.C.	
0.12	U <sub>3</sub> Ru <sub>4</sub> Al <sub>12</sub>	163985	$63.461(Cmcm')$	w/o	
Topology	 U=0 , LCEBR    U=2eV , TBD    U=4eV , LCEBR    U=6eV , LCEBR				

TABLE CCCXLVI. Topology phase diagram of U<sub>3</sub>Ru<sub>4</sub>Al<sub>12</sub>.

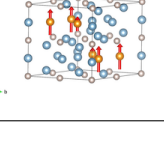
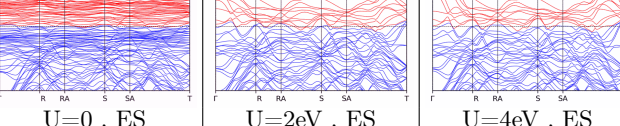
BCS ID	Formula	ICSD	MSG	T.C.	
0.149	Nd <sub>3</sub> Ru <sub>4</sub> Al <sub>12</sub>	*	$63.462(Cm'c'm)$	$\mathbb{Z}_2$	
Topology	 U=0 , ES    U=2eV , ES    U=4eV , ES    U=6eV , ES				

TABLE CCCXLVII. Topology phase diagram of Nd<sub>3</sub>Ru<sub>4</sub>Al<sub>12</sub>.

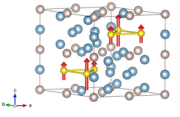
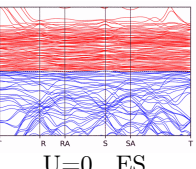
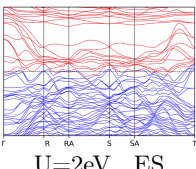
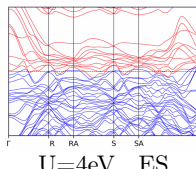
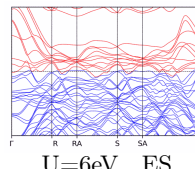
BCS ID	Formula	ICSD	MSG	T.C.	
0.173	Pr <sub>3</sub> Ru <sub>4</sub> Al <sub>12</sub>	*	63.462( $Cm'c'm$ )	$\mathbb{Z}_2$	
Topology	 U=0 , ES	 U=2eV , ES	 U=4eV , ES	 U=6eV , ES	

TABLE CCCXLVIII. Topology phase diagram of Pr<sub>3</sub>Ru<sub>4</sub>Al<sub>12</sub>.

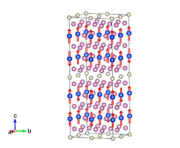
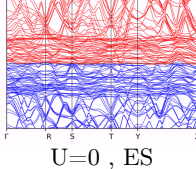
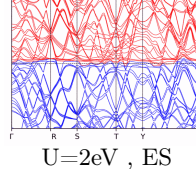
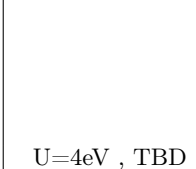
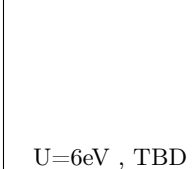
BCS ID	Formula	ICSD	MSG	T.C.	
3.3	Ho <sub>2</sub> RhIn <sub>8</sub>	*	63.464( $Cm'cm'$ )	$\mathbb{Z}_2\mathbb{Z}_2$	
Topology	 U=0 , ES	 U=2eV , ES	 U=4eV , TBD	 U=6eV , TBD	

TABLE CCCXLIX. Topology phase diagram of Ho<sub>2</sub>RhIn<sub>8</sub>.

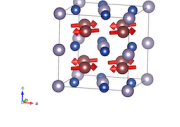
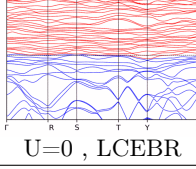
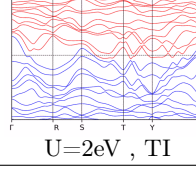
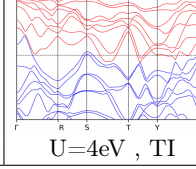
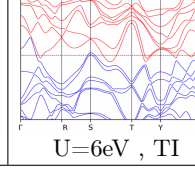
BCS ID	Formula	ICSD	MSG	T.C.	
1.200	U <sub>2</sub> Ni <sub>2</sub> Sn	*	63.466( $C_cmc_m$ )	$\mathbb{Z}_2$	
Topology	 U=0 , LCEBR	 U=2eV , TI	 U=4eV , TI	 U=6eV , TI	

TABLE CCCL. Topology phase diagram of U<sub>2</sub>Ni<sub>2</sub>Sn.

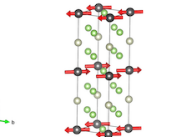
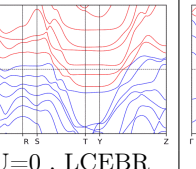
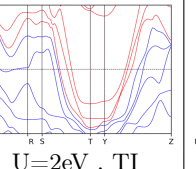
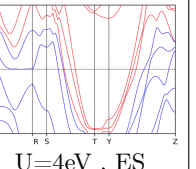
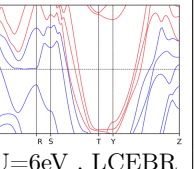
BCS ID	Formula	ICSD	MSG	T.C.	
1.262	NpRhGa <sub>5</sub>	*	63.466( $C_cmc_m$ )	$\mathbb{Z}_2$	
Topology	 U=0 , LCEBR	 U=2eV , TI	 U=4eV , ES	 U=6eV , LCEBR	

TABLE CCCLI. Topology phase diagram of NpRhGa<sub>5</sub>.

BCS ID	Formula	ICSD	MSG	T.C.	
1.195	Er <sub>2</sub> Ni <sub>2</sub> In	*	63.467( $C_a mcm$ )	$\mathbb{Z}_2$	
Topology	 U=0 , LCEBR      U=2eV , LCEBR      U=4eV , TI      U=6eV , LCEBR				

TABLE CCCLII. Topology phase diagram of Er<sub>2</sub>Ni<sub>2</sub>In.

BCS ID	Formula	ICSD	MSG	T.C.	
3.13	CeB <sub>6</sub>	67404	64.479( $C_a mca$ )	$\mathbb{Z}_2$	
Topology	 U=0 , LCEBR      U=2eV , TBD      U=4eV , TBD      U=6eV , TBD				

TABLE CCCLIII. Topology phase diagram of CeB<sub>6</sub>.

BCS ID	Formula	ICSD	MSG	T.C.	
1.188	CeRh <sub>2</sub> Si <sub>2</sub>	621959	64.480( $C_A mca$ )	$\mathbb{Z}_2$	
Topology	 U=0 , TI      U=2eV , LCEBR      U=4eV , ES      U=6eV , TI				

TABLE CCCLIV. Topology phase diagram of CeRh<sub>2</sub>Si<sub>2</sub>.

BCS ID	Formula	ICSD	MSG	T.C.	
0.141	TbGe <sub>2</sub>	56030	65.483( $Cm'mm$ )	w/o	
Topology	 U=0 , LCEBR      U=2eV , TBD      U=4eV , TBD      U=6eV , LCEBR				

TABLE CCCLV. Topology phase diagram of TbGe<sub>2</sub>.

BCS ID	Formula	ICSD	MSG	T.C.	
1.223	Tm <sub>2</sub> CoGa <sub>8</sub>	169773	65.489( $C_a$ mmm)	$\mathbb{Z}_2\mathbb{Z}_4$	
Topology					

TABLE CCCLVI. Topology phase diagram of Tm<sub>2</sub>CoGa<sub>8</sub>.

BCS ID	Formula	ICSD	MSG	T.C.	
1.106	Pr <sub>2</sub> CuO <sub>4</sub>	202884	66.500( $C_{Accm}$ )	$\mathbb{Z}_2$	
Topology					

TABLE CCCLVII. Topology phase diagram of Pr<sub>2</sub>CuO<sub>4</sub>.

BCS ID	Formula	ICSD	MSG	T.C.	
1.142	CeMgPb	*	67.510( $C_{Amma}$ )	$\mathbb{Z}_2$	
Topology					

TABLE CCCLVIII. Topology phase diagram of CeMgPb.

BCS ID	Formula	ICSD	MSG	T.C.	
0.16	EuTiO <sub>3</sub>	*	69.523( $Fm'mm$ )	w/o	
Topology					

TABLE CCCLIX. Topology phase diagram of EuTiO<sub>3</sub>.

BCS ID	Formula	ICSD	MSG	T.C.	
1.0.12	UAu2Si2	*	71.536( $Im'm'm$ )	$\mathbb{Z}_2\mathbb{Z}_2$	
Topology	 U=0 , ES      U=2eV , ES      U=4eV , ES      U=6eV , ES				

TABLE CCCLX. Topology phase diagram of UAu2Si2.

BCS ID	Formula	ICSD	MSG	T.C.	
2.28	NpNiGa5	*	74.559( $Imm'a'$ )	$\mathbb{Z}_2\mathbb{Z}_2$	
Topology	 U=0 , ES      U=2eV , ES      U=4eV , ES      U=6eV , ES				

TABLE CCCLXI. Topology phase diagram of NpNiGa5.

BCS ID	Formula	ICSD	MSG	T.C.	
1.59	KTb3F12	51125	84.58( $P_I4_2/m$ )	$\mathbb{Z}_4$	
Topology	 U=0 , TBD      U=2eV , LCEBR      U=4eV , LCEBR      U=6eV , LCEBR				

TABLE CCCLXII. Topology phase diagram of KTb3F12.

BCS ID	Formula	ICSD	MSG	T.C.	
0.107	Ho2Ge2O7	161912	92.111( $P4_12_12$ )	w/o	
Topology	 U=0 , LCEBR      U=2eV , LCEBR      U=4eV , LCEBR      U=6eV , LCEBR				

TABLE CCCLXIII. Topology phase diagram of Ho2Ge2O7.

BCS ID	Formula	ICSD	MSG	T.C.	
0.184	Nd <sub>5</sub> Si <sub>4</sub>	190404	92.114( $P4_12'_12'$ )	w/o	
Topology	 U=0 , ES	 U=2eV , ES	 U=4eV , ES	 U=6eV , ES	

TABLE CCCLXIV. Topology phase diagram of Nd<sub>5</sub>Si<sub>4</sub>.

BCS ID	Formula	ICSD	MSG	T.C.	
1.0.11	CeCoGe <sub>3</sub>	190701	107.231( $I4m'm'$ )	$\mathbb{Z}_2$	
Topology	 U=0 , LCEBR	 U=2eV , ES	 U=4eV , ES	 U=6eV , TBD	

TABLE CCCLXV. Topology phase diagram of CeCoGe<sub>3</sub>.

BCS ID	Formula	ICSD	MSG	T.C.	
2.26	PrCo <sub>2</sub> P <sub>2</sub>	73650	123.345( $P4/mm'm'$ )	$\mathbb{Z}_4\mathbb{Z}_4\mathbb{Z}_4$	
Topology	 U=0 , ES	 U=2eV , ES	 U=4eV , ES	 U=6eV , ES	

TABLE CCCLXVI. Topology phase diagram of PrCo<sub>2</sub>P<sub>2</sub>.

BCS ID	Formula	ICSD	MSG	T.C.	
1.162	NdMg	*	124.360( $P_c4/mcc$ )	$\mathbb{Z}_4$	
Topology	 U=0 , ES	 U=2eV , ES	 U=4eV , ES	 U=6eV , ES	

TABLE CCCLXVII. Topology phase diagram of NdMg.

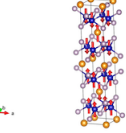
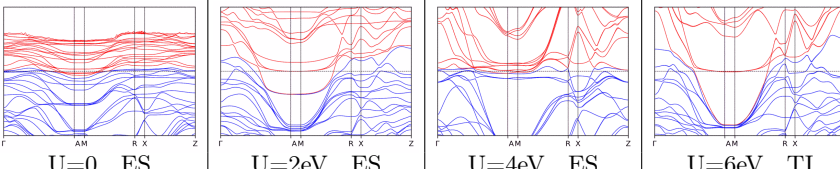
BCS ID	Formula	ICSD	MSG	T.C.	
1.251	NdCo <sub>2</sub> P <sub>2</sub>	73652	124.360( $P_c4/mcc$ )	$\mathbb{Z}_4$	
Topology					

TABLE CCCLXVIII. Topology phase diagram of NdCo<sub>2</sub>P<sub>2</sub>.

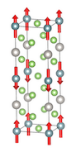
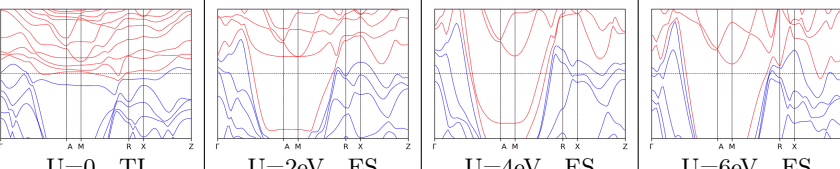
BCS ID	Formula	ICSD	MSG	T.C.	
1.255	UPtGa <sub>5</sub>	*	124.360( $P_c4/mcc$ )	$\mathbb{Z}_4$	
Topology					

TABLE CCCLXIX. Topology phase diagram of UPtGa<sub>5</sub>.

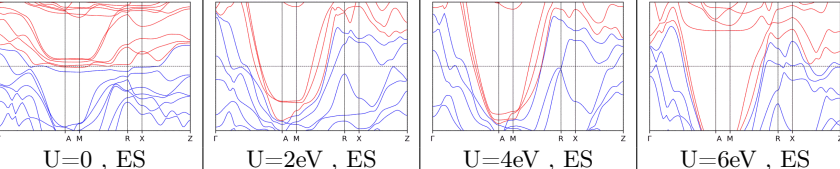
BCS ID	Formula	ICSD	MSG	T.C.	
1.261	NpRhGa <sub>5</sub>	*	124.360( $P_c4/mcc$ )	$\mathbb{Z}_4$	
Topology					

TABLE CCCLXX. Topology phase diagram of NpRhGa<sub>5</sub>.

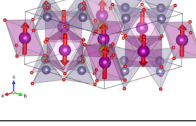
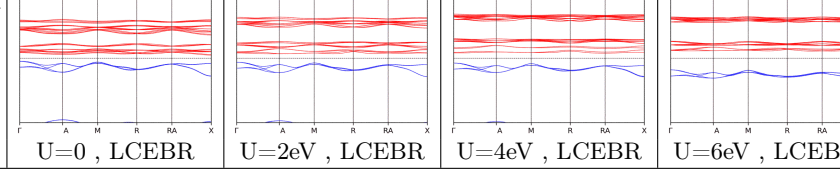
BCS ID	Formula	ICSD	MSG	T.C.	
0.189	CeMn <sub>2</sub> Ge <sub>4</sub> O <sub>12</sub>	*	125.367( $P4'/nbm'$ )	$\mathbb{Z}_2$	
Topology					

TABLE CCCLXXI. Topology phase diagram of CeMn<sub>2</sub>Ge<sub>4</sub>O<sub>12</sub>.

BCS ID	Formula	ICSD	MSG	T.C.	
2.14	NdMg	*	125.373( $P_C4/nbm$ )	$\mathbb{Z}_2$	
Topology					

TABLE CCCLXXII. Topology phase diagram of NdMg.

BCS ID	Formula	ICSD	MSG	T.C.	
1.253	CeCo <sub>2</sub> P <sub>2</sub>	85895	126.386( $P_I4/nnc$ )	$\mathbb{Z}_2$	
Topology					

TABLE CCCLXXIII. Topology phase diagram of CeCo<sub>2</sub>P<sub>2</sub>.

BCS ID	Formula	ICSD	MSG	T.C.	
0.80	U <sub>2</sub> Pd <sub>2</sub> In	106867	127.394( $P4'/m'bm'$ )	$\mathbb{Z}_2$	
Topology					

TABLE CCCLXXIV. Topology phase diagram of U<sub>2</sub>Pd<sub>2</sub>In.

BCS ID	Formula	ICSD	MSG	T.C.	
0.81	U <sub>2</sub> Pd <sub>2</sub> Sn	658413	127.394( $P4'/m'bm'$ )	$\mathbb{Z}_2$	
Topology					

TABLE CCCLXXV. Topology phase diagram of U<sub>2</sub>Pd<sub>2</sub>Sn.

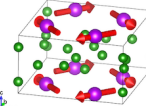
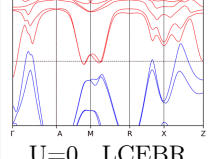
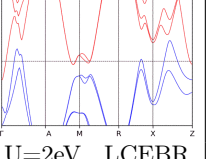
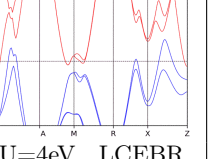
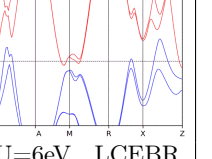
BCS ID	Formula	ICSD	MSG	T.C.	
0.9	GdB4	*	$127.395(P4/m'b'm')$	w/o	
Topology					

TABLE CCCLXXVI. Topology phase diagram of GdB4.

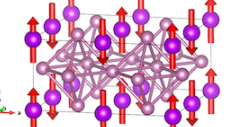
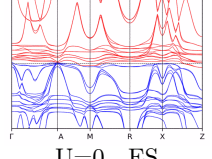
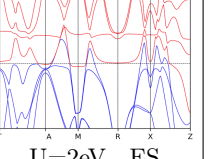
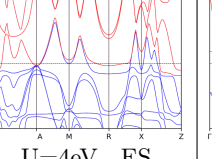
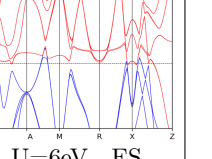
BCS ID	Formula	ICSD	MSG	T.C.	
1.81	GdIn3	*	$127.397(P_C4/mbm)$	$\mathbb{Z}_4\mathbb{Z}_4$	
Topology					

TABLE CCCLXXVII. Topology phase diagram of GdIn3.

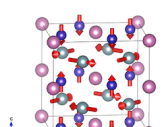
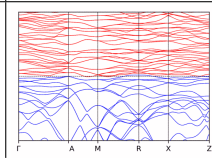
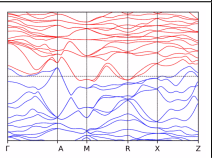
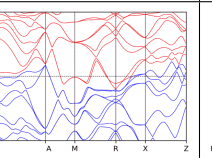
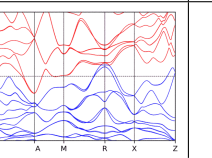
BCS ID	Formula	ICSD	MSG	T.C.	
1.102	U2Ni2In	*	$128.408(P_C4/mnc)$	$\mathbb{Z}_4$	
Topology					

TABLE CCCLXXVIII. Topology phase diagram of U2Ni2In.

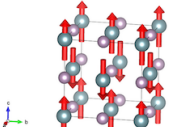
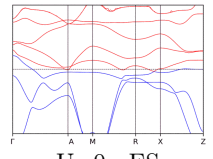
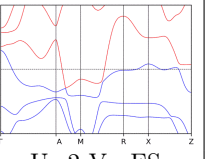
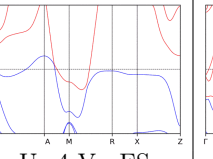
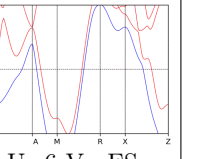
BCS ID	Formula	ICSD	MSG	T.C.	
1.160	UP	648255	$128.410(P_I4/mnc)$	$\mathbb{Z}_4$	
Topology					

TABLE CCCLXXIX. Topology phase diagram of UP.

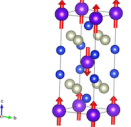
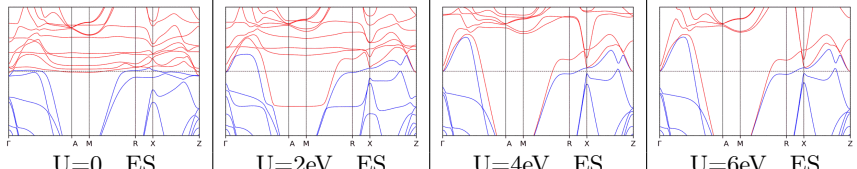
BCS ID	Formula	ICSD	MSG	T.C.	
1.187	TbRh2Si2	650329	128.410( $P_I4/mnc$ )	$\mathbb{Z}_4$	
Topology					

TABLE CCCLXXX. Topology phase diagram of TbRh2Si2.

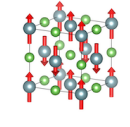
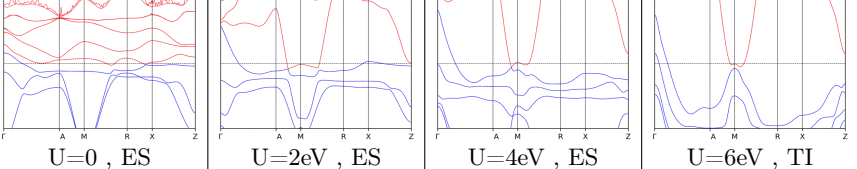
BCS ID	Formula	ICSD	MSG	T.C.	
1.208	UAs	*	128.410( $P_I4/mnc$ )	$\mathbb{Z}_4$	
Topology					

TABLE CCCLXXXI. Topology phase diagram of UAs.

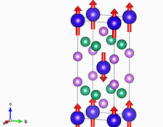
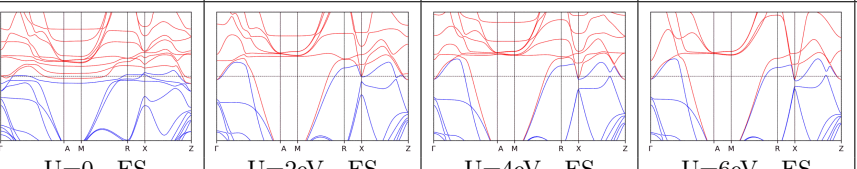
BCS ID	Formula	ICSD	MSG	T.C.	
1.21	DyCo2Si2	622705	128.410( $P_I4/mnc$ )	$\mathbb{Z}_4$	
Topology					

TABLE CCCLXXXII. Topology phase diagram of DyCo2Si2.

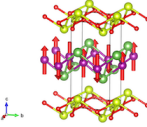
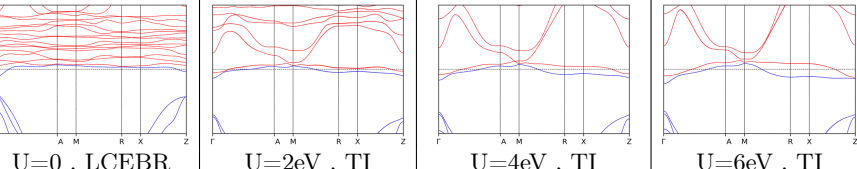
BCS ID	Formula	ICSD	MSG	T.C.	
0.186	CeMnAsO	195499	129.416( $P4'/n'm'm$ )	$\mathbb{Z}_2$	
Topology					

TABLE CCCLXXXIII. Topology phase diagram of CeMnAsO.

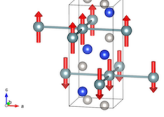
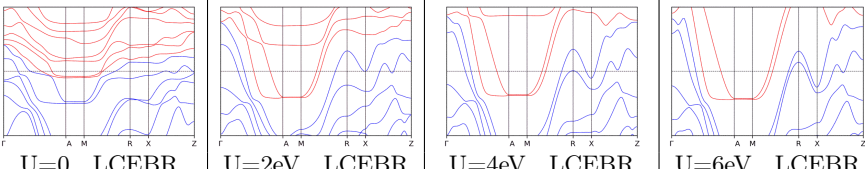
BCS ID	Formula	ICSD	MSG	T.C.	
0.194	UPt <sub>2</sub> Si <sub>2</sub>	57472	$129.419(P4/n'm'm')$	w/o	
Topology	 U=0 , LCEBR      U=2eV , LCEBR      U=4eV , LCEBR      U=6eV , LCEBR				

TABLE CCCLXXXIV. Topology phase diagram of UPt<sub>2</sub>Si<sub>2</sub>.

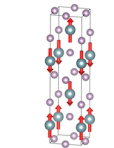
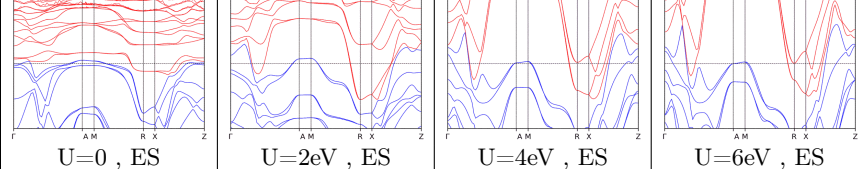
BCS ID	Formula	ICSD	MSG	T.C.	
1.215	UP2	77853	$130.432(P_c4/ncc)$	$\mathbb{Z}_2$	
Topology	 U=0 , ES      U=2eV , ES      U=4eV , ES      U=6eV , ES				

TABLE CCCLXXXV. Topology phase diagram of UP2.

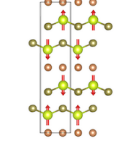
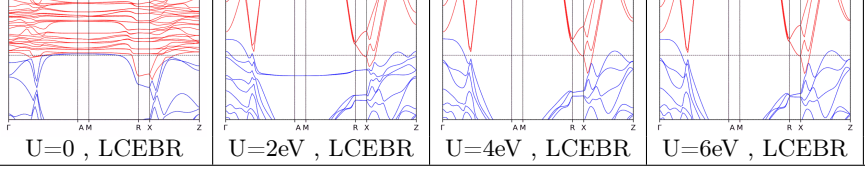
BCS ID	Formula	ICSD	MSG	T.C.	
1.271	CeSbTe	*	$130.432(P_c4/ncc)$	$\mathbb{Z}_2$	
Topology	 U=0 , LCEBR      U=2eV , LCEBR      U=4eV , LCEBR      U=6eV , LCEBR				

TABLE CCCLXXXVI. Topology phase diagram of CeSbTe.

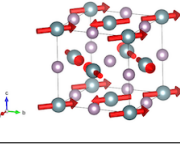
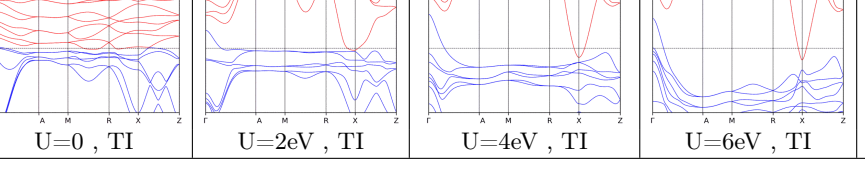
BCS ID	Formula	ICSD	MSG	T.C.	
2.13	UP	648255	$134.481(P_C4_2/nnm)$	$\mathbb{Z}_2$	
Topology	 U=0 , TI      U=2eV , TI      U=4eV , TI      U=6eV , TI				

TABLE CCCLXXXVII. Topology phase diagram of UP.

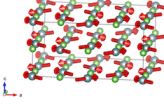
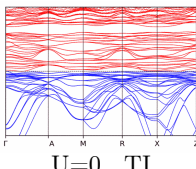
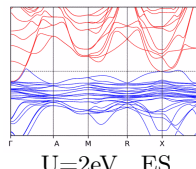
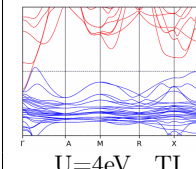
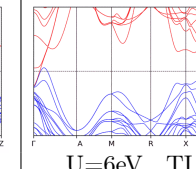
BCS ID	Formula	ICSD	MSG	T.C.	
2.20	UAs	*	134.481( $P_c4_2/nnm$ )	$\mathbb{Z}_2$	
Topology	 U=0 , TI	 U=2eV , ES	 U=4eV , TI	 U=6eV , TI	

TABLE CCCLXXXVIII. Topology phase diagram of UAs.

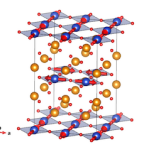
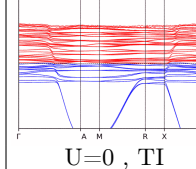
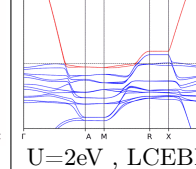
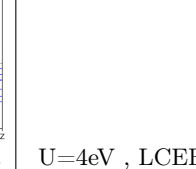
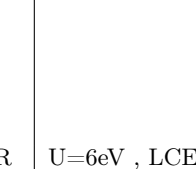
BCS ID	Formula	ICSD	MSG	T.C.	
2.6	Nd <sub>2</sub> CuO <sub>4</sub>	202885	134.481( $P_c4_2/nnm$ )	$\mathbb{Z}_2$	
Topology	 U=0 , TI	 U=2eV , LCEBR	 U=4eV , LCEBR	 U=6eV , LCEBR	

TABLE CCCLXXXIX. Topology phase diagram of Nd<sub>2</sub>CuO<sub>4</sub>.

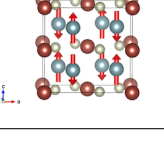
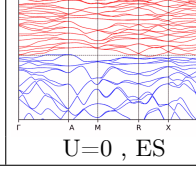
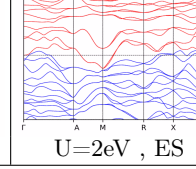
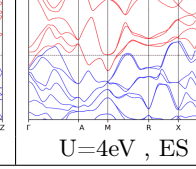
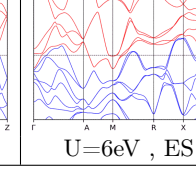
BCS ID	Formula	ICSD	MSG	T.C.	
1.103	U <sub>2</sub> Rh <sub>2</sub> Sn	246630	135.492( $P_c4_2/mbc$ )	$\mathbb{Z}_4$	
Topology	 U=0 , ES	 U=2eV , ES	 U=4eV , ES	 U=6eV , ES	

TABLE CCCXC. Topology phase diagram of U<sub>2</sub>Rh<sub>2</sub>Sn.

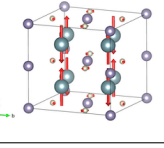
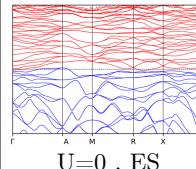
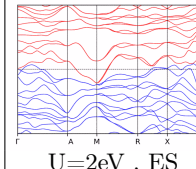
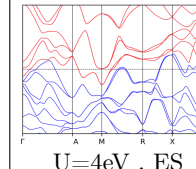
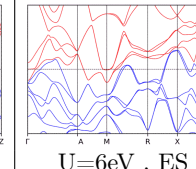
BCS ID	Formula	ICSD	MSG	T.C.	
1.207	U <sub>2</sub> Rh <sub>2</sub> Sn	*	135.492( $P_c4_2/mbc$ )	$\mathbb{Z}_4$	
Topology	 U=0 , ES	 U=2eV , ES	 U=4eV , ES	 U=6eV , ES	

TABLE CCCXCI. Topology phase diagram of U<sub>2</sub>Rh<sub>2</sub>Sn.

BCS ID	Formula	ICSD	MSG	T.C.	
1.254	UNiGa5	*	140.550( $I_c4/mcm$ )	$\mathbb{Z}_4$	
Topology	   				

TABLE CCCXCII. Topology phase diagram of UNiGa5.

BCS ID	Formula	ICSD	MSG	T.C.	
1.82	Nd2RhIn8	*	140.550( $I_c4/mcm$ )	$\mathbb{Z}_4$	
Topology	   				

TABLE CCCXCIII. Topology phase diagram of Nd2RhIn8.

BCS ID	Formula	ICSD	MSG	T.C.	
1.87	TbCo2Ga8	623196	140.550( $I_c4/mcm$ )	$\mathbb{Z}_4$	
Topology	   				

TABLE CCCXCIV. Topology phase diagram of TbCo2Ga8.

BCS ID	Formula	ICSD	MSG	T.C.	
0.154	Er2Ru2O7	97533	141.554( $I4'_1/am'd$ )	$\mathbb{Z}_2$	
Topology	   				

TABLE CCCXCV. Topology phase diagram of Er2Ru2O7.

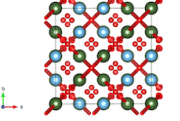
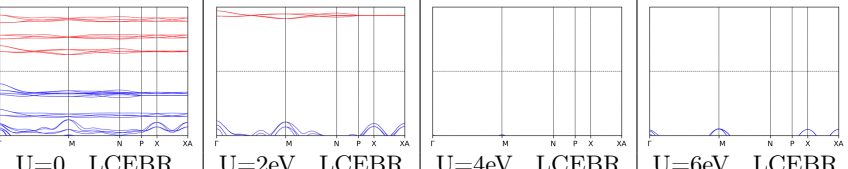
BCS ID	Formula	ICSD	MSG	T.C.	
0.29	Er <sub>2</sub> Ti <sub>2</sub> O <sub>7</sub>	24152	$141.554(I4'_1/am'd)$	$\mathbb{Z}_2$	
Topology	 U=0 , LCEBR    U=2eV , LCEBR    U=4eV , LCEBR    U=6eV , LCEBR				

TABLE CCCXCVI. Topology phase diagram of Er<sub>2</sub>Ti<sub>2</sub>O<sub>7</sub>.

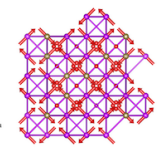
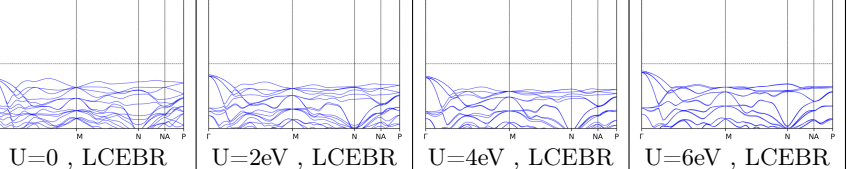
BCS ID	Formula	ICSD	MSG	T.C.	
0.47	Gd <sub>2</sub> Sn <sub>2</sub> O <sub>7</sub>	84753	$141.555(I4'_1/am'd')$	$\mathbb{Z}_2$	
Topology	 U=0 , LCEBR    U=2eV , LCEBR    U=4eV , LCEBR    U=6eV , LCEBR				

TABLE CCCXCVII. Topology phase diagram of Gd<sub>2</sub>Sn<sub>2</sub>O<sub>7</sub>.

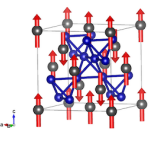
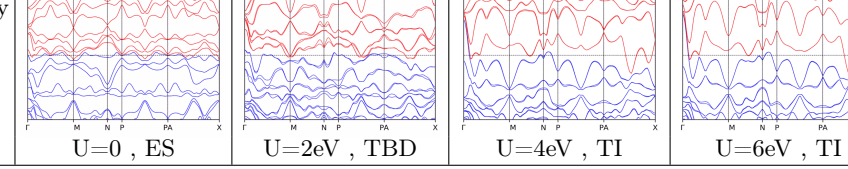
BCS ID	Formula	ICSD	MSG	T.C.	
0.126	NpCo <sub>2</sub>	102606	$141.556(I4'_1/a'm'd)$	$\mathbb{Z}_2$	
Topology	 U=0 , ES    U=2eV , TBD    U=4eV , TI    U=6eV , TI				

TABLE CCCXCVIII. Topology phase diagram of NpCo<sub>2</sub>.

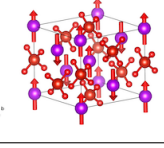
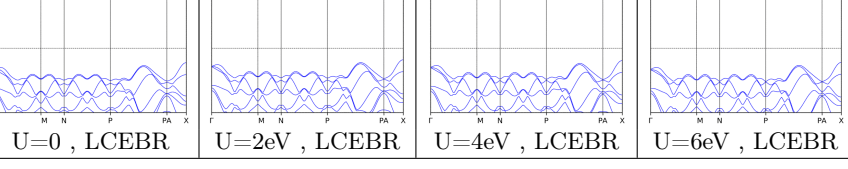
BCS ID	Formula	ICSD	MSG	T.C.	
0.198	GdVO <sub>4</sub>	238223	$141.556(I4'_1/a'm'd)$	$\mathbb{Z}_2$	
Topology	 U=0 , LCEBR    U=2eV , LCEBR    U=4eV , LCEBR    U=6eV , LCEBR				

TABLE CCCXCIX. Topology phase diagram of GdVO<sub>4</sub>.

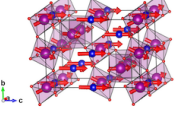
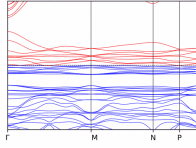
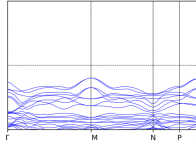
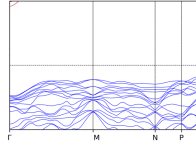
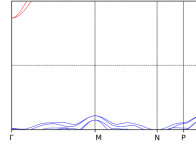
BCS ID	Formula	ICSD	MSG	T.C.	
0.151	Tm <sub>2</sub> Mn <sub>2</sub> O <sub>7</sub>	*	141.557( $I4_1/am'd'$ )	$\mathbb{Z}_2\mathbb{Z}_2$	
Topology	 U=0 , ES	 U=2eV , LCEBR	 U=4eV , LCEBR	 U=6eV , LCEBR	

TABLE CD. Topology phase diagram of Tm<sub>2</sub>Mn<sub>2</sub>O<sub>7</sub>.

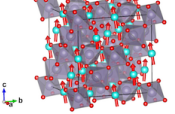
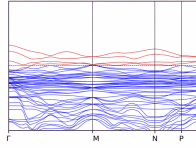
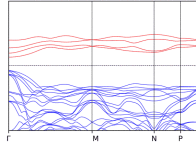
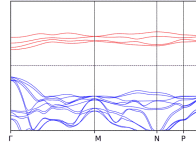
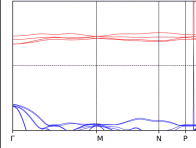
BCS ID	Formula	ICSD	MSG	T.C.	
0.157	Yb <sub>2</sub> Sn <sub>2</sub> O <sub>7</sub>	*	141.557( $I4_1/am'd'$ )	$\mathbb{Z}_2\mathbb{Z}_2$	
Topology	 U=0 , LCEBR	 U=2eV , LCEBR	 U=4eV , LCEBR	 U=6eV , LCEBR	

TABLE CDI. Topology phase diagram of Yb<sub>2</sub>Sn<sub>2</sub>O<sub>7</sub>.

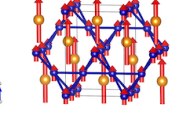
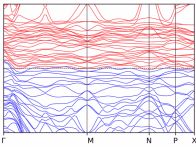
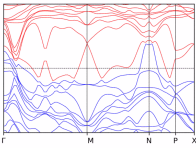
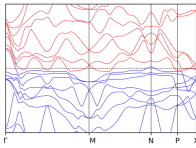
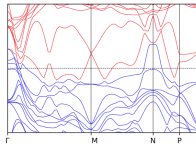
BCS ID	Formula	ICSD	MSG	T.C.	
0.227	NdCo <sub>2</sub>	246555	141.557( $I4_1/am'd'$ )	$\mathbb{Z}_2\mathbb{Z}_2$	
Topology	 U=0 , ES	 U=2eV , ES	 U=4eV , ES	 U=6eV , ES	

TABLE CDII. Topology phase diagram of NdCo<sub>2</sub>.

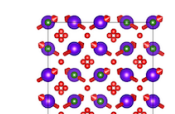
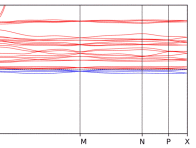
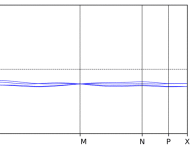
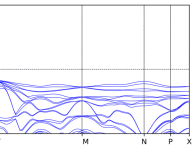
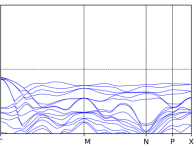
BCS ID	Formula	ICSD	MSG	T.C.	
0.48	Tb <sub>2</sub> Sn <sub>2</sub> O <sub>7</sub>	*	141.557( $I4_1/am'd'$ )	$\mathbb{Z}_2\mathbb{Z}_2$	
Topology	 U=0 , ES	 U=2eV , LCEBR	 U=4eV , LCEBR	 U=6eV , LCEBR	

TABLE CDIII. Topology phase diagram of Tb<sub>2</sub>Sn<sub>2</sub>O<sub>7</sub>.

BCS ID	Formula	ICSD	MSG	T.C.	
0.49	Ho <sub>2</sub> Ru <sub>2</sub> O <sub>7</sub>	96730	$141.557(I4_1/am'd')$	$\mathbb{Z}_2\mathbb{Z}_2$	
Topology	 U=0 , ES	 U=2eV , LCEBR	 U=4eV , LCEBR	 U=6eV , ES	

TABLE CDIV. Topology phase diagram of Ho<sub>2</sub>Ru<sub>2</sub>O<sub>7</sub>.

BCS ID	Formula	ICSD	MSG	T.C.	
0.51	Ho <sub>2</sub> Ru <sub>2</sub> O <sub>7</sub>	96730	$141.557(I4_1/am'd')$	$\mathbb{Z}_2\mathbb{Z}_2$	
Topology	 U=0 , TI	 U=2eV , LCEBR	 U=4eV , LCEBR	 U=6eV , LCEBR	

TABLE CDV. Topology phase diagram of Ho<sub>2</sub>Ru<sub>2</sub>O<sub>7</sub>.

BCS ID	Formula	ICSD	MSG	T.C.	
1.161	PrFe <sub>3</sub> (BO <sub>3</sub> ) <sub>4</sub>	*	155.48( $R_I32$ )	w/o	
Topology	U=0 , LCEBR	U=2eV , TBD	 U=4eV , ES	 U=6eV , LCEBR	

TABLE CDVI. Topology phase diagram of PrFe<sub>3</sub>(BO<sub>3</sub>)<sub>4</sub>.

BCS ID	Formula	ICSD	MSG	T.C.	
0.169	U <sub>3</sub> As <sub>4</sub>	42168	$161.71(R3c')$	w/o	
Topology	 U=0 , ES	 U=2eV , ES	 U=4eV , LCEBR	 U=6eV , LCEBR	

TABLE CDVII. Topology phase diagram of U<sub>3</sub>As<sub>4</sub>.

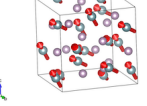
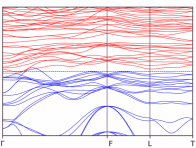
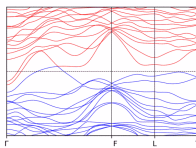
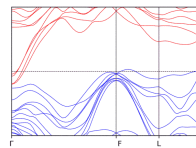
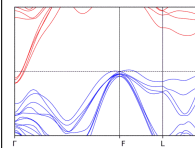
BCS ID	Formula	ICSD	MSG	T.C.	
0.170	U3P4	648243	161.71( $R3c'$ )	w/o	
Topology	 U=0 , ES	 U=2eV , ES	 U=4eV , LCEBR	 U=6eV , LCEBR	

TABLE CDVIII. Topology phase diagram of U3P4.

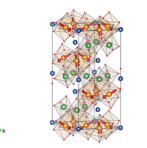
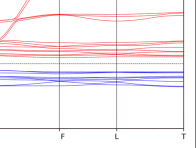
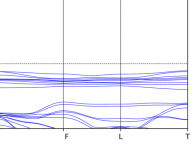
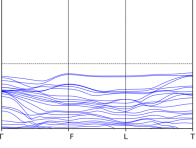
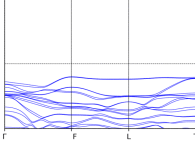
BCS ID	Formula	ICSD	MSG	T.C.	
0.167	Nd <sub>3</sub> Sb <sub>3</sub> Mg <sub>2</sub> O <sub>14</sub>	*	166.101( $R3m'$ )	$\mathbb{Z}_2\mathbb{Z}_4$	
Topology	 U=0 , LCEBR	 U=2eV , LCEBR	 U=4eV , LCEBR	 U=6eV , LCEBR	

TABLE CDIX. Topology phase diagram of Nd<sub>3</sub>Sb<sub>3</sub>Mg<sub>2</sub>O<sub>14</sub>.

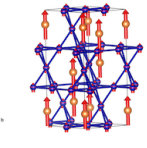
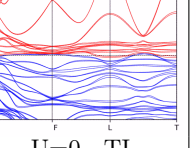
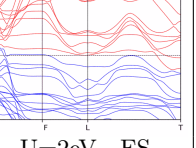
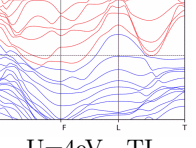
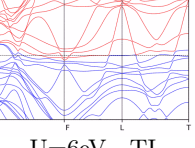
BCS ID	Formula	ICSD	MSG	T.C.	
0.228	TbCo <sub>2</sub>	152582	166.101( $R3m'$ )	$\mathbb{Z}_2\mathbb{Z}_4$	
Topology	 U=0 , TI	 U=2eV , ES	 U=4eV , TI	 U=6eV , TI	

TABLE CDX. Topology phase diagram of TbCo<sub>2</sub>.

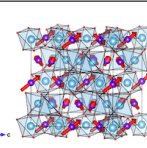
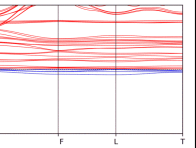
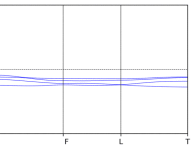
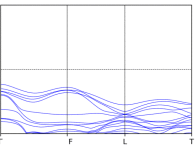
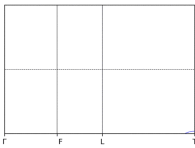
BCS ID	Formula	ICSD	MSG	T.C.	
0.77	Tb <sub>2</sub> Ti <sub>2</sub> O <sub>7</sub>	151747	166.101( $R3m'$ )	$\mathbb{Z}_2\mathbb{Z}_4$	
Topology	 U=0 , ES	 U=2eV , LCEBR	 U=4eV , LCEBR	 U=6eV , LCEBR	

TABLE CDXI. Topology phase diagram of Tb<sub>2</sub>Ti<sub>2</sub>O<sub>7</sub>.

BCS ID	Formula	ICSD	MSG	T.C.	
1.189	TbMg3	9750	167.108( $R_I3c$ )	$\mathbb{Z}_2$	
Topology	 U=0 , LCEBR		 U=2eV , LCEBR	 U=4eV , TBD	 U=6eV , TBD

TABLE CDXII. Topology phase diagram of TbMg3.

BCS ID	Formula	ICSD	MSG	T.C.	
0.32	HoMnO3	92838	185.197( $P6_3cm$ )	w/o	
Topology	 U=0 , LCEBR	 U=2eV , LCEBR	 U=4eV , LCEBR	 U=6eV , LCEBR	

TABLE CDXIII. Topology phase diagram of HoMnO3.

BCS ID	Formula	ICSD	MSG	T.C.	
0.33	HoMnO3	92838	185.197( $P6_3cm$ )	w/o	
Topology	 U=0 , LCEBR	 U=2eV , TBD	 U=4eV , TBD	 U=6eV , TBD	

TABLE CDXIV. Topology phase diagram of HoMnO3.

BCS ID	Formula	ICSD	MSG	T.C.	
3.8	NdZn	646083	222.103( $P_{In}3n$ )	$\mathbb{Z}_2$	
Topology	 U=0 , ESFD	 U=2eV , ES	 U=4eV , ES	 U=6eV , ESFD	

TABLE CDXV. Topology phase diagram of NdZn.

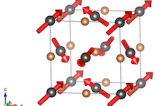
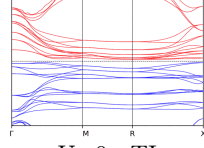
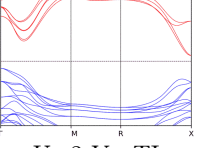
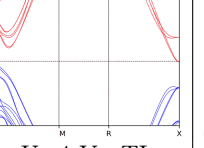
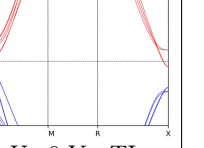
BCS ID	Formula	ICSD	MSG	T.C.	
3.12	NpSb	*	224.113( $Pn3m'$ )	$\mathbb{Z}_2$	
Topology	 $\Gamma - M - R - X$ $U=0, \text{TI}$	 $\Gamma - M - R - X$ $U=2\text{eV}, \text{TI}$	 $\Gamma - M - R - X$ $U=4\text{eV}, \text{TI}$	 $\Gamma - M - R - X$ $U=6\text{eV}, \text{TI}$	

TABLE CDXVI. Topology phase diagram of NpSb.

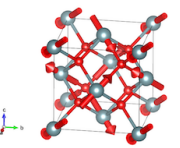
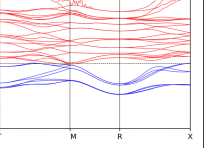
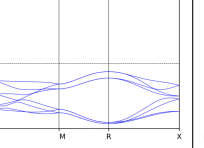
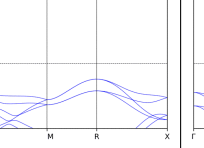
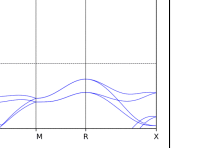
BCS ID	Formula	ICSD	MSG	T.C.	
3.2	UO <sub>2</sub>	647595	224.113( $Pn3m'$ )	$\mathbb{Z}_2$	
Topology	 $\Gamma - M - R - X$ $U=0, \text{ES}$	 $\Gamma - M - R - X$ $U=2\text{eV}, \text{LCEBR}$	 $\Gamma - M - R - X$ $U=4\text{eV}, \text{LCEBR}$	 $\Gamma - M - R - X$ $U=6\text{eV}, \text{LCEBR}$	

TABLE CDXVII. Topology phase diagram of UO<sub>2</sub>.

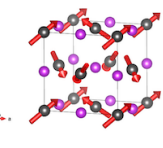
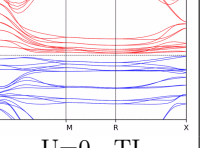
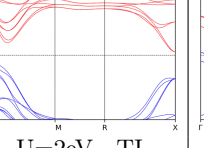
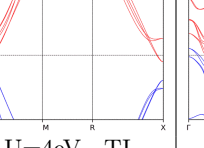
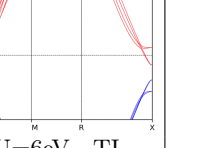
BCS ID	Formula	ICSD	MSG	T.C.	
3.7	NpBi	106952	224.113( $Pn3m'$ )	$\mathbb{Z}_2$	
Topology	 $\Gamma - M - R - X$ $U=0, \text{TI}$	 $\Gamma - M - R - X$ $U=2\text{eV}, \text{TI}$	 $\Gamma - M - R - X$ $U=4\text{eV}, \text{TI}$	 $\Gamma - M - R - X$ $U=6\text{eV}, \text{TI}$	

TABLE CDXVIII. Topology phase diagram of NpBi.

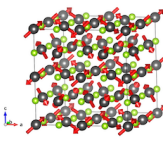
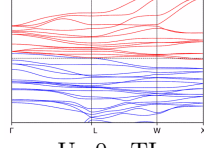
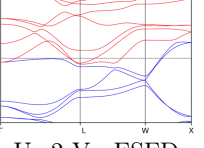
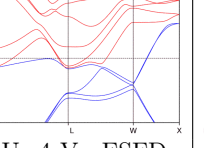
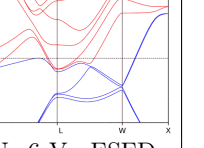
BCS ID	Formula	ICSD	MSG	T.C.	
3.10	NpSe	*	228.139( $F_Sd3c$ )	$\mathbb{Z}_2$	
Topology	 $\Gamma - L - W - X$ $U=0, \text{TI}$	 $\Gamma - L - W - X$ $U=2\text{eV}, \text{ESFD}$	 $\Gamma - L - W - X$ $U=4\text{eV}, \text{ESFD}$	 $\Gamma - L - W - X$ $U=6\text{eV}, \text{ESFD}$	

TABLE CDXIX. Topology phase diagram of NpSe.

BCS ID	Formula	ICSD	MSG	T.C.	
3.11	NpTe	*	228.139( $F_{sd}3c$ )	$\mathbb{Z}_2$	
Topology	 U=0 , TI	 U=2eV , ESFD	 U=4eV , ESFD	 U=6eV , ESFD	

TABLE CDXX. Topology phase diagram of NpTe.

BCS ID	Formula	ICSD	MSG	T.C.	
3.9	NpS	44382	228.139( $F_{sd}3c$ )	$\mathbb{Z}_2$	
Topology	 U=0 , ES	 U=2eV , ESFD	 U=4eV , ESFD	 U=6eV , ESFD	

TABLE CDXXI. Topology phase diagram of NpS.

BCS ID	Formula	ICSD	MSG	T.C.	
3.6	DyCu	*	229.143( $Im\bar{3}m'$ )	$\mathbb{Z}_4$	
Topology	 U=0 , TBD	 U=2eV , ES	 U=4eV , ES	 U=6eV , ES	

TABLE CDXXII. Topology phase diagram of DyCu.

- [1] Qi Wang, Yuanfeng Xu, Rui Lou, Zhonghao Liu, Man Li, Yaobo Huang, Dawei Shen, Hongming Weng, Shancai Wang, and Hechang Lei, "Large intrinsic anomalous hall effect in half-metallic ferromagnet  $\text{Co}_3\text{Sn}_2\text{S}_2$  with magnetic weyl fermions," *Nature communications* **9**, 1–8 (2018).
- [2] Enke Liu, Yan Sun, Nitesh Kumar, Lukas Muechler, Aili Sun, Lin Jiao, Shuo-Ying Yang, Defa Liu, Aiji Liang, Qianan Xu, *et al.*, "Giant anomalous hall effect in a ferromagnetic kagome-lattice semimetal," *Nature physics* **14**, 1125–1131 (2018).
- [3] MM Otrokov, II Klimovskikh, H Bentmann, D Estyunin, A Zeugner, ZS Aliev, S Gaß, AUB Wolter, AV Koroleva, AM Shikin, *et al.*, "Prediction and observation of an antiferromagnetic topological insulator," *Nature* **576**, 416–422 (2019).
- [4] Barry Bradlyn, L. Elcoro, Jennifer Cano, M. G. Vergniory, Zhijun Wang, C. Felser, M. I. Aroyo, and B. Andrei Bernevig, "Topological quantum chemistry," *Nature* **547**, 298–305 (2017).
- [5] M. G. Vergniory, L. Elcoro, Claudia Felser, Nicolas Regnault, B. Andrei Bernevig, and Zhijun Wang, "A complete catalogue of high-quality topological materials," *Nature* **566**, 480–485 (2019).
- [6] Tiantian Zhang, Yi Jiang, Zhida Song, He Huang, Yuqing He, Zhong Fang, Hongming Weng, and Chen Fang, "Catalogue of topological electronic materials," *Nature* **566**, 475–479 (2019).
- [7] Luis Elcoro, Benjamin J Wieder, Zhida Song, Yuanfeng Xu, Barry Bradlyn, and B Andrei Bernevig, "Magnetic topological quantum chemistry," arXiv preprint arXiv:2010.00598 (2020).
- [8] C. L. Kane and E. J. Mele, "Z<sub>2</sub> topological order and the quantum spin hall effect," *Phys. Rev. Lett.* **95**, 146802 (2005).
- [9] B Andrei Bernevig, Taylor L Hughes, and Shou-Cheng Zhang, "Quantum spin hall effect and topological phase transition in HgTe quantum wells," *Science* **314**, 1757–1761 (2006).
- [10] Haijun Zhang, Chao-Xing Liu, Xiao-Liang Qi, Xi Dai, Zhong Fang, and Shou-Cheng Zhang, "Topological insulators in Bi<sub>2</sub>Se<sub>3</sub>, Bi<sub>2</sub>Te<sub>3</sub> and Sb<sub>2</sub>Te<sub>3</sub> with a single dirac cone on the surface," *Nature physics* **5**, 438–442 (2009).
- [11] Timothy H Hsieh, Hsin Lin, Junwei Liu, Wenhui Duan, Arun Bansil, and Liang Fu, "Topological crystalline insulators in the SnTe material class," *Nature communications* **3**, 982 (2012).
- [12] A. Burkov and Leon Balents, "Weyl Semimetal in a Topological Insulator Multilayer," *Physical Review Letters* **107**, 127205 (2011).
- [13] Xiangang Wan, Ari M Turner, Ashvin Vishwanath, and Sergey Y Savrasov, "Topological semimetal and fermi-arc surface states in the electronic structure of pyrochlore iridates," *Physical Review B* **83**, 205101 (2011).
- [14] Gang Xu, Hongming Weng, Zhijun Wang, Xi Dai, and Zhong Fang, "Chern semimetal and the quantized anomalous hall effect in HgCr<sub>2</sub>Se<sub>4</sub>," *Phys. Rev. Lett.* **107**, 186806 (2011).
- [15] Zhijun Wang, Yan Sun, Xing-Qiu Chen, Cesare Franchini, Gang Xu, Hongming Weng, Xi Dai, and Zhong Fang, "Dirac semimetal and topological phase transitions in A<sub>3</sub>Bi(A=Na,K,Rb)," *Physical Review B* **85**, 195320 (2012).
- [16] Bohm-Jung Yang and Naoto Nagaosa, "Classification of stable three-dimensional Dirac semimetals with nontrivial topology," *Nature Communications* **5**, 4898 (2014).
- [17] Hongming Weng, Chen Fang, Zhong Fang, B Andrei Bernevig, and Xi Dai, "Weyl semimetal phase in noncentrosymmetric transition-metal monophosphides," *Physical Review X* **5**, 011029 (2015).
- [18] Shin-Ming Huang, Su-Yang Xu, Ilya Belopolski, Chi-Cheng Lee, Guoqing Chang, BaoKai Wang, Nasser Alidoust, Guang Bian, Madhab Neupane, Chenglong Zhang, *et al.*, "A weyl fermion semimetal with surface fermi arcs in the transition metal monopnictide TaAs class," *Nature communications* **6**, 7373 (2015).
- [19] S. M. Young, S. Zaheer, J. C. Y. Teo, C. L. Kane, E. J. Mele, and A. M. Rappe, "Dirac semimetal in three dimensions," *Phys. Rev. Lett.* **108**, 140405 (2012).
- [20] Robert-Jan Slager, Andrej Mesaros, Vladimir Juričić, and Jan Zaanen, "The space group classification of topological band-insulators," *Nature Physics* **9**, 98–102 (2013).
- [21] Chao-Xing Liu, Rui-Xing Zhang, and Brian K. VanLeeuwen, "Topological nonsymmorphic crystalline insulators," *Phys. Rev. B* **90**, 085304 (2014).
- [22] Zhijun Wang, Aris Alexandradinata, Robert J Cava, and B Andrei Bernevig, "Hourglass fermions," *Nature* **532**, 189–194 (2016).
- [23] Benjamin J Wieder, Barry Bradlyn, Zhijun Wang, Jennifer Cano, Youngkuk Kim, Hyeong-Seok D Kim, Andrew M Rappe, CL Kane, and B Andrei Bernevig, "Wallpaper fermions and the nonsymmorphic dirac insulator," *Science* **361**, 246–251 (2018).
- [24] Hoi Chun Po, Ashvin Vishwanath, and Haruki Watanabe, "Symmetry-based indicators of band topology in the 230 space groups," *Nature communications* **8**, 50 (2017).
- [25] Jorrit Kruthoff, Jan de Boer, Jasper van Wezel, Charles L. Kane, and Robert-Jan Slager, "Topological Classification of Crystalline Insulators through Band Structure Combinatorics," *Physical Review X* **7**, 041069 (2017).
- [26] Zhida Song, Tiantian Zhang, Zhong Fang, and Chen Fang, "Quantitative mappings between symmetry and topology in solids," *Nature Communications* **9**, 3530 (2018).
- [27] Eslam Khalaf, Hoi Chun Po, Ashvin Vishwanath, and Haruki Watanabe, "Symmetry indicators and anomalous surface states of topological crystalline insulators," *Phys. Rev. X* **8**, 031070 (2018).
- [28] Feng Tang, Hoi Chun Po, Ashvin Vishwanath, and Xiangang Wan, "Comprehensive search for topological materials using symmetry indicators," *Nature* **566**, 486–489 (2019).
- [29] Haruki Watanabe, Hoi Chun Po, and Ashvin Vishwanath, "Structure and topology of band structures in the 1651 magnetic space groups," *Science advances* **4**, eaat8685 (2018).

- [30] Max Hirschberger, Satya Kushwaha, Zhijun Wang, Quinn Gibson, Sihang Liang, Carina A Belvin, Bogdan Andrei Bernevig, Robert Joseph Cava, and Nai Phuan Ong, “The chiral anomaly and thermopower of weyl fermions in the half-heusler GdPtBi,” *Nature materials* **15**, 1161–1165 (2016).
- [31] Hao Yang, Yan Sun, Yang Zhang, Wu-Jun Shi, Stuart SP Parkin, and Binghai Yan, “Topological weyl semimetals in the chiral antiferromagnetic materials Mn<sub>3</sub>Ge and Mn<sub>3</sub>Sn,” *New Journal of Physics* **19**, 015008 (2017).
- [32] Hang Li, Shun-Ye Gao, Shao-Feng Duan, Yuan-Feng Xu, Ke-Jia Zhu, Shang-Jie Tian, Jia-Cheng Gao, Wen-Hui Fan, Zhi-Cheng Rao, Jie-Rui Huang, Jia-Jun Li, Da-Yu Yan, Zheng-Tai Liu, Wan-Ling Liu, Yao-Bo Huang, Yu-Liang Li, Yi Liu, Guo-Bin Zhang, Peng Zhang, Takeshi Kondo, Shik Shin, He-Chang Lei, You-Guo Shi, Wen-Tao Zhang, Hong-Ming Weng, Tian Qian, and Hong Ding, “Dirac surface states in intrinsic magnetic topological insulators EuSn<sub>2</sub>As<sub>2</sub> and MnBi<sub>2n</sub>Te<sub>3n+1</sub>,” *Phys. Rev. X* **9**, 041039 (2019).
- [33] DF Liu, AJ Liang, EK Liu, QN Xu, YW Li, C Chen, D Pei, WJ Shi, SK Mo, P Dudin, *et al.*, “Magnetic weyl semimetal phase in a kagomé crystal,” *Science* **365**, 1282–1285 (2019).
- [34] Ilya Belopolski, Kaustuv Manna, Daniel S Sanchez, Guoqing Chang, Benedikt Ernst, Jiaxin Yin, Songtian S Zhang, Tyler Cochran, Nana Shumiya, Hao Zheng, *et al.*, “Discovery of topological weyl fermion lines and drumhead surface states in a room temperature magnet,” *Science* **365**, 1278–1281 (2019).
- [35] Dongqin Zhang, Minji Shi, Tongshuai Zhu, Dingyu Xing, Haijun Zhang, and Jing Wang, “Topological axion states in the magnetic insulator MnBi<sub>2</sub>Te<sub>4</sub> with the quantized magnetoelectric effect,” *Phys. Rev. Lett.* **122**, 206401 (2019).
- [36] J.-R. Soh, F. de Juan, M. G. Vergniory, N. B. M. Schröter, M. C. Rahn, D. Y. Yan, J. Jiang, M. Bristow, P. Reiss, J. N. Blandy, Y. F. Guo, Y. G. Shi, T. K. Kim, A. McCollam, S. H. Simon, Y. Chen, A. I. Coldea, and A. T. Boothroyd, “Ideal weyl semimetal induced by magnetic exchange,” *Phys. Rev. B* **100**, 201102 (2019).
- [37] Simin Nie, Gang Xu, Fritz B Prinz, and Shou-cheng Zhang, “Topological semimetal in honeycomb lattice LnSI,” *Proceedings of the National Academy of Sciences* **114**, 10596–10600 (2017).
- [38] Jinyu Zou, Zhuoran He, and Gang Xu, “The study of magnetic topological semimetals by first principles calculations,” *npj Computational Materials* **5**, 1–19 (2019).
- [39] Guiyuan Hua, Simin Nie, Zhida Song, Rui Yu, Gang Xu, and Kailun Yao, “Dirac semimetal in type-iv magnetic space groups,” *Phys. Rev. B* **98**, 201116 (2018).
- [40] A.V. Shubnikov, N.V. Belov, W.T. Holser, and Institut kristallografi im. A.V. Shubnikova, *Colored Symmetry* (Macmillan, 1964).
- [41] Benjamin J. Wieder, Zhijun Wang, Jennifer Cano, Xi Dai, Leslie M. Schoop, Barry Bradlyn, and B. Andrei Bernevig, “Strong and fragile topological dirac semimetals with higher-order fermi arcs,” *Nature Communications* **11**, 627 (2020).
- [42] Yuanfeng Xu, Zhida Song, Zhijun Wang, Hongming Weng, and Xi Dai, “Higher-order topology of the axion insulator EuIn<sub>2</sub>As<sub>2</sub>,” *Phys. Rev. Lett.* **122**, 256402 (2019).
- [43] Benjamin J Wieder and B Andrei Bernevig, “The axion insulator as a pump of fragile topology,” arXiv preprint arXiv:1810.02373 (2018).
- [44] Liang Fu and C. L. Kane, “Topological insulators with inversion symmetry,” *Phys. Rev. B* **76**, 045302 (2007).
- [45] Frank Wilczek, “Two applications of axion electrodynamics,” *Physical review letters* **58**, 1799 (1987).
- [46] Xiao-Liang Qi, Taylor L Hughes, and Shou-Cheng Zhang, “Topological field theory of time-reversal invariant insulators,” *Physical Review B* **78**, 195424 (2008).
- [47] Roger S. K. Mong, Andrew M. Essin, and Joel E. Moore, “Antiferromagnetic topological insulators,” *Phys. Rev. B* **81**, 245209 (2010).
- [48] Andrew M. Essin, Joel E. Moore, and David Vanderbilt, “Magnetoelectric polarizability and axion electrodynamics in crystalline insulators,” *Phys. Rev. Lett.* **102**, 146805 (2009).
- [49] Taylor L. Hughes, Emil Prodan, and B. Andrei Bernevig, “Inversion-symmetric topological insulators,” *Phys. Rev. B* **83**, 245132 (2011).
- [50] Ari M. Turner, Yi Zhang, Roger S. K. Mong, and Ashvin Vishwanath, “Quantized response and topology of magnetic insulators with inversion symmetry,” *Phys. Rev. B* **85**, 165120 (2012).
- [51] Eslam Khalaf, “Higher-order topological insulators and superconductors protected by inversion symmetry,” *Phys. Rev. B* **97**, 205136 (2018).
- [52] Cai-Zhen Li, An-Qi Wang, Chuan Li, Wen-Zhuang Zheng, Alexander Brinkman, Da-Peng Yu, and Zhi-Min Liao, “Reducing electronic transport dimension to topological hinge states by increasing geometry size of dirac semimetal josephson junctions,” *Phys. Rev. Lett.* **124**, 156601 (2020).
- [53] Noam Morali, Rajib Batabyal, Pranab Kumar Nag, Enke Liu, Qiunan Xu, Yan Sun, Binghai Yan, Claudia Felser, Nurit Avraham, and Haim Beidenkopf, “Fermi-arc diversity on surface terminations of the magnetic weyl semimetal Co<sub>3</sub>Sn<sub>2</sub>S<sub>2</sub>,” *Science* **365**, 1286–1291 (2019).
- [54] K Kuroda, T Tomita, M-T Suzuki, C Bareille, AA Nugroho, Pallab Goswami, M Ochi, M Ikhlas, M Nakayama, S Akebi, *et al.*, “Evidence for magnetic weyl fermions in a correlated metal,” *Nature materials* **16**, 1090 (2017).
- [55] Nicodemos Varnava, Ivo Souza, and David Vanderbilt, “Axion coupling in the hybrid wannier representation,” *Phys. Rev. B* **101**, 155130 (2020).
- [56] Luis Elcoro, Barry Bradlyn, Zhijun Wang, Maia G. Vergniory, Jennifer Cano, Claudia Felser, B. Andrei Bernevig, Daniel Orobengoa, Gemma de la Flor, and Mois I. Aroyo, “Double crystallographic groups and their representations on the Bilbao Crystallographic Server,” *Journal of Applied Crystallography* **50**, 1457–1477 (2017).
- [57] Jennifer Cano, Barry Bradlyn, Zhijun Wang, L. Elcoro, M. G. Vergniory, C. Felser, M. I. Aroyo, and B. Andrei Bernevig, “Building blocks of topological quantum chemistry: Elementary band representations,” *Physical Review B* **97**, 035139 (2018).

- [58] M. G. Vergniory, L. Elcoro, Zhijun Wang, Jennifer Cano, C. Felser, M. I. Aroyo, B. Andrei Bernevig, and Barry Bradlyn, “Graph theory data for topological quantum chemistry,” Phys. Rev. E **96**, 023310 (2017).
- [59] Zhida Song, Sheng-Jie Huang, Yang Qi, Chen Fang, and Michael Hermele, “Topological states from topological crystals,” Science Advances **5** (2019), 10.1126/sciadv.aax2007.
- [60] Luis Elcoro, Zhida Song, and B. Andrei Bernevig, “Application of induction procedure and smith decomposition in calculation and topological classification of electronic band structures in the 230 space groups,” Phys. Rev. B **102**, 035110 (2020).
- [61] Wladimir A. Benalcazar, B. Andrei Bernevig, and Taylor L. Hughes, “Quantized electric multipole insulators,” Science **357**, 61–66 (2017).
- [62] Frank Schindler, Ashley M. Cook, Maia G. Vergniory, Zhijun Wang, Stuart S. P. Parkin, B. Andrei Bernevig, and Titus Neupert, “Higher-order topological insulators,” Science Advances **4**, eaat0346 (2018).
- [63] Frank Schindler, Zhijun Wang, Maia G. Vergniory, Ashley M. Cook, Anil Murani, Shamashis Sengupta, Alik Yu Kasumov, Richard Deblock, Sangjun Jeon, Ilya Drozdov, Hélène Bouchiat, Sophie Guéron, Ali Yazdani, B. Andrei Bernevig, and Titus Neupert, “Higher-order topology in bismuth,” Nature Physics **14**, 918–924 (2018).
- [64] Zhida Song, Zhong Fang, and Chen Fang, “(d-2)-Dimensional Edge States of Rotation Symmetry Protected Topological States,” Physical Review Letters **119**, 246402 (2017).
- [65] Josias Langbehn, Yang Peng, Luka Trifunovic, Felix von Oppen, and Piet W. Brouwer, “Reflection-Symmetric Second-Order Topological Insulators and Superconductors,” Physical Review Letters **119**, 246401 (2017).
- [66] Hoi Chun Po, Haruki Watanabe, and Ashvin Vishwanath, “Fragile Topology and Wannier Obstructions,” Physical Review Letters **121**, 126402 (2018).
- [67] Jennifer Cano, Barry Bradlyn, Zhijun Wang, L. Elcoro, M. G. Vergniory, C. Felser, M. I. Aroyo, and B. Andrei Bernevig, “Topology of Disconnected Elementary Band Representations,” Phys. Rev. Lett. **120**, 266401 (2018).
- [68] Barry Bradlyn, Zhijun Wang, Jennifer Cano, and B. Andrei Bernevig, “Disconnected elementary band representations, fragile topology, and Wilson loops as topological indices: An example on the triangular lattice,” Physical Review B **99**, 045140 (2019).
- [69] Junyeong Ahn, Sungjoon Park, and Bohm-Jung Yang, “Failure of Nielsen-Ninomiya Theorem and Fragile Topology in Two-Dimensional Systems with Space-Time Inversion Symmetry: Application to Twisted Bilayer Graphene at Magic Angle,” Physical Review X **9**, 021013 (2019).
- [70] Zhi-Da Song, Luis Elcoro, Yuan-Feng Xu, Nicolas Regnault, and B. Andrei Bernevig, “Fragile phases as affine monoids: Classification and material examples,” Phys. Rev. X **10**, 031001 (2020).
- [71] S. V. Gallego, J. M. Perez-Mato, L. Elcoro, E. S. Tasci, R. M. Hanson, K. Momma, M. I. Aroyo, and G. Madariaga, “MAGNDATA: towards a database of magnetic structures. I. The commensurate case,” Journal of Applied Crystallography **49**, 1750–1776 (2016).
- [72] G. Kresse and J. Furthmüller, “Efficient iterative schemes for ab initio total-energy calculations using a plane-wave basis set,” Phys. Rev. B **54**, 11169–11186 (1996).
- [73] Fabien Tran and Peter Blaha, “Accurate band gaps of semiconductors and insulators with a semilocal exchange-correlation potential,” Phys. Rev. Lett. **102**, 226401 (2009).
- [74] XiaoYu Deng, Lei Wang, Xi Dai, and Zhong Fang, “Local density approximation combined with gutzwiller method for correlated electron systems: Formalism and applications,” Phys. Rev. B **79**, 075114 (2009).
- [75] Jiacheng Gao, Quansheng Wu, Clas Persson, and Zhijun Wang, “Irvsp: to obtain irreducible representations of electronic states in the vasp,” arXiv preprint arXiv:2002.04032 (2020).
- [76] Nathan C Frey, Matthew K Horton, Jason M Munro, Sinéad M Griffin, Kristin A Persson, and Vivek B Shenoy, “High-throughput search for magnetic and topological order in transition metal oxides,” arXiv preprint arXiv:2006.01075 (2020).
- [77] Qiunan Xu, Zhida Song, Simin Nie, Hongming Weng, Zhong Fang, and Xi Dai, “Two-dimensional oxide topological insulator with iron-pnictide superconductor LiFeAs structure,” Phys. Rev. B **92**, 205310 (2015).
- [78] Dongfei Wang, Lingyuan Kong, Peng Fan, Hui Chen, Shiyu Zhu, Wenya Liu, Lu Cao, Yujie Sun, Shixuan Du, John Schneeloch, Ruidan Zhong, Genda Gu, Liang Fu, Hong Ding, and Hong-Jun Gao, “Evidence for majorana bound states in an iron-based superconductor,” Science **362**, 333–335 (2018).
- [79] Steve M. Young and Benjamin J. Wieder, “Filling-enforced magnetic dirac semimetals in two dimensions,” Phys. Rev. Lett. **118**, 186401 (2017).
- [80] Hoi Chun Po, Ashvin Vishwanath, and Haruki Watanabe, “Symmetry-based indicators of band topology in the 230 space groups,” Nature Communications **8**, 50 (2017).
- [81] J Zak, “Band representations of space groups,” Physical Review B **26**, 3010 (1982).
- [82] J Zak, “Berry’s phase for energy bands in solids,” Physical review letters **62**, 2747 (1989).
- [83] L Michel and J Zak, “Elementary energy bands in crystals are connected,” Physics Reports **341**, 377–395 (2001).
- [84] Chen Fang, Matthew J. Gilbert, and B. Andrei Bernevig, “Bulk topological invariants in noninteracting point group symmetric insulators,” Phys. Rev. B **86**, 115112 (2012).
- [85] Yoonseok Hwang, Junyeong Ahn, and Bohm-Jung Yang, “Fragile topology protected by inversion symmetry: Diagnosis, bulk-boundary correspondence, and wilson loop,” Phys. Rev. B **100**, 205126 (2019).
- [86] Juan L. Mañes, “Fragile phonon topology on the honeycomb lattice with time-reversal symmetry,” Phys. Rev. B **102**, 024307 (2020).
- [87] A. Alexandradinata, J. Höller, Chong Wang, Hengbin Cheng, and Ling Lu, “Crystallographic splitting theorem for band representations and fragile topological photonic crystals,” arXiv:1908.08541 [cond-mat, physics:physics] (2019), arXiv:

- 1908.08541.
- [88] J.M. Perez-Mato, S.V. Gallego, E.S. Tasci, L. Elcoro, G. de la Flor, and M.I. Aroyo, "Symmetry-Based Computational Tools for Magnetic Crystallography," *Annual Review of Materials Research* **45**, 217–248 (2015).
- [89] Guoqing Chang, Su-Yang Xu, Benjamin J. Wieder, Daniel S. Sanchez, Shin-Ming Huang, Ilya Belopolski, Tay-Rong Chang, Songtian Zhang, Arun Bansil, Hsin Lin, and M. Zahid Hasan, "Unconventional chiral fermions and large topological fermi arcs in RhSi," *Phys. Rev. Lett.* **119**, 206401 (2017).
- [90] Jennifer Cano, Barry Bradlyn, and MG Vergniory, "Multifold nodal points in magnetic materials," *APL Materials* **7**, 101125 (2019).
- [91] Guoqing Chang, Benjamin J Wieder, Frank Schindler, Daniel S Sanchez, Ilya Belopolski, Shin-Ming Huang, Bahadur Singh, Di Wu, Tay-Rong Chang, Titus Neupert, *et al.*, "Topological quantum properties of chiral crystals," *Nature materials* **17**, 978 (2018).
- [92] Ivo Souza, Nicola Marzari, and David Vanderbilt, "Maximally localized wannier functions for entangled energy bands," *Physical Review B* **65**, 035109 (2001).
- [93] MP Lopez Sancho, JM Lopez Sancho, JM Lopez Sancho, and J Rubio, "Highly convergent schemes for the calculation of bulk and surface green functions," *Journal of Physics F: Metal Physics* **15**, 851 (1985).
- [94] QuanSheng Wu, ShengNan Zhang, Hai-Feng Song, Matthias Troyer, and Alexey A. Soluyanov, "Wanniertools : An open-source software package for novel topological materials," *Computer Physics Communications* **224**, 405 – 416 (2018).
- [95] Feng Lu, JianZhou Zhao, Hongming Weng, Zhong Fang, and Xi Dai, "Correlated topological insulators with mixed valence," *Phys. Rev. Lett.* **110**, 096401 (2013).
- [96] Hongming Weng, Jianzhou Zhao, Zhijun Wang, Zhong Fang, and Xi Dai, "Topological crystalline kondo insulator in mixed valence ytterbium borides," *Phys. Rev. Lett.* **112**, 016403 (2014).
- [97] Yuanfeng Xu, Changming Yue, Hongming Weng, and Xi Dai, "Heavy weyl fermion state in CeRu<sub>4</sub>Sn<sub>6</sub>," *Phys. Rev. X* **7**, 011027 (2017).
- [98] K. Held, "Electronic structure calculations using dynamical mean field theory," *Advances in Physics* **56**, 829–926 (2007), <https://doi.org/10.1080/00018730701619647>.
- [99] Nicola Lanatà, Hugo U. R. Strand, Xi Dai, and Bo Hellsing, "Efficient implementation of the gutzwille variational method," *Phys. Rev. B* **85**, 035133 (2012).
- [100] Y. X. Yao, C. Z. Wang, and K. M. Ho, "Including many-body screening into self-consistent calculations: Tight-binding model studies with the gutzwille approximation," *Phys. Rev. B* **83**, 245139 (2011).
- [101] Nicodemos Varnava, Ivo Souza, and David Vanderbilt, "Axion coupling in the hybrid wannier representation," arXiv preprint arXiv:1912.11887 (2019).
- [102] Vladimir A. Benalcazar, B. Andrei Bernevig, and Taylor L. Hughes, "Electric multipole moments, topological multipole moment pumping, and chiral hinge states in crystalline insulators," *Physical Review B* **96**, 245115 (2017).